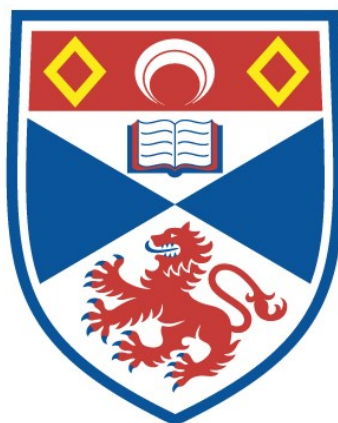# EXPLORING THE PROPERTIES OF SELECTIVELY FLUORINATED JANUS CYCLOHEXANE RINGS

Cihang Yu

A Thesis Submitted for the Degree of PhD
at the
University of St Andrews

2023

Exploring the Properties of Selectively Fluorinated Janus Cyclohexane Rings
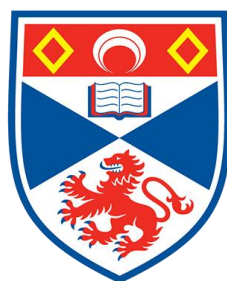
Cihang Yu

University of St Andrews

This thesis is submitted in partial fulfilment for the degree of

Doctor of Philosophy (PhD)

at the University of St Andrews

November 2022

Candidate's declaration

I, Cihang Yu, do hereby certify that this thesis, submitted for the degree of PhD, which is approximately 69,441 words in length, has been written by me, and that it is the record of work carried out by me, or principally by myself in collaboration with others as acknowledged, and that it has not been submitted in any previous application for any degree. I confirm that any appendices included in my thesis contain only material permitted by the 'Assessment of Postgraduate Research Students' policy.

I was admitted as a research student at the University of St Andrews in August 2017.

I received funding from an organisation or institution and have acknowledged the funder(s) in the full text of my thesis.

Date   19th Nov 2022   Signature of candidate

Supervisor's declaration

I hereby certify that the candidate has fulfilled the conditions of the Resolution and Regulations appropriate for the degree of PhD in the University of St Andrews and that the candidate is qualified to submit this thesis in application for that degree. I confirm that any appendices included in the thesis contain only material permitted by the 'Assessment of Postgraduate Research Students' policy.

Date   19th Nov 2022   Signature of supervisor

Permission for publication

In submitting this thesis to the University of St Andrews we understand that we are giving permission for it to be made available for use in accordance with the regulations of the University Library for the time being in force, subject to any copyright vested in the work not being affected thereby. We also understand, unless exempt by an award of an embargo as

i

requested below, that the title and the abstract will be published, and that a copy of the work may be made and supplied to any bona fide library or research worker, that this thesis will be electronically accessible for personal or research use and that the library has the right to migrate this thesis into new electronic forms as required to ensure continued access to the thesis.

I, Cihang Yu, confirm that my thesis does not contain any third-party material that requires copyright clearance.

The following is an agreed request by candidate and supervisor regarding the publication of this thesis:

Printed copy

No embargo on print copy.

Electronic copy

No embargo on electronic copy.

Date   19th Nov 2022   Signature of candidate

Date   19th Nov 2022   Signature of supervisor

Underpinning Research Data or Digital Outputs

Candidate's declaration

I, Cihang Yu, understand that by declaring that I have original research data or digital outputs, I should make every effort in meeting the University's and research funders' requirements on the deposit and sharing of research data or research digital outputs.

Date   19th Nov 2022   Signature of candidate

Permission for publication of underpinning research data or digital outputs

We understand that for any original research data or digital outputs which are deposited, we are giving permission for them to be made available for use in accordance with the requirements of the University and research funders, for the time being in force.

We also understand that the title and the description will be published, and that the underpinning research data or digital outputs will be electronically accessible for use in accordance with the license specified at the point of deposit, unless exempt by award of an embargo as requested below.

The following is an agreed request by candidate and supervisor regarding the publication of underpinning research data or digital outputs:

No embargo on underpinning research data or digital outputs.
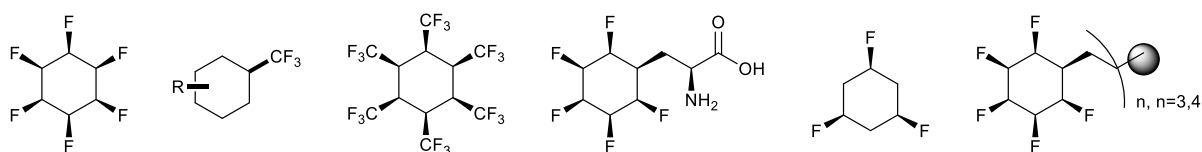
Date   19th Nov 2022   Signature of candidate

Date   19th Nov 2022   Signature of supervisor

Abstract

Janus face fluorocycloalkanes (JFC) represent a novel subject of study. The fluorinated electronegative face and the hydrogenated electropositive face of the rings create an extraordinarily high dipole moment which induces facial polarity. This thesis carries out various studies on this new class of compound.

In Chapter 1, a discussion of the background and general interest in fluorine chemistry is given. The role of fluorine in pharmaceutical chemistry is demonstrated. The most recent studies on the JFC are summarised and discussed, including their preparation and applications in ionic binding, supramolecular chemistry, and biological chemistry.

In Chapter 2, a recently reported stereoselective Rh-catalysed hydrogenation was further explored, and its substrate scope was extended to aryl–CF_3 to deliver facially polarised CF_3–cyclohexane motifs in high diastereoselectivity. The direct preparation of CF_3–containing cyclohexanes form a library of stereoselective motifs for further studies.

In Chapter 3, the study of facially polar CF_3–cyclohexane was extended to the preparation, properties and physiochemistry of all-*cis*-multi-CF_3 cyclohexanes with between 3 and 6 substituent CF_3 groups. The prepared all-*cis*-hexakis-CF_3–cyclohexane has a high barrier to ring inversion (27 kcal mol^{-1}), more than twice that of cyclohexane. This ring also coordinates chloride (Cl-) ion to the hydrogen face with a modest affinity constant (K = $10^3\,M^{-1}$).

In Chapter 4, the surface behaviour of the all-*cis*-hexafluorocyclohexane was studied on HOPG and gold surfaces. The reactivity of JFCs was studied, and a number of functional groups were installed onto the ring. of A novel amino acid of with a JFC side chain was prepared and

incorporated into peptide synthesis.

In Chapter 5, trifluoro substituted cyclohexanes were prepared. An unexpected triaxial preference was found in all-*cis*-1,3,5-trifluorocyclohexane and some of its derivatives. The conformational preferences of these derivatives were also investigated.

In Chapter 6, the JFC motifs were transformed into multi-dentate supramolecular architectures. The proposed frameworks were synthesized in modular approaches. The crystal structure of a number of the building blocks were demonstrated with voids in their supramolecular architectures.

Acknowledgement

Foremost, I would like to sincerely thank my supervisor, Prof David O'Hagan, for the opportunity to carry out my PhD research under his supervision and for all the support he has given me during my time at St. Andrews. His enthusiasm for organofluorine chemistry deeply influenced and encouraged me to persist in curiosity and motivation in this long journey of research. I thank his kindness, patience, and encouragement through the course of my PhD from the bottom of my heart. The research would be much difficult to progress without your guidance.

I would also like to thank all the DOH group members, past and present, for all the support and company in the group. It was of such valuable help, especially during the hard time of Biomolecular Science Building fire and the Covid-19 pandemic. I would especially thank Dr Qingzhi Zhang, Dr Marta Wojnowska, Dr Phillip Lowe, Dr Neil Keddie, Dr Nawaf Al-Maharik and Dr Davide Bello, Dr Rifahath Neyyappadath, for giving me advice throughout my PhD project; Dr Zeguo Fang, Dr Andrea Rodil, Dr Feng Xuan, Dr Joshua Clark, Dr Maria Rubaanu, Dr Tanya Bykova, Yohann Renault, Luca Dobson, Yawen Chen, Mengfan He, Tommy Poskin, Oluwayinka Oke, Dominic Spurling, Gleb Khrapach, William Sanders for their support and valuable discussions. I would thank all my friends in St. Andrews, in the CSC program, and in CSSA union. It has been a pleasure to know all the wonderful people in such a lovely town.

I would like to thank: Dr Tomas Lebl and Dr Siobhan Smith for all their help in the characterisation of NMR spectroscopy; Caroline Horsburgh, University Mass spectrometry facility, Alan Taylor, Edinburgh mass spectrometry centre, EPSRC national mass spectrometry centre Swansea for running mass spectrometry; Prof Alex Slawin, Dr David Cordes, Dr Yuri Andeev for solving the many challenging small crystal X-ray structures; Prof Russell Morris and Dr Gavin Peters for the porous material characterisation, DSC and BET measurement; Prof Michael Buehl for DFT computational studies in Chapter 3; Prof Christopher Baddeley and Dr Federico Grillo for Surface science experiments; Prof Douglas Philp on advice for binding affinity titration; Dr Robert Armstrong for conductivity experiments; Prof Matt Clarke for

hydrogenation facility and Prof Andrew Smith for hosting me in the aftermath of BMS fire; Prof Wuzong Zhou and Prof Nicholas Westwood for valuable help and advice in studying at St Andrews.

I would like to thank all the external collaborators: Prof Rodrigo Cormanich and Bruno Piscelli from the University of Campinas for their DFT calculations in Chapter 5; Dr Shigeyuki Yamada from Kyoto Institute of Technology for LC studies; Prof Gerd-Volker Röschenthaler and Dr Agnes Kütt from Jacobs University Bremen, for collaboration in Chapter 3; Prof Beate Koksch from Humboldt Universität of Berlin for tripeptide study; Prof Sebastien Thibaudeau from Université de Poitiers for superacid reaction study; Prof Terrance McMahon and Dr Scott Hopkins from the University of Waterloo for ionic affinity studies. All those talented collaborators informed and contributed to this work.

I would like to thank Prof Jinbo Hu for advising and help me to start my PhD study at St Andrews. I would not have such a wonderful research journey without that start. His resolute focus on research and kindness to people is always a respectful model.

I would like to specially thank my family, especially my parents, for their unconditional support and love. Thank you for all the supporting emotional and material, continuing through another side of the planet. I could not archive anything without you.

Finally, I must express my gratitude to my wife, Daian, for her continuous care, encouragement, and love. Everything would be much more difficult without your support. I am excited for our journey to commence next.

Funding

Research Data Outputs access statement

Research data underpinning this thesis are available at https://doi.org/10.17630/7310cff9-f312-4bcf-81c5-000ef10205e1

Abbreviations

[Rh]	Rh(CAAC)(COD)Cl catalyst
{X}	decoupling of nuclei X
ΔE	change in enthalpy
3D	three dimensional
a.u.	atomic units
AFM	atomic force microscopy
Asp(D)	aspartic acid
A-value	the ring flip Gibbs energy of chair conformers in monosubstituted cyclohexanes
ax	axial
b.p.	boiling point
BET	Brunauer-Emmett-Teller
Boc	*tert*-Butyloxycarbonyl
Bpin	Bis(pinacolato)diboron
CAACs	Cyclic (amino)(alkyl)carbene catalysts
cat.	Catalyst
cis-	this side of
CLM	cyno liver microsomes
COD	1,5-Cyclooctadiene
COF	covalent organic frameworks
conv.	Conversion
COSY	correlated spectroscopy
CuAAC	Copper-Catalysed Azide-Alkyne Cycloaddition
CyF_5	all *cis*-pentafluorocyclohexylalanine amino acids
D_0	bond disassociation energy
DBU	1,8-Diazabicyclo[5.4.0]undec-7-ene
DCM	dichloromethane
decomp.	Decomposition
DEPT	distortionless enhancement by polarisation transfer

DFT	density functional theory
DIBAL	Diisobutylaluminium hydride
DIPEA	N,N-Diisopropylethylamine
DIPA	diisopropylamine
Dipp	Diisopropylphenyl
DLM	dog liver microsomes
DMAP	4-Dimethylaminopyridine
DMF	N,N-Dimethylformamide
DMI	1,3-Dimethyl-2-imidazolidinone
DMSO	dimethyl sulfoxide
dr	diastereomeric ratio
DSC	differential scanning calorimetry
E_c	complexation energy
EDCI	1-Ethyl-3-(3-dimethylaminopropyl)carbodiimide
eq	equatorial
eq.	equivalent
Et2O	diethyl ether
eV	Electron volt
EXAFS	extended X-ray absorption fine structure
EXSY	exchange correlation
FEL	free electron laser
Fmoc	Fluorenylmethyloxycarbonyl protecting group
FTMS	Fourier transform mass spectrometry
FWHM	full width at half maximum
gMDCK	Madin-Darby canine kidney cell permeability measurement
HATU	Hexafluorophosphate Azabenzotriazole Tetramethyl Uronium
Hhep	human hepatocytes
HLM	human liver microsomal
HLM -N	human liver microsomal in absence of NADPH
HMBC	heteronuclear multiple bond correlation
HOE	heteronuclear overhauser enhancement

HOESY	heteronuclear overhauser effect spectroscopy
HOMO	highest occupied molecular orbital
HOPG	highly oriented pyrolytic graphite
HPLC	high-performance liquid chromatography
HREELS	high-resolution electron energy loss spectrometer
HSQC	heteronuclear single quantum coherence
$^{i}Pr_2NEt$	N,N-Diisopropylethylamine
IR	infrared
IRMPD	infrared multiple photon dissociation
JFC	Janus face cyclohexane
JOF	Janus face coordinating frameworks
K	association constant or Kelvin
K_a	affinity constant
K-edge	sudden increase in x-ray absorption
KinSol	kinetic solubility
LCDs	liquid crystalline displays
LDA	Lithium diisopropylamide
LED	light-emitting diode
LiHMDS	Lithium bis(trimethylsilyl)amide
Log $D_{7.4}$	distribution coefficient of compound in octanol versus in water at pH 7.4
Log P	partition coefficient
LSP	living supramolecular polymerisation
Lα	L-α line
m.p.	melting point
M.S.; MS	molecular sieves
m/z	mass-to-charge ratio
Mhep	mouse hepatocytes
MMP	matched molecular pair
MOF	metal organic frameworks
NA	not available

NADPH	nicotinamide adenine dinucleotide phosphate
NBO	natural bond orbital
NBS	N-Bromosuccinimide
^{n}BuLi	n-Butyllithium
NCHB	nonclassical hydrogen bond
NHC	N-Heterocyclic Carbene
NLO	non-linear optical
NMP	N-Methyl-2-pyrrolidone
NMR	nuclear magnetic resonance
NOE	nuclear Overhauser enhancement
NOESY	nuclear Overhauser effect spectroscopy
ONSU	N-hydroxysuccinimide ester
PBS	phosphate-buffered saline
PET	positron emission tomography
Phe(F)	phenylalanine
pK_a	Negative log of Ka
POM	polarising optical microscopy
ppm	parts per million
r.f.	retardation factor
r.t.	room temperature
RAIR	reflection absorption infrared
RAIRS	reflection absorption infrared spectroscopy
Rhep	rat hepatocytes
RLM	rat liver microsomes
rpm	revolutions per minute
SET	single electron transfer
S_N1	unimolecular nucleophilic substitution
S_NAr	nucleophilic aromatic substitution
STEM-EDS	scanning transmission electron microscopy – energy dispersive spectroscopy
STM	scanning tunnelling microscopy

syn-	on the same side
TB	twist boast
TBACl	tetrabutylammonium chloride
TBAF	tetrabutylammonium fluorine
TBAI	tetrabutylammonium iodide
TBAI	Tetra-n-butylammonium iodide
TBS	*tert*-butyldimethylsilyl
^{t}Bu	*tert*-butyl
TEM	transmission electron microscopy
Temp.	temperature
Tf	trifluoromethanesulfonyl
TFA	trifluoroacetic acid
THF	tetrahydrofuran
ThT	Thioflavin T
TLC	Thin-layer chromatography
TMS	trimethylsilyl
TPSA	topological polar surface area
trans-	on the other side
TS	transition states
TTMSS	Tris(trimethylsilyl)silane
Tyr(Y)	tyrosine
UV	ultraviolet
VIE	vertical ionisation energy
VT	variable temperature
XANES	X-ray absorption near-edge structure
XPS	X-ray photoelectron spectroscopy
β_0	hyperpolarisability
Δ CL$_{hep}$	change in hepatic clearance
λ	wavelength
χ	electron negativity

Contents

Chapter 1. Introduction

1.1 Fluorine element
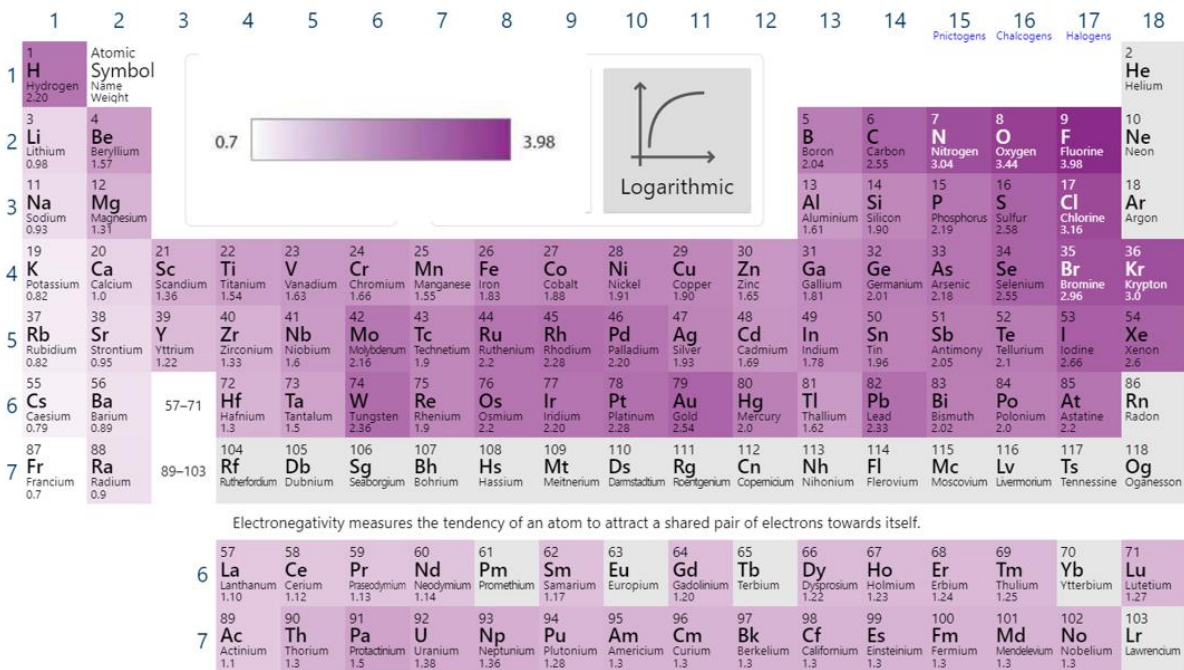
Figure 1-1 Periodic table of electronegativity by Pauling scale.[1]

Fluorine is the most electronegative element in the Periodic Table, assigned χ = 4.0 by Linus Pauling.[1] The fluorine atom has a Van der Waal radius of 1.46 Å, which is only larger than hydrogen 1.10 Å and helium 1.40 Å and is close to oxygen 1.58 Å.[2, 3] There is only one stable isotope, ^{19}F, found in nature. The element is the 13th most abundant element on earth, the most abundant of all of the halogens, and it exists mainly in the mineral forms of fluorspar and fluorapatite in the earth. [4]

Figure 1-2 Sample of mineral fluorspar.

Elemental fluorine (F_2) is highly reactive, and the synthesis and isolation of elemental fluorine became a major focus and challenge for chemists in the 19th Century. The extremely corrosive and highly toxic nature of both hydrogen fluoride (HF) and elemental fluorine meant that the isolation of elemental fluorine was extremely hazardous.[5] Frémy attempted the electrolysis of dry hydrogen fluoride from acidified potassium bifluoride and demonstrated the pure hydrogen fluoride was not conductive. In a modification of the electrolysis, elemental fluorine was finally isolated by Henri Moissan using a conductive mixture of potassium bifluoride and dry hydrogen fluoride. The work was viewed as such a landmark in the history of chemistry that Moissan was awarded the Nobel Prize of Chemistry in 1906, two months before his death.[6]

Figure 1-3 Henri Mossian and his electric furnace at the Faculté des Science, Université de Paris.[6]

In contrast to the abundance of mineral fluorides in the lithosphere, the natural occurrence

of organic fluorine in the biosphere is very low. This is because of the low solubility of fluoride minerals and consequently the low concentration (1.3 ppm) of fluoride in the ocean. This can be contrasted with chloride at 19,000 ppm. In addition, the high heat of hydration of fluoride renders it a poor nucleophile in water and suppresses its reactivity.[4, 7, 8] As a consequence, nucleophilic fluorination *in vivo* is very difficult and the appearance of organofluorine compounds in nature is uncommon. Only a handful of organic natural products which contain fluorine have ever been discovered and these are illustrated in Figure 1-4. [8]
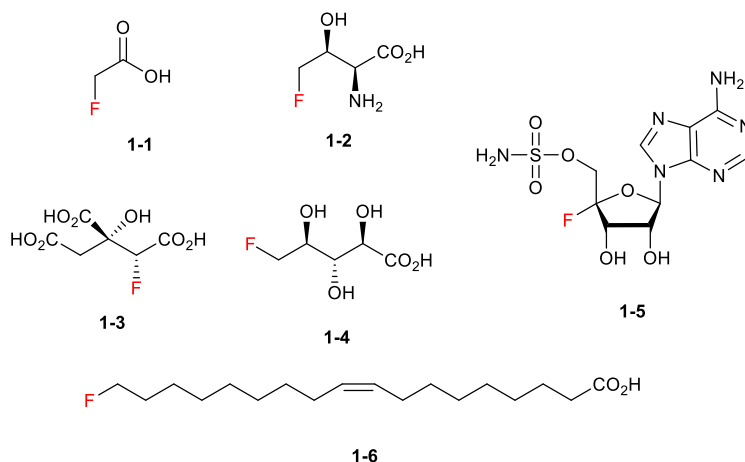
Figure 1-4 The known classes of organofluorine natural products.[8]

The only characterised fluorination enzyme, fluorinase, was first identified in 2002 in St. Andrews in a cell free extract of the bacterium *Streptomyces cattleya*.[9] This enzyme removes the hydration sphere around fluoride anion to facilitate a nucleophilic C–F bond formation on *S*-adenosyl-L-methionine (Scheme 1-1).[9, 10]
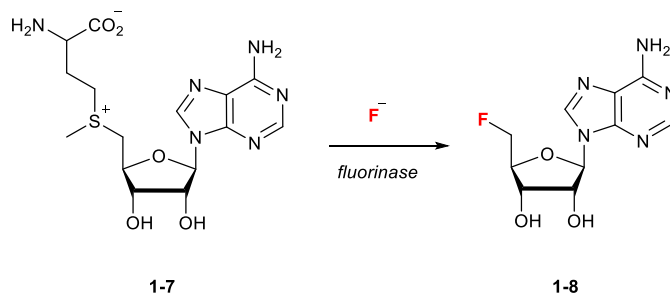
Scheme 1-1 The fluorinase reaction involves nucleophilic fluorination.

1.2 Organofluorine chemistry

Figure 1-5 Applications of organofluorine molecules.

Surprisingly, an element that is rare in the biosphere is intensively used in industrial production and daily life. More than 20 % of pharmaceutical and 30 % of agrochemical products contain at least one fluorine atom.[11, 12] Organofluorine molecules have been widely applied in positron emission tomography (PET), hydrophobic materials, aerospace materials, and liquid crystalline displays (LCDs).[4] The introduction of fluorine into organic molecules brings many advantages for tuning properties, due to the electronegative nature of fluorine and the stability of the C–F bond.

Van der Waals Radii/Å	H (1.2)	C (1.70)	N (1.55)	O (1.52)	**F (1.47)**
	Si (2.1)	P (1.8)	S (1.8)	Cl (1.74)	
Bond length/Å	C–H (1.09)	C–C (1.54)	C–N (1.47)	C–O (1.43)	**C–F (1.35)**
	C–Si (1.85)	C–P (1.84)	C–S (1.82)	C–Cl (1.77)	

Table 1-1 Van der Waals radii and average C–X bond lengths of some common elements.[2, 3]

The high electronegativity of the fluorine atom and the resultant electronegativity difference between carbon and fluorine, leads to the electrostatic character of the C-F bond. This generates a stable bond and also a relatively large dipole associated with the C–F bond.[7] On the other hand, the three lone pairs on fluorine are held tightly due to its high electronegativity, which results in a low donor ability and a very weak hydrogen bond

acceptor ability of organic bound fluorine.[7] The high charge density and low polarizability of fluorine in the C–F bond allows fluorine to tune the lipophilicity in pharmaceuticals development and for incorporation into hydrophobic materials. Perfluorinated materials are highly lipophobic and also hydrophobic and this leads to a large miscibility gap between fluorocarbons and hydrocarbons.[4]

Bond	Bond dissociation energy/k cal mol^{-1}
C–F	105.4
C–H	98.8
C–O	84.0
C–C	83.1
C–Cl	78.5
C–N	69.7

Table 1-2: Bond dissociation energy of common covalent bonds.[2, 7]

The C–F bond emerges as the strongest bond in organic chemistry with the highest average bond dissociation energy, D_0, of 105.4 kcalmol^{-1}.[7] This bond strength was discussed and rationalised by Wiberg,[13, 14] as less of a covalent interaction and more of an electrostatic attraction between $F^{\delta-}$ and $C^{\delta+}$ with formal charges and a very significant electrostatic character. This offers advantages when introducing fluorine into drug molecules and materials to improve metabolic, thermal and chemical stabilities.[4]

Moreover, the bond length of the C–F bond is short at only 1.35 Å (Table 1-1), due to the large bond energy of C–F bond and strong attraction between $F^{\delta-}$ and $C^{\delta+}$. And as discussed above, the fluorine atom is small with a Van de Waals radius of 1.47 Å. The small atomic radius and relatively short bond length makes the replacement of a hydrogen atom or a hydroxyl group effective with little steric change.[7] This offers advantages for pharmaceutical and medicinal chemistry applications which will be discussed in Chapter 1.4.

1.3 Conformation of C–F bonds

The introduction of the C–F bond into molecules can influence the conformation of organic compounds.[7] The strong dipole created by the C–F bond, and the negative electrostatic character on the fluorine atom, often influence molecular conformation by intermolecular and intramolecular electrostatic/dipole interactions.[7] By installation of a C–F bond adjacent to another charged atom or dipole, the conformation of potential drugs can be altered to adjust and improve the interaction and interference with targeted proteins.[15]

1.3.1 Dipole-Dipole interactions

1-9 trans   **1-9 cis**

favoured by 7.5 kcal mol^{-1}
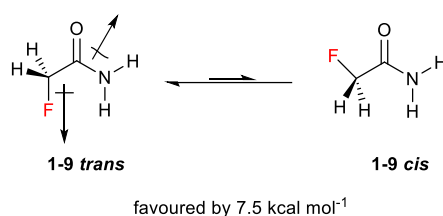
Figure 1-6 Calculated energy difference between *cis* and *trans* conformers of an α-fluoroamide **1-9**.[16]

The strong dipole-dipole interaction of the C–F bond influences the conformational behaviour of organofluorine compounds such as α-fluoroamides **1-9**.[16] The conformational preference is caused by the *anti*-periplanar relationship of the C–F and the carbonyl bond dipoles opposing each other; a phenomenon that extends to esters, ketones and aldehydes.[7]

1.3.2 Dipole-charge interactions and the electrostatic *gauche* effect
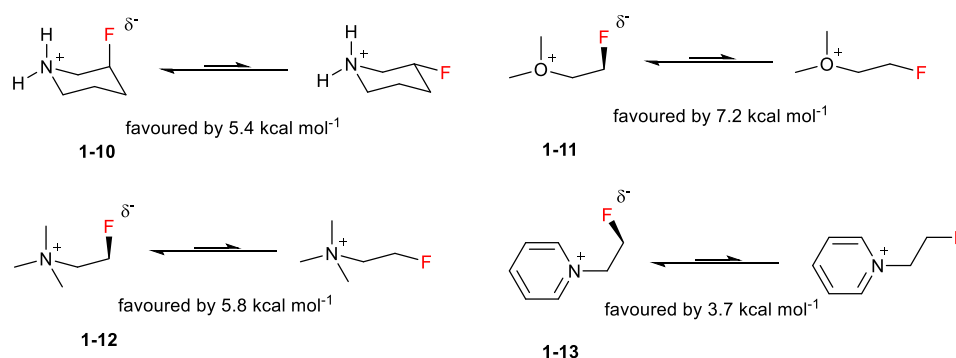
Figure 1-7 Charge-dipole interaction of C–F bonds.[7]

The interaction of C–F bond dipoles with formal charge has been measured and is significant.[7] The large axial preference (5.4 kcal mol^{-1}) of fluorine in the 3-fluoropiperidinium ring has been discussed.[17] Such an observation has been further studied in the cases of the strong *gauche* preference for protonated fluoroethylamine, fluoroethanol and fluoropyridium cations as illustrated in Figure 1-7. [18, 19]

1.3.3 Hyperconjugation
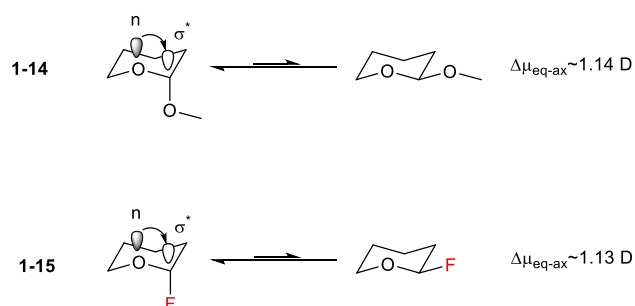
Figure 1-8 The anomeric effect for the C–O and C–F bond in α pyrans **1-14** and **1-15**.

Anomeric stabilisation is observed in **1-15** as a consequence of the low energy σ^*_{C-F} antibonding orbital, which is similar to that for C–O in the more classical anomeric effect. A

significant axial preference in 2-fluoropyran **1-15** arises due to the contribution of the lone pair (HOMO) from the ether oxygen into the σ^*_{C-F}, whilst this effect is most significant with fluorine relative to the other halogens as its strong electronegativity results in a closer energy gap with the oxygen lone pairs n and σ^*_{C-F} antibonding orbital.[7, 17] This stabilisation also effects the conformation of many fluorinated ether compounds.

1.3.4 *Gauche* effect

$\sigma_{C-H} \rightarrow \sigma^*_{C-F}$

Favored by 0.5-0.9 kcal mol^{-1}
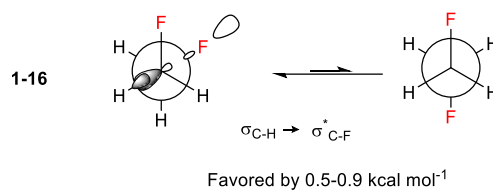
Figure 1-9 Hyperconjugation rational for the *gauche* preference of 1,2-difluoroethane **1-16**.

In the case of two vicinal C–F bonds, a preference for a *gauche* rather than an *anti*-conformation is observed, as established for 1,2-difluoroethane **1-16**.[20] In contrast, there is an *anti*-preference for vicinal C–Cl bonds or C–Br bonds in the 1,2-dihaloethane series.[7] For fluorine, the repulsion of two C–F dipoles is over-ridden by other stabilisation effects including $\sigma_{C-H}...\sigma^*_{C-F}$ hyperconjugative interactions, resulting in a *gauche* preference for of **1-16**. [7, 20]

1.4 Cyclohexane and conformational preferences with fluorine

1.4.1 Cyclohexane

The cyclohexane ring has a long history in the study of organic chemistry. Two years after Kekulé's cyclic benzene structure proposal in 1865, an early benzene reduction was attempted by Berthelot, in a reductive reaction using an excess of fuming hydroiodic acid at 275-280°C. The synthesis was reproduced by Baeyer, Wreden and Markovnikov, who proposed a C_6H_{12} formula of hexahydrobenzene, or cyclohexane, which was indeed misinterpreted as the product was methylcyclopentane.[21]
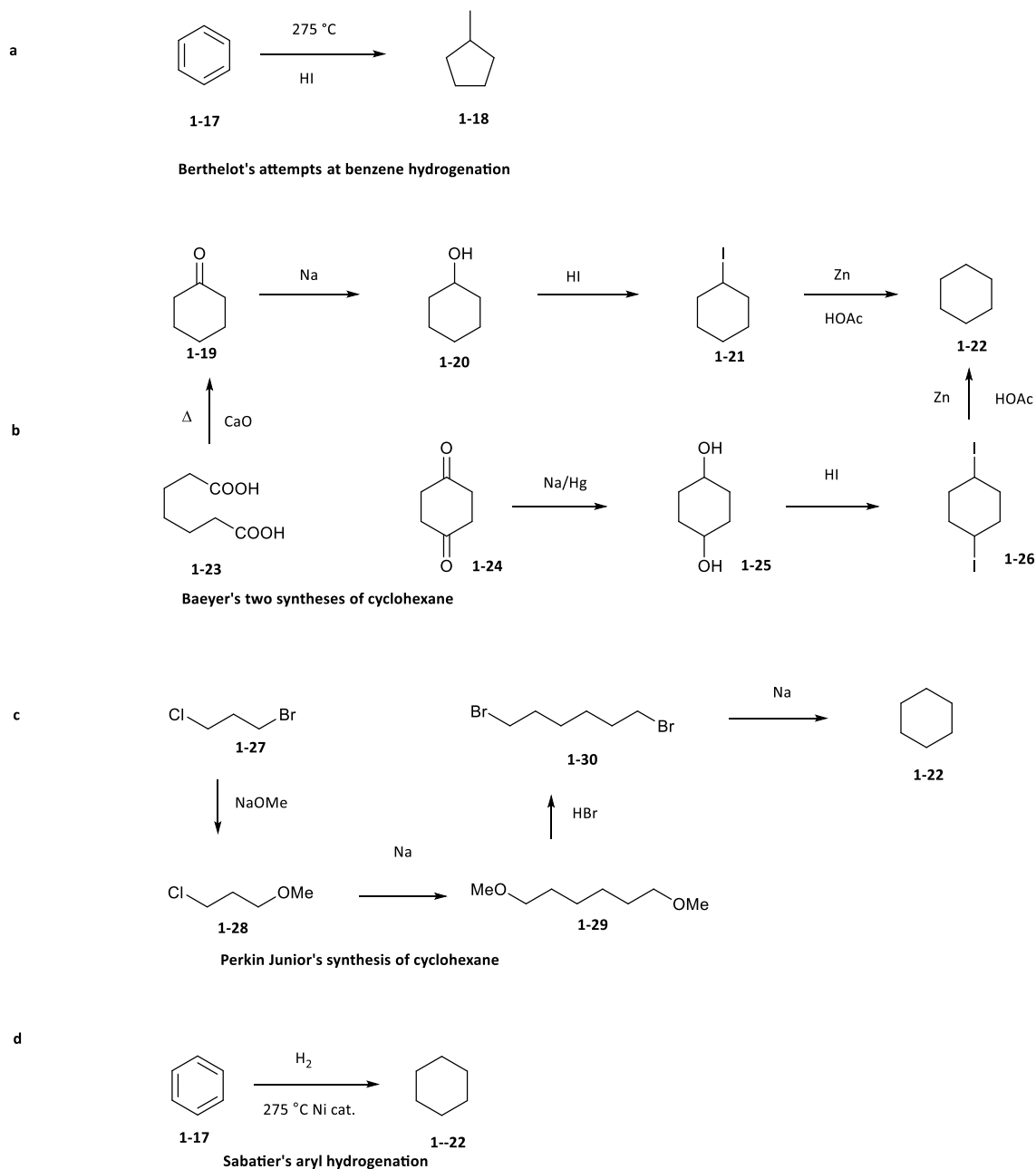
Figure 1-10 Historical synthesis (attempts) of cyclohexane.

In 1894, the synthesis of cyclohexane was achieved by Baeyer using a cascade reduction to pimelic acid or 1,4-cyclohexanedione.[22] At the same time Haworth and Perkin Jr. achieved a cyclisation using 1, 6-dibromohexane.[23] In the 20th Century, the catalytic hydrogenation reduction of benzene was finally achieved by Sabatier, by passing a mixture of benzene vapour and hydrogen in flow into a heated tube with a nickel catalyst.[24]

14

The assignment of the cyclohexane structure emerged from an intensity of interest over the past century. It was first assigned by Baeyer as a flat planar structure after his synthesis, and it was at this time that the name 'cyclohexane' was first used.[22] The structure developed from the Sashes's rigid chair structure to Hassel's 3D dimension model with flexible ring interconversion.[25, 26] And then the stereochemistry of cyclohexane derivatives containing a ring system, with axial and equatorial substituents became fully appreciated by Barton.[27]

1-22

Planer model   Rigid Chair model   Fling interconversion model
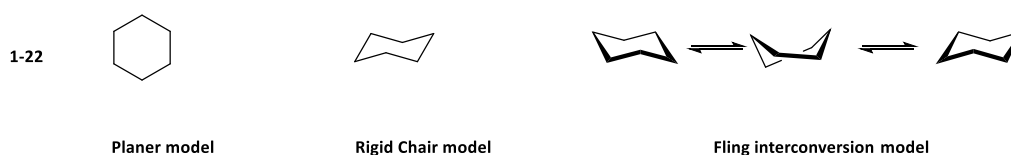
Figure 1-11 The conformational assignment of cyclohexane.

1.4.2 Cyclohexane conformation

Mono substitution of the cyclohexane ring leads to a non-equivalence of the axial and equatorial conformers in steric and energy terms as a consequence of steric repulsion, stereoelectronic effects and dipole distributions. The preferred conformation of a given ring is affected by the following factors (Figure 1-12):

(a) Steric 1,3-diaxial repulsion, (b) dipole minimisation, (c) solvation, (d) hyperconjugation and (e) charge-dipole or coulombic interactions.

small repulsion   large repulsion

1-30 eq   **1-30 ax**   **1-31 diaxial**   **1-31 di-equatorial**   **1-30 eq**

(a) Steric diaxial repulsion   **(b) dipole minimisation**   **(c) solvation**

1-30 eq   **1-32 diaxial**

(d) hyperconjugation   **(e) charge-diopole or coulombic interaction**
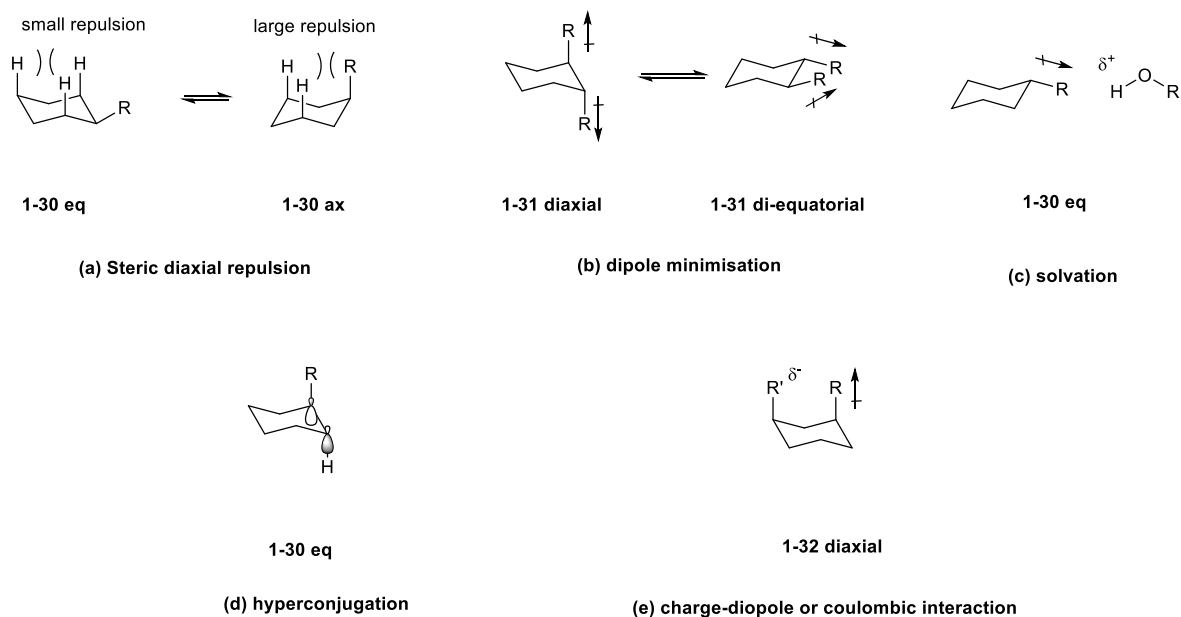
Figure 1-12 The conformation of substituted cyclohexanes.

1.4.2.1 **Mono-substituted cyclohexane**

The steric impacts of an individual substituent group is measured by their relative A-value. [28, 29] In the case of the single fluorine substituent as in fluorocyclohexane, the fluorine prefers the equatorial conformation, but the preference is small (0.10-0.42 kcal mol^{-1}) and is next to deuterium in terms of those substituents that form stable bonds to carbon.

1-30 eq   **1-30 ax**

favoured   **disfavoured**

ΔE =0.10-0.42 kcal mol

1-33 eq   **1-33 ax**
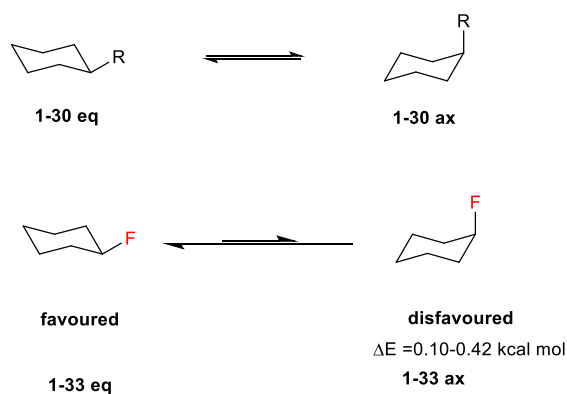
Figure 1-13 Ring interconversion of monosubstituted cyclohexanes.

16

Substituent	A Value (Kcal mol^{-1})
H	0.00
F	0.10-0.42
OH	0.52-1.04
Me	1.74-1.80
Cl	0.43-0.64
Br	0.38-0.67
Ph	2.80-2.90
^{t}Bu	>4.7

Table 1-3 A values of common substituents attached to cyclohexane.[28, 29]

1.4.2.2 **Multi fluoro-substituted cyclohexane**

In the case of di-substituted cyclohexanes with two of the same functional group, the energy levels of the different conformers can be equivalent or non-equivalent depending on the relative stereochemistry.
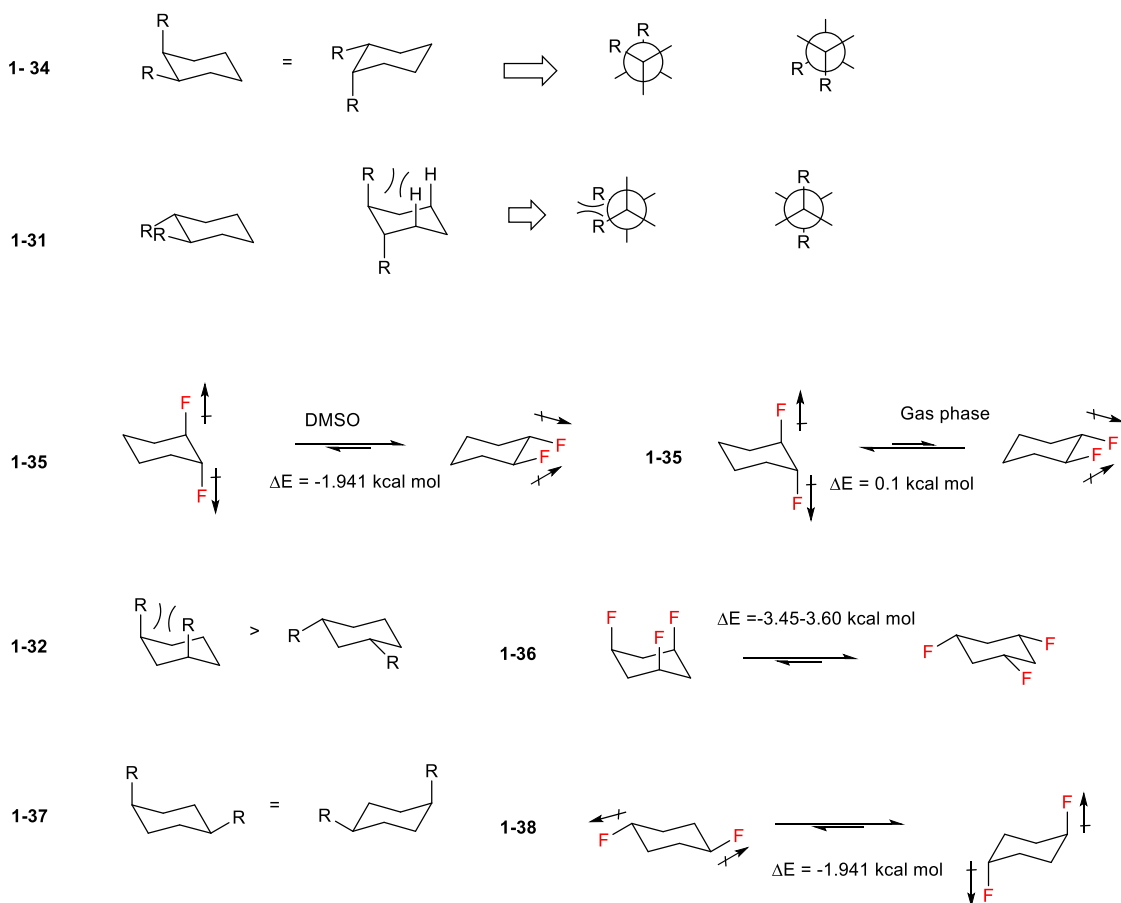
Figure 1-14 The conformation of bis-substituted cyclohexanes.

For a 1,2 di-substituted cyclohexane, when the two substituents have the *cis-* or *syn-* geometry, then the ring interconverts between two isoenergetic conformers, where one substituent adopts an axial orientation while the other adopts an equatorial orientation. However, when the 1,2 substituents have the *trans* or *anti* geometry, then there is a competition between diaxial and diequatorial conformers. For diequatorial, there is a repulsion of the two *gauche* substituents and for diaxial there are 1,3-diaxial repulsions with axial hydrogens. For polar substituents such as fluorine, dipole minimisation must also be taken into account. Studies on *trans*-1,2-difluorocyclohexane indicate that the diaxial conformation is preferred in the gas phase by 0.1 kcal mol^{-1} [30] whereas the di-equatorial conformation is preferred in DMSO solution.[31] It should be noted here that the diaxial conformer is also stabilised by hyperconjugative interactions with antiperiplanar hydrogens

which help counter 1,3-diaxial repulsion (see *gauche* effect).

For the 1,3 di-substituted fluorocyclohexane, a special example arises with the all-*cis*-1,3,5-trifluorocyclohexane prepared by arene hydrogenation[32] and the conformational preference was calculated by computational analysis which suggested that the tri-equatorial conformation is preferred by 3.45-3.60 kcalmol^{-1} over its tri-axial conformation.[33] This is largely due to electrostatic repulsion between the fluorines in the triaxial conformation.

For the 1,4 di-substituted fluorocyclohexane, the *cis* isomer again has two isoenergetic equivalent chair conformers after ring interconversion. For the *trans* isomer the di-axial conformation is preferred in the gas phase by 1.1 kcalmol^{-1}, and this arises from molecular dipole minimisation and coulombic attraction between C–F dipoles, as well as stabilising hyperconjugative interactions with antiperiplanar hydrogens.[30]

1.4.2.3 Fluorinated heterofunctionalised cyclohexane

The C–F bond interacts with other functional groups in a heterofunctionalised cyclohexane, and this can lead to unexpected changes in the conformational preference. For example, in the 2-fluoro-cyclohexanone, an axial preference for fluorine was observed in the gas phase by 0.45-0.6 kcal mol^{-1}. There are many factors involved in such a conformational preference and to overcome di-axial repulsion, including electrostatic repulsion of the C–F dipole, minimisation of the global molecular dipole and hyperconjugation. However, the equatorial C–F conformer is favoured in polar solvents such as DMSO which helps to screen intramolecular electrostatic attractions which are much stronger in the gas phase.[34]
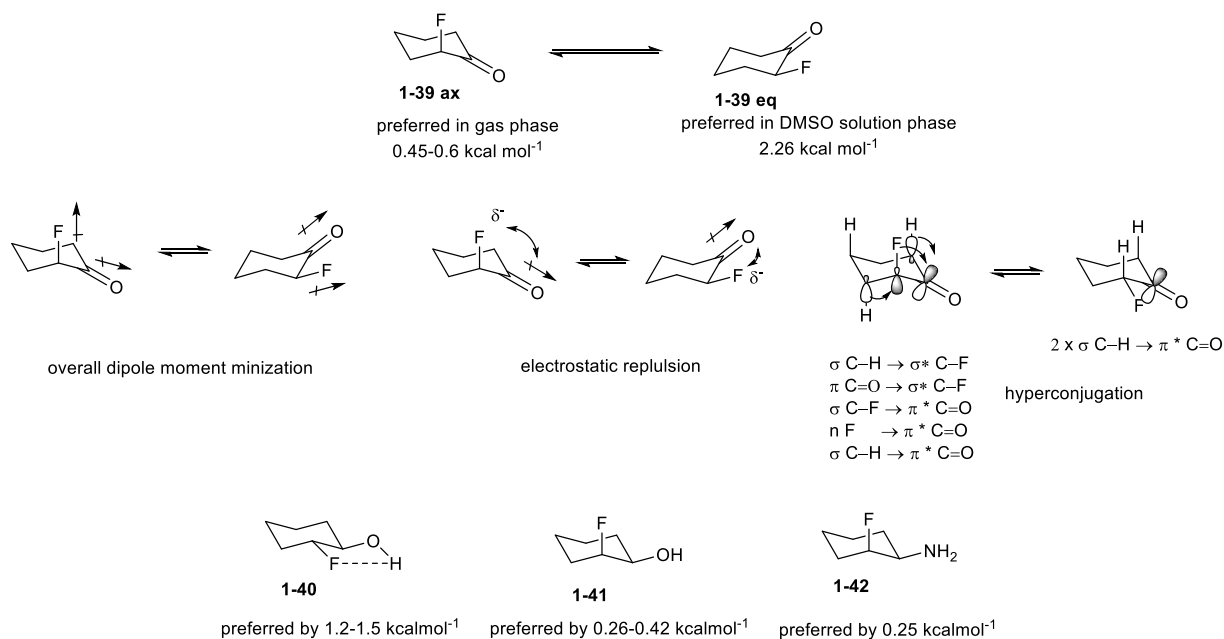
Figure 1-15 Conformation of di-substituted cyclohexanes with two different functional groups.

Some other classic examples of disubstituted fluorinated cyclohexane are listed in Figure 1-15. For *trans*—fluorocyclohexanol **1-40** the O–H …F can participate in a hydrogen bonding interaction, and this means that the more polar equatorial conformer becomes preferred. Hyperconjugation contributes to stabilisation of the axial C–F conformer of *cis*-2-fluorocyclohexanol and for *cis*-2-fluorocyclohexan-amine the axial conformer is slightly preferred.[35-37] The conformational preference of other substituted fluorocyclohexanes listed in Chapter 1.3 were already discussed above.

1.5 Organofluorine chemistry in pharmaceuticals applications

steric mimics

R—H ⟹ R—F
1-43   **1-44**

R—Me ⟹ R—CF$_3$
1-46   **1-47**

R—< ⟹ R—CF$_3$
1-50   **1-52**

electrostatic mimics

R—OH ⟹ R—F
1-45   **1-44**

1-48 ⟹ **1-49**

1-52 ⟹ **1-53**
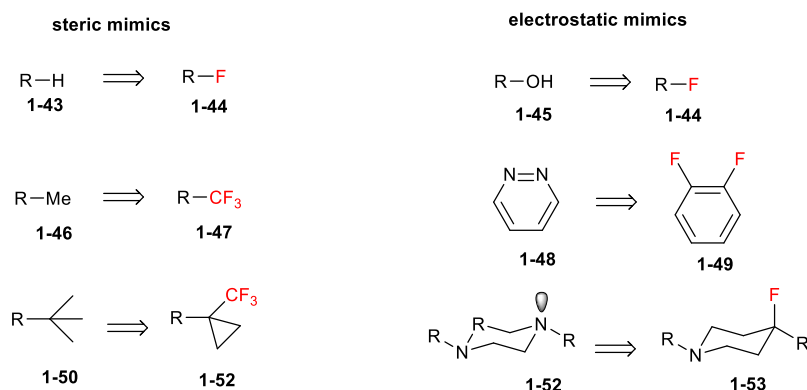
Figure 1-16 Examples of steric and electrostatic mimics for pharmaceuticals applications.[38]

The success of the isosteric substitution of C–F for C-H has been rationalised by the similar atomic radii and the close C–F and C-H bond length. The δ^- polarisation on $^{\delta+}C–F^{\delta-}$ bond can be viewed as an electronic mimic of a lone pair on a nitrogen atom or on the oxygen of a hydroxyl group. Replacement of fluorine containing motifs is not limited to fluorine for hydrogen. Other replacements have also met with success such as fluorine to nitrogen, C–F to C=O, fluorinated motifs to amides, sulphonamide, and urea, C–F to carbinol (C-OH), CF$_2$ motifs to oxygen, fluorine to nitrile.[38]

Moreover, in some of the well-established organofluorine motifs, both steric and polar similarity have resulted in other bio-isosteres of natural product's motifs. Vinyl fluorides **1-57** can mimic amides **1-56** sterically and electronically and similarly difluorotoluene **1-59** has been shown to mimic thymine **1-58**. [38-40]
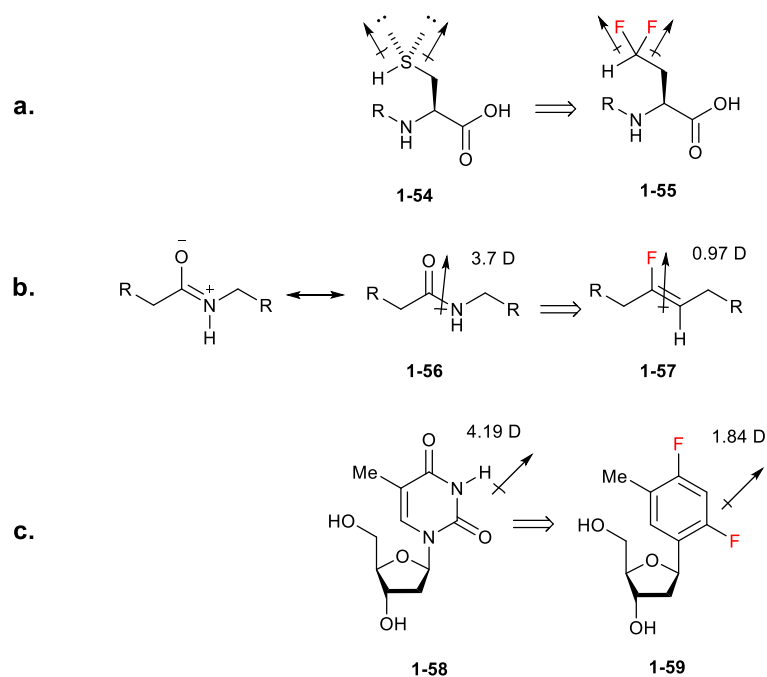
Figure 1-17 Examples of organofluorine compounds as steric and electronic mimics of natural products.

1.6 Multivicinal fluorine motifs
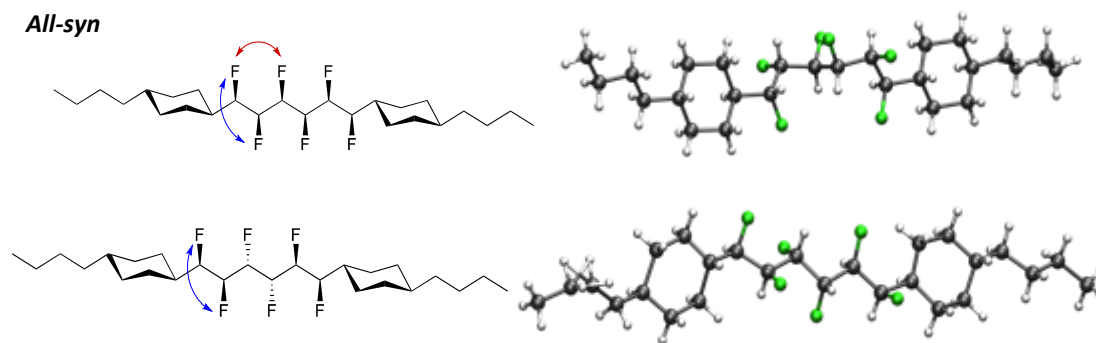
Figure 1-18 X-ray structure of all-*syn* **1-60** and *anti* **1-61** hexafluoroalkane.[41, 42]

The St Andrews group has had a strong interest in the synthesis and conformational analysis of multivicinal fluorine motifs. These rather unique fluorinated motifs have been explored in supramolecular chemistry, surface science studies, liquid crystals and physical organic chemistry studies more generally.[43]

Hunter *et al.* prepared two diastereoisomers of the linear hexa-fluoro alkyl motifs **1-60** and **1-61**. The favoured conformations accommodated a combination of 1,2-*gauche* effects and 1,3-dipolar repulsions (Figure 12).[41, 42] Diastereoisomer **1-60** had a helical conformation which arose because of 1,3-dipole repulsions and diastereoisomer **1-61** preferred an *anti*-zig-zag conformation as there is no 1,3-dipolar repulsions in that case.[41, 42]

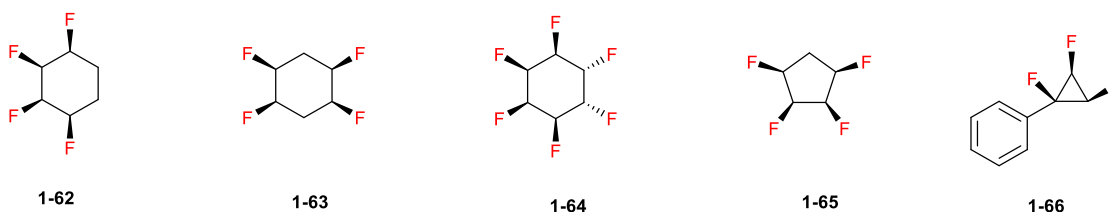**Figure 1-19** Multivicinal alicyclic fluorine motifs prepared in St Andrews.

Durie *et. al.* synthesized all-*syn*-1,2,3,4- and all-*syn*-1,2,4,5- tetrafluorocyclohexane **1-62, 1-63** as well as *η*-1,2,3,4,5,6-hexafluorocyclohexane **1-64**. Those organofluorine cyclohexanes show high melting points and **1-62** and **1-63** have large molecular dipole moments of about 5 D, which arise as they always have 1,3-diaxial C-F bonds, and this gives them particularly polar properties for an aliphatic. [43-45].

Multivicinal fluorine motifs have also been made with a range of functional groups with different stereochemistries. As shown in Figure 1-20, such motifs could be installed with hydroxyl, aldehyde and amine functional groups, and as single stereoisomers.[46, 47]
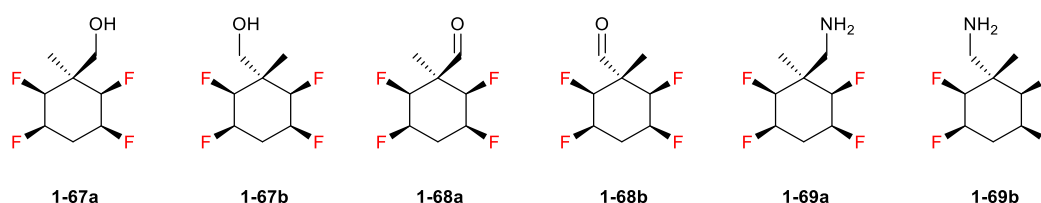
Figure 1-20 Functionalised all-*cis*-tetrafluoro cyclohexane motif.

All-*cis*-hexafluorocyclohexane **1-71** was synthesised by Keddie *et al.* in 2015 in 12 steps (Figure

16). Although this was a landmark compound it was only synthesised in a small amount due to the low yield of the 12-step process, which limited further studies. The distribution of 1,3,5-triaxial orientated C–F bonds and three triequatorial orientated C–F bonds in combination, form a fluorine face, and the other side of the cyclohexane, a hydrogen face. These faces are polarised, and this molecule emerged as the most polar aliphatic compound (μ = 6.2 D) known. Its unusual nature is exemplified in a melting point of over 200 °C.[48]
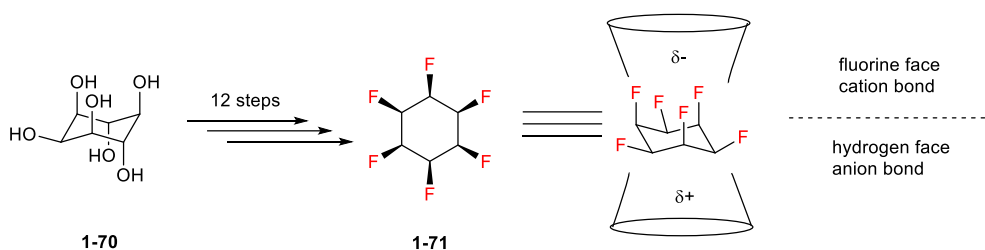
Figure 1-21 All-*cis*-hexafluorocyclohexane **1-71** has polarised faces.

1.6.1 Cyclic (amino)(alkyl)carbene rhodium catalysts

Cyclic (amino)(alkyl)carbene rhodium catalysts (CAACs) are of a group of NHC ligand catalyst which have attracted wide interest, but there were few organometallic catalysis studies[49] until the discovery of its special aryl hydrogenation properties by Wei *et al*.[50] Unlike most conventional homogenous catalysts which reduce the carbonyl bond predominately to deliver a benzyl alcohol **1-73** and subsequently to afford alkyl products **1-75** and **1-76**, the rhodium CAAC catalyst **[Rh]** (Scheme 1-2) displayed a unique and attractive property during the hydrogenation of benzaldehyde. It selectively hydrogenated the aromatic ring to a cyclohexane but retained the carbonyl bond to generate **1-74** and **1-78** (scheme 1-2).[50]
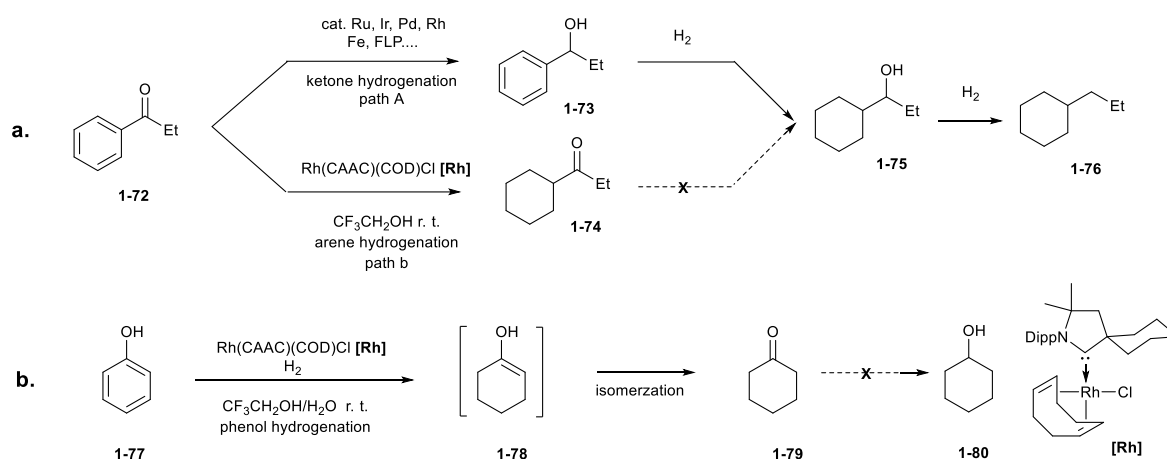
Scheme 1-2 Selective arene hydrogenation nature of Rh(CAAC)(COD)Cl **[Rh]**.

Following on from this, Wiesenfeldt *et al.* reported a breakthrough in the hydrogenation of fluoroarenes to fluorocyclohexanes by the application of catalyst **[Rh]**.[32] It is most common that, the transition metal catalysed hydrogenations of fluoroarenes are accompanied with defluorination due to ß-fluoride elimination therefore this protocol was exceptional in retaining the original aromatic fluorine as an aliphatic fluorine.[51] This protocol was extended to demonstrate the single step synthesis of multi-substituted and multi-fluorinated cyclohexanes on a relatively large scale by hydrogenation of the precursor aromatic.
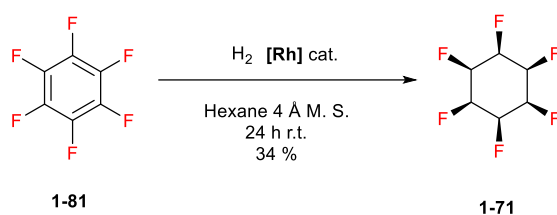
Scheme 1-3 One step synthesis of all-*cis*-hexafluorocyclohexane **1-71**.

This catalytic aryl hydrogenation opened up the prospects of access to a wide variety of the all-*cis*-multifluorinated cyclohexanes. The [Rh(COD)(CAAC)] catalyst could tolerate a range of functional groups, such as –OH, –OMe, –OTBS, –Bpin, –NHBoc, –COOMe and number of aromatic heteroaromatic substrates could be used such as fluoropyridines to make fluoropiperidines.[32, 52, 53]

Compounds: 1-82 (OTBS), 1-83 (OMe), 1-84 (NHBoc), 1-85 (CO₂Me), 1-86 (Bpin), 1-87 (NBoc), 1-88, 1-89, 1-90
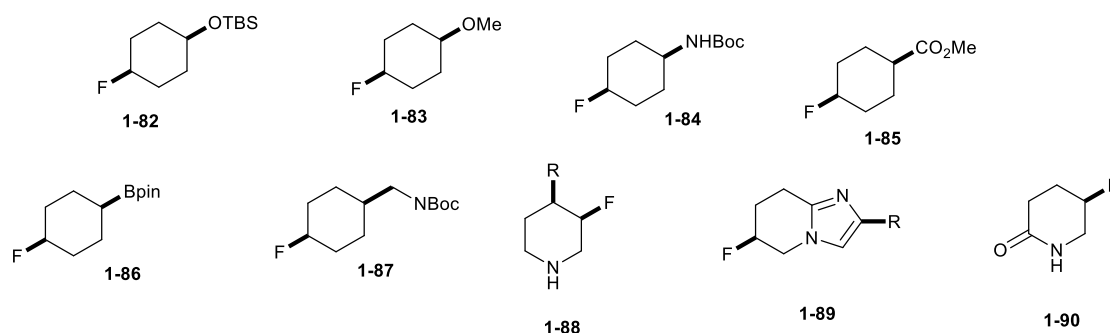
Figure 1-22 Examples of fluoroarene hydrogenations using the Zeng's catalyst **[Rh]**.

A mechanism study of the CAAC catalyst demonstrated that the active species during hydrogenation involves supported rhodium nanoparticles stabilized by the pyrrolidinium cation generated from the NHC ligand. The research compared the silica supported rhodium nanoparticles with prepared active catalyst **[Rh]**. The results indicated that the presence of NHC ligand improved the yield by 20-30 % to 86-90 % and reduced the defluorination from 20 % to 3 %, which suggested the advantage of the ligand species on the surface.[54]
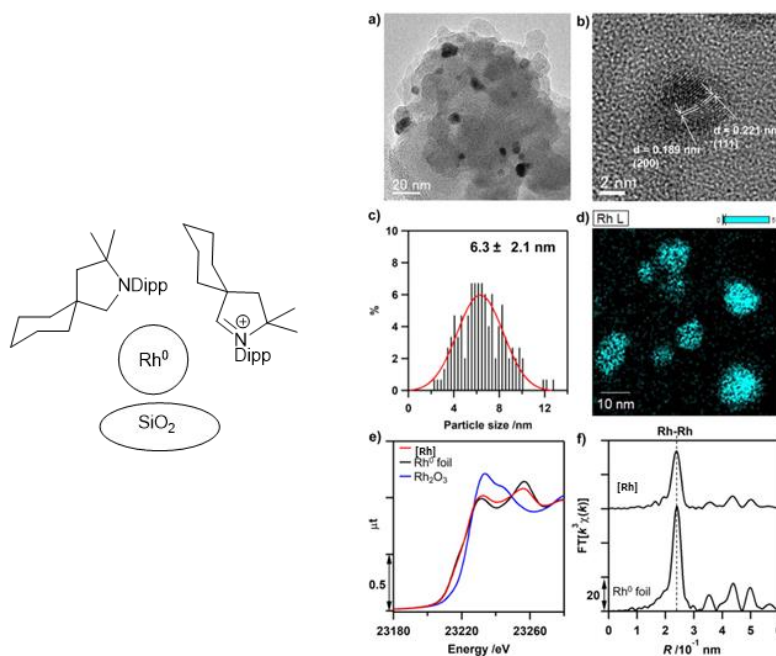
Figure 1-23 TEM images adapted from literature (a) and (b) of **[Rh]** with visible lattice structure (0.19 nm Rh(200), 0.22 nm Rh(111)). (c) Histogram showing the particle size distribution of **[Rh]**. (d) STEM-EDS image of **[Rh]** (blue, Rh Lα characteristic X-rays). (e) Rh K-edge XANES spectra of **[Rh]** (red), Rh(0) foil (black), and Rh₂O₃ (blue). (f) Rh K-edge EXAFS Fourier transforms of **[Rh]** and Rh(0) foil.[54]

26

1.6.2 Pharmaceutical application of polar fluorocyclohexanes

Metabolism studies with the fungus *Cunninghamella elegans* (model for human metabolism) was performed by Rodil *et al.*, which demonstrated benzylic hydroxylation as the main form of metabolism of **1-91** as shown in Scheme 1-4.
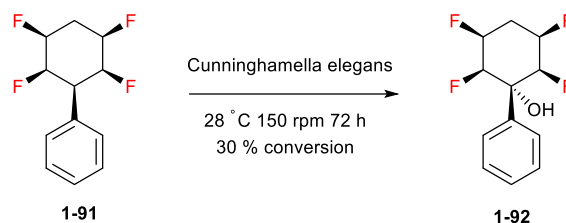
Scheme 1-4 Metabolic hydroxylation of compound **1-91**.

Three series of matched molecular pairs (MMPs) were recently prepared by Wang *et al*. of Genetech to examine the pharmacologic, physicochemical, and metabolic properties of Janus face cyclohexyl containing compounds as candidate motifs drug molecules. The result suggested that the all-*cis*-tetrafluorocyclohexyl motif led to improved solubility, lowered lipophilicity by 2 log units and enhanced metabolic stability in human liver microsomal HLM by Δ CL_{hep} reduced by 7 mL/min/kg. One drawback was that the Janus motif often lowered the permeability of the target molecules through cell membranes.[55]
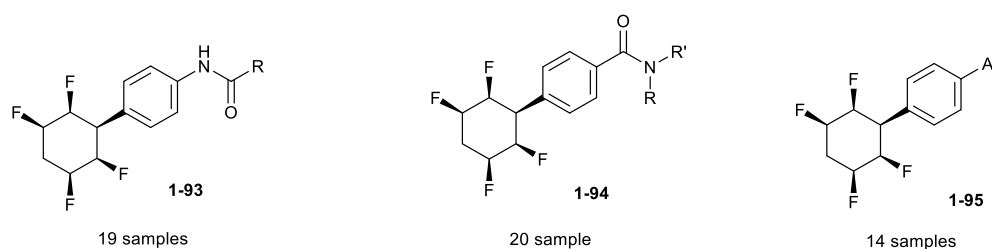
Figure 1-24 Examples of the matched pairs of Janus face cyclohexanes prepared for physicochemical and metabolic testing by Genentech.[55]

Overall, the Janus ring motifs have very similar properties to the frequently used motif morpholine, in terms of its physicochemical and metabolic stability profile, including its low

topological polar surface area (TPSA). This means the Janus motif could be a potential isosteric mimic to the morpholine ring in drug discovery with control of reduced TPSA and N/O atoms ratio.[55]
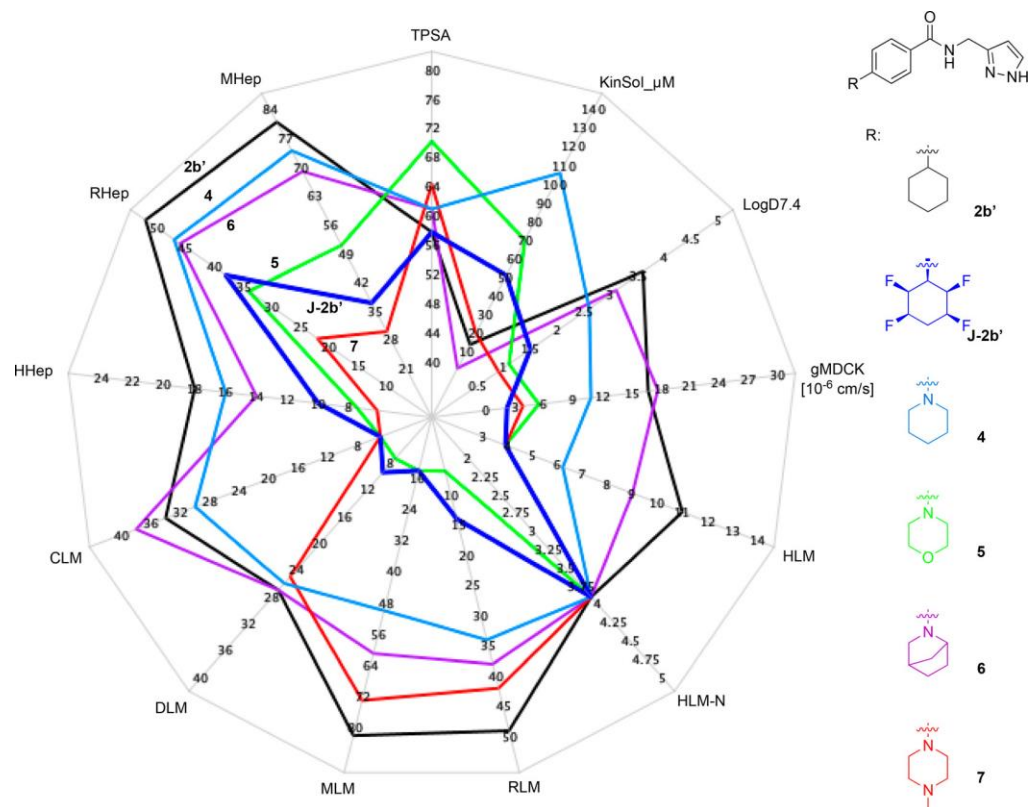
(TPSA = Toplogical polar surface area, KinSol = kinetic solublity, log$D_{7.4}$ distribution coefficient of compound in octanol versus in water at pH 7.4. gMDCK = Madin-Darby canine kidney cell permeability measurement. HLM = human liver microsomal, HLM -N = human liver microsomal in absence of NADPH, RLM= rat liver microsomes, DLM = dog liver microsomes, CLM= cyno liver microsomes, HHep=human hepatocytes, MHep = mouse hepatocytes, RHep = rat hepatocytes)[55]

Figure 1-25 Radar plot MMP analysis of Janus face analogue **1-96** with side chain 2b' (J-2b') versus analogues bearing different saturated (hetero)cycles adapted from literature.[55]

The lipophilicity of multi-vicinal fluorinated cyclohexyl motifs has been studied also by Log P measurements, where a decreasing Log P (increased polarity) was observed for tri-, tetra- and penta- fluoro cyclohexyl-benzenes respectively. Log P values are significantly lower relative to the aryl-cyclohexane and even biphenyl.[56, 57] For the cyclopropyl derivatives, the same Log P order and tendency was observed.[58, 59]

Log P	4.99	3.76	3.30	3.2	2.64	2.58
	1-97	1-98	1-99	1-100	1-101	1-91

Log P	3.4	2.73	2.56
	1-102	1-103	1-66
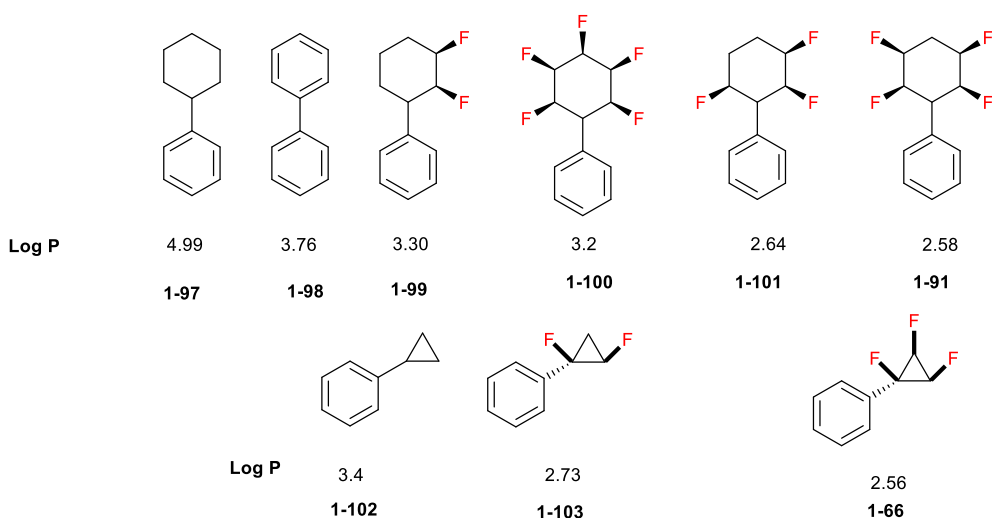
Figure 1-26 Log P values of selected alkyl and Janus face cyclohexanes as substituted benzenes.

1.6.3 Ionic binding

The distribution of 1,3,5-triaxial orientated fluorine atoms and 2,4,6-triequatorial orientated fluorine atoms in combination, form a fluorine face, and the other side of the cyclohexane, a hydrogen face. The two polarized faces introduce a Janus phase aspect, and the polarity has the potential to combine these rings on their different faces to complementary cations and anions respectively.

The binding affinity of all-*cis*-hexafluorocyclohexane **1-71** to ions in the gas phase was demonstrated by electrospray ionization and this generated complexes of **1-71** with sodium and chloride ions. These ions could be isolated in the ion chamber of a mass spectrometer. The isolated ions were then irradiated with a free electron laser (FEL) to generate infrared multiple photon dissociation (IRMPD) spectra. Complementary computational simulations were carried out (single point energy calculations at MP29(full)/6-311+G(2d,2p)). The complexes showed a strong binding affinity between the Janus cyclohexane and to Na$^+$ and Cl$^-$, with an affinity comparable to that of a crown ether to Na$^+$ and Brønsted and Lewis acids to Cl^{-1}.[60]
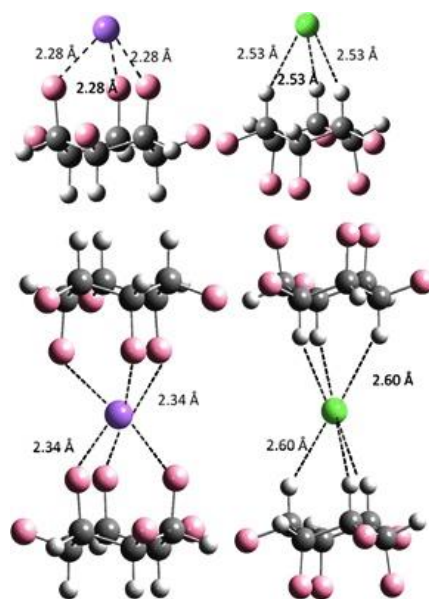
Figure 1-27 All-*cis*-hexafluorocyclohexane **1-71** binding with Na⁺(purple)Cl⁻(green) in the gas phase.[60]

The binding affinity of all-*cis*-hexafluorocyclohexane in solution were also determined by the titration of **1-71** with selected halogen anion and with tetrabutylammonium counter ions. A series of association constants (K) of the halogen anion in acetone solution were observed with a 1:1 stoichiometry. F⁻ (K = 600 ± 400 M⁻¹, decomposition of **1-71** occurs), Cl⁻ (K = 400 ± 40 M⁻¹), Br⁻ (K = 150 ± 7M⁻¹) and I⁻ (K = 37 ± M⁻¹). For the methoxyl substituted cyclohexane **1-105**, a similar 1:1 stoichiometry and association constant of K = 170 ±10 M⁻¹ to tetrabutylammonium chloride was observed which opens up applications for these rings as ligands for multidentate or macrocyclic structures for anion receptors. The strength of the binding affinity of **1-71** is moderate and dependent on the size of the anion and the dielectric constant of the solvent. [61]
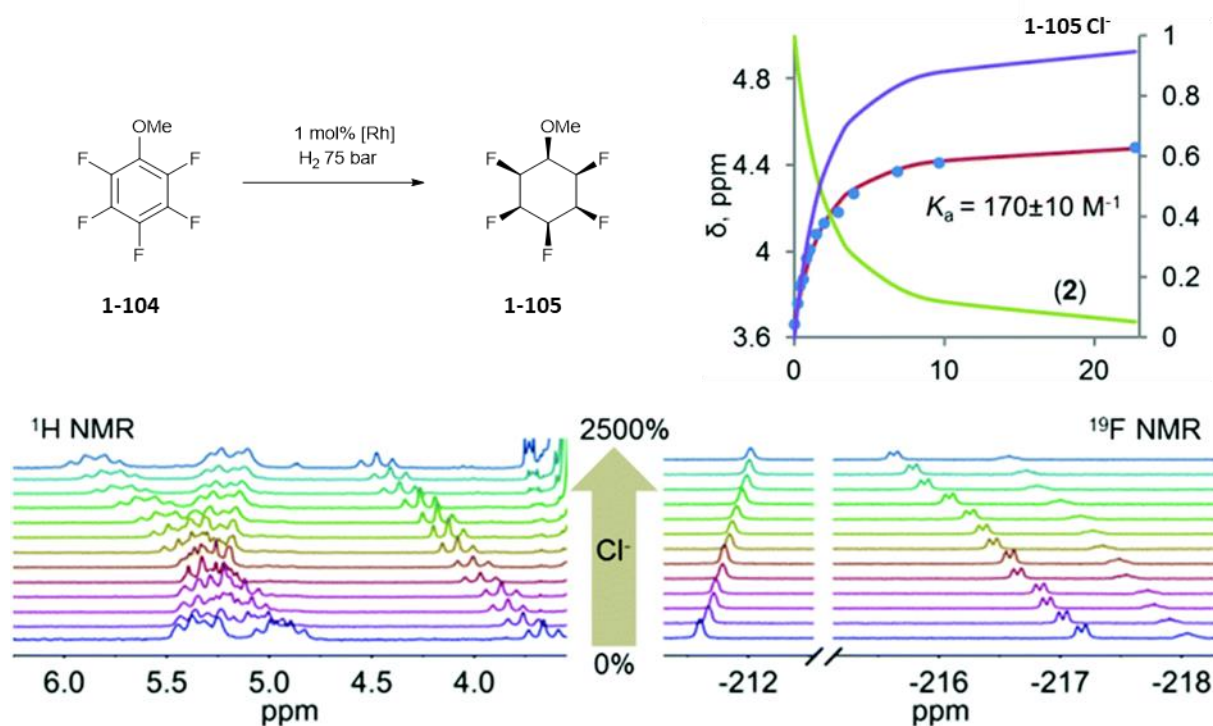
Figure 1-28 (a) Synthesis of **1-105** according to method reported by Wiesenfeldt *et al.*[32]; (b) binding isotherm and species concentration plot for the titration of **1-105** with TBACl. Blue spheres: experimental points, red line: fit according to 1 : 1 model, purple and green: mole fractions of corresponding species; (c) partial ^{1}H and ^{19}F NMR (acetone-d_6, 400 MHz, 293 K) stacked plots for the titration of **1-105** with TBACl.[61]

A co-crystal structure of **1-71** was solved with the tetraphenylphosphonium chloride ion and water. The crystal structure indicate a contact distance of the axial hydrogen in **1-71** of C–H…O in water with distance of 2.38 – 2.75 Å and a C–H …Cl⁻ distance of 2.98-3.18 Å, which is slightly longer than the gas phase calculation(Figure 1-29).[60, 61]
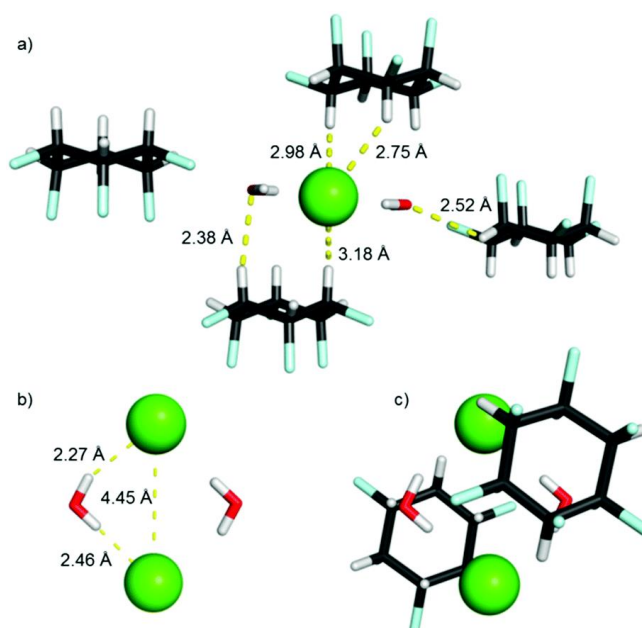
Figure 1-29 Solid state structure of the co-crystal of **1-71** with tetraphenylphosphonium chloride (cations omitted for clarity). (a) $(Cl^-)_2 \cdot (H_2O)_2$ coordinated to four molecules **1-71**; (b) structure of the $(Cl^-)2 \cdot (H_2O)_2$ cluster; (c) $(Cl^-)_2 \cdot (H_2O)_2$ cluster stacked between two molecules of **1-71**. Single crystals were obtained by the layering method (n-hexane/acetone + chloroform). Green: Cl; turquoise: F; red: O; grey: C; white: H.[61]

The facial polarisation of **1-71** resulted in a large macroscopic polarization of its crystal lattice, and this has been proposed to be a candidate building block for designing novel nonlinear optical materials.[62]
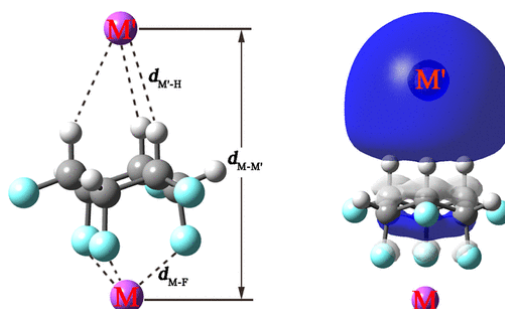
Figure 1-30 Geometric structure and HOMO of M·**1-71**·M' (M, M' = Li, Na, and K).[63]

Studies have indicated that complexes of organic alkalides $M^+ \cdot \textbf{1-71} \cdot M'^-$ (M, M'= Li, Na, K) form a new type of organic alkalide. Natural bond orbital (NBO) analysis found the NBO charges Q_M

on the metal are about $0.78 - 0.91$ |e| and Q_M' on M' are about -0.48 – -0.58 |e|. [63] A similar Q_M value was reported for lithium in (calix[4]pyrrole)M$^-$ complexes (M=Li, Na, K)[64] and the greater Q_M' value suggest a better potential for charge transfer between M and M', taking the advantage of its large facial polarity.

The complexation energies E_c of the M$^+$·**1-71**·M'$^-$ complexes are evaluated as large negative values (-95.8 to -139.0 kcal mol^{-1}) proving the strong and stable association between the three species. The VIE (vertical ionisation energy) values are about 2.96-3.83 eV indicating loosely bound diffuse electrons in such systems, and these are smaller than the ionisation energy of Cs atom (3.89 eV).

The HOMO orbital of the excitation M$^+$·**1-71**·M'$^-$ complexes were calculated by two-level models[65] and these were visualised, showing that the diffused excess electrons are mainly located around M'$^-$. Significant and large β_0 values of M$^+$·**1-71**·M'$^-$ alkalides were observed (3.49×10^4 to 1.45×10^6 a.u.), which are significantly larger than individual molecules of **1-71** with 127 a.u., suggesting that association of two alkali-metal atoms on the different faces of **1-71** greatly enhances its Non-Linear Optical (NLO) response and especially for potassides.[63] Such complex system are also employed to construct a number of superalkali-based alkalides and new variants of super alkalides with NLO response and stability.

1.7 Supramolecular nature of the Janus motif

The electropositive hydrogen face and the electronegative fluorine face, in the Janus cyclohexane rings, have a strong tendency to bind with each other through intermolecular interactions. Theory studies suggest that the energy of association or dimerization between two isolated **1-71** ring is ~8.2 kcal mol^{-1} (4.1 kcal mol^{-1} per ring) which is stronger than a good hydrogen bonding.[66]
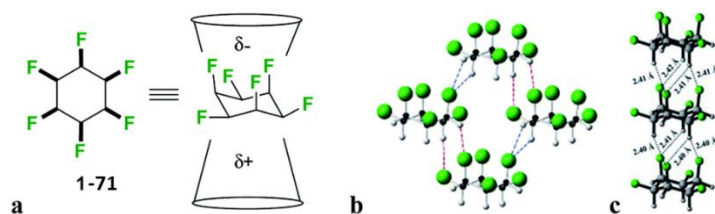
Figure 1-31 Hexafluorocyclohexane **1-71** (a) structure and non-equivalent facial polarity profile; (b) X-ray structure of the prototype Janus face all-*cis* hexafluorocyclohexane **1-71**; (c) theoretically predicted optimal molecular packing of **1-71** differs from the observed X-ray derived structure.[48, 62]
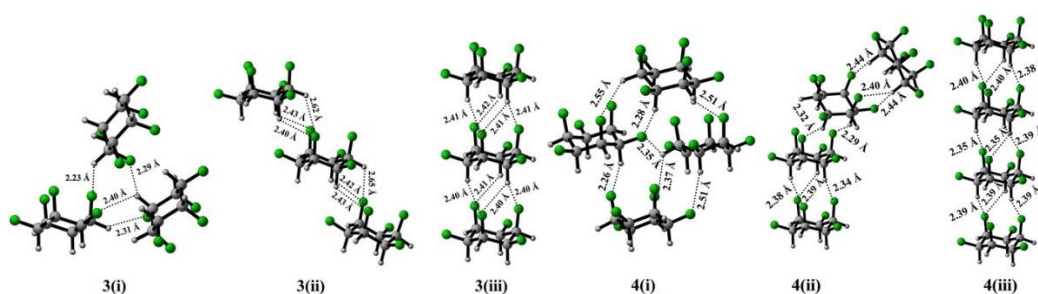
Figure 1-32 Optimized geometries for the timer 3- and tetramers 4- of **1-71** in different arrangements, that is, cyclic quartet, 3,4(i); slipped parallel stack, 3,4(ii); and completely parallel stacked, 3,4(iii). Selected bond lengths are shown in Å.[62]

The association energy between Janus rings is larger than that between two hexafluorobenzene rings (-4.6 kcal mol^{-1}), two benzene rings (-2.63 kcal mol^{-1}), and even the well-known association of hexafluorobenzene and benzene (-5.38 kcal mol^{-1}).[67, 68] The energy gained for stacking trimers of hexafluorocyclohexane rings is raised to ~20 kcal mol^{-1} (6.3 kcal mol^{-1} per ring) and further increased to ~30 kcal mol^{-1} for a tetramer (-7.7 kcal mol^{-1} per ring). The trend suggests the binding energy on self-association of the hexafluorocyclohexane rings will accommodate aggregation and polymerisation and promote supramolecular assembly. The average interaction energy per component converged at -20.9 kcal mol^{-1}.
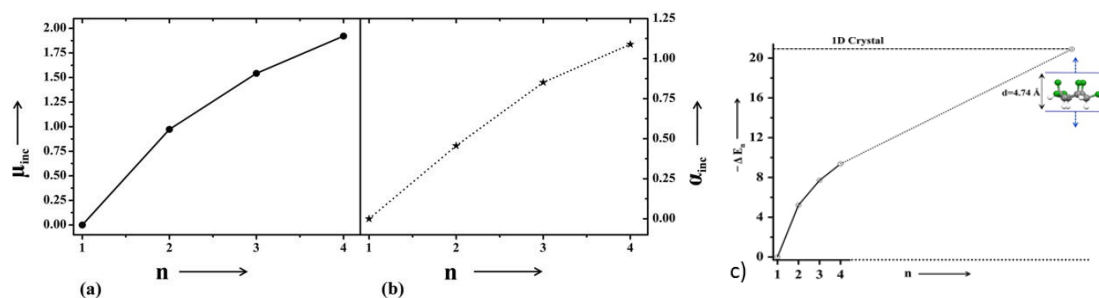
Figure 1-33 The configuration of the modelled 1D crystal of **1-71**, which has an asymptotic ΔE=−20.9 kcal mol^{-1}.

Increase of a) dipole moment (μ) b) polarization (α) and c) energy with respect to the number of molecules

of **1-71** in a complex in its energetically favourable orientation. Variation in calculated binding energies per

molecule (ΔE$_n$) in an aggregate of **1-71**.[62]

An increasing trend to overall polarity was also observed. From monomer to aggregated polymers, the polarity of rings system of all-*cis*-hexafluorocyclohexane **1-71** increased from 6.2 D (monomer) to 9.4 D(crystal asymmetric unit).[62]

A similar trend also applied to the overall polarizability of a 1 D crystal of **1-71**, and which resulted in a large macroscopic polarization, which the authors argue could be for designing novel nonlinear optical materials.[62]
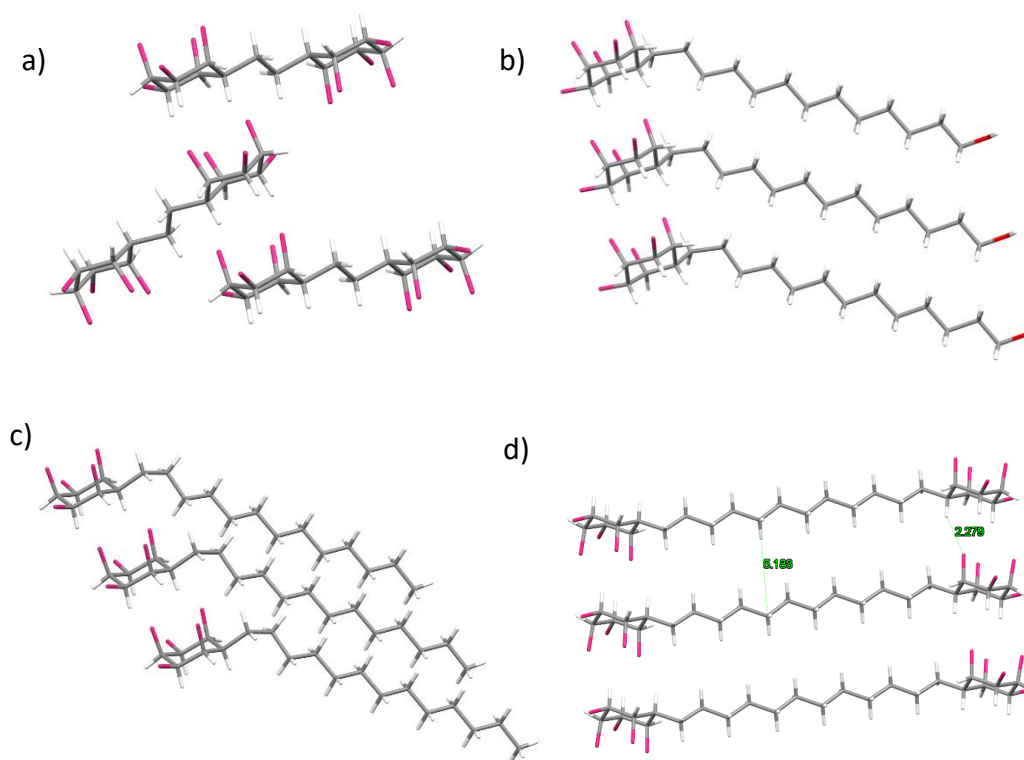
Figure 1-34 The supramolecular packing of alkyl substituted Janus face cyclohexanes and their crystal structures.[69]

The crystal structure of a number of both long alkyl chain and short alkyl chain substituted Janus face containing fluorocyclohexane rings, as well as number of bis-ring systems have been solved. These show a perpendicular packing of one ring over another. The interaction energy between the substituted rings remains at ~6-8 kcal mol^{-1} which is similar to the non-substituted all-*cis*-hexafluorocylohexane **1-71**. The substituted alkyl chains were found always to lie in an equatorial orientation to the cyclohexane ring while three C–F bonds sit axial, and this maintains a high net dipole moment relative to the ring flipped conformer. This polar arrangement is supported by the strong intermolecular associations between the Janus face rings as well as minimizing steric repulsions by forcing the alkyl group axial.

the ω-cyclohexyl **1-106 1-107**   ω –pentafluorocyclohexanol **1-108 1-109**
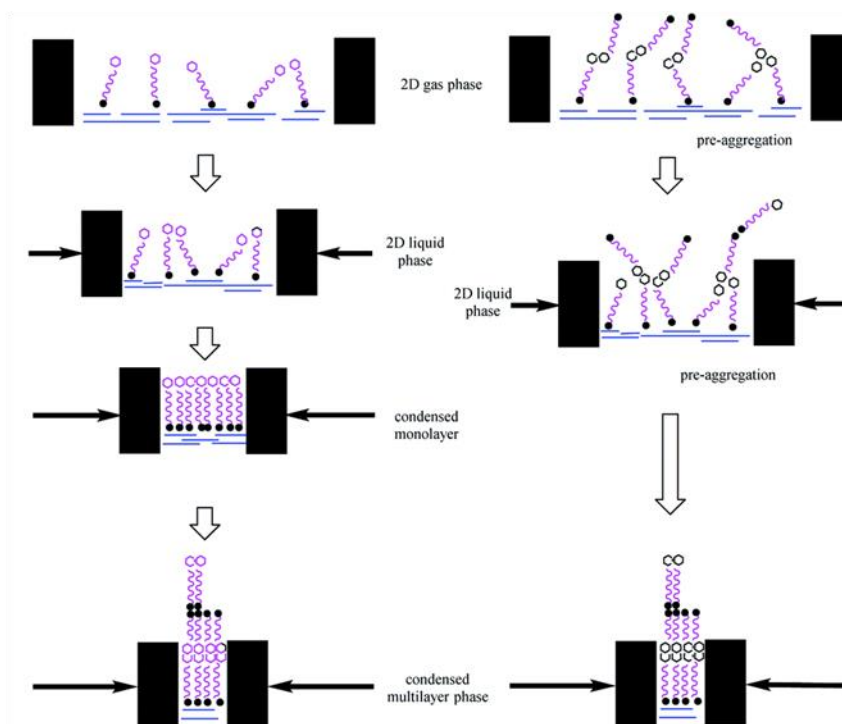
Figure 1-35 Schematic illustration of the Langmuir isotherm behaviour of the ω-cyclohexyl and ω-pentafluorocyclohexyl fatty acids on the water subphase.[69]

Langmuir isotherm analysis suggested that the Janus face cyclohexyl motif on the long chain fatty acid results in the molecules pre-aggregating and generating bilayers prior to compression, a behaviour which deviates from the non-fluorinated cyclohexyl fatty acids, which do not pre-aggregate.
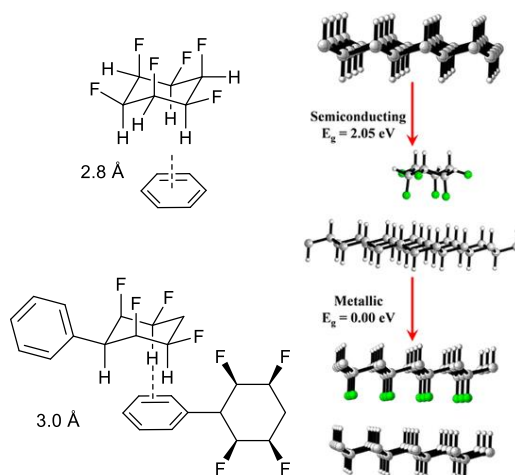
Figure 1-36 Janus face cyclohexane−π interaction with phenyl (left) and graphane.[70]

The Janus face motif shows a moderate interaction with aromatic rings by interaction of the aromatic with the electropositive hydrogen face. The energy of interaction of one molecule of **1-71** with a molecule of benzene was calculated at -7.9 kcal mol^{-1} and -6.4 kcal mol^{-1} at the MP2 and SCS-MP2 levels respectively,[71] with a calculated C–H…π distance of 2.8 Å. For the phenyl derivative of Janus face cyclohexane, the C–H…π interaction was identified in a solid-state crystal structure.

On a supramolecular level, **1-71** can pack between graphene and graphane in a sandwich structure through noncovalent interactions. The enhanced polarity of the axial C–H and C–F bonds contribute to the formation of a "triple decker" structure. The graphene band gap was reduced from 3.40 eV to 2.05 eV by coordination with **1-71**. Interaction with hydrofluorinated graphene shows a semi-conductivity with a band gap of about 3.0 eV, and with associations through a strong C–H …F–C interlayer with graphene to form a stable metallic bilayer.[70]

1-110
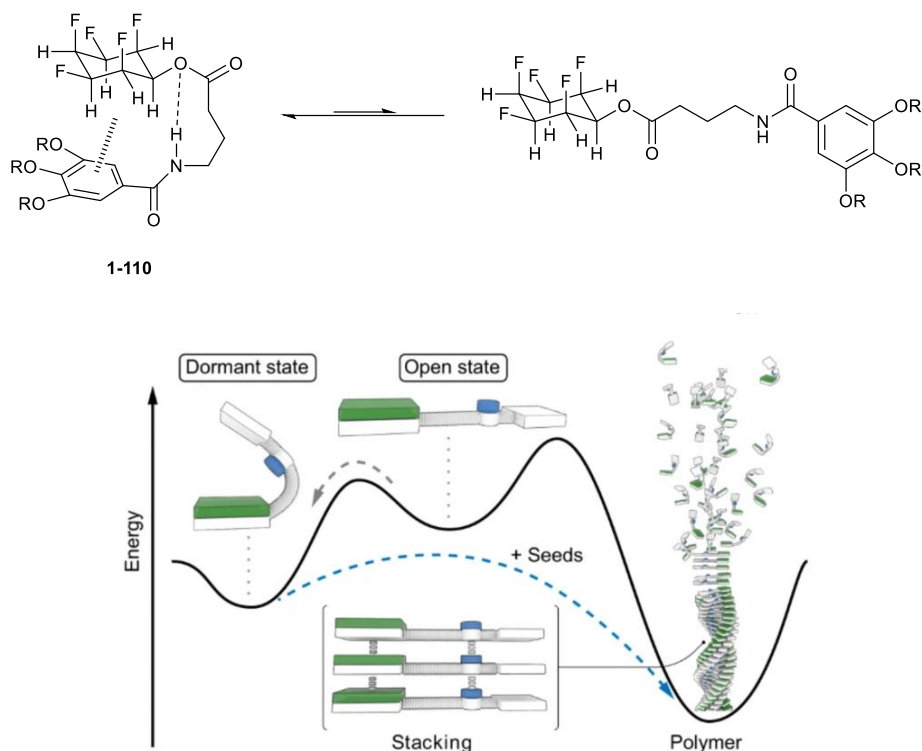
Figure 1-37 Top: General molecular design of the key monomer in a representative folded and unfolded state.

Bottom: schematic illustration of the partial energy profile of living supramolecular polymerisation (LSP).

Folding of a monomer into a dormant state inhibits spontaneous aggregation, whereas seeds can initiate LSP.

A supramolecular block copolymer was prepared by linking the all-*cis*-pentafluorocyclohexyl motif with derivatives of gallic acid though an ester bond, a short alkyl chain and amide bond. The monomer is a facially polarised fluorocyclohexane ring, engaging in an intramolecular hydrogen bonding, dipole-dipole and C–H …π interaction to form a dormant species. The flexible intramolecular interaction enabled living supramolecular polymerisation (LSP) which is under kinetic control for the self-assembly of nanofibres. These fibres can adjust in length and morphology depending on the position of the equilibrium. This study represents one of the first examples of supramolecular block copolymers synthesized from kinetically trapped monomers rather than off-pathway aggregation. Such behaviour offers a simple and novel facially polarized building block as an alternative to extended π systems or crosslinks through metal centers.[72]

39

1.8 References

1. L. Pauling, *The Nature of the Chemical Bond and the Structure of Molecules and Crystals: An Introduction to Modern Structural Chemistry*, Cornell University Press, Ithaca, NY, 1939.

2. A. Bondi, *J. Phys. Chem.*, 1964, **68**, 441-451.

3. R. S. Rowland and R. Taylor, *J. Phy. Chem.*, 1996, **100**, 7384-7391.

4. P. Kirsch, *Modern Fluoroorganic Chemistry: Synthesis, Reactivity, Applications*, Wiley-VCH, 2013.

5. J. N. R.Toon, and G. Gore, *Edu. Chem.*, 2011, 148-151.

6. A. Tressaud, *Angew. Chem. Int. Ed.*, 2006, **45**, 6792-6796.

7. D. O'Hagan, *Chem. Soc. Rev.*, 2008, **37**, 308-319.

8. D. O'Hagan and D. B. Harper, *J. Fluor. Chem.*, 1999, **100**, 127-133.

9. D. O'Hagan, C. Schaffrath, S. L. Cobb, J. T. G. Hamilton and C. D. Murphy, *Nature*, 2002, **416**, 279-279.

10. C. Dong, F. Huang, H. Deng, C. Schaffrath, J. B. Spencer, D. O'Hagan and J. H. Naismith, *Nature*, 2004, **427**, 561-565.

11. A. M. Thayer, *Chem. Eng. New Arch.*, 2006, **84**, 15-24.

12. J. Han, A. M. Remete, L. S. Dobson, L. Kiss, K. Izawa, H. Moriwaki, V. A. Soloshonok and D. O'Hagan, *J. Fluor. Chem.*, 2020, **239**, 109639.

13. K. B. Wiberg and P. R. Rablen, *J. Am. Chem. Soc.*, 1993, **115**, 614-625.

14. K. B. Wiberg, *Acc. Chem. Res.*, 1996, **29**, 229-234.

15. E. P. Gillis, K. J. Eastman, M. D. Hill, D. J. Donnelly and N. A. Meanwell, *J. Med. Chem.*, 2015, **58**, 8315-8359.

16. J. W. Banks, A. S. Batsanov, J. A. K. Howard, D. O'Hagan, H. S. Rzepa and S. Martin-Santamaria, *J. Chem. Soc.*, 1999, 2409-2411.

17. A. Sun, D. C. Lankin, K. Hardcastle and J. P. Snyder, *Chem. - Eur. J.*, 2005, **11**, 1579-1591.

18. C. R. S. Briggs, M. J. Allen, D. O'Hagan, D. J. Tozer, A. M. Z. Slawin, A. E. Goeta and J. A. K. Howard, *Org. Biomol. Chem.*, 2004, **2**, 732-740.

19. N. E. Gooseman, D. O'Hagan, M. J. Peach, A. M. Slawin, D. J. Tozer and R. J. Young, *Angew. Chem. Int. Ed.*, 2007, **46**, 5904-5908.

20. L. Goodman, H. Gu and V. Pophristic, *J. Phys. Chem. A*, 2005, **109**, 1223-1229.

21. E. W. Warnhoff, *J. Chem. Educ.*, 1996, **73**, 494.

22. A. Baeyer, *Liebigs Ann. Chem.* , 1894, 88-186.

23. R. D. H. William Henry Perkin Jr., *Ber. Deut. Chem. Ges*, 1894, 216-217.

24. J. B. S. P. Sabatier, *C. R. Hebd. Seaances Acad. Sci.*, 1901, 210-212.

25. B. O. O. Hassel, *Acta Chem. Scand.*, 1947, 929-943.

26. H. Sachse, *Chem. Ber.*, 1890, 1363-1370.

27. D. H. R. Barton, *J. Chem. Soc.*, 1953, 1027-1040.

28. S. H. W. E.L. Eliel, *Stereochemistry of organic compounds*, Wiley, New York, 1994.

29. N. J. H. S. Winstein, *J. Am. Chem. Soc.*, 1955, 5562-5578.

30. K. B. Wiberg, W. Hinz, R. M. Jarret and K. B. Aubrecht, *J. Org. Chem.*, 2005, **70**, 8381-8384.

31. M. P. Freitas, R. Rittner, C. F. Tormena and R. J. Abraham, *Spectrochimica Acta, Part A*, 2005, **61**, 1771-1776.

32. M. P. Wiesenfeldt, Z. Nairoukh, W. Li and F. Glorius, *Science*, 2017, **357**, 908-912.

33. E. Juaristi and R. Notario, *J. Org. Chem.*, 2016, **81**, 1192-1197.

34. F. Yoshinaga, C. F. Tormena, M. P. Freitas, R. Rittner and R. J. Abraham, *J. Chem. Soc.*, 2002, 1494-1498.

35. R. J. Abraham, T. A. D. Smith and W. A. Thomas, *J. Chem. Soc.*, 1996, 1949-1955.

36. E. A. Basso, L. A. Abiko, G. F. Gauze and R. M. Pontes, *J. Org. Chem.*, 2011, **76**, 145-153.

37. C. B. Francisco, C. S. Fernandes, U. Z. de Melo, R. Rittner, G. F. Gauze and E. A. Basso, *Beilstein J. Org. Chem.*, 2019, **15**, 818-829.

38. N. A. Meanwell, *J. Med. Chem.*, 2018, **61**, 5822-5880.

39. S. Couve-Bonnaire, D. Cahard and X. Pannecoucke, *Org. Biomol. Chem.*, 2007, **5**, 1151-1157.

40. E. T. Kool and H. O. Sintim, *Chem. Commun.*, 2006, 3665-3675.

41. L. Hunter, A. M. Z. Slawin, P. Kirsch and D. O'Hagan, *Angew. Chem. Int. Ed.*, 2007, **46**, 7887-7890.

42. L. Hunter, *Beilstein J. Org. Chem.*, 2010, **6**, 38.

43. A. J. Durie, A. M. Z. Slawin, T. Lebl and D. O'Hagan, *Angew. Chem. Int. Ed.*, 2012, **51**, 10086-10088.

44. A. J. Durie, A. M. Z. Slawin, T. Lebl, P. Kirsch and D. O'Hagan, *Chem. Commun.*, 2012, **48**, 9643-9645.

45. A. J. Durie, A. M. Z. Slawin, T. Lebl, P. Kirsch and D. O'Hagan, *Chem. Commun.*, 2011, **47**, 8265-8267.

46. T. Bykova, N. Al-Maharik, A. M. Z. Slawin and D. O'Hagan, *Org. Biomol. Chem.*, 2016, **14**, 1117-1123.

47. T. Bykova, N. Al-Maharik, A. M. Z. Slawin and D. O'Hagan, *Beilstein J. Org. Chem.*, 2017, **13**, 728-733.

48. N. S. Keddie, A. M. Slawin, T. Lebl, D. Philp and D. O'Hagan, *Nat. Chem.*, 2015, **7**, 483-488.

49. V. M. Marx, A. H. Sullivan, M. Melaimi, S. C. Virgil, B. K. Keitz, D. S. Weinberger, G. Bertrand and R. H. Grubbs, *Angew. Chem. Int. Ed.*, 2015, **54**, 1919-1923.

50. Y. Wei, B. Rao, X. Cong and X. Zeng, *J. Am. Chem. Soc.*, 2015, **137**, 9250-9253.

51. M. K. Whittlesey and E. Peris, *ACS Catal.*, 2014, **4**, 3152-3159.

52. T. Wagener, A. Heusler, Z. Nairoukh, K. Bergander, C. G. Daniliuc and F. Glorius, *ACS Catal.*, 2020, **10**, 12052-12057.

53. M. P. Wiesenfeldt, T. Knecht, C. Schlepphorst and F. Glorius, *Angew. Chem. Int. Ed.*, 2018, **57**, 8297-8300.

54. D. Moock, M. P. Wiesenfeldt, M. Freitag, S. Muratsugu, S. Ikemoto, R. Knitsch, J. Schneidewind, W. Baumann, A. H. Schäfer, A. Timmer, M. Tada, M. R. Hansen and F. Glorius, *ACS Catal.*, 2020, **10**, 6309-6317.

55. Y. Wang, W. Lee, Y.-C. Chen, Y. Zhou, E. Plise, M. Migliozzi and J. J. Crawford, *ACS Med. Chem. Lett.*, 2022, **13**, 1517-1523.

56. J. L. Clark, R. M. Neyyappadath, C. Yu, A. M. Z. Slawin, D. B. Cordes and D. O'Hagan, *Chem. - Eur. J.*, 2021, **27**, 16000-16005.

57. A. Rodil, S. Bosisio, M. S. Ayoup, L. Quinn, D. B. Cordes, A. M. Z. Slawin, C. D. Murphy, J. Michel and D. O'Hagan, *Chem. Sci.*, 2018, **9**, 3023-3028.

58. Z. Fang, D. B. Cordes, A. M. Z. Slawin and D. O'Hagan, *Chem. Commun.*, 2019, **55**, 10539-10542.

59. D. O'Hagan, *Chem. - Eur. J.*, 2020, **26**, 7981-7997.

60. B. E. Ziegler, M. Lecours, R. A. Marta, J. Featherstone, E. Fillion, W. S. Hopkins, V. Steinmetz, N. S. Keddie, D. O'Hagan and T. B. McMahon, *J. Am. Chem. Soc.*, 2016, **138**, 7460-7463.

61. O. Shyshov, K. A. Siewerth and M. von Delius, *Chem. Commun.*, 2018, **54**, 4353-4355.

62. S. M. Pratik, A. Nijamudheen and A. Datta, *Chemphyschem*, 2016, **17**, 2373-2381.

63. W.-M. Sun, B.-L. Ni, D. Wu, J.-M. Lan, C.-Y. Li, Y. Li and Z.-R. Li, *Organometallics*, 2017, **36**, 3352-3359.

64. W.-M. Sun, L.-T. Fan, Y. Li, J.-Y. Liu, D. Wu and Z.-R. Li, *Inorg. Chem.*, 2014, **53**, 6170-6178.

65. D. R. Kanis, M. A. Ratner and T. J. Marks, *Chem. Rev.*, 1994, **94**, 195-242.

66. S. M. Pratik, A. Nijamudheen and A. Datta, *ChemPhysChem*, 2016, **17**, 2373-2381.

67. P. R. Varadwaj, A. Varadwaj and B.-Y. Jin, *Phys. Chem. Chem. Phys.*, 2015, **17**, 31624-31645.

68. S. Tsuzuki, T. Uchimaru and M. Mikami, *J. Phys. Chem. A*, 2006, **110**, 2027-2033.

69. J. L. Clark, A. Taylor, A. Geddis, R. M. Neyyappadath, B. A. Piscelli, C. Yu, D. B. Cordes, A. M. Z. Slawin, R. A. Cormanich, S. Guldin and D. O'Hagan, *Chem. Sci.*, 2021, **12**, 9712-9719.

70. S. M. Pratik, A. Nijamudheen and A. Datta, *J. Phys. Chem. C*, 2017, **121**, 1752-1762.

71. R. A. Cormanich, N. S. Keddie, R. Rittner, D. O'Hagan and M. Bühl, *Phys. Chem. Chem. Phys.*, 2015, **17**, 29475-29478.

72. O. Shyshov, S. V. Haridas, L. Pesce, H. Qi, A. Gardin, D. Bochicchio, U. Kaiser, G. M. Pavan and M. von Delius, *Nat. Commun.*, 2021, **12**, 3134.

Chapter 2. Hydrogenation of trifluoromethylarene

2.1 Aims and objectives

The aim of this work was to study the hydrogenation of (trifluoromethyl)benzene derivatives using a Rh(CAAC)(COD)Cl **[Rh]** catalyst. The efficient direct hydrogenation of aryl CF_3 to alkyl CF_3 was not developed previously, and this could be a straightforward method to deliver synthetically more difficult cycloalkyl CF_3 compounds. This trifluoromethyl aryl hydrogenation reaction was studied exploring a range of substrates with different functional groups, to test the functional group tolerance of the reaction. The yield and the stereoselectivity of the hydrogenations were studied and optimised with an aim to offer an efficient and clean synthesis of a variety of pharmaceutical building blocks. Therefore, groups such as –OH, –NH, –COOH, which are amenable to subsequent conjugations and functional groups interconversions were included as well as the high value substituents such as $–OCF_3$.

The substrates of phenol, benzyl alcohol and aniline were protected first to prevent functional group coordination to the catalyst, or ketone formation via the formation of an intermediate enol (Scheme 1-3 b in Chapter 1, section 1.6.1).[1] Accordingly, protecting group were explored to facilitate the hydrogenation reaction.

2.2 Trifluoromethyl group

2.2.1 The trifluoromethyl group carbon atom

The trifluoromethyl group plays a significant role in pharmaceutical, agrochemical and materials chemistry research due to its unique properties such as high electron density, compact sterics, high hydrophobicity and lipophilicity as well as solubility.[2-5] There are a variety of blockbuster pharmaceuticals which contain at least one trifluoromethyl group, including Prozac **2-1**, Fluoridone **2-2**, Leflunomide **2-3**, Emend **2-4**, Meflouine **2-5**, Fludelone **2-6** and many others (Figure 2.1, Figure 2.2).
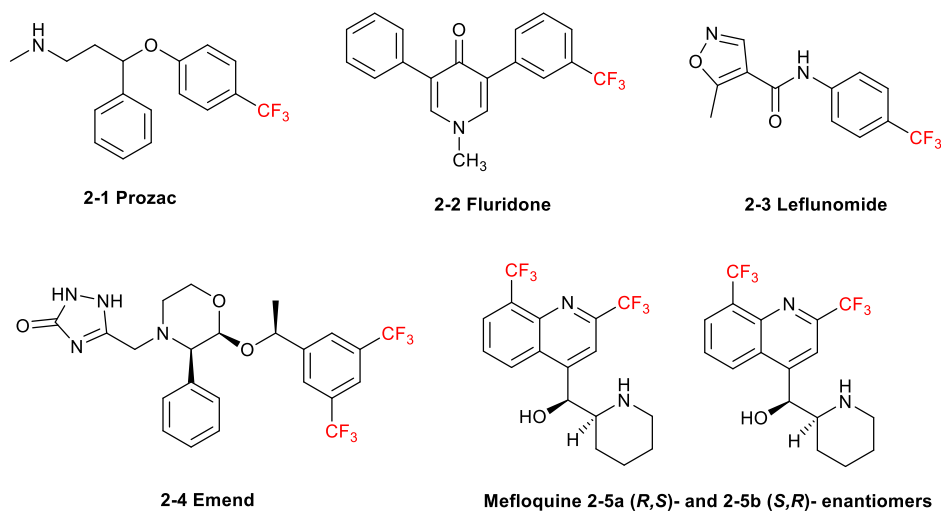

Figure 2-1 Important pharmaceuticals containing the trifluoromethyl group.

Fludelone illustrates an example of how the trifluoromethyl group facilitates research in medicinal chemistry. The substitution of a methyl group by the trifluoromethyl group on epothilone B derivatives increased metabolic stability, while retaining cytotoxic potency.[6, 7]
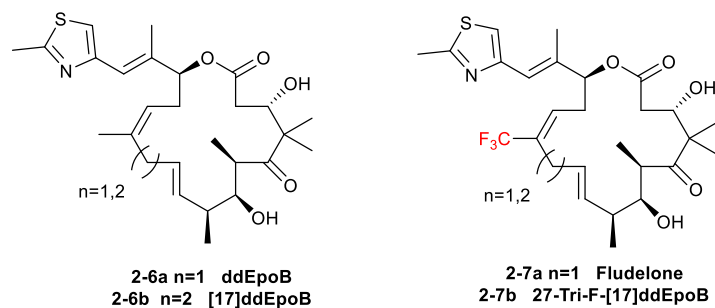
Figure 2-2 Evolution of Fludelone **2-6** and **2-7**.

Fluoroalkylation reactions often behave differently from traditional alkylation reactions. For example the Grignard reaction (Scheme 2-1a) and Williamson's ether synthesis (Scheme 2-1 b) do not work well with fluoroalkyl groups.[8-12] However methods for the introduction of a trifluoromethyl group have been developed for the efficient and straight forward introduction of fluorine atoms into motifs. [10, 13, 14]
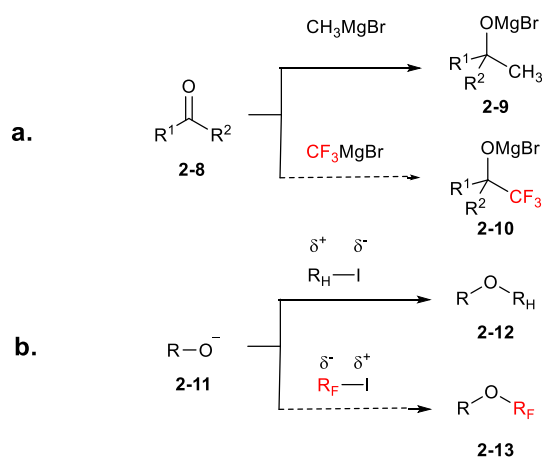
Scheme 2-1 Comparison of alkylation and fluoroalkylation.

This CF_3 group can be installed via transition metal mediated trifluoromethylations, radical trifluoromethylations and nucleophilic trifluoromethylations using commercially available reagents and relatively cheap starting materials (Scheme 2-2 a, b, c).[12, 15-17] Electrophilic trifluoromethylation has been applied to generate many challenging products such as –OCF_3, –NCF_3, –SCF_3, vinyl and alkyn–CF_3 (Scheme 2-2 d).[18, 19]

47
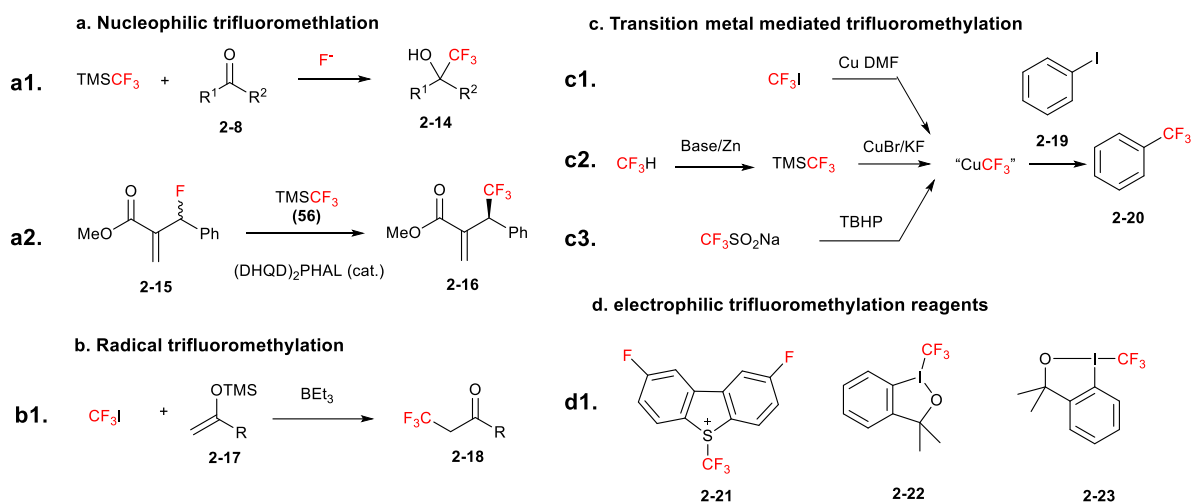
Scheme 2-2 Common trifluoromethylation strategies.

2.2.2 Previous studies on the hydrogenation of (trifluoromethyl)benzene derivatives

(Trifluoromethyl)benzene **2-20** was first synthesised in 1892[20] (Scheme 2-3 a), and the copper mediated trifluoromethylation of aromatic rings has been studied since the 1960s[21, 22] (Scheme 2-3 b). A study on the trifluoromethylation of carboxylic acids with SF_4 and consequent conformation studies on disubstituted cyclohexane was reported in 1967[23, 24] (Scheme 2-3 c).
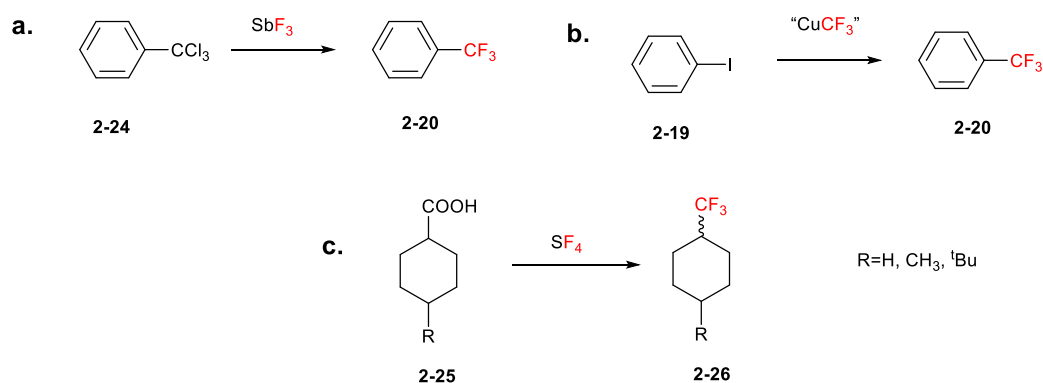
Scheme 2-3 Examples of trifluoromethylation on 6-membered rings.

Then there are several reports which have established the synthesis of di-functionalized trifluoromethyl groups on cyclohexane, with some limitations. For example, 1,2-*bis*(trifluoromethyl)cyclohexanes, *cis* **2-28** and *trans* **2-28** were prepared with $(CF_3)_2Te$, but without determination of the stereoselectivity (Scheme 2-4 a).[25] 1,2- and 1,3-*bis*(trifluoromethyl)cylcohexanes *cis* **2-32**, *trans* **2-32** and **2-33** have been made by deoxylfluorination of specific isomers of the precursor carboxylic acids using SF_4 at low temperature, while the yield and selectivity were shown to be substrate dependant.[26]
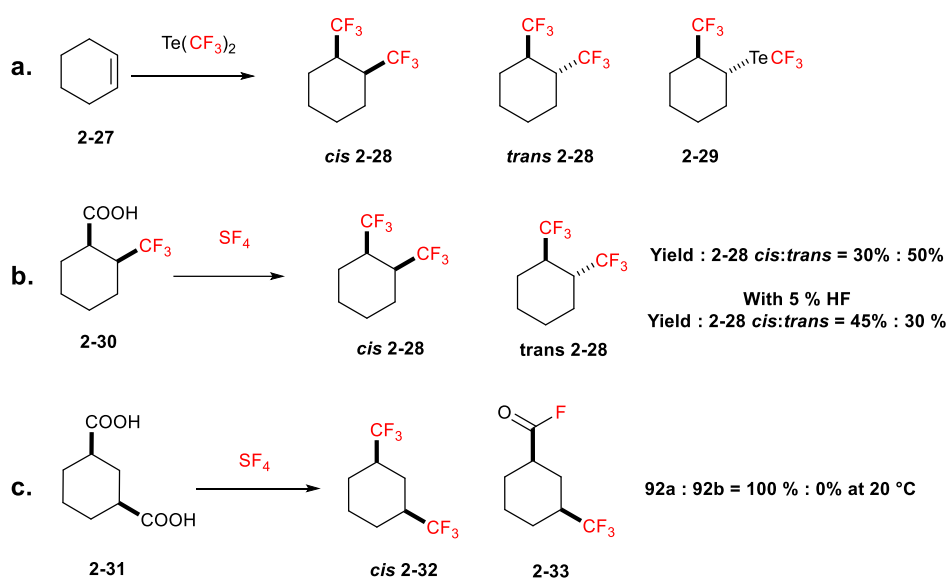
Scheme 2-4 Previous syntheses of difunctionalised trifluoromethylcyclohexanes.

Although asymmetric trifluoromethylations have recently been intensively studied,[27-29] there are only a few studies reported regarding the stereo-selective reduction trifluoromethyl hexane derivatives (Scheme 2-5). Collins *et al.* reported the *cis* hydrogenation of 1,2-*bis*(trifluoromethyl) octafluorocyclohexene **2-35** with a defluorinated product distribution (Scheme 2-5 a).[30] Carcenac *et al.* studied the hydrogenation of 1,4-perfluoroalkene **2-38** under ultrasound irradiation(Scheme 2-5 b)[31] and Takashi *et al.* reported the facially selective reduction of 2-(trifluoromethyl)cyclohexanone **2-39** with controlled diastereoselectivity (Scheme 2-5 c)[32]. The photo-induced reduction of 2-trifluoromethyl-cyclohexanone **2-39** was

studied by Semisch *et al.* but the reaction was not stereoselective (scheme 2-5 d).[33] Additionally, the Diel-Alder reaction product **2-43** from 2-heterosubstituted furan and hexafluoro-2-butyne was hydrogenated to generate the facially selective fluorinated building block **2-45** in high yield (Scheme 2-5 e).[34]
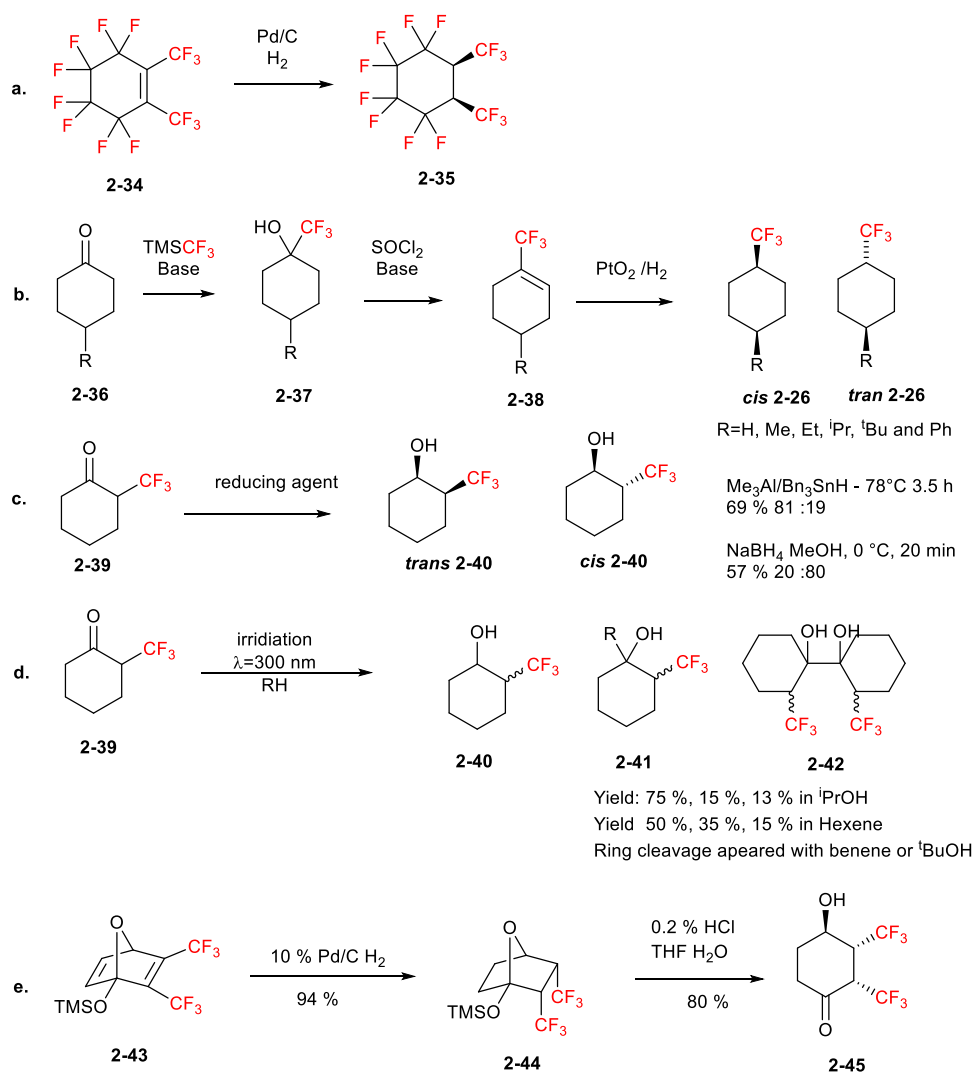
Scheme 2-5 Previous syntheses of functionalised (trifluoromethyl)cyclohexane derivatives.

Surprisingly, there are only a limited number of accounts in the literature regarding the aryl hydrogenation of (trifluoromethyl)benzene derivatives (Scheme 2-6). Previous hydrogenation reactions on such substrates have been studied predominately under heterogenous conditions. Zalesskaya *et al.* performed the hydrogenation of (trifluoromethyl)phenol **2-46**

with Raney Ni which yielded predominately *trans* isomers **trans 2-47** and defluorinated products (Scheme 2-6 a).[35] Alekseenko *et al.* studied the hydrogenation of trifluoromethylaniline **2-48**, as well as demonstrating the Pt catalysed hydrogenation to 1,2-bis(trifluoromethyl)cyclohexane *cis* **2-28**, yielding a major *cis* isomer.[26, 36] In both cases, the yield is not very high and the selectivity in 1,3- and 1,4- di-substituted substrates are low. Other research related to the hydrogenation of trifluoromethyl derivatives focused on the properties of heterogenous catalysts, using either simple (trifluoromethyl)benzene **2-20** as the substrate[37, 38] or retaining the (trifluoromethyl)arene unreduced.[39]
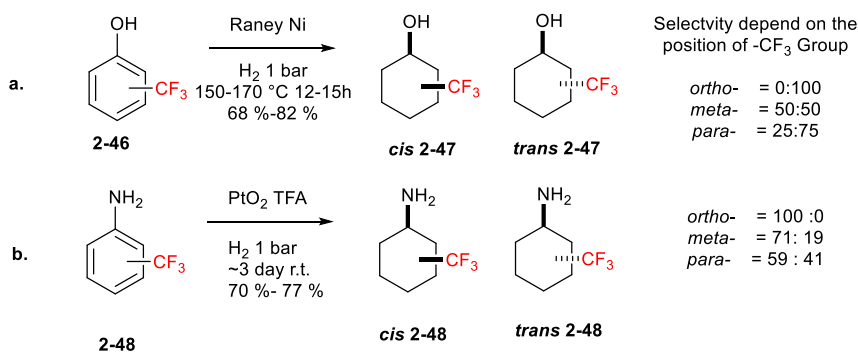
Scheme 2-6 Historical aryl hydrogenations of (trifluoromethyl)benzene derivatives.

2.2.3 Conformation of trifluoromethyl cyclohexanes
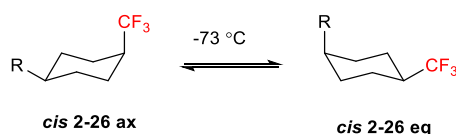
Scheme 2-7 Ring flipping of di-substituted cyclohexanes.

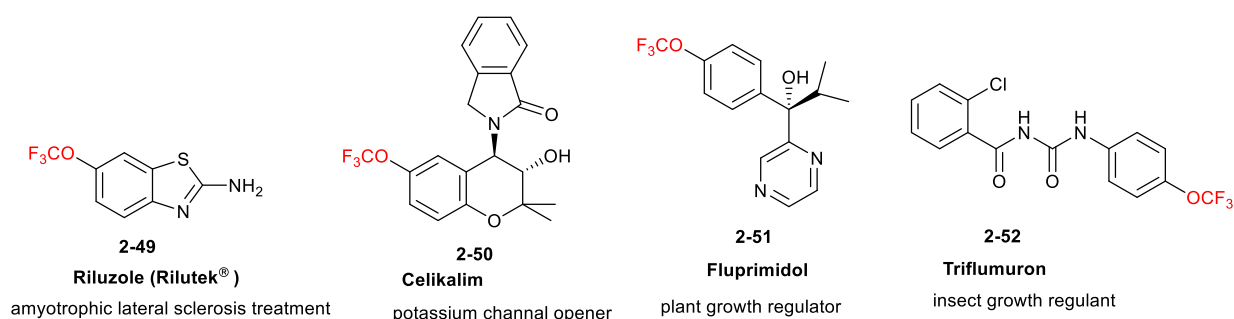The conformational preferences of the trifluoromethyl group on cyclohexanes was previously studied by Della *et al.* in 1967[24] and then more systematically by Carcenac *et al.* after 2000[31, 40-42]. Those studies concluded that the *A* value of the –CF$_3$ group is 2.37 kcal mol^{-1} from *K* =8.25 at -73 °C. By contrast the methyl group is 1.7 kcal mol^{-1}.[41-43] This research also revealed

that the coalesced fluorine peak in the ^{19}F NMR spectrum resolved to two peaks (-66 and -74 ppm) at low temperature indicating the equilibrium between the axial and equatorial $-CF_3$ conformers (Scheme 2-7 and Figure 2-4).

2.2.4 Trifluoromethyl groups bonded to heteroatoms

Trifluoromethyl groups directly linked to a heteroatom and especially OCF_3 and SCF_3, have attracted recent and significant interest, due to their unique properties as substituents, which have proven beneficial for pharmaceuticals and agrochemicals discovery.

For example, the trifluoromethoxyl group is metabolically stable in organisms, and it has a moderate lipophilicity of π_R =1.04. This makes such groups suitable for adjusting the chemophysical properties of drug molecules and insecticides by its long-range electron-withdrawing effects (σ_p =0.35 σ_m =0.38).[44]

2-49
Riluzole (Rilutek$^®$)
amyotrophic lateral sclerosis treatment

2-50
Celikalim
potassium channal opener

2-51
Fluprimidol
plant growth regulator

2-52
Triflumuron
insect growth regulant

Figure 2-3 Drugs containing the trifluoromethoxyl group.

However, the direct introduction of such groups is still under development. In the case of the OCF_3 group, the main challenge for direct introduction is the ready decomposition of precursor reagents into difluoro-phosgene and fluoride.[45]

In the case of SCF_3, although methods for the introduction of this group have been well developed in the past decade. However, many of those methodologies are rely on

nucleophilic, electrophilic or radical reactions on aromatic rings. So, aliphatic SCF$_3$ groups are less commonly prepared. Therefore, it become interesting to apply the rhodium CAAC catalyst in attempting the hydrogenation of hetero CF$_3$ aryl compounds to direct deliver hetero CF$_3$ aliphatic compounds.

2.3 Synthesis and conformations of (trifluoromethyl)cyclohexanes

2.3.1 Hydrogenation of (trifluoromethyl) benzene
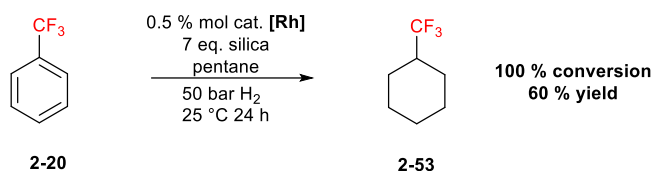
Scheme 2-8 Hydrogenation of (trifluoromethyl) benzene **2-53**.

In the first instance, catalytic hydrogenation of trifluoromethylbenzene **2-20** with Rh(CAAC)(COD)Cl **[Rh]** as a catalyst was explored at 50 bar H$_2$ in a steel autoclave. The reaction was followed by ^{19}F NMR (62.7 ppm) and showed a 100 % conversion from the aryl –CF$_3$ after 24 h. When the reaction was run with (trifluoromethyl)benzene as both the substrate and solvent, this showed only a 10 % conversion, and was not a significant improvement. Overall this demonstrated the ability of Rh(CAAC)(COD)Cl catalyst **[Rh]** to readily hydrogenate (trifluoromethyl)benzene **2-20** to afford (trifluoromethyl)cyclohexane **2-53**.

2.3.2 Hydrogenation of bis(trifluoromethyl)benzene

The substrate range was extended to bis(trifluoromethyl)benzene*s* and accordingly *ortho-*, *meta-* and *para-* di-substituted (trifluoromethyl)benzenes were explored as substrates for the hydrogenation reaction. The reaction again showed high conversions from aryl–CF$_3$ to alkyl–CF$_3$ products. The appearance of axial and equatorial –CF$_3$ groups in the ^{19}F-NMR spectra of

the products was not obvious at room temperature, however these signals could be resolved at low temperature (-75 °C).
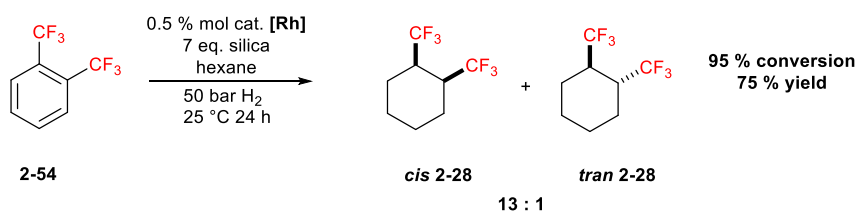
Scheme 2-9 Preparation of 1,2-bis(trifluoromethyl)cyclohexane **2-28**.
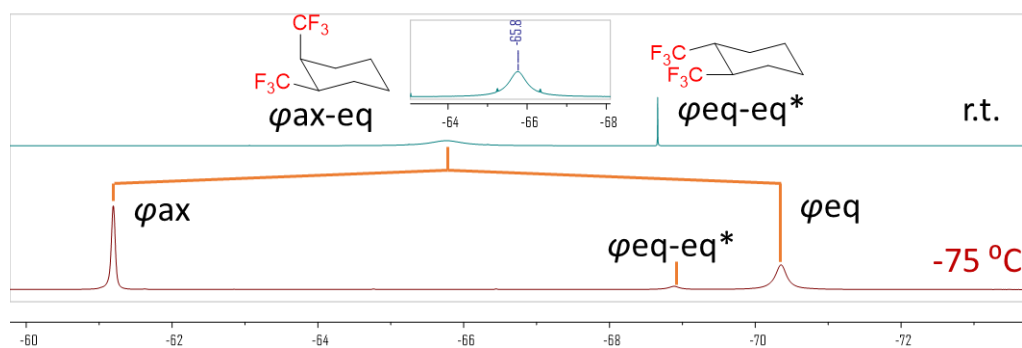
Figure 2-4 ^{19}F NMR spectra of *cis* **2-28** and *trans* **2-28** at -75 °C and room temperature (r.t.).

In the case of the *ortho* isomer **2-28** above, the ^{19}F {^{1}H} NMR at room temperature showed only a broad peak at -65 ppm however when the temperature was lowered to − 75 °C, this peak resolved into two peaks of equal intensity (1 : 1) at -61 ppm and -70 ppm with almost a 10 ppm separation (Scheme 2-9 and Figure 2-4).
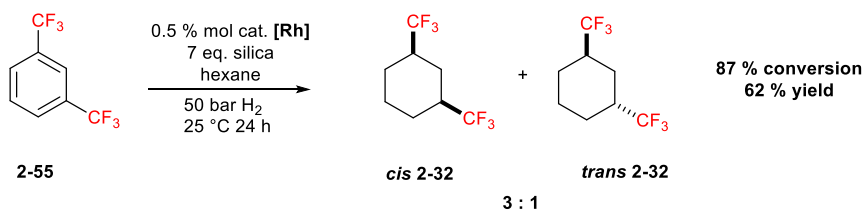
Scheme 2-10: Preparation of 1,3-bis(trifluoromethyl)cyclohexane **2-32**

In the case of the *meta*-isomer **2-32**, the aryl hydrogenation selectivity is lower than the *ortho*- and *para*- substrates. The major product ***cis* 2-32** has two equatorial –CF$_3$ groups in the most preferred conformation, at -74 ppm by ^{19}F NMR. The minor *trans* **2-32** product had a coalesced peak at -71 ppm which again becomes resolved at -75 °C, into two peaks at -66 ppm and -74 ppm respectively (Scheme 2-10 and Figure 2-5).
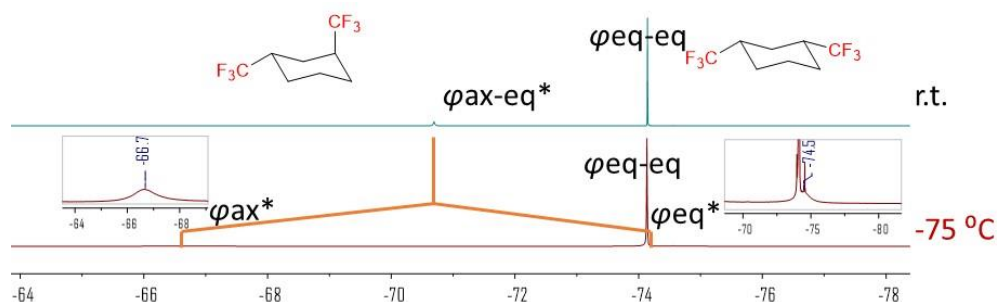
Figure 2-5 ^{19}F NMR spectra of ***cis* 2-57** and ***trans* 2-57** at -75 °C and at room temperature (r.t).

Finally, in the *para*-isomer **2-57**, generated the highest conversion of 100 % for the bis systems. The major product ***cis* 2-57** (-70 ppm) has a preferred conformation with one axial and one equatorial –CF$_3$ group as evidenced in the low temperature NMR spectrum, at -66 ppm and -74 ppm respectively (Scheme 2-11 and Figure 2-6).

Scheme 2-11 Preparation of 1,4-bis(trifluoromethyl)cyclohexane **2-57**.

Further resolution of this peak would require a lower temperature than -75 °C which was not experimentally feasible with the available NMR instruments. More generally these reactions proved the advantage of the CAAC catalyst on stereoselectivity on 1,2- and 1,4- disubstituted substrates.
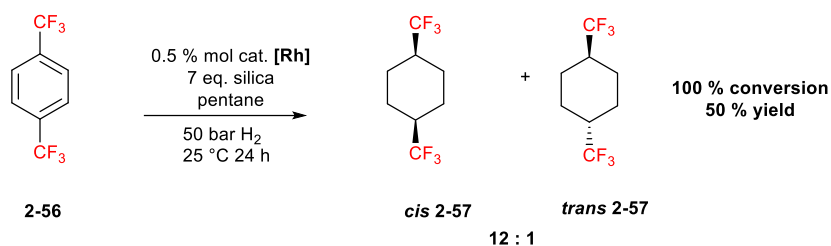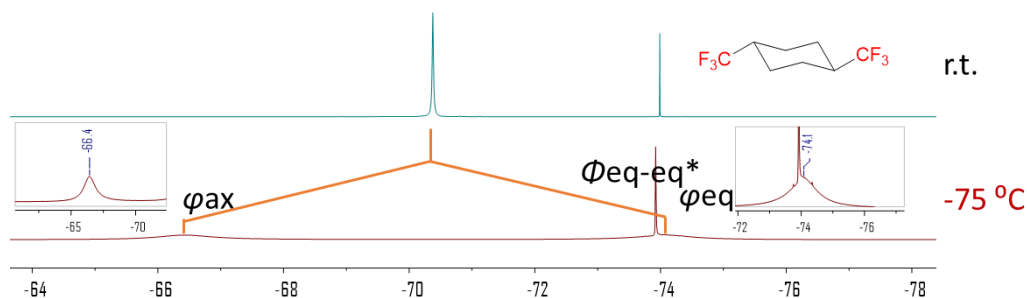
Figure 2-6 ^{19}F NMR spectra of *cis* **2-57** and *trans* **2-57** at -75 °C and room temperature (r.t.).

The stereo-selectivity of the aryl hydrogenation arises from the surface interaction between aryl substrate and catalytical surface.[46] In several further studies of the Rh-CAAC catalysed hydrogenation, its mechanism is proposed to be similar to heterogenous transition metal catalysed hydrogenation.[1, 46-49] The absorbed hydrogen atoms on the catalyst surface add across to the C=C double bond (Scheme 2-12 a).
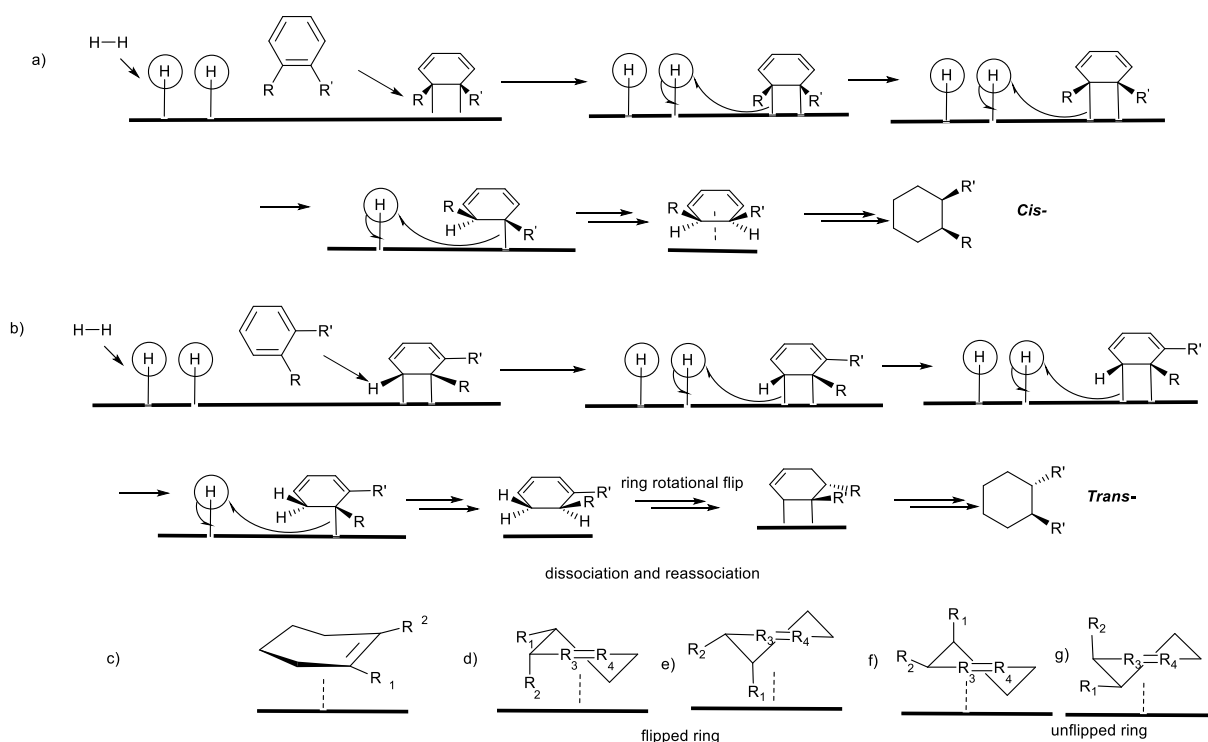

Scheme 2-12: A mechanism of the Rhodium catalysed hydrogenation reaction.

56

The *trans-* products were formed from the partially hydrogenated intermediates cyclohexadienes and cyclohexenes. As shown in Scheme 2-12 (b), the intermediates olefin ring flips and reassociates to the catalyst surface through the opposite face of the ring. During the process, the hydrogen atoms transfer to different faces, resulting in a *trans*-configuration of the R and R' groups.

The stereoselectivity of the hydrogenations were excellent with 1,2-disubstitued substrates (Scheme 2-12 c). The 1,3-disubstituted substrates gave the lowest stereoselectivity most likely due to generating higher energy of 1,3 di-axial intermediates with the direct *syn*-hydrogenation (Scheme 2-12 d, R1 and R3 are substituted). The 1,4-disubstituted substrates had an intermediate stereoselectivity promoted by the large steric resistance (Scheme 2-12 e, R1 and R4 are substituted).[46]

2.3.3 Hydrogenation of trifluoromethylphenol

A series of hydrogenation reactions was explored on phenols to try to generate trifluoromethylcyclohexanols. As reported in the literature, phenols required protection in order to prevent enol isomerisation.[50] Accordingly a *tert*-butyldimethylsilyl (TBS) group was used to protect a series of (trifluoromethyl)phenol substrates as illustrated in Scheme 2.13.
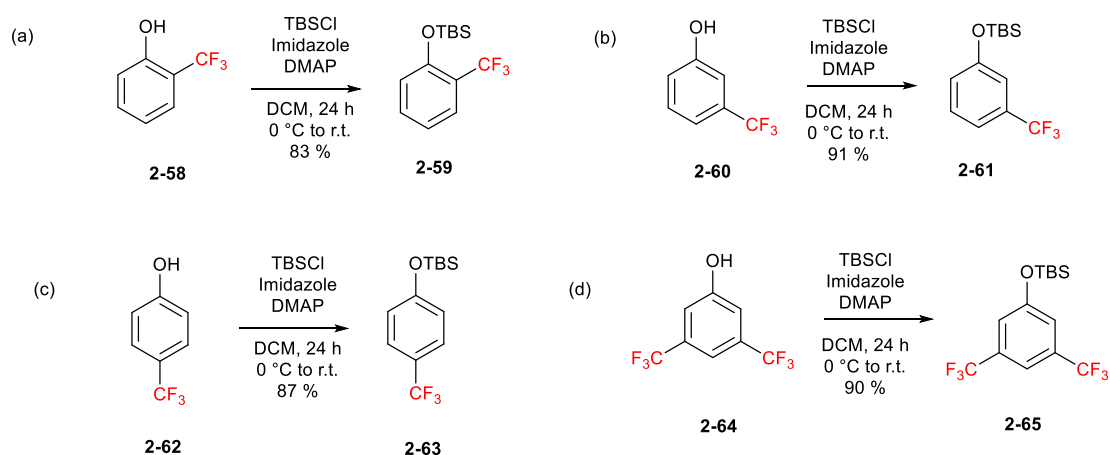
Scheme 2-13 TBS group protection of (trifluoromethyl)phenols.

57

Aryl hydrogenation reactions with catalyst **[Rh]** were then explored on these TBS protected substrates. The hydrogenation progressed successfully in each case, converting the TBS protected phenols to TBS protected cyclohexanol ethers, generally in good yield and high selectivity.
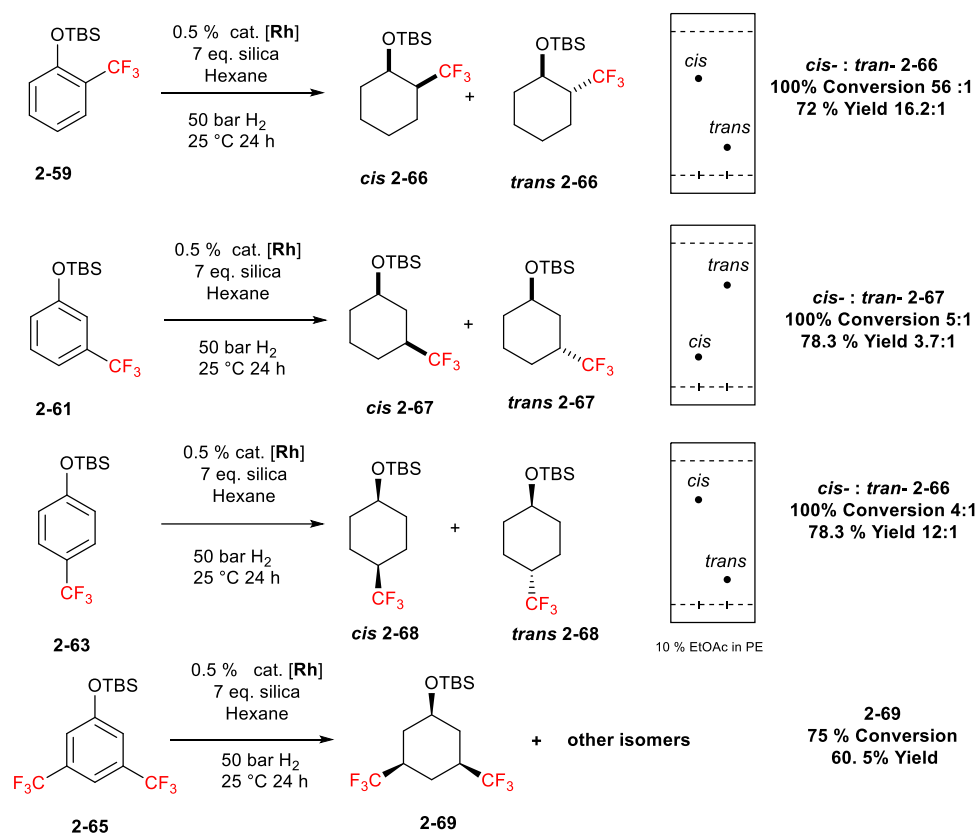
Scheme 2-14 Preparation and TLC outcomes of TBS protected (trifluoromethyl)cyclohexanols.

The major *cis* and minor *trans* isomers of TBS-protected cyclohexanol could be readily purified and separated by column chromatography. Experimentally it was observed that product *cis* **2-67** is much more polar than the other two *cis* products *cis* **2-66** and *cis* **2-68** (Scheme 2-14) Again, the high conversion and selectivity of the 1,2 and 1,4-substituted substrates suggests the efficient application of the CAAC catalyst **[Rh]**.

In order to prove the relative stereochemistry and the utility of the *cis*-trifluoromethyl cyclohexanol motif, the TBS protected cyclohexanol was deprotected with TBAF, as illustrated

in Scheme 2.15.
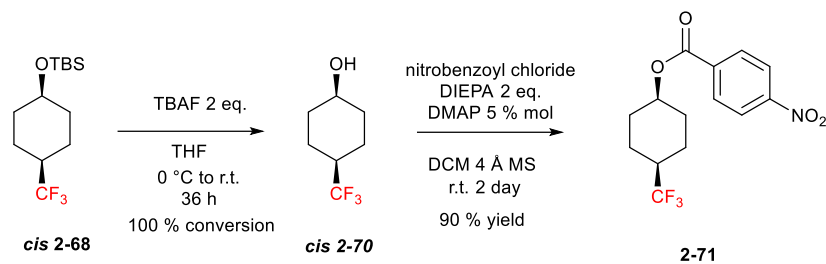
Scheme 2-15 Deprotection following esterification of compound **2-68**.

Subsequently a nitro-benzoyl ester derivative **2-71**, was prepared and this ester could be crystallised. The resultant X-ray crystal structure confirmed the *syn*-stereochemistry, with both substituents on the same face of the cyclohexane ring.
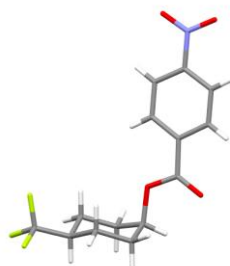
Figure 2-7 Crystal structure of product **2-71** showing the *syn* stereochemistry.

A solution ^{1}H-NMR nuclear Overhauser enhancement (NOE) experiment on 3,5 bis-(trifluoromethyl)cyclohexanol ether **2-69** was in good agreement with the stereochemistry revealed in the X-ray structure. Irradiation of the proton, geminal to the ether oxygen (H-C-O-SiR$_3$) correlated with the axial H–CCF$_3$ proton, consistent with the *syn* stereochemistry as illustrated in Figure 2-8.
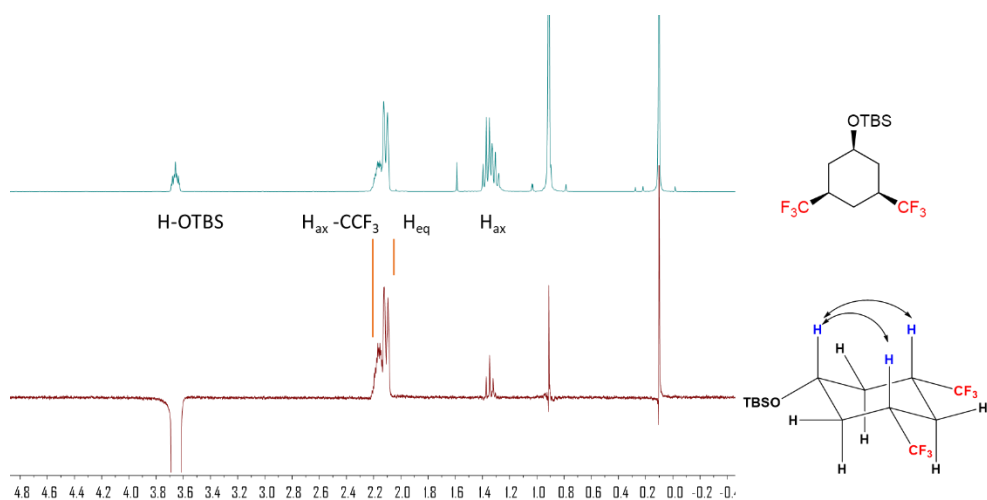
Figure 2-8 NOE experiment of cyclohexane **2-69**.

2.3.4 The direct hydrogenation of isomers of (trifluoromethyl)phenol

Direct aryl hydrogenation of the *ortho, meta* and *para* isomers of trifluoromethyl phenol was explored without phenol protection. The outcomes are summarised in Scheme 2.16.
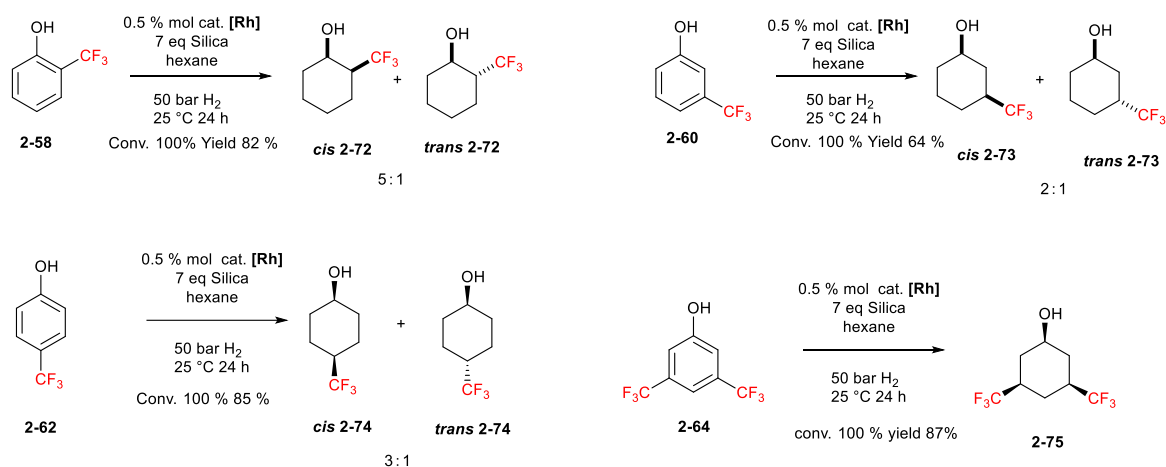
Scheme 2-16 Direct arylhydrogenation of trifluoromethoxyl phenols.

These reactions proved to be very successful with full conversion of starting materials, although conversions were lower relative to reactions with the silyl ether protected substates. It should be noted that the cyclohexyl alcohols are relatively volatile compounds and they

slowly sublime at room temperature and there are losses during work up. It was notable too that the stereoselectivity of these direct hydrogenation reactions is significantly lower compared to that of the silyl ethers. Presumably this is due to the steric impact of the large silyl protecting group during the hydrogenation process. However, the direct hydrogenation of the phenols gives overall higher yields relative to the three-steps silyl protection-hydrogenation-deprotection protocol.

2.3.5 Hydrogenation of trifluoromethoxy aromatics

The trifluoromethoxy group ($-OCF_3$) is a long-range electron-withdrawing group[51] and is emerging as an important functional group in pharmaceuticals research.[27] However, trifluoromethoxylation methods are limited and require toxic reagents and high cost (eg. of $PhSO_3CF_3$).[15] Therefore, an efficient method to introduce aliphatic OCF_3 groups is attractive and would extend the range of compounds containing this group beyond the more common aromatics. So, hydrogenation substrates were extended to (trifluoromethoxy)benzene **2-76** and its derivatives.
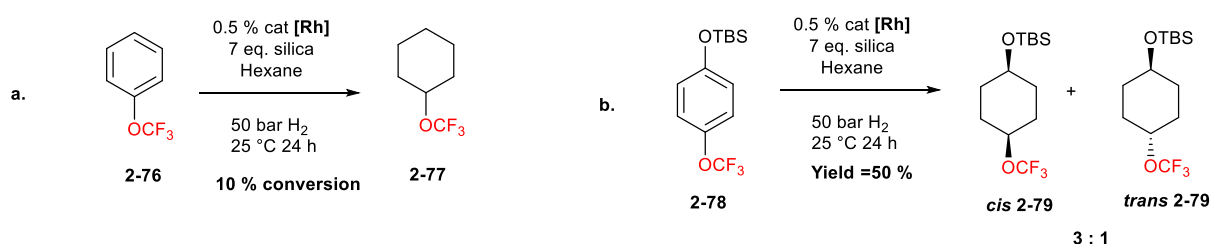
Scheme 2-17 Preparation of (trifluoromethoxy) cyclohexane **2-77** and (trifluoromethoxy) cyclohexan-4-TBS silyl ether **2-79**.

An initial reaction obtained 10% conversion of **2-76** to **2-77**. Developing the TBS ether protocols to this series, the protected phenol **2-78** was then subject to aryl hydrogenation and this gave a 50 % yield and a product ratio of 3:1 presumably of the *syn-* and *anti-* products respectively. For the major product, a ^{1}H-NMR NOE experiment showed a correlation

between the two protons at the substituted positions on the ring consistent with the *syn* stereochemistry. The trifluoromethoxy aromatic hydrogenation reactions were extended to explore the functional group tolerance of the reaction.
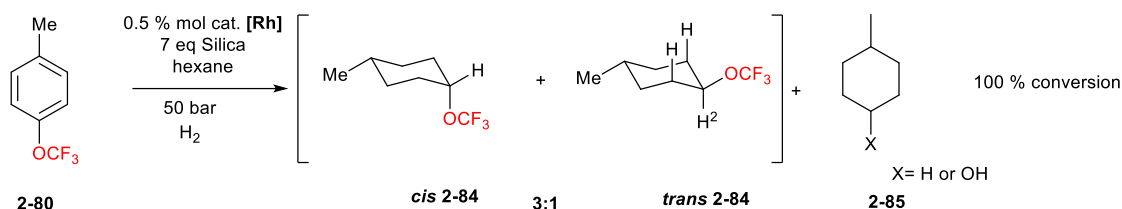
Scheme 2-18 Preparation of trifluoromethoxy 4-methyl cyclohexane **2-84**.

Accordingly, a methyl substituent was explored in substrate **2-80**. This substrate showed a full conversion with no aromatic proton signals left as judged by the ^{1}H-NMR of the crude product. The coupling constant, on the tertiary proton geminal to the trifluoromethoxy group, suggested a 3:1 isomer distribution of *cis and trans* **2-84**. The *syn* product was identified as major product. The large coupling constant (11.1 Hz) of this geminal proton in the minor product indicates an antiparallel relationship to the vicinal axial proton and this is consistent only with the *trans* products (Figure 2-9). It is proved difficult to separate this product from the hexane solvent due its low boiling point. In addition, a side product of C–O bond cleavage is suggested, as there was a high polarity spot observed on TLC, with r.f. value closed to cyclohexanol. No ^{19}F signal was observed for this by-product and the identity of this product was not confirmed.

1H NMR (500 MHz, Chloroform-*d*) δ 4.49 (tt, *J* = 4.5, 2.7 Hz, 3H), 4.12 (tt, *J* = 11.1, 4.5 Hz, 1H).
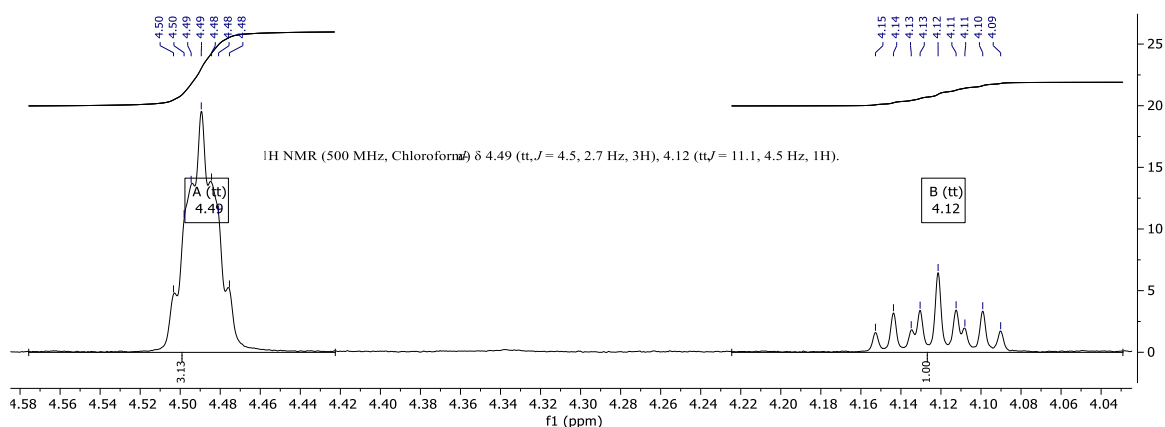
Figure 2-9 ^{1}H-NMR spectrum, of the hydrogenation product **2-84**.
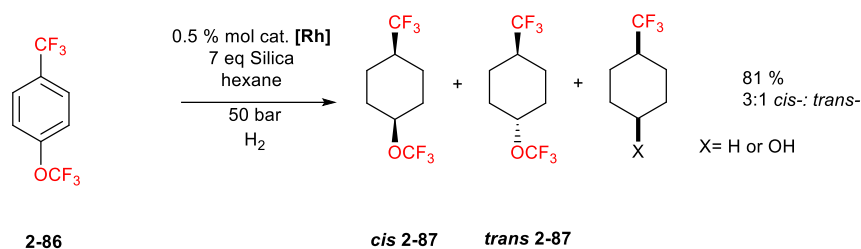
Scheme 2-19 Prepration of 1-trifluoromethoxyl-4-trifluoromethyl cyclohexane.

Unexpectedly the reaction shows higher conversion compared to the unsubstituted trifluoromethoxy benzene, either with an electron withdrawing CF₃ group or electron donating methyl group. The 1,4-disubstituted cyclohexane, which has a relatively high boiling point could be separated from solvent. The isolation of its *cis* and *trans* isomers was challenging but possible, and each isomer was characterised. The reaction has a 3:1 distribution of *cis-* : *trans-* selectivity which is similar to the methyl starting material.
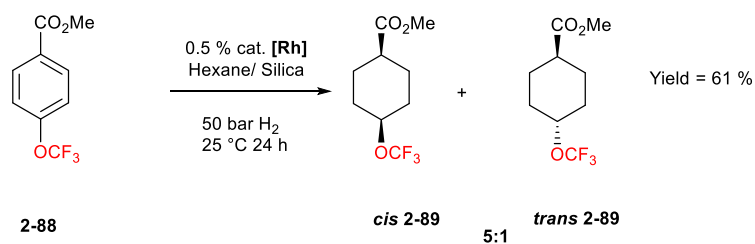
Scheme 2-20 Preparation of methyl 4-(trifluoromethoxy)cyclohexane carboxylate **2-89**.

63

Aryl hydrogenation of the methyl ester **2-88** shows an improved selectivity of *cis* product (5:1 *cis* to *trans* ratio). The higher selectivity compared to the methyl or trifluoromethyl groups suggests a more significant influence on stereochemistry from the ester functionality despite a lower yield (25 %). This may be due to the chelating potential of the carbonyl with the catalyst.
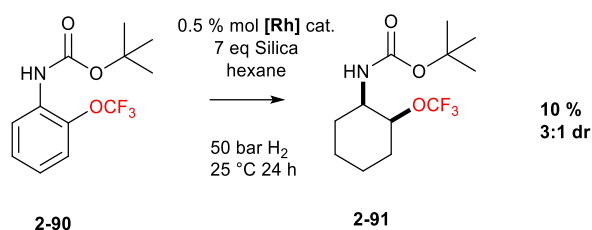
Scheme 2-21 Preparation of 2-trifluoromethoxylcyclohexylcarbamate **2-91**.

Aryl hydrogenation of carbamate **2-90** required an extended reaction time and molecular sieves, and even then, it was a poor reaction which only afforded the cyclohexane product 2-91 in 10 % yield.

In a further elaboration, a liquid crystal type product **2-93** was generated by aryl hydrogenation of the aromatic precursor **2-92** (Scheme 2-22). X-Ray structure analysis of the product showed that the two original cyclohexyl rings had retained their *trans* geometry, while the aromatic ring was reduced to generate a *cis* cyclohexyl ring. In the structure the OCF$_3$ group is axial, a conformation that is presumably dictated by the preference of the adjoining cyclohexyl ring to lie equatorial. In the X-ray structure, the –CF$_3$ group is pointing away from the alkyl chain, as might be expected on steric grounds.
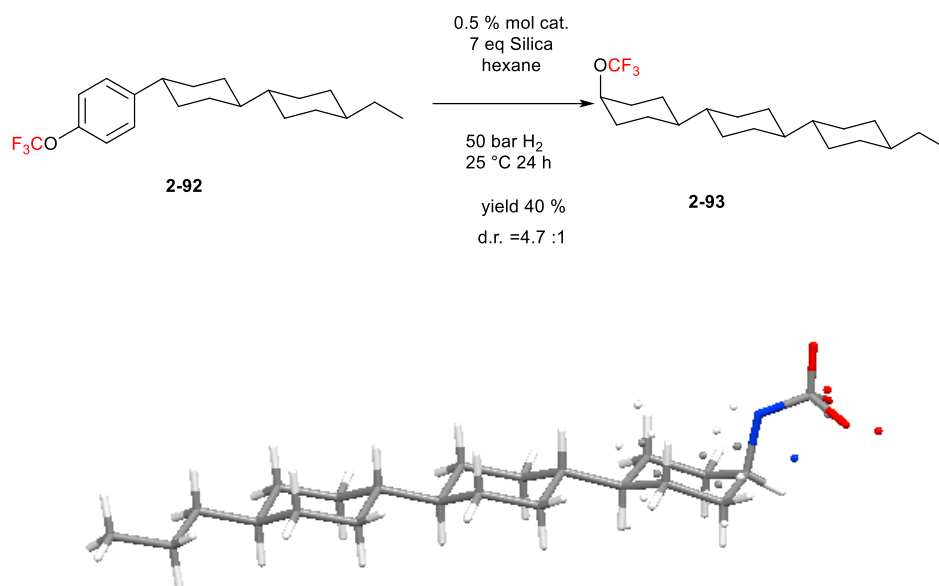
Scheme 2-22 Synthesis and X-ray structure of trifluoromethoxy-cyclohexyl liquid crystal motif **2-93**.

A DSC-POM measurement was carried out on compound **2-93** in collaboration with Dr. Yamada in Kyoto. However, no liquid crystal phase was observed with compound **2-93**. An elongation of the ethyl side chain was suggested to improve the potential of liquid crystal behaviour, although this was not pursued.
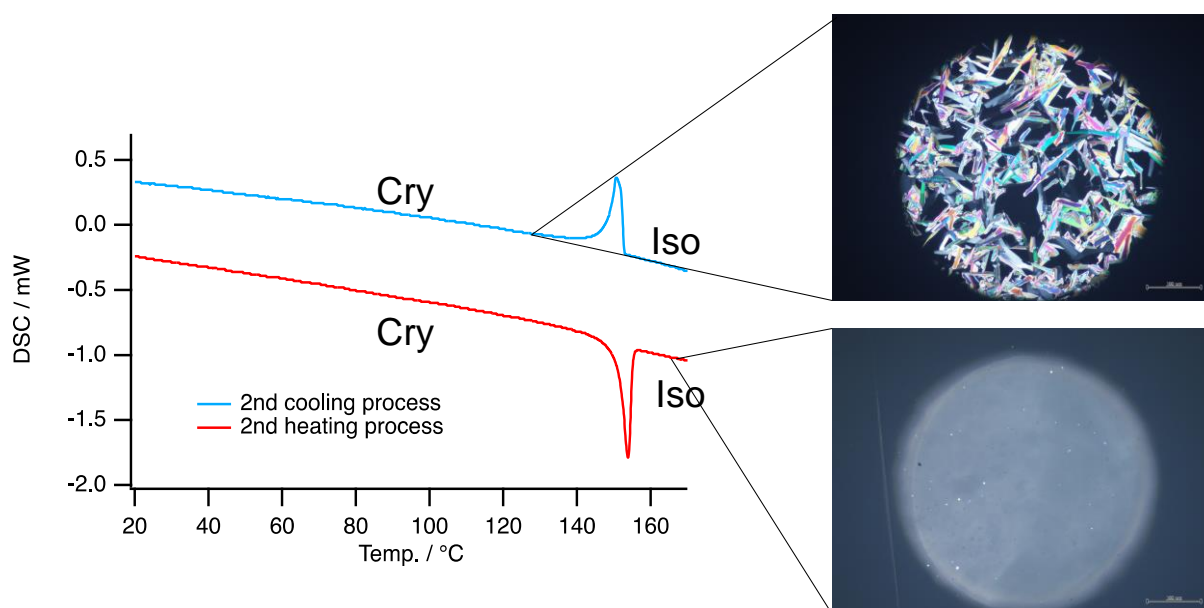
Phase transition	Temp. / °C	ΔH / kJ mol^{-1}	ΔS / J K^{-1}mol^{-1}
Cry - Iso	149	-8.07	-54.2
Iso - Cry	153	7.60	49.7

Figure 2-10 DSC and POM measurement of compound **2-93** (Dr.Yamada, Kyoto).

2.3.6 Attempted aryl hydrogenation of aryl-SF₅ and aryl-SF₃ substrates

Pentafluorosulfanyl aromatics are inert to aryl hydrogenation using standard palladium catalysts. Harsh reduction conditions such as a Birch reduction conditions will result in the decomposition of the SF$_5$ group to sulfides (Scheme 2-23 c).[52] A common method to prepare aliphatic SF$_5$ involves the oxidative cleavage of aromatic derivatives or to employ of SF$_5$X addition.[53] Therefore, the hydrogenation of aryl SF$_5$ compounds to afford alkyl SF$_5$ compounds becomes a novel objective.
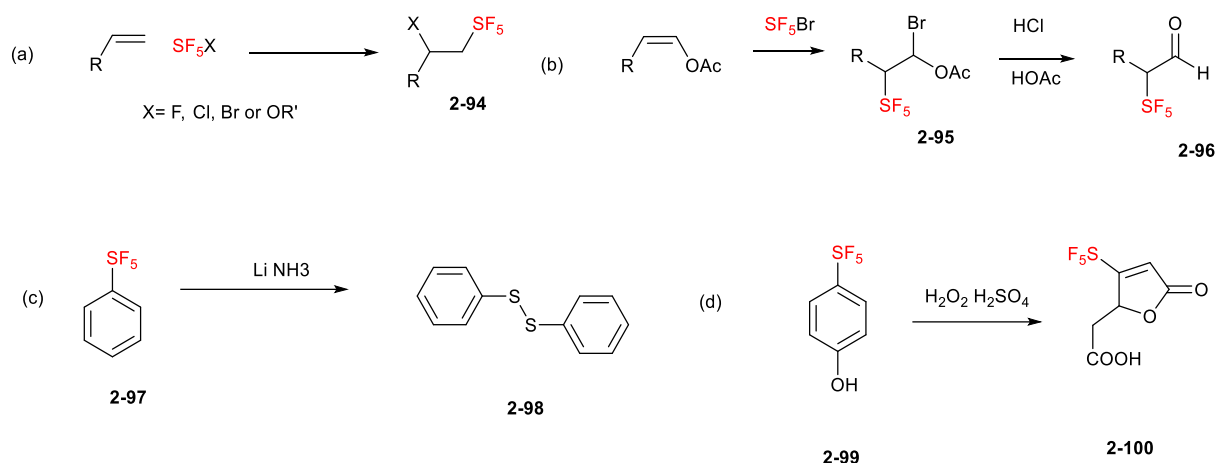
Scheme 2-23 Reported methods to aliphatic SF₅ compounds.
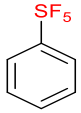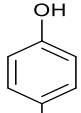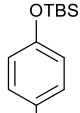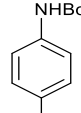
A novel approach to aliphatic SF₅ compounds might involve Rh(COD)CAAC **[Rh]** catalysed aryl hydrogenations, therefore the hydrogenation of a series of SF₅ containing aromatics was explored as an extension to the above investigations.

The standard conditions for Rh(COD)CAAC **[Rh]** hydrogenation were tested on (pentalfluorosulfanyl)benzene, however this was unsuccessful and the starting material was recovered after on work up. It appeared too that the Rh catalyst converted to Rhodium nanoparticles, coated across the silica gel additive.

Free amines or unprotected phenols did not undergo arene hydrogenation. In the case of aniline, rhodium nanoparticles did not form, consistent with the conditions for pentafluoroaniline and trifluoromethyl aniline hydrogenation where protecting groups are necessary.

O-Silyl and N-Boc protection was carried out on the candidate substrates, and this could be achieved in good yields. A series of conditions were then screened on both of these substrate classes, however, none of the desired product was observed under the established hydrogenation conditions. Higher catalyst loadings, or raised temperature only resulted in the deprotection of **2-100** and **2-101**. The more polar solvent DCM was investigated to avoid any
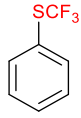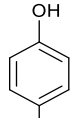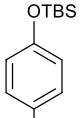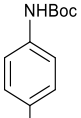
possible insoluble intermediates due to the SF$_5$ group, however rhodium nanoparticles did not form in DCM solution.

	Conditions	2-97	2-99	2-100	2-101
a	400 mg 4 Å MS. 2ml hexane per mmol 0.2 mol% cat	NA	NA	NA	NA
b	400 mg 4 Å silica. 2ml hexane per mmol 0.2 mol% cat	NA	NA	NA	NA
c	1 g 4 Å MS. 14 ml hexane per mmol 0.2 mol% cat	NA	NA	Decomp.	Decomp.
d	1 g silica 14 ml hexane per mmol 0.2 mol% cat	NA	NA	Decomp.	Decomp.
e	400 mg 4 Å ms. 2 ml hexane per mmol 2% mol cat	NA	NA	Decomp.	Decomp.
f	400 mg silica, 2 ml hexane per mmol 2 % mol cat	NA	NA	Decomp.	Decomp.
g	400 mg silica. 2ml DCM per mmol 0.2 mol% ca	NA	NA	NA	NA
h	400 mg silica. 2ml hexane per mmol 0.2 mol% cat 50 °C	NA	NA	Decomp.	Decomp.

Aa* NA= Starting material recovered

Table 2-1 Condition explored for the hydrogenation of SF$_5$– phenyl derivatives.

Aryl trifluoromethyl thioether (-SCF$_3$) substrates were also explored, however a more complicated outcome was observed. Under mild hydrogenation conditions, starting material was recovered. Increasing the catalyst loading led to either the decomposition of the SCF$_3$ group or deprotection of N-Boc/O-silyl groups. There was only one set of conditions for **2-105**, where there was a trace of an aliphatic product observed, and this was after one week (7 days) of hydrogenation (** in Table 2-2).

	Conditions	SCF$_3$ (2-102)	OH / SCF$_3$ (2-103)	OTBS / SCF$_3$ (2-104)	NHBoc / SCF$_3$ (2-105)
a	400 mg 4 Å MS. 2ml hexane per mmol 0.2 mol% cat	NA	NA	NA	NA
b	400 mg silica 2ml hexane per mmol 0.2 mol% cat	NA	NA	NA	NA
c	1 g 4 Å MS. 14 ml hexane per mmol 0.2 mol% cat	NA	NA	Partial Decomp.	Partial Decomp.
d	1 g silica 14 ml hexane per mmol 0.2 mol% cat	NA	NA	Decomp.	Decomp.
e	400 mg 4 Å ms. 2 ml hexane per mmol 2% mol cat	NA	NA	Decomp.	Decomp.
f	400 mg silica, 2 ml hexane per mmol 2 % mol cat	NA	NA	Decomp.	Decomp.
g	400 mg silica. 2ml DCM per mmol 0.2 mol% ca	Decomp.	Decomp.	Decomp.	Decomp.
h	400 mg 4A sillica. 2ml hexane per mmol 0.2 mol% cat 50 °C 3 day	Decomp.	NA	Decomp.	Decomp. **trace product.

Aa* NA= Starting material recovered

Table 2-2 Condition of the hydrogenation of the –SCF$_3$ phenyl derivatives.

The unsuccessful screening of SCF$_3$ substituted phenyl derivatives is likely due the potential coordination of sulfur with the rhodium metal. Another possible reason of inactivity is the Lewis basicity of the sulfide group which forms adducts with Lewis acid in the hydrogenation reaction. [50]

There are perhaps several behind the unsuccessful hydrogenation of SF$_5$ substituted phenyl derivatives. One is the steric-electric bulkiness of the SF$_5$ preventing the aryl ring from associating with the catalyst. Another is the exceptional electron-withdrawing effect of the SF$_5$ (σ_p=0.68) which may reduce the electron density of the π system and caused low reactivity. [54]

2.4 Conclusion

In conclusion, aryl hydrogenation reactions with the CAAC catalyst **[Rh]** generated (trifluoromethyl)cyclohexyl and (trifluoromethoxy)cyclohexyl motifs with good *cis*-stereoselectivity and generally in high conversions. The hydrogenation reaction worked also

on sterically bulky and electron deficient substrates and afforded highly stereoselective all-*cis* trifluoromethyl cyclohexanes. The motifs that were synthesised here offer interesting compounds for further studies in physical organic chemistry, medicinal chemistry and may have applications in surface science.

During the course of this work, Zeng's lab published the hydrogenation of aryl-CF$_3$ substrates to cyclohexanes, including many of the examples explored here. The disclosure undermined the novelty of this work for publication.[55] So, at that point, a focus was placed on the preparation of tetrakis- and hexakis- trifluoromethyl cyclohexanes, discussed in the next Chapter.

2.5 References

1. M. P. Wiesenfeldt, T. Knecht, C. Schlepphorst and F. Glorius, *Angew. Chem. Int. Ed.*, 2018, **57**, 8297-8300.

2. K. Müller, C. Faeh and F. Diederich, *Science*, 2007, **317**, 1881-1886.

3. K. L. Kirk, *Org. Process Res. Dev.*, 2008, **12**, 305-321.

4. M. Hird, *Chem. Soc. Rev.*, 2007, **36**, 2070-2095.

5. N. A. Meanwell, *J. Med. Chem.*, 2018, **61**, 5822-5880.

6. A. Rivkin, K. Biswas, T.-C. Chou and S. J. Danishefsky, *Org. Lett.,* 2002, **4**, 4081-4084.

7. A. Rivkin, T.-C. Chou and S. J. Danishefsky, *Angew. Chem. Int. Ed.*, 2005, **44**, 2838-2850.

8. R. D. Chambers, *Fluorine in organic chemistry*, Blackwell Pub., Oxford, 2004.

9. K. Uneyama, *Organofluorine Chemistry*, Blackwell Pub., Oxford, UK, 2006.

10. C. Ni and J. Hu, *Chem. Soc. Rev.*, 2016, **45**, 5441-5454.

11. T. Liang, C. N. Neumann and T. Ritter, *Angew. Chem. Int. Ed.*, 2013, **52**, 8214-8264.

12. P. Kirsch, *Modern Fluoroorganic Chemistry: Synthesis, Reactivity, Applications*, Wiley-VCH, 2013.

13. X. Liu, C. Xu, M. Wang and Q. Liu, *Chem Rev*, 2015, **115**, 683-730.

14. J.-A. Ma and D. Cahard, *J. Fluor. Chem.*, 2007, **128**, 975-996.

15. M. Zhou, C. Ni, Y. Zeng and J. Hu, *J. Am. Chem. Soc.*, 2018, **140**, 6801-6805.

16. T. Nishimine, H. Taira, E. Tokunaga, M. Shiro and N. Shibata, *Angew. Chem. Int. Ed.*, 2016, **55**, 359-363.

17. Q.-Y. Chen and S.-W. Wu, *Chem. Commun.*, 1989, 705-706.

18. J. Charpentier, N. Früh and A. Togni, *Chem. Rev.*, 2015, **115**, 650-682.

19. S. Barata-Vallejo, B. Lantaño and A. Postigo, *Chem. - Eur. J.*, 2014, **20**, 16806-16829.

20. F. Swarts, *Bull. Acad. Roy. Belg.*, 1892, **24**, 474.

21. V. C. R. McLoughlin and J. Thrower, *Tetrahedron*, 1969, **25**, 5921-5940.

22. Y. Kobayashi and I. Kumadaki, *Tetrahedron Lett.*, 1969, **10**, 4095-4096.

23. W. R. Hasek, W. C. Smith and V. A. Engelhardt, *J. Am. Chem. Soc.*, 1960, **82**, 543-551.

24. E. W. Della, *J. Am. Chem. Soc.*, 1967, **89**, 5221-5224.

25. D. Naumann, B. Wilkes and J. Kischkewitz, *J. Fluor. Chem.*, 1985, **30**, 73-87.

26. A. N. Alexeenko and V. P. Nazaretian, *J. Fluor. Chem.*, 1994, **69**, 241-247.

27. J.-A. Ma and D. Cahard, *Chem. Rev.*, 2004, **104**, 6119-6146.

28. V. Bizet, T. Besset, J. A. Ma and D. Cahard, *Curr. Top. Med. Chem.*, 2014, **14**, 901-940.

29. X. Yang, T. Wu, R. J. Phipps and F. D. Toste, *Chem. Rev.*, 2015, **115**, 826-870.

30. D. Collins, R. Stephens and J. C. Tatlow, *J. Fluor. Chem.*, 1986, **32**, 213-227.

31. Y. Carcenac, M. Tordeux, C. Wakselman and P. Diter, *J. Fluor. Chem.*, 2005, **126**, 1347-1355.

32. O. Takashi, F. Mayumi and M. Keiji, *Chem. Lett.*, 1998, **27**, 817-818.

33. C. Semisch and P. Margaretha, *Helv. Chim. Acta*, 1984, **67**, 664-668.

34. G.-D. Zhu, M. A. Staeger and S. A. Boyd, *Org. Lett.*, 2000, **2**, 3345-3348.

35. A. N. B. I. M. Zalesskaya, E. P. Saenko, Y. A. Eialkov, L. M. Yagupolskii, *Zhur. Org. Khim.* , 1980, **16**, 1194-1202.

36. A. N. Alekseenko, K. Denis, O. Lukin, P. K. Mykhailiuk, O. V. Shishkin and Y. M. Pustovit, *Synthesis*, 2012, **44**, 2739-2742.

37. A. Lefranc, Z.-W. Qu, S. Grimme and M. Oestreich, *Chem. - Eur. J.*, 2016, **22**, 10009-10016.

38. M. Fang, N. Machalaba and R. A. Sánchez-Delgado, *Dalton Trans.*, 2011, **40**, 10621-10632.

39. B. Y. Kara, B. Kılbaş and H. Göksu, *New J. Chem.*, 2016, **40**, 9550-9555.

40. Y. Carcenac, P. Diter, C. Wakselman and M. Tordeux, *Magn. Reson. Chem.*, 2006, **44**, 617-623.

41. Y. Carcenac, P. Diter, C. Wakselman and M. Tordeux, *New J. Chem.*, 2006, **30**, 442-446.

42. Y. Carcenac, M. Tordeux, C. Wakselman and P. Diter, *New J. Chem.*, 2006, **30**, 447-457.

43. E. L. Eliel and T. J. Brett, *J. Am. Chem. Soc.*, 1965, **87**, 5039-5043.

44. A. Tlili, F. Toulgoat and T. Billard, *Angew. Chem. Int. Ed.*, 2016, **55**, 11726-11735.

45. H. Ge, H. Liu and Q. Shen, in *Organofluorine Chemistry*, 2021, pp. 99-172.

46. J.-F. Sauvage, R. H. Baker and A. S. Hussey, *J. Am. Chem. Soc.*, 1960, **82**, 6090-6095.

47. M. P. Wiesenfeldt, Z. Nairoukh, W. Li and F. Glorius, *Science*, 2017, **357**, 908-912.

48. D. Moock, M. P. Wiesenfeldt, M. Freitag, S. Muratsugu, S. Ikemoto, R. Knitsch, J. Schneidewind, W. Baumann, A. H. Schäfer, A. Timmer, M. Tada, M. R. Hansen and F. Glorius, *ACS Catal.*, 2020, **10**, 6309-6317.

49. T. Wagener, A. Heusler, Z. Nairoukh, K. Bergander, C. G. Daniliuc and F. Glorius, *ACS Catal.*, 2020, **10**, 12052-12057.

50. Y. Wei, B. Rao, X. Cong and X. Zeng, *J. Am. Chem. Soc.*, 2015, **137**, 9250-9253.

51. E. Castagnetti and M. Schlosser, *Chem. - Eur. J.*, 2002, **8**, 799-804.

52. N. Vida, T. Pastýříková, B. Klepetářová and P. Beier, *J. Org. Chem.*, 2014, **79**, 8906-8911.

53. G. Haufe, *Tetrahedron*, 2022, **109**, 132656.

54. J. M. W. Chan, *Journal of Materials Chemistry C*, 2019, **7**, 12822-12834.

55. X. Zhang, L. Ling, M. Luo and X. Zeng, *Angew. Chem. Int. Ed.*, 2019, **58**, 16785-16789.

Chapter 3. Janus face all-*cis* 1,2,4,5-tetrakis(trifluoromethyl)- and all-*cis* 1,2,3,4,5,6-hexakis(trifluoromethyl)- cyclohexanes

3.1 Introduction

It is aesthetically pleasing to consider the preparation of cyclohexanes with six identical substituents on each of the six carbons. Such analogues have nine configurational isomers and there are 13 conformational isomers in total.[1, 2] Among all of these possible isomers, a special situation draws attention, and that is when all six substituent groups have an all *cis* configuration, alternatively known as the all-*syn* stereochemistry. Those isomers have equivalent chair conformers on inter-conversion, and among all of the other isomers, they are highest in energy, due to the threefold 1,3-steric repulsions between three axial groups.

Only a small number of all-*cis* hexa substituted cyclohexanes have previously been synthesised and studied. These are the hexa-hydroxy **3-5** and its corresponding hexa-acetate **3-6** and then hexa-benzoyl ester **3-7**.[3] The hexakis-carboxylic acid **3-2** and its corresponding hexa-methyl **3-3** and hexa-benzoyl esters **3-4** have also been prepared. [4, 5]Finally, the hexa-methyl **3-1**[6] and most recently the hexafluoro-cyclohexane **3-8**[7] have been prepared and their X-ray structures recorded. Other all-*syn* hexa-halogenated cyclohexanes have only been reported in computational studies,[1, 2] although there is a special case in this general class of compounds with lindane **3-9**, which is a hexa-chlorocyclohexane, that has been produced on a tonne scale from the direct chlorination of benzene, as an insecticide, but is now discontinued.[8]
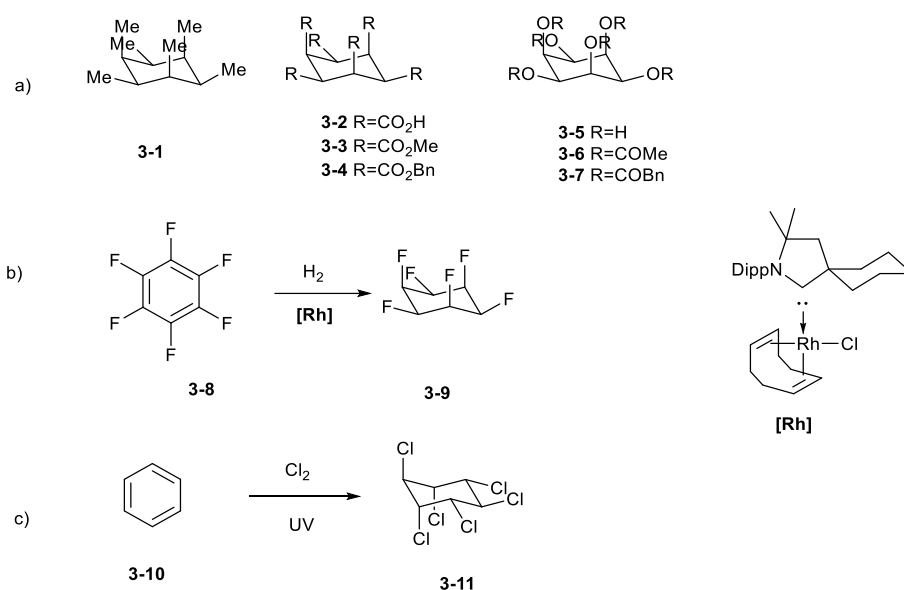
Figure 3-1 (a) Previous examples of all-*syn*-hexa-substituted cyclohexanes; (b) catalytical synthesis of

novel Janus face all-*syn*-hexafluorocyclohexane;(c) synthesis of the insecticide lindane.

3.2 Aims and objective

As discussed in the introduction, it became interesting to synthesis cyclohexane with multiple

CF_3 groups, especially as the all-*syn* hexakis isomer would be the most sterically demanding

of the all-*syn* series so far. This isomer would be predicted to have Janus face polar properties.

The relatively large –CF_3 groups would generate a larger negatively polarised face compared

to hexafluorocyclohexane **3-9**. The preparation of this analogue could be addressed by aryl

hydrogenation of CF_3-hexakis benzene **3-22** using Zeng's RhCAAC catalyst **[Rh]**, although it

was anticipated that it may be difficult to achieve aryl hydrogenation due to the steric impact

of the –CF_3 groups. In order to support this approach, computational and simulation methods

were applied to analyse the properties of the resultant cyclohexanes and to assess if a

synthetic approach would be plausible.

3.3 Results and discussion

3.3.1 All-*cis-* tris and tetrakis CF$_3$ cyclohexanes

The all-*cis*-1,3,5-tris(trifluoromethyl) cyclohexane **3-13** and all-*cis*-tetrakis(trifluoromethyl) cyclohexane **3-15** were prepared following Zeng's aryl hydrogenation method using Zeng's catalyst. The reactions proved to be straightforward and generated the desired products without much difficulty as summarised in Scheme 3-1.
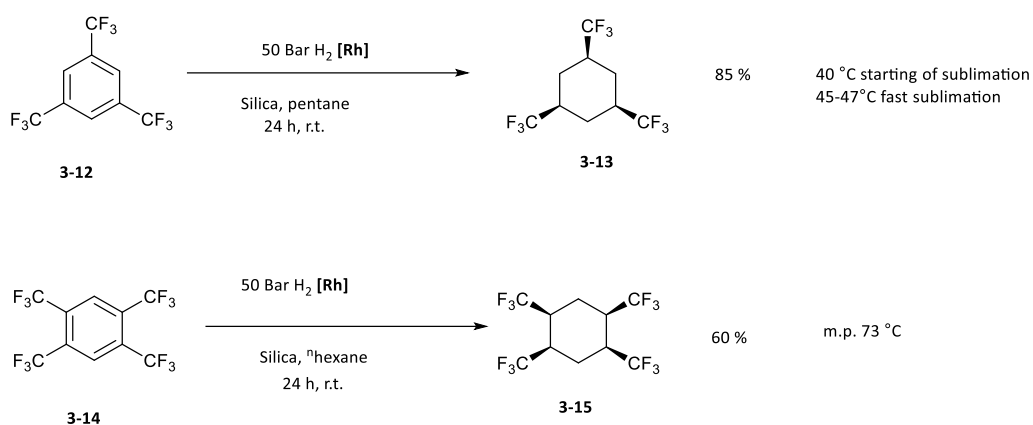

Scheme 3-1 Synthesis of trifluorocyclohexanes **3-13** and **3-15**.

The synthesis of cyclohexane **3-13** was achieved in an 85 % yield and cyclohexane **3-15** was recovered in a 60 % yield and each are crystalline compounds. Cyclohexane **3-13** behaves as a highly crystalline material, which refines its structure in a sealed container equilibrating between the gas and solid phase over time. It continually changes its form in the sealed tube. Cyclohexane **3-13** has a predominantly equatorial –CF$_3$ conformation with a highly shielded ^{19}F NMR shift of δ -72.3 ppm.
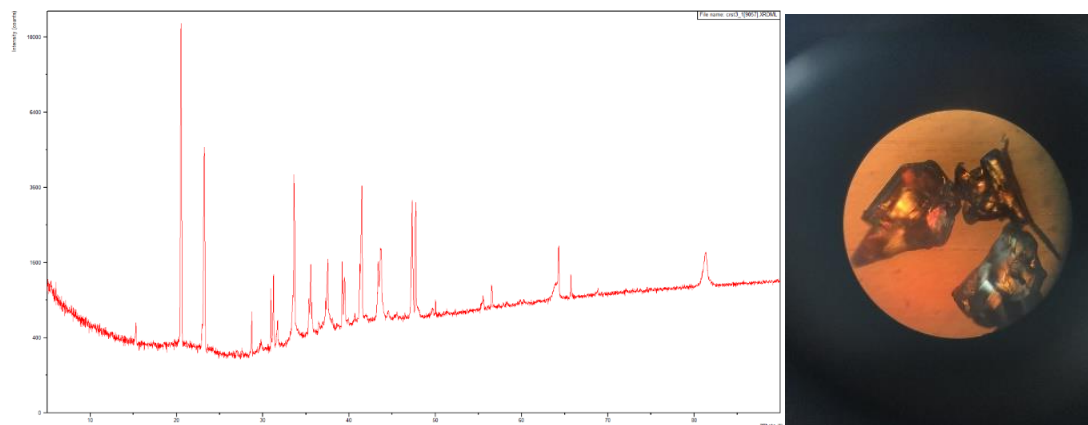
Figure 3-2 The X-ray powder diffraction spectrum **of 3-13** and image of a crystal of **3-13**.

Interestingly given the high quality of the crystalline material, a single crystal X-ray structure could not be resolved. This difficulty is very likely caused by the low barrier of rotation along the packing axis. On the other hand, a single crystal X-ray structure of tetrakis CF_3–cyclohexane **3-15** was determined successfully as shown below.
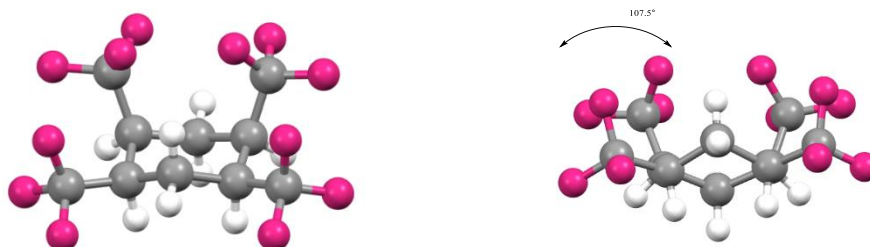

Figure 3-3 *The* single crystal structure of **3-15**.

An image of the solid-state structure of **3-15** is shown in Figure 3-3. The structure shows a near classical chair conformation for the cyclohexane with two 1,3 di-axial and two 1,3-di-equatorial CF_3 groups. The steric and electrostatic repulsion of the di-axial CF_3 groups is obvious in the large angle of 107.5° associated with the 1,3-diaxial splay (CF_3^{ax} –C–C –CF_3^{ax}), and angle which differs significantly from cyclohexane itself at 90°.

A variable temperature (VT) $^{19}F\{^{1}H\}$ - NMR of **3-15** was recorded (Figure 3-4). The –CF_3 groups

show an equivalence in chemical shift at room temperature, which suggest rapid ring inversion on the NMR relaxation time scale. However, at the lower temperature of -75 °C, ring inversion is slowed down sufficiently to distinguish the axial and equatorial –CF$_3$ groups, consistent with the X-ray structure (Figure 3-3). [9-11]
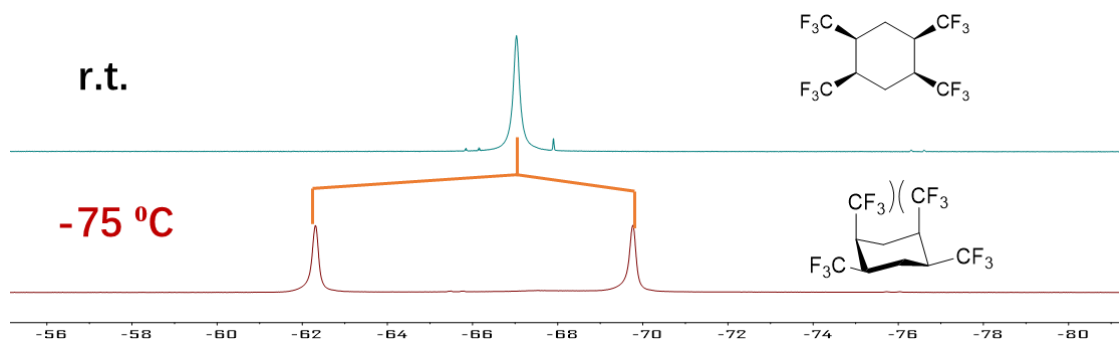
Figure 3-4 ^{19}F{^{1}H}- NMR of **3-15** at r.t. and at -75 °C.

A stepwise VT NMR was then carried out at 4 °C intervals and an Eyring plot analysis of the chemical shift non-equivalence was plotted. The coalescence temperature was not determined due to the complicated NMR pattern near coalescence. The barrier to ring interconversion was calculated to have a ΔG of ≈ 10.3 kcalmol^{-1}, which was unexpectedly lower than the classical barrier for cyclohexane interconversion (≈ 11 kcal mol^{-1}). Although unexpected, this may be due to a higher energy ground state relative to the highest point in the energy profile, relative to cyclohexane. [12, 13.]

$$\ln\frac{k}{T} = \frac{-\Delta H^\ddagger}{R}\left(\frac{1}{T}\right) + \ln\frac{\kappa k_\mathrm{B}}{h} + \frac{\Delta S^\ddagger}{R}$$

Equation 3-1 The Eyring equation

In the Eyring plot a reciprocal parameter was involved. The ln(k/T) was plotted vs. $1/T$ to evaluate the ΔH from the slope and ΔS value from the intercept. As the intercept is where $1/T$ = 0 or T = ∞, therefore the value of the entropy is unreliable.[14] Literature statistical analysis of Eyring equation argues that the standard errors of ΔH and ΔS in the least-squares analysis

is not accurate. This underlying reason is that the temperature range of the measurement is only a small fraction of the actual absolute temperature.[15]

The unusual off-centre coalescence (by 3 ppm) of the axial and equatorial −CF$_3$ signals from ^{19}F{^{1}H} NMR during the variable temperature experiment scale is conspicuous. This asymmetry suggests the presence of a minor high energy conformer with a significant population, contributing to the signal in the low temperature NMR solution. It was concluded that this is most likely to be a relatively stable interconverting "twist boat" conformer. This was investigated by computation.
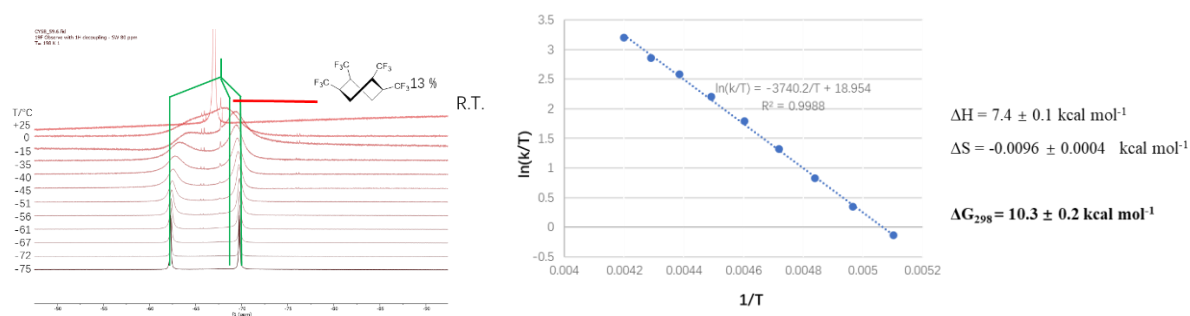
Figure 3-5 the variable temperature VT-^{19}F{^{1}H} NMR spectrum of **3-15** and the corresponding Eyring plot.

A DFT (B3LYP-D3) computational analysis was carried out to establish the energy barriers along the ring interconversion process of **3-15**. Specifically, to investigate the unexpectedly low energy observed in the Eyring plot Figure 3-5. This work was carried out by Professor Michael Buehl of the School of Chemistry, University of St Andrews. The DFT calculations indicated that the barrier to ring interconversion is about 12 kcal mol^{-1}, which is consistent with the sterically demanding -CF$_3$ groups. Computation also identified that the "twist boat" conformation has an energy (1.1 kcal mol^{-1}) only slightly higher than the ground state "chair" conformation (0 kcal mol^{-1}).
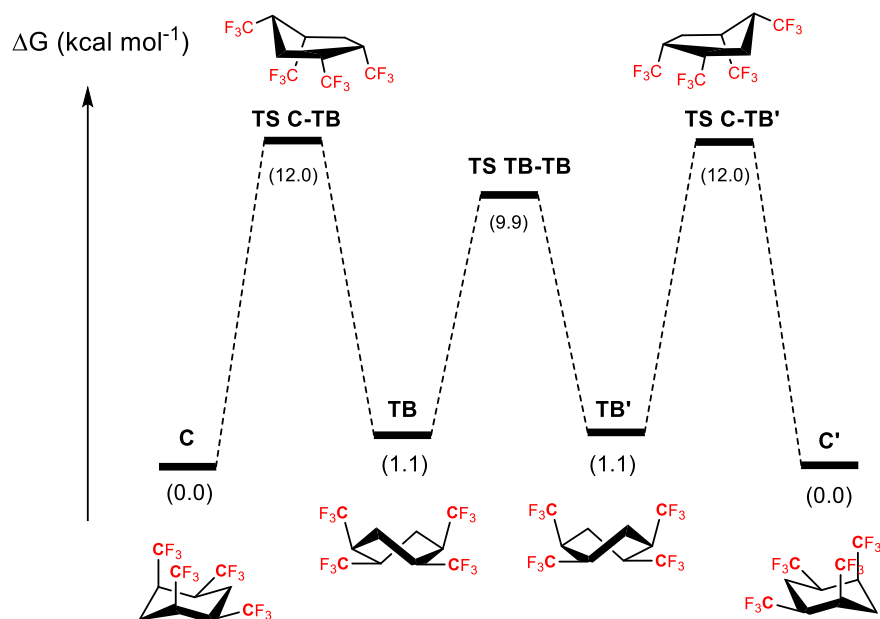
Figure 3-6 DFT (B3LYP-D3/3–311+G**/CPCM(CH2Cl2)//B3LYP-D3/6-31G* level) computed profile of the relative energy of intermediates for the ring interconversion of **3-15**.

This small energy difference estimates that there will be 13.5 % population of "twist boat" in solution and that it will make a significant contribution to the ^{19}F-NMR spectrum in solution under ambient conditions, as was observed in the VT-NMR study. The observation of a relatively large population of "twist boat" conformer of 1,2,4,5-tetrakis(trifluoromethyl)cyclohexane **3-15** is also consistent with other sterically demanding substituents on cyclohexane. For example 1,2,4,5-tetrakis(isopropyl)cyclohexane **3-16** has a *more stable* twist boat conformation than its chair conformer.[13]

The computational experiments suggest that the ring flip process of **3-15** is not an elementary process, which might complicate the measurement in VT study.[16] The presence of relatively large population of twisted boat form of **3-15** at cryogenic temperature with similar relative energy level of chair forms of **3-15** contributes into the exchange of signal and the simulated relaxation rate. Those factors could potential effected the NMR kinetic measurement which is differed from expected value.
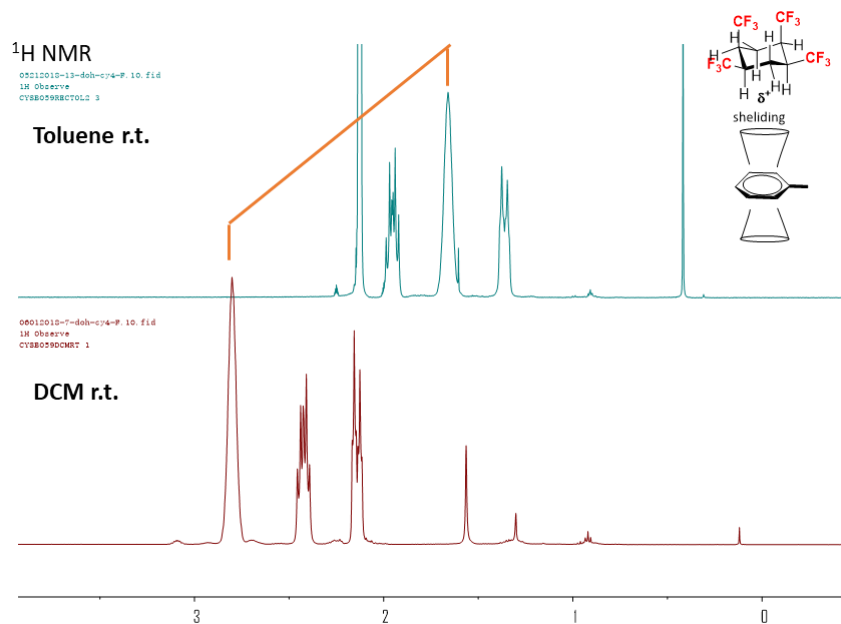
Figure 3-7 Comparison of ¹H-NMR of cyclohexane **3-15** *in d₂-DCM and d₈-toluene*.

¹H NMR experiments in various solvents were carried out on cyclohexane **3-15** in order to analyse the π shielding effect on the cyclohexane ring. ¹H-NMR shifts were recorded in d_2-DCM and d_8-toluene. Comparative ¹H-NMR spectra show a relative 0.6 ppm downfield shift of the H_{ax} protons in toluene and the CH_2 hydrogens signals coalesced with a downfield shift of 1.2 ppm. These downfield shifts are evidence of an interaction between the electropositive face of the cyclohexane ring of **3-15** and the π-face of toluene, which induces an anisotropy of the local magnetic field due to the aromatic ring current.

3.3.2 All-*cis* hexakis-CF₃ cyclohexane

After the preparation of cyclohexane **3-15** by direct hydrogenation in satisfactory yield, it became an objective to prepare the all-*cis*-hexakis-(CF₃) cyclohexane **3-30**. It follows that this will involve the direct aryl hydrogenation of the hexakis CF₃ benzene **3-26** as the more promising approach, although there was a concern regarding success given that there are so many sterically bulky CF₃ groups. At the outset the first challenge however was to prepare hexakis CF₃ benzene **3-26**, the required substrate for direct hydrogenation. One approach

81

envisaged a trimerization of hexafluorobut-2-yne **3-20** to generate **3-26**. Hexafluorobut-2-yne **3-20** has previously been prepared.[17]
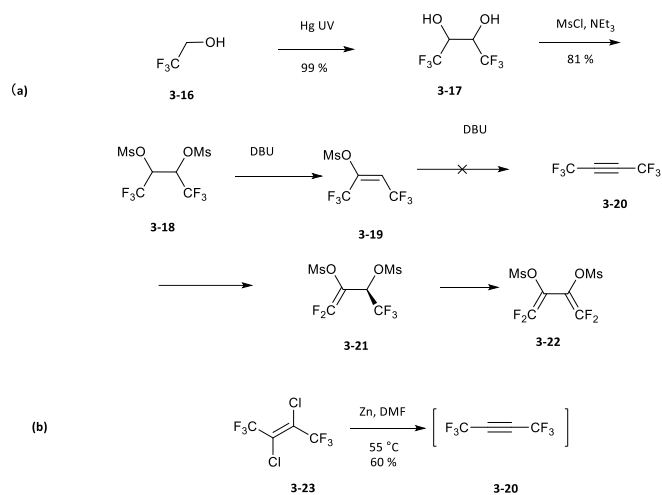
**Scheme 3-2** Synthesis of hexafluorobut-2-yne **3-20**.[17]

In the first approach the dimesylated derivative **3-18**, which is prepared from the mesylation of 1,1,1,4,4,4-hexafluoro-butan-1,2-diol **3-17,** was treated with base. A significant intensity for a geminal CF_2 alkene was observed by ^{19}F NMR at -86 ppm as the major product,[18] however there was no indication that the desired acetylene had formed.

In a second approach, commercially available 2,3-dicholoro perfluoro-but-2-ene **3-23** was treated with freshly activated zinc. The reaction provided a 60 % conversion to the desired acetylene **3-20** as evidenced by a signal in the ^{19}F-NMR spectrum at -55 ppm. This value is in agreement with the literature.[19] An argon flow was passed through the reaction mixture to carry **3-20** into a reaction flask equipped with dry ice/acetone cooled condenser for the trimerisation reaction.
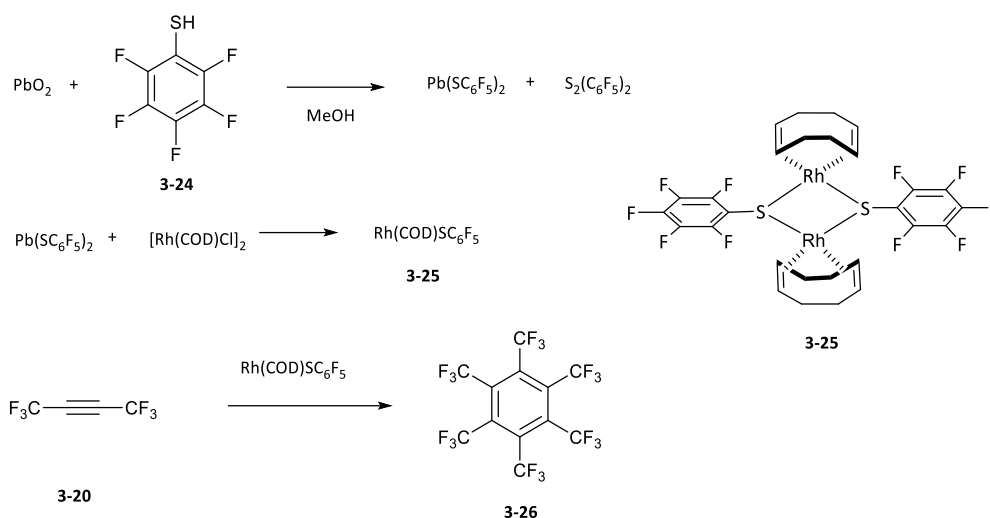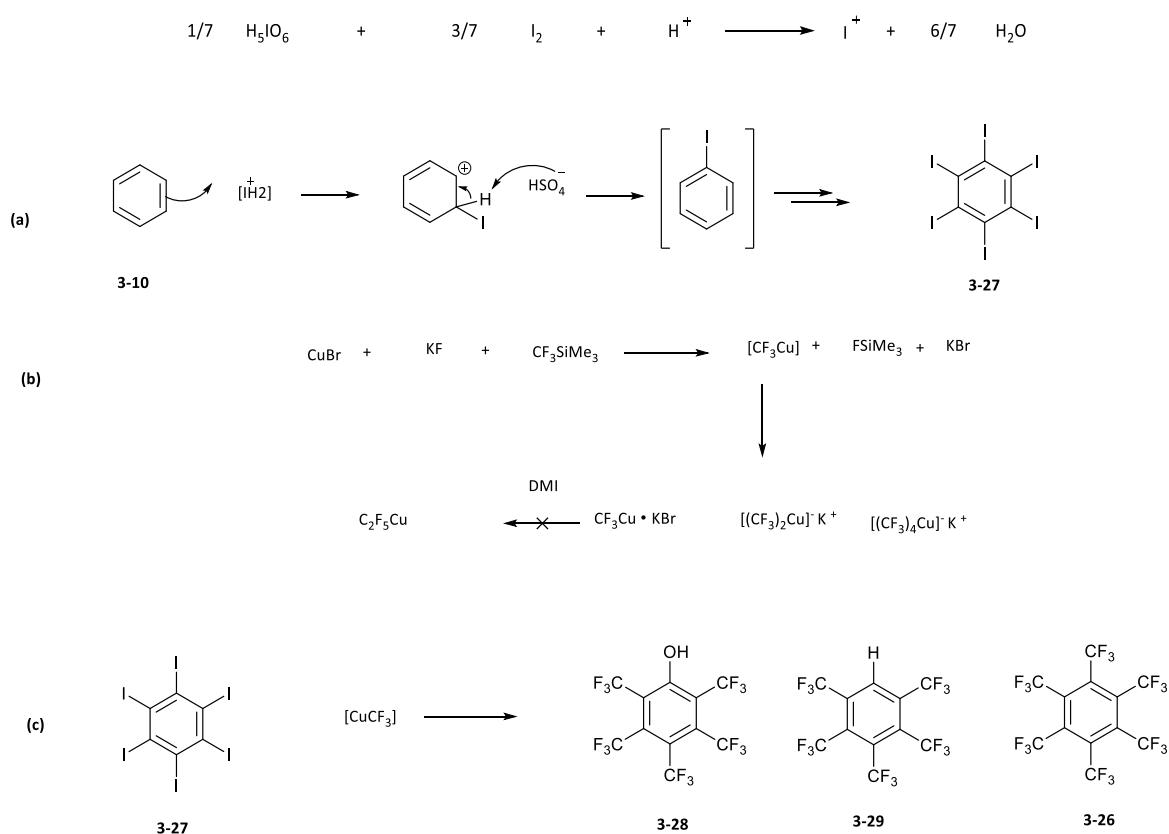
Scheme 3-3 Cyclisation synthesis of hexakis-CF₃-benzene **3-26**.

A Rh pentafluorosulfide catalyst was prepared for the catalytic trimerisation of **3-20** described in literature.[20] Accordingly lead oxide was converted to lead pentafluorophenylsulfide[21] and the resultant lead pentafluorosulfide was converted to the cyclooctadiene complex **3-25**.[22] The hexafluoro-but-2-yne that was prepared earlier was submitted to trimerisation in a benzene solution under argon. However, only a trace of the product was observed in the reaction mixture by ^{19}F NMR. The product proved difficult to separate from the reaction, particularly from unreacted hexafluoro-2,3-dichloro-but-ene and DMF. The volatile nature of the desired product **3-26** to sublimation further reduced the amount of available product. Only 20 mg of **3-26** and with the presence of trace DMF was obtained by this protocol starting from 1.4 g of **3-23**.
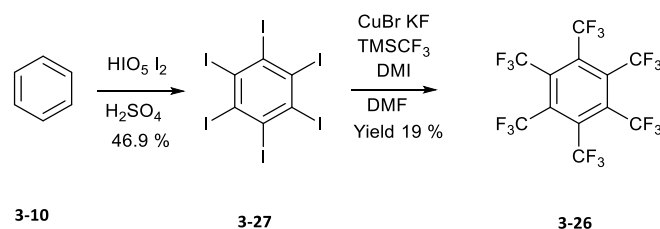
Scheme 3-4 Synthesis of hexakis-CF₃ benzene **3-26**.

83

An alternative synthesis approach was explored applying a literature method to prepare **3-26**.[23] This involved exhaustive copper mediated trifluoromethylation of per-halogenated benzene. Hexabromo-benzene is commercially available and was explored initially in a per-trifluoromethylation reaction. In the event, trifluoromethylation was sluggish and the reaction did not yield the fully trifluoromethylated product. Only pentakis-CF$_3$ benzene derivatives were identified by ^{19}F NMR after reaction work up. This is perhaps due to the poor reactivity of the hexabromobenzene with CuCF$_3$ particularly as trifluoromethylation progresses. In an effort to increase reactivity hexa-iodobenzene was prepared. This was achieved by periodination of benzene with iodine and periodic acid in concentrated sulfuric acid via electrophilic aromatic substitution.[24]


Scheme 3-5 Synthesis of hexaiodobenzene and trifluoromethylation of hexakis-CF$_3$ benzene **3-26**.

The resultant periodinated benzene was isolated in 41% yield after recrystallisation. It was then submitted to the copper mediated per-trifluoromethylation reaction. For these

reactions the CuCF$_3$ was generated *in situ* and monitored by ^{19}F{^{1}H}-NMR.[25] 1,3-Dimethyl-2-imidazolidinone (DMI) was used instead of N-methyl-2-pyrrolidone (NMP) as a solvent to better stabilise the CF$_3$Cu from forming difluorocarbene and by extension CuC$_2$F$_5$. In the event the trifluoromethylation reaction delivered aromatic products in a 1:2:1 ratio and these were separated by recrystallisation and then sublimation to yield the desired product **3-26**. 100 mg of **3-26** was isolated in a 20 % yield.

The resultant hexakis-CF$_3$ benzene was submitted to hydrogenation under a range of conditions to explore efficiency. The first reactions used Yagupolski's method[26] for the direct hydrogenation with a platinum catalyst in TFA, however only starting material was recovered after the reaction (Scheme 3-6 a).

Under Rh(CAAC)(COD) catalysed conditions, various solvents were tested. A reaction in hexane suffered from relatively poor solubility of the substrate, which adsorbed onto silica during the reaction. Reactions in DCM, THF and diethyl ether suffered in preventing the formation of the required active rhodium nanoparticles.
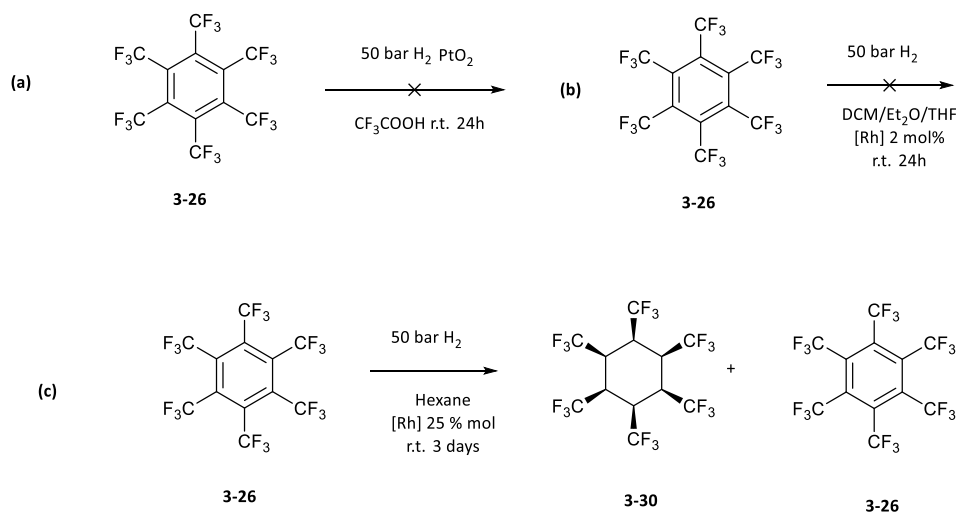

Scheme 3-6 Approaches to aryl hydrogenation of hexakis-CF$_3$ benzene.

In the extended reaction time of the hydrogenation method using Zeng's **[Rh]** catalyst, only a

trace of a product was apparent in the ^{1}H{^{19}F} NMR and the ^{1}H-^{19}F HMBC NMR spectra. As shown in Figure 3-8, the two broad signals were observed at 2.8 and 3.6 ppm. The two broad signals become resolved after ^{19}F decoupling in the–CF$_3$ region (-55 to -75 ppm). The two triplets couple to each other with a typical gauche $^3J_{\text{H-H}}$ coupling constant of 5.24 Hz which is evidence of the presence of cyclohexane **3-30**.
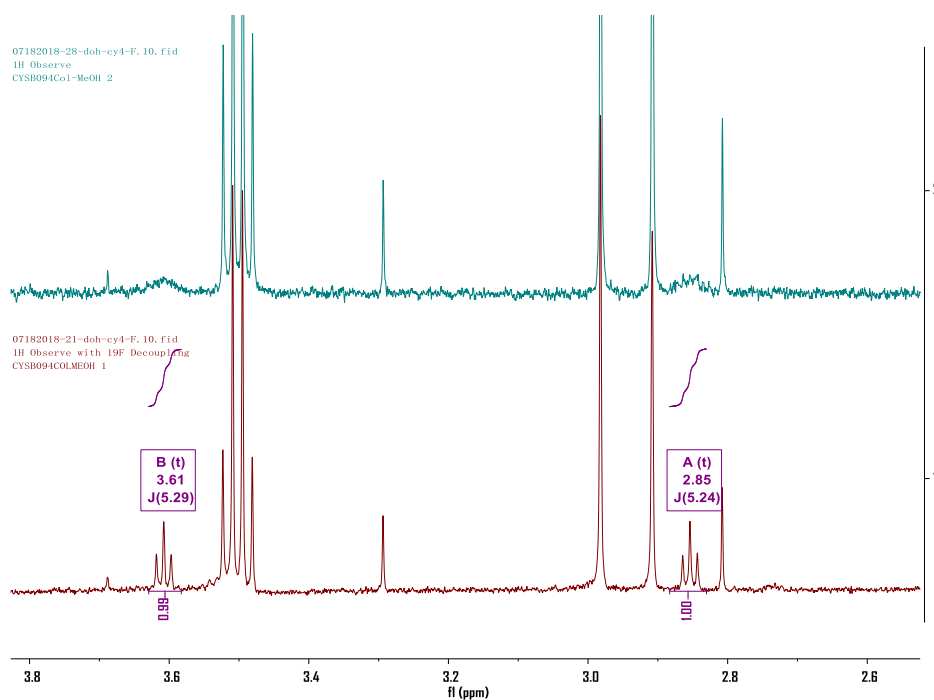

Figure 3-8 The ^{1}H-NMR (upper trace) and ^{1}H{^{19}F}-NMR (lower trace) after aryl hydrogenation of **3-26**.

The conversion to product under these reaction conditions was less than 5 %, therefore the reaction required to be pushed to a higher conversion. Accordingly, the reaction was heated to 50°C and was monitored by ^{19}F-NMR. This resulted in conversion to the required product of about 10 % over a week in the autoclave, and there was a full consumption of starting material after a 3-week period (Scheme 3-7). The purification of the product proved challenging as **3-30** is not UV active and it is inert from TLC stains due to the lack of reactivity from the electron withdrawing trifluoromethyl groups. Purification was carried out by carefully flush column chromatography using pentane and diethyl ether as eluents, and followed then by DCM, monitoring fractions continuously by ^{19}F NMR.
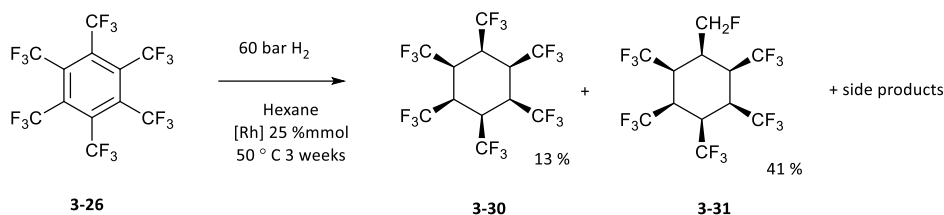
Scheme 3-7 Aryl hydrogenation of **3-23** gave cyclohexanes **3-30** and **3-21**.

A major product was isolated in 41 % yield. The structure was solved by NMR analysis and ultimately by X-ray crystallography. Unexpectedly it contained only five CF_3 groups along with one CFH_2 group. All substituents retained the *cis* stereochemistry despite one $-CF_3$ group suffering from a hydrodefluorination reaction. The ^{19}F NMR of **3-31** shows four distinct peaks, with an upfield CFH_2 fluoromethyl peak at over -200 ppm, an axial CF_3 peak downfield at -59 ppm, and two equatorial CF_3 groups in two environments around -65 ppm. The integration of the fluorinated group in a ratio of 1:2:2:1 for CFH_2: $_{ax}CF_3$: $_{eq}CF_3$: $_{eq}CF_3'$ is consistent with the proposed structure of the product **3-31**. The three CF_3 groups adopting an equatorial position suggests that the fluoromethyl group is pointing axial under ambient conditions.
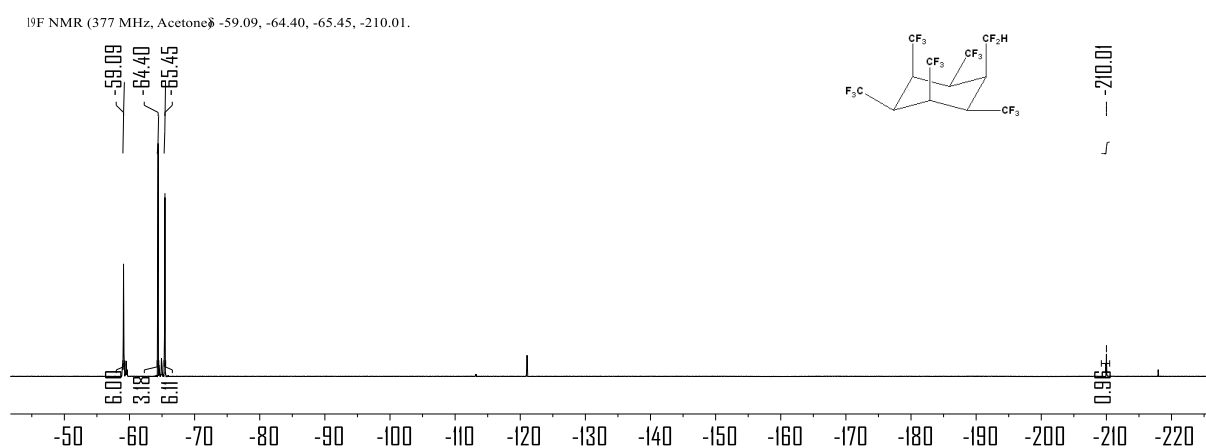
Figure 3-9 ^{19}F NMR of cyclohexane **3-31**.

The ^1H NMR and $^1H\{^{19}F\}$ NMR of the product also corresponds well with the structure of **3-31** with two fluoromethyl protons, two equatorial and three axial protons in two environments,

and one equatorial proton coupled to four protons. In the ^{1}H$\{^{19}$F$\}$ NMR, with ^{19}F decoupling in –CF$_3$ region, the ^{1}H peaks showed a coupling constant around 5 Hz as shown in Figure 3-10. The absence of any large antiperiplanar coupling is consistent too with the all-*cis* configuration of the major product.
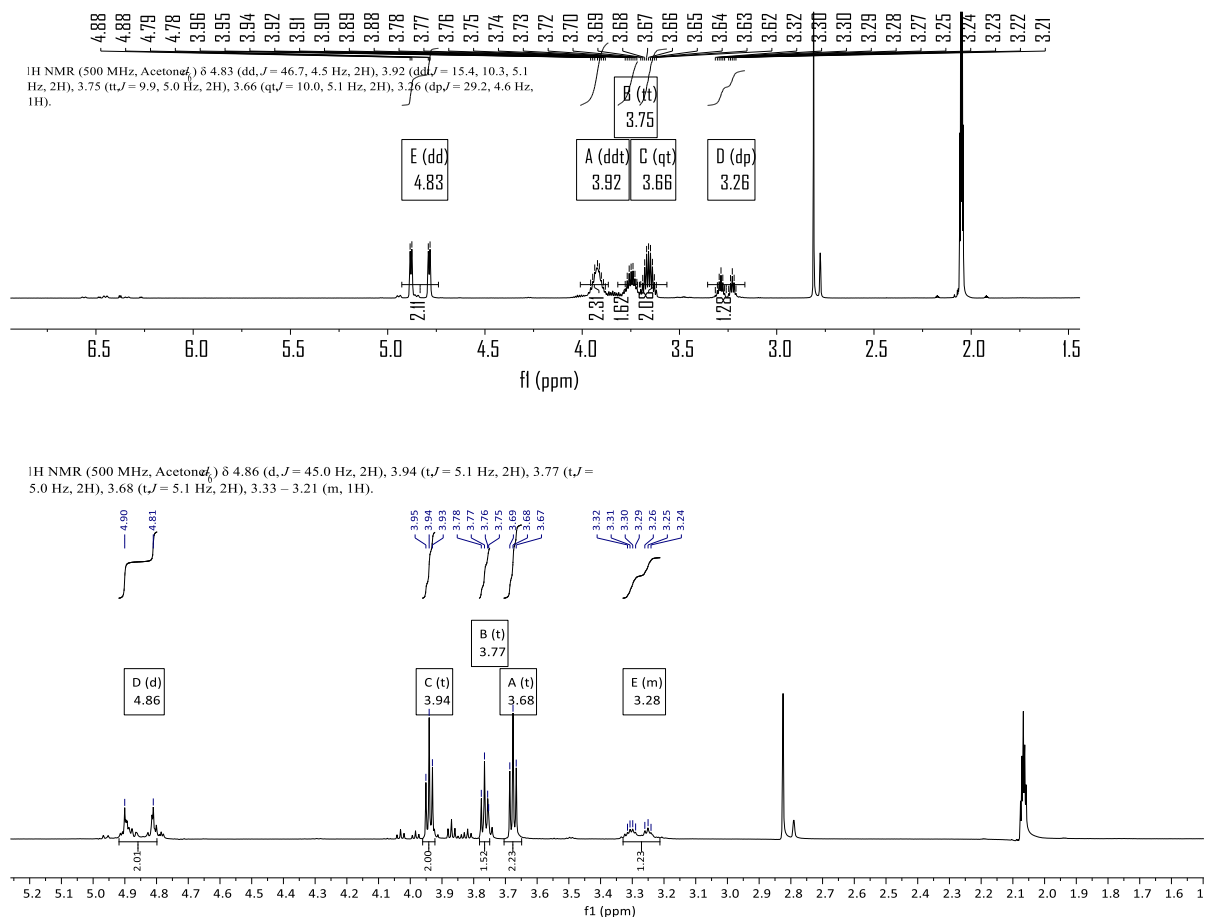
Figure 3-10 the ^{1}H and ^{1}H$\{^{19}$F$\}$ NMR of compound 3-31.

The structure of **3-31** was further confirmed by single crystal X-ray analysis, and the overall structure proved quite difficult to distinguish from the expected target product **3-30**. However, guided by NMR, the electron density at one of the axial substituents had a significant lower electron density than the other axial CF$_3$ groups, and that density is pointing away from the
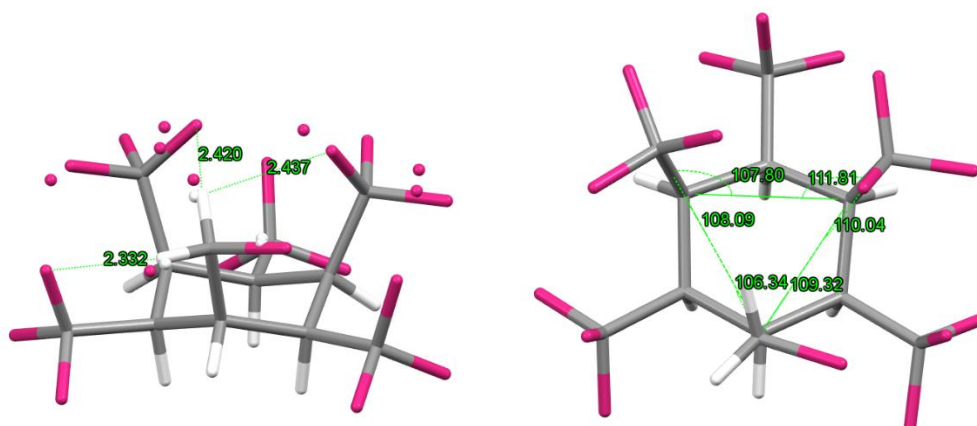
centre of the ring.

Figure 3-11 The X-ray structure of **3-31**.

This suggested that there is a fluoromethyl group and that the fluorine is pointing away from the sterically congested diaxial CF$_3$ groups. The co-aligned crystal packing lattice of **3-31** indicates that the dipole associated with the fluoromethyl group dictates long range order. The di-axial splay angle of the CFH–C–C(CF$_3$) (106.3-109.3, average of 107.8) is significantly lower than the value of CF$_3$–C–C(CF$_3$) (from 107.8 to 111.8, average of 109.4) consistent with a reduced steric impact.

In the low polarity fraction from column chromatography, a co-eluting fraction of the **3-31** was isolated and which contained the lactam **3-32**, derived from the CAAC ligand. This product was isolated, and an X-ray crystal structure was solved. The lactam came from corruption of the CAAC catalyst ligand after oxidation of the carbene centre. The fraction containing complexed **3-31** had a significant polarity difference to that when pure **3-31** eluted.
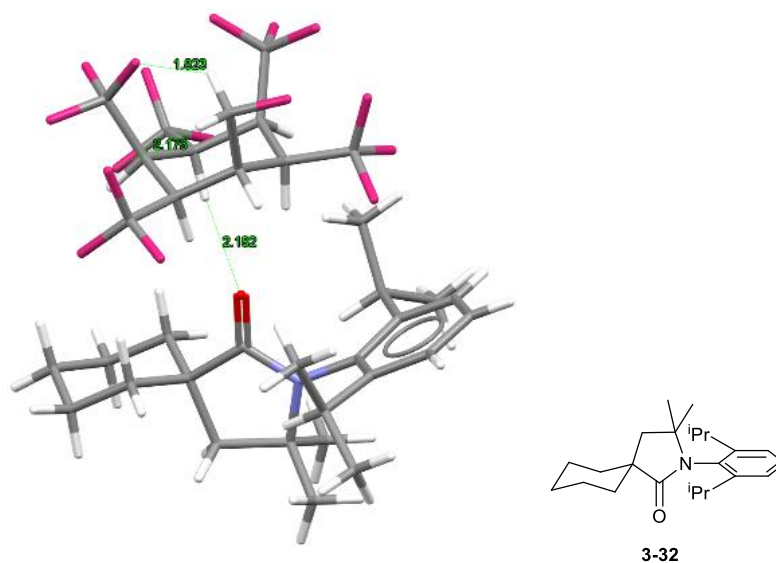
Figure 3-12 The X-ray single crystal structure of co-complex **3-31** and lactam **3-32**.

The crystal structure of **3-31** shows hydrogen bond lengths of 2.18 Å and 2.38 Å between the carbonyl oxygen and two axial protons, suggesting two strong hydrogen bonds to the hydrogen face of the Janus cyclohexane. The H_2CF in the fluoromethyl group has a contact distance of about 2.4 Å and 1.82 Å to the nearest axial CF_3 group, which represent very short C-H...F–C contacts even considering the free rotation dynamics of the CF_3 group. The unstrained di-axial splay angle of the fluoromethyl group at 105.5° in the co-complex structure is lower than the value of the un-coordinated form of 106.3° shown in Figure 3-11. But the average splay angle value of the substituent groups is similar to coordinated 109.0° versus uncoordinated 108.9°.

The desired hexakis CF_3-cyclohexane **3-30** was isolated by chromatography from the DCM fraction in 13 % yield as a rather amorphous material. Low-temperature evaporation of solvent was necessary in order to obtain a pure sample of **3-30** which indicated the ready sublimation of the product. The material was tested on a hot-stage microscope as well as by DSC measurements (Figure 3-13), and both analyses suggested that the compound has a melting range of between 47 - 51°C.
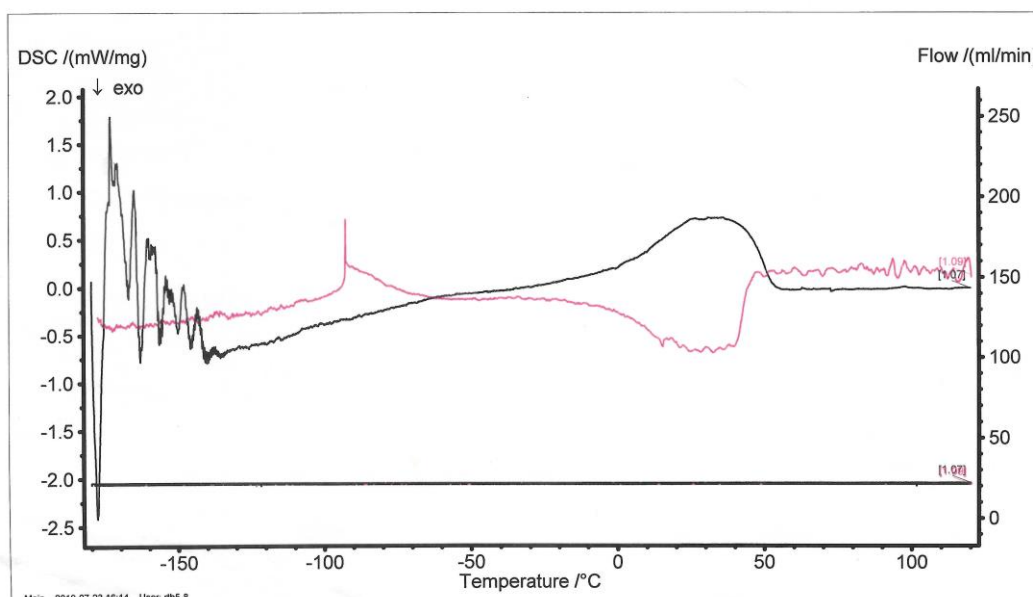
Figure 3-13 DSC measurement of **3-30**.

As shown in Figure 3-14, the ^{1}H NMR of the cyclohexane **3-30** shows two broad signals at δ 2.85 ppm and δ 3.68 ppm. Coupling from fluorine was ruled out by ^{1}H{^{19}F}-NMR where two sets of peaks, which are clear triplets, with a coupling constant ($^3J_{H-H}$) of 5.3 Hz, were recorded, essentially as expected. Two set of CF_3 groups (axial and equatorial) are observed in the ^{19}F NMR in a 1:1 integration ratio. The axial protons are upfield at δ 2.85 ppm on the upfield and with an expected larger coupling constant ($^3J_{H-F}$) of 9.0-9.8 Hz while the equatorial protons are at δ 3.68 ppm with no large H–F coupling constant observed.

91
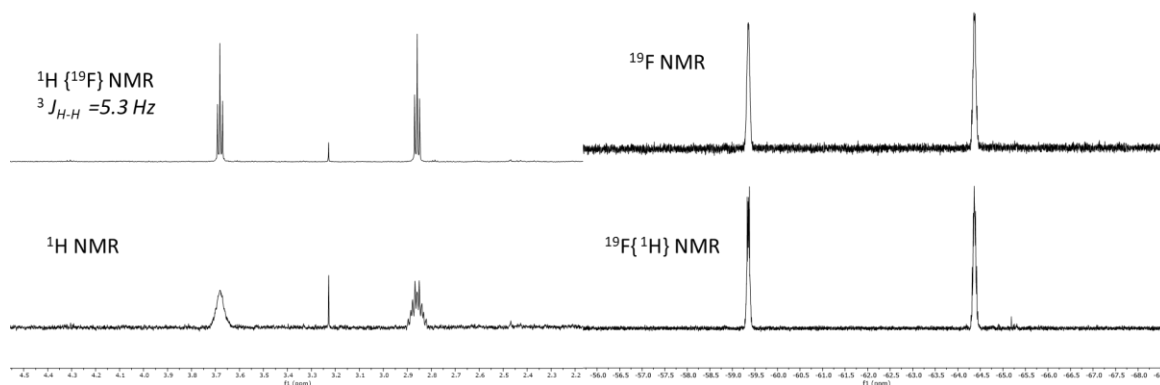
Figure 3-14 the NMR spectrum of hexakis CF_3-cyclohexane **3-30**.
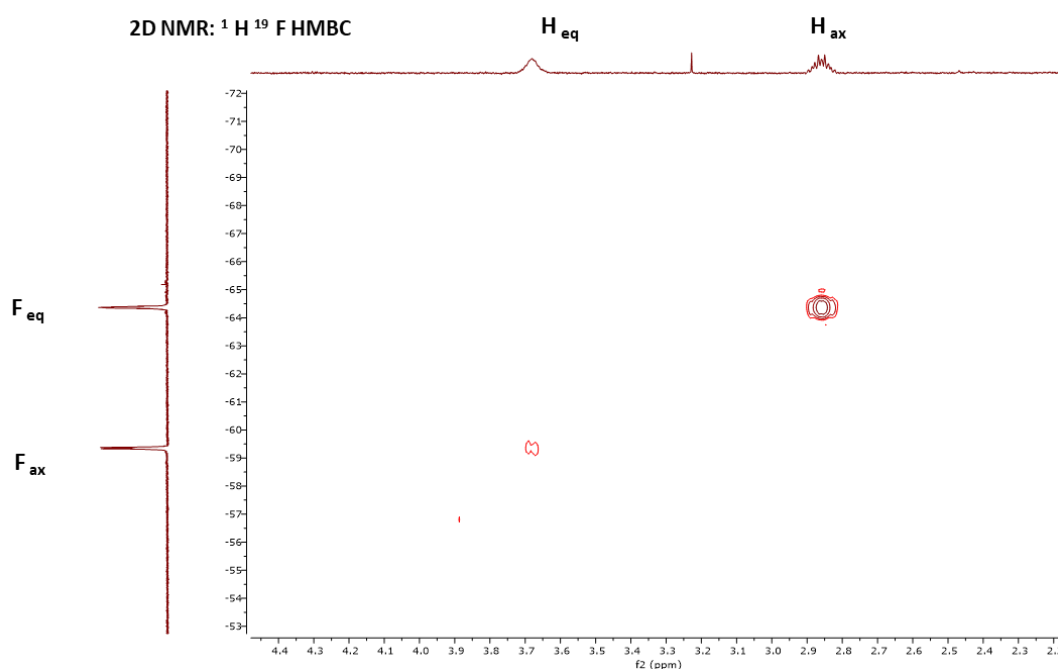
Figure 3-15 ^{1}H -^{19}F HMBC NMR of **3-30**.

The axial CF_3 are downfield in the ^{19}F-NMR spectrum relative to the equatorial CF_3 which are upfield. This is as expected and consistent with the literature where the axial CF_3's are more deshielded and agrees with the general chemical shift difference of axial to equatorial CF_3.[9] The correlation of the axial protons coupling to equatorial CF_3's is supported by ^{1}H - ^{19}F HMBC NMR shown in Figure 3-15.
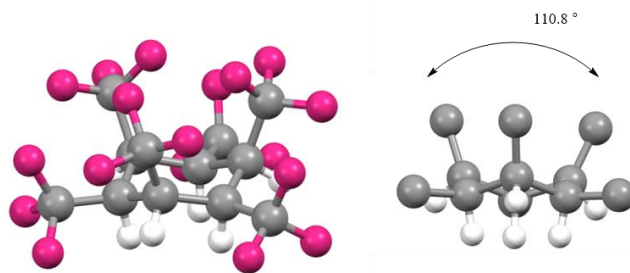
Figure 3-16 X-ray single crystal structure of **3-30.**

An X-ray single crystal structure of **3-27** was obtained and this proved that the cyclohexane ring adopts a flattened chair conformation. This is clearly caused by steric crowding due to repulsion between the axial CF_3 groups. The observed diffraction data revealed that the tri-axial CF_3 groups are showing a splay ($CF_3 –C–C–CF_3$) angle of about 110.8 °, averaged from 107.9° to 113.2°. The axial-axial splay angle (110.8 °) of **3-30** is significantly different from an ideal cyclohexane ring where this angle is 90°, and it is wider than the value of 105.5° observed in the all-*cis*-hexamethylcyclohexane **3-1** crystal structure. It is also greater than the angle found in the cyclohexane **3-31** which averaged only 108.9º where CFH_2 replaced axial CF_3.[6, 27] This is entirely consistent with the larger steric impact of CF_3 over CFH_2.
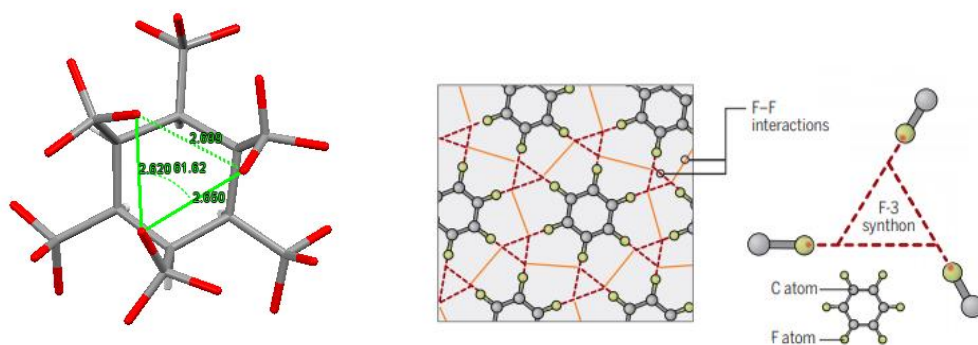

Figure 3-17 Projection view of the X-ray single crystal structure of **3-30** (left); the windmill F-3 synthon of

hexafluorobenzene on Ag (1 1 0).

The projection view of the structure of **3-30** shows the three C–F bonds that point over the ring are also perhaps making halogen bonds with each other as they appear to direct towards

93

the halogen σ-hole (Figure 3-17). This forms a windmill shape or triangle synthon, similar to hexafluorobenzene on a silver surface. [28] The geometry of the three axial CF_3 groups which are perpendicular to the cyclohexane ring results in close intramolecular contacts which are comparable to intermolecular interactions in hexafluorobenzene along the 2D surfaces.

A computational study, carried out by Professor Michael Buehl at the University of St Andrews, mapped an electrostatic potential of **3-30** using the B3LYP/6-31G* method. This indicated a large and diffuse electronegative area associated with the CF_3 groups on one side of the ring. By contrast, a significant but concentrated area of electropositive charge was apparent on the opposite side of the ring associated with the hydrogen face. The overall dipole moment of **3-30** is 4.0 D, a value significantly lower than the all-*cis*-hexafluorocyclohexane **3-9** at 6.2 D. This is presumably due to the polar asymmetry of **3-30** with a more diffuse electronegative face and a concentrated electropositive region.
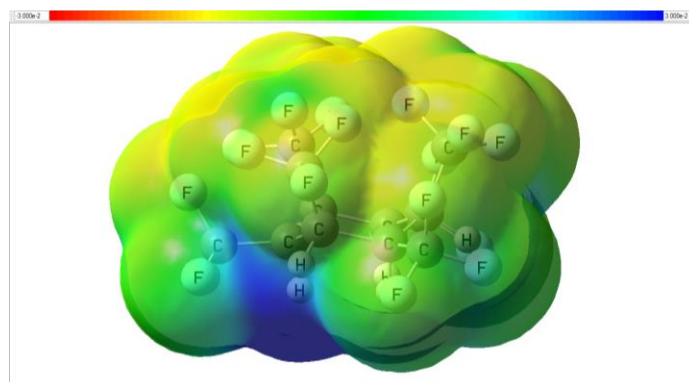
Figure 3-18 DFT calculation electrostatic potential map of **3-30** illustrates a focused positive charge density (blue) on the hydrogen face carried out by Prof. Michael Buehl, School of Chemistry.

The Janus face aspects of cyclohexane **3-30** were further investigated by experimental measurements. Variable solvent NMR experiments were carried out to investigate the interaction between different solvents by observing relative chemical shifts changes by ^{1}H NMR for the H_{ax} and H_{eq} hydrogens.
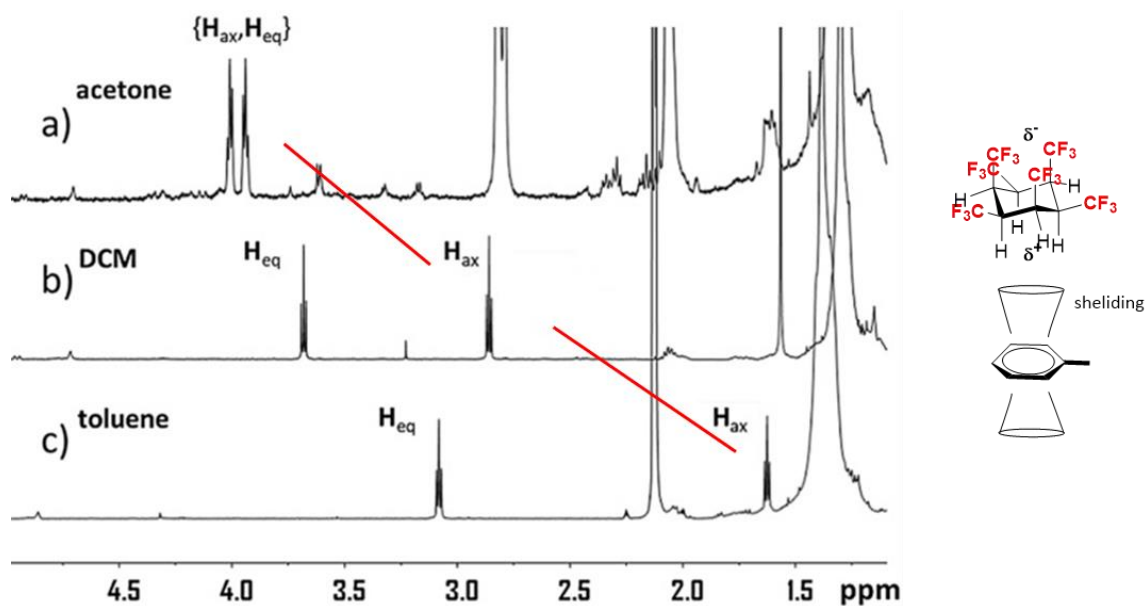
Figure 3-19 NMR comparison of cyclohexane **3-30** in *d*-acetone, *d*-DCM and *d*-toluene.

The spectra are compared in Figure 3-19. A strong upfield shift from DCM to toluene was observed for all of the hydrogens. The magnitude of the shift for the axial protons ($\Delta\delta$ H_{ax} 1.25 ppm) is significantly larger than that for the equatorial protons ($\Delta\delta$ H_{eq} = 0.6 ppm). This is caused by the aromatic ring of toluene associating with the electropositive hydrogen face of **3-30** and inducing a significant anisotropic effect predominantly on the axial hydrogens, as they will be in closer contact on average with the aromatic ring.
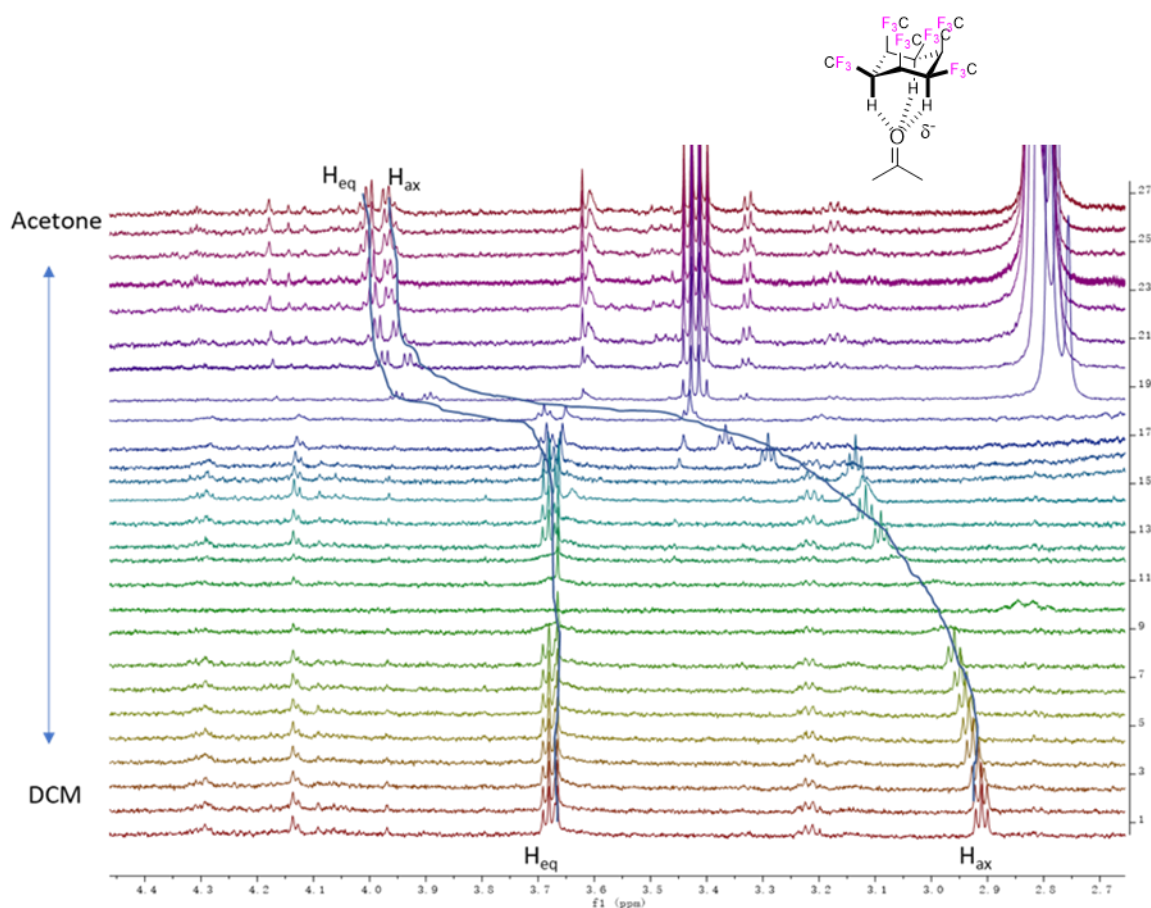
Figure 3-20 ^{1}H{^{19}F} NMR of **3-30 in solvents progressing from** *d*-acetone to *d*-DCM.

In contrast, a significant downfield shift was observed, predominantly for the axial protons, when changing the solvent from DCM to acetone. This is consistent with hydrogen bonding between the axial protons of **3-30** and the carbonyl of the solvent and is consistent with the coordination observed in the X-ray structure (Figure 3-12) where the hydrogen face of **3-31** coordinated to the carbonyl of the amide derived from the carbene catalyst.
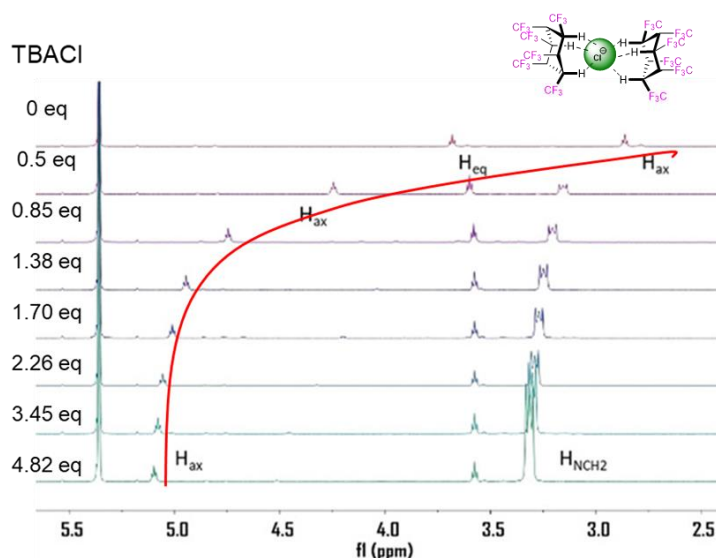
Figure 3-21 Titration of **3-30** over TBACl in DCM monitored by $^1H\{^{19}F\}$ NMR.

A series of titration experiments was carried out to examine the binding potential of **3-30** towards anions. In the first instance, cyclohexane **3-30** was titrated with chloride ions by exposing to tetrabutylammonium chloride (TBACl) in a DCM solution. Due to the difficulty to preparing cyclohexane **3-30**, there was only a few milligrams of material. Only one titration experiment was carried out with freshly isolated **3-30**. Accordingly, TBACl solution was added stepwisely to **3-30** in DCM solution. It took more than 5 equivalents of TBACl to reach the maximum chemical shift change for the H_{ax} signals in **3-30** by ^1H NMR.

The titration was monitored progressively by ^1H NMR as shown in Figure 3-21. A clear chemical shift change of $\Delta\delta H_{ax}$ = 2.4 ppm was observed after 2 equivalents of Cl$^-$ had been added, and again predominantly associated with the axial protons. The chemical shift changes of both axial and equatorial protons become stable at this limit. A chemical shift crossover of the H_{ax} and H_{eq} protons was observed during the titration process. The H_{ax} and H_{eq} protons were assigned relative to the CF$_3$ signals and their corresponding cross peaks in the ^1H-^{19}F HMBC spectrum, as showed in Figure 3-22.

97
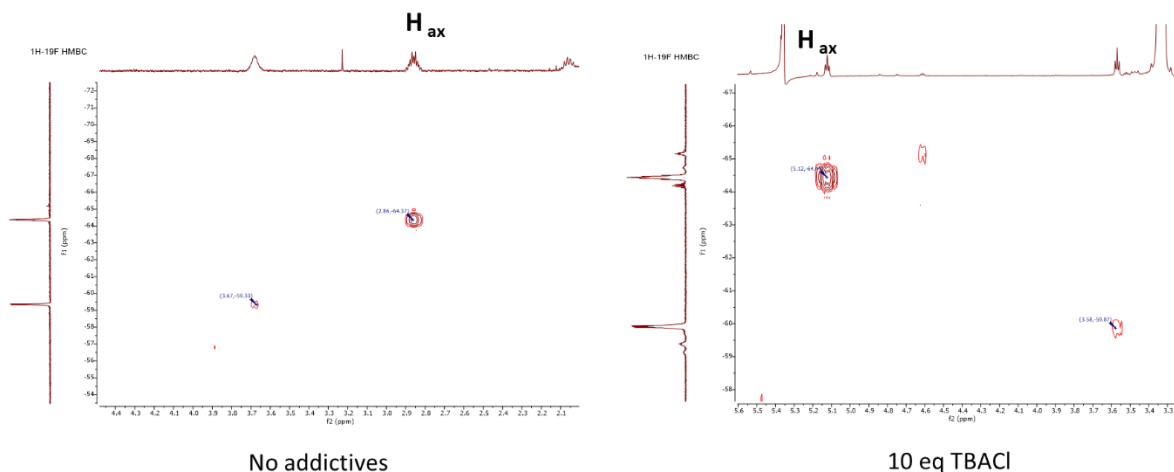
Figure 3-22 Comparison of ^{1}H ^{19}F HMBC NMR of **3-30** without additive and with 10 eq. TBACl.

The data of TBACl to **3-30** ratios and related ^{1}H NMR chemical shifts were matched using the Bindfit tool.[29] The ^{1}H NMR chemical shift change of H_{ax} in **3-30** was used as it shifted to the greatest extend during the titration . A limitation of the data collected is the limited number of most valid points between 0.5 to 0.8 equivalents in the host-guest interaction model. Nevertheless, a series of notable chemical shift changes in the ^{1}H NMR spectra were observed between 1 to 5 equivalents of TBACl, and these suggested the integrity of the host-guest interaction of **3-30** and chloride ion. The points on the titration plot illustrated in Figure 3-21 have a non-linear correlation, and this is useful in establishing the binding affinity and fitting to an appropriate host guest model.
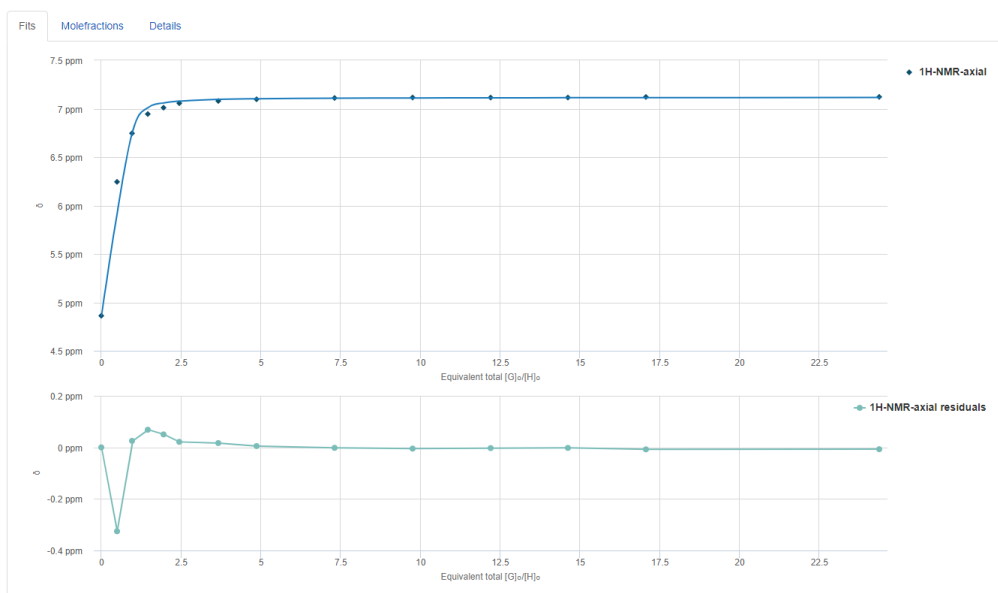
Figure 3-23 Titration of **3-30** fitted to an invalid 1:1 host to guest model.

Several common host vs guest coordination models were fitted with the data set to examine the stoichiometry. The titration plot shows the host to guest interaction do not follow an intuitive 1:1 model, as an invalid value was observed of K = 16299.3 M^{-1} with errors bar of ± 114.6 % (Figure 3-23). Similarly, the host : guest = 1 : 2 model was ruled out also due to a large error (>131 %).
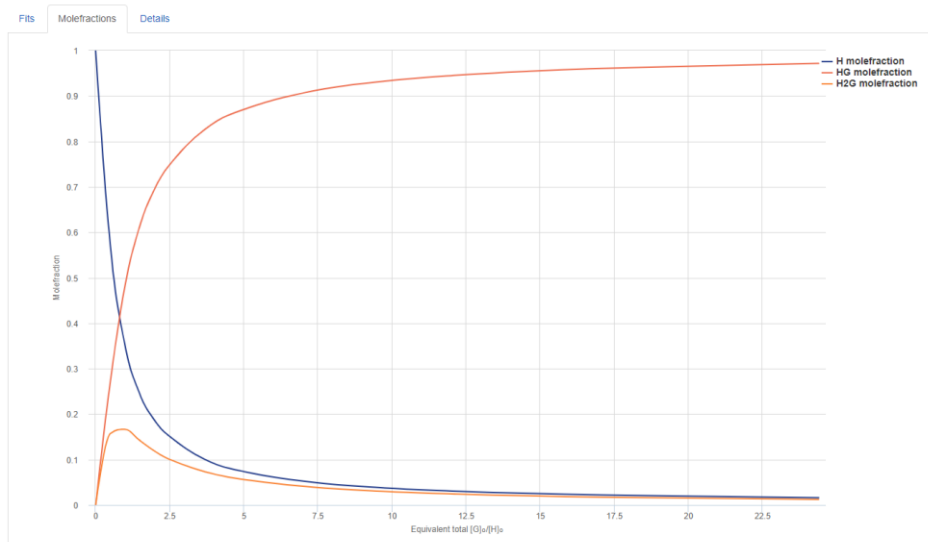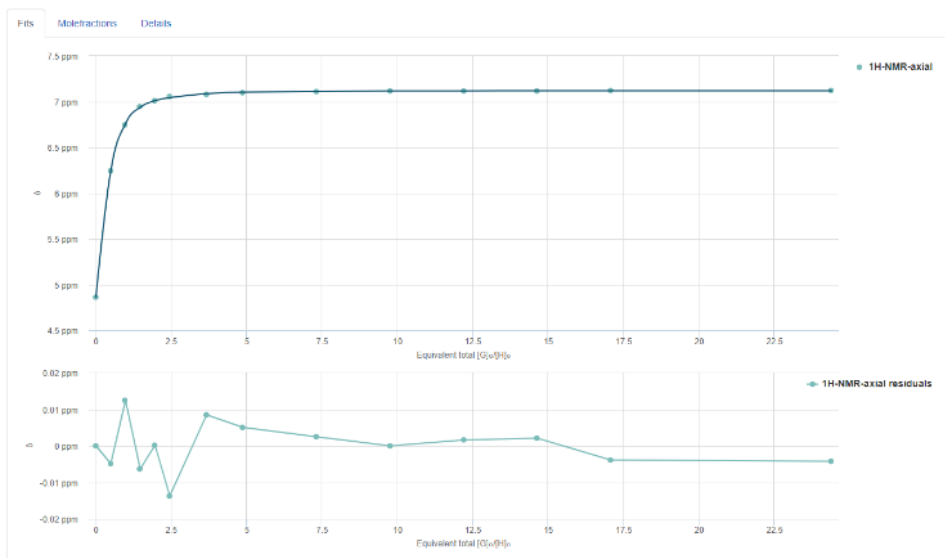
Figure 3-24 Top: The titration of **3-30** over TBACl in DCM monitored by ^{1}H{^{19}F} NMR and fitted into host : guest = 2 : 1 model in Bindfit. Bottom: The plot of host (H): guest (G) species of **3-30** : TBACl against the equivalents of TBACl.

A host : guest = 2 : 1 coordination model fitted the titration outcome most accurately. An association constant for chloride ion was measured at $K_{11} \approx 1274.5$ M^{-1} ± 18.5 % and $K_{12} \approx$ 192.8 M^{-1} ± 9.9 %. A secondary coordination suggested that **3-30** binds chloride ion in 2-fold ratio. The relatively small error bar gives the greatest confidence in this model.[30] The in Figure

3-34 shows the ratio change of **3-30** from 1 to 2 equivalents of TBACl.

The equilibrium between [H], [HG] and [H$_2$G] species results in a second order relationship of [H] to the chemical shift change.[31] The number of measurements taken between 1 to 5 equivalents of guest becomes useful in order to fit the second order correlation. However, more precisely titration experiments in the 0.5 to 0.8 equivalent range would provide a more accurate measurement of the binding affinity between chloride ion and **3-30**.
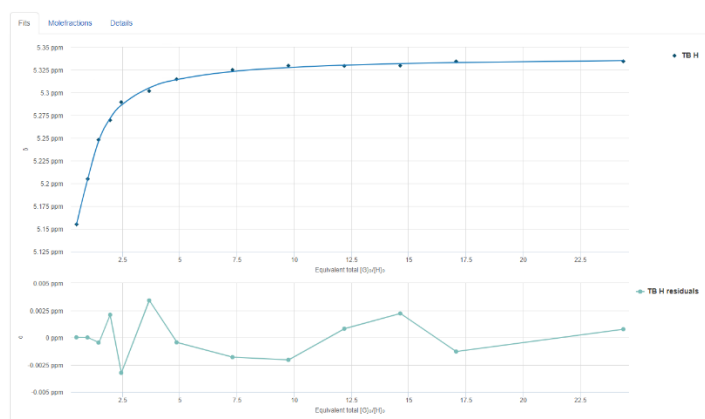
Figure 3-25 Titration of **3-30** fitted in an invalid 2:1 host to guest model by proton at NC$\underline{H}_2$-. Chemical shift of ^{1}H NMR was added +2 ppm for Bindfit input file correction as described.

The proton signals associated with the α NCH$_2$'s of the tetrabutylammonium ion was also used to fit the titration curves. A host : guest 2 : 1 association model was observed as well, with equilibrium constant, K_{11} = 4580.4 M^{-1} ± 12.6 % and K_{12} = 595.5 M^{-1} ± 9.4 %. These values suggest that the association affinity constant measured through the NCH$_2$ proton shifts is close in the magnitude to that from the **3-30** H$_{ax}$ measurement. However, the fit is less reliable due to less of a ^{1}H NMR chemical shift change across the experiment. For the same reason, the signal from the H$_{eq}$ protons of **3-30** was not used in the fit.

2 : 1 Host to guest complexes were observed by electrospray ionization (ESI) mass

spectrometry as well, where [2M+Cl]⁻ ions were detected for both **3-30** and **3-31**.
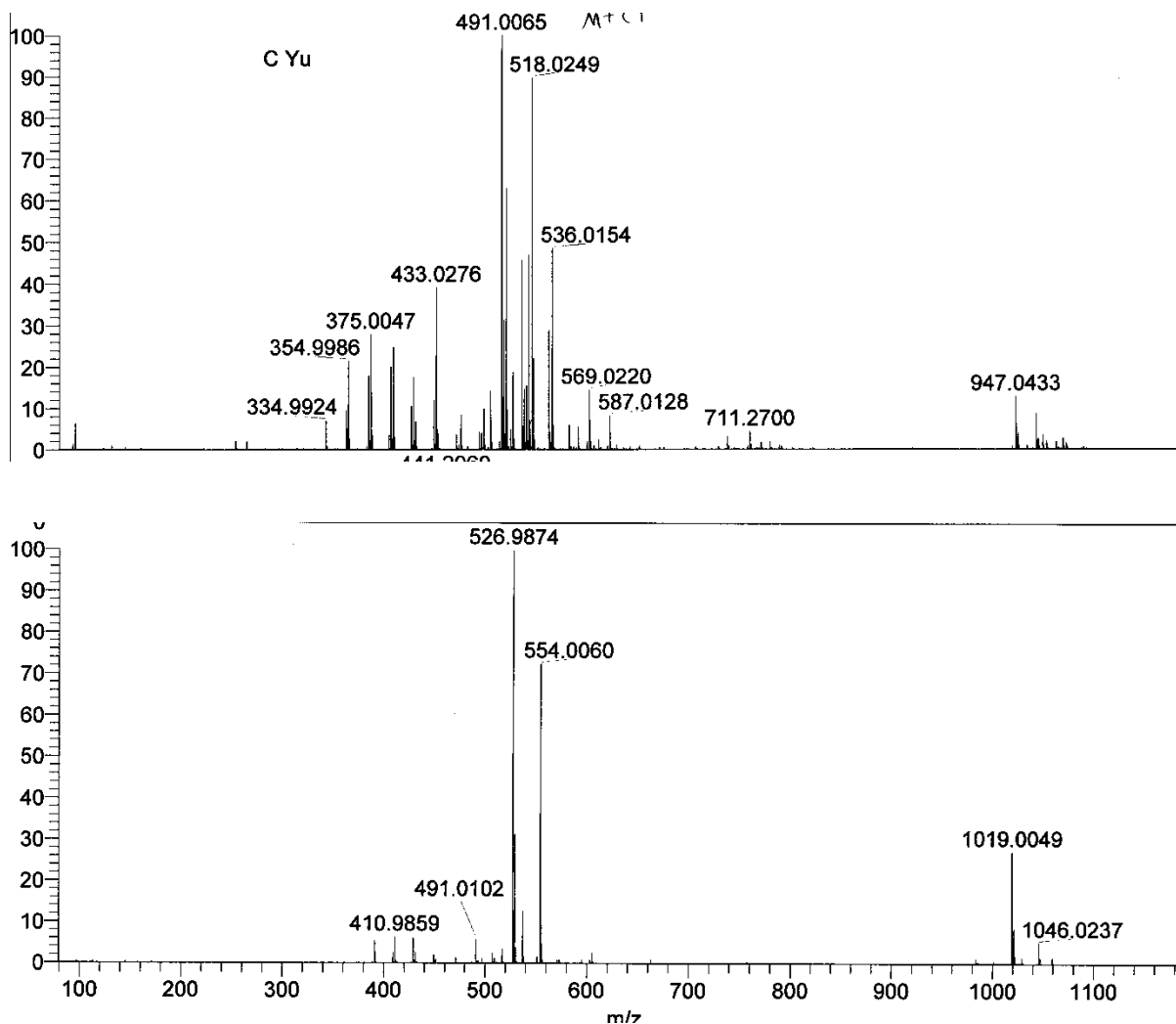
Figure 3-26 FTMS ESI -P. 518 for [**3-31**+Cl], 947 for [2***3-31**+Cl](top); 526 for [**3-30**+Cl], and 1019 for [2***3-30**+Cl], isotope patterns were consistent with the presence of chloride ion(bottom).

A similar ¹H NMR titration experiment for fluoride was carried out with tetrabutylammonium fluoride. This indicated a lower affinity in a 1:1 model. The titration against fluoride ion was also monitored by ¹⁹F NMR. An ordered decomposition of **3-30** was observed after exposure to two equivalents of TBAF. The observation appeared to involve the exocyclic β-dehydrofluoro elimination with fluoride acting as a base. Endocyclic β-dehydrofluoro was

102

previously observed when all-*cis*-hexafluorocyclohexane **3-9** was titrated with fluoride.[30]
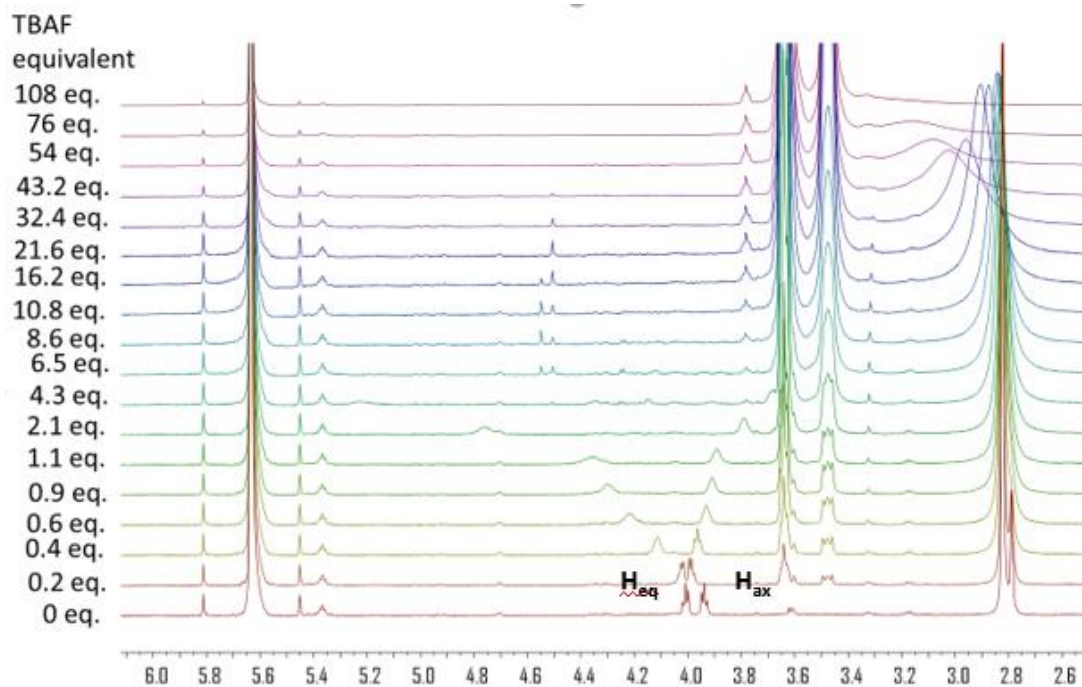
Figure 3-27 Titration of **3-30** over TBAF monitored by $^1H\{^{19}F\}$ NMR.
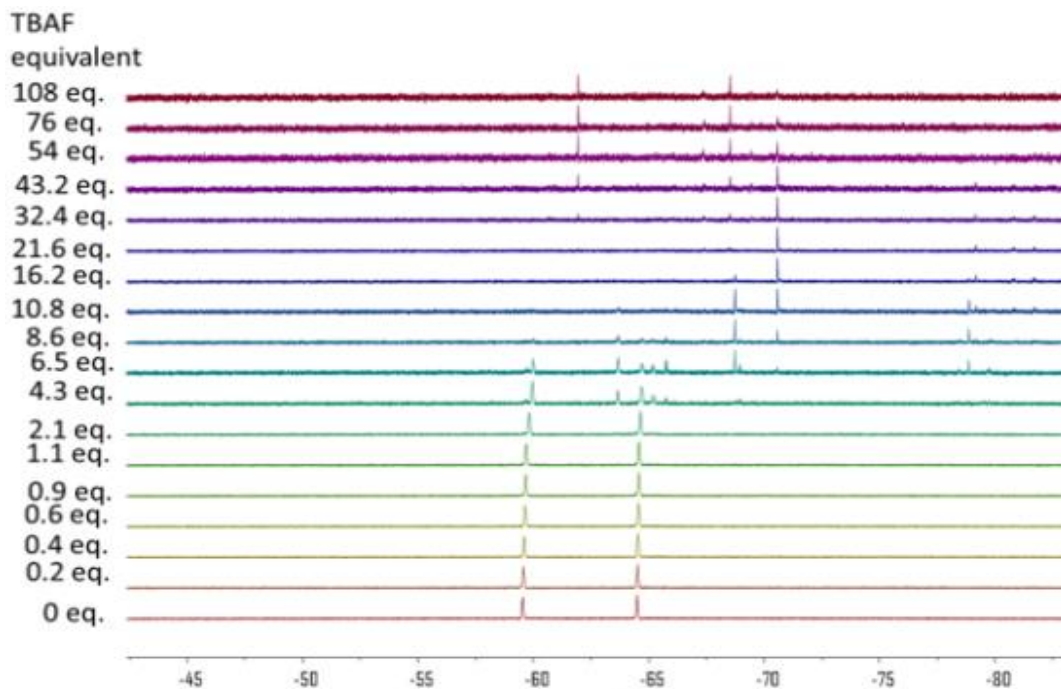
Figure 3-28 Titration of **3-30** over TBAF monitored by $^{19}F\{^1H\}$ NMR.
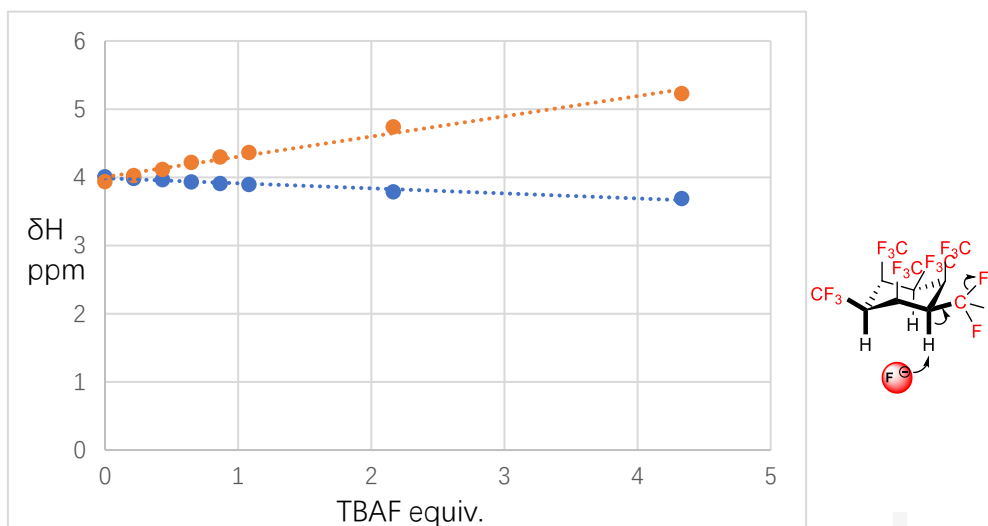
Figure 3-29 Plot of concentration of TBAF (equivalent) versus chemical shift δH in ppm.

The titration curve for TBAF was fitted to a 1:1 host guest model. An association constant of K= 118.1 M^{-1} was calculated by reference to the changes in the H_{ax} chemical shifts and a value of K= 199.4 M^{-1} was calculated by reference to the changes in the H_{eq} chemical shifts, over the range of 0 eq. to 4 eq. of TBAF. The 2-fold difference in association constant values is reasonably related to a relatively low binding affinity and the differences in the chemical shift ranges of the two sets of protons, and perhaps a greater accuracy can be applied to the data from the H_{ax} chemical shift data.

The titration of compound **3-30** with iodide shows a further lowering in affinity which ΔδH was only achieved after addition of 200 eq. of TBAI. Presumably the large atomic radius of iodide and the soft charge has poor affinity towards the concentrated charged positive face.
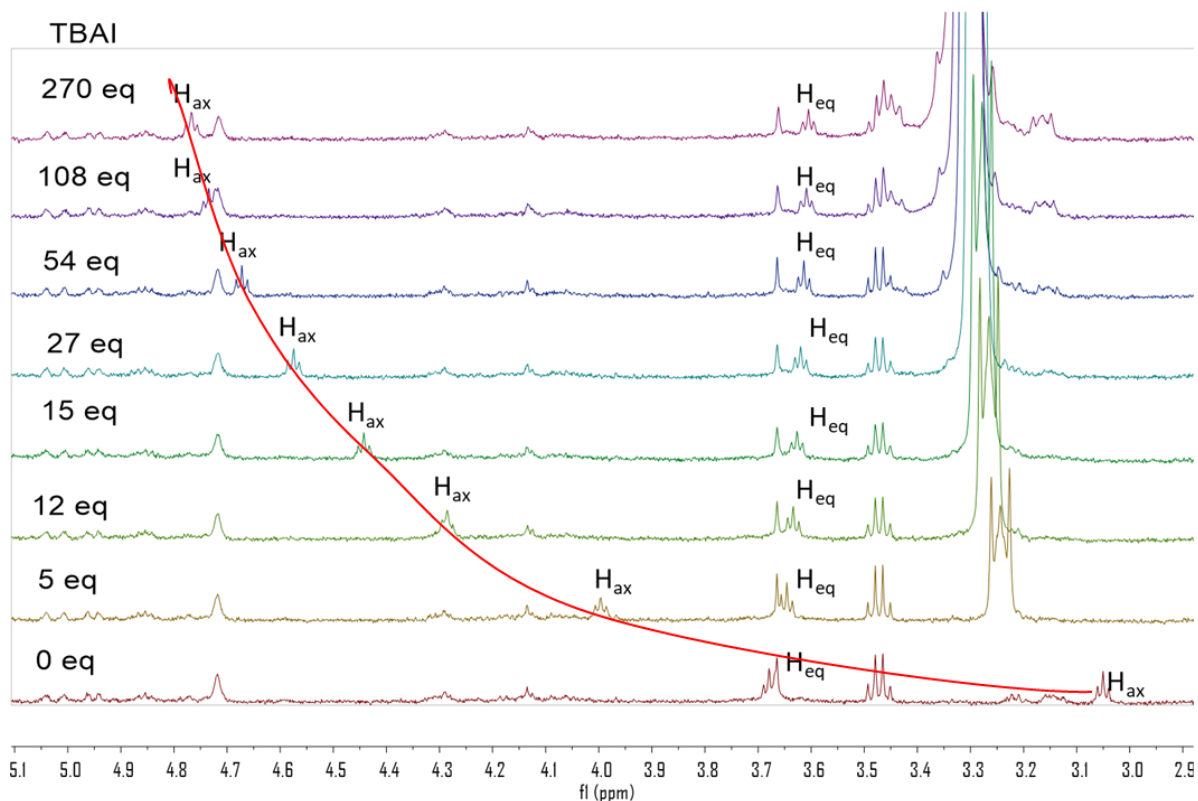
Figure 3-30 The ^{1}H{^{19}F} NMR of the titration of **3-30** over TBAI.

The barrier to interconversion of the cyclohexane **3-30** was first investigated experimentally by VT-NMR measurements. The spectra were recorded by changing temperature across the temperature range -80 °C to +80°C, however no significant changes in chemical shifts in the ^{1}H-NMR or ^{19}F{^{1}H}-NMR was observed. Two further experiments exploring exchange correlation (EXSY) NMR experiments for ^{1}H and ^{19}F nuclei were conducted, however no polarisation transfer was detected even at the highest temperature of 80 °C. This indicated that the barrier to ring inversion for **3-30** is high and the rate of ring interconversion is too slow in the NMR time scale to be observed.
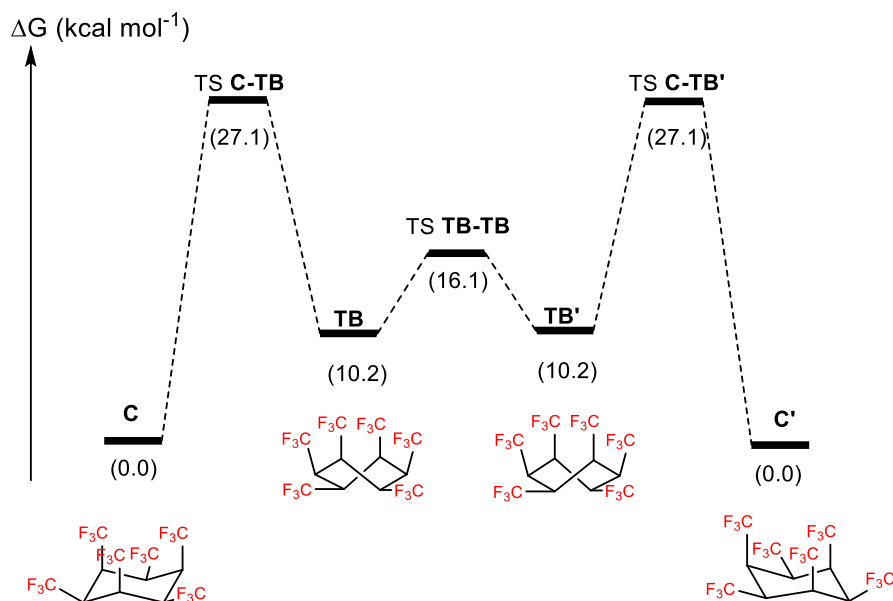
Figure 3-31 Profile of relative energies (kcal mol^{-1}) of intermediates and transition states for the interconversion of cyclohexane **3-30** between chair (**C**) and twist-boat (**TB**) conformers, with their mirror images (**C'** and **TB'**, respectively—note that **TB** and **TB'** are enantiomers. Free energies at 298 K (in kcal mol^{-1}) at the B3LYP-D3/3–311+G(d,p)/CPCM(CH2Cl2)//B3LYP-D3/6-31G(d) level.

Given the challenges with NMR, in order to gain some estimate of the barrier to ring inversion, a computational (DFT) study was carried out with the B3LYP-D3 method. This was conducted by Prof Michael Buehl of the School of Chemistry at the University of St Andrews (Figure 3-31). This evaluated the transition states (TSs) that are likely to be involved in the minima of the force field. The lowest energy transition state that was found was a boat structure involved in the transition between two enantiomeric twist boast (TB) conformers. The $\Delta G^{\ddagger}$ corresponding to the twist-boat intermediate was 5.9 kcal mol^{-1}. Twist-boat and chair minima are known to interconvert via a half-chair structure. In this case that structure for **3-30** was very high in energy and the highest barrier on the conformation profile was a $\Delta G^{\ddagger}$ = 27.1 kcal mol^{-1} at room temperature. At the highest theory level tested, involving a continuum model to simulate DCM as the solvent, the twist boat conformer of **3-30** is calculated to be significantly higher in energy level than the chair conformation by ΔG^{0} = 10.2 kcal mol^{-1} at room temperature. The detailed interconverting pathway for ring flipping was not tracked

due to the complexity involved in deconvoluting the complexity of additional intermediates and transition states, which arise due to the –CF$_3$ groups interlocking. This is due to steric and electric repulsion between fluorine atoms on two axial –CF$_3$ groups. However, it could be concluded that there is a significantly higher ring flip energy for the interconversion process than that found for hexamethyl-or hexafluoro cyclohexane **3-1** and **3-9**. With a barrier to ring inversion of $\Delta G^{\ddagger} = 27.1$ kcal mol^{-1}, cyclohexane **3-30** appears to be the most sterically hindered analogue of an all-*cis* hexakis substituted cyclohexane that has been prepared to date, and nearly three times that found for cyclohexane (10.8 kcal mol^{-1}).

The B3LYP method is one of the most famous hybrid density function theory model, including Hartree–Fock exchange, local exchange, gradient exchange correction, local correlation, and gradient correlation correction. [32] B3LYP is known to be a reliable and versatile method for calculating molecular properties such as geometries, energies, and vibrational frequencies. [33] The calculation is considered relative reliable in large basis set. However, it should be noticed that large number of atoms in the **3-30** molecule which lead to the complicity to DFT calculation, especially for the C–F bonds in the branches.

The large barrier to ring inversion calculated in the DFT study with solvent correction was in good agreement that the experimental observation by ^{1}H NMR which had resolved signal at raised temperature as well as the absence of cross peaks in the raised temperature EXSY NMR spectrum. The calculated dipole and with a non-symmetrical charge distribution is consistent with the observed affinity of **3-30** toward chloride ion.

3.3.3 Pentakis(2,3,4,5,6)trifluoromethylcyclohexan-1-ol

It became interesting to prepare derivatives of all-hexakis-trifluoromethyl cyclohexane **3-30** to explore incorporation into more advanced molecular architectures. To this end aryl hydrogenation of pentakis(trifluoromethyl)phenol **3-28** became an objective, as the resultant cyclohexanol has the potential to be derivatised through the alcohol group. This target also

became appropriate as the major product of the trifluoromethylation reaction of **3-27** is the pentakis(trifluoromethyl)phenol **3-28** and thus it became available for aryl hydrogenation experiments.
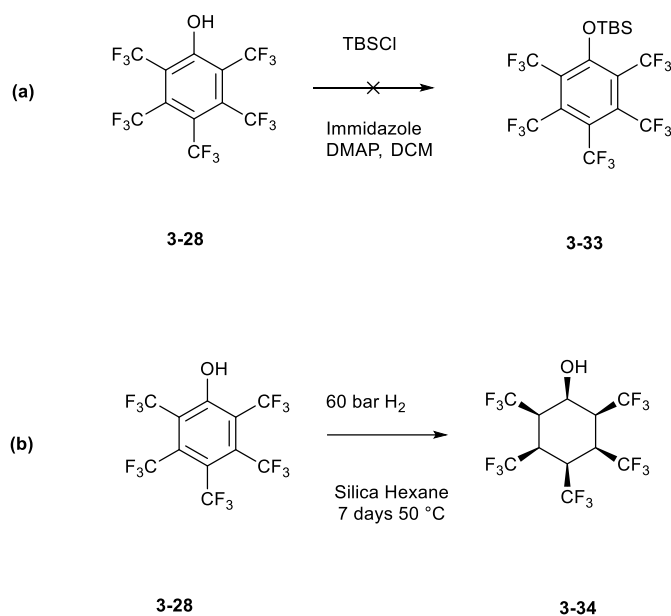
Scheme 3-8 Anticipated reactions of **3-28**.

Firstly, the TBS was investigated as a protecting group for the phenol. As discussed by Glorius and as observed in Chapter 2, it is shown that TBS protected phenol ethers were generally good substrates for aryl hydrogenation.[34] However, in this case, reaction of TBS-Cl with phenol **3-33** was extremely sluggish and did not convert to the desired silyl ether. The product which could be observed by TLC during the reaction, and it immediately decomposed to starting material **3-28** after contact with moisture in the air. In view of this, reactions were explored using phenol **3-28** directly for aryl hydrogenation without any protection. The reaction proceeded but with moderate conversion only, and with some starting material remaining unreacted. Also, a significant amount of hydrodefluorination side products were observed during the reaction. Cyclohexanol **3-34** was successfully hydrogenated under similar conditions to those previously applied to the preparation of cyclohexane **3-30**.
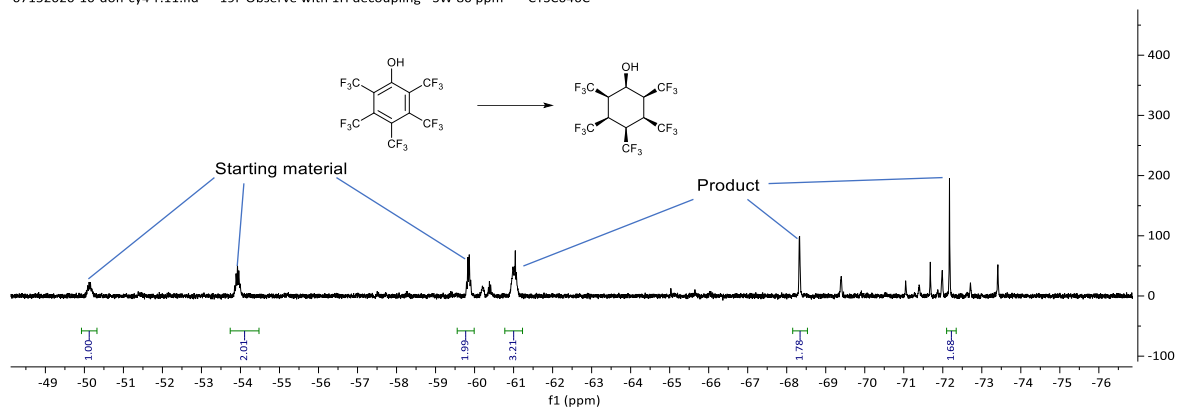
Figure 3-32 the ^{19}F NMR of product mixture after direct aryl hydrogenation of **3-34**.

It can be seen in Figure 3-32 that the aromatic CF_3 signals at -50 to -60 ppm in the ^{19}F-NMR spectrum were converted to cycloalkyl CF_3's with axial and equatorial CF_3 in the range -60 to -70 ppm. This is consistent with previous examples (e.g. **3-30**) and literature values of alkyl CF_3 groups.[9-11] The three peaks at -50 ppm, -54 ppm and -60 ppm match to the starting phenol.
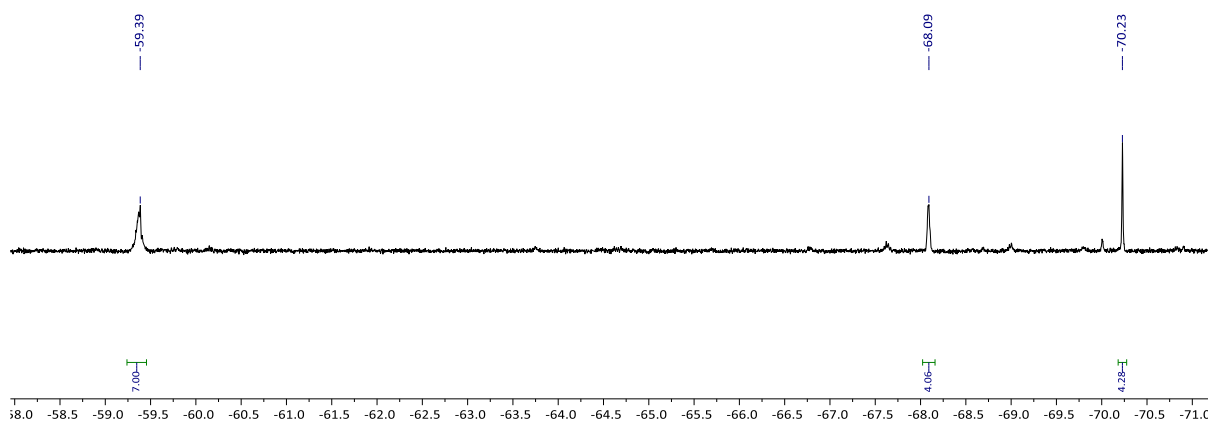
Figure 3-33 ^{19}F NMR spectrum of **3-34**.

The major fraction isolated showed three ^{19}F-NMR signals at -59.4, -68.1 and -70.2 ppm, demonstrating aryl hydrogenation. The integration of the three aliphatic -CF_3 signals shows a ratio of CF_3 ax : CF_3 eq : CF_3' eq = 7 : 4 : 4. This ratio suggests the presence of –OH axial and –OH equatorial species in a ratio of 2:1.

109

Purification of the product proved to be difficult, as the hydrodefluorination side products with high polarity and co-eluted with the desired product. The level of the side product generated during the long hydrogenation, makes this hydrogenation an inefficient method to deliver compound **3-34**, certainly in high yield as required for the preparation of functional molecules.

3.4 Summary

In summary, a range of all-*cis* multi-vicinal CF_3 containing cyclohexanes were prepared with all the substituents on one face of the ring. For compound **3-13**, the chair conformation is lowest in energy according to NMR studies. Cyclohexane **3-15** has a twist conformation which is close in energy to the ground state chair conformation and accordingly, it is relevant in solution. VT-NMR studies are consistent with that predicted by theory. Cyclohexane **3-30** has the highest barrier (27 kcalmol^{-1}) to ring interconversion of any cyclohexane known so far. The stereochemical distribution of the CF_3 groups in **3-30** led to a large and diffuse electronegative hemisphere on the -CF_3 dominated face and a much more concentrated arc of electropositive charge on the hydrogen face. This molecule shows modest binding affinity towards halide ions (F$^-$, Cl$^-$, Br$^-$ & I$^-$) and also acetone indicating coordination to the area of electropositive charge, and it represents a novel Janus face cyclohexane.[35]

3.5 References

1. Q. Luo, K. R. Randall and H. F. Schaefer, *RSC Adv.*, 2013, **3**, 6572-6585.

2. V. Umadevi, N. Santhanamoorthi and L. Senthilkumar, *Comput. Theor. Chem.*, 2014, **1049**, 55-61.

3. S. J. Angyal and D. J. McHugh, *J. Chem. Soc.*, 1957, 3682-3691.

4. S. Brückner, L. Malpezzi Giunchi, G. Di Silvestro and M. Grassi, *Acta Crystallographica Section B*, 1981, **37**, 586-590.

5. M. Farina, M. Grassi and G. Di Silvestro, *J. Am. Chem. Soc.*, 1985, **107**, 5100-5104.

6. H. Werner, G. Mann, M. Mühlstädt and H. J. Köhler, *Tetrahedron Lett.*, 1970, **11**, 3563-3566.

7. N. S. Keddie, A. M. Slawin, T. Lebl, D. Philp and D. O'Hagan, *Nat. Chem.*, 2015, **7**, 483-488.

8. K. Nolan, J. Kamrath and J. Levitt, *Pediatric Dermatology*, 2012, **29**, 141-146.

9. E. W. Della, *J. Am. Chem. Soc.*, 1967, **89**, 5221-5224.

10. Y. Carcenac, P. Diter, C. Wakselman and M. Tordeux, *New J. Chem.*, 2006, **30**, 442-446.

11. Y. Carcenac, M. Tordeux, C. Wakselman and P. Diter, *New J. Chem.*, 2006, **30**, 447-457.

12. S. H. W. E.L. Eliel, *Stereochemistry of organic compounds*, Wiley, New York, 1994.

13. J. Weiser, O. Golan, L. Fitjer and S. E. Biali, *J. Org. Chem.*, 1996, **61**, 8277-8284.

14. J. H. Espenson, *Chemical kinetics and reaction mechanisms*, McGraw-Hill, New York ;, 2nd edn., 1995.

15. G. Lente, I. Fábián and A. J. Poë, *New J. Chem.*, 2005, **29**, 759-760.

16. E. V. Anslyn and D. A. Dougherty, *Modern physical organic chemistry*, University Science Books, Sausalito, Calif, 2006.

17. H. N. C. Wong, Y. I. D. Xing, Y. F. Zhou, Q. Q. Gong and C. Zhang, *Synthesis*, 1984, **1984**, 787-790.

18. C. Bakewell, A. J. P. White and M. R. Crimmin, *Angew. Chem. Int. Ed.*, 2018, **57**, 6638-6642.

19. C. Zhang, X. Jia and H. Quan, *J. Fluor. Chem.*, 2016, **191**, 77-83.

20. J. J. Garcia, C. Sierra and H. Torrens, *Tetrahedron Lett.*, 1996, **37**, 6097-6098.

21. M. E. Peach, *Can. J. Chem.*, 1968, **46**, 2699-2706.

22. R. Saleedo and H. Torrens, *Transition Met. Chem.*, 1980, **5**, 247-249.

23. A. Kütt, V. Movchun, T. Rodima, T. Dansauer, E. B. Rusanov, I. Leito, I. Kaljurand, J. Koppel, V. Pihl, I. Koppel, G. Ovsjannikov, L. Toom, M. Mishima, M. Medebielle, E. Lork, G.-V. Röschenthaler, I. A. Koppel and A. A. Kolomeitsev, *J. Org. Chem.*, 2008, **73**, 2607-2620.

24. D. L. Mattern, *J. Org. Chem.*, 1984, **49**, 3051-3053.

25. D. J. Burton and Z.-Y. Yang, *Tetrahedron*, 1992, **48**, 189-275.

26. A. N. B. I. M. Zalesskaya, E. P. Saenko, Y. A. Eialkov, L. M. Yagupolskii, *Zhur. Org. Khim.* , 1980, **16**, 1194-1202.

27. N. S. Keddie, A. M. Z. Slawin, T. Lebl, D. Philp and D. O'Hagan, *Nat. Chem.*, 2015, **7**, 483-488.

28. Z. Han, G. Czap, C.-l. Chiang, C. Xu, P. J. Wagner, X. Wei, Y. Zhang, R. Wu and W. Ho, *Science*, 2017, **358**, 206-210.

29. D. Brynn Hibbert and P. Thordarson, *Chem. Commun.*, 2016, **52**, 12792-12805.

30. O. Shyshov, K. A. Siewerth and M. von Delius, *Chem. Commun.*, 2018, **54**, 4353-4355.

31. P. Thordarson, *Chem. Soc. Rev.*, 2011, **40**, 1305-1323.

32. J. Tirado-Rives and W. L. Jorgensen, *J. Chem. Theo. Thermodyn.*, 2008, **4**, 297-306.

33. B. G. Johnson, P. M. W. Gill and J. A. Pople, *J. Chem. Phys.*, 1993, **98**, 5612-5626.

34. M. P. Wiesenfeldt, T. Knecht, C. Schlepphorst and F. Glorius, *Angew. Chem. Int. Ed.*, 2018, **57**, 8297-8300.

35. C. Yu, A. Kütt, G.-V. Röschenthaler, T. Lebl, D. B. Cordes, A. M. Z. Slawin, M. Bühl and D. O'Hagan, *Angew. Chem. Int. Ed.*, 2020, **59**, 19905-19909.

Chapter 4. Further investigations of the Janus-face fluorocyclohexane motif

4.1 Further exploration on all-*cis*-hexafluoro-cyclohexanes

4.1.1 Introduction of all-*cis* hexafluorocyclohexane

As discussed, in 2015 Keddie *et. al.* reported a 12 step synthesis (Scheme 4-1) of all-*cis* hexafluorocyclohexane **4-3** [1] and this was modified to a one-step-synthesis using a Rh NHC catalyst **[Rh] 4-6**. A variety of functional groups were tolerated, some on a reasonable reaction scale.[2] This development enabled access to this class of materials for further study.
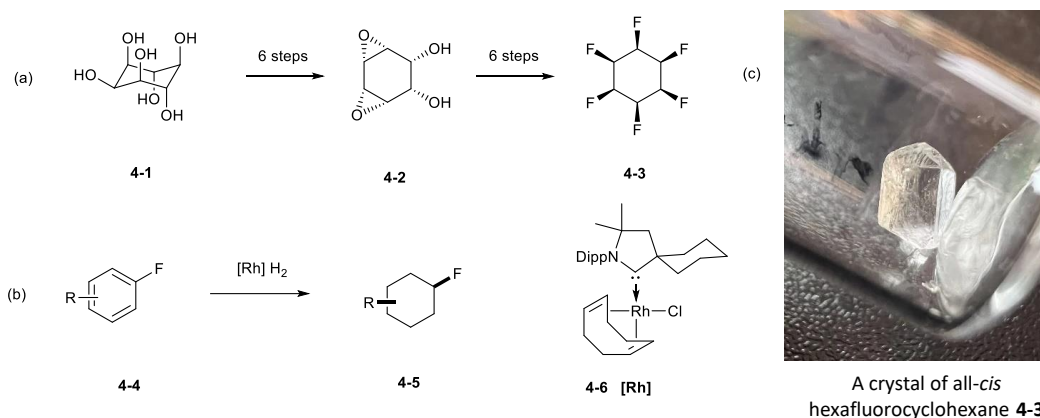
Scheme 4-1 Syntheses of the Janus fluorocyclohexanes.

4.1.2 Optimisations of the synthesis of all-*cis* hexafluorocyclohexane 4-3

The reaction condition reported by Wiesenfeldt *et al.* using 2.5 eq. of silica offered a low yield (34%) of **4-3** on a small reaction scale.[2] Therefore, a condition screening exercise was carried out to optimise the selectivity and yield. In most of the reactions summarised in Table 4-1, the starting material, hexafluorobenzene **4-7** was retained. In some cases, targeted products of **4-5** were founded, but in low conversions as judged by ^{19}F NMR. Flushing with polar

solvents suggested that products were retained on 4 Å molecular sieves. In the cases using an increased reaction pressure or elongated reaction time, this led to a mixture of hydrodefluorinated products such as **4-8**, **4-9** and other defluorinated products, all resulting in lower yields.
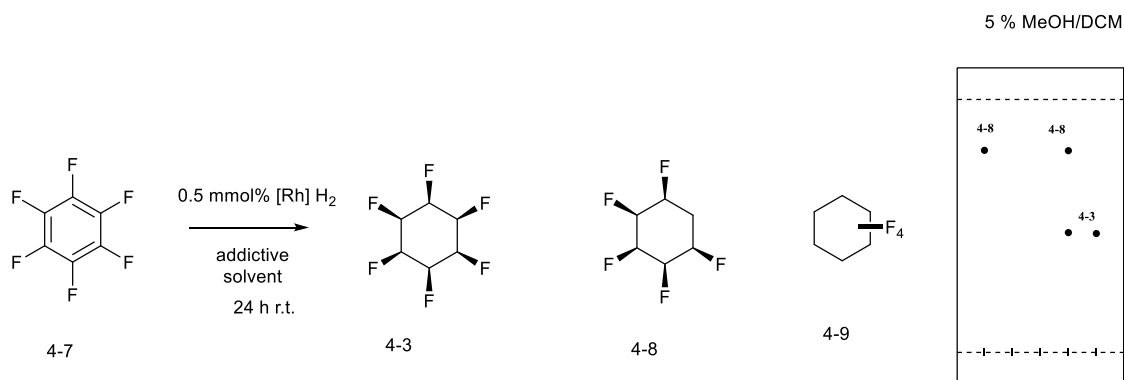
Scheme 4-2 Synthesis of all-*cis* hexafluorocyclohexane **4-3** by aryl hydrogenation and reaction side products. TLC of column fractions shows the co-ordinating species **4-8** and **4-3** are present.

In order to improve the yield of the reaction in Scheme **4-2**, a number of optimisations were explored. The reactions, which use molecular sieves, require significant volume of solvent to separate product from the absorbing solid residue. This led to a significant amount of product loss. The use of highly polar and high boiling point solvents also led to a decreased yield. Therefore, the reaction was performed with silica added, so it could be directly submitted to column chromatography, for ease of work up.

The screening of reaction conditions suggested that the raised temperature or increased catalyst loading would result in increased hydrodefluorination product **4-8**. The by-product **4-8** is mainly caused by β-dehydrofluorination during a reductive elimination step, followed by a hydrogenation of alkene.[2] There is evidence suggesting that the elongation of the reaction time would potentially convert product **4-3** to by-product **4-8**. This is possible due to the occurrence of dehydrofluorination products which would be followed by a hydrogenation of the alkene. However further investigations are required.

Entry	additive	modification	solvent	4-3	4-8
a	2.5 eq. silica		hexane	20%	< 5%
b	2.5 eq. 4 Å MS		hexane	25% *	< 5%
c	2.5 eq. silica		DCM	N.A.	N.A
d	2.5 eq. 4 Å MS		DCM	N.A	N.A
e	7 eq. silica		Hexane	95 %	< 5%
f	7 eq. silica	2 mmol % Rh	Hexane	91 %	10%
g	7 eq. 4 Å MS		Hexane	90 % *	< 5%
h	7 eq. silica	3 days	hexane	80 %	15 %
i	7 eq. silica	50 °C	hexane	85 %	12%
j	7 eq. Silica		DCM	<10%	N.A
k	7 eq. 4 Å MS		DCM	<10%	N.A
l	7 eq. silica,	1 g scale	Hexane	89%	< 5%
m	7 eq. 4 Å MS	1 g scale	Hexane	80%	< 5%

*Product was adsorbed onto sieves and caused lower isolated yield

**Table 4-1** Optimisation of the preparation of **4-3.**

Products **4-3** and **4-8** show very different behaviour on column chromatography from their TLC profiles. A significant polarity difference emerged between pure **4-3** and **4-8** where there is always a large coeluted component of **4-8** and **4-3** isolated after clearance of independent **4-3**. Significant amounts of the all-*cis*-hexafluorocyclohexane **4-3** also appeared in the lower polarity mobile phase (100% DCM experimental vs 5 % MeOH in DCM expected).

This might be due to cluster formation between **4-3** and **4-8**, or self-assembling of molecules of **4-3**. The separation of **4-3** and **4-8** required repeated columns. Pentane was added to co-evaporate traces of the residual solvent, and a significant amount of **4-3** was lost under the high vacuum due to its propensity to sublime (10% over night). A later publication from the Glorius lab, reported an improvement of hydrogenation of hexafluorobenzene to generate **4-3** in 88 % yield.[3]

4.1.3 The melting point and sublimation of all-*cis*-hexafluorocyclohexane 4-3

Different results on the melting point of **4-3** were reported by Keddie *et al.* (206 °C) and Wiesenfeldt *et al.* (decomposition at 274 °C only).[1, 2] In order to assess this discrepancy a melting point measurement was carried out carefully with a pure recrystallised sample of **4-3**. Under ambient conditions, compound **4-3** started to be sublimed around 200 °C. The sublimation process was significantly accelerated when the temperature was raised to 205 °C. This assessment confirmed a significant melting point observed at 214-216 °C which was followed by colourisation and decomposition with subsequent heating.

### 4.1.4 Synthesis of per-deuterated all-*cis*-hexafluorocyclohexane 4-3 D
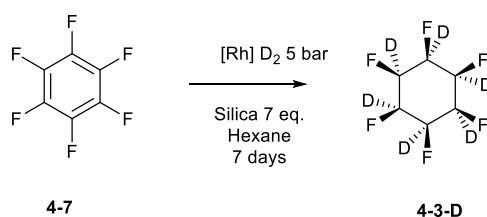
Scheme 4-3 Synthesis of perdeuterated-all-*cis* hexafluorocyclohexane.

A deuterated version of hexafluorocyclohexane was prepared with the aim of examining the influence of perdeuteration on its polarity. Due to the high cost of deuterium gas at high pressure, a test reaction was carried out with lower pressure deuterium gas but with an elongated reaction time relative to hydrogenation. In the event, the conversion was low with a distribution of various defluorination by-products, however around a 70% yield of the deuterated ring could still be isolated.

Meanwhile, a collaborative DFT calculation performed by Prof. Terrance McMahon of the University of Waterloo in Canada, suggested there is no significant difference in the C–H and C–D bond length is **4-3** and consequently no difference in the dipole moment of deuterated

4-3. The computed electronic energies for perdeuterated cyclohexane **4-3** with cations or anions show less than 0.01 kJ mol^{-1} difference.
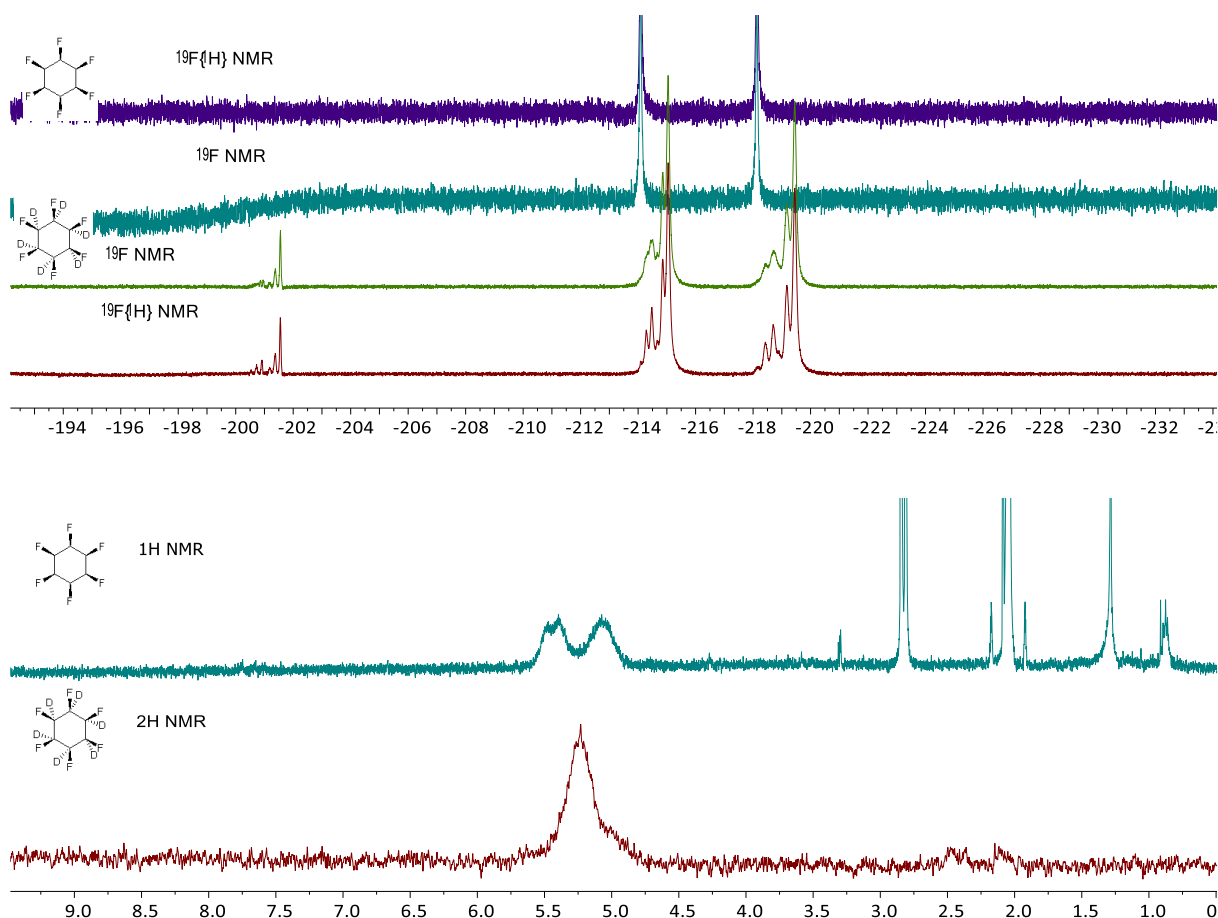
Figure 4-1 ^{1}H, ^{2}H and ^{19}F NMR of the cyclohexane **4-3** and **4-3 D**

A comparison of the ^{1}H NMR and ^{2}D NMR spectra referenced to d_6-acetone for cyclohexanes **4-3** and **4-3 D** showed no change in the chemical shift of the proton/deuterium Δδ. The ^{2}H NMR of **4-3 D** is measured at low resonance frequency, and the axial and equatorial deuterium nuclei are in fast exchange, therefore the peak at 5.25 ppm was not resolved as in **4-3**. The ^{19}F NMR shows a significant heavy atom upfield shift of ~ 1 ppm. The satellite signals suggest impurities of partially protonated/deuterated species such as $C_6F_6D_5H$ or $C_6F_6D_4H_2$ etc, showing chemical shifts of ΔδF proportional to the level of deuteration. These observations are in agreement with the reported isotope effects in H-F…D hydrogen bonding.[4] The axial fluorine at -219 ppm is shifted by 1.30 ppm and the equatorial fluorine at -214 ppm is shifted

0.96 ppm due to the axial fluorine having a stronger correlation to the adjacent proton and a larger coupling constant to the antiperiplanar vicinal protons.

4.2 Surface science study of all-*cis* hexafluoro-cyclohexane

In order to understand the physical chemistry of all-*cis*-hexafluorocyclohexane on surfaces, a gram of cyclohexane **4-3** was prepared by aryl hydrogenation. The surface studies were carried out in close collaboration with Dr Federico Grillo and Professor Christopher Baddeley at the University of St Andrews.

4.2.1 Computational studies

A model of all-*cis*-hexafluorocyclohexane was made using the Gaussian 03 software package, and the geometrically optimised vibration frequencies were calculated using the DFT 6-311G method.[5] The DFT calculation was carried out at a preliminary level. The frequencies of the calculated vibrational spectrum were corrected for the intrinsic over-estimation of the method used to overcome the intrinsic error in simulation. The resulting spectrum is attached below in Figure 4-2 for comparison and interpretation of the experimental data.
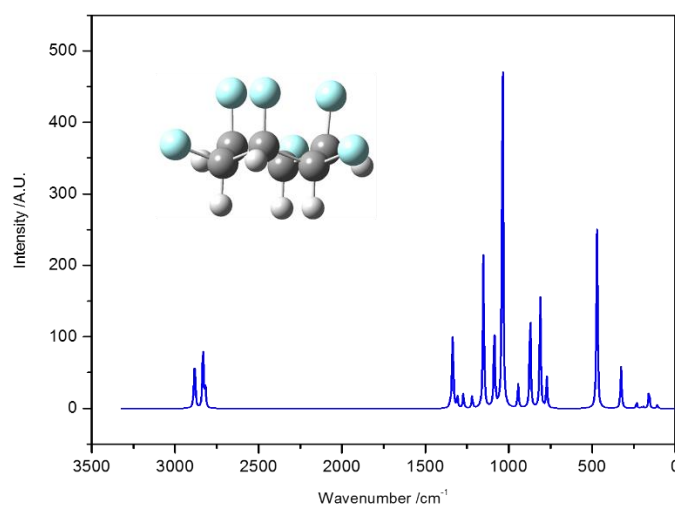

Figure 4-2 Optimized geometry and calculated vibrational spectrum of all-*cis*-hexafluorocyclohexane **4-3**.

The simulation of the vibrational spectrum was conducted with the aim of determining resonance assignments and then for a comparison with the experimental measurements. The calculated and experimental spectra are in good agreement.

4.2.2 Experiments using Reflection Absorption Infrared Spectroscopy (RAIRS)

A number of experiments were carried out using reflection absorption infrared spectroscopy (RAIRS) to explore the surface behaviour of **4-3**. RAIRS is a surface-sensitive spectroscopy so could be used to study the vibrational behaviour of molecules associated with a surface. It can inform on structure, orientation of molecules as well as the nature of their it interaction with metal surface, and this benefits from the measurements taken from reflection irradiation of the surface rather than transmission.[6]

A solution of 1 μM of all-*cis* hexafluorocyclohexane **4-3** was prepared in analytical grade acetone. The Au(111) crystal surface was flame annealed with a Bunsen burner and used to collect both a RAIR background spectrum and a gas phase spectrum. The surface of Au(111) was immersed three times in a solution of all-*cis*-hexafluorocyclohexane for 5 min each time and RAIRS were collected for each immersion. The resulting spectra are shown in Figure 4-3 with similar peaks attributed to the signals shown in the presence of acetone. The peaks around 3000 cm^{-1} are assigned to C-H stretches, around 1735 cm^{-1} to the C=O symmetric stretch, around -1365 cm^{-1} to C-H out of plane bends and around 1215 cm^{-1} to the in-plane C=O bend. The fine pattern shows an acetone related signal which is due to co-crystallisation of adducts of **4-3**.
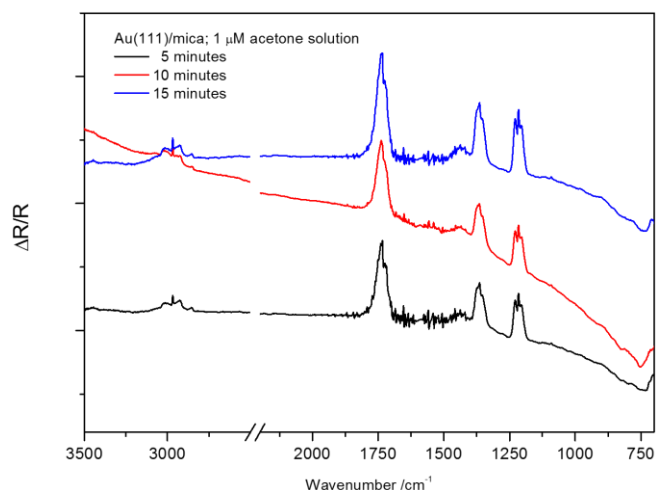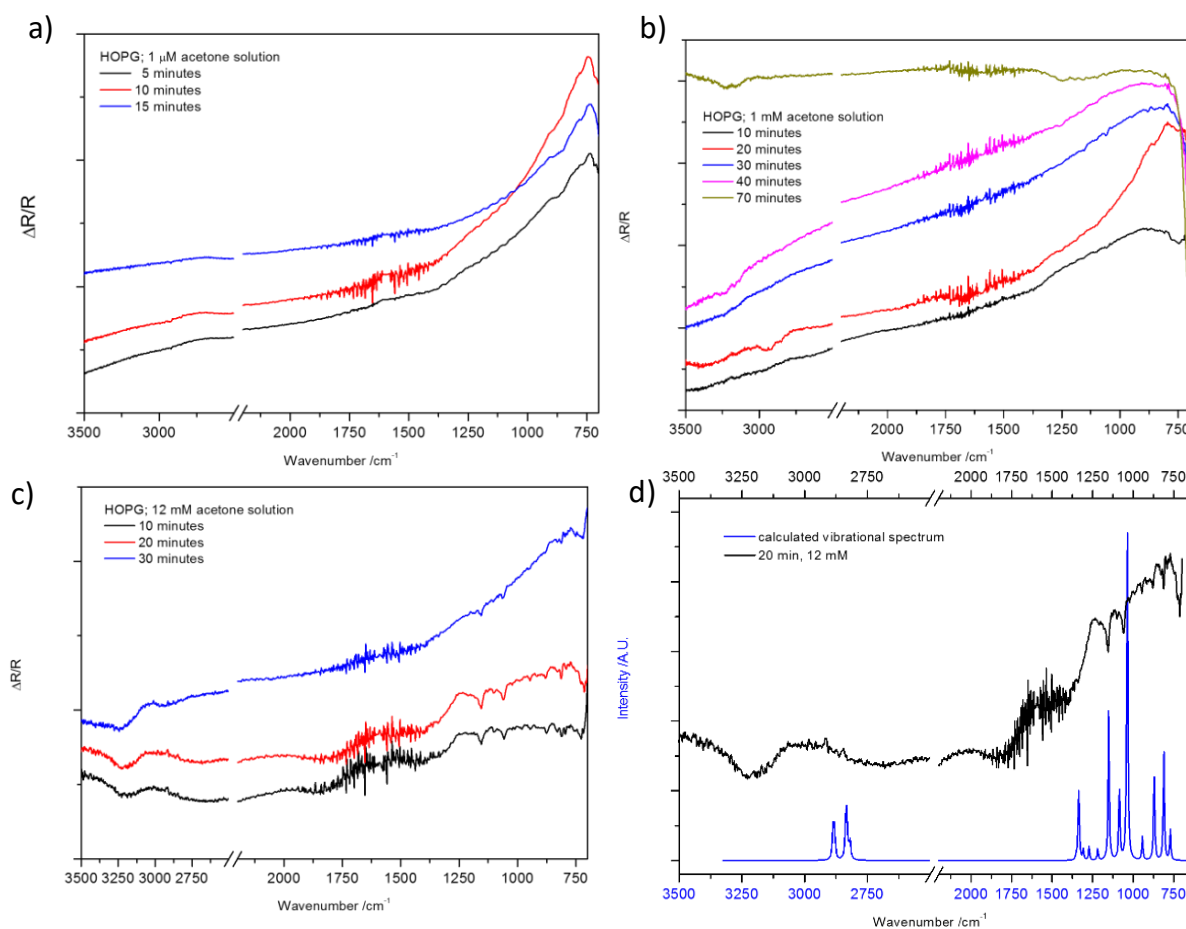
Figure 4-3 RAIR spectra collected upon immersion of an Au(111)/mica crystal on a 1 μM acetone solution of

all-*cis*-hexafluorocyclohexane **4-3**.

However, no significant band assigned to **4-3** was observed in the RAIRs spectrum. This is most likely because the signal is supressed by the large amount of acetone associated with the surface. And the observed crystal cluster of **4-3** on gold surface suggests a propensity for **4-3** to self-assemble on the gold surface. The signal for **4-3** could be potentially enhanced by increasing the immersion time.

In an attempt to reduce the excess of acetone associated on gold surface, less polar solvents were explored, however **4-3** proved insoluble. Other methods such as sublimation or chemical vapor deposition (CVD) could potentially be investigated.

To reduce the influence of acetone solvent with surface, the experiment was carried out on a different surface. A clean Highly Oriented Pyrolytic Graphite (HOPG) single crystal substrate was used to collect the RAIR background and gas phase spectra. The crystal was immersed three times in 1 μM solution of all-*cis* hexafluorocyclohexane **4-3** each for 5 minutes, and each time a measurement was taken. The spectra only show gas phase species (water and CO_2) while there was only a trace of vibration signal present at low intensity around 865-765 cm^{-1}.

Figure 4-4 RAIR spectra collected upon immersion of an HOPG crystal in a solution of all-*cis* hexafluorocyclohexane **4-3** (a) in a 1 μM acetone solution, (b) and with extend time; (c) on a 12 mM acetone solution. (d) Experimental RAIR spectrum collected upon immersion of HOPG in a 12 mM acetone solution of **4-3** for 20 min compared with the calculated vibrational spectrum.

After the same treatment of three immersions, both samples on Au(111) and HOPG were analysed *via* XPS however there we no signals recorded that related to organic bound fluorine.

The concentration of the immersion solution was increased to 1 mM and the focus was placed on HOPG due to the strong acetone signal from the Au(111) surface. The HOPG surface was cleaned and used to record a background IR gas phase spectrum. The HOPG surface was then immersed in a solution of all-*cis*-hexafluorocyclohexane **4-3** four times at 10 minutes each. A clear vibrational band at 765 cm^{-1} was observed after the first immersion. After the 2nd

immersion a signal at 2900 cm^{-1} appeared, and only after the 3rd immersion was the signal of all-*cis* hexafluorocyclohexane observed at 3250 cm^{-1}, 1150 cm^{-1}, 1060 cm^{-1} and below 800 cm^{-1} (Figure 4-4 a).

The 4th immersion did not enhance any signal intensity except broadening of the absorption at 3250 cm^{-1}. An intensive immersion was performed by extending the exposure time of the HOPG in all-*cis* hexafluorocyclohexane **4-3** solution to a further 30 minutes. A further increase of signal at 3250 cm^{-1} was observed as well as the further broadening of the band between 1300 and 1020 cm^{-1}. A small amount of a white intensity of all-*cis* hexafluorocyclohexane **4-3** solid/crystal was observed on the HOPG surface, while a very small signal relating to organic-fluorine was observed by XPS (Figure 4-4 b).

Observed /cm^{-1}	Calculated /cm^{-1}	Assignment
3200 – 3250	-	O-H (H-bonded, ice on detector)
2916	2886	C-H equatorial stretch, very weak
2845	2832	C-H axial stretch, very weak
1155	1152	C-H equatorial bend + C-F axial stretch, ↓
1099	1084	C-H axial bend + C-F axial stretch, weak ↑
1060	1035	Stretch C-F equatorial, strong
947	942	Ring breathing, asym, strong ↑
879	869	Ring breathing, asym
812	810	Ring breathing, sym, strong ↑
792	771	Ring torsion

Table 4-2 Comparison between experimental and calculated IR frequencies and their assignments for **4-3**; arrows indicate the direction of the calculated total dipole moment derivative with reference to the geometry in Figure 4-2.

In order to maximise the all-*cis*-hexafluorocyclohexane **4-3** related signals, the concentration of the immersion solution was increased to 12 mM. The HOPG surface was cleaned and recorded for background and gas phase IR spectra. The surface was immersed three times again and recorded as shown in Figure 4-4c. All-*cis*-hexafluorocyclohexane related signals were observed after the first immersion as shown in Table 4-2. All vibrational signals were

enhanced after the 2nd immersion, which decreased after the 3rd immersion when crystals of all-*cis*-hexafluorocyclohexane **4-3** formed on the HOPG surface. Figure 4-4d was plotted to compare the theoretically calculated spectra in Figure 4-2 with the experimental spectra recorded after the 2nd immersion.

The DFT calculated vibrational spectrum wavenumbers were similar to those observed in RAIRS. A strong C–F bond stretch was observed. It is suggested that the **4-3** ring is parallel to the HOPG surface. Relatively large differences were observed between computational and observed values of C–H axial, C–H equatorial and C–F equatorial stretches in **4-3**. This observation suggests that the hydrogen face is more likely interacting with the HOPG surface.

 However, as the limited signal intensity observed of **4-3**, the interaction of **4-3** with HOPG surface was not fully assigned. Therefore, it is difficult to identify that the orientation of fluorine face is point toward surface or away from the surface. Future investigation of orientation could be potentially assigned by comparing experimental data with DFT simulation of vibrational spectrum **4-3** associated with surface on two different faces on large basis set. And, higher resolution of RAIRS could be potentially achieved by optimisation of deposition method in future.

### 4.2.3 Investigation using XPS (X-ray photoelectron spectroscopy)

To further confirm the affinity of **4-3** with crystal surfaces, X-ray photoelectron spectroscopy experiments were carried out. This could offer information such as the elemental composition and chemical bonding on the surface.[7]

RAIRS measurement were conducted after the immersion of the Au(111)/mica surface and the HOPG crystal surface in a 1 μM solution, of **4-3** in acetone for 15 minutes. In the event, no signals related to the presence of fluorine were observed. However, to investigate the presence of C-F vibrations, XPS measurements were taken after immersion of the HOPG

surface in 1 mM and 12 mM solutions of **4-3**. Organo-fluorine signals were apparent as shown in Figure 4-5.

The fluorine 1s region does not show any signals after immersion in the 1 μM solution, while after immersion in 1 mM solution a peak at 687 eV, with full width at half maximum 3.22 eV appears. The peak intensity and full width at half maximum (FWHM) increased after exposure of the HOPG surface to a 12 mM solution.

Two components with maxima at 686.3 eV and 684.1 eV of similar intensity and FWHM (2.75 eV), can reasonably fit under the curve, implying that two different F environments are present. This can have different interpretations: Possibilities are F axial vs F equatorial environments, F closer to HOPG vs F further away, multilayer growth (with one set of molecules orientated one way and another set orientated the opposite way). The latter hypothesis stems from the observation of white deposits.
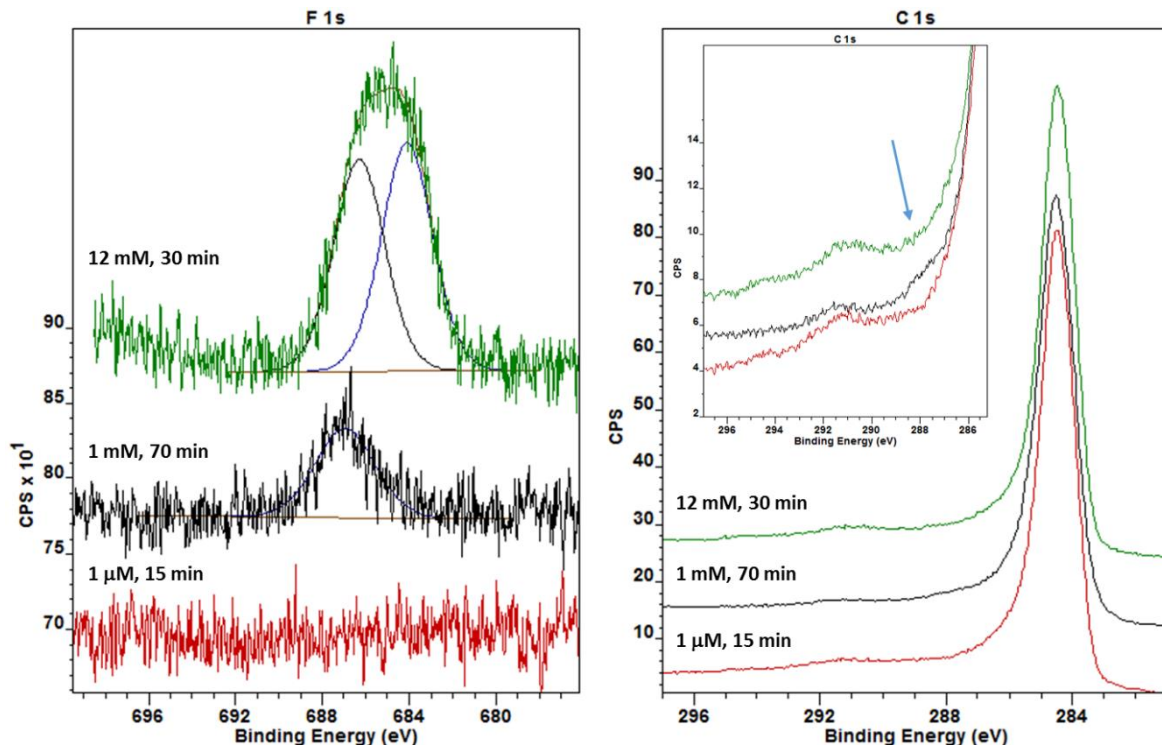
Figure 4-5 F 1s and C 1s XPS spectra collected upon immersion of an HOPG in acetone solution of **4-3**; concentrations and total immersion times.

124

The C 1s region of the XPS spectrum is more complicated, as the main carbon peak is due to HOPG (and is used for the binding energy scale calibration, 284.5 eV). The XPS handbook [7] reports a C signal related to a F environment, as in CHF, to be at ~287.8 – 290.2 eV. Perhaps this is the shoulder to the high binding energy side of the C 1s peak (indicated by an arrow in the inset). The peak seen at ~291.1 eV is attributed to a $\pi \rightarrow \pi^*$ transition typical of carbon in aromatic compounds.

The XPS spectra proves the presence of **4-3** on the HOPG surface with sufficient immersion. This is further confirmed by F_{ax} and F_{eq} signals at higher immersion concentrations. The presence of **4-3** is consistent with a reasonable fit with the FWHM of the overall F signal. The C signal is relatively poorly resolved due to excess carbon atoms in the HOPG surface.

4.2.4 Vacuum studies

The Au(111) crystal surface was selected for vacuum studies as it is easy to clean and it interacts strongly with fluorine atoms. The Au(111) surface was cleaned under vacuum by sputtering with argon ions and annealing to about 800 K for further investigation.

The vacuum experiments were performed in a capillary tube inserted into a ceramic crucible, mounted under vacuum and heated *via* a Ta filament (0.15 mm). Calibration was carried out by subliming a crystal of all-*cis*-hexafluorocyclohexane **4-3** directly into a quadrupolar mass spectrometer. A signal at m/z 193 amu matched the molecular weight of **4-3** (192.1+1) and was observed with a current of 0.8 A and voltage of 1.26 V.

Vibrational spectroscopy in vacuum was carried out on a high-resolution electron energy loss spectrometer (HREELS, VSW HIB1001), which was operated in the specular geometry with a primary beam (6 eV) at room temperature. It is a surface sensitive technique that use a high energy electron beam to probe the properties of surface material. Therefore, the vibrational and electronic properties of the sample could be characterised. The data analysis and

interpretation are very similar to IR for practical purposes, while the wavenumber (energy loss/cm^{-1}) range is broader (0-4500 cm^{-1} vs 800-4500 cm^{-1}) with poorer resolution (FWHM about 45-50 cm^{-1} vs 4 cm^{-1}). The advantage of HREELS is that the M–C, M–N and M–O (M = metal) vibrations are accessible. The fundamental selection rules for active vibrations are similar to IR, however additional rules for surface sections are applied. Only vibrations with a dynamic dipole moment normal or close to normal to the surface are active on the surface.

Three successive measurements on clean Au(111) surfaces were made, for 20 min, 30 min and 120 min in a total of 170 minduration under a pressure of 5 x 10^{-8} mbar. The resultant spectra, compared to the calculated spectrum are illustrated in Figure 4-6 and reported in Table 4-3. Spectra were normalised to the intensity of the elastic peak. Gas phase DFT calculations of an isolated molecule was performed using the B3LYP functional and the 6-311G basis set, as implemented in Gaussian 09. Geometry optimisation was carried out after which the vibrational spectra were calculated. Energy scales were corrected according to the literature to compensate for the over-estimation due to the functional/basis set combination.[5, 8] Calculated peaks were convoluted with Gaussian functions having FWHM of 50 cm^{-1}. In order to simulate the decrease in sensitivity at increased energy loss, typical of HREELS, each intensity was divided by its corresponding frequency empirically.
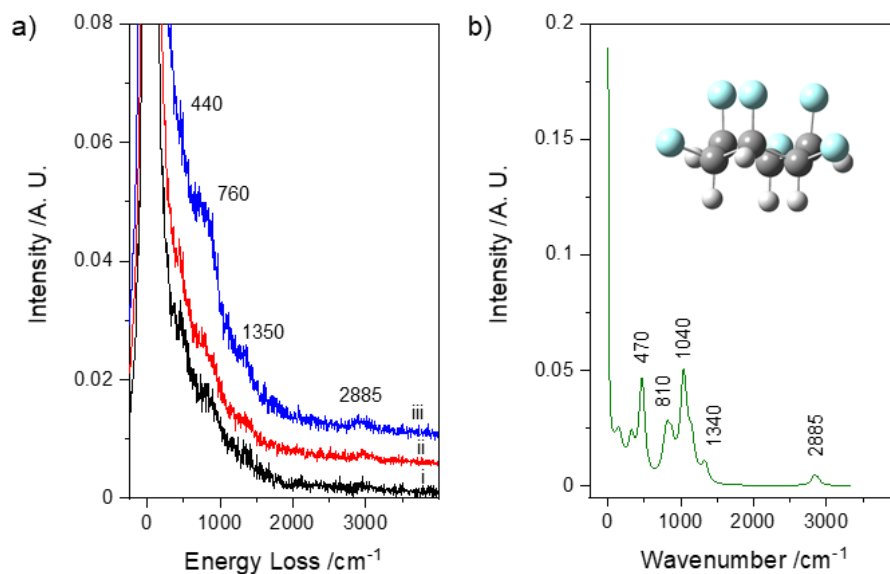
Figure 4-6 a) HREEL spectra collected following deposition of **4-3** on Au(111) at room temperature. i) 20 min; ii) additional 30 min; iii) additional 120 min. b) vibrational spectrum calculated via DFT methods; in the inset, optimised geometry of **4-3** colour coded: H, light grey; C, dark grey; F, light blue.

Experimental	Calculation	Assignment
2885	2885	CH stretch; both
1350	1340	CH out-of-plane bend; both
	1080	CH in-plane bend; CF-stretch; axial
	1040	CH in-plane bend; CF-stretch; equatorial
760	810	Ring breathing
440	470	Ring twist

Table 4-3 Observed vibrations (cm^{-1}) and comparison with calculated assignments.

Weak broad signals were observed in the spectra which is interpreted as a low coverage of **4-3** or disorder or possibly diffusing species. The predicted C–H in plane bend band and C–F stretch band around 1060 cm^{-1} were not observed in the experimental spectra. This might be because dipole moments are parallel to the **4-3** ring plane which suggests that the fluorocyclohexane ring should be parallel to the Au (111) surface.

Overall, the experimental wavenumbers are close to the computationally estimated values. However due to the nature of low resolution and high FWHM of HREELS, the signal broadening and error is relatively large. The signal intensity of **4-3** might be improved in future

by optimising the decomposition method with controlled single or multi layers of crystal growth.

Imaging in vacuum was carried out on a variable temperature Scanning Tunnelling Microscope (VT STM-Omicron) operating at room temperature with tungsten tips. **4-3** was tested on the Au(111) surface under the same conditions and evaporation source used for the vibrational spectroscopy measurements. The visualisation of **4-3** on surface might give information of interaction between gold atoms with **4-3** or its crystal cluster.

The clean Au(111) single crystal before dosing shows a typical herringbone reconstruction.[9] This is due to the peculiar characteristic of Au(111) and its ability to accommodate 4% more atoms in the surface layer, with respect to the second layer. This results in a uniaxial compression along close packed directions, so that atomic lines raised by about 1/3 Å run along ⟨11-2⟩ equivalent directions. No other surface defects were observed before deposition, as shown in cross section in Figure 4-7.
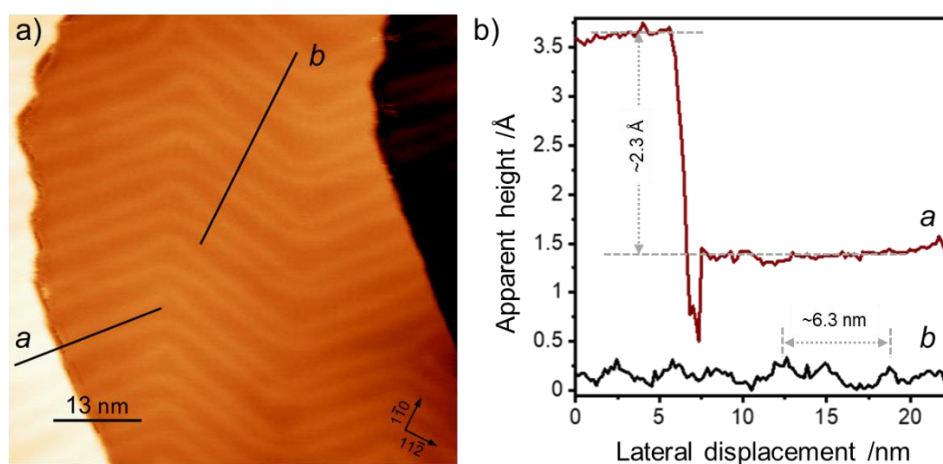
Figure 4-7 a) STM image of clean Au(111); 63.5 × 63.5 nm^2, -1.5 V, 0.5 n Å; b) Cross section measurements as indicated in a): a indicates a measured step height of about 2.3 Å; b shows the periodicity along the $[1\bar{1}0]$ direction, about 6.3 nm.

128

Upon deposition of **4-3** for 5 min at 0.76 A × 1.13 V, initial features in the form of protrusions and depressions likely appear on terraces, as shown in Figure 4-8 as a black arrow. A higher magnification area is shown in Figure 4-8 b. Higher magnification areas, collected at a reversed bias are shown in Figure 4-9; these features do not seem to change their appearance.
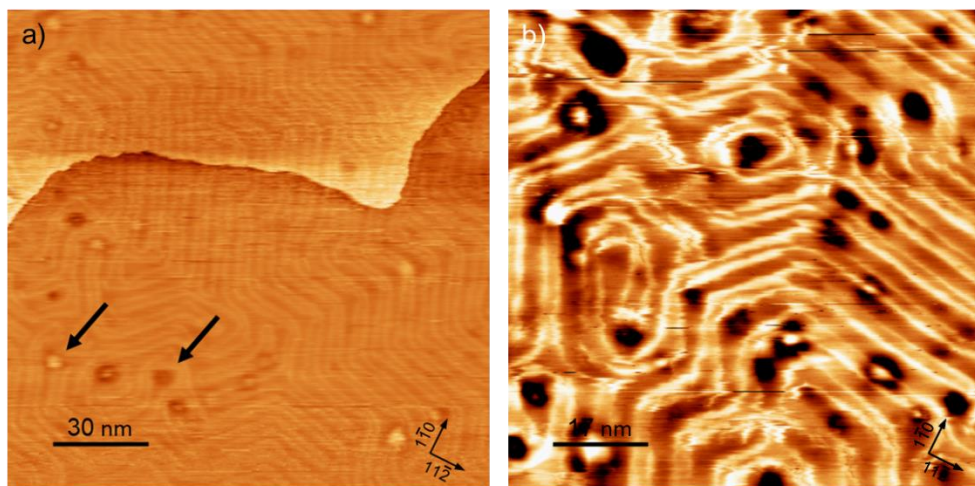

Figure 4-8 STM image showing a low coverage preparation of **4-3** on Au(111); a) bright and dark features are highlighted with black arrows. A) 30× 30 nm^2, -0.7 V, 0.1 nA; b) 87 × 87 nm2, -0.5 V, 0.15 nA.

The darkest area surrounding a bright feature on the mid-left side of Figure 4-9 seems to have a truncated triangular shape, which is an uncommon occurrence on a threefold symmetric surface. The other darker areas seem to have a more circular shape, with an average diameter of about 8 nm, whereas the electronic height of the inner and brighter core is lower, or at best just below, the height of the terrace.

Although such features can only be seen after molecular deposition, there are a few potential origins of such phenomena. One hypothesis is that such features represent small clusters of **4-3** adsorbed on the surface; the different contrast can be a sign of the molecule being orientated with the axial F atoms pointing towards or away from the surface. This could generate a different contrast, as tunnelling would occur through a different series of orbitals. No molecular resolution was obtained. Another hypothesis is that **4-3** can displace gold atoms,

in fact the herringbone reconstruction seems distorted after adsorption, and the brighter features may be the result of the agglomeration of such atoms to form a cluster. In this case the surrounding darker halo could represent the molecules, possibly diffusing around the cluster.
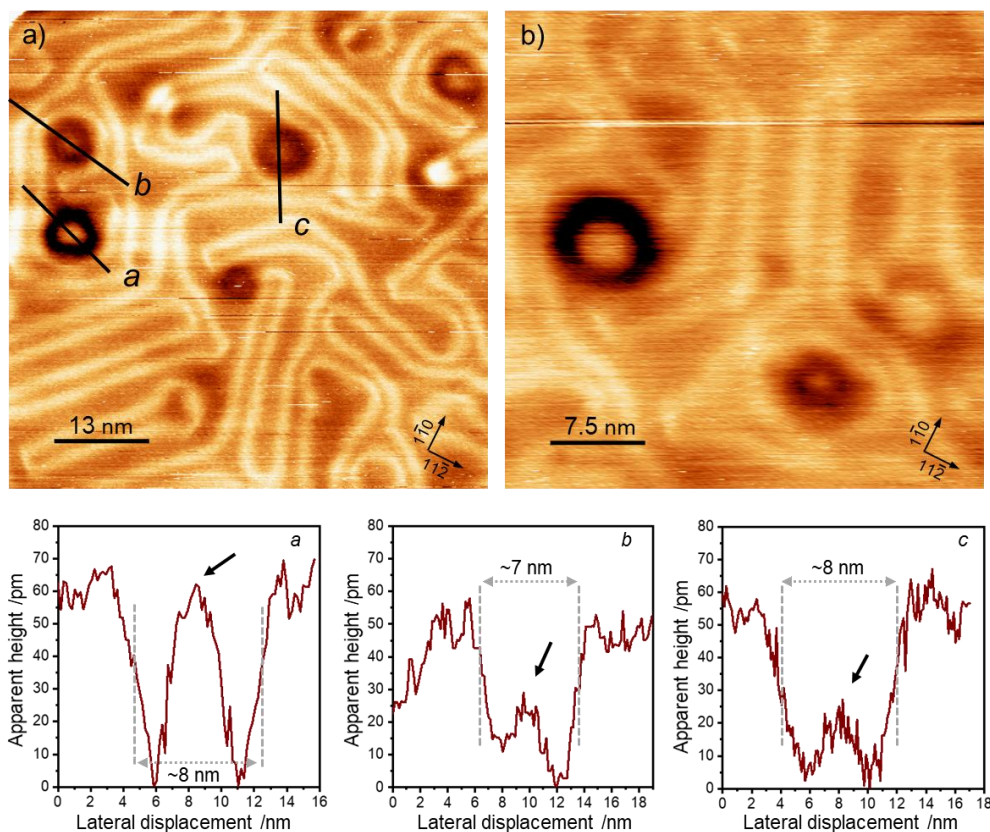
Figure 4-9 STM images showing bright features surrounded by dark areas. a) 65 × 65 nm2, -0.4 V, 0.28 nA; b) 37.5 × 37.5 nm2, 1 V, 0.2 nA. on the bottom row, line profiles as in a); the black arrows indicate the position of the features with brighter contrast.

A very high coverage preparation was achieved by depositing for 15 min at 0.8 A × 1.41 V. The surface is fully covered by a thick layer of organic deposits which do not display any order. Tunnelling was extremely difficult. Any attempt to desorb the excess molecules by annealing (up to 160 °C) was unsuccessful.

The full establishment of the physical interaction of **4-3** with gold or HOPG surface would

need further investigation, which including and not limited to the optimisation of deposition of **4-3** in varied solvent/vapor conditions, the multilayers growth control, the orientation and intermolecular interactions characterisation, and higher resolution of XPS, HREELS, AFM and SEM measurements.

4.3 Synthesis of derivatives of Janus-face fluorocyclohexyl functional derivatives

4.3.1 Reactivity study on Janus face fluorocyclohexane

It became of interest to explore the reactivity of the selectively fluorinated cyclohexyl ring as the functionalisation of the cyclohexane rings could offer access to different Janus face compounds.

4.3.1.1 Janus face fluorocyclohexane interaction with base

The hydrogens on the hydrogen face of a Janus face fluorocyclohexane ring are electron deficient. Therefore, there is a possibility that these protons could be extracted by a base if the kinetic process is faster than the β-fluorine elimination. In the event, however, the reaction shows a high conversion to exclusively 1,2,4-trifluorobenzene **4-17** by ^{1}H and ^{19}F NMR.
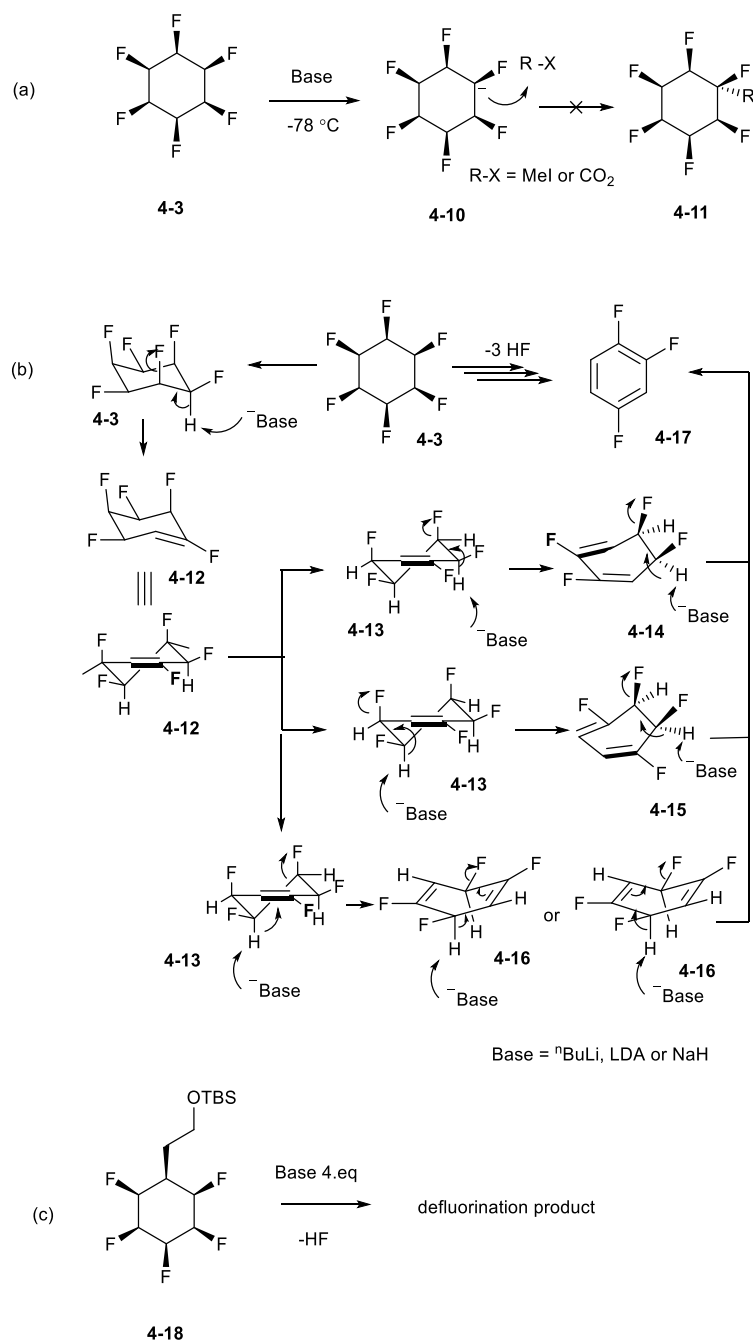
Scheme 4-4 (a*)* Deprotonation of **4-3**, (b) The proposed mechanism of formation **4-17**. (c) Dehydrofluorination

of all-*cis*-pentafluorocyclohexyl silyl ether was described in literature.[10]

A proposed mechanism of the defluorination process of **4-3** is illustrated in Scheme 4-4. All-*cis*-hexafluorocyclohexane **4-3** undergoes β-fluorine elimination. Defluorination will occur exclusively through the axial hydrogens by an E_2 elimination mechanism which requires an anti-periplanar relationship between H and F. The resultant intermediated **4-13** is drawn as a

half chair geometry which has two axial protons and its antiperiplanar elimination would be straightforward. Compound **4-16** could undergo a 1,4-elimination, and either pathway would result in trifluoro-benzene **4-17**.

Base	pK_a (H_2O)	Solvent	Stable (1 h)
Pyridine	5	$CHCl_3$	Yes
Triethylamine	11	$CHCl_3$	Yes
^{i}Pr$_2$NEt	11	$CHCl_3$	Yes
Piperidine	12	$CHCl_3$	Yes
NaOH	14	Water/DMSO	Yes
NaOMe	16	THF	90 %
^{t}BuONa	17	THF	No
LiHMDS	26	THF	No
NaH	35	THF	No
LDA	36	THF	No
^{n}BuLi	~50	THF	No

Table 4-4 Stability of silyl ether **4-18** in various bases at r.t. and in the literature.[10]

As reported by Clark *et. al.*, Janus face fluorocyclohexyl rings are compatible with mild nitrogen bases, however defluorination is observed with strong bases p*Ka* > 16.[10, 11] A number of experiments in Chapter 6 demonstrated that NaH is tolerated if only 1 equivalent of base is added and there is a substituent with a more acidic proton. It remains challenging to find a suitable base to deprotonate **4-3** and lead to a successful reaction with an electrophile.

4.3.1.2 Interaction of the Janus face fluorocyclohexane 4-3 with a super acid

A collaboration was carried out with Prof. Thibaudeau at the University of Poitiers in France. Compounds **4-3** and **4-19** were prepared on a relatively large scale (~1 g each) and reacted

with superacid media of HF/SbF$_5$ in a 1:1 ratio at -50 °C.

For the reaction with compound **4-3**, the formation of SbF$_6^-$ was observed around -125 ppm. The ^{1}H, ^{19}F NMR and ^{1}H-^{19}F HMBC suggested a partially activated species such as **4-20**. A ratio of 2:3 with F$_{ax}$: F$_{eq}$ was observed which suggested an averaged signal with one axial fluorine coordinating with SbF$_6^-$ and shifted downfield. No significant decomposition occurred suggesting that compound **4-20** might be able to react with nucleophiles.
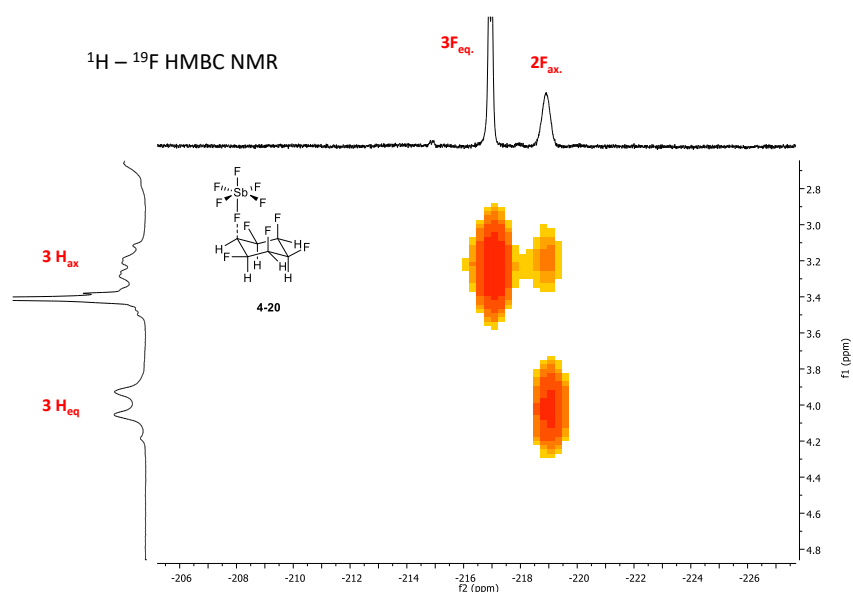
Figure 4-10 The ^{1}H-^{19}F *in-situ* NMR at -50 °C monitoring the reaction of **4-3** in superacid media.

For the reaction with compound **4-19**, defluorination was observed. In the ^{13}C NMR, a carbocation -**C**$^+$H- peak was assigned at 218.7 ppm while the vinyl carbons in F**C**=C–C$^+$H- was assigned at 211.6 ppm and FC=**C**–C$^+$H at 138.7 ppm. The ^{1}H- and ^{19}F- 2D NMR spectra suggest formation of carbocation **4-25**.
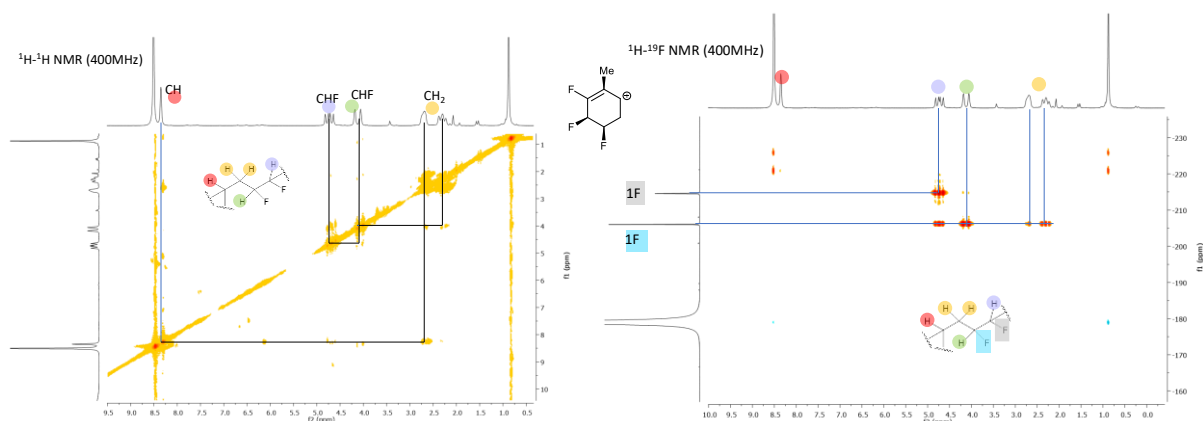
Figure 4-11 the ^{1}H-^{19}F *in-situ* NMR at -50 °C monitoring the reaction of **4-3**.

A putative reaction mechanism is proposed as illustrated in Scheme 4-5. E1 Elimination of the electron rich axial F in compound **4-19** generates carbocation **4-21** and then elimination occurs to form a more stable carbocation **4-23** with the positive charge stabilised by an adjacent π bond. The conjugated carbocation **4-25** appears to be the most favoured species stabilised by the adjacent electron rich alkene.
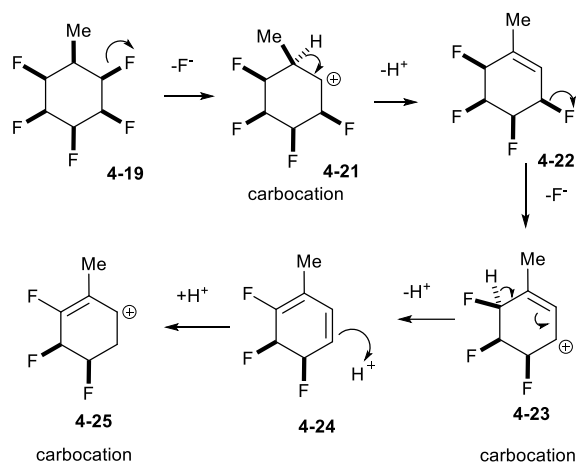
Scheme 4-5 Proposed mechanism for putative carbocation **4-25**.

The reaction of compounds **4-3** and **4-19** with superacids demonstrates the formation of carbocations from Janus face fluorocyclohexanes. It remains to trap the carbocation with nucleophiles, which would support the above hypothesis and may offer an approach to Janus

face cyclohexyl derivatives.

4.3.1.3 Exploration of halogenation of all-*cis*-hexafluorocyclohexane 4-3

A series of reaction conditions was explored in an attempt to halogenate **4-3**, and particularly by a radical process. **4-3** is inert to elemental bromine and iodine, even at raised temperature (100 °C), with or without UV irradiation. The radical initiator NBS, was explored. In all attempts, only a trace conversion was observed, even after heating in a solution of CBr_4 at 200 °C. The product, indicated by the ^{19}F-NMR signal (Figure 4-12), could not be isolated by chromatography.
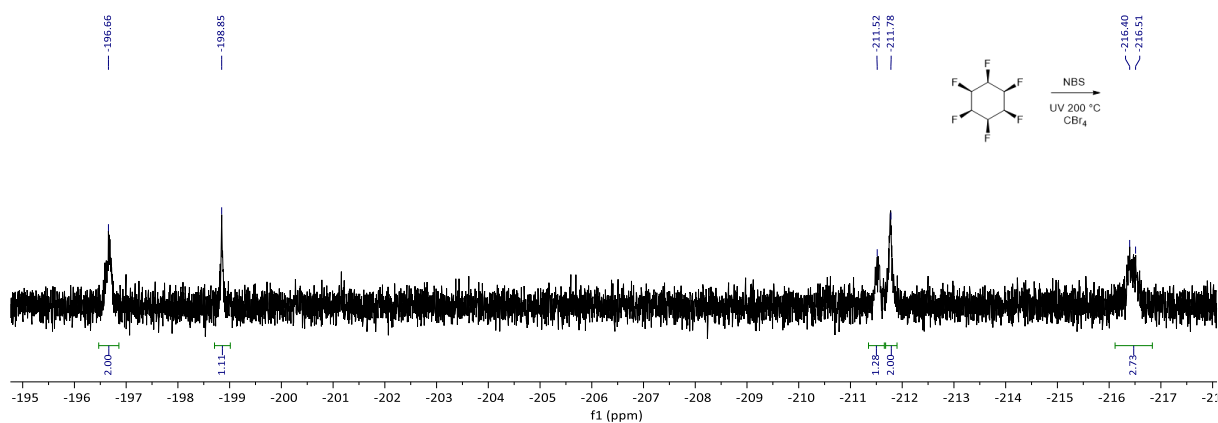
Figure 4-12 ^{19}F NMR spectrum of the NBS reaction with **4-3**.

4.3.2 Synthesis of amine derivatives of Janus-face fluorocyclohexyl motifs

It became an objective to develop routes to amines carrying Janus face fluorocyclohexanes due to their potential in bio-conjugation and as building blocks for medicinal chemistry research. The pentafluoro-aniline **4-26** and pentafluorophenyl-ethylamine **4-27** were used as substrates due to their commercial availability. Aryl hydrogenation attempts of the aniline or amines were unsuccessful without protecting groups on the nitrogen (Scheme 4-6).

136
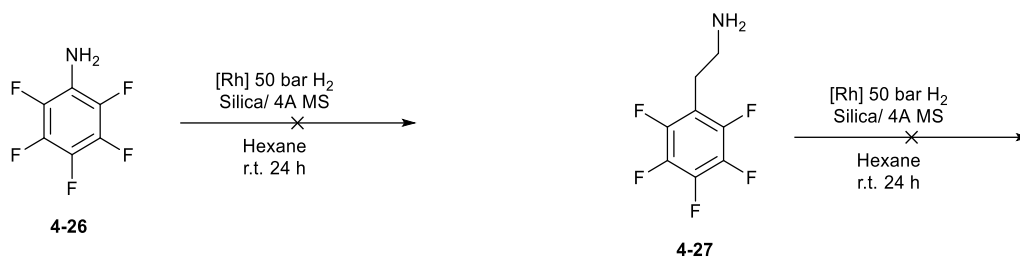
Scheme 4-6 Direct aryl hydrogenation of **4-26** and **4-27** failed without N-protection.

The preparation of the NHBoc protected amine **4-28** proved challenging. A number of conditions were attempted for the preparation of **4-28** and **4-31**, however without a strong base and a high temperature, there was no conversion to N-Boc protected product. In addition, when a high temperature was used, over protection on the amine occurs as the dominant product, even when only 1 equivalent of Boc-anhydride was added. This presumably arises because once the first Boc group is installed in **4-28**, the nitrogen can be more readily deprotonated for a second acylation.
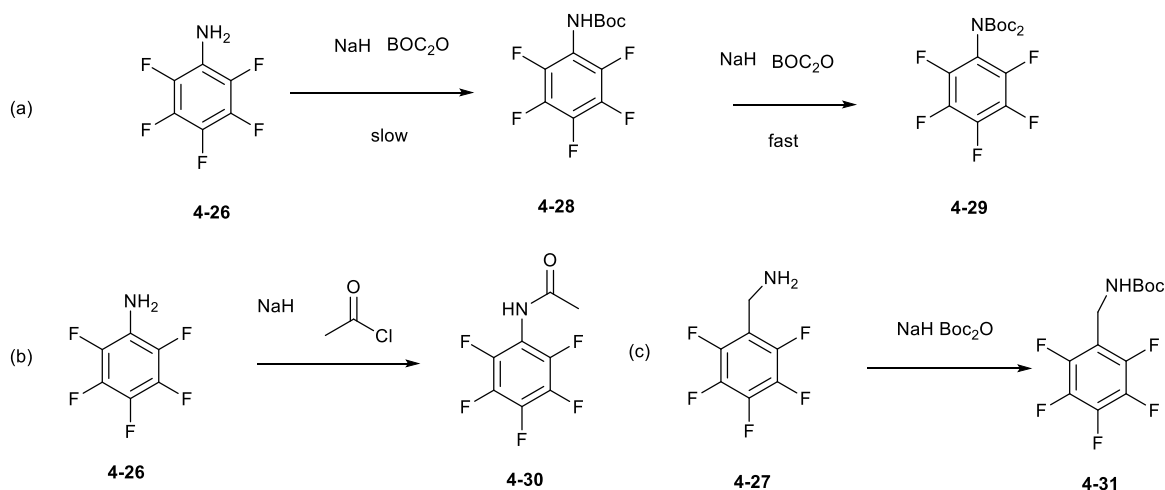
Scheme 4-7 Protection of the amine derivatives.

Strong bases such as sodium hydride or ^{n}BuLi was used to prepare the amide salt, such that the deprotonated anion avoids over protection. This method resulted in a low yield of NHBoc-protected pentafluoro-aniline **4-28** with a number of side products bring formed.

Defluorination occurred as a side reaction in the preparation of the Boc-pentafluoro-aniline **4-28**.

Aryl hydrogenation of the Boc-protected amines remained challenging. Success was achieved only with raised temperature or extended reaction times and hydro-defluorination was significant during the hydrogenations.

The acetyl group was explored as another protecting group for **4-30**. As acetic anhydride is not nucleophilic enough, the pentafluoro-aniline protection was achieved by reaction of pentafluoroaniline with acetyl chloride and sodium hydride (Scheme 4-7 b).
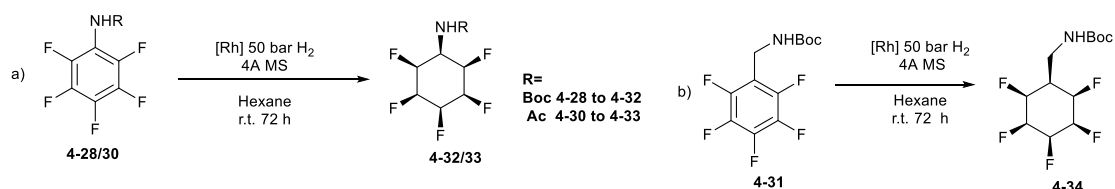
Scheme 4-8 Aryl hydrogenations of protected amines.

The hydrogenation of acetyl aniline **4-30** proceeded in low yield. Only a trace amount of product was observed by ^{19}F NMR. The Boc protected amine **4-28** and **4-31** could be hydrogenated to the desired cyclohexanes **4-32** and **4-34** in 26 -27 % yield in a slightly modified reaction. This involved an extended reaction time (72 h) or a raised temperature (50 °C) and with supporting additives of 4 Å molecular sieves.

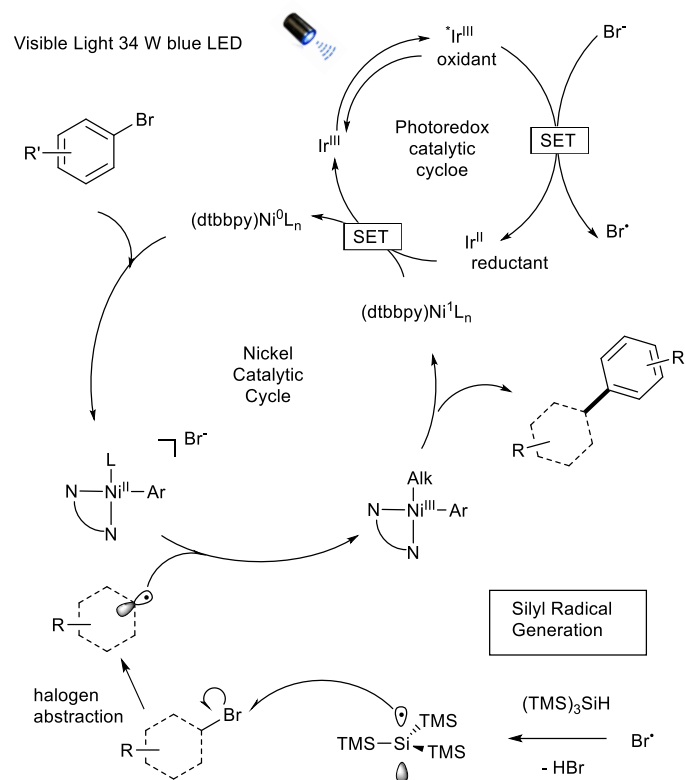### 4.3.3 MacMillan photoredox coupling reactions
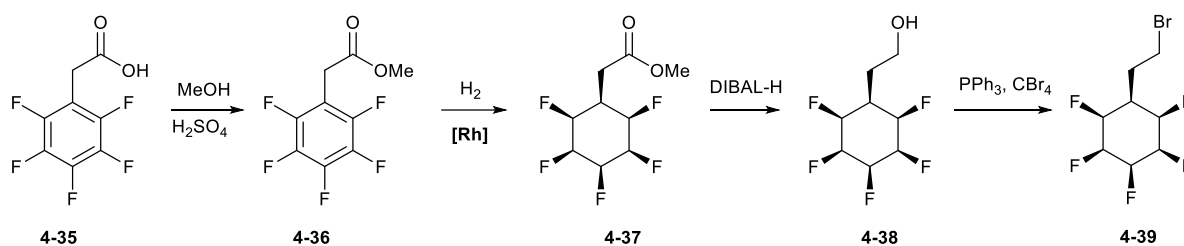
Scheme 4-9 Previous syntheses to Janus face fluorocyclohexyl building blocks.[6]

Pentafluorophenylacetic acid is a useful starting material to functionalised Janus face fluorocyclohexane rings leading to the corresponding carboxylic ester and acid, alcohol and the primary bromide products **4-35**– **4-39** as shown in Scheme 4.9 .[10]
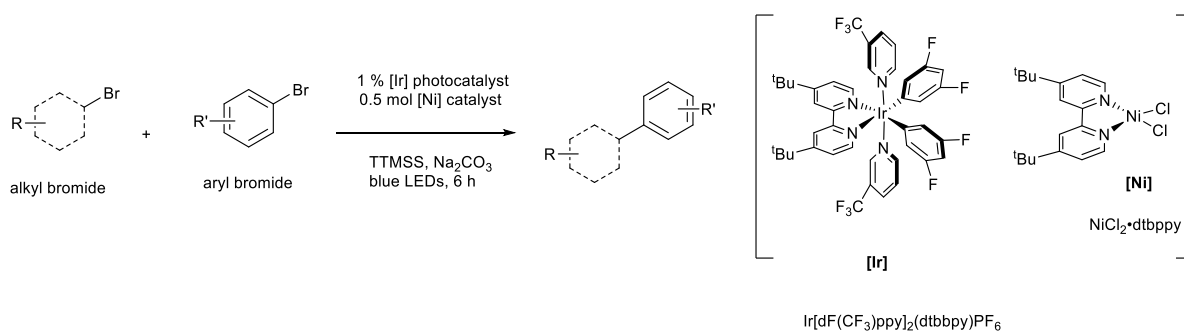

Scheme 4-10 MacMillan photoredox coupling between sp^2 arly halide and sp^3 alkyl bromide.[12]

The primary alkyl bromide **4-39** is obviously an interesting building block both as a standard electrophile but also for transition metal catalysed cross coupling reactions. The MacMillian photoredox cross coupling reaction shown in Scheme 4-10 was explored to couple the bromide **4-39** with an aryl bromide. The absence of palladium in the coupling conditions should also minimize unwanted hydrodefluorination side reactions.[13]

Scheme 4-11 Mechanistic cycle for silyl-mediated Ni cross-coupling.[12]

The MacMillan photoredox coupling between a sp^3 and a sp^2 carbon was demonstrated by using tris(trimethylsilyl)silane under metalla-photoredox catalysis as shown in Scheme 4-11. A photocatalytic generated silyl radical is proposed to abstract the halide from the alkyl bromide and to generate an active nucleophilic radical for coupling. It was already demonstrated that the alkyl bromide could be primary, secondary or tertiary.[12]
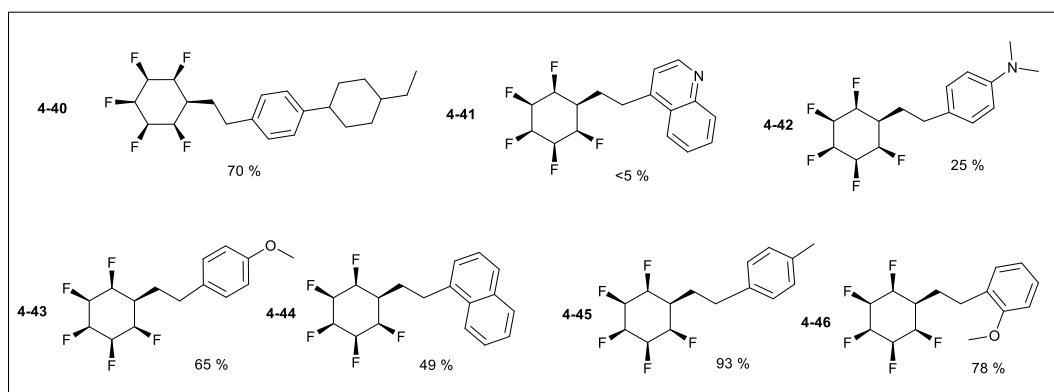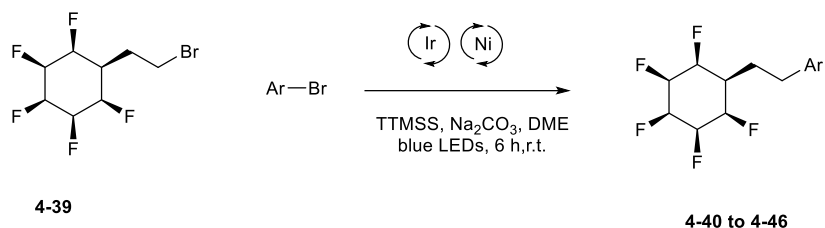
Scheme 4-12 Janus face fluorocyclohexane derivatives synthesised by the MacMillan photo-redox protocol.

Modification of the reaction conditions was made by diluting the substrate concentration. This was because the solubility of bromide **4-39** is low in the solvent 1,2-dimethoxyethane. A number of substrates were subjected to photoredox cross coupling as shown in Scheme 4-12. The reaction afforded products in moderate yield with non-functionalised alkyl substrates. However, the reaction conversion with the quinoline ring was noticeably lower, perhaps due to coordination with the catalysts.

4.4 Janus face fluorocyclohexane in amino acids and peptides

4.4.1 Introduction

As discussed in Chapter 1, the Janus face fluorocyclohexyl motif shows an extraordinary polarity and may find a role in drug development. Since the aryl hydrogenation approach allows access to 1 g scale preparations after optimisation, a direct aryl hydrogenation of the aromatic ring in L-(*S*)- pentafluorophenylalanine **4-47** became possible. Success would deliver all-*cis*-pentafluorocyclohexylalanine amino acids (**CyF₅**) such as **4-48** and **4-51**. The highly unusual side chain would introduce entirely unique properties for an amino acid and allow its introduction into peptides.
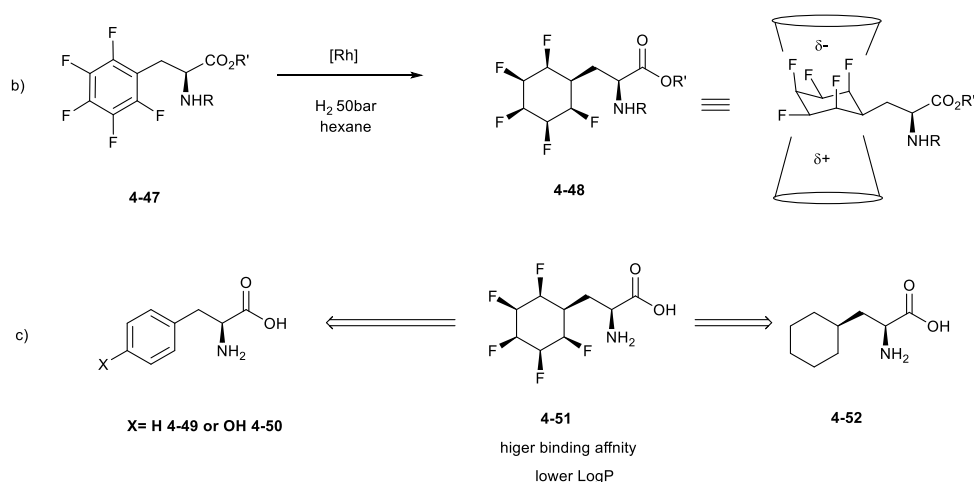
Scheme 4-13 Approach to fluorocyclohexyl amino acids.

The hydrogen face in these fluorocyclohexanes have an affinity for aromatic rings (gas phase ~6-7 kcal mol^{-1}) involving C–H...π interactions.[1, 14] The fluorocyclohexane ring also shows strong affinity with ions in the gas, solution and solid phases.[11, 15] Such behaviour suggested that an amino acid would become a versatile unit for the introduction of the ring into peptides and proteins. A key focus of the project therefore aimed to explore such an approach and also to investigate interactions with polar amino acid side chains.

142
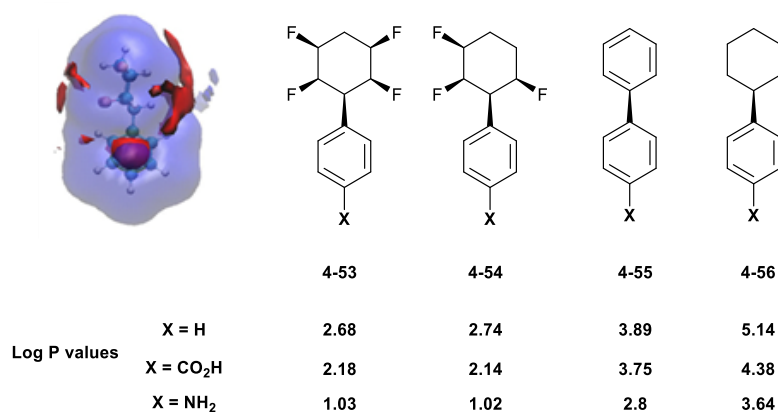
Figure 4-13 Association of water (red) around the aryl tetrafluorocyclohexyl motif. Water associates with the hydrogen face of the ring.

The Janus face fluorocyclohexane ring has an important aspect in that polarity increases with an increasing number of fluoromethylene (-CHF-) groups. The phenyl, benzoic acid or aniline derivates of Janus face fluorocyclohexanes, carrying up to four fluorines shows a reduction of up to ~2.5 units in Log Ps compared to the corresponding non-fluorinated cyclohexyl derivatives. A molecular dynamics study indicated that the increase in polarity and consequentially decreased Log P, emerged because of water association through hydrogen bonding to the hydrogen face the fluorocyclohexane ring. The association benefits from fluorines polarising the geminal fluoromethylene hydrogens.[16] Therefore, the Janus face fluorocyclohexyl building blocks become able to provide a binding site without a significant increase in log P, which is otherwise generally problematic for aliphatic motifs.

These fluorocyclohexane rings are also dissimilar to typical aryl rings, as there is a significant difference in polarity and partial charge on each side of the ring. The electropositive and electronegative faces represent a novel physicochemical profile without obvious counterparts or analogues elsewhere. The ring system could potentially interact with charged or polarised groups on the surface of proteins. Therefore, the Janus face ring interactions are potentially interesting for pharmaceutical chemistry.

143

4.4.2 Aims and objectives

A combination of Janus face fluorocyclohexane ring containing amino acids, dipeptides and tripeptides was envisaged, to prepare a structural series predisposed to form supramolecular assemblies at neutral pH in buffer.[17, 18] It is known that tripeptides can generate supramolecular macroscopic assemblies (gels) which have been analysed by TEM, AFM and X-ray structure analysis.
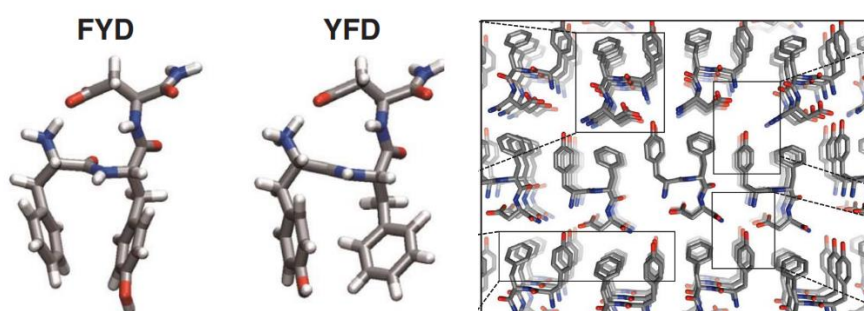
Figure 4-14 Previously described conformations for FYD and YFD peptides and a crystal structure (FYD), showing different interfaces in a lattice.[17, 18]

The primary target structures for this study followed closely the structures of the reported tripeptides developed by Lampel and Frederix *et.al*. [17, 18] These tripeptides had C-terminal carboxamide (RCONH$_2$) containing phenylalanine (**F**), aspartic acid (**D**) and tyrosine (**Y**) residues, amino acids that are predisposed to self-assembly at pH 8 in phosphate buffer. For example, the **FYD** tripeptide was revealed to adopt the conformation shown in Figure 4-14, and this conformation can reasonably be expected to be reinforced when **F** (phenylalanine) or **Y** (tyrosine) is replaced by an amino acid containing a Janus face fluorocyclohexane ring. The aim of this aspect of the project was to prepare a range of tripeptides by rearranging **D**, **F**, **Y**, **CyF$_5$** and other amino acids as illustrated in Figure 4-15. It was envisaged that the tripeptides could be constructed by either solution or solid phase peptide synthesis.[19, 20]

Figure 4-15 Target peptide structures.

4.4.3 Synthesis of 1,2,3,4,5-all-*cis*-pentafluorocyclohexyl-alannine (CyF₅)

At the outset, test reactions were explored for aryl hydrogenations in an effort to obtain the Janus face cyclohexyl version of phenylalanine.

Scheme 4-14 Preparation of protected amino acid Boc-F₅Phe-OMe **4-48**.

Commercially available Boc-pentafluorophenylalanine **4-58** was converted to its methyl ester by trimethylsilyl azomethane, a reaction that occurred in quantitative yield. An initial attempt using standard fluoroaryl hydrogenation conditions showed no conversion to the desired product and therefore conditions screening was carried out to try to optimise the reaction.

Entry	Addictves	solvent	Conditon	yield
a	7 eq. Silica	hexane	1 day r.t.	N.A.
b	450 mg 4 Å MS	hexane	1 day r.t.	N.A.
c	7 eq. Silica	THF	1 day r.t.	N.A.
d	7 eq. Silica	DCM	1 day r.t.	N.A.
e	7 eq. Silica	Et2O	1 day r.t.	N.A.
f	7 eq. Silica	hexane	1 day 50 °C	N.A.
g	7 eq. Silica	hexane	3 day r.t.	10 %
h	450 mg 4 Å MS	hexane	3 day r.t.	30 %
i	450 mg 4 Å MS	hexane	1 week r.t.	25 %
j	1 g 4 Å MS	hexane	3 day r.t.	45 %

Table 4-5 Reaction conversions of the preparation of **4-48**.

Aryl hydrogenation of substrate **4-47** was very poor although compared with silica, 4 Å MS offered higher yields. The reaction could be scaled up to about a 3 mmol scale. Further scaling reduced the yield dramatically, most probably due to poor stirring in the pressurised autoclave.
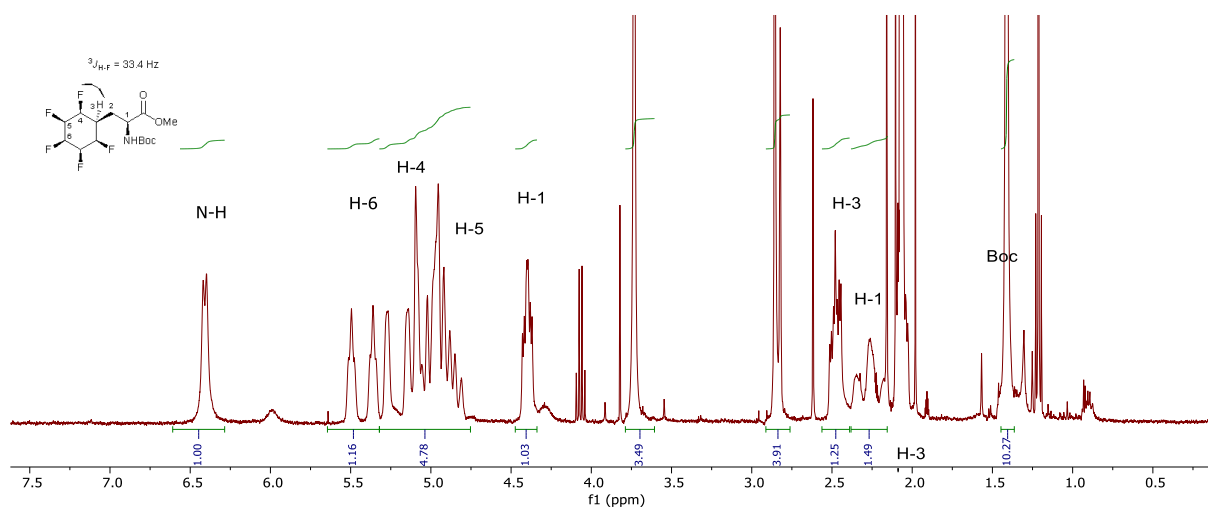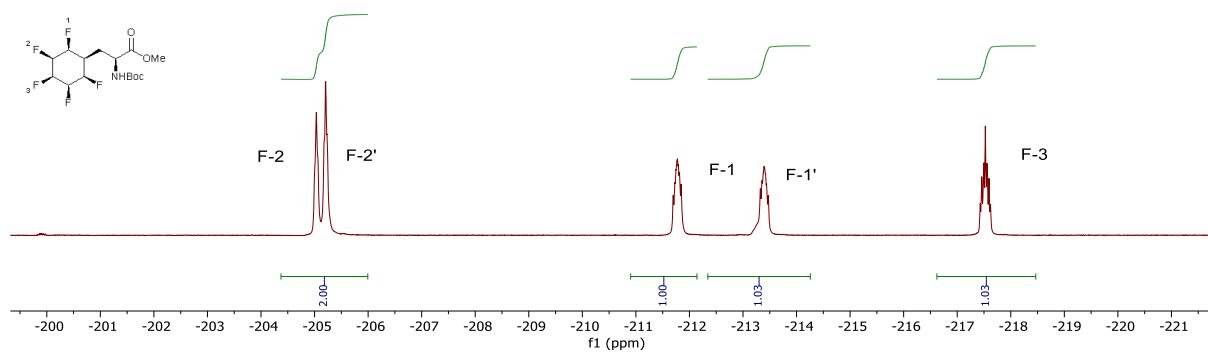
Figure 4-16 The ^1H and ^{19}F NMR of Boc-**CyF$_5$**-OMe **4-48**.

An X-ray derived structure (Figure 4-17) of product **4-48** was obtained after recrystallisation in methanol and DCM. The three fluorines at positions 2, 4 and 6 adopt an axial orientation, despite electrostatic repulsion between the fluorine atoms. There are strong intermolecular contacts such as hydrogen bonding, where the carbonyl-to N-H distance is about 2.03 Å.
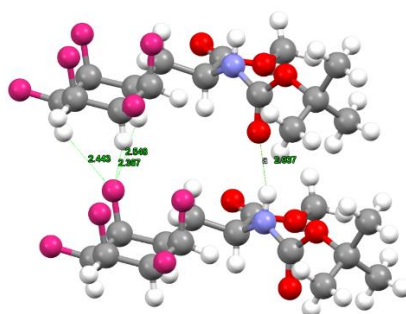
Figure 4-17 X-ray structure of Boc-**CyF$_5$**-OMe **4-48**.

One of the axial fluorines is sitting underneath the hydrogen face of the Janus ring and makes contact with all three axial protons evenly (CF...H-C 2.4 Å) forming a triangular pyramid. These contacts indicate strong self-assembling interactions associated with the Janus ring.

A few derivatives of protected amino acids (**4-48** to **4-60**) were prepared with ethyl or *t*-butyl ester protection or N-methyl protection on the amino group. However, no improvement in the aryl hydrogenation yield was observed with those protecting groups.

Protection group	Addictves	yield
-Boc -OMe **4-48**	450 mg 4 Å MS	40%
-Boc -OEt **4-58**	450 mg 4 Å MS	N.A.
-Boc -O^{t}Bu **4-59**	450 mg 4 Å MS	defluorination
-NMe -OMe **4-60**	450 mg 4 Å MS	N.A.

Table 4-6 Protecting group scan for aryl hydrogenations.

4.4.4 Preparation of all-*cis*-pentafluorocyclohexylalanine derivatives

Various deprotection methods were explored on the hydrogenated product **4-49** to release the functional groups for peptide assembly reactions.
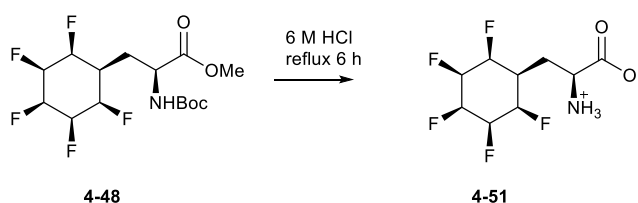
Scheme 4-15 Hydrolysis of **4-48** to amino acid **4-51** and its zwitterion structure.

Aqueous HCl was used to hydrolyse the methyl ester on the carboxylate side and remove the Boc group on the amine side. ^{19}F -NMR indicated a 95 % conversion to the desired amino acid **4-51**, with only traces of defluorination. A crystal structure presents as a zwitterion, and unexpectedly HCl is not retained as an adduct, which was presumably removed under high vacuum on work up.
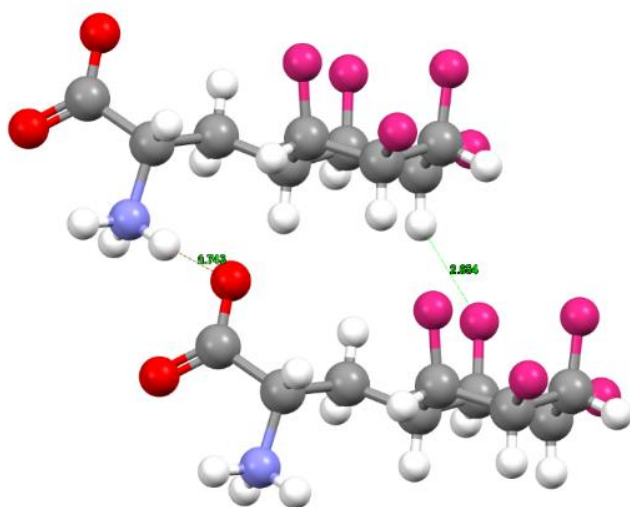
Figure 4-18 X-ray structure of **4-51.**

By comparison with protected amino acid **4-48** the $N^+H^-\ldots O=C$ (carbonyl) distance in **4-51** is much shorter (1.74 Å compared with **4-48** for 2.0 Å). The fluorine face of the cyclohexyl ring is further away from the hydrogen face, caused presumably by stronger ionic bonding and Janus face fluorocyclohexyl packing.

The N-Boc group could be safely removed after treatment with TFA. NMR showed only a trace of defluorination and the product was isolated as a gel and used neat for further transformations.
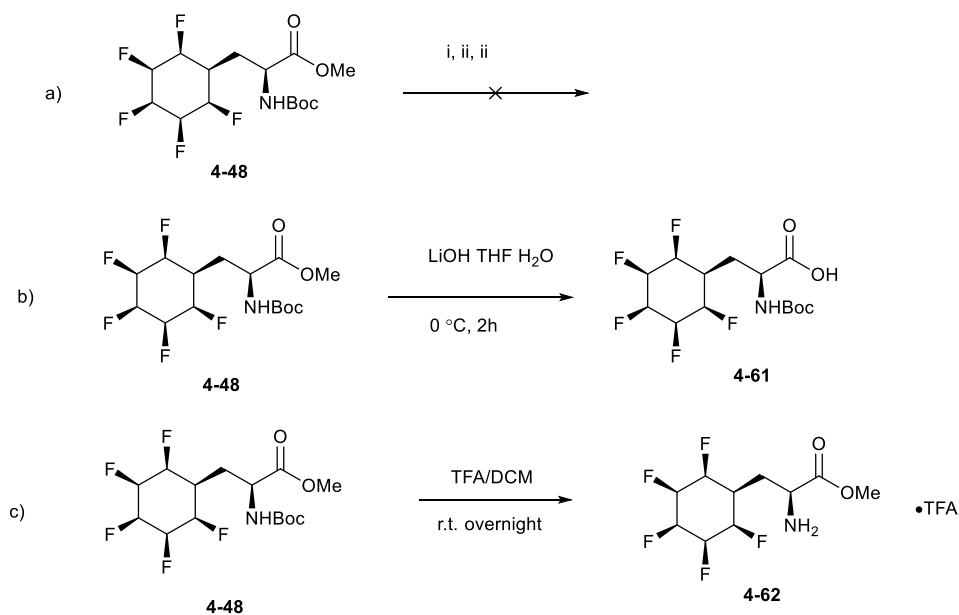
Scheme 4-16 Selective deprotection of **4-48**. (a) i) MeI, r.t., overnight, ii) BF₃ ·Et₂O, r.t., overnight, iii) KOH, 2 h; (b) Methyl ester deprotection by 2 eq. LiOH·H₂O, THF, H₂O, 0 °C, 2 h; (c) Boc deprotection by TFA.[10]

The selective hydrolysis of methyl esters with base is difficult as the conditions lead to defluorination. Most strong inorganic bases are not compatible with the all-*cis*-pentafluoro-cyclohexyl ring. Deprotection with methyl iodide was also attempted, however the methyl group was retained. Mildly basic conditions were explored with lithium hydroxide at low temperature. The reaction was successful and gave product in 85 % yield and with only a trace of starting material. The lithium salt is not present in the crystal structure of **4-61** after workup and recrystallisation.
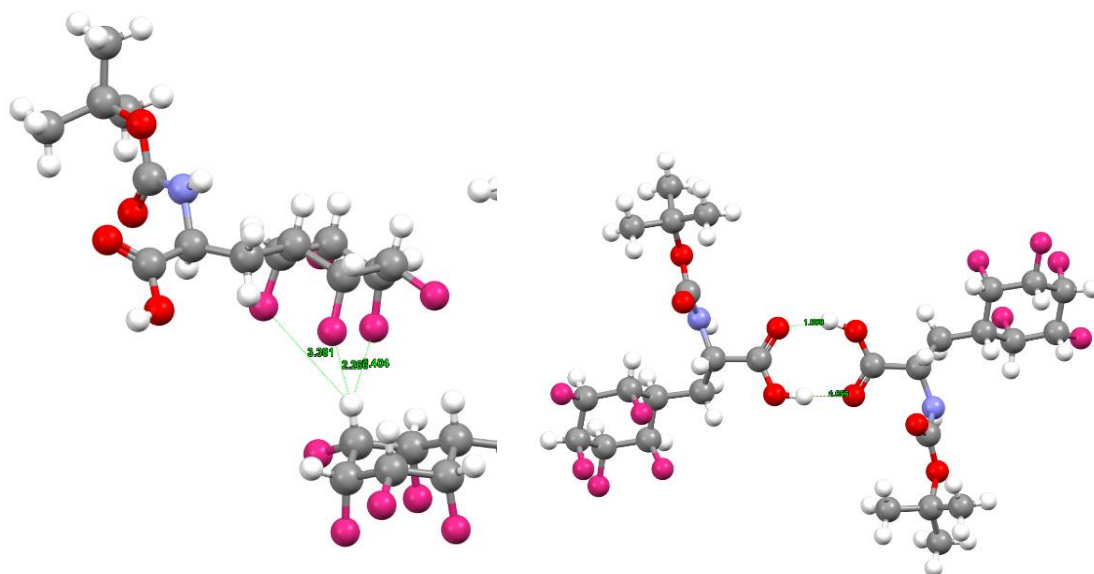
Figure 4-19 X-Ray structure of **4-61**.

The crystal structure of **4-61** shows close contact of the axial hydrogen to the axial fluorine with a 2.26-2.49 Å contact distance. This orders the packing arrangement of the Janus rings. Unlike other derivatives, the N-H has only a very weak (2.69 Å) association with the carbonyl group in this structure.
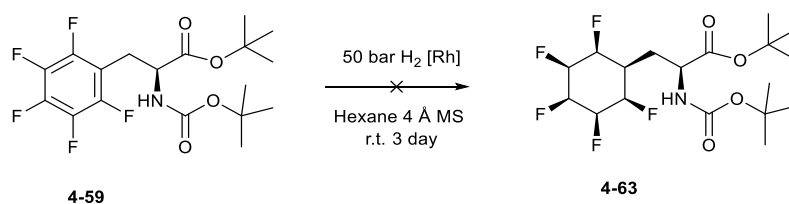
Scheme 4-17 Synthesis of compound **4-63** Boc-**CyF$_5$**-O^{t}Bu.

As illustrated in Table 4-6, Boc-**CyF$_5$**-OB^{t}Bu **4-63** was prepared by direct aryl hydrogenation, to explore any steric effect of the t-butyl groups on the rhodium catalyst hydrogenation reaction. However, the reaction showed no improvement in conversion.
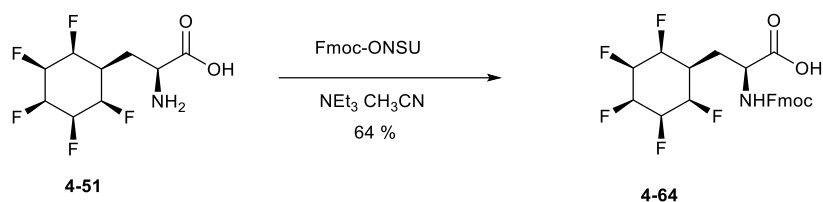
Scheme 4-18 Synthesis of Fmoc protected **4-64**.

The Fmoc protected amino acid was prepared after full deprotection of **4-51** to the free amino acid and reprotection with Fmoc-ONSU. The reaction was efficient and there was only a trace of the Fmoc residue which was removed after several columns and a recrystallisation. The Fmoc-protected **4-64** is particularly useful for direct solid-phase peptide synthesis and its synthesis in this form is important for inclusion in peptides.

The hydrophobicity of the Fmoc-CyF$_5$-OH **4-64** was studied by reverse phase HPLC in collaboration with the Koksch group at the Freie University in Berlin. The retention time of the Fmoc-protected amino acid was plotted against the van der Waal (vdW) volume of the side chain. Fmoc-CyF$_5$-OH **4-64** behaved significantly differently from comparative amino acids where it is much less hydrophobic (more polar) than the corresponding cyclohexyl amino acid, valine, fluorinated Phe derivatives and even Phe itself.[21] The hydrophobicity of CyF$_5$ **4-64** is similar to β-branched valine, which is unexpected given that the vdW volume of the CyF$_5$ side chain is nearly 3 times greater than that of valine.
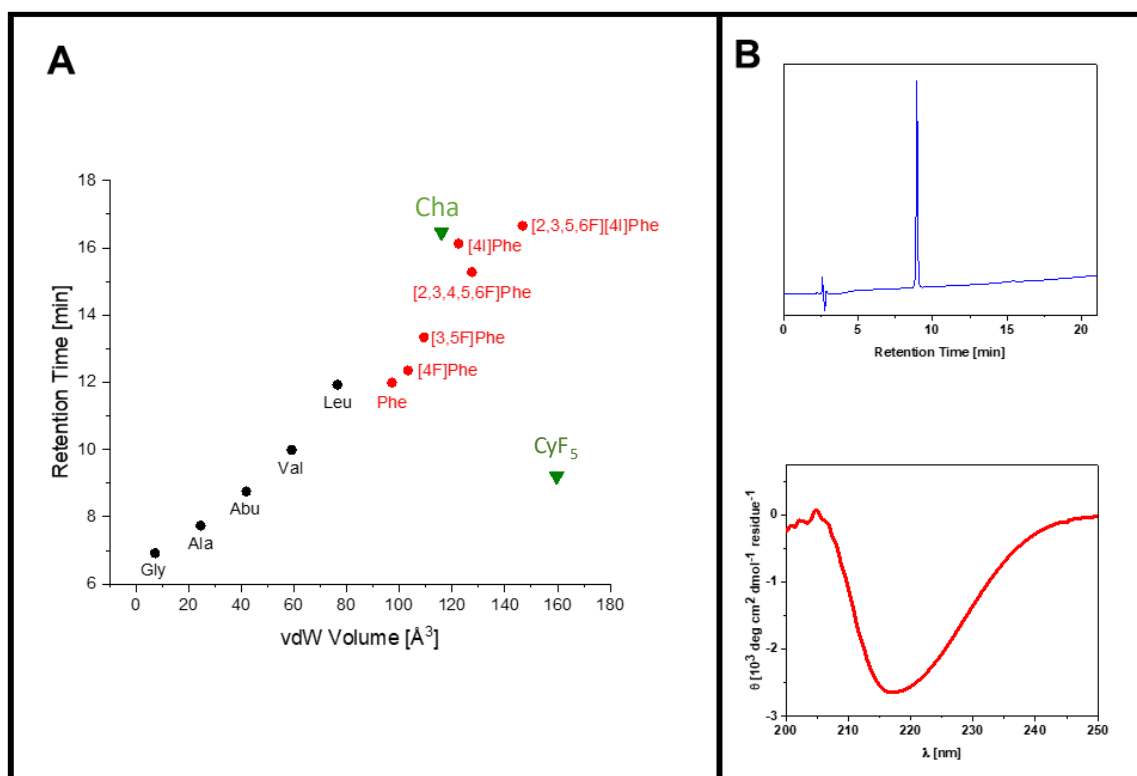
Figure 4-20 A) HPLC retention times versus vdW of various amino acids. B) The retention time of **4-64**.

An imidazolidinone was prepared from the all-*cis* pentafluorocyclohexylalanine **4-64**. The target product was prepared in about a 50% overall yield after deprotection of **4-48** followed by a protocol previously described in the literature and summarised in Scheme 4-19.[22]
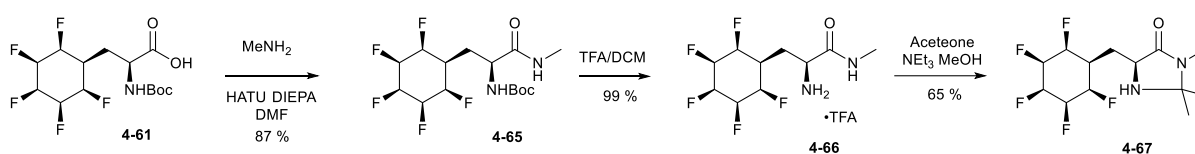

Scheme 4-19 Synthesis of imidazolidinone **4-67**.

The X-ray single crystal structure of **4-67** was obtained and is illustrated in Figure 4-21. It can be seen that the three C–F bonds at the 1,3,5 positions show a tri-axial orientation in the structure which is anticipated to have a higher net dipole that the C–F triequatorial conformation and is presumably dictated by the preference for the side chain to lie equatorially.

153
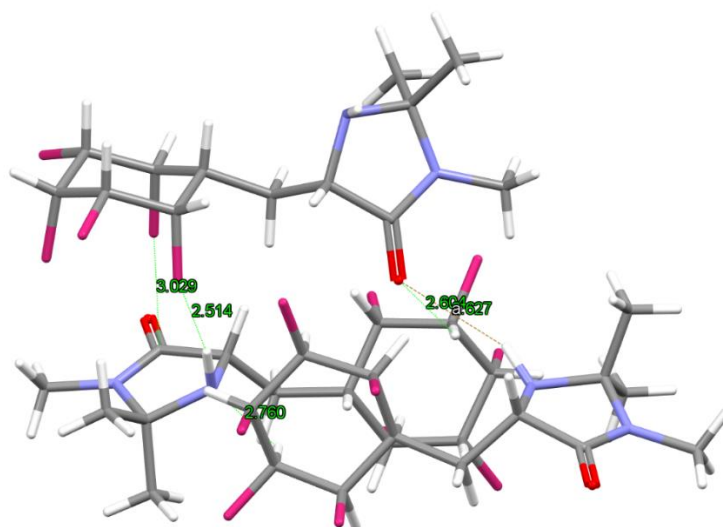
Figure 4-21 X-ray crystal structure of **4-67**.

A cyclic trimer arrangement was found in the crystal structure of **4-67**. One fluorocyclohexyl ring is arranged parallel to the imidazolidinone ring with a distance of ~4.50 Å. The fluorine face of the ring is pointing towards the imidazolidinone ring with short contact distances. The axial C–F … H–N distance is 2.51 Å and C–F …C=O 3.03 Å to the carbonyl of the ring. Another fluorocyclohexyl ring contacts the imidazolidinone ring through its hydrogen face, with a contact distance of the axial C–H …N–H of 2.76 Å. The product is enantiomerically pure and therefore this imidazolidinone could be developed as a chiral catalyst incorporating the Janus face fluorocyclohexyl ring to benefit intermolecular coordination.

4.4.5 Hydrogenation of fluorocyclohexyl containing dipeptides
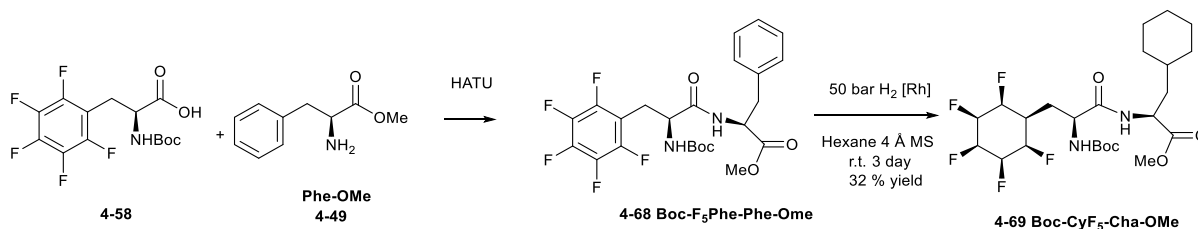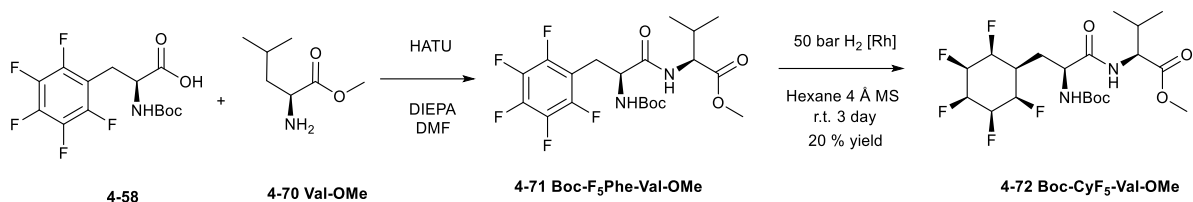
Scheme 4-20 Direct aryl hydrogenation of fluorocyclohexyl containing dipeptides.

Dipeptide **4-69** was prepared by HATU coupling of amino acids **4-58** and **4-49** to deliver dipeptide **4-68** carrying an aromatic side chain. This was then followed by direct aryl hydrogenation in a 20% yield. Dipeptide **4-72** was prepared following a similar protocol. The resultant Janus face containing peptide was prepared in 32 % yield. These hydrogenations demonstrated the tolerance of rhodium hydrogenation to dipeptides containing amino acids with neutral side chains. The hydrogenated dipeptides are fine powders and form gels easily in solution. These gels form fibres when solvent is removed or apolar solvent added.
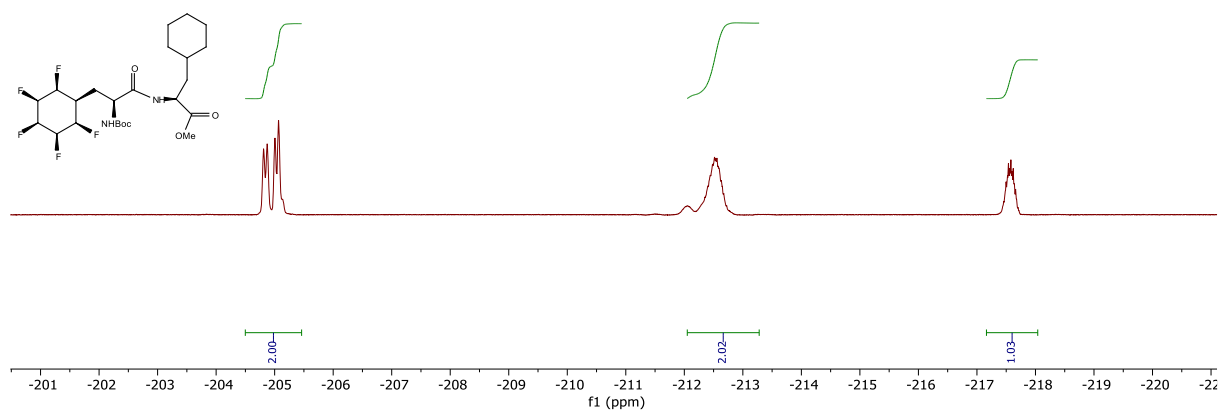
Figure 4-22 The ^{1}H-NMR and ^{19}F NMR of dipeptide **4-69**.

The peaks at 7.7 and 6.3 ppm in the ^{1}H-NMR indicate the amide protons and those between 5.5-4.5 ppm shows typical hydrogens in all-*cis* pentafluorocyclohexyl rings. The peak at 5.5 ppm suggests the fluorocyclohexyl ring is sitting with a 2,4,6-trifluoro axial orientation as the most electronic deficient proton (equatorial) is downfield. This conformation is also consistent with the ^{19}F NMR. The three axial fluorines are at upfield and the two equatorial

fluorines have distinct chemical shifts, as they are non-equivalent due to the presence of the chiral centre in the side arm.

4.4.6 Solution phase peptide synthesis

Solution phase peptide syntheses were explored to prepare peptide containing Janus face cyclohexyl ring in large quantity. To avoid harsh reaction conditions which may lead defluorination or racemisation, such as preparation of carbonyl chloride, or reaction involve strong bases, mild amide conjugation methods were tested. A low reactivity of 1-Ethyl-3-(3-dimethylaminopropyl)carbodiimide (EDCI) coupling between the all-*cis* pentafluorocyclohexylalanine with natural amino acids was observed in test reactions. And it proved difficult to separate hydroxybenzotriazole (HOBt) from the coupled product. Therefore, hexafluorophosphate azabenzotriazole tetramethyl uranium (HATU) coupling with diisopropylethylamine (DIPEA) was used to promote amide bond formation. Several dipeptides and then their consequent tripeptides were prepared using the HATU coupling methodology.

4.4.6.1 Synthesis of tripeptide Tyr-Phe-CyF₅
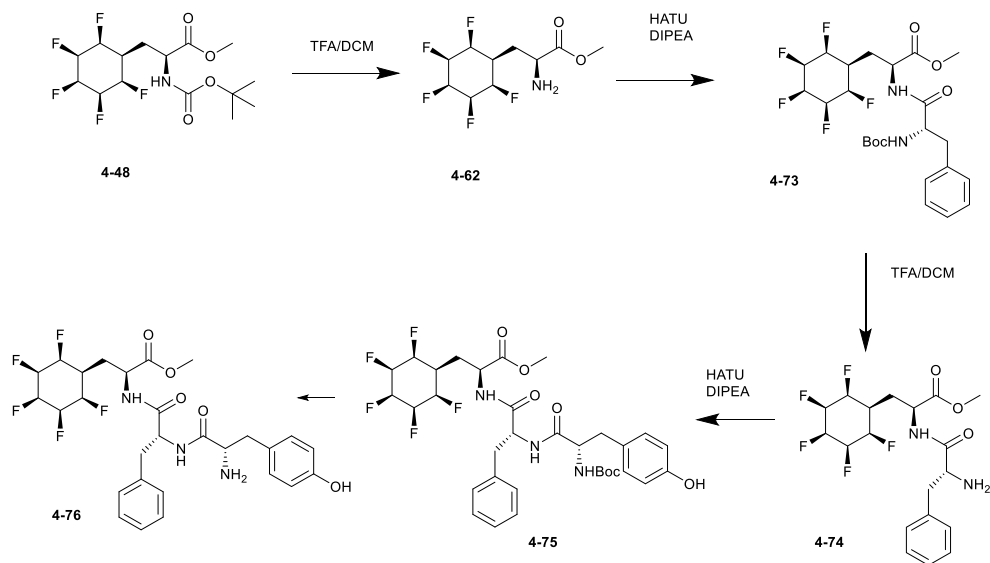
Scheme 4-21 Synthesis of tripeptide **4-76**.

Two examples of tripeptides were prepared in a stepwise manner. Di-protected all-*cis* pentafluorocyclohexylalanine **4-48**, was selectively deprotected with TFA in DCM as described previously. The excess TFA was removed under high vacuum, where a stoichiometric amount of TFA was retained. A solution of the activated compound **4-73** in DMF was treated with HATU and Boc-Phe **4-73**. The product was columned and characterised before progressing to the coupling step. Unlike the starting material **4-48**, which is soluble only in polar solvents, **4-73** is soluble in solvents such as EtOAc/chloroform/DCM. The product is a white solid, which forms a gel in solution. A ^{13}C DEPT-NMR experiment showed poor resolution of the aromatic and fluorocyclohexyl ring carbons due to C–F coupling, whereas a better signal was observed by HSQC and HMBC cross coupling as the signal is enhanced by proton correlation.
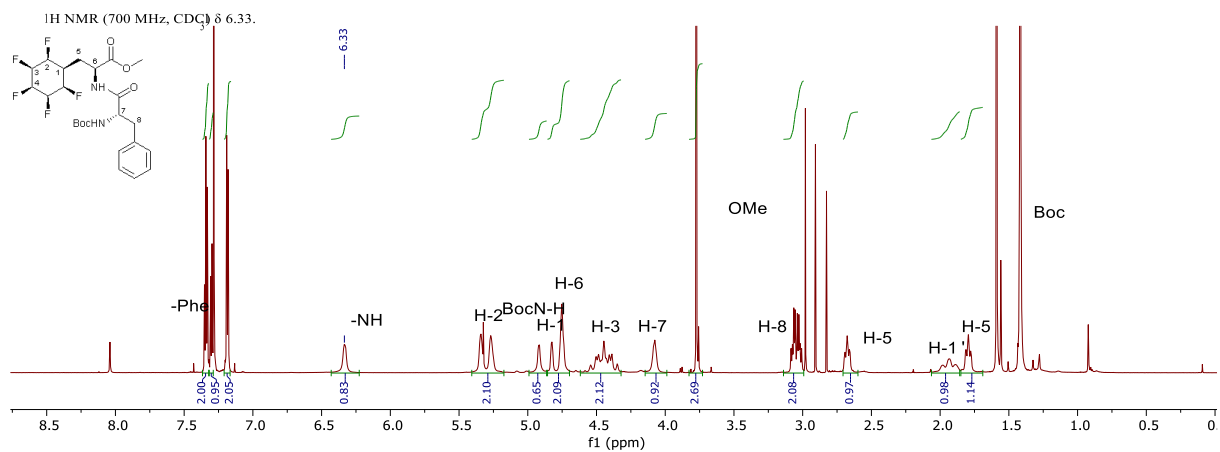
Figure 4-23 The ^{1}H NMR of Boc-Phe-CyF$_5$-OMe **4-73**.

The ^{1}H-NMR spectra in Figure 4-23 of the dipeptide **4-73** shows complexity. The signals between 7.0 - 7.5 ppm are assigned to the aromatics of the phenylalanine side chain. The signal assigned to the *ortho* proton is a doublet with an integration of one. The $^3J_{H-F}$ coupling constant of 26 Hz associated with H1 suggests an antiperiplanar relationship to the adjacent fluorine. This indicates that the fluorocyclohexyl ring retains its most polar 2,4,4' C−F triaxial conformation.
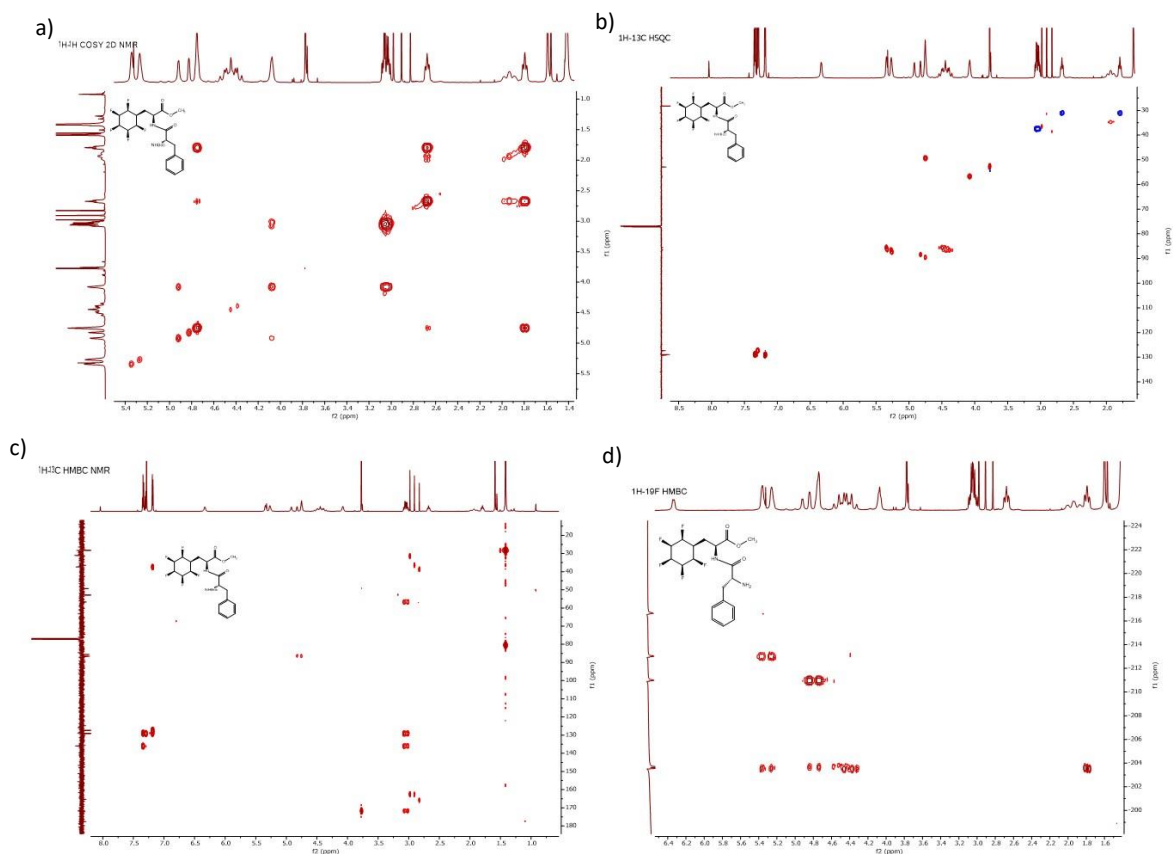
Figure 4-24 2D NMR of dipeptide Boc-Phe-CyF$_5$-OMe **4-73** (a) ^{1}H-^{1}H COSY, (b) ^{1}H-^{13}C HSQC, (c) ^{1}H-^{13}C HMBC and (d) ^{1}H-^{19}F HMBC.

The three signals between 4.5-5.5 ppm match well with the all-*cis* pentafluorocyclohexyl pattern. The peak distribution pattern is different from that found in acetone solution where the terminal CHF proton has the most downfield signal. Due to rapid ring inversion and solvent effects, the ^{1}H-NMR signals of the fluorocyclohexyl ring poorly couple to each other in the ^{1}H-^{1}H COSY and ^{1}H-^{13}C HMBC spectra. The coupling relationships were assigned using the ^{1}H-^{13}C HSQC with DEPT spectra. The two H-5 protons have different chemical shifts by ~ 0.8 ppm indicating the different electromagnetic nature of the two Janus faces.
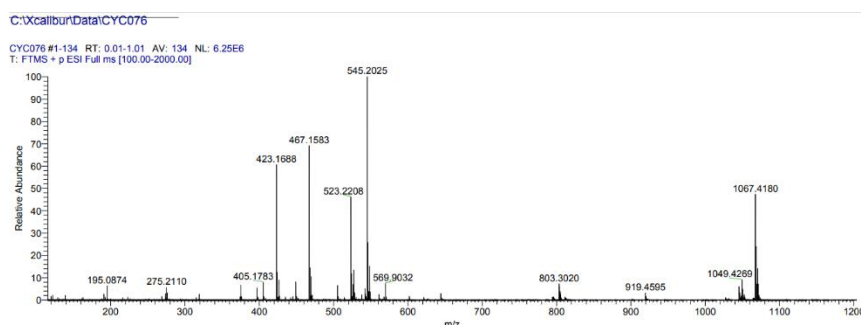
Figure 4-25 Mass spectrum of dipeptide Boc-Phe-CyF$_5$-OMe **4-73**.

In the mass spectrum for **4-73**, the exact mass of 545.2025 matches to the expected value (545.2046) for [M+Na]$^+$ within about 2ppm , while the ion at 523.2208 matches that expected for [M+H]$^+$ with 523.2226 again at only around 2ppm variance.

In order to progress, dipeptide **4-73** was treated with TFA, then volatiles were removed under vacuum, and the product was then reacted with HATU activated Boc-Tyr-OH. The resultant tripeptide **4-75** was no longer soluble in chloroform, so more polar solvents, acetonitrile or methanol were required to bring the compound into solution.
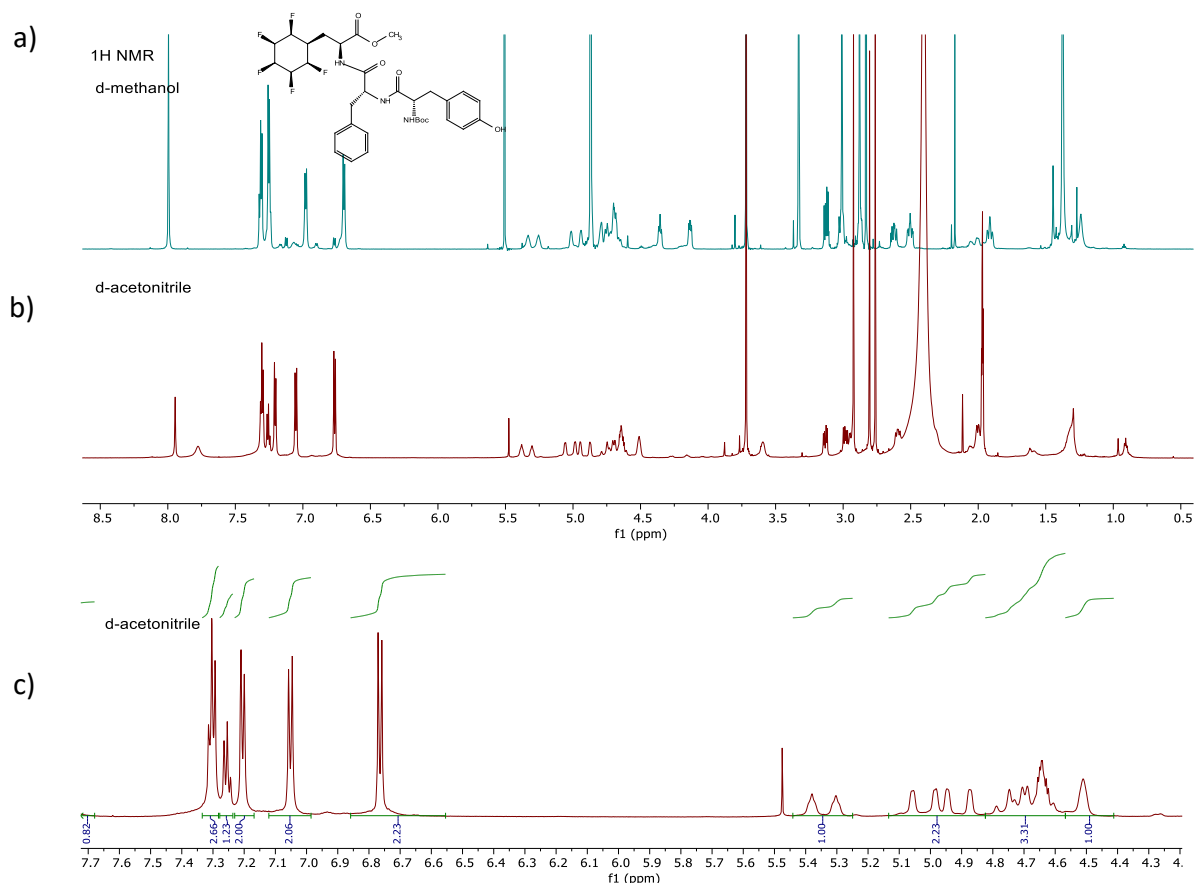
Figure 4-26 Sections of the ¹H NMR of tripeptide Boc-Tyr-Phe-CyF₅-OMe **4-75** in d-Methanol and d-acetonitrile.

The ¹H NMR of **4-75** in acetonitrile shown in Figure 4-26 shows diagnostic signals between 4 -8 ppm. The signals around 7.5-7.2 are consistent with the phenyl ring, and the two sets of doublets at 7.05 and 6.75 ppm indicate the para substitution of the phenol ring in tyrosine. The signals in the 5.4-4.4 ppm region are typical of the Janus fluorocyclohexane ring and the overall integration assigns well to the 1:1:1 ratio expected for each amino acid component of the peptide. The solvent residues from acetonitrile prevented further assignment of the aliphatic region, therefore, deuterated methanol was used as the solvent to reveal the signals under the acetonitrile solvent peaks.
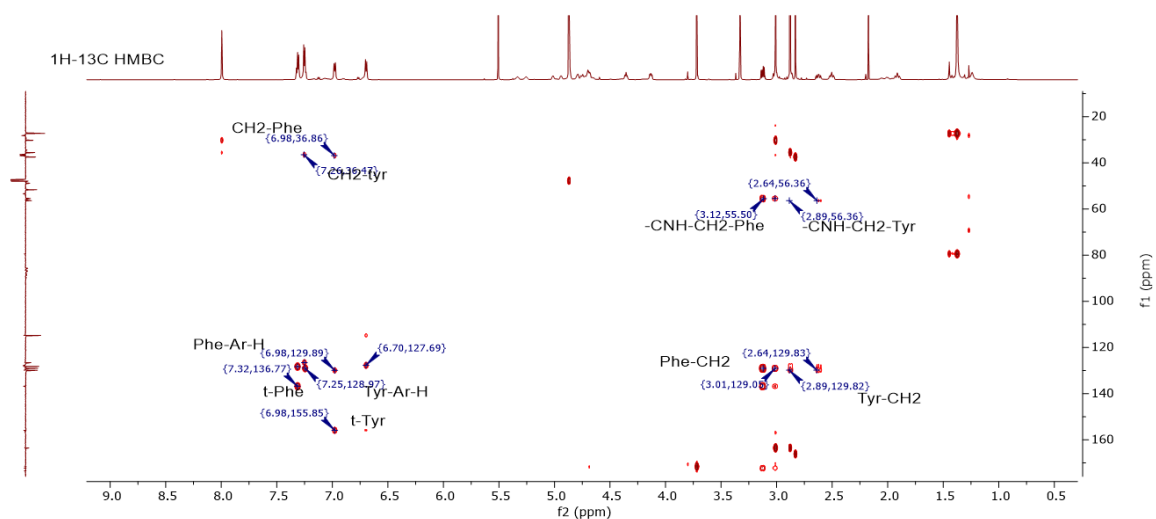
Figure 4-27 ^{1}H-^{13}C HMBC NMR of tripeptide Boc-Tyr-Phe-CyF$_5$-OMe **4-75**.

The ^{1}H - ^{13}C HSQC shows a strong $^2J_{H-C}$ coupling indicating two tyrosine Ar-H carbons and three phenylalanine Ar-H carbons. And then the ^{1}H-^{13}C HMBC reveals cross coupling between the CH$_2$ (α) next to the aromatic carbon and the CH (β) next to amino carbon, which suggest that the peak at 36.5ppm is coupled to Phe and 36.9ppm also coupled to Tyr, allowing the CH$_2$ protons next to the aromatic to be assigned.
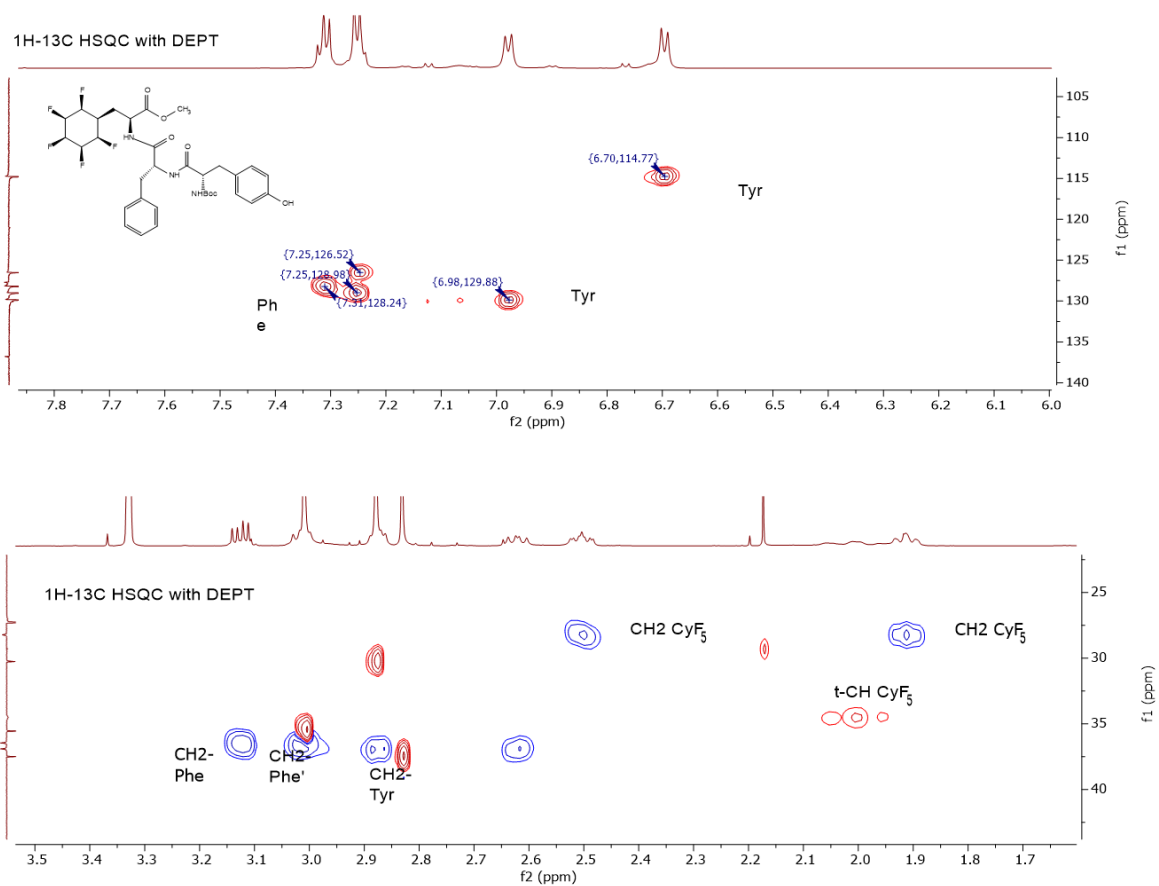
Figure 4-28 ^{1}H-^{13}C HSQC with DEPT NMR of tripeptide Boc-Tyr-Phe-CyF$_5$-OMe **4-75**.

The HSQC with carbon DEPT spectra shows some evidence of the distribution of the alkyl protons on the amino acids. Cross peaks shows that the two triplets at 2.51ppm and 1.92 ppm correlate to the same carbon, while the two protons on CH$_2$ carbon overlap with signals from the solvent residue, at 3.01 ppm and 2.87 ppm respectively.
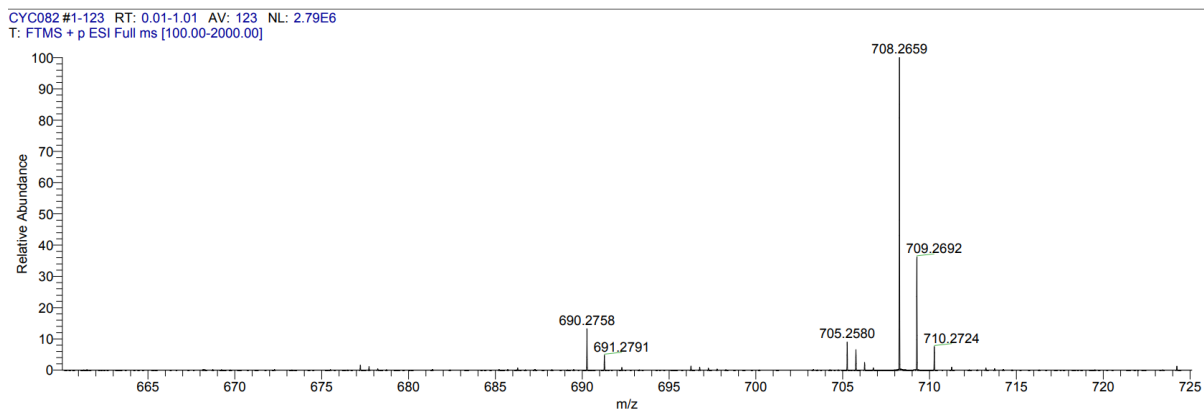
Figure 4-29 Mass spectrum of tripeptide Boc-Tyr-Phe-CyF$_5$-OMe **4-75**.

The mass spectrum recorded in positive ion mode shows a distinct peak for [M+Na]$^+$ of 708.2659 m/z while the calculated value is 708.2684, and this is about a 2 ppm accuracy.

Removal of the Boc group was carried out to generate tripeptide **4-75** and to release the free amine. The ^{1}H NMR shows that the tripeptide **4-76** has a very similar pattern to tripeptide **4-75**, while the disappearance of the Boc group and the shift of H-9 are apparent.
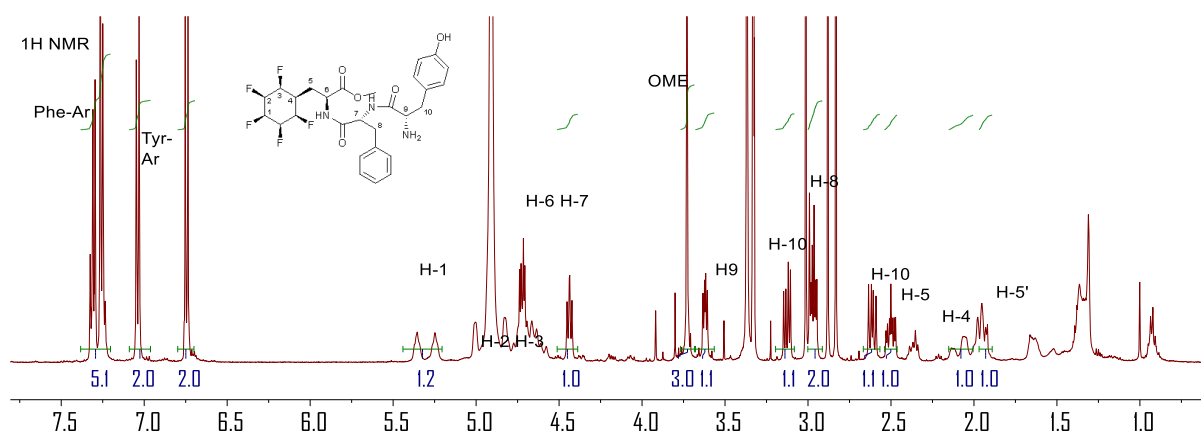
Figure 4-30 ^{1}H NMR of tripeptide Tyr-Phe-CyF$_5$-OMe **4-76.**

HPLC analysis was used to assess the purity of tripeptide **4-76** and to further purify the tripeptide. The product tripeptide **4-76** had a retention time of 18 min and proved to be of high purity, however the HPLC purified tripeptide had low solubility.
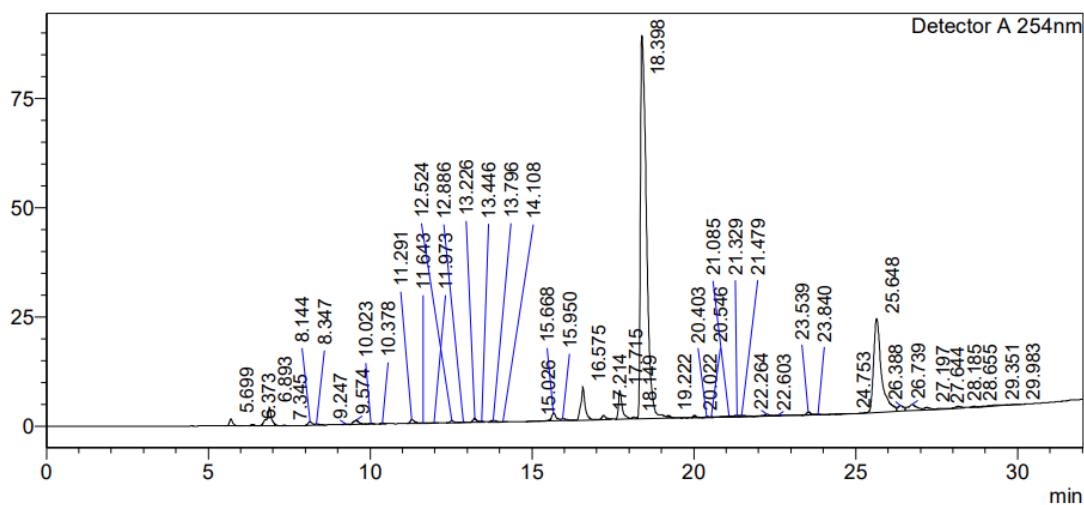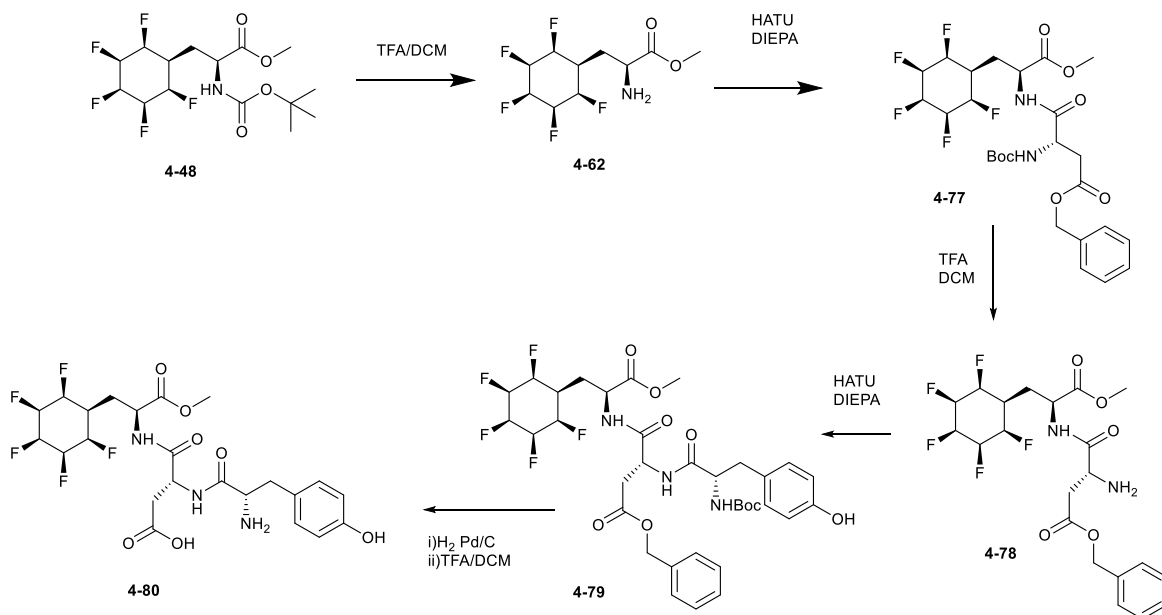
<Chromatogram>

mV

Figure 4-31 Semi-prep HPLC analysis of tripeptide **4-76**, 15-95 % (water/acetonitrile).

4.4.6.2 Synthesis of tripeptide Tyr-Asp-CyF$_5$

Scheme 4-22 The synthesis of tripeptide Tyr-Asp-CyF$_5$ **4-80**.

A similar procedure was carried out to prepare the negatively charged tripeptide **4-80**, containing an aspartic acid unit. The preparation started with Boc group deprotection of **4-48**

165

in TFA/DCM, followed by a HATU coupling with Boc protected aspartic acid Boc-Asp(OBz)-OH which had a benzyl protected side chain.
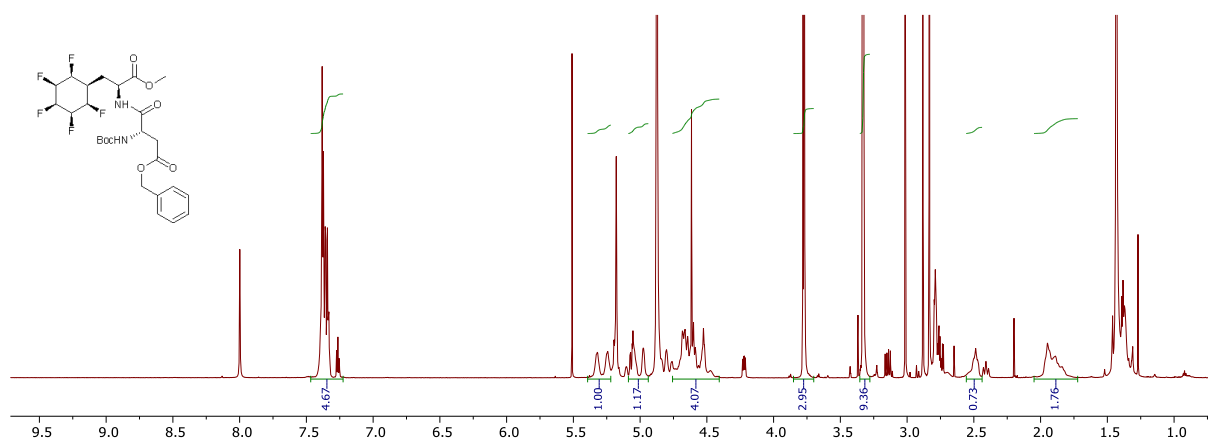
**Figure 4-32** ^{1}H NMR of dipeptide Boc-Asp(Bz)-CyF$_5$-OMe.

The ^{1}H NMR spectrum of the product dipeptide **4-77** clearly shows the benzyl aromatic protons around 7.3 ppm and the all-*cis*-pentafluorocyclohexyl protons around 5 ppm. Dipeptide **4-77** was deprotected and carried through to the next step of the synthesis. Mass spectrometry confirmed the composition of dipeptide **4-77**. A distinct peak of [M+Na]$^+$ was observed at 603.2076 m/z which was only 3 ppm at variance to the calculated mass of 603.2101 m/z
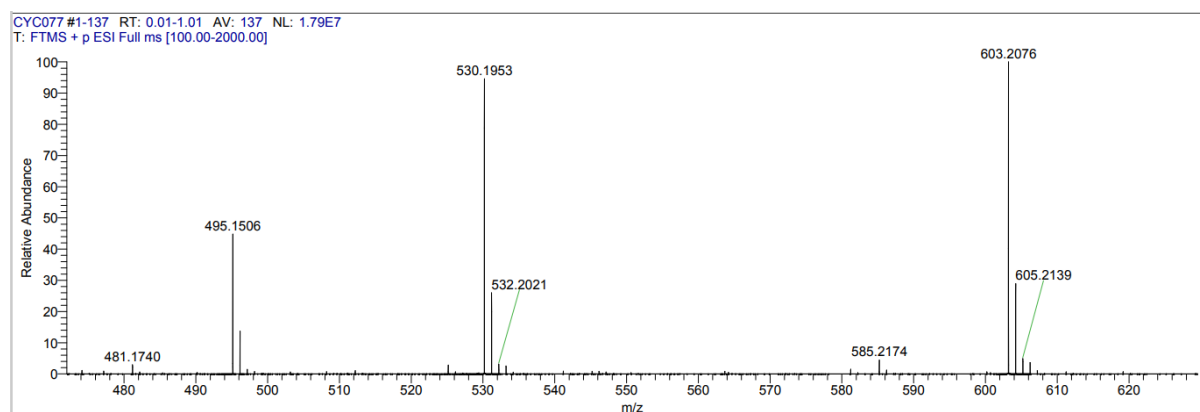
**Figure 4-33** Mass spectrum of Boc-Asp(Bz)-CyF$_5$-OMe **4-77**.

Dipeptide **4-77** was deprotected to generate **4-78**, which was then coupled with Boc protected tyrosine. The product was purified by column chromatography. The ^{1}H-^{13}C HSQC NMR spectrum was used to confirm the tyrosine and benzyl aromatic carbons through the characteristic doublets for *para* substitution in the phenol moiety of tyrosine, and also the benzyl Ph signal. The benzyl CH$_2$ at 5.17 ppm and the tyrosine CH$_2$ signals could also be identified. The ^{1}H-1 shows an antiperiplanar geometry to the adjacent axial fluorine as evidenced by the large $^3J_{H-F}$ coupling of 32.8 Hz.
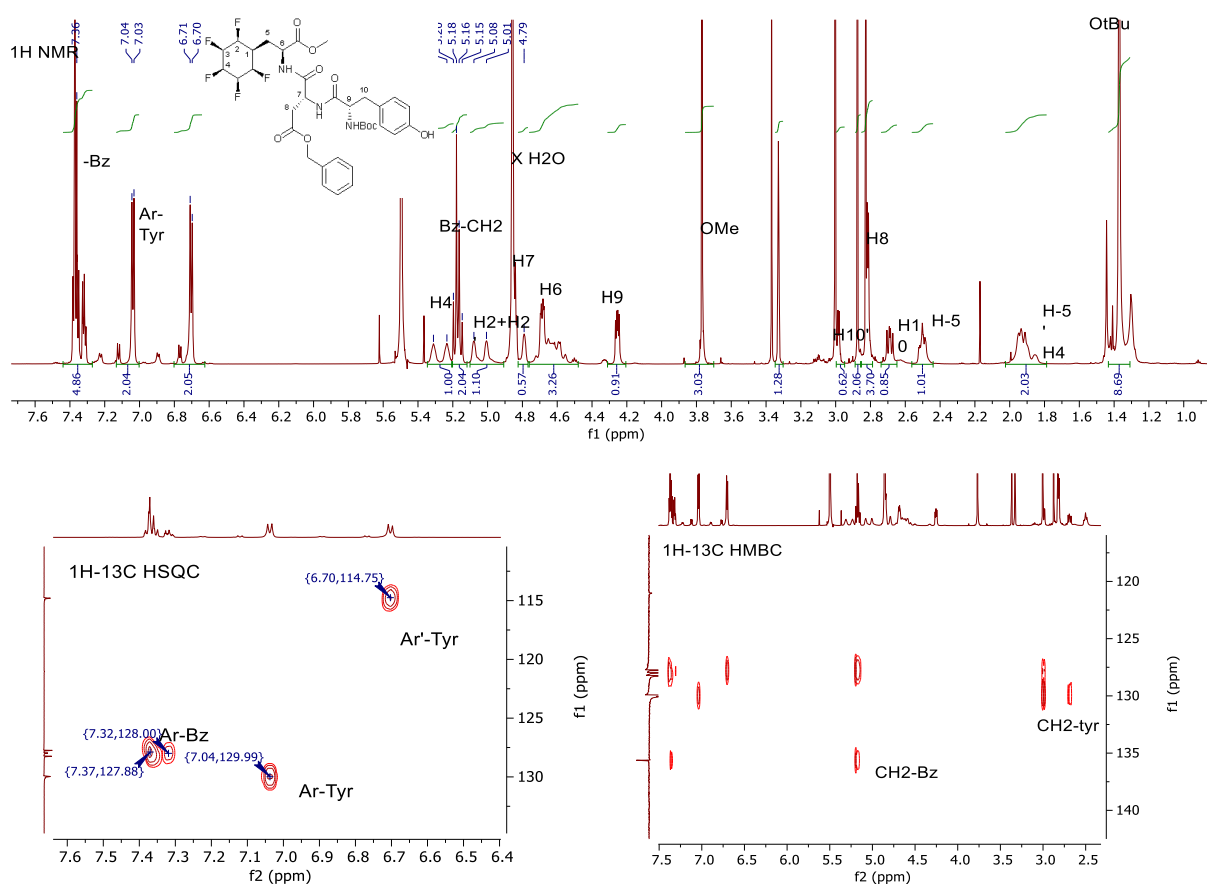
Figure 4-34 The ^{1}H, ^{1}H-^{13}C HSQC with DEPT, and ^{1}H-^{13}C HMBC NMR of dipeptide **4-77**.

Tripeptide **4-79** was deprotected by a palladium catalysed hydrogenation to cleave the benzyl group. The Boc group was then hydrolysed by treatment in TFA/DCM. The integrity of the tripeptide was confirmed by ^{1}H and ^{19}F NMR as illustrated in Figure 4-34. The resultant tripeptide **4-80** showed a poorer solubility than tripeptide **4-76**, even in methanol. The poor

solubility may be caused by the strong charge affinity of the Janus face fluorocyclohexyl ring with other polar groups in these tripeptides.
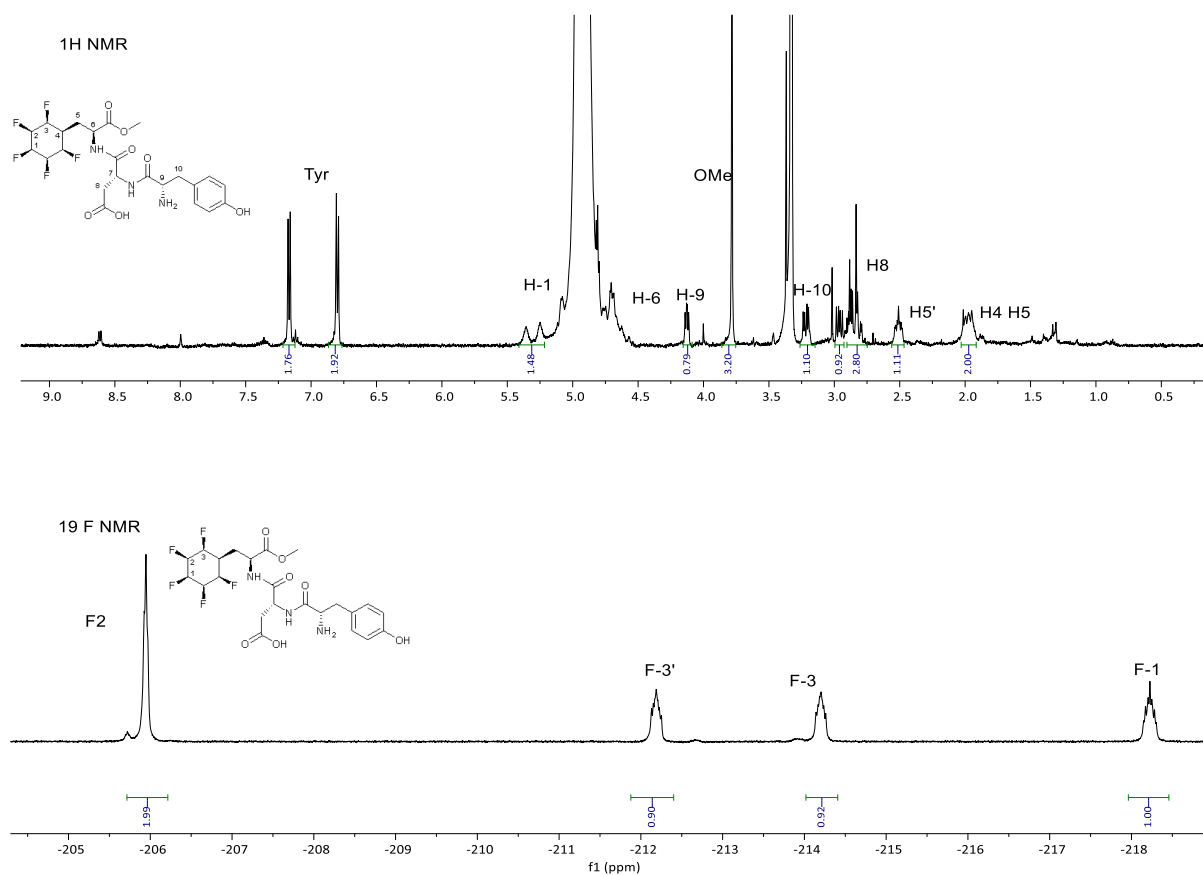
Figure 4-35 ^{1}H and ^{19}F NMR of tripeptide Tyr-Asp-CyF$_5$-OMe **4-80**.

Similarly, HPLC analysis was used to assess the purity of tripeptide **4-80** and to further purify the tripeptide. The product tripeptide **4-80** had a retention time of 16 min and proved to be of high purity, however the HPLC purified tripeptide had low solubility.

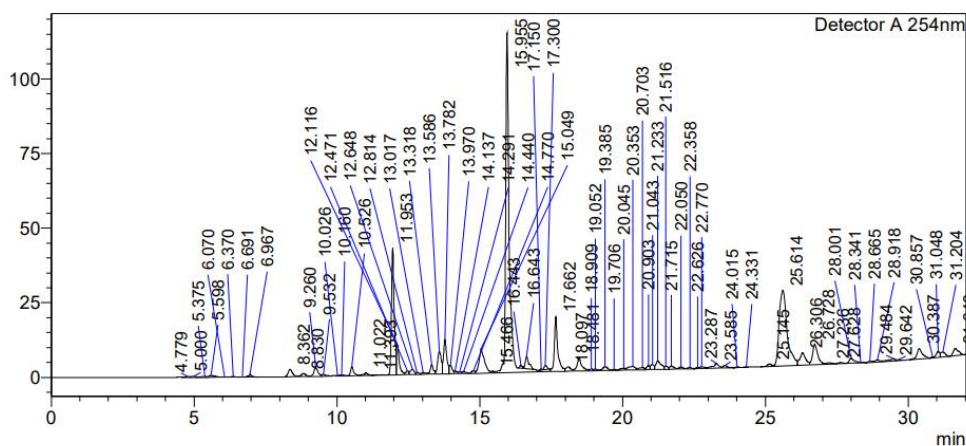**Figure 4-36** Semi-prep HPLC analysis of tripeptide **4-80**, 15-95 % (water/acetonitrile).

4.4.6.3 The synthesis of CyF$_5$-Tyr linked tripeptide

In order to explore the practicality of preparing tripeptides containing all-*cis*-pentafluorocyclohexyl motifs with a varied combination of amino acids, the dipeptide intermediate **4-82** was synthesised on a larger scale. This involved HATU coupling, however a significant by product emerged from coupling through the phenol hydroxyl group. The reaction was optimised by reducing the amount of HATU to one equivalent.[23] In this way dipeptide **4-82** was generated and, on work up, it formed a hydro gel type consistency in polar solvents turning into an amorphous residue when the apolar solvent hexane was added. In the latter case, the product generated fibres when the solvent was completely removed.
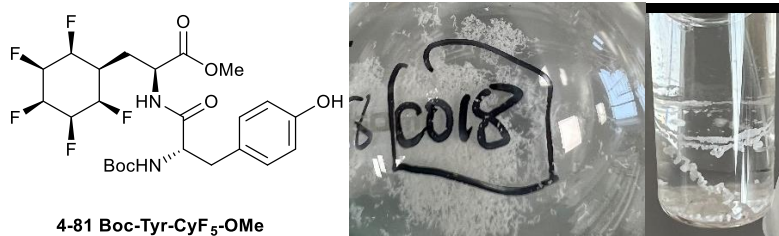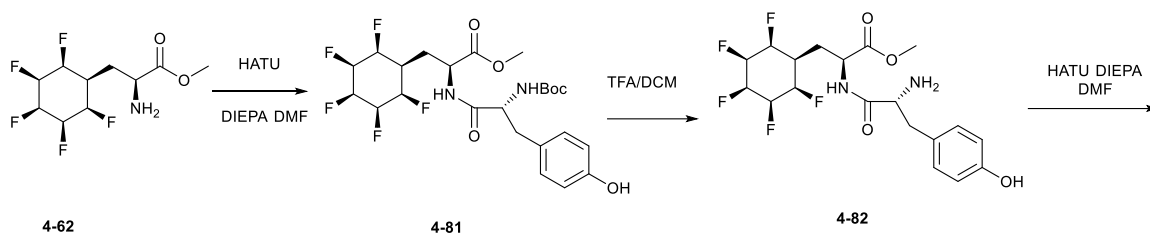
Figure 4-37 Dipeptide **4-81** and a visual indication of its amorphous behaviour in the solid and solution phase.

Four protected tripeptides were prepared by HATU coupling from dipeptide **4-81**. They all show strong affinity to the C_{18} stationary phase in HPLC and they are all poorly soluble in water even after deprotection. The low solubility and tailing in their HPLC elution profiles led us to switch to more feasible purifications by preparative TLC.
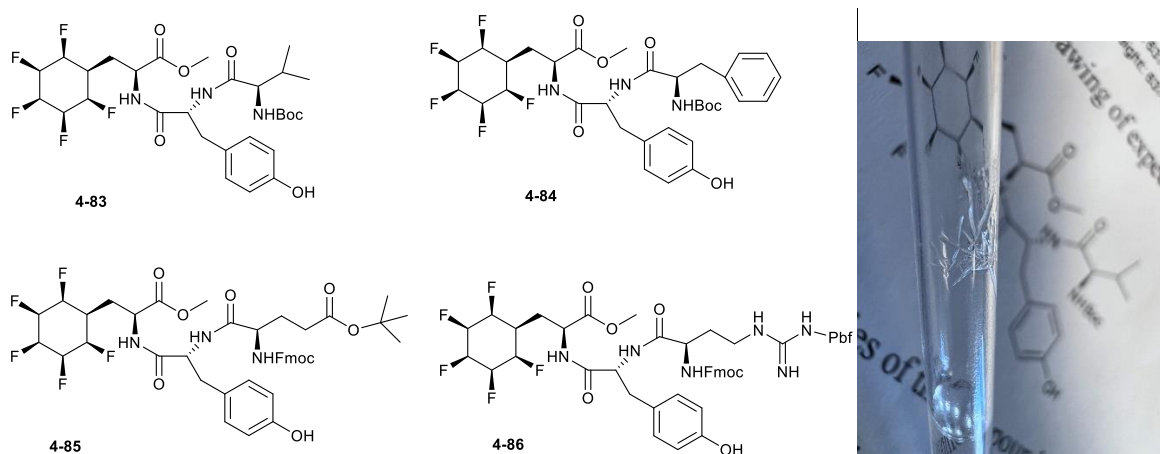

Figure 4-38 Tripeptides with the CyF$_5$-Tyr sequence. A nanocrystal fibre of Boc-Val-Tyr-CyF$_5$-OMe **4-83** (right).

170

4.4.7 NMR experiments investigation through space coupling

The six tripeptides that were prepared were dissolved in the most suitable solvent in each case and subjected to NOE and HOE NMR experiments to assess through space interactions/coupling between Janus face fluorocyclohexyl rings and the other amino acid side chains. This is discussed below for each peptide.
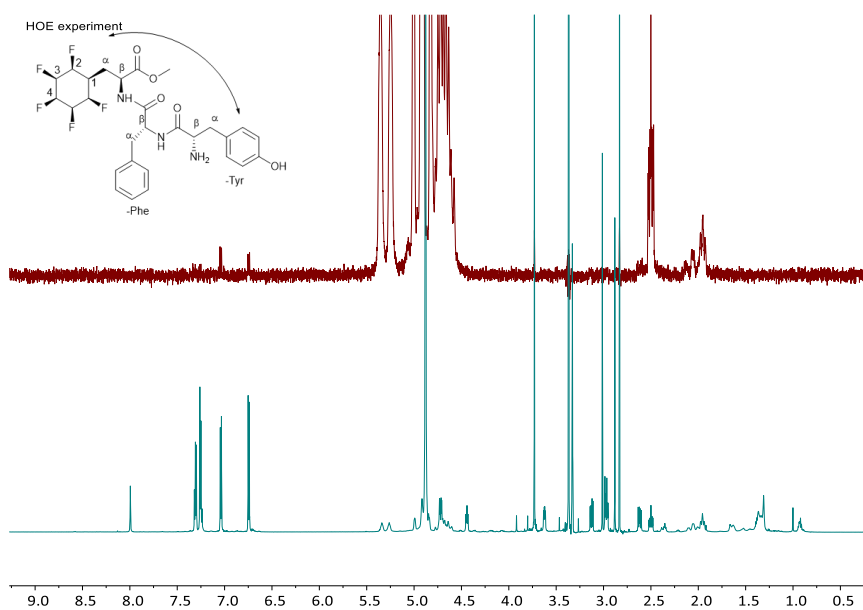
4.4.7.1 Tyr-Phe-CyF$_5$-OMe 4-76

For tripeptide Tyr-Phe-CyF$_5$-OMe **4-76**, the NOE experiment was carried out with irradiation on the 4-proton of the cyclohexane ring. The 4-H proton is sitting with an equatorial orientation and pointing away from the peptide chain and is most likely to contact other side chains. The NOE experiment shows the 4-H proton in **4-76** is indeed interacting in this way and with the *ortho*-H proton of the tyrosine aromatic. This matches with the previous observation that the Janus face fluorocyclohexane ring tends to have an affinity for aromatic rings and is consistent with 4-H making a through space contact as illustrated in Figure 4-39 (top right). This is suggests an intermolecular interaction involved in the antiparallel packing of the two rings as the correlation between 4-H and *ortho*-H.
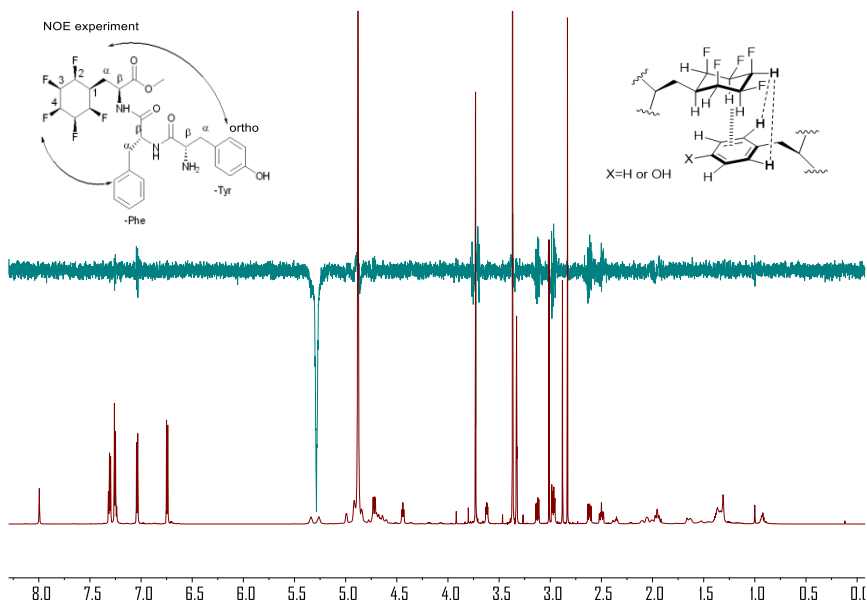
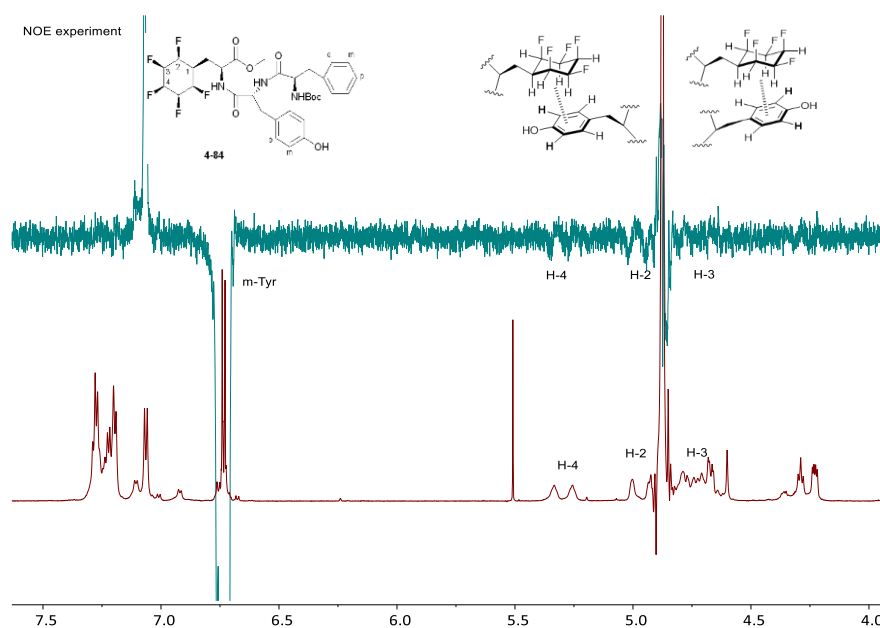**Figure 4-39** NOE experiment of the tripeptide Tyr-Phe-CyF$_5$-OMe **4-76**.

The HOE experiment was carried out by broad irradiation of the fluorines on the fluorocyclohexyl ring and shows a strong interaction between the fluorines and the tyrosine phenol protons. Weak interactions between the Phe aryl protons and these fluorines were barely observed.

Figure 4-40 HOE experiment of tripeptide Tyr-Phe-CyF$_5$-OMe **4-76.**
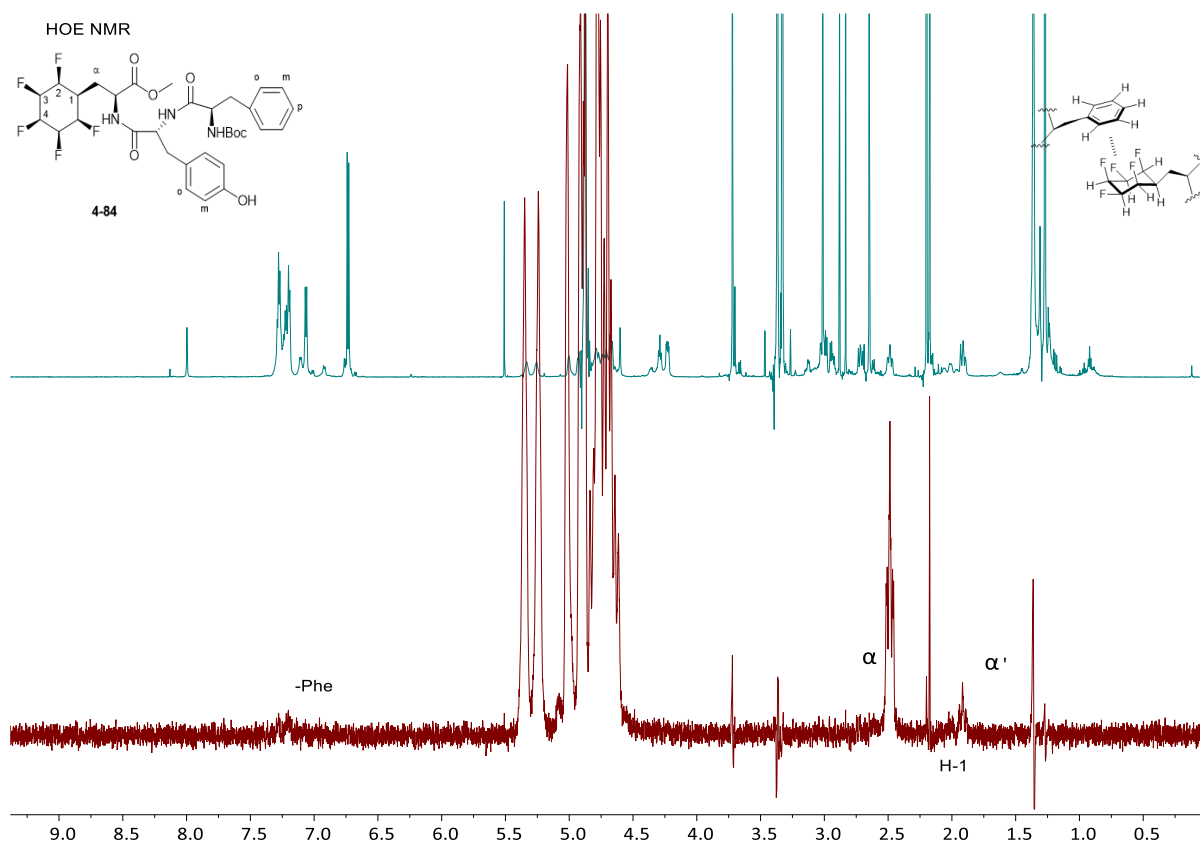
4.4.7.2 Boc-Phe-Tyr-CyF₅-OMe 4-84

For tripeptide Phe-Tyr-CyF₅ **4-84**, the NOE experiment was performed by irradiation of the *meta* protons on the tyrosine phenol. These *meta* protons are separated from any other aromatic signals and respond strongly with NOE irradiation.

Figure 4-41 The NOE experiment of tripeptide Boc-Phe-Tyr-CyF₅-OMe **4-84**.

Unlike tripeptide **4-76**, the NOE experiment for **4-84** showed strong correlations between the tyrosine aryl *meta* protons and all of the protons on the hydrogen face of the Janus ring. The correlation could be either intermolecular or intramolecular. The Tyr to CyF₅ correlation is much stronger than the Tyr-Phe correlation, as no Phe correlation signal was observed by NOE. On the face of it, this indicates a stronger affinity between Janus face fluorocyclohexane with aromatic rings rather than Phe-Phe interactions which are less obvious here.

Figure 4-42 HOE experiment of Boc-Phe-Tyr-CyF₅-OMe **4-84**.

The ¹H-¹⁹F HOE NMR shows the exclusive correlation between the irradiated fluorines and the aryl ring of phenylalanine. The correlation between fluorine to tyrosine is not observed here. The other tripeptides **4-80**, **83**, **85** and **86** synthesised in this project, showed only weak correlations between the aromatic side chains and Janus ring as judged by HOESY and NOESY NMR. **4-85** HOEXY shows a correlation between fluorine and ᵗbutyl group, and very weakly to tyrosine *ortho*-aromatic protons. In the HOEXY NMR, the fluorine of **4-85** and **86** is correlated to the Fmoc group in their structure.

Through space NMR indicated a strong correlation between the terminal CyF₅ and terminal aryl side chain. The presence of non-aromatic side chain is interrupting such –Ar to Janus ring interactions on the NMR correlation scale.

## 4.4.8 Aggregation and assembly properties of JFC peptides

In the collaborative program with Prof. Koksch's lab in Berlin, they investigated some aspects of the supramolecular properties of the amino acids and in particularly around all-*cis* pentafluorocyclohexylalanine (**4-51** CyF$_5$). The Fmoc protected CyF$_5$ **4-64** was coupled to L-(*S*)-phenylalanine, and the resultant dipeptide was fully deprotected and purified by HPLC. The CyF$_5$-Phe **4-87** product and its analogue Phe-Phe **4-88** were submitted to a Thioflavin T fluorescence assay to investigate their aggregation properties.
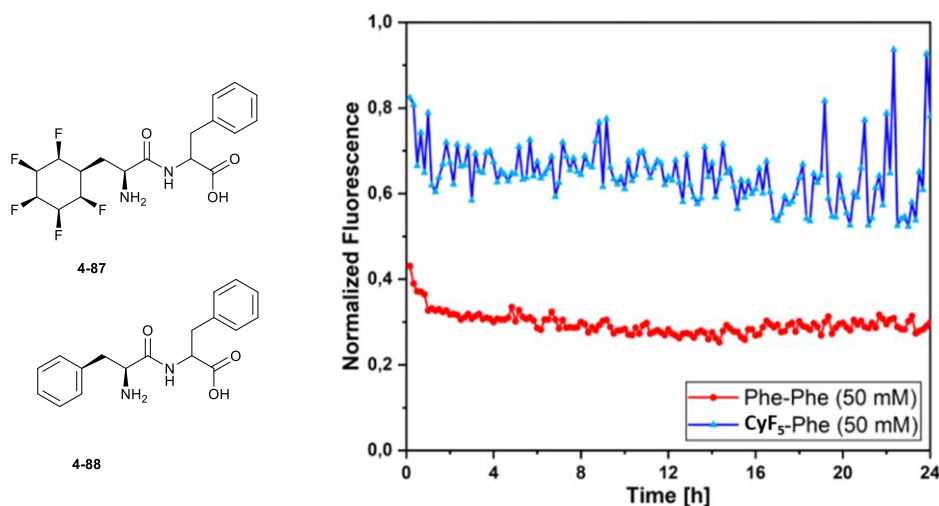
Figure 4-43 Thioflavin T assay. Peptides were incubated at 37 °C with orbital shaking for 2 sec (amplitude: 2 mm, 280.8 rpm) before each measurement (10 min intervals), dissolved in pH 7.4, 10 mM PBS buffer containing 20 µM thioflavin T. The fluorescent dye gives a strong fluorescence upon binding to amyloids caused by rotational immobilization. Fluorescence emission was measured at 485 nm and normalized with respect to its maximum value.

As illustrated in Figure 4-43, the CyF$_5$-Phe **4-87** shows an enhanced fluorescence emission by comparison with Phe-Phe **4-88**. However, no aggregation kinetics profile was detected to indicate a dynamic process. Subsequently, dipeptide CyF$_5$-Phe **4-87** was submitted to

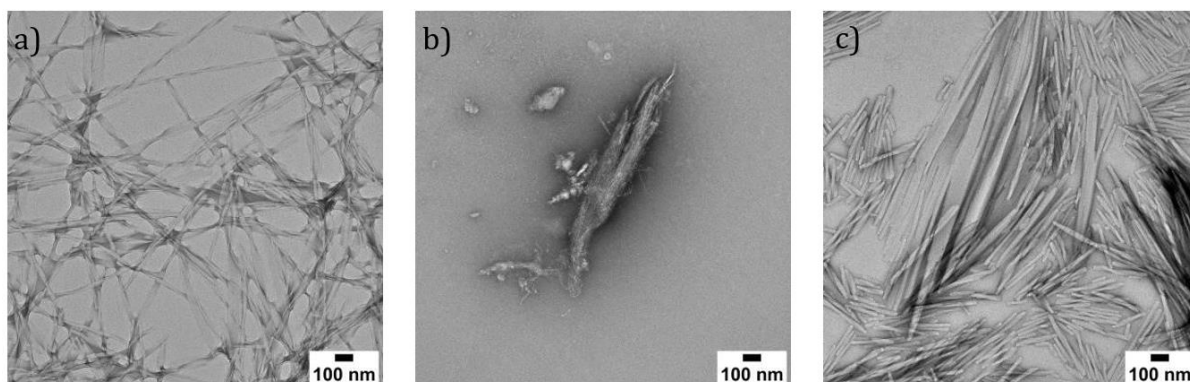transmission electron microscopy (TEM) and it was measured by Dr. Boris Schade (Humbholt University).
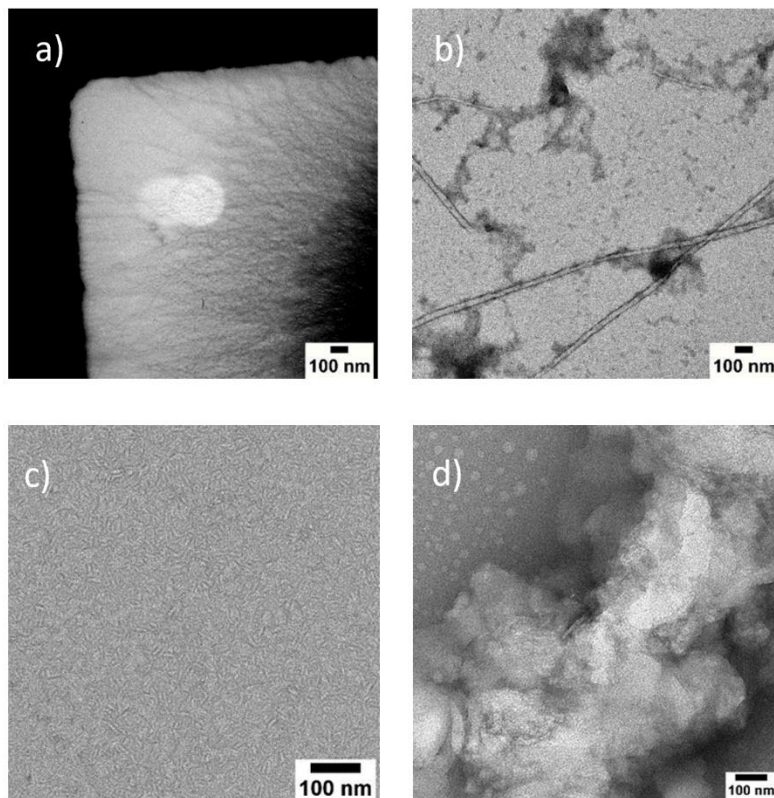
Figure 4-44 Negative-staining transmission electron microscopy (TEM) images of probes in PBS Buffer (+ 20 µM ThT) indicates the formation of fibrils. Samples: a) CyF$_5$Phe; [50 mM], b) CyF$_5$Phe; [5 mM], c) PhePhe; [50 mM], d) PhePhe; [5 mM]. Image data were recorded using a 4k×4k Ceta CMOS camera.

The TEM images in Figure 4-44 show the formation of nano fibre structures, which again indicate a self-assembling propensity of the Janus face containing dipeptide structures. The CyF$_5$ amino acid was then used for the preparation of the hexapeptide NFGAIL[21] and variant structures for further investigation of their respective aggregation kinetics. For this case study, the phenylalanine residue was varied and replaced with the various phenyl analogues as

shown in Figure 4-44.

Figure 4-45 Structural representation of NFGAIL variants.

The hexapeptides were then synthesised using solid phase Fmoc synthesis in the standard manner and the product hexapeptides were purified by HPLC. They were then submitted to the thioflavin T fluorescence assay. Ammonium acetate was used as a buffer to maintain compatibility with previous studies.[21]

Figure 4-46 a) Retention times (RP-HPLC assay) for Fmoc-protected amino acids plotted against the vdW volume of their side chains. The retention time (tR) of amino acids acts as an experimentally defined dimension of hydrophobicity b)-d) The kinetic profile of NGGAIL and its variants on thioflavin T assays at different molarities.

As illustrated in Figure 4-45, the kinetic profile of NFGAIL, N-Cha-GAIL and NF5Phe-GAIL behaves proportionally to the measured hydrophobicity of the side chain as determined by their vdW's volumes. The tendency is aligned with the relationship between aggregation kinetics and hydrophobicity proposed in previous NFGAIL studies.[21] The morphology of the aggregated NFGAIL, N-Cha-GAIL and N-F5PheGAIL was analysed in TEM spectroscopy.

Figure 4-47 Negative-staining transmission electron microscopy (TEM) images of selected NFGAIL solutions in ammonium acetate buffer (10 mM, pH~7) show the formation of amyloid fibrils. Samples: a) NFGAIL; [4 mM] b) N-Cha-GAIL; [4 mM] c) N-F5Phe-GAIL; [4 mM].

As shown in Figure 4-46, N-CyF$_5$-GAIL does not follow the hydrophobicity-vdW trend observed previously (Figure 4-20).[21] This is because the fluorocyclohexyl ring appears to slow the aggregation process significantly. One possibility for such an observation is a change in the β-sheet geometry of phenyl analogues in the antiparallel orientation to Janus face fluorocyclohexyl ring formed in N-CyF$_5$ does not fit any base stacking or facial dipole to π interaction.[24] Another possibility is water associated with the Janus face fluorocyclohexyl ring has hydrogen bonding potential to the facial polarised ring.[16, 21]
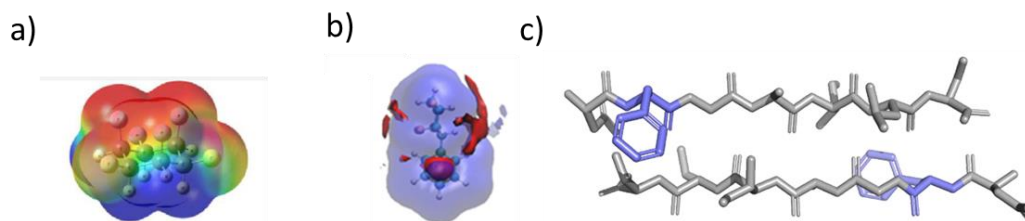
Figure 4-48 a) Representation of the electrostatic potential map of Janus face fluorocyclohexane[1] b) Water associated with Janus face fluorocyclohexyl ring, c) Crystal structure of NFGAILS (PDB 5E5V) with highlighted phenyl analogue positions.

4.5 Summary

In summary, the properties, and applications of Janus face fluorocyclohexane rings were further developed in this project. The unusual surface behaviour of the Janus face fluorocyclohexyl motif was demonstrated on the Au (111) crystal. The preparation of the all-*cis* hexa- and penta- fluorocyclohexane building blocks was optimised and a number of functional groups were installed on-to the ring, and consequently versatile coupling methods and functional group interconversions could deliver this motif to drug discovery programmes and supramolecular assembly. A role for Janus face fluorocyclohexyl ring in the biochemistry context was demonstrated by all-*cis* pentafluorocyclohexylalanine (CyF$_5$) and its peptide analogue which were prepared and studied in peptides. The strong binding affinity of the Janus face fluorocyclohexyl ring, the large facial polarity and the tunable hydrophobicity present exciting prospects of future biological and pharmaceutical applications.

4.6 References

1. N. S. Keddie, A. M. Z. Slawin, T. Lebl, D. Philp and D. O'Hagan, *Nat. Chem.*, 2015, **7**, 483-488.

2. M. P. Wiesenfeldt, Z. Nairoukh, W. Li and F. Glorius, *Science*, 2017, **357**, 908-912.

3. M. P. Wiesenfeldt, T. Knecht, C. Schlepphorst and F. Glorius, *Angew. Chem. Int. Ed.*, 2018, **57**, 8297-8300.

4. P. Schah-Mohammedi, I. G. Shenderovich, C. Detering, H.-H. Limbach, P. M. Tolstoy, S. N. Smirnov, G. S. Denisov and N. S. Golubev, *J. Am. Chem. Soc.*, 2000, **122**, 12878-12879.

5. T. Kasahara, H. Shinohara, Y. Oshima, K. Kadokura, Y. Uriu, C. Ohe and K. Itoh, *Surf. Sci.*, 2004, **558**, 65-79.

6. C. R. Arumainayagam, H.-L. Lee, R. B. Nelson, D. R. Haines and R. P. Gunawardane, *Surf. Sci. Rep.*, 2010, **65**, 1-44.

7. J. F. Moulder and J. Chastain, *Handbook of X-ray Photoelectron Spectroscopy: A Reference Book of Standard Spectra for Identification and Interpretation of XPS Data*, Physical Electronics Division, Perkin-Elmer Corporation, 1992.

8. G. W. T. M.J. Frisch, H.B. Schlegel, G.E. Scuseria, M.A. Robb, J.R. Cheeseman, G. Scalmani, G. Barone, B. Mennucci, G.A. Petersson, *Gaussian 09, Revision D.01*, Gaussian, Inc, Wallingford CT, 2013.

9. C. Wöll, S. Chiang, R. J. Wilson and P. H. Lippel, *Phys. Rev. B*, 1989, **39**, 7988-7991.

10. J. L. Clark, R. M. Neyyappadath, C. Yu, A. M. Z. Slawin, D. B. Cordes and D. O'Hagan, *Chem. - Eur. J.*, 2021, **27**, 16000-16005.

11. B. E. Ziegler, M. Lecours, R. A. Marta, J. Featherstone, E. Fillion, W. S. Hopkins, V. Steinmetz, N. S. Keddie, D. O'Hagan and T. B. McMahon, *J. Am. Chem. Soc.*, 2016, **138**, 7460-7463.

12. P. Zhang, C. C. Le and D. W. C. MacMillan, *J. Am. Chem. Soc.*, 2016, **138**, 8084-8087.

13. M. K. Whittlesey and E. Peris, *ACS Catal.*, 2014, **4**, 3152-3159.

14. R. A. Cormanich, N. S. Keddie, R. Rittner, D. O'Hagan and M. Bühl, *Phys. Chem. Chem. Phys.*, 2015, **17**, 29475-29478.

15.   O. Shyshov, K. A. Siewerth and M. von Delius, *Chem. Commun.*, 2018, **54**, 4353-4355.

16.   A. Rodil, S. Bosisio, M. S. Ayoup, L. Quinn, D. B. Cordes, A. M. Z. Slawin, C. D. Murphy, J. Michel and D. O'Hagan, *Chem. Sci.*, 2018, **9**, 3023-3028.

17.   A. Lampel, S. A. McPhee, H.-A. Park, G. G. Scott, S. Humagain, D. R. Hekstra, B. Yoo, P. W. J. M. Frederix, T.-D. Li, R. R. Abzalimov, S. G. Greenbaum, T. Tuttle, C. Hu, C. J. Bettinger and R. V. Ulijn, *Science*, 2017, **356**, 1064-1068.

18.   P. W. J. M. Frederix, G. G. Scott, Y. M. Abul-Haija, D. Kalafatovic, C. G. Pappas, N. Javid, N. T. Hunt, R. V. Ulijn and T. Tuttle, *Nat. Chem.*, 2015, **7**, 30-37.

19.   M. Amblard, J.-A. Fehrentz, J. Martinez and G. Subra, *Mol. Biotechnol.*, 2006, **33**, 239-254.

20.   A. Isidro-Llobet, M. N. Kenworthy, S. Mukherjee, M. E. Kopach, K. Wegner, F. Gallou, A. G. Smith and F. Roschangar, *J. Org. Chem.*, 2019, **84**, 4615-4628.

21.   S. Chowdhary, J. Moschner, D. J. Mikolajczak, M. Becker, A. F. Thünemann, C. Kästner, D. Klemczak, A.-K. Stegemann, C. Böttcher, P. Metrangolo, R. R. Netz and B. Koksch, *ChemBioChem*, 2020, **21**, 3450-3450.

22.   Deepa and S. Singh, *Adv. Synth. Catal.*, 2021, **363**, 629-656.

23.   E. I. Vrettos, N. Sayyad, E. M. Mavrogiannaki, E. Stylos, A. D. Kostagianni, S. Papas, T. Mavromoustakos, V. Theodorou and A. G. Tzakos, *RSC Adv.*, 2017, **7**, 50519-50526.

24.   A. B. Soriaga, S. Sangwan, R. Macdonald, M. R. Sawaya and D. Eisenberg, *J. Phys. Chem. B*, 2016, **120**, 5810-5816.

Chapter 5. Unexpected triaxial C–F preference in all-*cis*-1,3,5-trifluorocyclohexane motifs

5.1 Background and aim
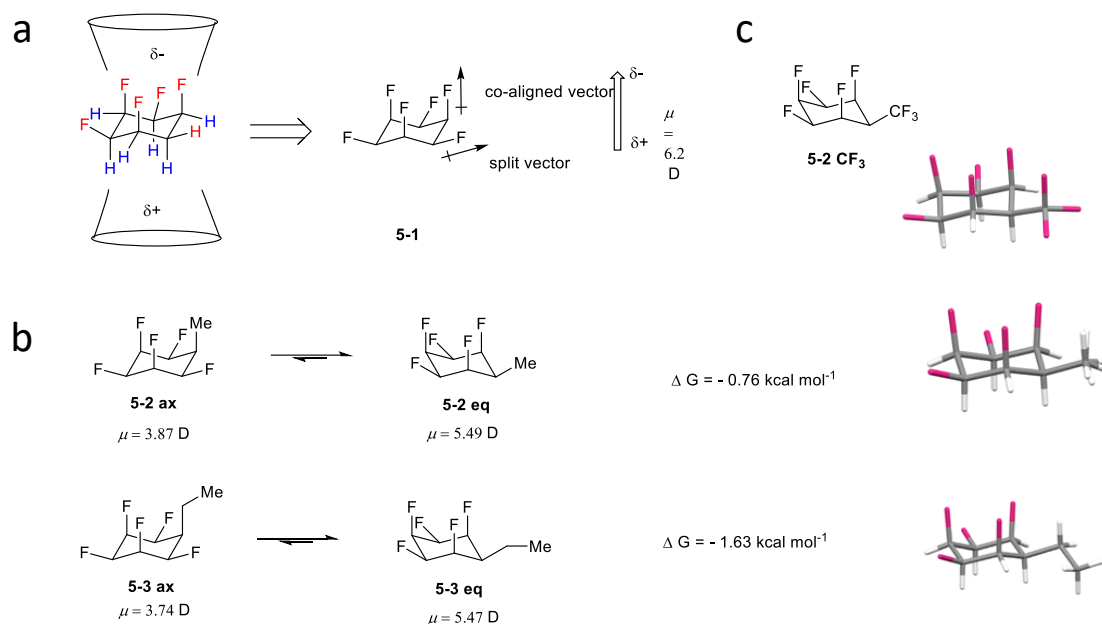
Figure 5-1 (a) Calculated (M06L-D3/aug-cc-pVTZ level) equilibrium energies between *axial/equatorial* conformers of alkyl substituted all-*cis* 1,2,3,4,5,-pentafluorocyclohexanes 3 and 4; (b) solid state X-ray structures of 5-2 CF_3 (upper) , 5-2 (mid) and 5-3 (bottom). In each case the equatorial conformer is favoured.

As discussed in the Introduction, in the classical conformational equilibria of un-strained substituted cyclohexane rings, the favoured lower energy conformer tends to adopt the maximum number of bulky substituent groups in an equatorial orientation, to minimise steric and electrostatic repulsion of 1,3 diaxial interactions.[1-5]

It is worth noting that, in most of the single crystal structures of all-*cis*-pentafluorocyclohexane derivatives reported, the substituent groups adopt an equatorial orientation in their favoured conformers despite the strong electrostatic repulsion between

three axial C–F dipoles. This even extends to less sterically demanding alkyl chains such as methyl and ethyl substituted Janus face cyclohexanes (JFCs). Such a conformational preference is stabilised by the intermolecular interactions between JFCs rings, and it is assisted with the steric relaxation. Computational studies indicated that the alkyl substituent in JFCs favour an equatorial conformation in the gas phase as well.[6]

The origin of the all-*cis* hexafluorocyclohexane **5-1** polarity lies in the tri-axial alignment of three C-F bonds, a situation that is always maintained in the chair conformations. The molecular dipole associated with the tri-equatorial C-F conformer is significantly reduced as the individual C-F dipoles counteract and equalise.[7]

It was of immediate interest to study the conformational preference of the all-*cis*-fluorocyclohexyl motif but with fewer fluorines. The favoured conformation of lesser substituted JFC rings should be dictated by intramolecular interactions in the gas phase and solution and then also intermolecular interactions in the condensed solid state.

The aim of the project was to prepare a library of all-*cis* multifluorinated cyclohexane derivatives and to demonstrate their conformational preferences both experimentally and by computation. The favoured conformations of these derivatives were studied by X-ray crystal structure analysis in the solid state, NMR for solution, and DFT calculations to estimate gas phase behaviour.
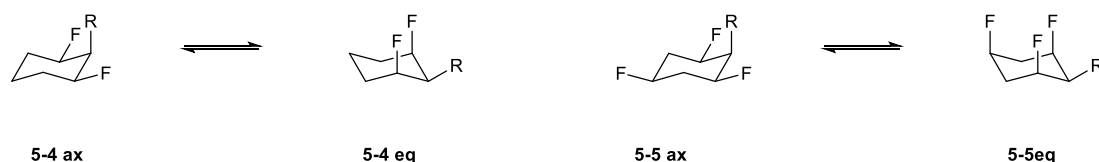
Scheme 5-1 Ring flip profile of 1,3 difluoro and 1,3,5 trifluoro cyclohexyl motifs.

The 1,5 difluoro and 1,3,5 trifluoro, mono-substituted (R – group) cyclohexyl rings **5-4** and **5-5** were of most interest. The favoured chair conformers of such motifs mainly depends on

competition between the electrostatic repulsion of di-axial C-F bonds and 1,3-diaxial H…R repulsions. Those conformers where an equatorial R-group is favoured will generate building blocks with a high net dipole moment and good facial polarity, but with fewer fluorine atoms. Deriving high polarity from fewer fluorine atoms would be potentially useful for applications in supramolecular chemistry and in motifs for drug development.

5.2 Results and discussion

5.2.1 Non-substituted Janus face cyclohexane rings

A series of all-*cis*-multifluorocyclohexanes were readily prepared by direct aryl hydrogenation of the corresponding fluoroarene as described by Wiesenfeldt *et al.*[8] Cyclohexanes **5-8**, **10**, **12** were already reported in the literature and their conformational preferences have already been studied. In these cases, ring interconversions generate iso-energetic conformers. [9, 10]
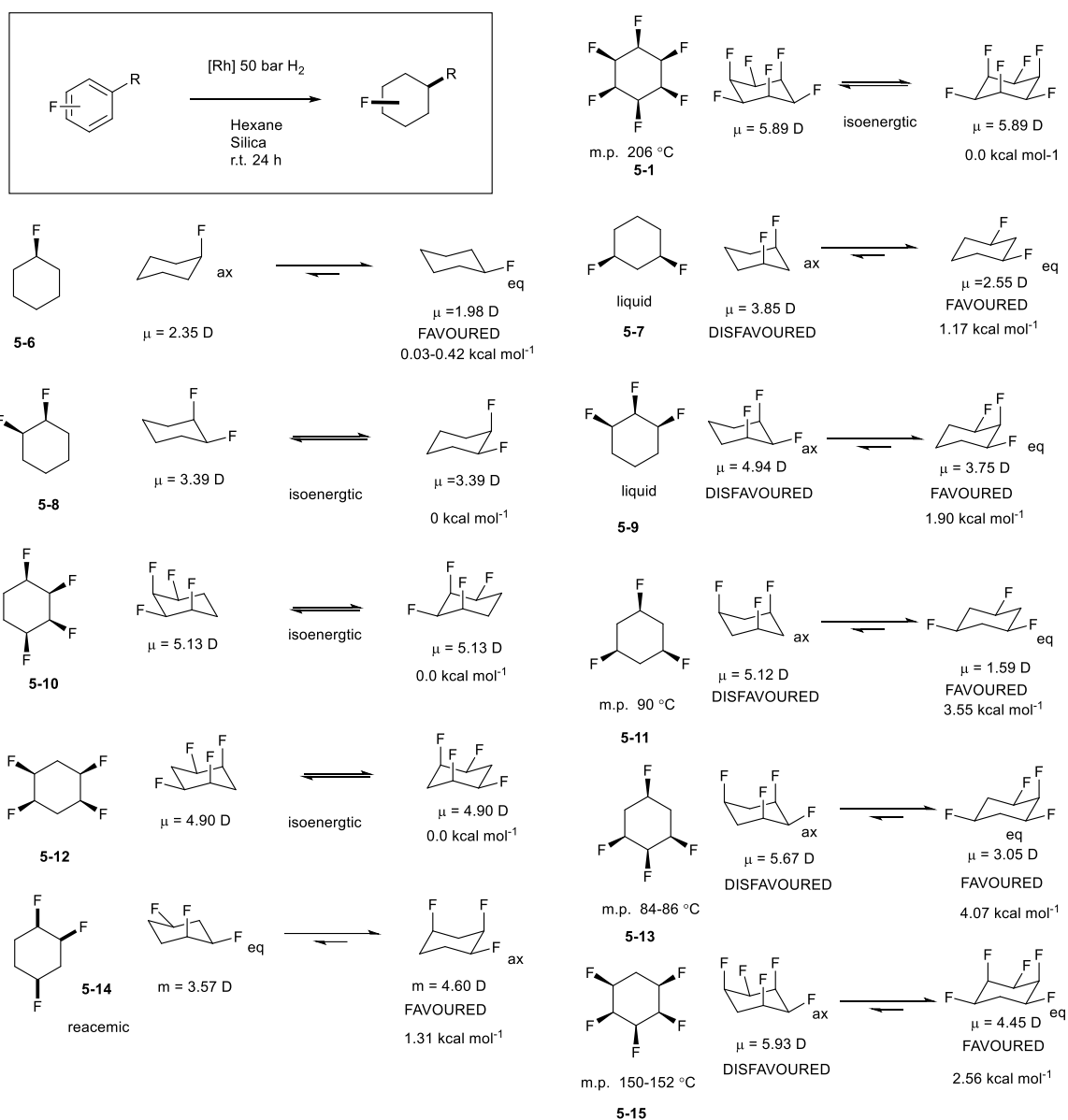
Figure 5-2 Dipole moment and relative energies of all-*cis*-fluorocyclohexane. [11] Comparative properties

calculated at the DF-MP2/ccpVTZ level of theory at MP2/DZP geometric, dipole moment based on SCF/cc-

96vtz from literature value, PBE0-D3/def2-TZVP//B3LYP-D3/def2-TZVP level of theory recalculated for **5-6, 9,**

10, 11.

The gas phase conformational preferences of cyclohexanes **5-1, 11, 13** and **15** were

recalculated using the PBE0-D3/def2-TXVP//B3LYP-D3/def2-TZVP level of theory by our

collaborators led by Prof. Rodrigo Cormanich of the University of Campinas. The B3LYP-

D3/def2-TZVP level was chosen for the geometry optimisation and frequency calculation

since it resulted in an accurate representation of the geometries which were observed in the related synthetic compounds. Also, the PBE0-D3/def2-TZVP level was chosen for single point energy calculations as it accommodated with lowest mean absolute error. Cyclohexanes **5-1**, **7**, **9**, **11**, **13** and **15** were prepared by the direct hydrogenation of the corresponding fluoro-arenes in order to study their liquid phase and solid phase conformations experimentally.
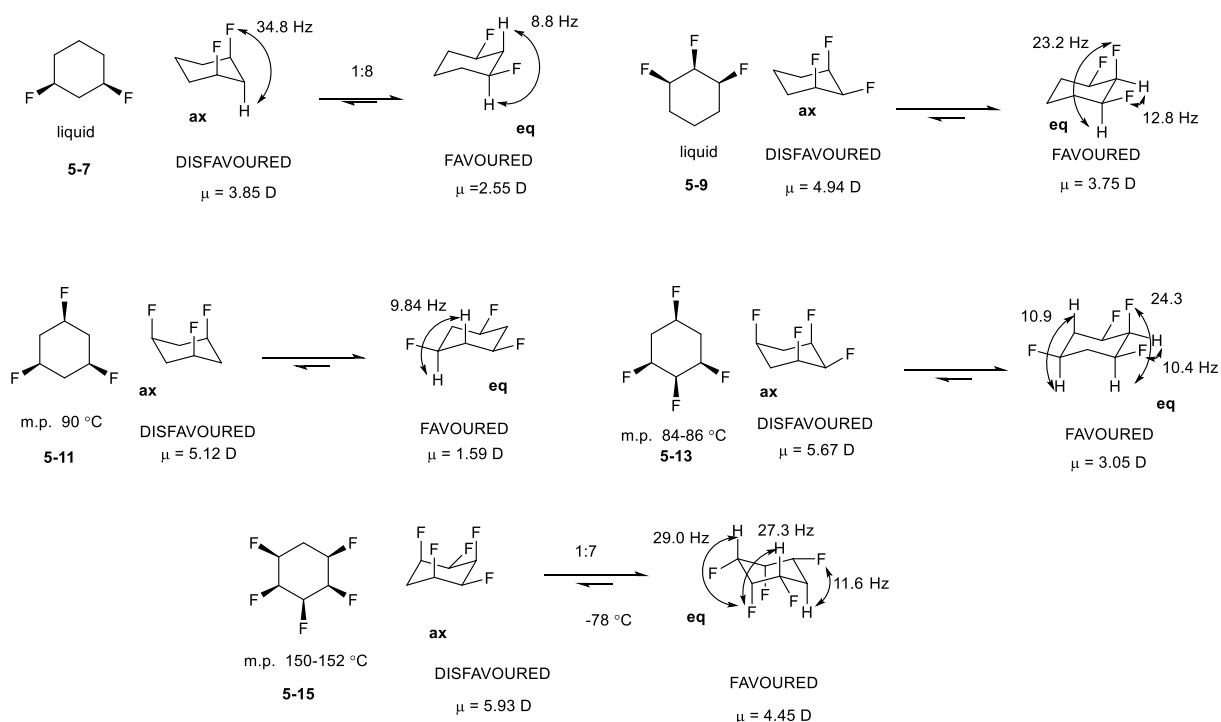
Figure 5-3 Conformational preferences observed for all-*cis* fluorocycloalkanes in solution and key coupling constant assignments for the favoured conformers.

Cyclohexanes **5-7** and **5-9** are liquids at room temperature which suggests relatively weak intermolecular interactions between the molecules. The preferred conformation of compounds **5-7** and **5-11** in DCM, have the C–F bonds equatorial in the chair conformation. This was established from the relatively large coupling constant between adjacent vicinal protons of $^3J_{H–H} = 8.8$ Hz, which suggests an anti-periplanar geometry (Figure 5-3). Compound **5-7** shows a 8:1 C–F equatorial to C–F axial ratio, which is evidenced by the large $^3J_{H–F}$ antiperiplanar coupling constant of 34.8 Hz in d_2-DCM at room temperature in the minor

conformer. Compounds **5-9** and **5-13** have a dominant equatorial conformation in *d*-chloroform. The geometry could be assigned from the $^3J_{\text{H-F}}$ coupling constant of 12.8 Hz between H-2 to F-1 and F-3, as well as the large ($^3J_{\text{H-F}}$ 23.2 Hz) coupling value between H-1 and the adjacent F-2 indicating that they are antiperiplanar.
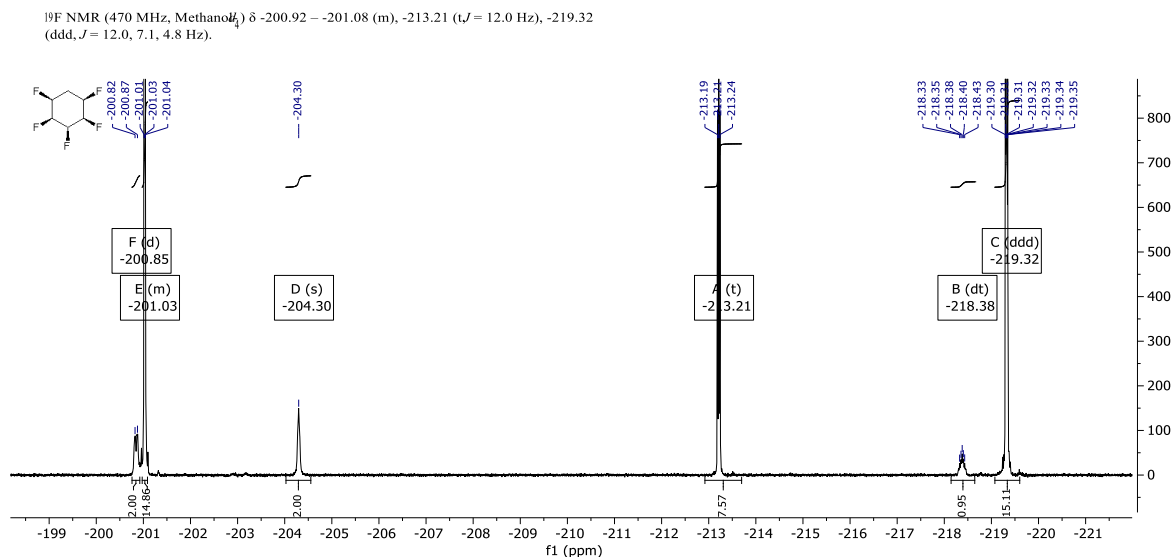

Figure 5-4 ^{19}F NMR of **5-15** at -78 °C which shows the resolved axial and equatorial conformers.

Compound **5-15** undergoes rapid ring interconversion at room temperature and generates an average spectrum. In the ^{19}F NMR, three peaks are observed at room temperature while two of the signals observed from -213.7 to -214.8 ppm and -216.7 to -219.4 ppm are broad. These broad signals are however resolved at low temperature (− 78 °C) and the ^{1}H-NMR shows two sets of signals corresponding to the axial and equatorial conformers in a 7:1 ratio favouring the equatorial conformation.

Figure 5-5 Sample of compound **5-11** indicating ready sublimation on the bench.

Compounds **5-11** and **5-15** have a unique behaviour equilibrating between the solid state and the gas phase. This cyclohexane undergoes ready sublimation and recondensation in a sealed sample bottle. As shown in the Figure 5-5, the powdered solid **5-11** self-assembles into fine needle like crystals, and a similar phenomenon was apparent for cyclohexane **5-15** but on a slower time scale.
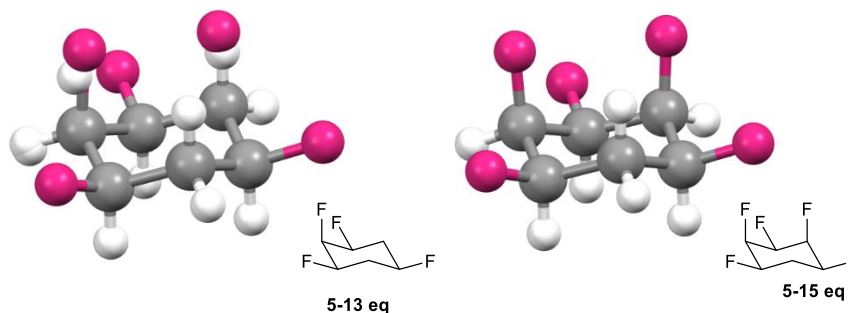
Figure 5-6 The X-Ray structures of cyclohexanes **5-13** and **5-15**. Both have an equatorial preference in the solid state.

Compound **5-13** shows an expected solid-state conformation with three equatorial fluorines. The two symmetrical axial positions are occupied by the remaining fluorine with a ~ 50 % occupancy. The crystal structure of **5-13** is in agreement with the equatorial preference observed in solution by NMR. Compound **5-15** has a similar disordered crystal structure, in which the axial positions are only partially occupied by fluorine, due to the axial proton location averaged by rotation along the ring axis. The near full occupancy of 1,3,5 equatorial positions demonstrated the equatorial conformation of cyclohexane **5-15** in the solid phase.
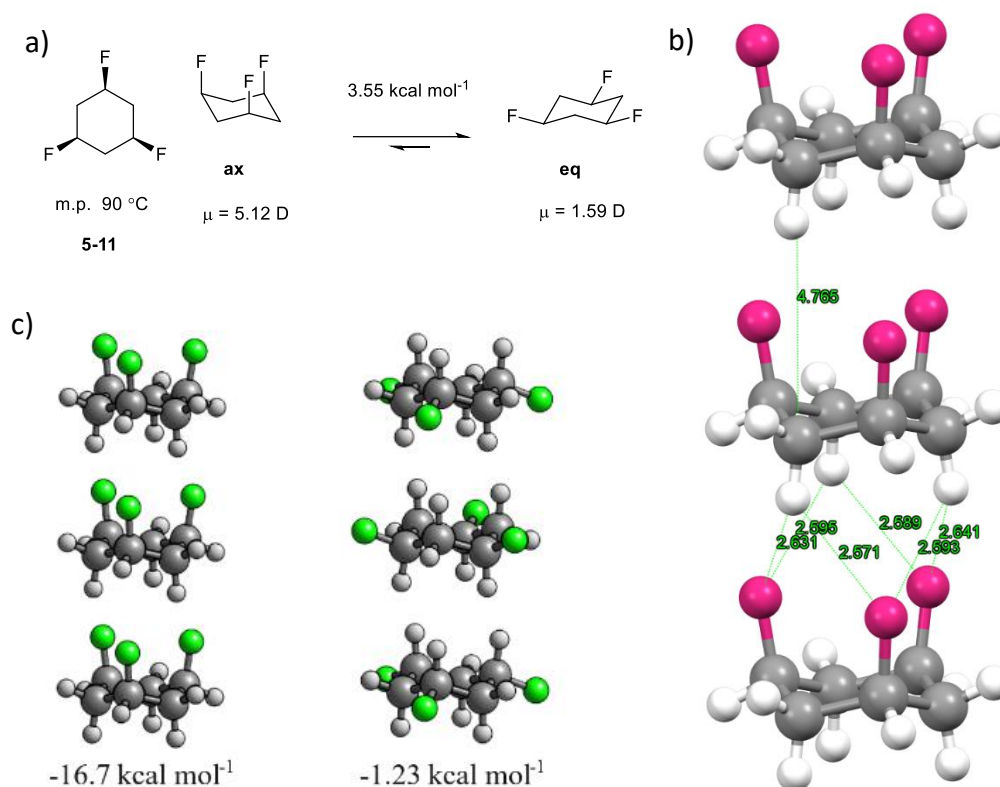
Figure 5-7 (a) Calculated equilibrium energy in the gas phase, with dipole moments (D) of both axial and equatorial conformers of **5-11**. (b) Section (3 molecules) of the X-Ray structure of **5-11** showing the tri-axial conformation in the solid state. (c) Computational analysis of the energies gained from condensation of tri-axial and tri-equatorial **5-11** conformers arranged similarly to the X-ray structure.

A striking observation was found in the solid-state structure of **5-11** shown in Figure 5-7, where the tri-axial C–F geometry was preferred in the stacking pattern. This was unexpected as the triequatorial (C–F bonds) conformer is significantly preferred in the gas phase by 3.55 kcal mol^{-1}. Also, the axial conformer has a significantly higher dipole moment (axial μ = 5.12 D vs. equatorial μ = 1.59 D).

In order to rationalise this observation, a DFT calculation of the association energies resulting on trimerisation of **5-11** in the gas phase was carried out with both tri-equatorial and tri-axial conformers. These calculations were carried out in the lab of Prof Rodrigo Cormanich at the

University of Campinas in Brazil. The molecules were arranged with one ring stacked on top of the another, to approximate the arrangement in the crystal structure. A London-dispersion corrected Hartree Fock method (HFLD)[12] was used and the aug-cc-pVTZ basis was set as implemented in ORCA 5.03[13] for its high accuracy between the DLPNO-CCSD and DLPNO-CCSD(T) schemes and fast basis set convergence.
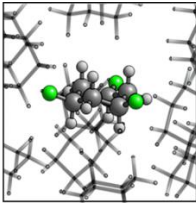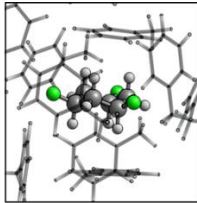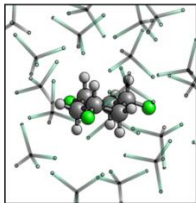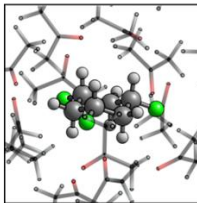
A striking difference between the axial and equatorial conformers, for the association energy in the packing arrangement was observed. The interaction energy in bringing three isolated tri-axial molecules of **5-11** together was -16.7 kcalmol^{-1} whereas the energy was much less (-1.23 kcalmol^{-1}) after condensing three tri-equatorial conformers. The stabilisation observed in the packed structure is derived from the inherent polarity and consequent intermolecular electrostatic attraction between the ring faces. The electronegative fluorine face with co-aligned C–F dipole moments interacts with the electrostatic positive hydrogen face of an adjacent molecule. The value of about ~8.0 kcal mol^{-1} for each of the two interactions in bringing three molecules together matches the magnitude already evaluated for **5-1**[14]. The tri-equatorial conformer of **5-11** is far less stabilised when rings come together as the rings are significantly less polar.

Figure labels:
20-30 Hz, F, F ~170 Hz, F, H, **5-11 ax**
~10 hz, 9.84 Hz, H, F, F, F, H, ~180 Hz, **5-11 eq**

F, F, F, m.p. 90 °C, **5-11**

DISFAVOURED
μ = 5.12 D

FAVOURED
μ = 1.59 D
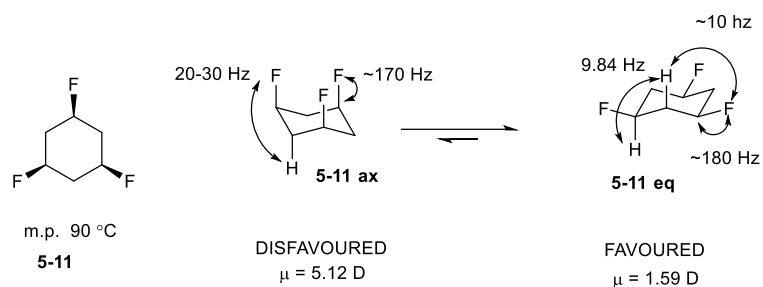
NMR solvent	δ ^{1}H ppm	$^3J_{H-H}$ coupling CH<u>F</u>–H$_{ax}$	$^2J_{H-F}$ coupling	$^1J_{C-F}$ coupling	Solvent dielectric constant ε
d-Acetone	4.70	11.6	47.1	173.5, 16.1	20.7
d-DCM	4.58	9.4	45.8		8.9
Chloroform-*d*	4.55	10.2	46.4	176.0, 14.9	4.8
d-tolune	3.65	11.0	47.3	176.9, 17.0	2.4
d-cyclohexane	4.27	11.2	47.3	179.4 16.7	2.0

Table 5-1 Chemical shift (δ) and key coupling constants for compound **5-11** in different deuterated solvents.

The solution phase behaviour of **5-11** was explored in some detail. The ^{1}H NMR in d-cyclohexane d_2-DCM, chloroform-*d*, d_8-toluene d_6-acetone and d_4-methanol all indicated a predominant tri-equatorial conformation, as no large $^3J_{H-F}$ values were observed. Typical antiperiplanar HC–CF $^3J_{H-F}$ coupling constants are in the range of 20-35 Hz. For compound **5-11**, in the various solvents, values in the range of 4.5-11.5 Hz $^3J_{H-F}$ were observed suggesting a *gauche* relationship between fluorine and the vicinal hydrogen (HC–CF).[15-17] In the ^{13}C NMR spectra of **5-11,** a change in $^1J_{C-F}$ coupling constant with the polarity of the solvent was observed. As the signals for the axial and equatorial conformers coalesce due to rapid ring interconversion, the $^1J_{C-F}$ coupling constant is an average of the **5-11 eq** and **5-11 ax** conformer populations.

Figure 5-8 Experiment and theory (M06L/pcJ-1//M06L/pc-1) derived $^1J_{CF}$ NMR-coupling constants for **5-11** tend to lower values with increasing polarity of the solvent.

The coupling constant of $^1J_{C\text{-}F}$ is 179.4 Hz in the least polar solvent (*d*-cyclohexane) reduces as the solvents become more polar. The value in d_8-toluene is 176.9 Hz, in d-chloroform it is 176.0 Hz and a $^1J_{C\text{-}F}$ value of 173.5 Hz is observed in the most polar d_6-acetone. Such a tendency can be rationalised in terms of the Perlin effect.[18-20] The Perlin effect is the phenomenon where the axial C–F bond has a smaller $^1J_{C\text{-}F}$ coupling constant than the equatorial C–F bond. It has been argued that this is due to hyperconjugation which is maximised for an axial fluorine as it is antiperiplanar to two C–H bonds, which are donating electron density into the $\sigma^*_{C\text{-}F}$ antibonding orbital. This weakens and elongates the C–F bond a little, resulting in a reduced $J_{C\text{-}F}$ coupling constant. This effect only applies to axial C–F bond.

The observed values of $^1J_{C\text{-}F}$ coupling constants were reduced with increasing dielectric constant ε of the solvent, as shown in Table 5-1 and Figure 5-7. This is consistent with the fact that more polar solvent will accommodate the more polar conformer and increase its

population in solution. Computation suggested a 50:50 ratio of the axial to equatorial conformers in acetone, which is the most polar ($\varepsilon = 20.7$) solvent that was explored. Similarly, in the ^{19}F NMR in d_2-DCM, the coalesced peak was resolved into two broad signals at -78 °C indicating an approximate ratio of 40:60 of the axial to equatorial conformer.

## 5.2.2 All-*cis* 3,4,5 trifluoro substituted cyclohexanes

A series of variously substituted fluorocyclohexanes were prepared by direct aryl hydrogenation. The substituent groups selected were methoxyl (–OMe), hydroxyl (–OH), acetamide (NHMe), carbamate (NHBoc) and a carbonyl ester (COOMe). The C–O and C–N bonds are the most common heteroatoms found in organic chemistry, and therefore these derivatives were selected as they could be deprotected and transformed into their corresponding esters or amides for supramolecular applications or drug development projects.
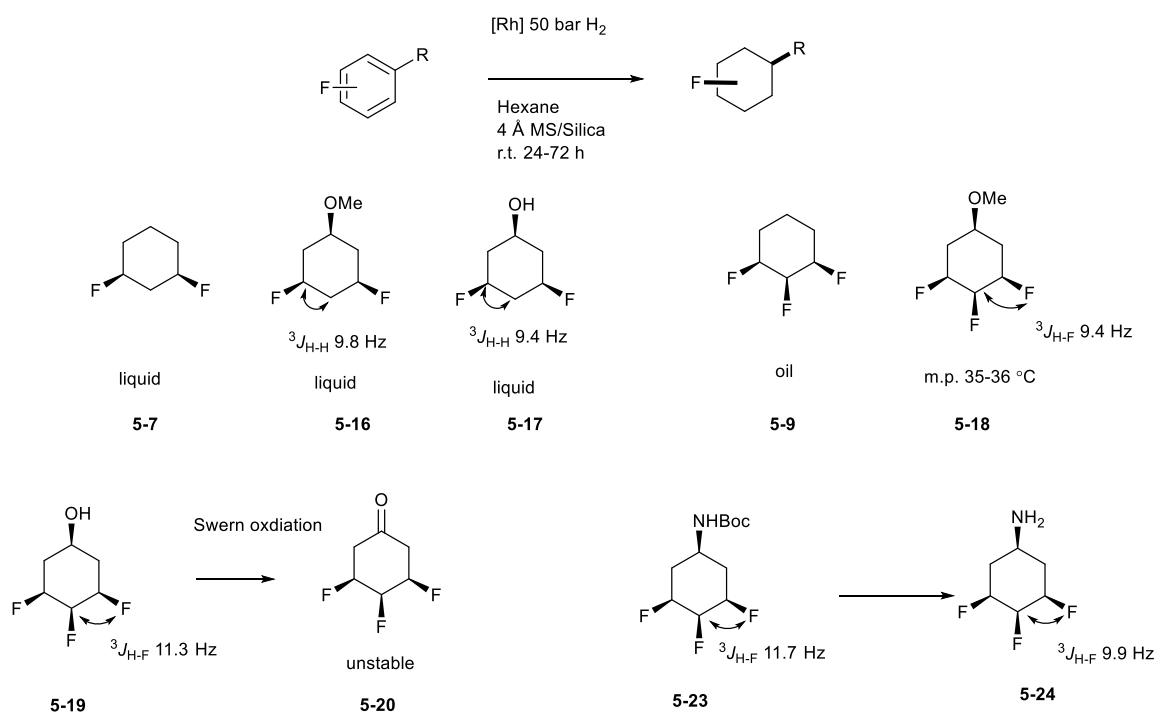
Figure 5-9 Key coupling constants of all-*cis*-3,5 difluoro and 3,4,5 tri-fluorocycloalkane derivatives suggests the equatorial conformation is preferred in solution.

At the outset, a number of derivatives of cyclohexanes **5-7** and **5-9** were prepared. As discussed previously, **5-7** and **5-9** have a conformational preference where the C–F bonds adopt an equatorial orientation, and this results in a predominant di-equatorial species. Compounds **5-16** and **5-17** are 1,3,5 tri-substituted and have the potential to co-align their dipoles in a condensed phase.

In the ^{1}H NMR spectra of compounds **5-16**, **5-17**, **5-18**, **5-19**, and **5-23**, large $^3J_{\text{H-H}}$ values were observed for the geminal (-CHX-) proton attached to the substituted carbon of the C–O and C–F bonds, suggesting an axial orientation for the C-H bond. Therefore, the substituent in the 1,2,3 trifluorocyclohexane motifs have an equatorial preference in solution. These compounds are liquid at room temperature indicating that they do not readily crystallise.
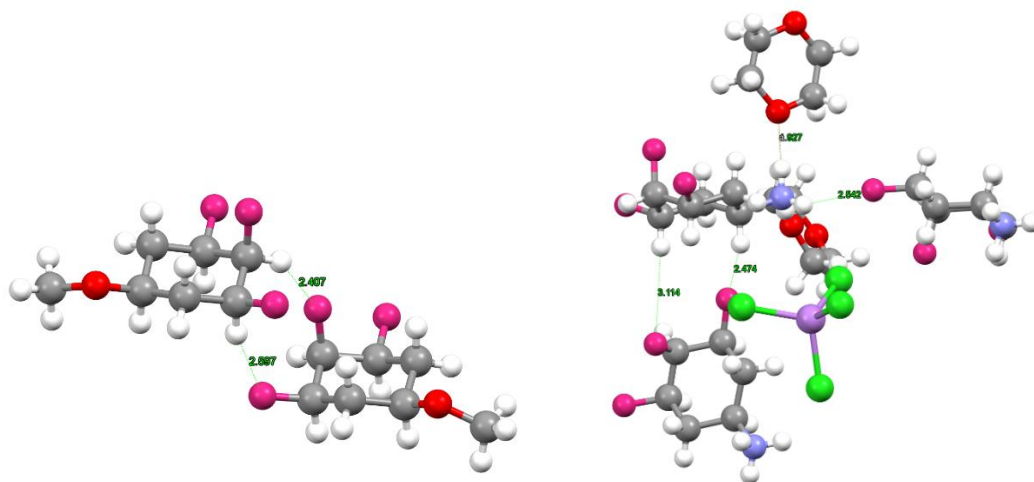
Figure 5-10 The X-ray crystal structures of **5-18** and **5-24** show an equatorial substituent.

The crystal structure of **5-18** in Figure 5-10 shows a predominant equatorial conformation in the solid state, perhaps as expected. The cyclohexyl ring arrangements in the solid state of **5-18** is not so ordered and deviates from the more regular stacking of the rings. However relatively short C–H...F–C contact distances of CH$_{\text{ax}}$...$_{\text{eq}}$FC = 2.60 Å and CH$_{\text{eq}}$...$_{\text{ax}}$FC = 2.41Å are observed in intermolecular contacts.

Compound **5-19** could be converted to ketone **5-20** by a Swern oxidation. The resultant

ketone **5-20** was stable in solution for one week and offers an intermediate for further

conversion.

The crystal structure of free amine **5-24** also shows an equatorial conformation for the

amine substituent. Amine **5-24** co-crystallised with $FeCl_4$ and dioxane, which were added

during the deprotection procedure. A short contact $CH_{ax...eq}FC$ distance of 2.47 Å of the

hydrogen face axial proton to the underneath perpendicular equatorial C–F bond was

observed indicating a stabilising interaction.

5.2.3 All-*cis*-1,3,5 trifluoro substituted cyclohexanes

A library of 1,3,5-trifluorocyclohexane derivatives was prepared to explore the potential for

co-aligning three axial C–F bonds. Such conformations have a large dipole moment but with

fewer fluorine atoms. It is of interest to explore the factors which may influence a propensity

towards a tri-axial arrangement of C–F bonds with fewer fluorines.
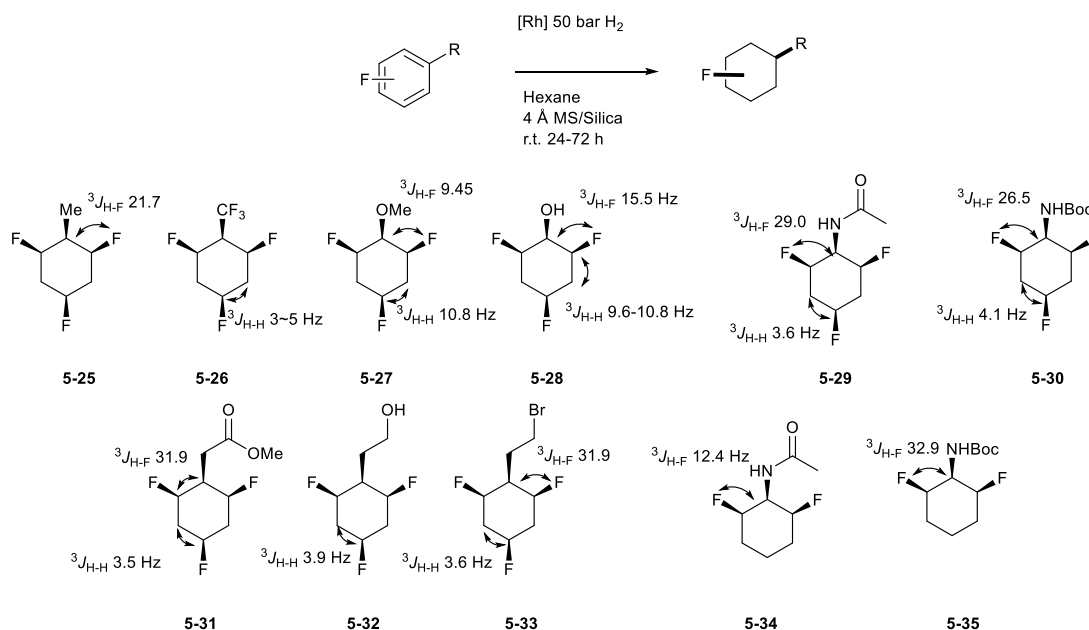
Figure 5-11 All-*cis*- 1,3,5 trifluorocyclohexane derivatives prepared by aryl hydrogenation. Key coupling

constants were assigned by ^{1}H and ^{19}F NMR to determine solution conformations.

The methyl substituted trifluoromethylcyclohexane **5-25** was found to adopt a similar tri-equatorial conformational preference to **5-11** in the gas phase (Figure 5-13 a). An exception arose with **5-25 ax** where the solution NMR in d-chloroform indicated a large $^3J_{\text{H-F}}$ coupling constant of 21.7 Hz for the CHMe proton, indicative of an axial conformation. Conformer **5-25 ax** is the only conformer found in the solid phase X-ray crystal structure. DFT calculations indicate that in the gas phase **5-25 eq** is less polar than **5-11 eq**. The equatorial conformer of **5-11** with an axial orientation of the methyl group is favoured in the gas phase by 1.98 kcalmol^{-1}. The gas phase simulated interaction energy, gained from the trimerisation of three molecules of **5-25** close to the crystal lattice arrangement, indicates a significant energy difference between the tri-axial C–F conformer (-16.62 kcalmol^{-1}) and the tri-equatorial C–F conformer (-9.24 kcalmol^{-1}). The more polar conformer results in much greater supramolecular stabilisation and consequentially adoption of axial C–F bonds in the condensed phase.
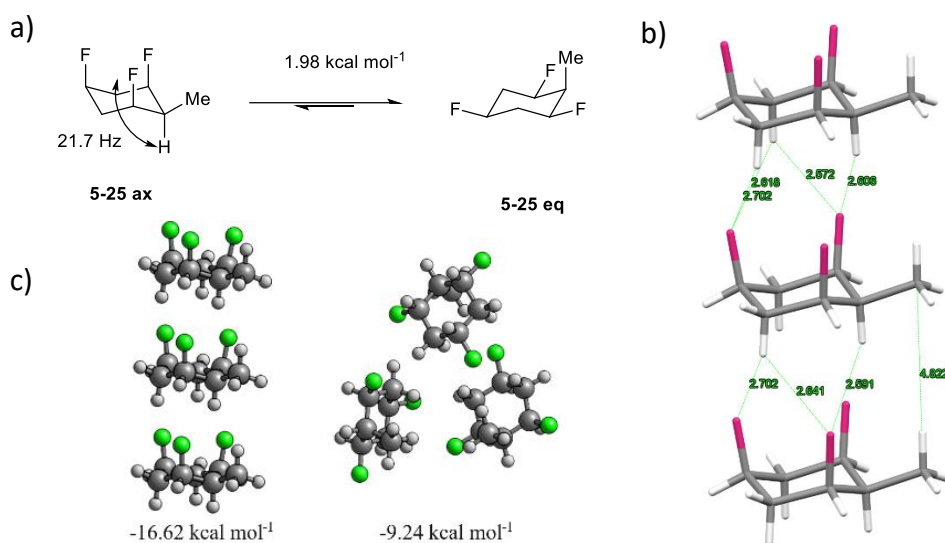
Figure 5-12 Equilibrium energies (a), X-Ray structure (b) computational analysis indicating the energy gained from condensation of tri-axial and tri-equatorial conformer of **5-25**.

It is noted that the equatorial conformer of **5-25eq** (Me axial) could not achieve a local

minimum by parallel packing, and the optimised geometry is a less organised arrangement. This is almost certainly due to the steric influence of the axial methyl group which is hindering the parallel packing of the cyclohexane ring. In contrast the solid-state arrangement of tri-axial C–F cyclohexane with the sterically relaxed equatorial methyl group is facilitated.
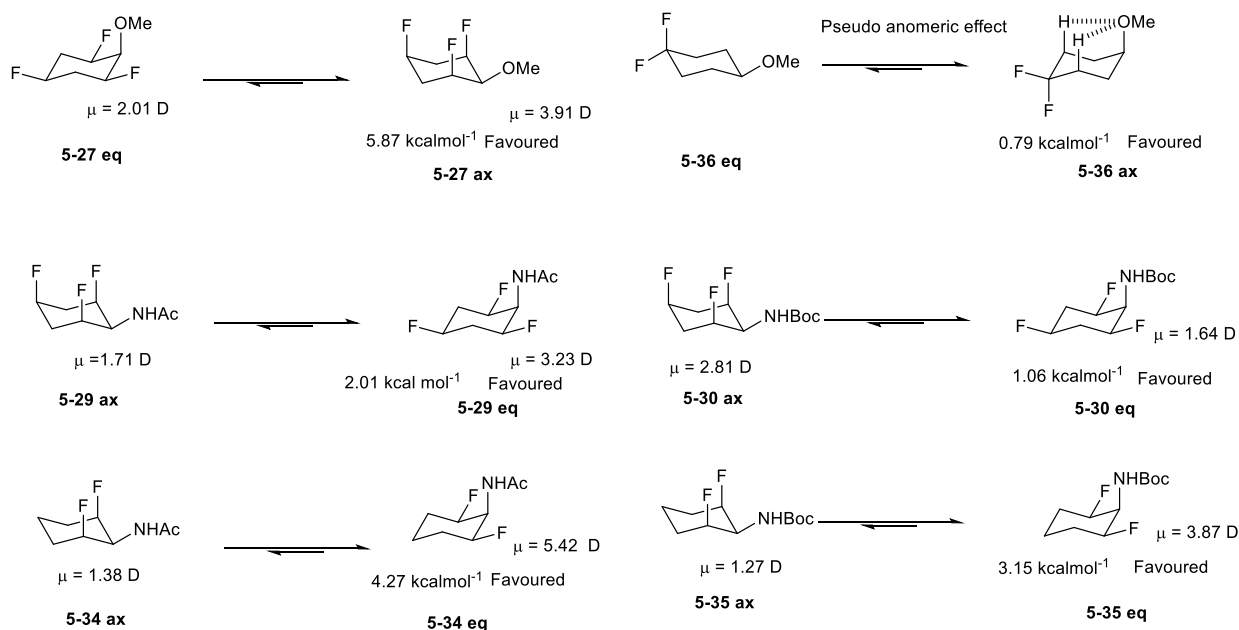
Figure 5-13 The equilibrium energy and dipole moment of both axial and equatorial conformers of **5-25**, **29**, **30**, **34**, **35** and **36.**

The OMe group of methoxycyclohexane **5-27** has a significantly favoured equatorial (OMe) conformation in the gas phase by 5.87 kcalmol^{-1}. Compound **5-27** is one of the few derivatives of 1,3,5-trifluorocyclohexane with a crystal structure where the three C–F bonds adopt a triequatorial arrangement in the solid state. This is consistent with the unexpected behaviour of 4,4-difluoro-methoxycyclohexane **5-36**, which also prefers a conformation where the methoxyl group adopts an axial orientation. That phenomenon was described as a pseudo-anomeric effect.[21, 22] The axial preference arose due to the accommodation of electrostatic nonclassical hydrogen bonds (NCHBs) between the axial methoxyl oxygen and the electropositive 1,3-di-axial hydrogens, due to the inductive effect of the fluorines, in the **5-36 ax** conformer. Such NCHB interactions may also dictate the **5-25 eq** conformer here and this

could account for the different behaviour of **5-27** in the solid state relative to other substituted 1,3,5-trifluorocyclohexanes. Another factor weakening the tri-axial C–F supramolecular interaction in **5-27** is the small dipole moment *difference* between **5-25 eq** (2.01 D) and **5-25 ax** (3.91 D).
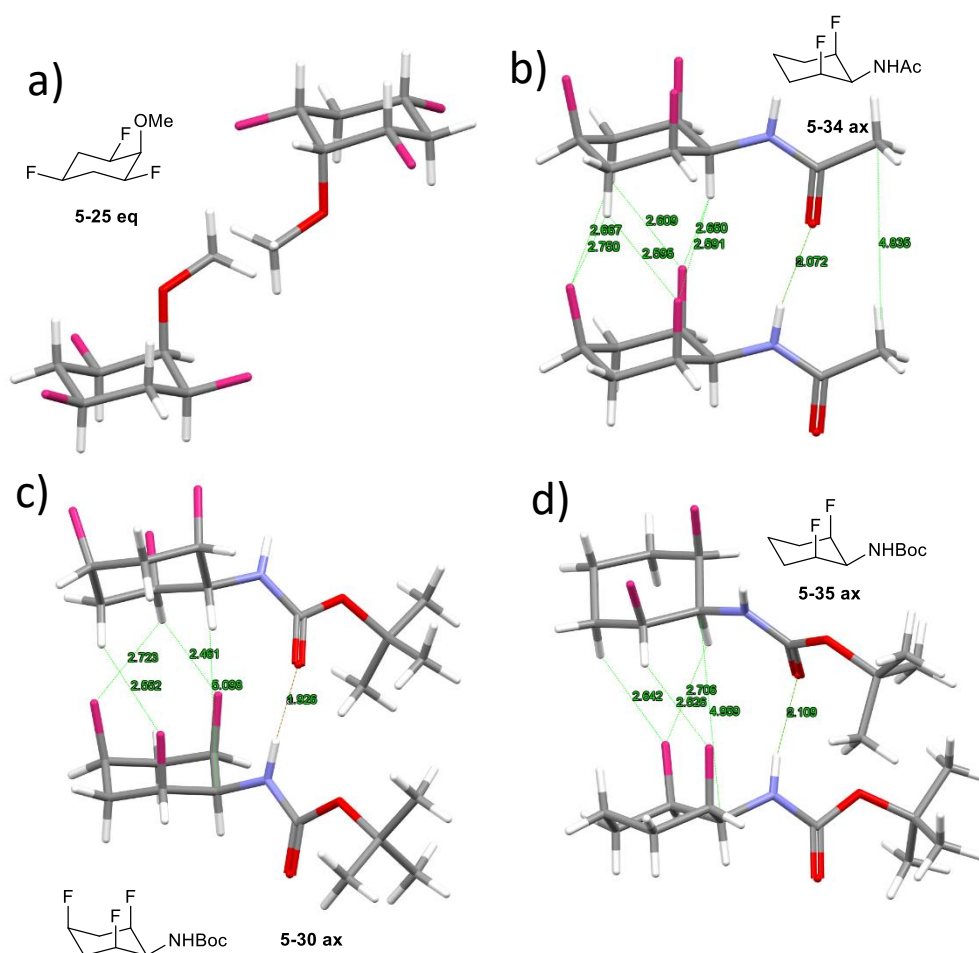
**Figure 5-14** X-Ray structures of **5-25**, **34, 30** and **35**.

The conformations of amino substituted 1,3,5-trifluorocyclohexanes were explored. The crystal structures of acetamide **5-29** and carbamate **5-30** were recorded and are illustrated in Figure 5-14. In each case these derivatives adopt a tri-axial C–F preference in the solid-state condensed phase and the C–N substituent is lying an equatorial orientation. Unlike the all-*cis* 1,3,5-trifluorocyclohexane rings that support a low energy equatorial conformer in the gas

phase, the amino substituted **5-29** and **5-30** have a significant preference for the tri-axial C–F conformers in the gas phase. Unlike the methyl and methoxy groups, the acetamide and carbamate groups are over-riding the electrostatic repulsion between fluorine atoms. The "*gauche effect*" is one of the significant factors involved in such stabilisation.
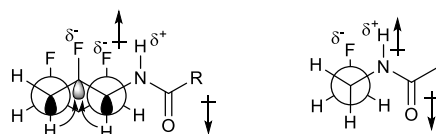
Figure 5-15 Fluorine *gauche* effect in **5-29** and **5-30 ax** (left) and 2-fluoroacetamide (right).

As previously discussed in Chapter 1 (Section 1.3.2), an amide substituent tends to orientate *gauche* to a vicinal fluorine. Such observations in **5-29** and **5-30** are consistent with well-known stereoelectronic effects in organofluorine chemistry and particularly that 1,2-difluoroethane **1-16** has a lower energy *gauche* than *anti* conformer, which is favoured by ~0.8 kcalmol^{-1} in the gas phase. This is exclusive to the organo-fluorine bond since 1,2-dichloro, 1,2-dibromo and 1,2-diiodoethanes have a favoured *anti* conformation. The major factor attributed to the *gauche* effect involves the σ_{C-H} … σ_{C-F} antiperiplanar hyperconjugation. Other factors such as electrostatic interactions between the 1,3 $^{\delta-}$F–C $^{\delta+}$ in 1,2-difluoroethane and steric repulsion also contribute to the conformational preference.[21, 23] The *gauche* effect is also enhanced if the fluorine is vicinal to a strong electron withdrawing group such as acetamide.[24-26] The energy gained for such stabilisation in 2-fluoroethylacetamide is 1.78 kcal mol^{-1} which is double the value of the classical 1,2 difluoroethane *gauche* effect.
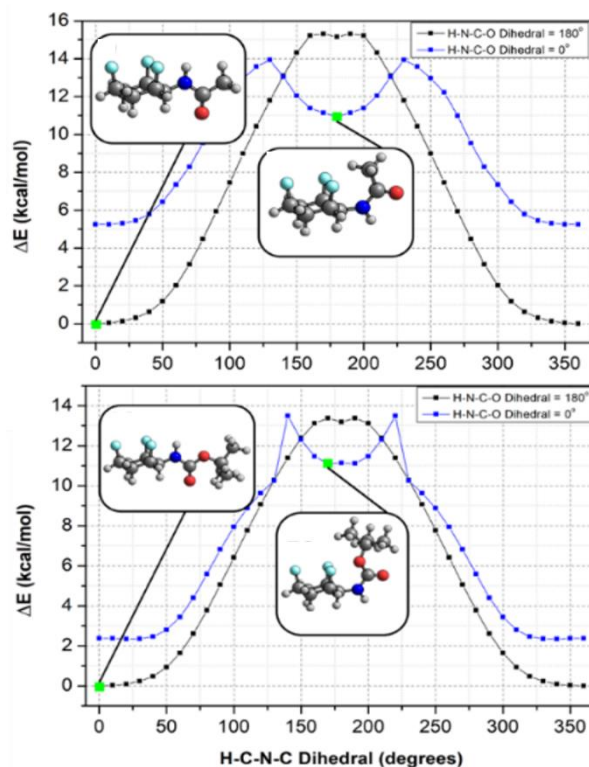
Figure 5-16 Rotational energy profiles for triaxial **5-29 ax** and **5-30 ax**. H-N-C-O dihedral angles of 180° are favoured with deep energy wells for conformers with N-H *syn* and C=O *anti* to axial C-F bonds.

Rotational energy force fields were calculated (Prof Rodrigo Cormanich, University of Campinas, Brazil) rotating around the C–NHAc and C–NHBoc bonds for both the tri-axial and tri-equatorial conformers of compound **5-29** and **5-30**. In all cases, the *trans* (*anti*) geometry of the C=O dipole to the C–F dipole was observed in the lowest energy conformers. It follows that the N–H bond is oriented parallel to the C–F bonds while the C=O bond is facing the opposite direction. Both compounds **5-29** and **5-30** have their lowest energy conformers, with minimised overall dipole moments, in a steep energy well of 14-15 kcal mol^{-1}. Such a geometry also enables an electrostatic attraction between the adjacent fluorine and N–H hydrogen, hence the system gains stability from both stereoelectronic and electrostatic effects.

When the substituent groups have a large steric influence on the cyclohexyl ring, the tri-axial

C–F conformer becomes predominant in solution, as shown for **5-31**, **5-32** and **5-33**. Large ^3J H-F coupling constant values of 32 Hz were found between the hydrogen on the tertiary carbon and the adjacent fluorine. Therefore, such motifs could be used in drug discovery, polymer and supramolecular materials to influence conformation and polarity to improve performance.

As both compounds **5-29** and **5-30** prefer tri-axial C–F bonds, the influence of removing the distal fluorine was explored in compounds **5-34** and **5-35**. It was envisaged that this would reduce electrostatic repulsion between the C–F bonds relative to the tri-axial C-F system. The results are summarised in Figure 5-11 and show that the removal of the third fluorine significantly increased the relative equilibrium energy for the acetamide (-4.27 kcal mol^{-1}) and for the carbamate (-3.15 kcalmol^{-1}) for the favoured C–F diaxial conformation in gas phase.

5.3 Summary

In conclusion, a range of all-*cis*-fluorocyclohexanes with C–F bonds at different positions were synthesised by aryl hydrogenation and their relative conformation energies studied by DFT calculations, NMR and X-ray structural studies. The unexpected tri-axial C–F conformation in 1,3,5 trifluorocyclohexane was found in the solid state overriding the calculated stabilisation energy ~3.5-3.7 kcal mol^{-1} for the corresponding equatorial conformation in the gas phase. This behaviour demonstrates the strong intermolecular interactions in the condensed phase for 1,3,5-trifluorocyclohexane and most of its derivatives, which could be useful in the design of supramolecular structures. Such effects could be enhanced by electron-withdrawing substituent groups, such as acetamide and carbamate, by further influencing conformation through the stereoelectronic *gauche* effect. In certain combinations, the overall dipole moment minimization, electrostatic attraction and stereoelectronic repulsion of substituent groups can override the tri-axial fluorine repulsion and extend the tri-axial C–F conformational preference into the solution phase and also in the gas phase.[27]

5.4 References

1. E. W. Warnhoff, *J. Chem. Educ.*, 1996, **73**, 494.

2. B. O. O. Hassel, *Acta Chem. Scand.*, 1947, 929-943.

3. D. H. R. Barton, *J. Chem. Soc.*, 1953, 1027-1040.

4. S. H. W. E.L. Eliel, *Stereochemistry of organic compounds*, Wiley, New York, 1994.

5. N. J. H. S. Winstein, *J. Am. Chem. Soc.*, 1955, 5562-5578.

6. J. L. Clark, A. Taylor, A. Geddis, R. M. Neyyappadath, B. A. Piscelli, C. Yu, D. B. Cordes, A. M. Z. Slawin, R. A. Cormanich, S. Guldin and D. O'Hagan, *Chem. Sci.*, 2021, **12**, 9712-9719.

7. N. S. Keddie, A. M. Z. Slawin, T. Lebl, D. Philp and D. O'Hagan, *Nat. Chem.*, 2015, **7**, 483-488.

8. M. P. Wiesenfeldt, Z. Nairoukh, W. Li and F. Glorius, *Science*, 2017, **357**, 908-912.

9. A. J. Durie, A. M. Z. Slawin, T. Lebl, P. Kirsch and D. O'Hagan, *Chem. Commun.*, 2012, **48**, 9643-9645.

10. A. J. Durie, A. M. Z. Slawin, T. Lebl, P. Kirsch and D. O'Hagan, *Chem. Commun.*, 2011, **47**, 8265-8267.

11. Q. Luo, K. R. Randall and H. F. Schaefer, *RSC Adv.*, 2013, **3**, 6572-6585.

12. C. Bannwarth, S. Ehlert and S. Grimme, *J. Chem. Theo. Thermodyn.*, 2019, **15**, 1652-1671.

13. F. Neese, F. Wennmohs, U. Becker and C. Riplinger, *J. Chem. Phys.*, 2020, **152**, 224108.

14. S. M. Pratik, A. Nijamudheen and A. Datta, *Chemphyschem*, 2016, **17**, 2373-2381.

15. A. Lawer and L. Hunter, *Eur. J. Org. Chem.*, 2021, **2021**, 1184-1190.

16. Y. Lizarme-Salas, A. D. Ariawan, R. Ratnayake, H. Luesch, A. Finch and L. Hunter, *Beilstein J. Org. Chem.*, 2020, **16**, 2663-2670.

17. L. Hunter, P. Kirsch, A. M. Z. Slawin and D. O'Hagan, *Angew. Chem. Int. Ed.*, 2009, **48**, 5457-5460.

18. A. C. Tsipis, *New J. Chem.*, 2022, **46**, 13940-13952.

19. J. M. Silla, M. P. Freitas, R. A. Cormanich and R. Rittner, *J. Org. Chem.*, 2014, **79**, 6385-6388.

20. V. V. S. Wolfe B. M. Pinto, R. Y. N. Leung, *Can. J. Chem.*, 1969, **68**, 1051.

21. B. A. Piscelli, D. O'Hagan and R. A. Cormanich, *Phys. Chem. Chem. Phys.*, 2021, **23**, 5845-5851.

22. B. A. Piscelli, W. Sanders, C. Yu, N. Al Maharik, T. Lebl, R. A. Cormanich and D. O'Hagan, *Chem. - Eur. J.*, 2020, **26**, 11989-11994.

23. J. C. R. Thacker and P. L. A. Popelier, *J. Phys. Chem. A*, 2018, **122**, 1439-1450.

24. D. Y. Buissonneaud, T. van Mourik and D. O'Hagan, *Tetrahedron*, 2010, **66**, 2196-2202.

25. N. E. J. Gooseman, D. O'Hagan, M. J. G. Peach, A. M. Z. Slawin, D. J. Tozer and R. J. Young, *Angew. Chem. Int. Ed.*, 2007, **46**, 5904-5908.

26. J. W. Banks, A. S. Batsanov, J. A. K. Howard, D. O'Hagan, H. S. Rzepa and S. Martin-Santamaria, *J. Chem. Soc.*, 1999, 2409-2411.

27. C. Yu, B. A. Piscelli, N. A. Maharik, D. B. Cordes, A. M. Z. Slawin, R. A. Cormanich and D. O'Hagan, *Chem. Commun.*, 2022, DOI: 10.1039/D2CC05058G.

Chapter 6. Towards Janus face coordinating organic frameworks

6.1 Introduction

6.1.1 Background to framework materials
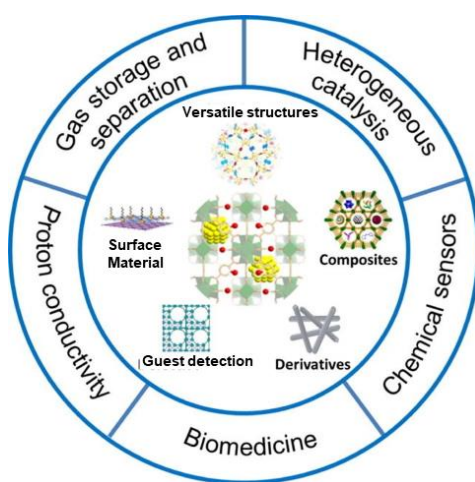
Framework organic materials are a class of synthetic porous crystalline compounds which are emerging as attractive functional materials. Two widely studied framework materials are Covalent Organic Frameworks (COFs) and Metal Organic Frameworks (MOFs), which have developed extensively in the past decades. This is due to their attractive properties such as structural versatility, long range order, high porosity for gas absorption, and tuneable functionality for host-guest interactions.[2, 3]

The ability to design such molecular architectures allows control of properties such as pore size, surface area, charge conductivity and thermal stability. Such porous materials assembled from simple building blocks offers potential in bio-imaging, bio-sensing and drug delivery applications.[4]

More recently, a catalogue of flexible frameworks constructed by hydrogen bonding, so called hydrogen-bonded organic frameworks (HOFs) were established. The HOFs material have many unique properties such as mild synthesis conditions, solution processability, self-assembling properties, and as a consequence, self-healing, and regeneration potential. [5-8]

6.1.2 Classes of framework materials
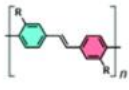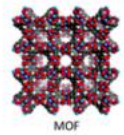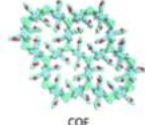
Example	Advantages	Disadvantages	Chemical interaction detection
carbon nanotube	• High surface-to-volume ratio • High aspect ratio • Excellent stability • High density of reactive sites • Good thermal stability • Compatible with device miniaturization	• Requirement of chemical modification to enhance selectivity • Difficulty in establishing reliable electrical contacts • Difficulty in purification • Limited structure and precision control	• Electrochemical • Chemiresistive • Optical detection
graphene	• Large surface-to-volume ratio • Good optical transparency • Excellent mechanical flexibility • Good functionalization ability • Potential for good processability • Compatible with ultra-thin silicon channel technology	• Zero bandgap • Lack of effective analyte binding sites in its pure form	• Electrochemical • Chemiresistive
metal oxide	• Strong analyte binding • Good mechanical strength • Good thermal stability • Easy to interface with solid-state devices • Good designability to improve selectivity	• Low surface area • Difficulty with miniaturization • Slow dynamics of analyte transport	• Chemiresistive • Electrochemical
conjugated polymer	• Feasibility of introducing an analyte receptor • Collective (molecular wire) effect for amplified sensitivity • Wide tunability of conductivity • Good processability	• Possibility of swelling during measurement • Limited solubility in aqueous solution • Dependence on design for selectivity	• Fluorescence • Conductometric • Potentiometric • Colorimetric
MOF	• Large surface area and porous structure • Atomically precise structure • Abundant active sites • Tunable pore geometry, surface chemistry, and physical properties	• Stability in harsh environment • Challenge in the fabrication of materials into devices • High cost of large-scale production	• Fluorescence • Electrochemical • Chemiresistive • Electromechanical
COF	• Large surface area and porous structure • Tunable pore geometry, surface chemistry, and physical properties • Abundant active sites • Potential for atomically precise structure • Generally contains light and earth-abundant elements • Potential to be highly stable	• Limited processability • Challenge in the synthesis of material with high crystallinity and controlled morphology • High cost of large-scale production	• Fluorescence • Colorimetric • Electrochemical • Chemiresistive • Crystallography
HOF	• High crystallinity • Versatile modularity • Solution processability • Self assembling, self healing and regeneration	• Limited functional groups tolerance • Sensitive to chemical conditions • Relatively small pore volume	• Fluorescence • Colorimetric • Electrochemical • Crystallography

Figure 6-2 A summary of framework materials from the review of Meng and Mirica.[9]

Porous compounds have been developed by many different approaches as illustrated in Figure 6-2 above. Among the large variety of porous materials, MOFs and COFs share advantages in controlling surface area, pore size, active sites, thermal and chemo stability, as their structures can be engineered. The tunability and processability of HOFs also has attracted much attention over the past decades.

### 6.1.3 Janus face cyclohexanes as supramolecular self-assembling motifs

As discussed in Chapter 1, Section 1.6.3, and section 1.7, the Janus face motif interacts face to face with an association energy of about ~8.2 kcalmol^{-1} between the two rings. This is stronger than a good hydrogen bond (~5.0 kcal mol) and significantly larger than the association between two hexafluorobenzene rings (-4.6 kcal mol^{-1}), between two benzene rings (-2.63 kcal mol^{-1}) and between one benzene ring and one hexafluorobenzene ring (-5.38 kcal mol^{-1}).[10, 11] The energy of condensed and stacked trimers and tetramers of these rings in the gas phase is lower than the isolated molecules by ~20 and ~30 kcalmol^{-1} respectively. Also, there is an increasing trend in overall polarity from the monomer to the aggregated structures of all-*cis* hexafluorocyclohexane from 6.2 D to 9.4 D.[12] Therefore it becomes feasible to consider self-assembled superstructures using Janus rings but with a stronger interaction energy relative to hydrogen bonding materials (HOF).

Janus face cyclohexanes[13] have been shown to adopt supramolecular structures by crystallography, theory and Langmuir isotherm studies[14], and this has been applied to a number of supramolecular applications such as living polymerisation (LSP), semiconductivity in 2D-hetero-structures sandwiched by graphene sheets[15] and in non-linear optical materials (NLO).[16]

6.1.4 Framework material design

Topology design requires supramolecular assembly in three dimensions.[3, 17] In order to

establish a scaffold and generate a porous structure (Figure 6-3), a suitable monomer is required which has the potential to associate non-covalently and in 3D.
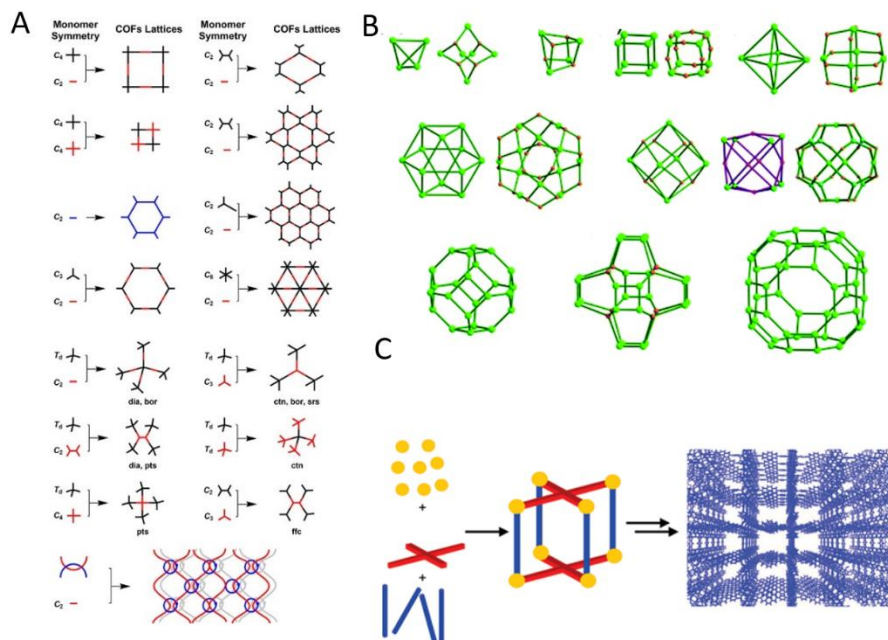
Figure 6-3 Reviewed topology diagrams for COF, HOF (A) and MOF (B) and general scheme for framework synthesis (C). Figure adapted from the literature.[1-4, 6, 9, 17, 18]

6.2 Aims and objectives

The aim of this aspect of the project was to explore the potential to generate supramolecular frameworks using self-associations of the Janus face fluorocyclohexane ring systems as illustrated in Figure 6-4 below.

Figure 6-4 Proposed coordination for constructing Janus ring supramolecular frameworks.

The Janus rings have both electrostatically charged positive and negative faces with the potential to self-associate into 3D frameworks. The strong interactions between the fluorine and hydrogen faces make it possible to connect stereo-divergent centres. Therefore, it was of interest to explore if this interaction would be sufficient to drive supramolecular assembly and negate the requirement for the typical functional groups such as carboxylates or alkyne/nitrile groups, which are common in COFs or MOFs.

The Janus face motif, and especially the pentafluorocyclohexyl motif, has an affinity for polar solvents, however any lattice should be resistant to dissociation in non-polar solvents, and it was anticipated they should be able to maintain a lattice. In addition, the stable C-F bond and the hydrophobic nature of these organofluorine building blocks should confer thermal stability and chemical resistance to any supramolecular assembly. The solubility and the binding affinity of the Janus rings could be controllable by adjusting the solvent system,[19] and thus reversible assembly and disassembly could become of feature of such materials.

6.3 Ligand synthesis

In order to connect 3D cores to the Janus cyclohexanes, a chemically stable bond is required, and ideally it should be formed in good yield. A number of connecting bond types are illustrated in Figure 6-5, which at the outset became candidates to explore.
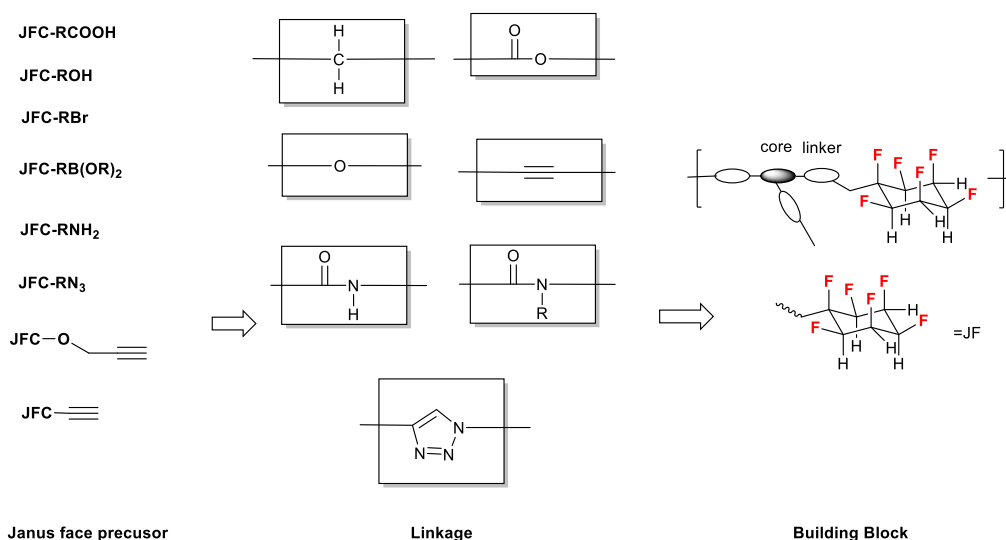
Figure 6-5 Ligand synthesis toward building blocks for 3D assembly.

For ester or amide bond formation, the originating carboxylate could be either attached to the Janus fluorocyclohexyl motif or alternatively amines and alcohols carrying the Janus cyclohexane could be utilized as building blocks. In order to synthesise a Janus carboxylate, the most straight-forward synthesis would involve direct hydrogenation of an ester of pentafluoro-phenylacetic acid **6-2**, as already developed by Clarke *et al.*[20]
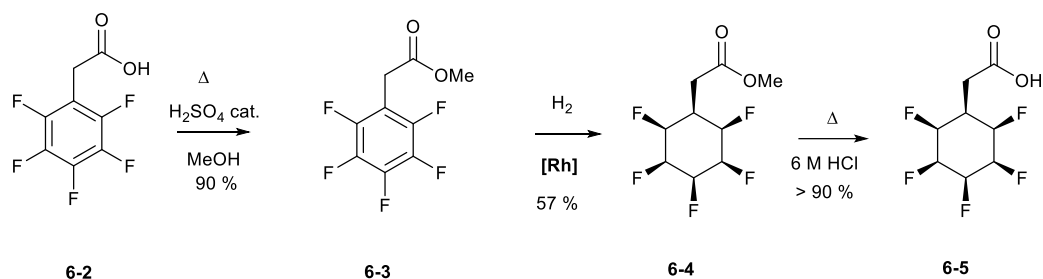
Scheme 6-1 Preparation of Janus face fluorocyclohexyl carboxylic acid **6-5**.

Accordingly, pentafluoro-phenylacetic acid **6-2** was refluxed in methanol to generate the methyl ester **6-3**. The aryl ring of the resultant ester was hydrogenated using Zeng's catalyst. The hydrogenated product **6-4** was then hydrolysed by refluxing in 6 M HCl to release the free carboxylic acid. Carboxylic acid **6-5** proved to be suitable for amide and ester coupling reactions and several functional group interconversions.
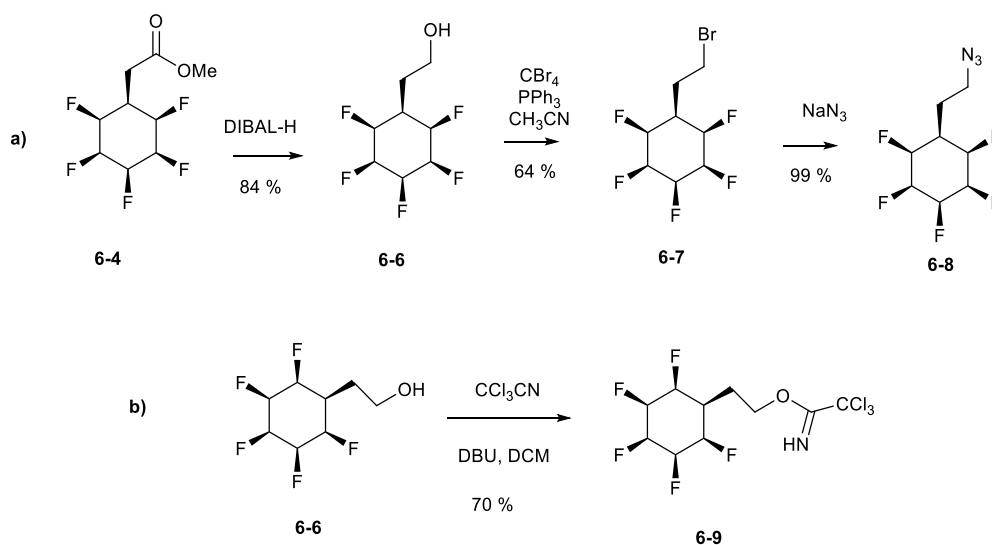
Scheme 6-2 Preparation of Janus face fluorocyclohexyl linkers.

Alkyl bromide **6-7** was prepared on a relatively large scale and became particularly useful for alkylation reactions. In addition to acting as a good electrophile, bromide **6-7** also proved suitable for photo-redox cross coupling/radical reactions.
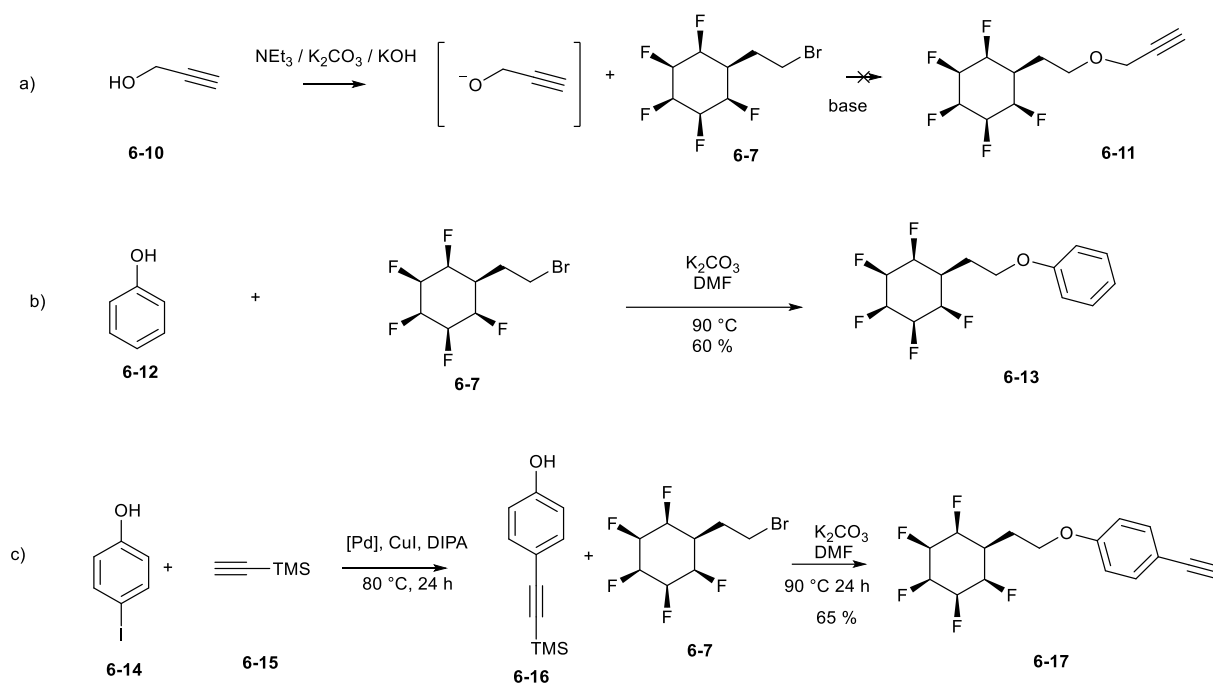
Scheme 6-3 Preparation of Janus face cyclohexyl derivatives with alkyne groups.

It was attractive to append an alkyne group in some manner to the Janus cyclohexane to enable Sonogashira or 'click' chemistry. This was initially explored by trying to prepare a propargyl ether with alkyl bromide **6-7**. However, the reaction of **6-7** with the alkoxylate of propargyl alcohol failed. This is almost certainly due to the strong base required to deprotonate the alcohol, as defluorination of the Janus face fluorocyclohexyl ring occurs under those conditions.

An exploratory reaction was conducted between phenol and the alkyl bromide **6-7** under mildly basic conditions. The reaction was successful with full conversion and ether **6-13** could be isolated in 65 % yield. This protocol demonstrated C–O bond formation with alkyl bromide **6-7** under mildly basic conditions.

The phenylacetylene ether **6-17** could be prepared by a Sonogashira reaction followed by a Williamson ether synthesis reaction of the protected ethynylphenol **6-16** with alkyl bromide **6-7**. The protecting TMS group on **6-17** is removed spontaneously in a cascade under basic

reaction conditions, which avoids the extra step required to prepare and handle unstable ethynylphenol **6-30**.
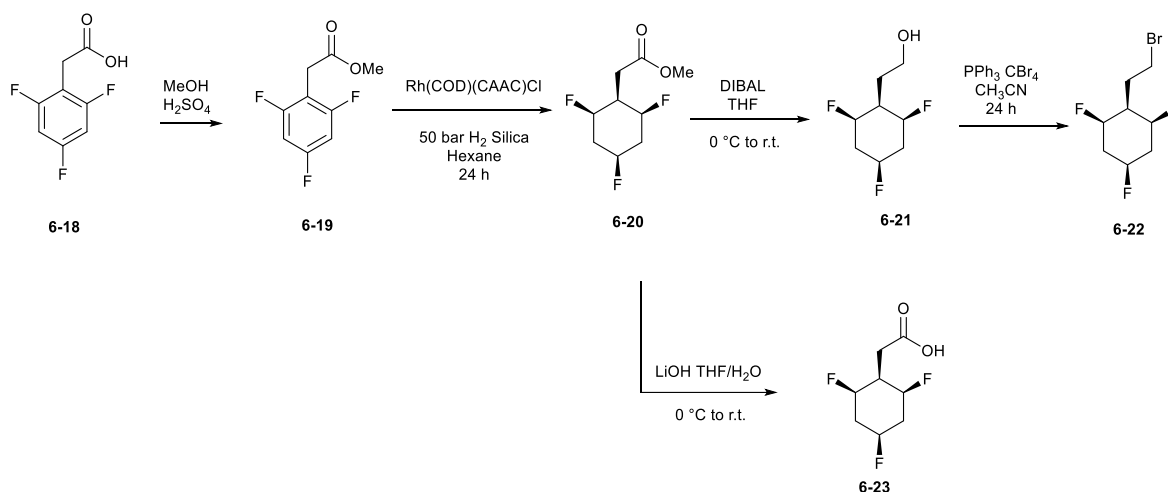
Scheme 6-4 Synthesis of all-*cis*-1,3,5-trifluorocyclohexyl ligands.

As discussed in Chapter 5, the all-*cis*-1,3,5 trifluorocyclohexyl motif could offer a simplified version of the Janus face fluorocyclohexyl motif, with a similar molecular dipole (5.1-5.6 D) but with less fluorine.

A series of 1,3,5-all-*cis*-trifluorocylohexyl motifs were prepared in a similar manner to the all-*cis*-pentafluorocyclohexyl motif. A low yield only was recovered after aqueous HCl hydrolysis of **6-20** to generate carboxylic acid **6-23**, and this was not successful due to the propensity of **6-23** for sublimation. As an alternative approach, methyl ester **6-20** was carefully hydrolysed under mildly basic conditions with LiOH, and this afforded a high yield of **6-23**.

All-*cis* 1,3,5-trifluorocyclohexyl motifs generally show higher solubility compared to the all-*cis* pentafluorocyclohexyl motifs, and this may offer some advantages in synthesis.

6.4 Core synthesis

6.4.1 Tripodal branch cores

Only one tripodal building block was tested in this project, essentially as such a design is 'flat' and will not generate 3D-architectures. This is not consistent with the aim of this aspect of the project.

(a) commercial avaliable C3 core **6-24**

(b) C3 toplogy building block in rigid COF/MOF

(c) C3 toplogy building block in flexible structure

(d) Parallel layers stacking of janus face cyclohexyl motifs
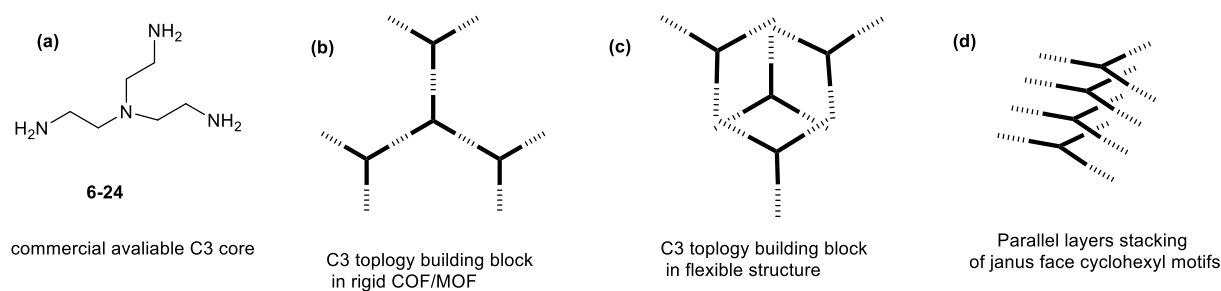
Figure 6-6 The tripodal structure of the building blocks.

The flexible self-assembly of the Janus face cyclohexyl motif will easily fill up the free space through thermodynamically favoured close contacts (Figure 6-6 c), rather than that expected from an ideal rigid head-to-head alignment in a scaffold structure (Figure 6-6 b). The face-to-face stacking of the targeted C3 building block leads to a further reduction of porous space. Such building blocks are promising for 2D and surface materials, however the core was not developed in this project.

6.4.2 3D-branched cores with T_4 symmetry

Tetra-aniline **6-24** and tetra-bromide **6-27** are commercially available and readily accessible. Therefore, a number of functional core compounds for crosslinking were prepared from these two tetraphenyl methane derivatives.
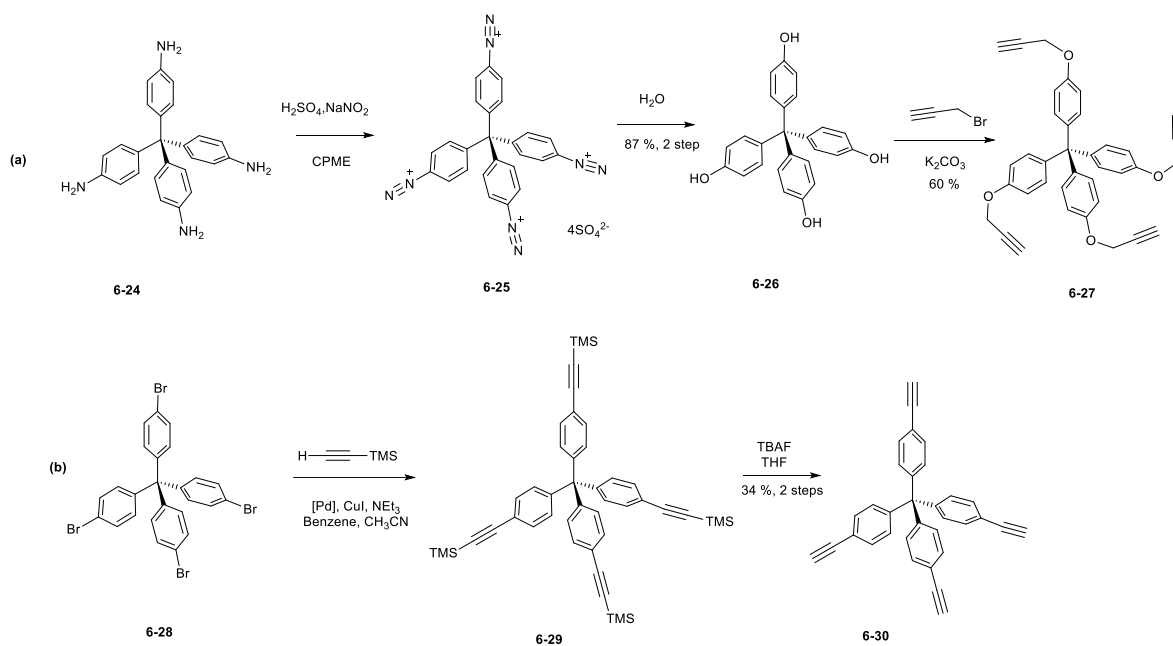
Scheme 6-5 Synthesis of 3D-branched cores with T$_4$ symmetry.

As illustrated in Scheme 6-5, the tetra(*p*-aniline)methane **6-24** could be easily activated by diazonium formation to prepare tetra(*p*-phenol)methane **6-26**.[21] Phenol **6-26** was used in the construction of a C–O bond linkage by ether formation or ester bond formation. Tetra propargyl ether **6-27** was prepared from tetra phenol **6-26** in 60 % yield.

The tetra(*p*-bromophenyl)methane **6-28** is a good candidate 3-D core building block for extension by aryl cross coupling reactions. Accordingly, the tetra(*p*-ethynylphenyl)methanes **6-29** and **6-30** were prepared from **6-28** by a Sonogashira reaction followed by deprotection, and the products were progressed to Heck or for CuAAC cross coupling reactions.
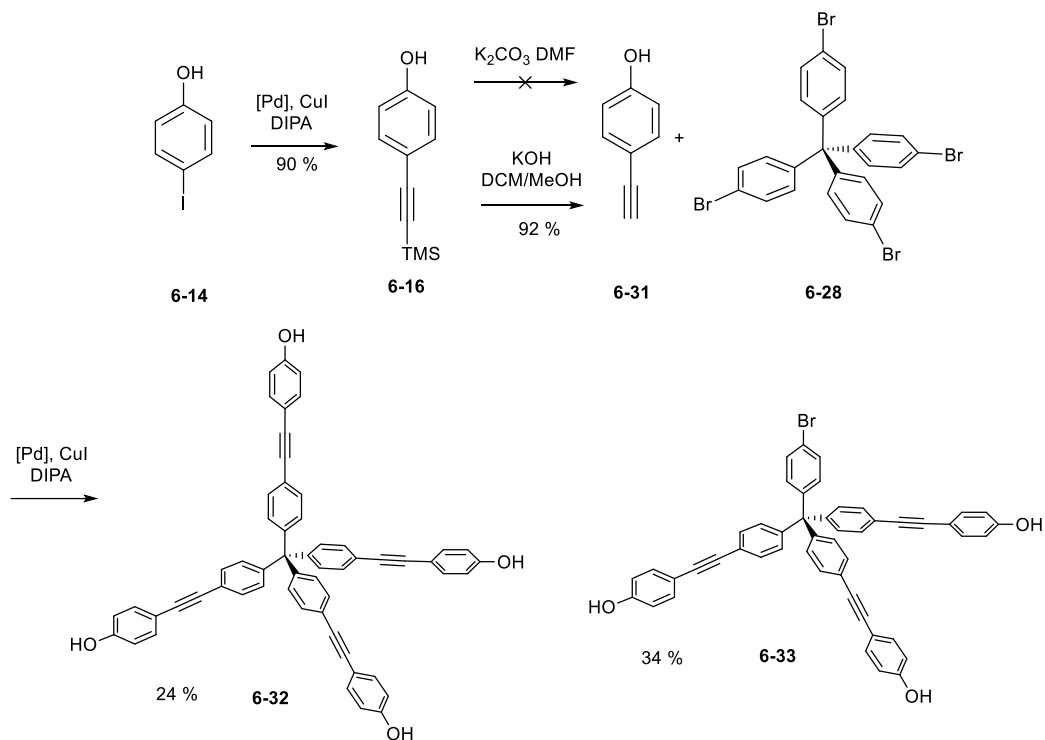
Scheme 6-6 Synthesis of elongated tetraphenyl 3D branched cores with T_4 symmetry.

In order to prepare an elongated 3D core building block, a Sonogashira reaction was applied to the tetra(*p*-bromophenyl)methane **6-28**. The TMS protected ethynylphenol **6-16** was rapidly deprotected by potassium hydroxide to form ethynylphenol **6-31**, while slower deprotection methods or storage leads to polymerisation and decomposition of **6-31**. The resultant ethynyl **6-31** was used immediately after preparation and purification in the next step of the Sonogashira reaction to generate tetraphenol **6-32** in 24 % yield. Due to the poor reactivity of the aryl bromide and a homocoupling, by-product **6-33** was generated in 34 % yield as well.

Another strategy to construct a 3D building block involved starting with an adamantane core. Tetrabromo-adamantane **3-34** was prepared following the method reported by Ging *et al.*[22] **6-36** is a candidate for S_N1 reactions as well as a range of transition metal mediated aryl cross coupling reactions.

Tetrabromo-adamante **6-35** is efficiently converted to the tetrahydroxy-adamantane **6-36** [23] and the yield could be improved by extensive Soxhlet extraction. Tetrahydroxyl-adamantane **6-36** proved to be a versatile intermediate and was used for a number of Williamson ether synthesis reactions. Additionally, adamantane **6-34** could be extended to a rigid 3D building block after the introduction of an additional phenyl spacer. The tetra-iodo scaffold **6-41** was prepared via a fourfold Friedel-Crafts reaction, followed by electrophilic aromatic substitution with iodine. The resultant tetra aryl iodide could then be used for number of cross coupling reactions. [24]

The tetraphenol building block **6-39** was constructed by electrophilic aromatic substitution with anisole in the presence of a Brønsted acid. The resulting mixture of *ortho-* and *para-* products was an inevitable outcome of this reaction. This presented a challenging separation which required careful column chromatography, but in the end, the desired tetra-4-methoxylphenyl adamantane **6-38** was successfully isolated. The methoxyl ethers of **6-38** could then be deprotected by treatment with BBr_3 to provide the tetra-phenol **6-39**.
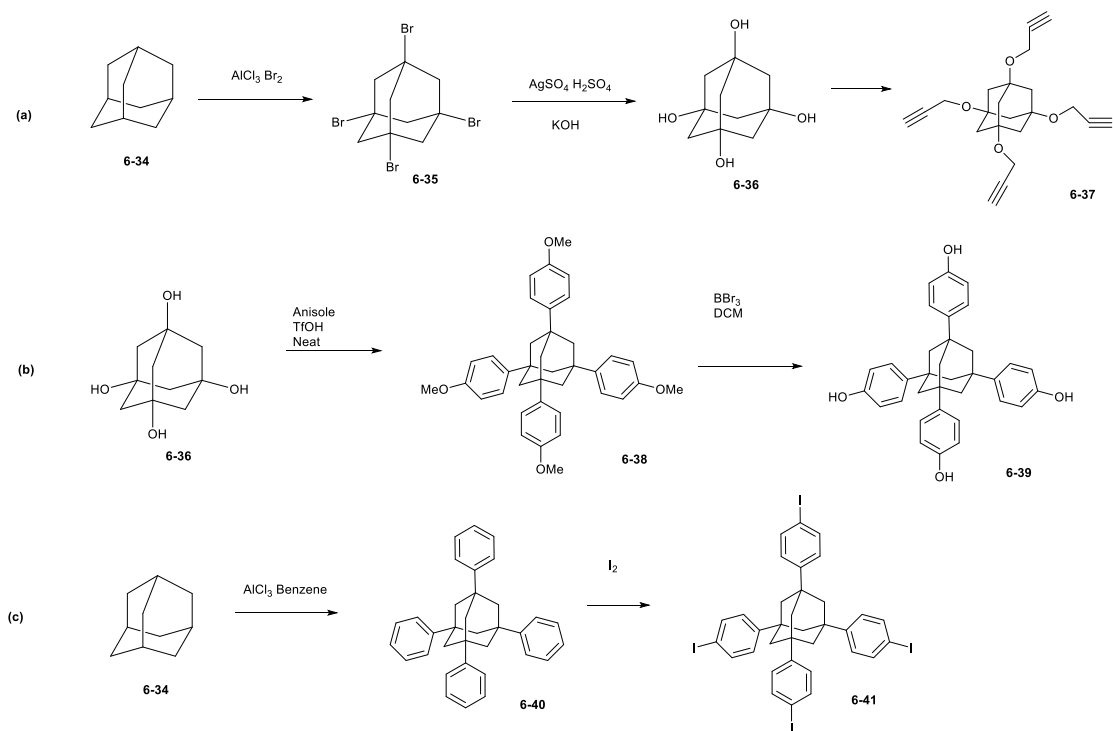
Scheme 6-7 Synthesis of adamantane and derived building blocks.

An alternative 4-fold 3D-scaffold could be prepared starting from pentaerythritol **6-42**. This was elaborated by propargyl ether formation using propargyl bromide. The resultant tetra-acetylene **6-43** offered a useful intermediate for Heck and CuAAC 'click' reactions to assemble the desired 3D building blocks for supramolecular assembly.
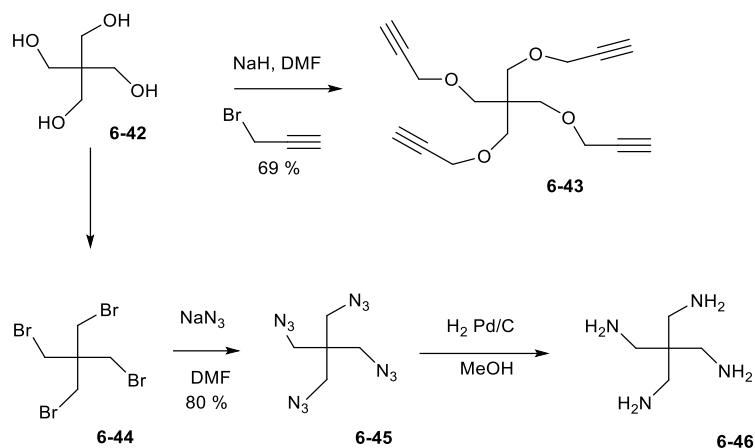
Scheme 6-8 Synthesis of pentaerythritol derivatives 3D branched core.

Another series of useful compounds were prepared by commercially available pentaerythritol tetrabromide **6-44**. The tetrabromide **6-44** could be converted to the tetra-azide **6-45** after treatment with sodium azide. Tetra azide **6-45** is clearly a candidate for 'click' reactions, combining with acetylenes. The azide moieties in **6-45** can also be reduced by hydrogenation to generate tetra-amine **6-46** and other useful building blocks.

6.4.3 3D-branched cores with D_{3d} symmetry centre

An accessible 3D branched building block with a D_{3d} centre is the commercially available tetraphenol **6-47**. The tetraphenol **6-47** is amenable to a variety of C–O bond construction reactions and here it was transformed to tetra- acetylene **6-48** in 50 % yield.
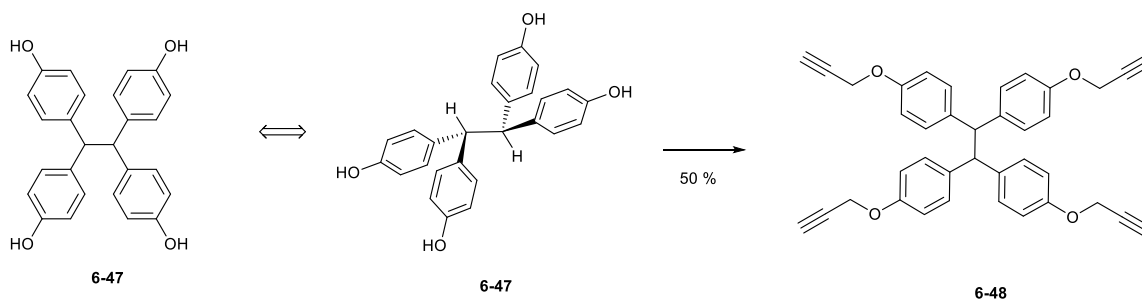
Scheme 6-9 Synthesis of a 3D branched core with D_{3d} symmetry.

6.4.4 3D-branched cores with S_4 symmetry centre
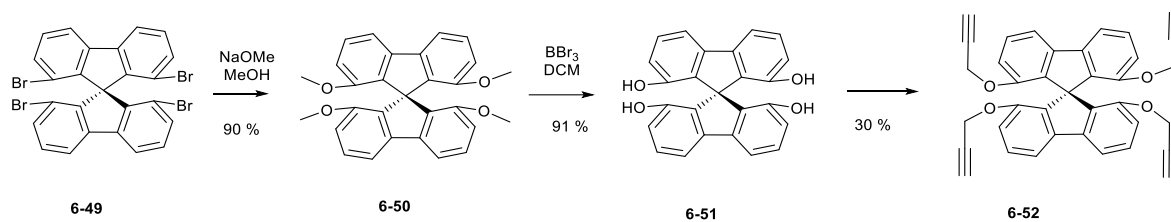
Scheme 6-10 Synthesis of a 3D building block with S_4 symmetry.

The commercially available spiro-tetrabromide **6-49** offers a good 3D core building block for aryl coupling reactions. A number of functional group interconversions were carried out in a similar manner to that described in Chapter 6.4.2. Tetra-bromide **6-49** was converted into tetra-methoxylphenyl **6-50** by an S$_N$Ar substitution reaction in 90% yield. The resultant tetramethoxylphenyl **6-50** was deprotected to afford tetraphenol **6-51** in 91% yield, and this could be used now for C–O bond linkage. Accordingly, tetraacetylene **6-52** was prepared from the **6-51** by alkylation with propargyl bromide in 30 % yield.

6.5 Synthesis of the building blocks

6.5.1 Amide linked assemblies

A test synthesis was explored initially with commercially available amine **6-24**. As shown in Figure 6-10. The carboxylic acid was activated by HATU and reacted with triethyltriamine **6-24**. The reaction gave a 79 % yield of tri-amide **6-53** after recrystallisation.
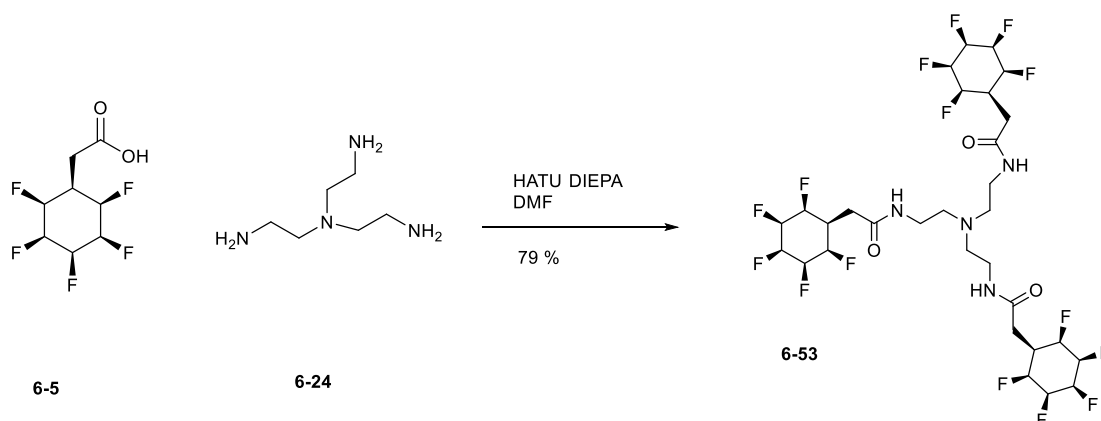
Scheme 6-11 Synthesis of tripodal building block **6-53**

Tri-amide **6-53** has very poor solubility in most polar solvents such as DMSO, DMF, or acetone, and is almost insoluble in any non-polar solvent. Attempts at recrystallisation of **6-53** only resulted in the generation of an amorphous fine powder, which was hard to re-dissolve.
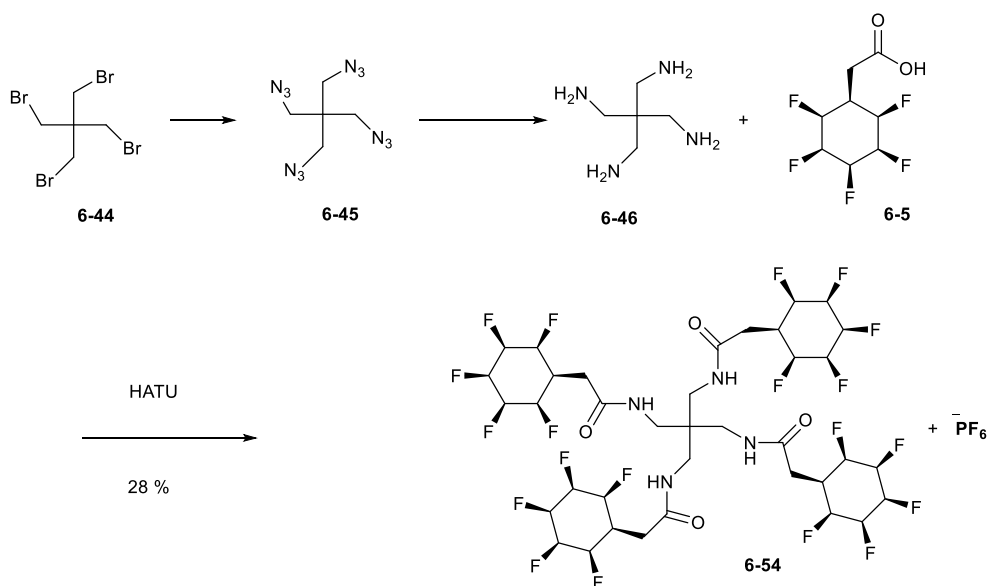
Scheme 6-12 Synthesis of tetra-amide building blocks **6-54**

In a similar approach, **6-54** was synthesised via HATU coupling of carboxylic acid **6-5** and tetrakis(aminomethyl)methane **6-46**. The product **6-54** co-eluted with DMF, DIPEA and HATU reagents during chromatography, however, after removal of the DMF *in vacuo* at high

temperature, DIPEA and much of the HATU could be washed away with chloroform.

19F NMR (659 MHz, Acetone-d_6) δ -205.33 (d, J = 38.1 Hz), -211.80, -217.52.
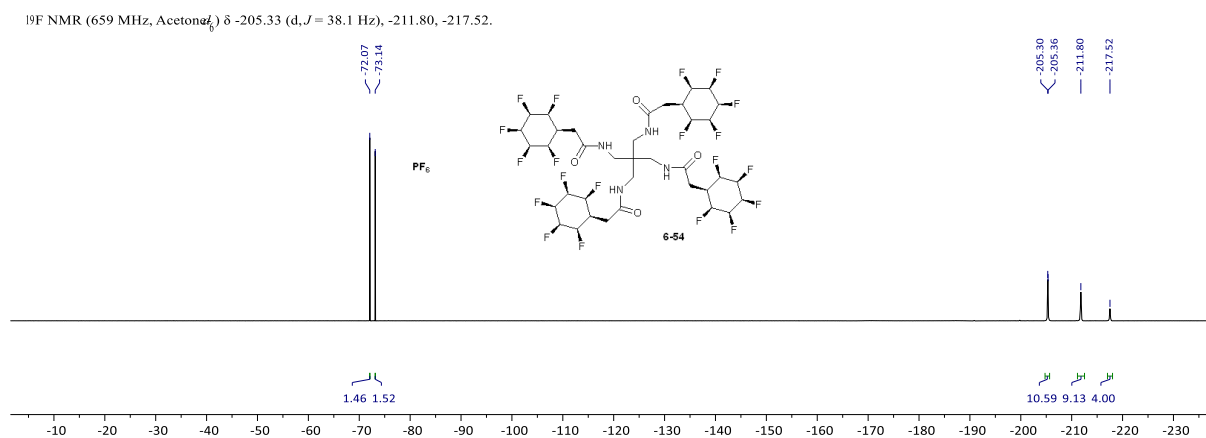
Figure 6-7 ^{19}F NMR of the tetra-amide **6-54** combined with PF$_6^-$ ion

A relatively pure sample of **6-54** was isolated after centrifugation, and a 2:1 stoichiometric amount of the phosphorous hexafluoride ion (PF$_6^-$) ion was evident combined with **6-54**, even after several rounds of chromatography. This observation agrees with the strong binding affinity of Janus face cyclohexyl rings towards charged ions. The positively charged counterion was not identified on ^{1}H and ^{19}F NMR.

The 4-fold scaffolded tetra-amide **6-54,** based on the penta-erythrial motif adopts a near pyramidal geometry in the solid state. The crystal structure of tetra-amide **6-56** prepared from a Ugi multi-component reaction involving tetra-isocyanide **6-55** reported by Buteara *et al.*, has a similar 4-fold structure to tetra-amide **6-54**.[25] The reported crystal structure of the analogue shows a pyramidal geometry with a "windmill" like arrangement of its side chains. The molecule may associate to a guest molecule through these coordinating side chains. Therefore, the tetra-amide **6-54** emerged as a promising target.
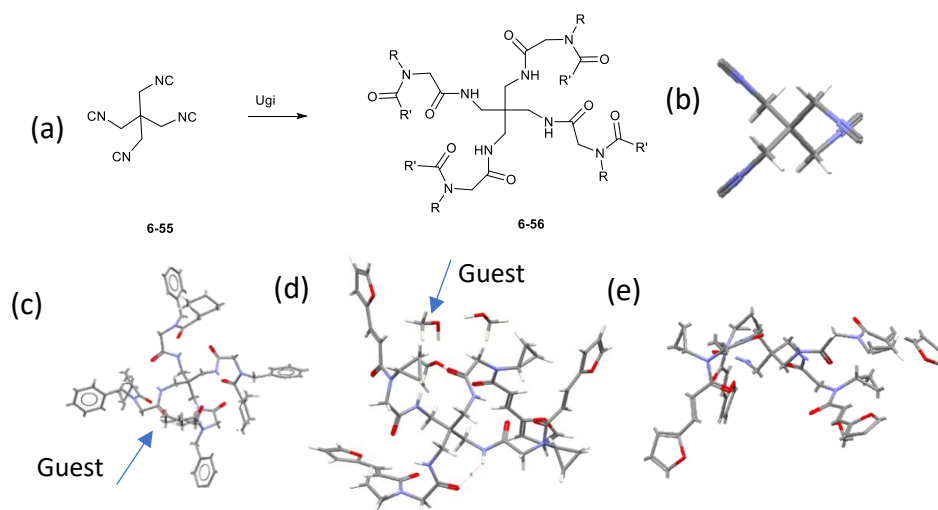
Figure 6-8 (a) Synthesis of tetra-amide **6-56** in 4-fold structure reported Buteara *et al.*; (b) simplified crystal structure of tetra-isocyanide **6-55** and tetra-amide **6-56** core; (c) guest cyclohexanol molecule in tetra-amide **6-56**;(d) the projected view of "windmill" shape of 4 side chains in **6-56**, (e) pyramidal C_1 geometry of the **6-56**.[25]

With the aim of extending the coordination potential to the Z-axis, a tetrahedral core with a more rigid structure was explored using the HATU coupling method. Again, the reaction resulted in reasonable yields of 55% and 75% respectively. Amide **6-57** has a tetrahedral geometry suitable for coordination and lattice formation. The resultant product **6-57** was purified by recrystallisation from acetone/DCM or a higher yield could be achieved after column chromatography. A single crystal was grown and submitted for X-ray diffraction.
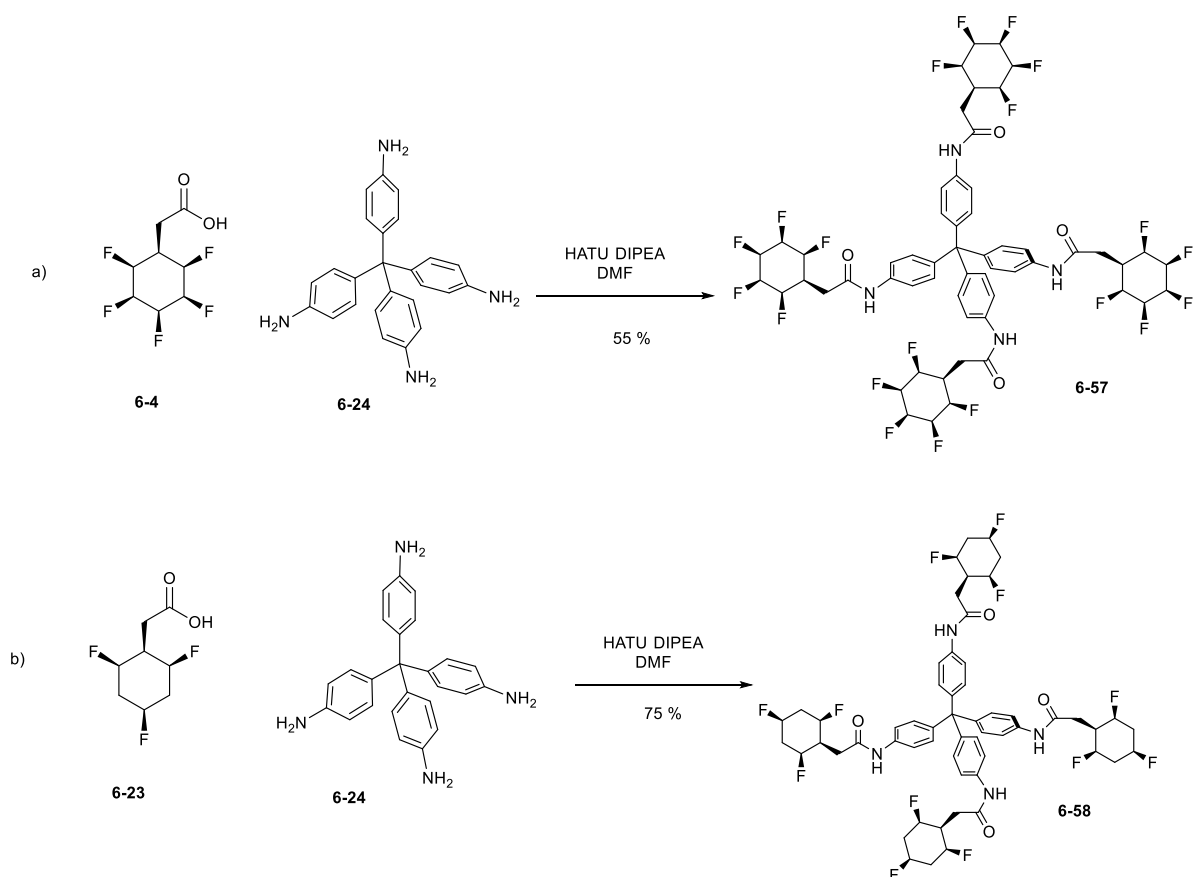
Scheme 6-13 Synthesis of tetra-amide **6-57** and **6-58**

The crystal structure of **6-57** shows a lattice structure emanating from the tetrahedral scaffold of the building block. As shown in Figure 6-9, the N-H amide to carbonyl oxygens show short contacts (2.2 Å) consistent with good hydrogen bonding, while the all-*cis* pentafluorocyclohexyl rings, trimerised with zig-zag packing (Figure 6-9 d). C–H…F–C contacts with distances of 2.4-2.5 Å (shortest 2.35 Å) were observed between two parallel intermolecular Janus face fluorocyclohexane rings. Two scaffolds are separated by about 2.8-3.5 Å between Ar–H…H–Ar and 9.0 Å between two spiro centres. The rigid T_4 tetraphenyl core supports void spaces which constitute about a 12 % porous volume. This is three times bigger than HOFs' porous volume in earlier design of 4 %.[5]
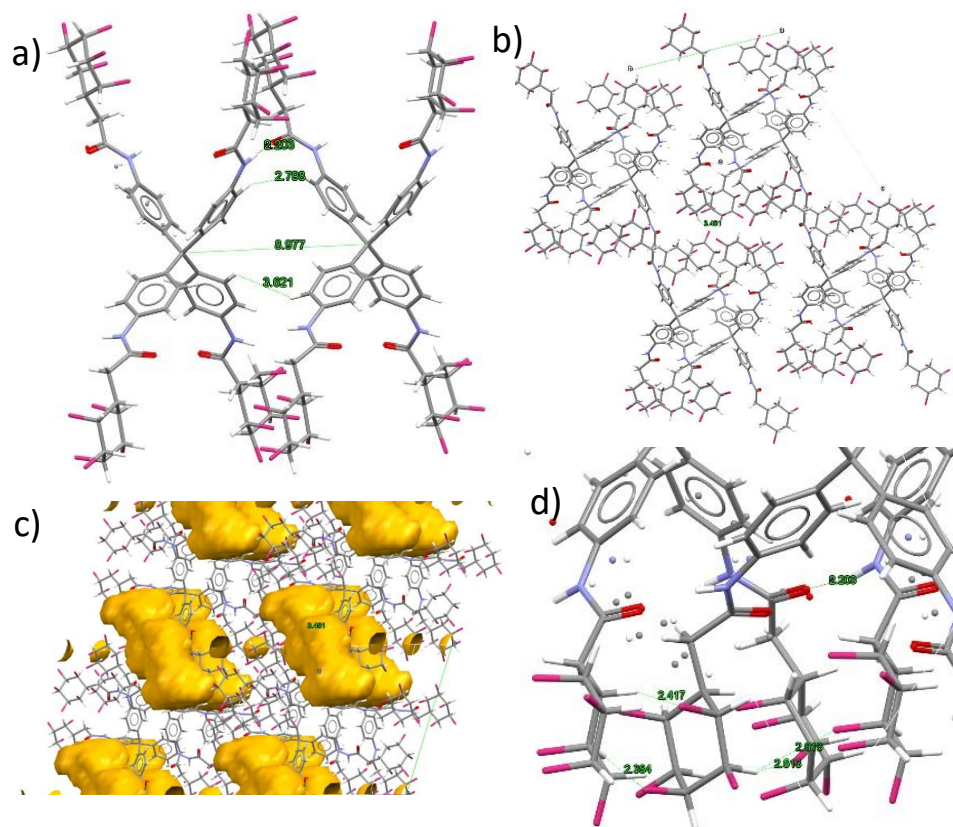
Figure 6-9 The Xray crystal structure of tetra-amide **6-57**. (a) Measured intermolecular bond distances; (b) The unit cell of **6-57** crystal structure; (c) Void space of **6-57** crystal structure; (d) trimerisation arrangement of Janus rings.

In the solution phase, the ^{1}H ^{19}F HMBC NMR shows strong cross peaks between the aromatic protons of the phenyl rings to the fluorine atoms on the Janus face fluorocyclohexyl rings. These correlations indicate intermolecular interactions between the rings in solution.
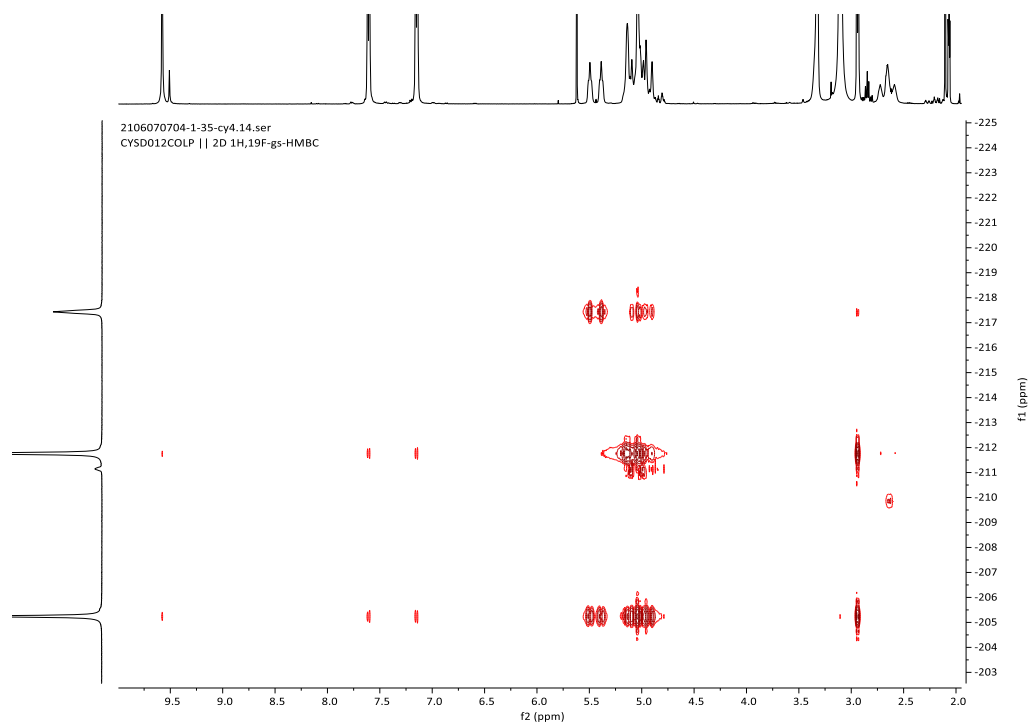
Figure 6-10 The ^{1}H-^{19}F NMR spectrum of tetra-amide **6-57**

A hexafluorophosphate ^{19}F signal was found in the ^{1}H{^{19}F}-NMR, showing a 1:6 stoichiometry of the PF$_6^-$ ion to tetra-amide **6-57**. This suggested the association of the PF$_6^-$ ion with the tetra-amide building blocks **6-57**, again indicating strong ionic binding affinity with the Janus face fluorocyclohexane ring consistent with previous observations.[13, 26]
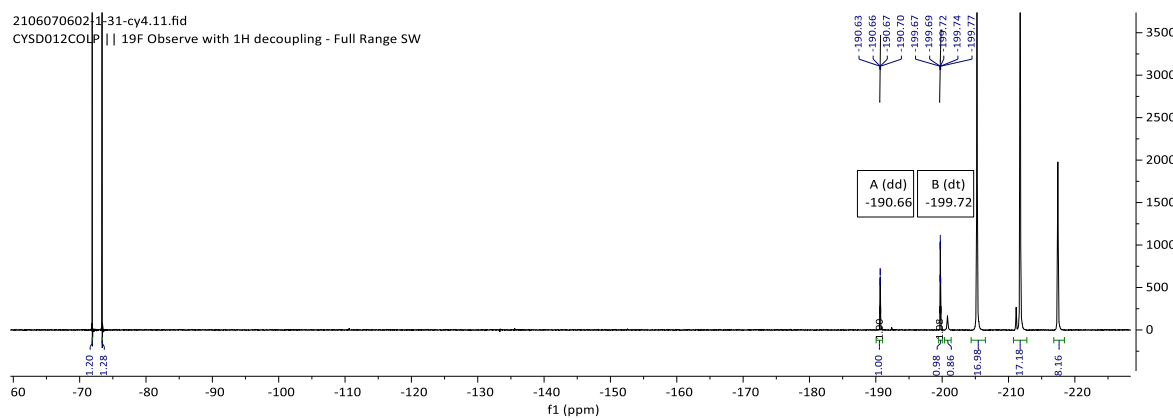
Figure 6-11 ^{19}F NMR of tetra-amide **6-57** combined with PF$_6^-$

One of the drawbacks of these amide coupled structures, is that the amine bond is a hydrogen-bond donor, and this competes with the Janus rings for supramolecular connectivity through intermolecular hydrogen bonding interactions. Accordingly, the N-Me analogue of *N*-tetra-amide **6-59** was prepared in order to explore removing the capacity of the amide to hydrogen bond.

In order to achieve this, an exhaustive methylation was explored by treatment with NaH and MeI. The reaction time was kept short, and the reaction temperature was cooled to avoid any potential elimination of the hydrogen fluoride from the Janus rings. The reaction is summarised in Scheme 6-14 and product **6-59** could be recovered in good yield (80%). Purification of **6-59** was achieved by recrystallisation. N-Methylamide **6-59** was crystallised from DMF solution and a powder X-ray analysis could be achieved from the refined solid.
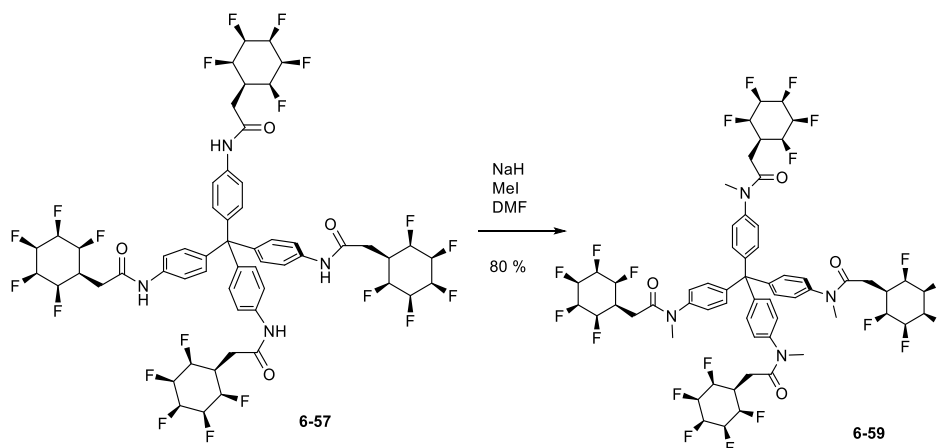
Scheme 6-14 The methylation of **6-57** to tetra N-methyl amide **6-59**.

Tetra N-methylamide **6-59** has much lower solubility when compared to **6-57**, presumably due to the absence of the amide as a hydrogen bonding donor. This also resulted in a lower crystallinity of tetra N-methyl amide **6-59**. X-Ray powder diffraction of **6-59** was conducted on the recrystallised product. The observed diffraction pattern of **6-59** shows a similar pattern to the simulated structure obtained from single crystal structure data of tetra amide **6-57**.

The key peaks at 5 Ɵ, 7 Ɵ and 8Ɵ are similarity distributed, suggesting that tetra amide **6-57** and tetra N-methyl amide **6-59** have a similar lattice symmetry.
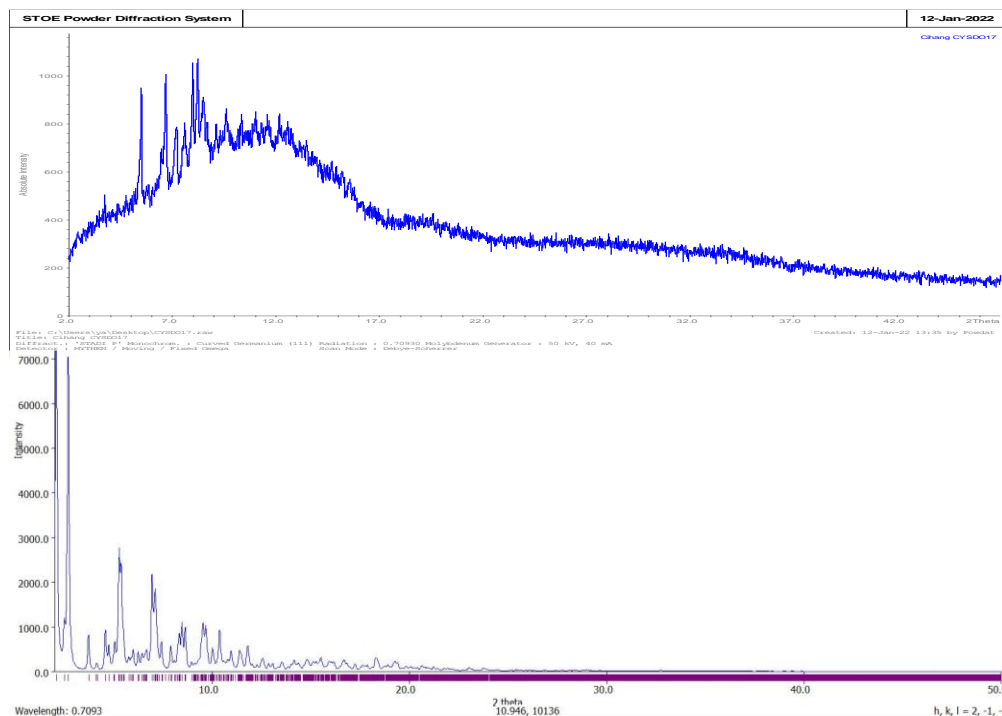
Figure 6-12 Powder diffraction pattern of tetra N-methyl amide **6-59** (top) and simulated diffraction pattern of tetra-amide **6-57** from single crystal structure (bottom).

Both tetra-amides **6-54** and **6-57** show strong intermolecular interactions between Janus face fluorocyclohexyl rings with PF_6^- ion. Amide **6-54** shows a 2:1 ratio with the PF_6^- ion after several rounds of column chromatography and **6-57** shows a 5:1 ratio with the PF_6^- ion. Notably, the satellite signals of **6-57** at -190 ppm and -200 ppms in ^{19}F NMR suggest that a Janus face fluorocyclohexyl ring interacts with the PF_6^- ion in the solution phase. This again indicates a strong interaction between the Janus face fluorocyclohexyl building blocks and the PF_6^- anion.
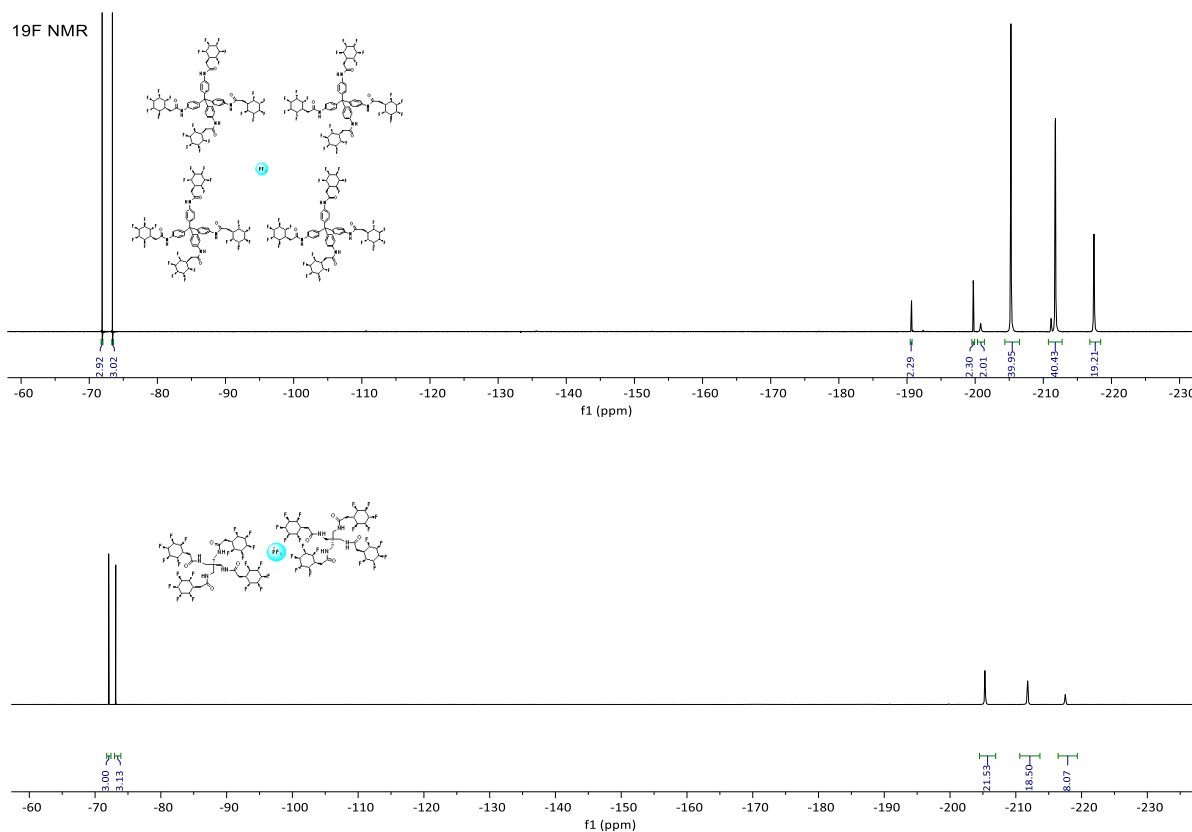
Figure 6-13 ^{19}F NMR of tetra-amide **6-54** (bottom) and **6-57** (top) combined with PF$_6^-$

The all-*cis* 1,3,5-trifluorocyclohexyl analogue of tetra-amide building block **6-58** was prepared by a similar approach with tetra-amide **6-57**. The tetra-amide **6-58** was isolated in an improved yield of 75 %, which benefited from the good solubility of all-*cis* 1,3,5-trifluorocyclohexane ring. A BET gas uptake measurement was carried out on tetra-amide **6-58**. A plateau of was observed clearly in the isotherm plot. A surface area of 9 m^2 g^{-1} was calculated from this measurement, and this is in agreement with the ~12 % porous volume in the **6-57** crystal structure. This outcome indicated some potential to construct porous frameworks with these Janus face fluorocyclohexyl rings.
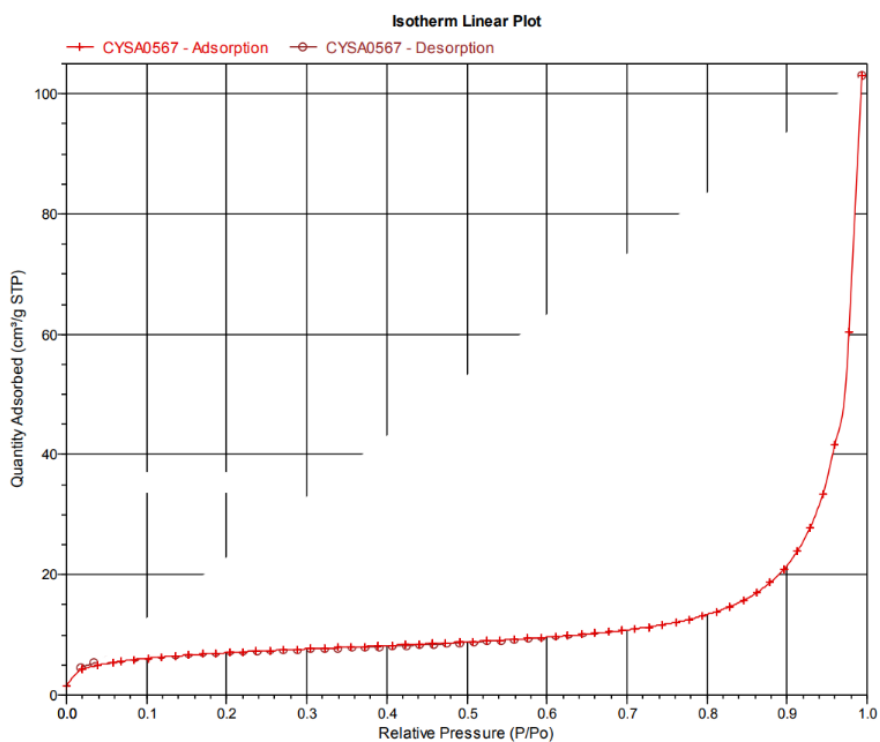
Figure 6-14 BET measurement of tetra-amide **6-58**

6.5.2 Ether building blocks

6.5.2.1 Alkyl -O- Alkyl ether

Ether C-O bond formation is an attractive approach in which to prepare scaffolds containing Janus-face motifs. The advantage of an ether bond is that it is chemically stable and offers a simple connection without the complexity of a functional group that can independently interact in a supramolecular assembly.
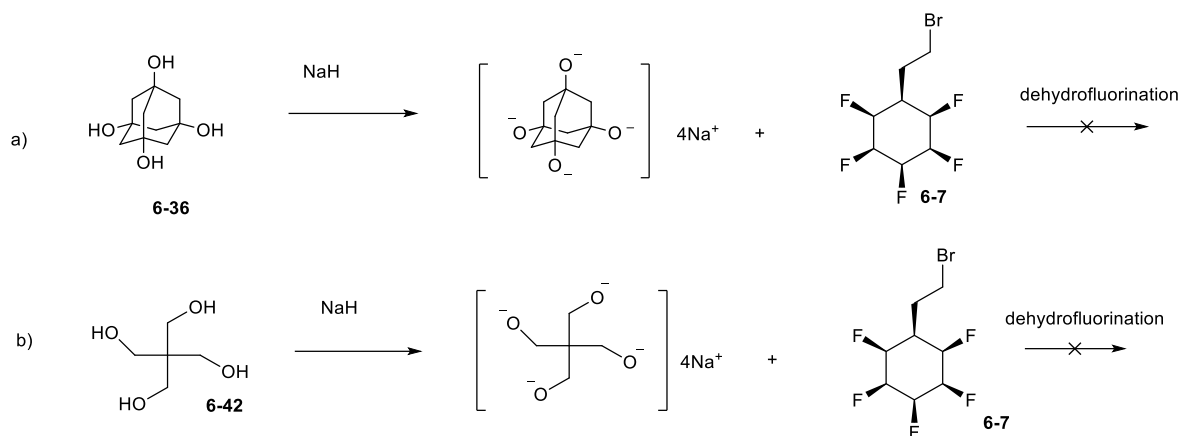
Scheme 6-15 Approaches to synthesis alkyl–O–alkyl ether building blocks.

An initial approach used sodium hydride as a base to deprotonate tetra-ol **6-36**, and then react with alkyl bromide **6-7**. However, the conversion was poor and alkyl bromide **6-7** was largely recovered. There was also some suggestion from ^{1}H and ^{19}F NMR that dehydrofluorination had occurred when heating and when an elongated reaction time was applied, due to the presence of signals consistent with vinyl and aromatic protons, as discussed in Chapter 4.
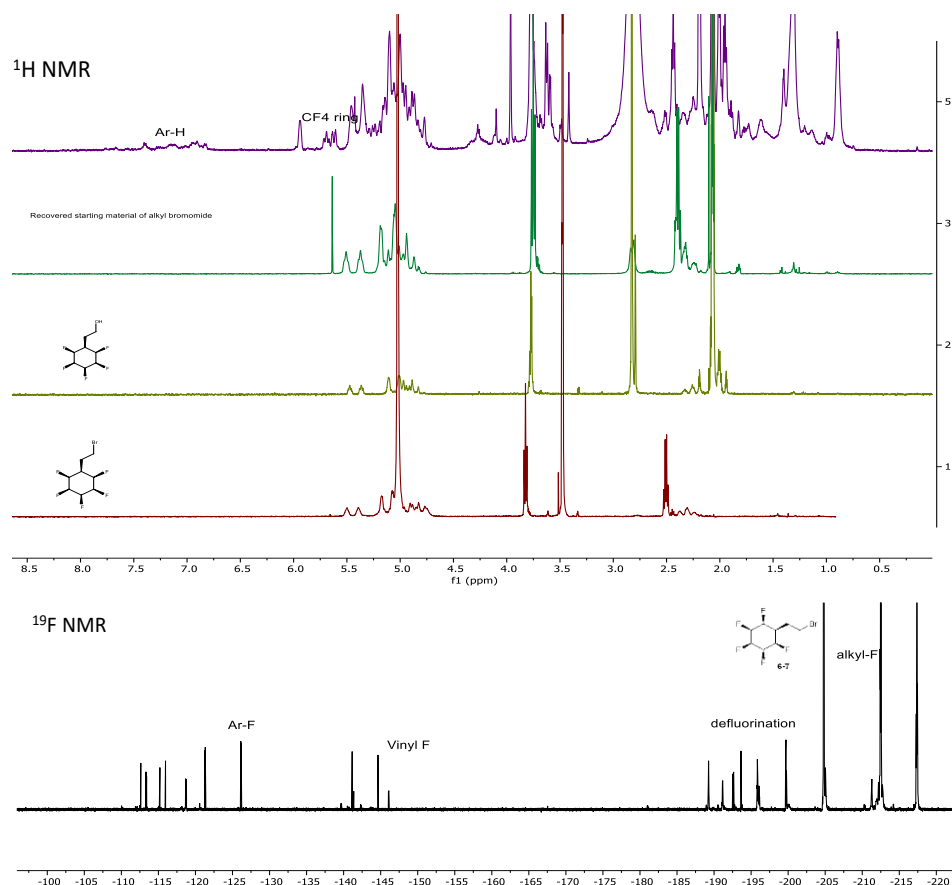
Figure 6-15 ¹H and ¹⁹F NMR spectra demonstrated the conversion and by-products of reactions in scheme 6-15.

As shown in Scheme 6-16, another approach to the desired ethers was explored by reacting trichloroacetamide **6-9** with the tetra-ol under acidic conditions. However no desired product formed and only BF₃ coordinated **6-9** and traces of hydrolysed product **6-21** were observed.
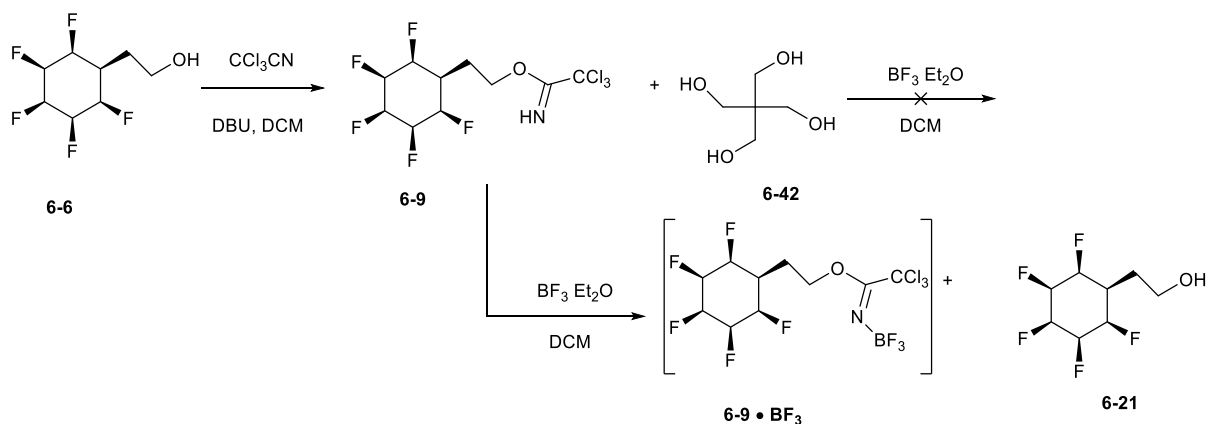
Scheme 6-16 Approach for the synthesis of an alkyl–O–alkyl ether building block with trichloroacetamide.

6.5.2.2 Aryl-O-alkyl ether

Given the poor outcomes from deprotonation of aliphatic alcohols, attention focused on the preparation of phenol ethers, the phenol being more acidic with a pKa ~10 versus that of ~pKa 16 for an aliphatic alcohol. The decreased basicity for example should reduce dehydrofluorination side reactions.
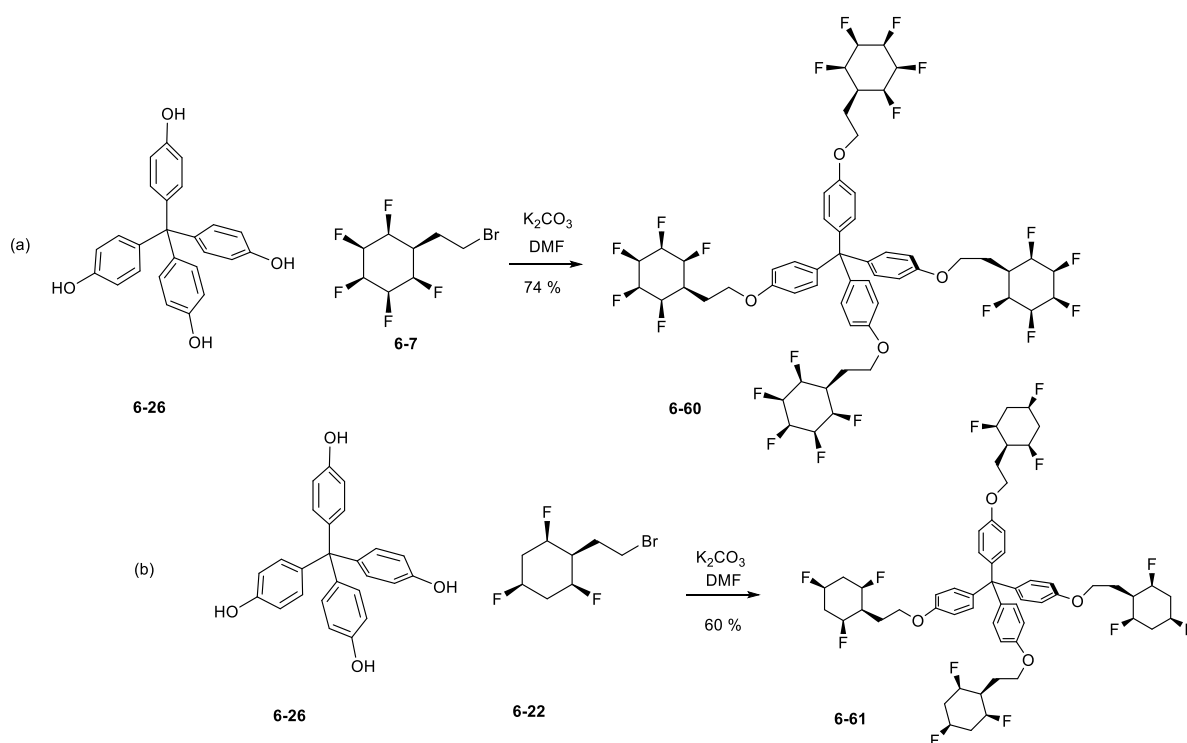
Scheme 6-17 Synthesis of tetraphenyl ether building block **6-60** and **6-61**.

As shown in Scheme 6-17, the tetraphenyl ether **6-60** was prepared via a Williamson's ether synthesis under mild K_2CO_3 conditions. The reaction offered a 74 % yield after column chromatography or about 65 % yield from recrystallisation only. An all-*cis* 1,3,5-trifluorocyclohexyl tetraphenyl ether analogue **6-61** was prepared by a similar approach in 60 % yield. The tetraphenyl ether **6-61** is a fine crystal solid similar to **6-60**. The all-*cis* 1,3,5 trifluorocyclohexyl ring makes **6-61** more soluble in less polar solvents compared to all-*cis*-pentafluorocyclohexyl **6-60** and this benefits also from fewer fluorine atoms in the cyclohexane ring.

234
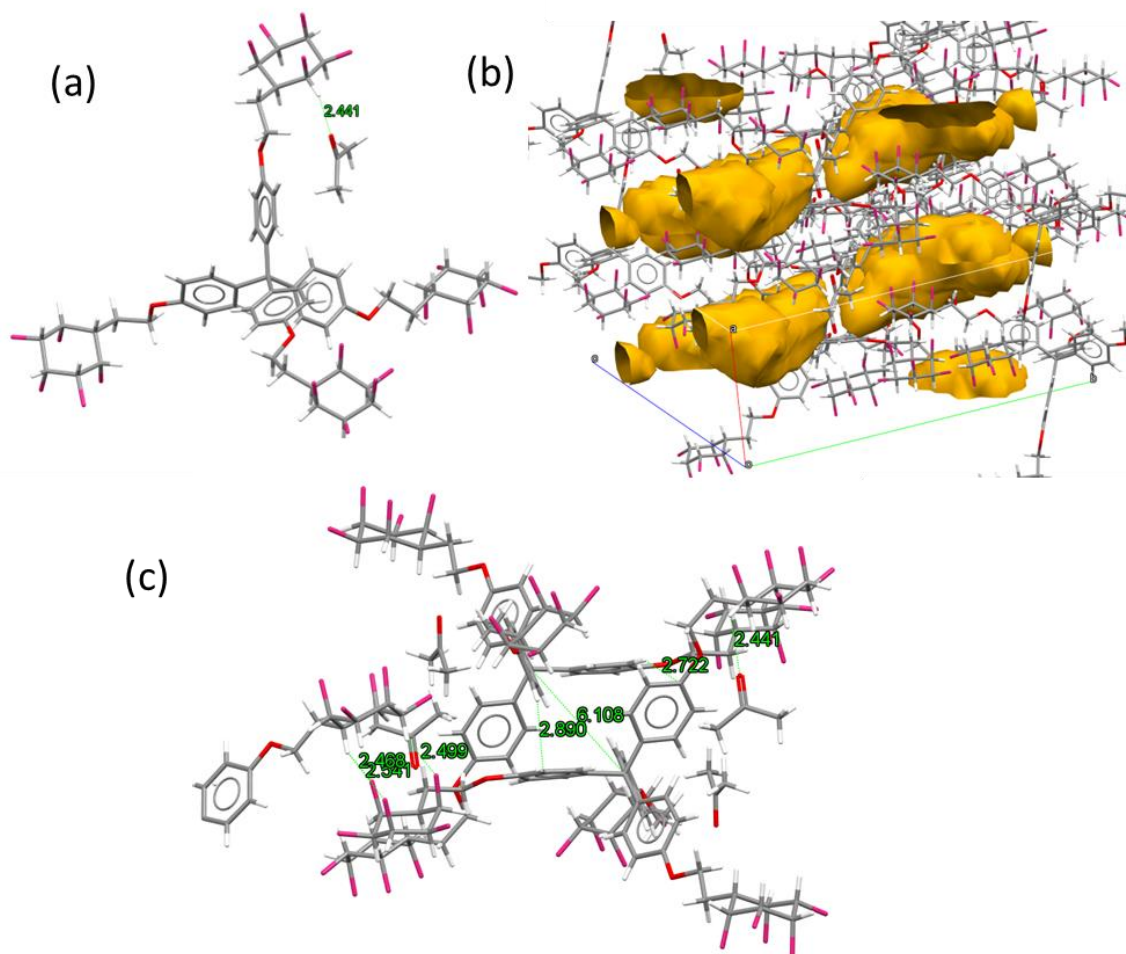
Figure 6-16 X-Ray crystal structure of **6-60**, (a) The monomer **6-60** with guest solvent molecule of acetone; (b) void space in crystal structure of **6-60**; (c) the intramolecular contact distance of **6-60**.

The X-ray crystal structure of tetraphenyl **6-60** is shown in Figure 6-16. The hydrogen face of the Janus face fluorocyclohexyl ring has a contact distance of C–H...O=C of 2.4 Å with co-crystallised acetone molecules, showing a strong association with the carbonyl guest molecule as expected. There are more than 3 acetone molecules present in the unit cell, and a 11.3 % void volume proved the porosity of the **6-60** building blocks. The Janus face fluorocyclohexyl ring is parallel packed contacting with another ring intermolecularly with a C–H...F–C distance of 2.4-2.5 Å and 4.5 Å between the ring planes (Figure 6.16, c, left). The phenyl ring is perpendicular T shaped and with a distance of 2.9 Å to the C–H to an aromatic

ring. The π…π interactions and herein the coordinating geometry of the building block **6-60** resulted in a close core to core distance of 6.1 Å between two **6-60** building blocks. The crystal structure suggests a slightly smaller porous volume for the framework than tetra-amide **6-57**. Therefore, the elongation of the tetraphenylether **6-60** building block become of obvious interest.
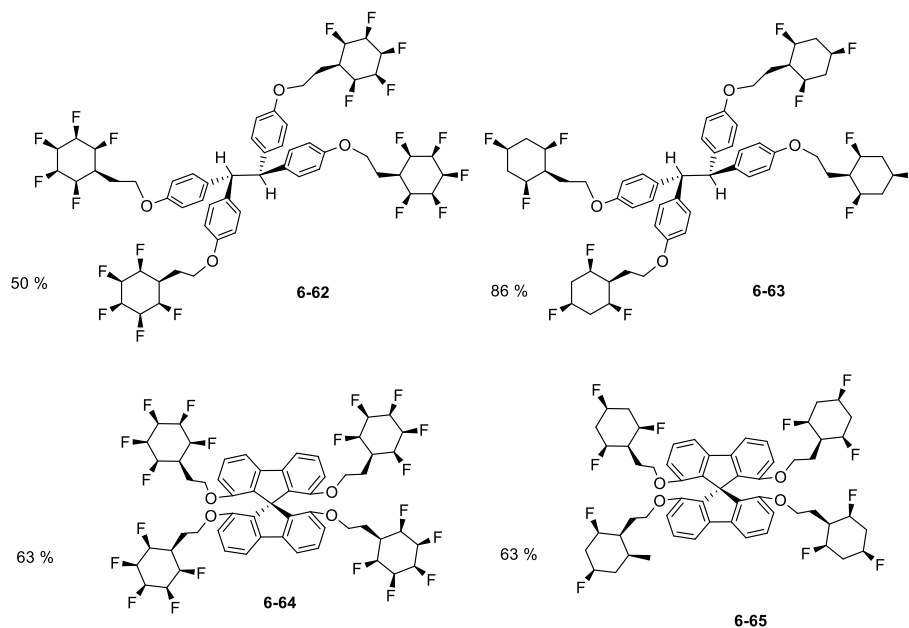
Figure 6-17 Alkyl–O–alkyl ether building blocks with D_{3d} and S_4 centres.

D_{3d} and S_4 centre scaffolds were synthesised from tetraphenol cores **6-47** and **6-51** a similar approach to that of the T_4 centred **6-60** and **6-61**. The resultant products are listed in Figure 6-17. The reaction had moderate yields from 50 % to 86 % as listed. Building blocks **6-64** and **6-65** are crystalline as expected, and the X-ray single crystal structure was not obtained yet due to the crystal size. The building blocks **6-62** and **6-63** forms fine needles, perhaps caused by the supramolecular structure. The observation is consistent with fibre formation of Janus face flouorocylohexyl peptides as discussed in Chapter 4 and the reported living supramolecular polymerisation with Janus face containing monomers.[19]

6.5.2.3 Diphenyl acetylene T_4 building block
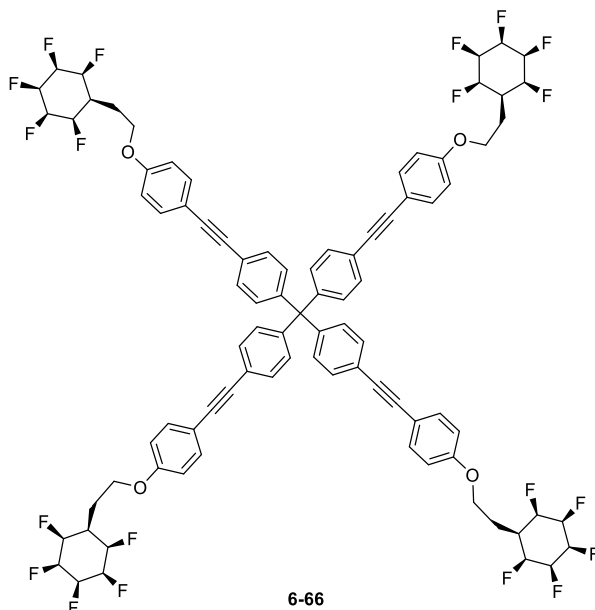
Figure 6-18 Supramolecular building blocks tetrakis-(diphenylacetylene) **6-66** with T_4 symmetry.

The next development of the project aimed to elongate the linkage between the Janus face fluorocyclohexane rings and its core. A synthetic target became the bis-acetylene **6-66** shown in Figure 6-18.
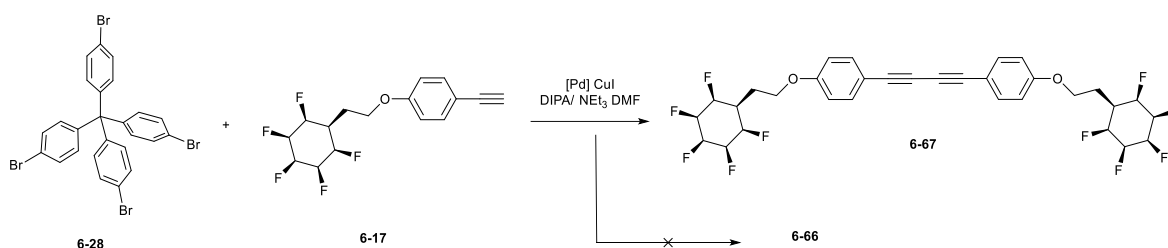
Scheme 6-18 Synthesis of diphenylacetylene **6-67** using a Sonogashira reaction.

The initial strategy envisaged coupling ethynyl phenol ether **6-17** with the tetra-arylbromide **6-28** in a four-fold Sonogashira protocol. In the event, there was a high conversion to a poorly soluble product which could be isolated after the reaction. The product was only soluble in DMSO, and although not confirmed unambiguously, the ^{1}H-NMR was consistent with

formation of homo-coupled product **6-67**. This was most likely due to the high reactivity of the terminal acetylene groups over the aryl bromide in this palladium catalysed process.

In another retrosynthesis approach as discussed Section 6.4.2, arylbromide **6-28** was coupled to freshly prepared ethynyl-phenol **6-31**. The reaction generated the tri-substituted product **6-33**, presumably due to the low reactivity of the aryl bromide (Scheme 6-6).
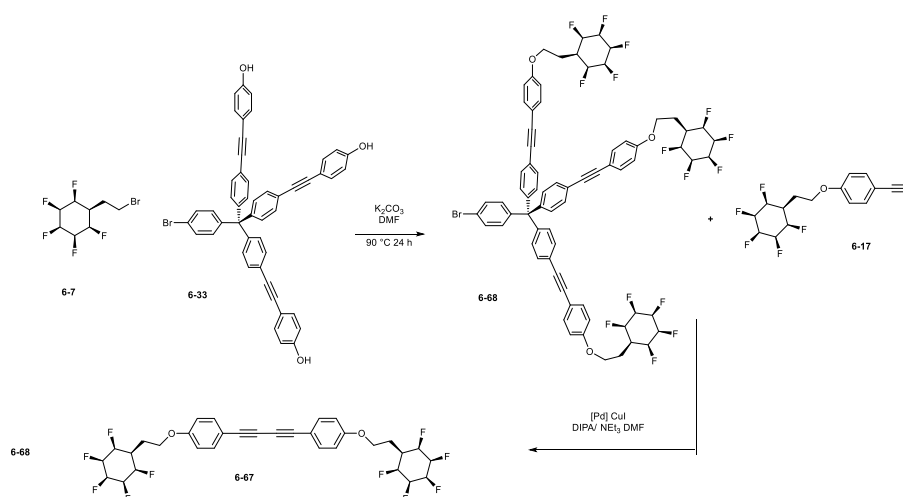
Scheme 6-19 Approach of synthesis diphenylacetylene **6-66** from tripodal core **6-33**.

To explore this further, the major product triphenol **6-33** was converted to aryl bromide **6-68**. This aryl bromide **6-68** was then committed to a further one-to-one Sonogashira reaction with **6-17**. This resulted only in the homocoupling product **6-67** and starting material **6-68** was also recovered from the reaction, again indicative of the low reactivity of the aryl bromide.

The C3 symmetry building block **6-68** shows no gas absorption properties in preliminary BET measurements.

Scheme 6-20 Synthesis of tetrakis(diphenylacetylene) building block **6-66**

Due to the poor reactivity of the terminal alkyne with phenyl bromide, the minor product **6-32** presented as the most accessible option to access a C_4 elongated scaffold. The product shows a low polarity behaviour, especially by column chromatography with the presence of trace DMF/acetone. The target building block **6-66** was isolated in 43 % yield as a white amorphous solid.

Figure 6-19 ^{1}H NMR of tetra(diphenylacetylene) **6-66**

The size of the tetraphenyl **6-66** crystal expanded significantly upon absorbing solvent. The water signal in **6-66** ^{1}H NMR splits, similarly the methanol –OH signal in **6-60** has a resolved

coupling to a methyl group. Those behaviours indicate association between targeted frameworks with guest molecules.

6.5.2.4 Adamantane core building blocks

Another strategy explored to elongate the tetraphenyl ether **6-60** building block was to replace the central spiro carbon with an adamantane cage, to retain the overall symmetry of the building block. As shown is Scheme 6-21(a), the first approach to prepare **6-69** involved a four-fold electrophilic substitution of **6-36** with phenyl ether **6-13** in the presence of a Brønsted acid. In the event, the reaction did not afford the desired product of **6-69**, perhaps due to the low solubility of **6-13** in the reaction.
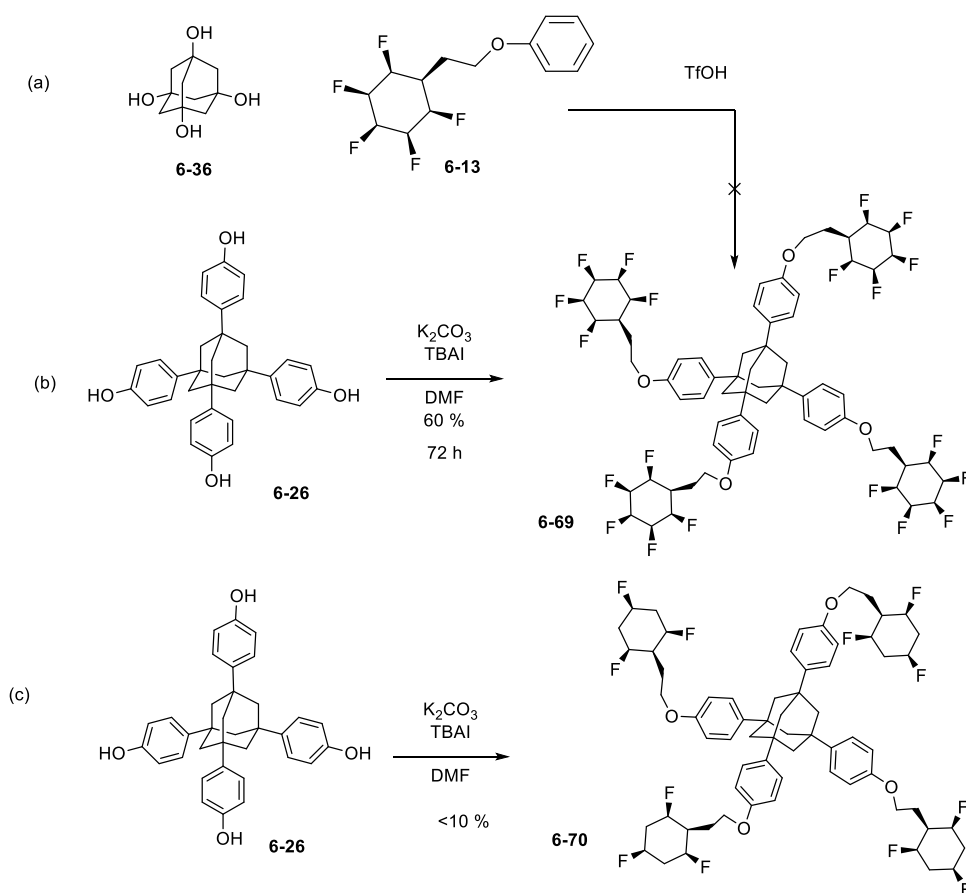
Scheme 6-21 Synthesis of tetraphenyl ether building blocks with an adamantane core

An alternative approach was applied involving firstly the synthesis of tetraphenyhydroxyl adamantane **6-26** described in Scheme 6-7 (b) in Section 6.4.2. Tetraphenyl ether **6-69** was synthesised in a fourfold Williamson's ether synthesis reaction. Extended reaction times and addition of the surfactant TBAI was necessary for good conversion to **6-26**, and the resubmission of the crude product with additional alkyl bromide and base significantly improved the yield of **6-69** to 60 %. A lower yield of less than 10 % was obtained for the all-*cis*-1,3,5 trifluorocyclohexyl analogue **6-70** as illustrated in Scheme 6-21.

A BET measurement was carried out with framework **6-69**. However very limited nitrogen uptake was measured <3 m^3 g^{-1} indicating limited porosity, although this may be also a consequence of an inability to displace solvents. [18] The purification, recrystallisation and activation of frameworks **6-69** was performed, however gas uptake was not improved.
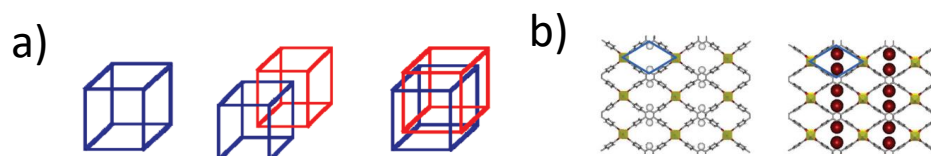
Figure 6-20 (a) Cartoon representations of the noncatenated framework, 2 non catenated frameworks, 2 catenated framework with interwoven structure ;(b) Representation of activated framework with pore free volume and deactivated framework with pore filled by absorbates.

6.5.3 Triazole linkage scaffold
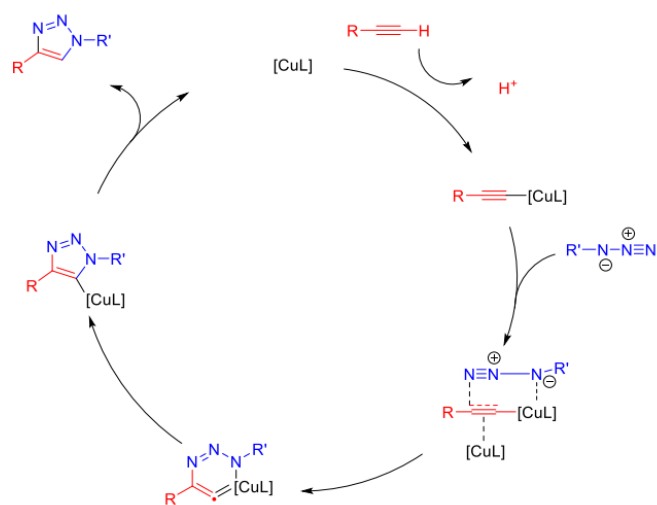
Scheme 6-22 The catalytical mechanism of the CuAAC 'click' reaction adapted from Hein and Fokin.[27]

The triazole linkage can be achieved by the CuAAC mediated 'click' reaction between an alkyl azide and a terminal alkyne.[27] Two retrosynthesis approaches are applicable listed in Scheme 6-22, each with the Janus face motif pre-installed on either the azide or acetylene component of the 'click' substrates. Care was taken as there is some danger in handling azides particularly with high N/C ratios (Scheme 6-23).
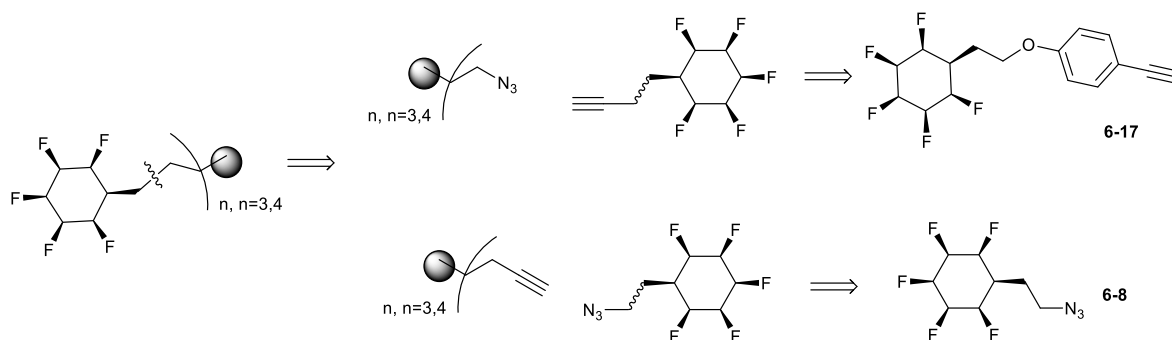
Scheme 6-23 Retrosynthesis approach to triazole linked framework building blocks.

6.5.3.1 Synthesis of the 4-fold alkyne scaffolds
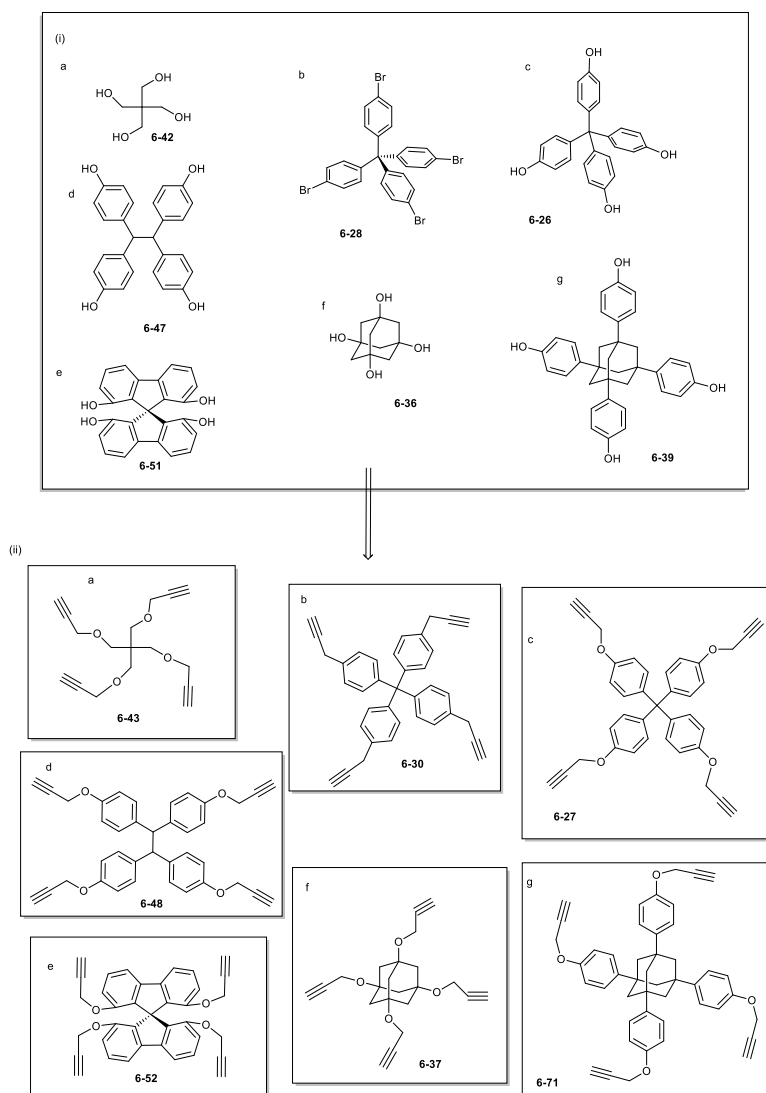
Scheme 6-24 Synthesis of the 4-folds alkyne scaffolds, entry (i) starting material, (ii) targeted tetra-alkyne.

The 4-fold acetylene scaffold cores (Scheme 6-24, ii) were prepared following literature protocols from pre-prepared alcohol/bromide intermediates (Scheme 6-24, i). Potassium carbonate mediated Williamson ether syntheses were applied and in most cases with phenol substrates. Products were formed in reasonable yields. Harsher reaction conditions, using sodium hydride, were applied in the case of alkyl alcohols **6-42** and **6-36**, and a Sonogashira reaction was applied in the case of **6-28**.

6.5.3.2 Triazole linkage scaffolds
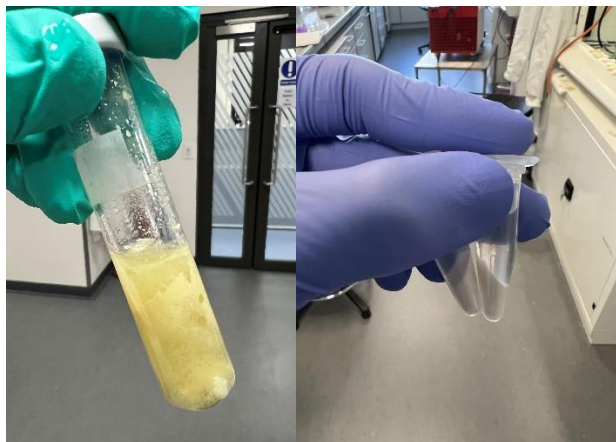
Figure 6-21 'Click' synthesis of tetrakis-triazole building blocks.

The product alkynes were then converted to the corresponding triazole scaffolds using a 'click' reaction. In each case the products precipitated out of the reaction mixture, and they could be purified simply by washing and then centrifugation, which gave products in a decent yield and purity.

Entry of product	Scheme 6-24, tetrakis-alkyne	Scheme 6-25, 'click' reaction
a	69 %	87 %
b	34 %	89 %
c	60 %	98 %
d	50 %	92 %
e	30 %	66 %
f	17 %	39 %
g	40 %	83 %

Table 6-1 Yield of reactions in Scheme 6-24; preparation of tetrakis-alkyne and in Scheme 6-25; 'Click' CuAAC coupling to tetrakis-triazole building blocks.

A series of triazole scaffold products (Scheme 6-25) were prepared and the yields are summarized in Table 6-1. Moderate yields of about 50 % were obtained for the synthesis of 4-fold alkyne core substrates and excellent yields above 80 % were obtained for the 'click' reaction, with the exception of entry f where the yields were low for both steps. The

Williamson's ether synthesis of **6-37** was less favoured presumably due to the large steric hindrance of the tertiary alcohol. The CuAAC 'click' reaction has a low yield towards **6-77**, this is because the higher solubility of **6-77** leads to product lost during work up. The tetrakis-triazole **6-77** is more soluble than other tetrakis-triazoles due to the absence of a phenyl group, which leads to the absence of π interactions within the building blocks, and consequently low enthalpy gain during precipitation of **6-73**.
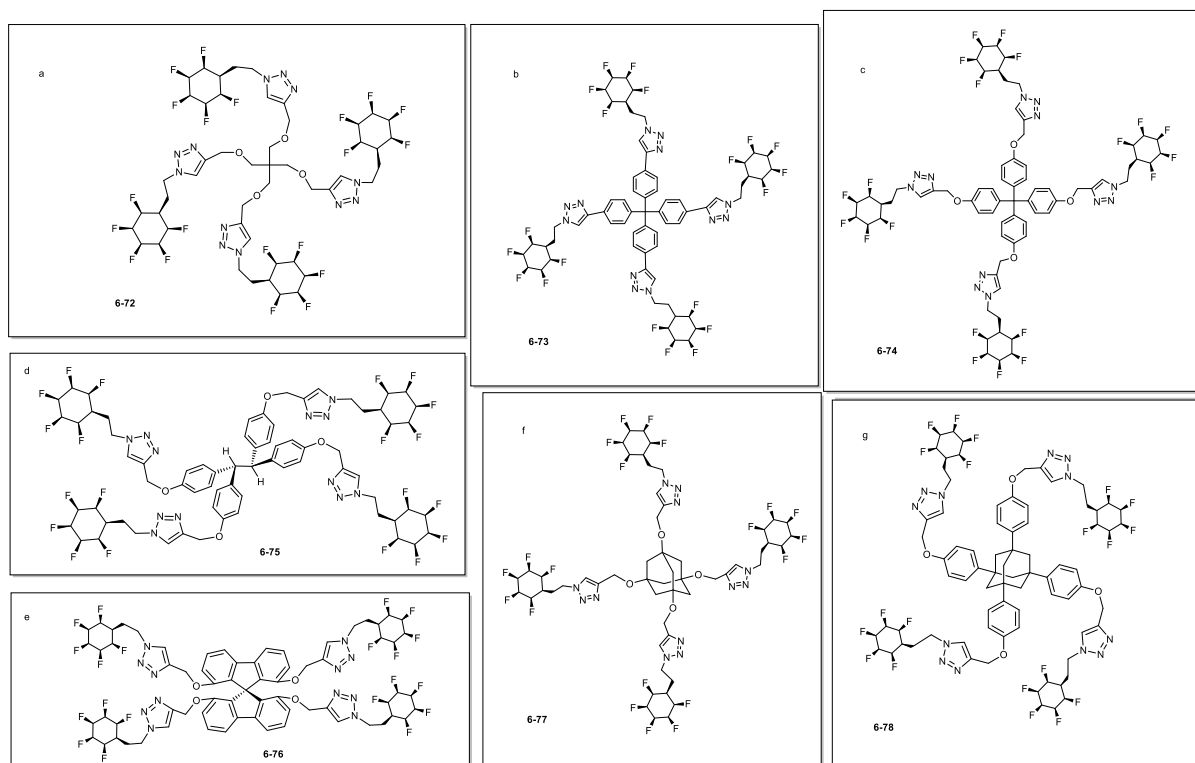
Scheme 6-25 The analogues of tetrakis-triazole building blocks prepared by "click" reaction

The ^{1}H NMR signal of the triazole has a downfield singlet which indicates a high stereoselectivity of the CuAAC reaction. This benefits from the large steric hindrance on the tetrakis-alkyne core and ruled out 1,5-cyclolisation, which makes the cycloaddition only afford 1,3 cycloaddition products as expected.
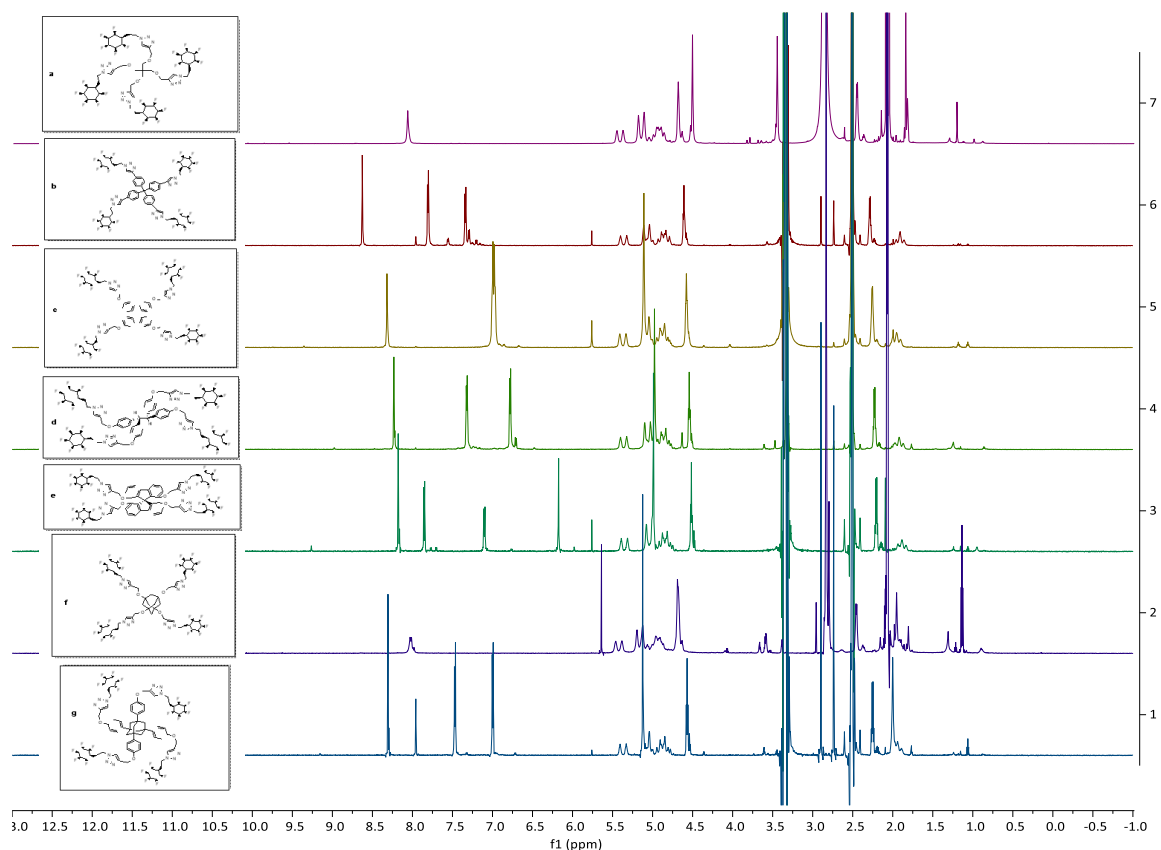
Figure 6-22 ^{1}H NMR of the tetrakis-triazole building blocks. The triazole proton signal is around δ 8 ppm and the Janus face cyclohexyl protons are near 5 ppm. From top to bottom Scheme 6-25 a to g.

The tetrakis-triazole frameworks are fine powders in most cases and framework **6-75** is a fibre which is consistent with the behaviour of other tetraphenylethane building blocks. X-Ray powder diffraction analysis was carried out on a fine powder of **6-74**, and the spectra is shown in Figure 6-23. The X-ray diffraction pattern suggests that the building blocks of **6-74** form a crystalline matrix in the solid state. The large FWHM of the broad peak suggests that the size of the crystals are small, which is consistent with observations made by microscopy.
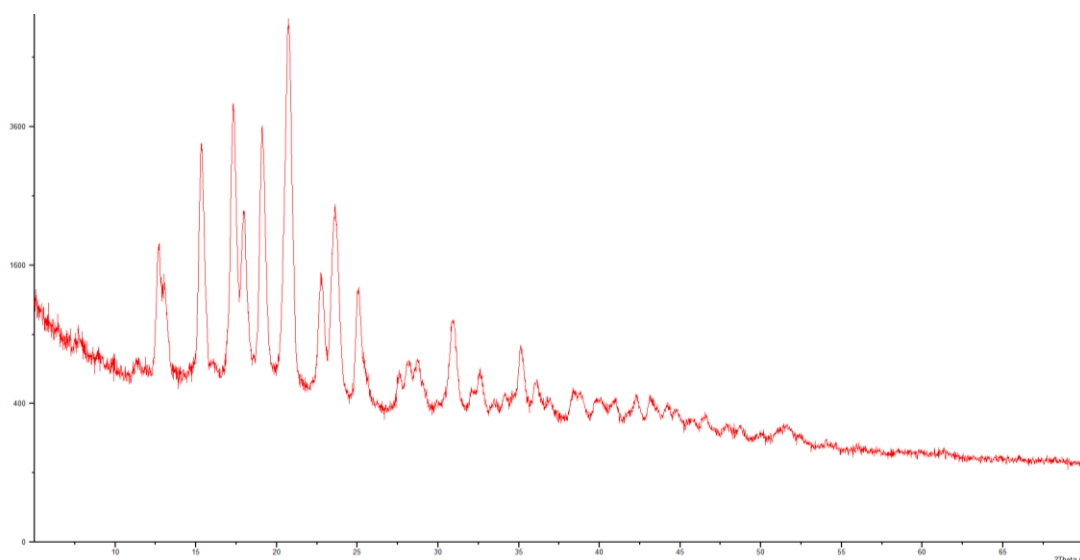
Figure 6-23 Xray powder diffraction pattern of tetrakis-triazole framework material **6-74**.

6.6 Summary

In summary, a range of supramolecular building blocks containing Janus face fluorocyclohexane motifs were synthesised in versatile strategies and generally with good yields. The building blocks were designed and proved to assemble into framework materials with face-to-face interactions between rings to generate so called Janus organic frameworks (JOFs). This offers a novel linking methodology for supramolecular chemistry. The framework materials are selectively soluble in a small range of solvents, which enabled the guest molecules to exchange in the porous volume as well as post-editing of the frameworks. The solvent processibility benefiting from the reversible association of Janus face rings is tested and proven. These assemblies are more promising than HOFs in term of stability due to the stronger interconnection interactions between Janus face rings relative to hydrogen bonds. The self-assembling nature of the building blocks forms porous and crystalline frameworks. The strong binding affinity of the JOF materials toward dipoles and ions was also evidenced by single crystal diffraction structures and solution phase NMR. And preliminary space volumes have been successfully designed into the superstructure, and voids were confirmed by X-ray and supported by BET measurements.

6.7 References

1.   L. Jiao, J. Y. R. Seow, W. S. Skinner, Z. U. Wang and H.-L. Jiang, *Mater. Today*, 2019, **27**, 43-68.

2.   A. E. Baumann, D. A. Burns, B. Liu and V. S. Thoi, *Chem. Commun.*, 2019, **2**, 86.

3.   N. Huang, P. Wang and D. Jiang, *Nat. Rev. Mater.*, 2016, **1**, 16068.

4.   X. Ma, M. Lepoitevin and C. Serre, *Mater. Chem. Front.*, 2021, **5**, 5573-5594.

5.   Q. Huang, W. Li, Z. Mao, L. Qu, Y. Li, H. Zhang, T. Yu, Z. Yang, J. Zhao, Y. Zhang, M. P. Aldred and Z. Chi, *Nat. Commun.*, 2019, **10**, 3074.

6.   L. Chen, B. Zhang, L. Chen, H. Liu, Y. Hu and S. Qiao, *Materials Advances*, 2022, **3**, 3680-3708.

7.   B. Wang, R.-B. Lin, Z. Zhang, S. Xiang and B. Chen, *J. Am. Chem. Soc.*, 2020, **142**, 14399-14416.

8.   J. F. Moulder and J. Chastain, *Handbook of X-ray Photoelectron Spectroscopy: A Reference Book of Standard Spectra for Identification and Interpretation of XPS Data*, Physical Electronics Division, Perkin-Elmer Corporation, 1992.

9.   Z. Meng and K. A. Mirica, *Chem. Soc. Rev.*, 2021, **50**, 13498-13558.

10.   P. R. Varadwaj, A. Varadwaj and B.-Y. Jin, *Phys. Chem. Chem. Phys.*, 2015, **17**, 31624-31645.

11.   S. Tsuzuki, T. Uchimaru and M. Mikami, *J. Phys. Chem. A*, 2006, **110**, 2027-2033.

12.   S. M. Pratik, A. Nijamudheen and A. Datta, *Chemphyschem*, 2016, **17**, 2373-2381.

13.   O. Shyshov, K. A. Siewerth and M. von Delius, *Chem. Commun.*, 2018, **54**, 4353-4355.

14.   J. L. Clark, A. Taylor, A. Geddis, R. M. Neyyappadath, B. A. Piscelli, C. Yu, D. B. Cordes, A. M. Z. Slawin, R. A. Cormanich, S. Guldin and D. O'Hagan, *Chem. Sci.*, 2021, **12**, 9712-9719.

15.   S. M. Pratik, A. Nijamudheen and A. Datta, *J. Phys. Chem. C*, 2017, **121**, 1752-1762.

16.   R. Bano, M. Arshad, T. Mahmood, K. Ayub, A. Sharif, S. Perveen, S. Tabassum, J. Yang and M. A. Gilani, *J. Phys. Chem. Solids*, 2022, **160**, 110361.

17. K. Geng, T. He, R. Liu, S. Dalapati, K. T. Tan, Z. Li, S. Tao, Y. Gong, Q. Jiang and D. Jiang, *Chem. Rev.*, 2020, **120**, 8814-8933.

18. O. K. Farha and J. T. Hupp, *Acc. Chem. Res.*, 2010, **43**, 1166-1175.

19. O. Shyshov, S. V. Haridas, L. Pesce, H. Qi, A. Gardin, D. Bochicchio, U. Kaiser, G. M. Pavan and M. von Delius, *Nat. Commun.*, 2021, **12**, 3134.

20. J. L. Clark, R. M. Neyyappadath, C. Yu, A. M. Z. Slawin, D. B. Cordes and D. O'Hagan, *Chem. - Eur. J.*, 2021, **27**, 16000-16005.

21. T. Taniguchi, M. Imoto, M. Takeda, T. Nakai, M. Mihara, T. Iwai, T. Ito, T. Mizuno, A. Nomoto and A. Ogawa, *Heteroat. Chem*, 2015, **26**, 411-416.

22. G. S. Lee, J. N. Bashara, G. Sabih, A. Oganesyan, G. Godjoian, H. M. Duong, E. R. Marinez and C. G. Gutiérrez, *Org. Lett.*, 2004, **6**, 1705-1707.

23. H. Stetter and M. Krause, *Liebigs Ann. Chem.*, 1968, **717**.

24. X. Wang, S.-m. Lu, J. Li, Y. Liu and C. Li, *Catal. Sci. Technol.*, 2015, **5**, 2585-2589.

25. R. Butera, A. Shrinidhi, K. Kurpiewska, J. Kalinowska-Tłuścik and A. Dömling, *Chem. Commun.*, 2020, **56**, 10662-10665.

26. B. E. Ziegler, M. Lecours, R. A. Marta, J. Featherstone, E. Fillion, W. S. Hopkins, V. Steinmetz, N. S. Keddie, D. O'Hagan and T. B. McMahon, *J. Am. Chem. Soc.*, 2016, **138**, 7460-7463.

27. J. E. Hein and V. V. Fokin, *Chem. Soc. Rev.*, 2010, **39**, 1302-1315.

Chapter 7. Experimental

7.1 General experimental

All reactions were carried out under argon or nitrogen atmosphere with standard Schlenk techniques unless otherwise specified. The reaction glassware was flame dried or oven dried overnight and cooled under vacuum. Commercially available chemicals were purchased from Acros, Alfa Aesa, Apollo Scientific, Fisher Scientific, Fluorochem, Manchester Organics, Sigma Aldrich, Strem Chemicals, and TCI (UK) and used as received unless otherwise stated. Anhydrous solvents such as DCM, diethyl ether, THF, toluene and hexane were dried in a solvent purification system (Mbraun MB SPS-200). Anhydrous DMF, DMI, NMP, pentane and benzene were purchased as dry solvent and used as received. Room temperature refers to the temperature range 15-27 $^\circ$C. The heating temperatures are measure as the temperature of an oil bath or Drysyn heating block surround.

Hydrogenation reactions were performed in high pressure autoclaves at indicated pressure and temperature. The hexane used for the hydrogenation reactions was degassed bubbling argon for 1 hour over powdered 4 Å molecular sieves and left for 1 day under argon before use. The reaction mixture was loaded to a dry reaction vessel equipped with a magnetic stirring bar and transferred to the Autoclave under argon. *In vacuo* refers to the use of a rotary evaporator with a membrane pump to 30-50 mbar at 40 $^\circ$C unless otherwise stated.

^{1}H, ^{13}C and ^{19}F NMR spectra were recorded on a Bruker AVIII-HD 700 Hz with Cryo Probe Prodigy TCI (^{1}H, 700 MHz, ^{13}C, 176 MHz, ^{19}F, 659 MHz), a Bruker AVIII 500 Hz with Cyro Probe Prodigy BBO, or a Bruker AVIII-HD 500 Hz with SmartProbe BBFO+ (500 MHz ^{1}H, 125 MHz ^{13}C, and 470 MHz for ^{19}F) or Bruker AV 400 Hz with BBFO probe (400 MHz ^{1}H, 100 MHz ^{13}C, 161 MHz and 376 MHz for ^{19}F). NMR analyses were carried out at room temperature in indicated deuterated solvents unless otherwise noted. Chemical shifts data were reported as δ units of

ppm corrected by the solvent residue peak[1] and coupling constants, *J*, are reported in Hz. Multiplicities are indicated by: s for singlet, d for doublet, t for triplet, q for quartet and m for multiplet and br. for broad brand. Analytical thin layer chromatography was carried out on aluminium backed Merck TLC silica gel 60 F$_{254}$ plates. These plates were visualised using UV light at 254 nm wavelength, dyed by potassium permanganate or phosphomolybdic acid followed by heating. Flush column chromatography was performed with Sigma-Aldrich silica gel, 60 Å pore size and 230-400 mesh, 40-63 μm particle size under 5 psi compressed air. Melting points were measured on an Electrothermal 9100 melting point apparatus, a Griffin electric thermal melting point apparatus with thermometer or hot stage microscopy with thermometer reading uncorrected.

Mass spectra measurements were carried at either the University of St Andrews Mass Spectrometer Facility, University of Edinburgh Mass Spectrometer Facility or the EPSRC National Mass Spectrometry Service Center at Swansea using given methods.

Synthesis of Rh(CAAC)(COD)Cl, [Rh]

The preparation of Rh(CAAC)(COD)Cl **[Rh]** was carried out according to the reported literature[2,3] with modification. Commercially available ligand (CAAC)·2HCl was used instead of the synthetic carbene salt (CAAC)HCl, therefore 1 more equivalent of base was added.

Rh-CAAC-COD-Cl **[Rh]**
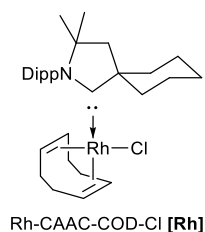
[Rh(COD)Cl]$_2$ precursor (161 mg, 0.326 mmol, 0.5 eq.), carbene salt CAAC·2HCl (250 mg, 0.691 mmol, 1 eq.) and KHMDS (262 mg, 0.983 mmol, 4 eq.) were added to a Schlenk tube in a glove box under nitrogen atmosphere. Dry THF (15 ml) was added dropwise over 10 min to the

vigorously stirring solid/suspension mixture. The suspension was stirred for another 10 min at -78 °C, after which the cooling dry ice/acetone bath was removed. After stirring for 16 h at r.t., the reaction mixture was filtered, the residue was washed with THF (10 ml), concentrated, dried under high vacuum, dissolved in diethyl ether, adsorbed on silica gel and purified by column chromatography once or twice (pentane/diethyl ether 19:1). After evaporation of the solvent, the complex was triturated from a concentrated DCM (0.1 ml) with pentane to yield desired complex as yellow powder. Yield 55 %. ^{1}H NMR (400 MHz, Chloroform-*d*): δ = 7.45–7.37 (m, 2H), 7.14 (dd, *J* = 1.6, 6.4 Hz, 1H), 5.24 (t, *J* = 7.2 Hz, 1H), 4.60 (q, *J* = 8.0 Hz, 1H), 3.92–3.86 (m, 1H), 3.45–3.43 (m, 1H), 2.92–2.84 (m, 2H), 2.63–2.45 (m, 3H), 2.28–2.25 (m, 1H), 2.14–2.11 (m, 1H), 2.01–1.92 (m, 3H), 1.78–1.73 (m, 7H), 1.58–1.55 (m, 2H), 1.49 (s, 3H), 1.44–1.35 (m, 3H), 1.26–1.22 (m, 9H), 1.19 (s, 3H), 0.94 (d, *J* = 6.8 Hz, 3H).

7.2 Chapter 2

7.2.1 Synthesis of substrates

TBS protected alcohols

TBS-protection of phenols was carried out according to the literature.[4]

General procedure for TBS-protection:

Phenol (1 eq, 5.3 mmol), 4-dimethylaminopyridine (0.1 eq., 65 mg, 0.5 mmol), and imidazole (1.6 eq, 580 mg, 8.5 mmol) were dissolved in dry DCM 15 ml. The solution was cooled with an ice bath. Tert-butyldimethylsilyl chloride (1.1 eq, 880 mg, 5.8 mmol) was added and the suspension was stirred overnight and allowed to warm up to room temperature (about 20 °C) The reaction was filtered, and the filtrate was evaporated under reduced pressure. The concentrated mixture was re-dissolved in 50 ml diethyl ether, cooled in an ice bath and then acidified with 0.5 M HCl to pH=1. The organic layer was separated and washed with brine 3

times, dried over sodium sulphate, filtered, and concentrated *in vacuo*. The residue was purified by column chromatography.

1-[[(1,1-Dimethylethyl)dimethylsilyl]oxy]-2-(trifluoromethyl) benzene 2-59
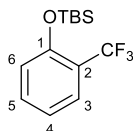
Trifluoromethyl phenol (1 eq, 860 mg, 5.3 mmol), 4-dimethylaminopyridine (0.1 eq, 65 mg, 0.535 mmol), and imidazole (1.6 eq, 580 mg, 8.5 mmol) were dissolved in dry DCM 15 ml. The solution was cooled with an ice bath. *Tert*-butyldimethylsilyl chloride (1.1 eq, 880 mg, 5.8 mmol) was added and the suspension was stirred overnight and allowed to warm up to room temperature (about 20 °C) The reaction was filtered, and the filtrate was evaporated under reduced pressure. The concentrated mixture was re-dissolved in 50 ml diethyl ether, cooled in an ice bath and then acidified with 0.5 M HCl to pH=1. The organic layer was separated and washed with brine 3 times, dried over sodium sulphate, filtered, and concentrated again under reduced pressure. The residue was purified by column chromatography with pure petroleum ether, r.f. ~0.8, affording a colourless oil 1.33 g, yield 82 %.

^{1}H NMR (700 MHz, Chloroform-d) δ 7.55 (dd, *J* = 7.8, 1.8 Hz, 1H, H-3), 7.39 (td, *J* = 7.7, 1.8 Hz, 1H, H-5), 6.99 (t, *J* = 7.6 Hz, 1H, H-4), 6.92 (d, *J* = 8.2 Hz, 1H, H-6), 1.02 (s, 9H, C(CH$_3$)$_3$), 0.28 (s, 6H, Si(CH$_3$)$_2$). ^{13}C NMR (176 MHz, Chloroform-d) δ 154.1 (C-1), 133.0 (C-5), 127.3 (q, *J* = 5.2 Hz, C-3), 124.0 (q, *J* = 272.3 Hz, CF$_3$), 121.3 (q, *J* = 29.9 Hz, C-2) 120.5 (C-4), 119.7 (C-6) 25.6 (C(CH$_3$)$_3$), 18.3 (C(CH$_3$)$_3$), -4.1 (Si(CH$_3$)$_2$). ^{19}F NMR (659 MHz, Chloroform-d) δ -61.89. The compound NMR data match the reported literature.[5] FTMS -P ESI *m/z* calculated for [M]$^-$ 276.1157, [M+H]$^-$ 277.1236; found 277.0876

1-[[(1,1-Dimethylethyl)dimethylsilyl]oxy]-3-(trifluoromethyl) benzene 2-60
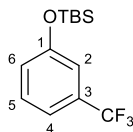

The reaction was carried out according to the standard procedure for TBS silyl protection.

A colourless oil (1.47 g) was obtained, 91 %, ^{1}H NMR (500 MHz, Chloroform-d) δ 7.34 (t, *J* = 7.9 Hz, 1H, H-5), 7.21 (d, *J* = 7.7 Hz, 1H, H-4), 7.08 (s, 1H, H-2), 7.00 (dd, *J* = 8.2, 2.4 Hz, 1H, H-6), 1.00 (s, 9H, Si^{t}Bu), 0.22 (s, 6H, SiMe$_2$). ^{13}C NMR (126 MHz, Chloroform-d) δ 156.1 (C-1), 132.0 (q, *J* = 32.2 Hz, C-3), 130.0 (C-5), 124.1(q, *J* = 272.2 Hz, CF$_3$), 123.5 (C-6), 118.1 (q, *J* = 3.8 Hz, C-4), 117.2 (q, *J* = 3.7 Hz, C-2), 25.7 (C(CH$_3$)$_3$), 18.3 (C(CH$_3$)$_3$), -4.4 (Si(CH$_3$)$_2$). ^{19}F NMR (470 MHz, Chloroform-d) δ -62.72. FTMS -P ESI *m/z* calculated for [M]$^-$ 276.1157, [M+H]$^-$ 277.1236; found 277.0876,

1-[[(1,1-Dimethylethyl)dimethylsilyl]oxy]-4-(trifluoromethyl) benzene 2-63
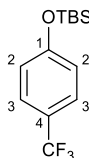
The reaction was carried out according to the standard for TBS silyl protection. A colourless oil (1.40 g), 87 % was obtained.

^{1}H NMR (500 MHz, Chloroform-d) δ 7.50 (d, *J* = 8.4 Hz, 2H, H-2), 6.91 (d, *J* = 8.4 Hz, 2H, H-3), 1.01 (s, 9H, Si^{t}Bu), 0.24 (s, 6H, SiMe$_2$). ^{19}F NMR (470 MHz, Chloroform-d) δ -61.54. 13C NMR (126 MHz, Chloroform-d) δ 158.7 (C-1), 127.0 (q, *J* = 3.8 Hz, C-3), 124.6 (q, *J* = 271.2 Hz, CF$_3$) 123.6 (q, *J* = 32.6 Hz, C-4), 120.3 (C-2), 25.7 (C(CH$_3$)$_3$), 18.4 (C(CH$_3$)$_3$), -4.3 (Si(CH$_3$)$_2$). The NMR spectra agree with reported values.[4] FTMS -P ESI *m/z* calculated for [M]$^-$ 276.1157, [M+H]$^-$

277.1236; found 277.0876

1-[[(1,1-Dimethylethyl)dimethylsilyl]oxy]-3,5-bis(trifluoromethyl) benzene 2-64
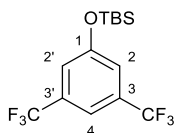
The reaction was carried out according to the standard procedure for TBS silyl protection. A colourless oil was obtained (1.64 g) was obtained, about 90 % yield.

^{1}H NMR (500 MHz, Chloroform-d) δ 7.46 (s, 1H, H-4), 7.23 (s, 2H, H-2), 1.00 (s, 9H, Si^{t}Bu), 0.25 (s, 6H, SiMe$_2$). ^{19}F NMR (470 MHz, Chloroform-d) δ -63.0. ^{13}C NMR (126 MHz, Chloroform-d) δ 156.7 (C-1), 133.0 (q, J = 33.3 Hz, C-3), 123.3 (q, J = 272.8 Hz, CF$_3$), 120.4 (C-2), 115.0 (C-4), 25.6 (C($\underline{C}$H$_3$)$_3$), 18.3 ($\underline{C}$(CH$_3$)$_3$), -4.4 (Si(CH$_3$)$_2$). FTMS -P ESI m/z calculated for [M]$^-$ 344.1031, [M+H]$^-$ 345.1109; found 345.0748,. TOF MS Cl+: m/z calculated for [M+] 344.1031 found 344.1035.

1-[[(1,1-Dimethylethyl)dimethylsilyl]oxy]-4-(trifluoromethoxy)benzene 2-78
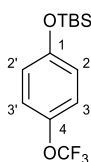
The reaction was carried out according to the standard procedure for TBS silyl protection. A colourless oil (1.40 g) was obtained, yield 88 %.

^{1}H NMR (500 MHz, Chloroform-d) δ 7.08 (m, 2H, H-3), 6.89 – 6.73 (m, 2H, H-2), 0.99 (s, 9H, Si^{t}Bu), 0.20 (s, 6H, SiMe$_2$). ^{13}C NMR (126 MHz, Chloroform-d) δ 154.4 (C-1), 143.3 (C-4), 122.5 (C-2), 120.9 (C-3), 120.7 (q, J = 256.0 Hz, OCF$_3$), 25.7 (C($\underline{C}$H$_3$)$_3$), 18.3 ($\underline{C}$(CH$_3$)$_3$), -4.4 (Si(CH$_3$)$_2$). ^{19}F NMR (470 MHz, Chloroform-d) δ -58.4. The NMR spectrum is agreement with reported

date. TOF MS Cl+: *m/z* calculated mass for [M+] 292.1106; found 292.1109.

Tert-butyldimethyl(4-(pentafluorosulfaneyl)phenoxy)silane 2-100
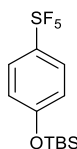
Compound **2-100** was prepared by the general TBS protection method. A colourless liquid (653 mg) was obtained. The product was used into next step directly. Yield 98 %. ^{1}H NMR (500 MHz, Chloroform-*d*) δ 7.65 (d, *J* = 9.1 Hz, 2H), 6.87 (d, *J* = 9.2 Hz, 2H), 1.01 (s, 9H), 0.26 (s, 6H). ^{19}F NMR (470 MHz, Chloroform-*d*) δ 86.32 (p, *J* = 150.2 Hz), 64.14 (d, *J* = 150.2 Hz). ^{13}C NMR (126 MHz, Chloroform-*d*) δ 158.1, 147.1, 127.6, 119.6, 34.2, 25.5, -4.4. FTMS -P calculated 333.0773, observed 333.0541.

Tert-butyldimethyl(4-((trifluoromethyl)thio)phenoxy)silane 2-104
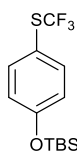
Compound **2-104** was prepared by the generally TBS protection method, and a colourless liquid (597 mg) was obtained, yield 97 %. ^{1}H NMR (500 MHz, Chloroform-*d*) δ 7.52 (d, *J* = 8.6 Hz, 2H), 6.87 (d, *J* = 8.7 Hz, 2H), 1.00 (s, 9H), 0.24 (s, 6H). ^{19}F NMR (470 MHz, Chloroform-*d*) δ -43.84. ^{13}C NMR (126 MHz, Chloroform-*d*) δ 158.4, 138.3, 129.6 (q, *J* = 308 Hz), 121.1, 115.6, 34.2, 25.6, -4.4. HRMS +P Ms [M] 308.0872, calculated 308.0878.

Boc protected anilines/amines

General procedure for Boc protection[6]: To a solution of the aniline (2 mmol) in 30 ml THF, Boc anhydride (2.5 mmol, 1.25 eq.), was added slowly under nitrogen. The reaction was

exothermic and left to stir for overnight. The reaction was monitored by TLC, and the reaction was heated under reflux if necessary. Potassium carbonate/NEt$_3$ in toluene was used as indicated. The reaction was concentrated *in vacuo* and subjected to column chromatography for purification. For larger scale reactions, the product could be purified by distillation.

Tert-butyl (4-(pentafluorosulfaneyl)phenyl)carbamate 2-101
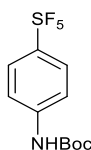
Compound **2-101** was prepared via the standard Boc protection procedure on a 2 mmol scale. A white solid product (411 mg) was obtained, yield 64 %.

^{1}H NMR (400 MHz, Chloroform-*d*) δ 7.66 (d, *J* = 9.2 Hz, 2H), 7.44 (d, *J* = 8.8 Hz, 2H). ^{19}F NMR (377 MHz, Chloroform-*d*) δ 86.59 − 84.38 (m), 63.67 (d, *J* = 150.2 Hz). ^{13}C NMR (101 MHz, Chloroform-*d*) δ 155.7, 152.1, 141.3, 127.0, 117.4, 28.3, 27.4. ^{19}F NMR (377 MHz, Chloroform-*d*) δ 87.34 − 84.30 (m), 63.67 (d, J = 150.2 Hz). FTMS -P [M-H], 318.0588, observed, cal. 318.0592.

Tert-butyl (4-((trifluoromethyl)thio)phenyl)carbamate 2-105
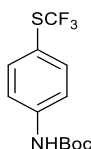
Compound **2-105** was carried out according to the standard Boc protection procedure on a 2 mmol scale. A white solid product (533 mg) was obtained with 91 % yield.

^{1}H NMR (400 MHz, Chloroform-*d*) δ 7.57 (d, *J* = 8.7 Hz, 2H), 7.43 (d, *J* = 8.7 Hz, 2H), 6.59 (s, 1H), 1.52 (s, 9H). ^{19}F NMR (377 MHz, Chloroform-*d*) δ -43.56. ^{13}C NMR (101 MHz, Chloroform-

d) δ 151.3, 141.1, 137.6, 118.8, 81.1, 28.3. ^{19}F NMR (377 MHz, Chloroform-*d*) δ -43.56. FTMS -P overved [M-H], 292.0623, cal 292.0627.

Tert-butyl (2-(trifluoromethoxy)phenyl)carbamate 2-90
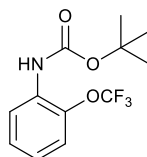
Compound **2-90** was prepared according to the literature described method. [6]

The aniline substrate (5 mmol) and the Boc anhydride (7.5 mmol) were refluxed in toluene overnight. The product was purified by distillation. A white solid (1.2 g) was obtained in 90 % yield, product was used without further purification.

^{1}H NMR (700 MHz, Chloroform-*d*) δ 7.27 – 6.96 (m, 3H), 6.87 – 6.48 (m, 1H), 3.89 (s, 1H), 1.63 – 1.50 (m, 9H).^{19}F NMR (659 MHz, Chloroform-*d*) δ -57.77. FTMS -P observed [M-H] 276.0854, cal. 276.0853.

7.2.2 Hydrogenation of (trifluoromethyl)benzene derivatives

General Procedure for hydrogenation reaction

Rh(CAAC)(COD)Cl **[Rh]** (2.9 mg, 0.5 mol %) was charged to an oven-dried 10 ml microwave tube equipped with a cross shape stirring bar and oven-dried silica gel (140 mg), unless otherwise noticed. The solid mixture was evacuated and charged with argon three times, after which hexane (2.0 ml) and the liquid substrate (1.0 mmol) were added under argon. The glass vial was placed in a high-pressure steel autoclave under argon with open cap. The Autoclave was pressurized and depressurized with hydrogen gas three times and then the pressure was charged to 50 bar. The reaction mixture was stirred at 25 °C in an oil bath for 24 h. Afterwards,

the autoclave was depressurized slowly and carefully. The crude NMR sample was taken by filtering aliquots of the reaction mixture through cotton wool followed by flushing with deuterated chloroform/acetone/methanol or if only ^{19}F NMR was being measured with non-deuterated solvent. The crude reaction mixtures containing 4 Å MS were filtered, flushed with sufficient amount of DCM/Acetone/Methanol (4 ml of each), and concentrated in *vacuo*. The residue was dissolved again in DCM, absorbed onto silica and subjected to column chromatography. In case of silica as an additive, the reaction mixture was dried *in vacuo* and subjected to column chromatography directly. Column chromatography with the indicated solvent was applied to obtain pure products.

(Trifluoromethyl)cyclohexane 2-53
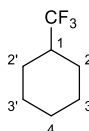
(Trifluoromethyl)benzene was filtered through a packed of silica under argon before use. The Rh(CAAC)(COD)Cl (2.9 mg, 0.5 mol %) was loaded into an oven-dried 10 ml microwave tube equipped with a cross shape stirring bar and oven-dried 4 Å MS beads (140 mg). Dry pentane (2 ml) was added to the rector, then (trifluoromethyl)benzene (146 mg, 1 mmol, 1eq.) was added dropwise to the reaction mixture. The reaction vessel was flushed three time with hydrogen gas before being charged with 50 bar of hydrogen. The reaction was then heated with stirring for 24 h, and then the hydrogen was released carefully. The reaction mixture was filtered through cotton wool and washed with 6 ml of pentane. The solvent was removed on a Kugelrohr distillation apparatus. The product was obtained as a colourless oil (90 mg), full conversion according to ^{19}F NMR, yield 59 %. a trace of pentane was not separated from the product, which was a volatile compound.

^{1}H NMR (500 MHz, Chloroform-*d*) δ 1.1–1.4 (m, 6H), 1.6–2.0 (m, 5H) ^{19}F NMR (470 MHz,

Chloroform-*d*) δ -74.2. ^{13}C NMR (126 MHz, Chloroform-*d*) δ 128.0 (q, *J* = 278.5 Hz, CF$_3$), 42.2 (q, *J* = 26.3 Hz, C-1), 25.7 (C-3), 25.3 (q, *J* = 2.5 Hz C-2), 25.2 (C-4). The NMR spectra match to reported data[7]. To assign the alkyl proton region from the overlapping solvent peaks, a reaction was run neat, and 10 % conversion was obtained. MS EI +: *m/z* calculated for [M+] 152.0813; found 152.0811.

1,2-Bis(trifluoromethyl)cyclohexane 2-28

cis- **2-28**   *trans-* **2-28**
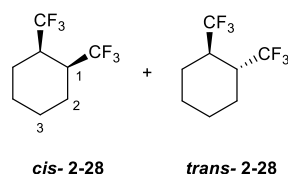
The reaction was carried out according to the general procedure for hydrogenation of (trifluoromethyl)cyclohexanes. The reaction was performed with hexane and silica. A colourless oil (165 mg) was obtained, 95 % conversion and 75 % yield, as a volatile compound. The two isomers and trace solvent are not separable and only peaks of the major isomer *cis-* **2-28** are listed.

^{1}H NMR (500 MHz, Chloroform-*d*) δ 2.66 – 2.46 (m, 2H, H-1), 2.01 (m, 2H, H$_{eq}$-2), 1.79-1.70 (m, 2H, H$_{eq}$-3), 1.70-1.60 (m, 2H, H$_{ax}$-2), 1.49 (m, 2H, H$_{ax}$-3). ^{13}C NMR (126 MHz, Chloroform-*d*) δ 126.8 (q, *J* = 280.5 Hz, CF$_3$), 40.2 (q, *J* = 28.3, 27.2 Hz, C-1), 23.5 (C-2), 22.7 (C-3).^{19}F NMR (470 MHz, Chloroform-*d*, room temperature) δ -65.76 (br.) ^{19}F NMR (470 MHz, CD$_2$Cl$_2$, -75 ^{o}C) δ -61.2, (CF$_3$-axial), -70.4(CF$_3$- equatorial). ^{19}F NMR for **2-28 trans** observed around δ-68.7 in both condition.

EI +p: *m/z* calculated for [M-HF] $^+$ 199.9867 [M-HF-F]$^+$ 180.9883, found 200.0653

1,3-Bistrilfluoromethylcyclohexane 2-32

cis- 2-32   tran 2-32
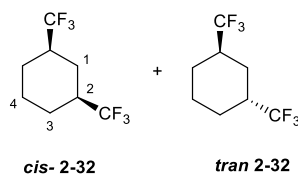
The reaction was performed with hexane and silica. The reaction was carried out according to used procedure for compound **2-28**. A colourless oil (136 mg) was obtained, 87 % conversion, 62 % yield, volatile compound. The two isomers and trace solvent are not separable, only peaks of major isomer **cis-2-32** are reported.

^{1}H NMR (500 MHz, Chloroform-*d*) δ 2.22 – 2.15 (m, 2H), 2.10 (m, 2H, H-2), 2.06 – 1.97 (m, 3H), 1.70 – 1.64 (m, 1H). 1.26-1.36 (m, 4H); ^{13}C NMR (126 MHz, Chloroform-*d*) δ 127.3 (q, J = 278.4 Hz, CF_3), 41.1 (q, J = 27.3 Hz, C-2) 24.4 (C-3), 24.0 (C-1), 23.7 (C-4) ^{19}F NMR (470 MHz, Chloroform-*d*, r.t.) δ -74.1.^{19}F NMR (470 MHz, CD_2Cl_2, -75°C) δ -74.1.

Compound **trans 2-32** ^{19}F NMR (470 MHz, Chloroform-*d*, r.t.) δ -70.7

EI +p full ms: *m/z* calculated for [M-HF]+ 199.9867, [M-HF-F]+ 180.9883; found 200.0662 and 181.0678

1,4-Bis-(trifluoromethyl)cyclohexane 2-56

cis- 2-56   tran- 2-56
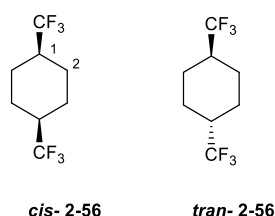
The reaction with performed with pentane and silica. The procedure was carried out according to the general procedure for (trifluoromethyl)cyclohexane. A colourless oil (110 mg)

was obtained, 100 % conversion and 50 % yield. Volatile compound. Only peaks of major isomer are listed in ^{1}H and ^{13}C NMR. Trace of solvent was azeotropic and not removed completely. Volatile compound. Only peaks of major isomer *cis-* **2-56** are reported.

^{1}H NMR (500 MHz, Chloroform-*d*) δ 2.31 – 2.13 (m, 2H, H-1), 1.93 – 1.79 (m, 4H, H_{eq}-2), 1.76 – 1.61 (m, 4H, H_{ax}-2). ^{13}C NMR (126 MHz, Chloroform-*d*) δ 128.1 (q, *J* = 279.6 Hz, CF_3), 38.5 (q, *J* = 26.4 Hz, C-1), 21.6 (C-2). ^{19}F NMR (470 MHz, Chloroform-*d*, r.t.) δ -70.4 (d, *J* = 8.0 Hz). ^{19}F NMR (470 MHz, CD_2Cl_2, -75 °C) δ -66.5, -74.1.

Compound **trans 2-56** ^{19}F NMR (470 MHz, Chloroform-*d*, r.t.) δ -74.0

EI +p full ms: *m/z* calculated for [M-HF-F]$^+$ 180.9883, [M-HF]$^+$ 199.9867; found 181.0633 and 200.0637

cis-2-(Trifluoromethyl)cyclohexanol *tert*-butyldimethylsilyl ether *cis* 2-66
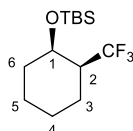
The reaction was carried out according to the general procedure, 4 Å M. S. beads (140 mg) and hexane was used. The reaction mixture was filtered, flushed with DCM and dry loaded onto silica for column chromatography, r. f. 0.7 with pure hexane. A colourless oil (203 mg) was obtained, yield 72 %.

^{1}H NMR (500 MHz, Chloroform-*d*) δ 4.27 (s, 1H, H-1), 2.06 – 1.92 (m, 1H, H-2), 1.90 – 1.72 (m, 3H, H_{eq}-3, 4, 6), 1.72 – 1.60 (m, 2H, H_{eq}-5, H_{ax}-3), 1.49 – 1.39 (m, 1H, H_{ax}-5), 1.34 (m, 1H, H_{ax}-6), 1.30 – 1.18 (m, 1H, H_{ax}-4), 0.90 (s, 9H, Si^{t}Bu), 0.04 (d, *J* = 7.5 Hz, 6H, SiMe$_2$).

^{13}C NMR (126 MHz, Chloroform-*d*) δ 127.2 (q, *J* = 279.9 Hz, CF_3), 64.5 (C-1), 46.9 (d, *J* = 74.1

Hz, C-2), 33.6 (C-6), 25.8 (C($\underline{C}H_3$)$_3$), 25.1 (C-4), 19.6 (C-3), 19.3 (C-5), 18.1 ($\underline{C}$(CH$_3$)$_3$), -4.3 (SiMe), -5.3 (SiMe').

^{19}F NMR (470 MHz, Chloroform-d) δ -69.52 (d, J = 9.1 Hz).

TOF MS ASAP+: m/z calculated for [M+H] 283.1705, found 283.1701
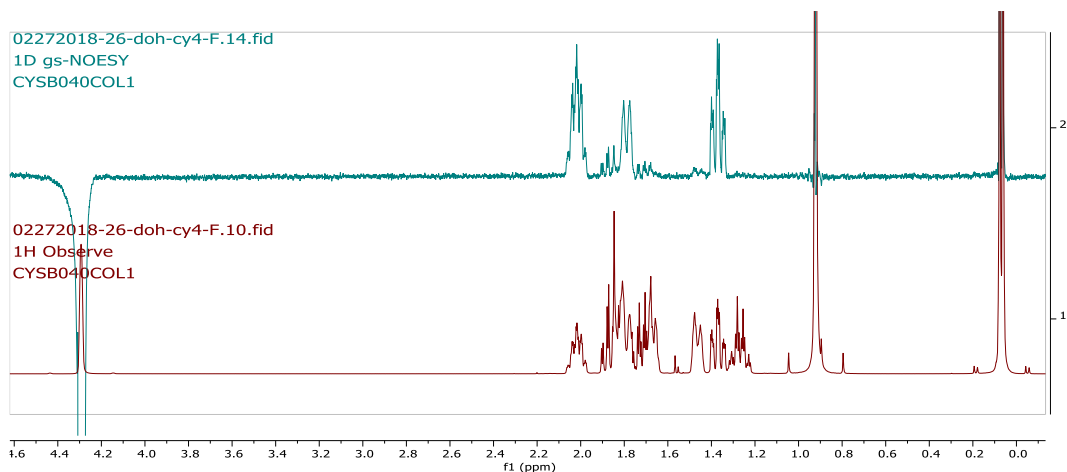
NOE experiment on compound *cis 2-66*

A NOE experiment was performed irradiating H-1, and this showed that H$_{ax}$-3, 5, H$_{eq}$-2 wer correlated.

trans-2-(Trifluoromethyl)cyclohexanol *tert*-butyldimethylsilyl ether *tran* 2-66
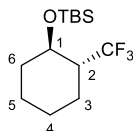
***Trans* 2-66** was obtained as a byproduct during the preparation of *cis* **2-66**, r.f. 0.1 with pure hexane. Trace <1 %

^{1}H NMR (700 MHz, Chloroform-d) δ 3.70 (td, J = 9.6, 4.4 Hz, 1H, H-1), 2.10 – 2.01 (m, 1H, H-2),

2.01 – 1.95 (m, 1H) 1.95 –1.86 (m, 1H H_{eq}-6), 1.80 – 1.63 (m, 2H), 1.44 – 1.10 (m, 4H, H_{ax}), 0.87 (s, 9H, Si^{t}Bu), 0.06 (s, 3H, SiMe), 0.04 (s, 3H, SiMe').^{13}C NMR (176 MHz, Chloroform-d) δ 127.4 (q, J = 281.0 Hz, CF$_3$), 69.7 (C-1), 48.8 (q, J = 23.7 Hz, C-2), 35.8 (C-6), 29.9 (C($\underline{C}$H$_3$)$_3$), 25.9, 24.4 (q, J = 3.0 Hz, C-3), 24.3, 24.1, 18.0 ($\underline{C}$(CH$_3$)$_3$), -4.1 (SiMe'), -5.0 (SiMe).

^{19}F NMR (470 MHz, Chloroform-d) δ -67.9 (d, J = 8.5 Hz).

TOF MS ASAP+: m/z calculated for [M+H] 283.1705, found 283.1702

cis-3-(Trifluoromethyl)cyclohexanol _tert_-butyldimethylsilyl ether _cis_ 2-67
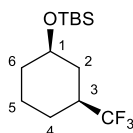
The same procedure used for with compound **2-66** was carried out, and the product was columned with pure hexane, r.f. 0.2. and flushed with 10 % EtOAc if necessary. A colourless oil (172 mg) was obtained, yield 61 %. ^{1}H NMR (500 MHz, Chloroform-d) δ 3.55 (m, 1H, H-1), 2.04 (m, 2H, H-3, H_{eq}-2), 1.92 – 1.79 (m, 2H, H_{eq}-4, 6), 1.39 – 1.12 (m, 5H), 0.88 (s, 9H, Si^{t}Bu), 0.06 (s, 6H, SiMe$_2$).

^{13}C NMR (126 MHz, Chloroform-d) δ 127.4 (q, J = 278.5 Hz, CF$_3$), 70.3 (C-1), 41.2 (q, J = 26.9 Hz, C-3), 35.5 (C-6), 34.6 (br. C-2), 26.0 (C($\underline{C}$H$_3$)$_3$), 24.2 (br. C-4), 23.0 (C-5), 18.3 ($\underline{C}$(CH$_3$)$_3$), -4.5 (SiMe), -4.5 (SiMe').^{19}F NMR (470 MHz, Chloroform-d) δ -73.6 (d, J = 8.1 Hz).

TOF MS ASAP+: m/z calculated for [M+H] 283.1705, found 283.1701

trans-3-(Trifluoromethyl)cyclohexanol _tert_-butyldimethylsilyl ether _trans_ 2-67
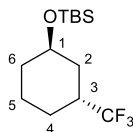
The reaction was carried out according to the standard procedure for CF_3 aryl hydrogenation.

Byproduct of compound **2-67**, r.f. value 0.7 in pure hexane. A colourless oil, 17 % yield

^{1}H NMR (500 MHz, Chloroform-_d_) δ 4.14 (s, 1H, H-1), 2.49 (m, 1H, H-3), 1.98 – 1.81 (m, 2H, H_{eq}-2,4), 1.81 – 1.68 (qt, _J_ = 13.2, 3.7 Hz, 1H, H_{eq}-5), 1.68 – 1.61 (d, _J_ =13.5 Hz, 1H, H_{eq}-6) 1.61 – 1.50 (m, 1H, H_{ax}-5), 1.40 (td, _J_ =12.7, 2.3 Hz, H_{ax}-2) 1,34 (tdd, _J_ =13.4, 4.3, 2.3 Hz, H_{ax}-6), 1.24 (qd, _J_ = 12.7, 3.9 Hz, 1H, H_{ax}-4), 0.89 (s, 9H, Si^{t}Bu), 0.04 (d, _J_ = 2.6 Hz, 6H, SiMe$_2$). ^{13}C NMR (126 MHz, Chloroform-_d_) δ 128.3 (q, _J_ = 278.1 Hz, CF_3), 65.4 (C-1), 36.3 (q, _J_ = 26.6 Hz, C-3), 32.6 (C-6), 32.5 (q, _J_ = 2.0, C-2), 25.8 (C($\underline{C}H_3$)$_3$), 24.6 (q, _J_ = 2.5, C-4), 18.7 (C-5), 18.0 ($\underline{C}$(CH$_3$)$_3$), -4.9 (SiMe), -5.0 (SiMe'). ^{19}F NMR (470 MHz, Chloroform-_d_) δ -73.8 (d, _J_ = 9.2 Hz).

TOF MS ASAP+: _m/z_ calculated for [M+H] 283.1705, [M-H] found 281.1548; found 281.0518

cis-4-(Trifluoromethyl)cyclohexanol _tert_-butyldimethylsilyl ether _cis_ 2-68
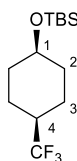
Compound **_cis_ 2-68** was prepared was carried out according to the standard CF_3 hydrogenation conditions. A colourless oil (203 mg) was obtained, yield 72%. ^{1}H NMR (700 MHz, Chloroform-_d_) δ 4.00 (p, _J_ = 3.0 Hz, 1H, H-1), 2.03 – 1.91 (m, 1H, H-2), 1.82 – 1.71 (m, 4H, H_{eq}2,3), 1.66 – 1.59 (m, 2H, H_{ax}-3), 1.47 – 1.37 (m, 2H, H_{ax}-2), 0.89 (s, 8H), 0.04 (s, 5H). ^{13}C NMR (176 MHz, Chloroform-_d_) δ 127.9 (q, _J_ = 278.5 Hz, CF_3), 65.2 (C-1), 41.6 (q, _J_ = 26.4 Hz, C-

4), 32.2 (C-2), 25.9 (C($\underline{C}H_3$)$_3$), 19.0 (C-2), 18.2 ($\underline{C}$(CH$_3$)$_3$), -4.8 (SiMe$_2$).^{19}F NMR (470 MHz, Chloroform-d) δ -73.9 (d, J = 8.5 Hz).

TOF MS ASAP+: m/z calculated for [M+H] 283.1705, found 283.1706

trans-4-(Trifluoromethyl)cyclohexanol _tert_-butyldimethylsilyl ether _trans_ 2-68
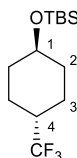
The c0ompound **2-68** was carried out according to the standard CF$_3$ hydrogenation conditions. 6 % yield, by product of **2-68**. ^{1}H NMR (400 MHz, Chloroform-d) δ 3.66 − 3.44 (m, 1H, H-1), 1.98 − 1.84 (m, 5H, H-4, H$_{eq}$-2,3), 1.41 − 1.22 (m, 4H, H$_{ax}$-2,3), 0.87 (s, 9H, Si^{t}Bu), 0.06 (s, 6H, SiMe$_2$). ^{13}C NMR (126 MHz, Chloroform-d) δ 127.9 (q, J = 278.4 Hz, CF$_3$), 70.6 (C-1), 41.1 (d, J = 26.6 Hz, C-4), 34.4 (C-2), 23.6 (d, J = 2.4 Hz, C-3), 23.7 (C($\underline{C}H_3$)$_3$), 18.3 ($\underline{C}$(CH$_3$)$_3$), -4.5 (SiMe$_2$). ^{19}F NMR (376 MHz, Chloroform-d) δ -73.3.

TOF MS ASAP+: m/z calculated for [M+H] 283.1705, [M-H] for 281.1548; found 283.1364 and 281.1552

cis-3,5-Bis(Trifluoromethyl)cyclohexanol _tert_-butyldimethylsilyl ether 2-69
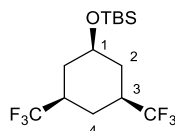
Compound **2-69** was prepared according to the standard CF$_3$ hydrogenation conditions. A colourless oil (100 mg) was obtained, yield 60 %.

^{1}H NMR (500 MHz, Chloroform-d) δ 3.63 (tt, J = 10.8, 4.3 Hz, 1H, H-1), 2.30 − 2.04 (m, 5H, H-

3, H_{eq}-2,4), 1.46 – 1.22 (m, 3H, H_{ax}-2,4), 0.88 (s, 9H, Si^{t}Bu), 0.07 (s, 6H, SiMe$_2$).^{13}C NMR (126 MHz, Chloroform-*d*) δ 126.8 (q, *J* = 278.3 Hz, CF$_3$), 68.6 (C-1), 39.6 (q, *J* = 27.8 Hz, C-3), 33.9 (C-2), 25.8 (C(CH$_3$)$_3$), 23.3 (br., C-4), 18.1 (C(CH$_3$)$_3$), -4.6 (SiMe$_2$).^{19}F NMR (470 MHz, Chloroform-*d*) δ -73.5 (d, *J* = 7.7 Hz).

TOF MS ASAP+: *m/z* calculated for [M+H] 351.1579, [M+2H] 352.1603; found 351.1577, 352.1609

7.2.3 Deprotection and esterification of TBS-protected cyclohexanol

4-*cis*-Trifluoromethyl-cyclohexan-1-ol *cis- 2-70*
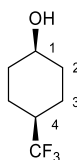
The deprotection of the TBS protected cyclohexanol was conducted according to a literature procedure.[2] TBS protected cyclohexanol *cis* **2-68** (0.2 mmol), was dissolved in dry THF (2 ml), then TBAF (2 eq.) was added dropwise at -20 °C. The reaction mixture was stirred below 0 °C for 12 hours then allowed to warm up to room temperature. The reaction was allowed to be stirred for maximum further 24 h, followed by TLC with phosphomolybdic acid (PMA). The reaction was quenched with 1 M HCl and purified by column (1:1 diethyl ether/pentane), r.f. 0.4. The solvent was concentrated but trace residue was not removed due to the volatility of compound **2-70**. The product was used directly for next step. 100 % conversion by ^{19}F NMR.

4-*cis*-(Trifluoromethyl)cyclohexyl 4-nitrobenzoate 2-71
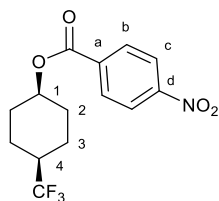
Compound *cis* **2-70** (0.11 mmol, 17 mg) was transferred into a Schlenk tube and dissolved in dried DCM (2 ml), 4 Å M. S. (15 mg), 4-nitro-benzoyl chloride (1 eq.), DIPEA (1.5 eq). DMAP (2 mol%), were added in sequence at 0 °C. The reaction was stirred at r.t. for 2 days (gives a yellow reaction mixture). The crude product could be recrystallised in hot pentane as well. The yellow impuritiy could be removed by column chromatography, 10 % EtOAc/pentane, 0.5 r.f. White crystal 29 mg was obtained, 90 % yield.

^{1}H NMR (500 MHz, Chloroform-*d*) δ 8.31 (dt, *J* = 8.9, 2.0 Hz, 2H, H-c), 8.21 (dt, *J* = 8.9, 2.0 Hz, 2H, H-b), 5.43 – 5.19 (m, *J* = 2.2, 1H, H-1), 2.27 – 2.08 (m, 3H, H-4, H-2), 1.89 (m, H-3), 1.83 – 1.62 (m, 4H, H-2, H-3). ^{19}F NMR (470 MHz, Chloroform-*d*) δ -73.79 (d, *J* = 8.4 Hz). ^{13}C NMR (126 MHz, Chloroform-*d*) δ 164.0 (-CO$_2$), 150.1 (C-d), 136.0 (C-a), 130.8 (C-b), 127.6 (q, *J* = 278.7, 278.3 Hz, CF$_3$). 123.8 (C-c), 70.0 (C-1), 41.0 (q, *J* = 27.0 Hz, C-4), 28.6 (C-2), 19.9 (q, *J* = 2.9 Hz, C-3). MS ASAP +p APCI SOLID: *m/z* calculated for [M+H]$^+$ 318.0950, [M+2H]$^+$ 319.0984; found 318.0948, 319.0982. The structure was confirmed by X-ray crystallography.

7.2.4 Direct hydrogenation of trifluorophenol

cis- 2-(Trifluoromethyl)cyclohexan-1-ol, *cis*- 2-72
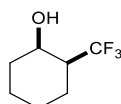
The reaction was carried out according to the standard procedure for CF$_3$ aryl hydrogenation.

The purification was performed by column chromatography with DCM, and a colourless oil (138 mg) was obtained in 82 % yield.

^{1}H NMR (500 MHz, Chloroform-d) δ 4.34 (t, J = 3.0 Hz, 1H, C$\underline{H}$OH), 2.10 (dddd, J = 12.8, 9.2, 3.8, 2.1 Hz, 1H, HCF3), 1.98 – 1.53 (m, 8H). ^{19}F NMR (471 MHz, Chloroform-d) δ -69.77.
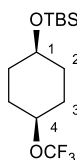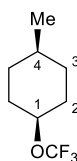
cis-3-(Trifluoromethyl)cyclohexan-1-ol *cis* 2-73
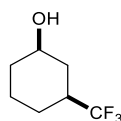
The reaction was carried out according to the standard procedure for CF$_3$ aryl hydrogenation, and a colourless oil (108 mg) was obtained in 64 % yield with d:r ratio 2:1; only peaks of the major product are listed.

^{1}H NMR (500 MHz, Chloroform-d) δ 4.27 – 4.08 (m, 1H, C$\underline{H}$OH), 2.52 (dtd, J = 12.3, 8.9, 3.6 Hz, 1H, CHCF$_3$), 2.26 – 1.64 (m, 8H). ^{19}F NMR (470 MHz, Chloroform-d) δ -73.67

4-*cis*-Trifluoromethyl-cyclohexan-1-ol *cis- 2-70*
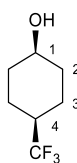
Compound **2-70** could also be obtained by the direct hydrogenation of 4-trifluoromethyl-phenol, columned chromatography was performed by flushing with DCM, and this gave a colourless solid (107 mg), 85 % yield, 3:1 *d.r.* ratio. 48-50°C m.p.

^{1}H NMR (400 MHz, Chloroform-d) δ 4.08 (t, J = 3.2 Hz, 1H, H-1), 2.03 (m, 1H, 4-H), 1.91 – 1.83 (m, 2H, H-2), 1.82 – 1.65 (m, 4H, H-4), 1.60 – 1.48 (m, 2H, H-2). ^{19}F NMR (377 MHz, Chloroform-d) δ -73.62 (d, J = 8.4 Hz). ^{13}C NMR (176 MHz, Chloroform-d) δ 126.9, (CF$_3$, by ^{1}H-^{13}C HMBC),

65.1 (C-1), 41.4 (q, *J* = 26.6 Hz, C-4), 31.4, 19.0.

Mass: Exp. Value 168.0762 GC/MS EI+, theoretical value: 168.0763

4-*trans*-Trifluoromethyl-cyclohexan-1-ol *trans*- 2-70
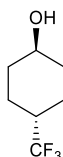
The reaction was carried out according to the standard procedure for CF_3 aryl hydrogenation; (36 mg), 85 % total yield. 3:**1**

Compound ***trans* 2-70** was isolated as the side product of preparation of ***cis*- 2-70**

^{1}H NMR (500 MHz, Chloroform-*d*) δ 3.62 (tt, *J* = 10.6, 4.3 Hz, 1H), 2.15 – 2.05 (m, 2H), 2.00 (dq, *J* = 13.0, 2.7 Hz, 3H), 1.47 – 1.35 (m, 2H), 1.33 – 1.24 (m, 2H). ^{19}F NMR (470 MHz, Chloroform-*d*) δ -73.34. ^{13}C NMR (176 MHz, Chloroform-*d*) δ 127.6 (q, *J* = 278.7 Hz), 69.8, 53.5, 41.0 (q, *J* = 26.7 Hz), 33.9, 23.4. Mass: GC/MS EI+ Observed 168.0762 calculated:168.0762.

All-*cis*-3,5-bis(trifluoromethyl)cyclohexan-1-ol 2-75
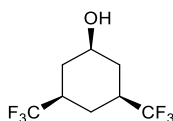
The reaction was carried out according to the standard procedure for CF_3 aryl hydrogenation, a colourless solid (205 mg) was obtained after column chromatography from DCM, m.p. 66-68 °C, 87 % yield.

^{1}H NMR (300 MHz, Methanol-*d*₄) δ 4.88 (d, *J* = 3.8 Hz, 2H), 3.67 (tt, *J* = 11.2, 4.3 Hz, 1H), 2.41 (dh, *J* = 16.1, 4.2 Hz, 2H), 2.25 – 2.10 (m, 2H), 2.09 – 1.98 (m, 1H), 1.45 – 1.06 (m, 4H).^{19}F NMR

(282 MHz, MeOD) δ -75.20. HRMS Calculated 235.0563[M-H] Observed -p [M-H] 235.0562

7.2.5 Hydorgenation of trifluoromethoxyl benzene

**cis-4-(Trifluoromethoxyl)cyclohexanol *tert*-butyldimethylsilyl ether 2-79**

The reaction was carried out according to the standard procedure for CF$_3$ aryl hydrogenation. A colourless oil (150 mg) with 50 % yield obtained. 4:1 d.r. **Cis 2-79** (120 mg) was obtained. **Trans 2-79 (**30 mg) was obtained as side product.

^{1}H NMR (500 MHz, Chloroform-*d*) δ 4.22 (td, *J* = 8.6, 4.3 Hz, 1H, H-4), 3.80 (dt, *J* = 5.9, 2.9 Hz, 1H, H-1), 1.96 (ddt, *J* = 12.7, 8.4, 4.9 Hz, 2H, H$_{eq}$-2), 1.71 (ddd, *J* = 10.6, 8.1, 4.7 Hz, 4H, H$_{ax}$-2, H$_{eq}$-3), 1.58 – 1.43 (m, 2H, H$_{ax}$-3), 0.89 (s, 9H, Si^{t}Bu), 0.04 (s, 6H, SiMe$_2$). ^{13}C NMR (126 MHz, Chloroform-*d*) δ 121.9 (q, *J* = 253.7 Hz, CF$_3$), 76.5 (C-4), 66.6 (C-1), 31.2 (C-4), 27.7 (C-1), 25.9 (C(CH$_3$)$_3$), 18.2 (C(CH$_3$)$_3$), -4.7 (SiMe$_2$).^{19}F NMR (470 MHz, Chloroform-*d*) δ -57.7. The experiment of NOE shows a weak correlation between H-1 and H-4 suggesting the *cis*-conformation of the products.

TOF MS ASAP+: *m/z* calculated for [M+H] 299.1654, [M+2H] 300.1678, [M+3H] 301.1649; found 299.1652, 300.1675, 301.1649.

cis-1-Methyl-4-(trifluoromethoxy)cyclohexane *cis* 2-84

The reaction was carried out according to the standard procedure for CF$_3$ aryl hydrogenation, the reaction ran to full conversion. However, the volatile product could not be separated from the solvent residue. Conversion recorded from diagnostic signal of Ar-H and tertiary Alkyl-H.

^{1}H NMR (500 MHz, Chloroform-*d*) δ 4.49 (tt, *J* = 4.5, 2.7 Hz, 1H, H-1), 1.98 (m, 2H, H-2). ^{19}F NMR (471 MHz, Chloroform-*d*) δ -57.84.

cis 1-(Trifluoromethoxy)-4-(trifluoromethyl)cyclohexane *cis*- 2-86
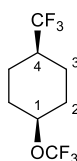
The reaction was carried out according to the standard procedure for CF$_3$ aryl hydrogenation, 55 % yield (135 mg) obtained as a colourless oil. *Trans* and *cis* product could not be separated by column chromatography. Only major peaks were reported.

^{1}H NMR (700 MHz, Chloroform-*d*) δ 4.49, (s, 1H, H-COCF3) δ 1.99(m, 2H, axial H2) δ 1.55(m, 5 H, 4H of 2,3 and 1 H of 4) δ 1.33 (2H of H2) ^{19}F NMR (659 MHz, Chloroform-*d*) δ -57.74. ^{13}C NMR (176 MHz, Chloroform-*d*) δ 122.6, 121.1, 75.1, 32.4, 30.4, 28.6.

Methyl *cis*-4-(trifluoromethoxy)cyclohexane-1-carboxylate *cis*-2-89
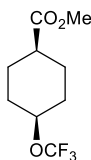
The reaction was carried out according to the standard procedure for CF$_3$ aryl hydrogenation and a colourless liquid (139 mg) was obtained, 61 %.

^{1}H NMR (500 MHz, Chloroform-*d*) δ 4.45 (dt, *J* = 5.2, 2.3 Hz, 1H), 2.55 − 2.38 (m, 1H), 1.96

(dddd, *J* = 24.3, 14.0, 9.9, 4.2 Hz, 4H), 1.82 – 1.76 (m, 2H), 1.72 – 1.62 (m, 2H). ^{19}F NMR (470 MHz, Chloroform-*d*) δ -57.96. ^{13}C NMR (126 MHz, Chloroform-*d*) δ 175.3, 122.7, 74.4, 51.7, 41.1, 29.8, 23.3.

EI Accu found [226.0806] cal [226.0811]

trans-4-Ethyl-4''-_cis_-(trifluoromethoxy)-1,1':4',1''-_trans_-tercyclohexane 2-93
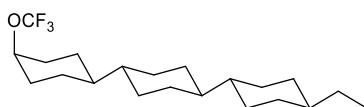
Compound **2-93** was isolated by very long column chromatography with pentane, as a white volatile solid (144 mg), 40 % yield, m.p. 150-154 °C.

^{1}H NMR (500 MHz, Chloroform-*d*) δ 4.50 (s, 1H), 1.99 (d, *J* = 13.0 Hz, 2H), 1.74 (dt, *J* = 24.2, 10.2 Hz, 8H), 1.49 (s, 1H), 1.47 – 1.38 (m, 2H), 1.32 (q, *J* = 7.3 Hz, 3H), 1.22 – 0.79 (m, 18H). ^{19}F NMR (470 MHz, Chloroform-*d*) δ -57.65. ^{13}C NMR (126 MHz, Chloroform-*d*) δ 75.3, 23.8, 20.1, 39.9, 30.3, 14.4, 22.6, 33.6.

tert-Butyl (_cis_-2-(trifluoromethoxy)cyclohexyl)carbamate 2-91
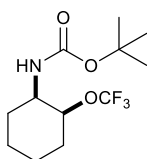
Compound **2-91** obtained with 4 Å MS was purified as a white solid. yield<10 %, 78 °C m.p.

^{1}H NMR (500 MHz, Chloroform-*d*) δ 4.45 (s, 1H), 3.48 (s, 1H), 2.44 – 2.13 (m, 2H), 1.97 – 1.84 (m, 3H),1.47 (s, 9H) 1.32 – 0.91 (m, 3H). ^{19}F NMR (470 MHz, Chloroform-*d*) δ -73.72. ^{13}C NMR (126 MHz, Chloroform-*d*) δ 129.5, 127.2 (q, J =281 Hz), 79.4, 48.6, 32.7, 32.1, 29.8, 29.3, 24.1, FTMS, +P, observed [M]283.2643, calculated 283.1695.

7.3 Chapter 3

Hexa-iodobenzene 3-27
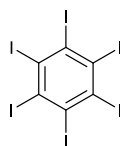
The reaction was conducted according to a literature conditions. [8] Sublimed iodine was used for the reaction. The scaling up of the reaction resulted a low yield and an inseparable impurity. NMP (10 ml) and H_2O (0.5-1 ml) was used for recrystallisation of the crude product on a small scale batch (100 mg) and offered orange fine powder (1.9 g). Literature melting point, decomposition from 385 to 420 ^oC. Found decomposition temperature from 380 - 395 ^oC. Yield 46.9 %. ^{13}C NMR (126 MHz, DMSO) δ 121.8. TOF MS EI+: *m/z* [M]$^+$ calculated for 833.4268; found in 833.4282.

Hexakis(trifluoromethyl)benzene 3-26
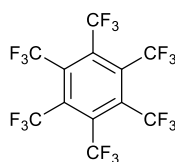
The reaction was conducted was carried out according to a scaling down reaction procedure from the literature.[9] and white crystal was obtained after distillation, extraction and recrystallisation in 19 % yield. ^{19}F NMR (377 MHz, Chloroform-*d*) δ -51.7 in agreement reported value. M.p. reported 210-220 ^oC in a sealed capillary, observed sublimation at 200.5 to 201.2 ^oC in an open capillary.

FTMS +p APCI, ASAP: *m/z* calculated for [M]$^+$ 485.9713, [M-F]$^+$ 466.9729, observed 466.9718.

Penta(trifluoromethyl)phenol 3-28
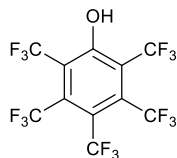
The product was obtained the side product during the preparation of **3-26**. The remaining residue after evaporation was extracted with diethyl ether, dried over MgSO$_4$, filtered over a silica pad and sublimed over H$_2$SO$_4$ to afford compound **3-28**. as a white powder. Yield 15 %.

^{19}F NMR (377 MHz, Methanol-d_4) δ -51.08 (hept, J = 17.5 Hz), -53.79 (hept, J = 17.1 Hz), -59.01 (q, J = 17.0 Hz).

All-*cis*-1,3,5-tris(trifluoromethyl)cyclohexane 3-13
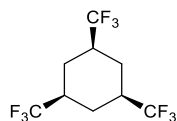
The reaction was carried out according to the general procedure of substrate (1 g) with silica (10 g). The reaction mixture was subjected to column on pentane directly after the reaction. A white solid, sublimation and condensation at room temperature and slowly at -20 °C affording transparent needle crystals (630 mg), yield 60 %. M.p. 45-47 °C (accomplished with sublimation).

^{1}H NMR (500 MHz, Chloroform-d) δ 2.24 (m, 6H, J=11.58/3.35 (t) with 19F decoupling), 1.40 (q, J = 12.7 Hz, 3H). ^{19}F NMR (470 MHz, Chloroform-d) δ -73.86 (d, J = 7.4 Hz). ^{13}C NMR (126 MHz, Chloroform-d) δ 126.4 (q, J = 278.4 Hz), 39.9 (q, J = 28.3 Hz), 24.6 – 21.1 (m).

All-*cis*-1,2,4,5-Tetrakis(trifluoromethyl)cyclohexane 3-15
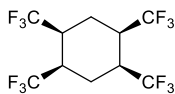
The reaction was carried out according to the general procedure with 450 mg of silica. Reaction mixture was dried and subjected to column directly, 10 % EtOAc/hexane. The white solid (214 mg) was washed with cooled pentane and then recrystallised in hot pentane/DCM. 60 % yield.

^{1}H NMR (700 MHz, Chloroform-*d*) δ 2.72 (br., 4H, HCCF$_3$), 2.40 (dt, *J* = 14.9, 8.7 Hz, 2H, H$_{eq}$-CH$_2$), 2.10 (dt, *J* = 15.1, 5.5 Hz, 2H, H$_{ax}$-CH$_2$). ^{13}C NMR (176 MHz, Chloroform-*d*) δ 125.5 (q, *J* = 280.5 Hz, CF$_3$), 38.2 (q, *J* = 32.3 Hz, CCF$_3$), 20.3 (CH$_2$). ^{19}F NMR (377 MHz, Chloroform-*d*, r.t.) δ -66.9. ^{19}F NMR (470 MHz, CD$_2$Cl$_2$, -75 °C) δ -62.3, -69.8. White needle, m. p. 72.4 °C to 72.6 °C. CI -p full mass: *m/z* calculated for [M-H]$^-$ 355.0362 found 355.0192.

All-*cis* 1,2,3,4,5,6-Hexakis-(trifluoromethyl)cyclohexane 3-30
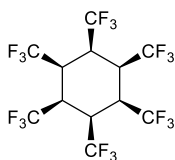
Oven-dried silica gel (7 eq, 210 mg), hexakis-(trifluoromethyl) benzene **3-26** (0.5 mmol, 243 mg) and Rh(CAAC)(COD)Cl (20% mmol, 57 mg) were charged to an oven-dried glass microwave tube (50 ml) equipped with a magnetic stirring bar. The glass vial was placed in a high-pressure stainless-steel autoclave under argon with an open cap and then hexane (20 ml) was injected into the reaction mixture. The autoclave was pressurized and depressurized with hydrogen gas three times and then the pressure was charged to 60 bar from a master cylinder of hydrogen (200 bar). The autoclave containing the reaction was placed in a stirred oil bath at 60 °C for 2 weeks. At the end of this time the autoclave was then depressurized

slowly and carefully.

The crude reaction mixtures containing silica gel was filtered, washed with pentane (5 column volumes), 5% diethyl ether (10 column volumes), 10% diethyl ether (10 column volumes), and then DCM. The contents of each fractions were analysed by $^{19}F\{^{1}H\}$ NMR and clean fractions were isolated and the solvent was removed at reduced pressure to leave the product residue (13 %, 31 mg).

$^{1}H\{^{19}F\}$ NMR (500 MHz, Methylene Chloride-d_2) δ 3.65 (t, J = 5.3 Hz, 3H equatorial H), 2.82 (t, J = 5.3 Hz, 3H, axial H). ^{19}F NMR (470 MHz, CD$_2$Cl$_2$) δ -59.33, -64.37. ^{13}C (37.00 C- CF$_3$ eq , 46.44 C-CF$_3$ ax, 123.25-CF$_3$ by HSQC and HMBC, ESI: 526.9864 [M+Cl]$^-$.

All-*cis*-1,2,3,4,5-pentakis(trifluoromethyl)-6-fluoromethyl-cyclohexane 3-31
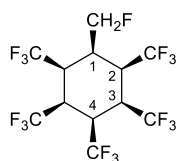
Compound **3-31** was isolated as the major product of reaction during the preparation of compound **3-30**. A pale white solid (42 mg) was obtained in 40 % yield. $^{1}H\{^{19}F\}$ NMR (500 MHz, Acetone-d_6) δ 4.83 (dd, J = 46.7, 4.5 Hz, 2H, CH$_2$F), 3.92 (ddt, J = 15.4, 10.3, 5.1 Hz, 2H, H-3), 3.75 (tt, J = 9.9, 5.0 Hz, 1H,H-4), 3.66 (qt, J = 10.0, 5.1 Hz, 2H, H-2), 3.26 (dp, J = 29.2, 4.6 Hz, 1H,H-1). $^{19}F\{^{1}H\}$ NMR (377 MHz, Acetone) δ -59.09, -64.40, -65.45, -210.01.) ^{13}C NMR: 78.82 CH$_2$F, 44.72 C-2, 44.28 C-4, 36.45 C-3, 33.28 C-1. ESI 491.0065 [M+Cl]$^-$

**All-*cis*-1,2,3,4,5-pentakis(trifluoromethyl)-phenol 3-34**
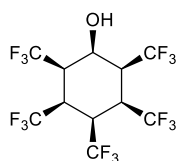
The reaction was carried out using the the same aryl hydrogenation conditions used for the preparation **3-30** with substrate **3-28**. The product was submitted to column chromatography for purification, hexane (10CV) followed by DCM to 2% MeOH in DCM. ^{1}H NMR (700 MHz, Chloroform-*d*) δ 4.33 (t, *J* = 6.7 Hz, 2H), 4.11 (d, *J* = 6.5 Hz, 1H), 3.77 (s, 1H), 2.79 (t, *J* = 8.3 Hz, 2H). ^{19}F NMR (470 MHz, Chloroform-*d*) δ -59.39, -68.08, -70.23.

Experimental (VT-^{19}F-NMR) determination of ring inversion barrier for 3-15

^{19}F-NMR spectra in MeOD were recorded on a Bruker AVANCE 500MHz spectrometer equipped with a 5mm QNP-probe across the temperature range 196 – 240 K. Complete line shape analysis was carried out using the Bruker TopSpin D-NMR module.

T	k	1/T	ln(k/T)
196.0	172.14	0.0051	-0.1298
201.3	283.54	0.0050	0.342341
206.6	472.24	0.0048	0.826551
211.9	790.37	0.0047	1.316433
217.2	1296.66	0.0046	1.786637
222.6	2029.00	0.0045	2.209877
228.1	3020.82	0.0044	2.583631
233.1	4083.90	0.0043	2.863555
238.1	5849.45	0.0042	3.201412

Table 7-3-1 Temperature dependence of the rate constant of the ring interconversion for cyclohexane **3-15**
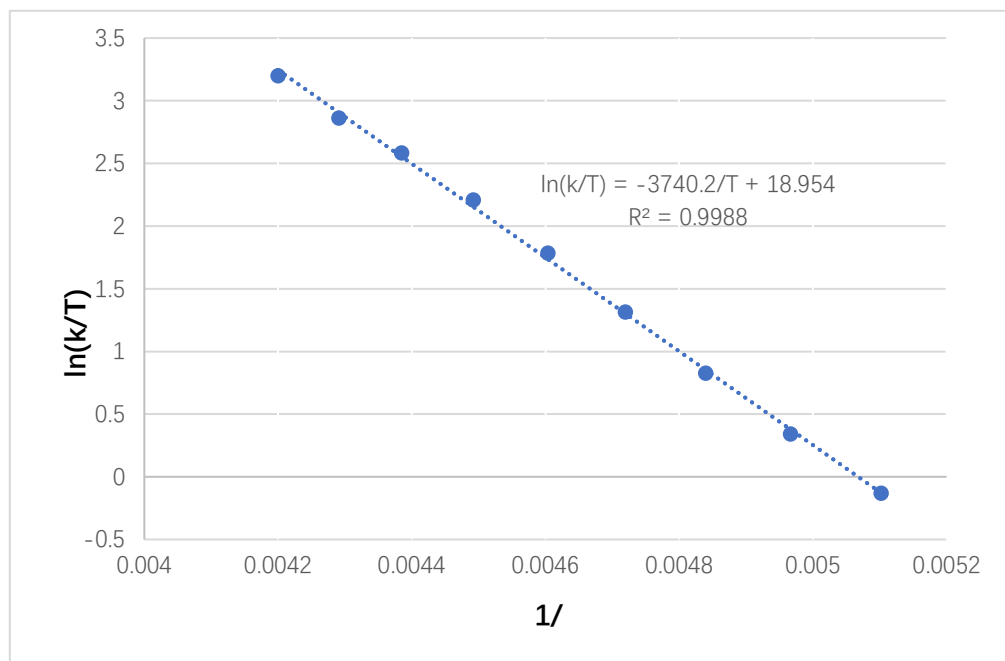
Figure 7-3-1 Fitting experimental data to the Erying equation provided the following parameters for ring interconversion;

$\Delta H = 31.1 \pm 0.4$ kJmol^{-1} $= 7.4 \pm 0.1$ kcal mol^{-1}

$\Delta S = -0.040 \pm 0.002$ kJ mol^{-1} $= -0.0096 \pm 0.0004$ kcal mol^{-1}

$\Delta G_{298} = 43.0 \pm 1.0$ kJ mol^{-1} $= 10.3 \pm 0.2$ kcal mol^{-1}

Halide ion and acetone titrations with cyclohexane 3-30

Titrations of halide ion; F$^-$ (from TBAF, tetrabutylammonium fluoride), Cl$^-$ (from TBACl, tetrabutylammonium chloride), I$^-$ (from TBAI, tetrabutylammonium iodide), and acetone were conducted. Binding affinities for chloride and iodide were calculated using the Bindfit[ia] software; (http://app.supramolecular.org/bindfit/ see P. Thordarson, *Chem. Soc. Rev.*, **2011**, *40*, 1305 -1323)

All experiments were performed with a 500MHz NMR instrument at r.t.. H$_{ax}$ and H$_{eq}$ represent the signals for the axial and equatorial protons for compound **3-30**. H$_{NCH}$ represents the N(C$\underline{H}_2$CH$_2$CH$_2$CH$_3$)$_4$ proton of the tetrabutylammonium group. Compound **3-30** is designated as the *host* molecule in each titration.

7.4 Chapter 4

7.4.1 General procedure for hydrogenation in chapter 4

Fluoroarene substrate (1 mmol), oven dried silica (450 mg)/ 4Å MS (1g, for amino acids), Rhodium CAAC catalyst (1 mol %) and dry hexane (10 ml) were added under argon to a 100 ml glass tube vessel. The reaction vessel was placed in a 150 ml stainless steel autoclave. The autoclave was pressurised and de-pressurised with 5 bar hydrogen three times before being chargedd to 50 bar of hydrogen. The reaction mixture was stirred at room temperature for 24 h, or 72 h for amino acids, after which the autoclave was de-pressurised. The reaction mixture was flushed with DCM, acetone or methanol onto silica, dried and submitted to column chromatography.

All-*cis*-hexafluorocyclohexane 4-3
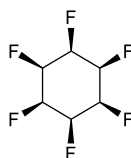
The cyclohexane **4-3**, (also refer to **1-71**, **3-9**, **5-1**, and **6-1**), was prepared using the standard procedure for aryl hydrogenation with silica. Reaction was purified by column chromatography, (Acetone/DCM; TLC on 5 % MeOH, DCM). Product obtained as a white solid (183 mg). 95 % yield, m. p. 214-216 °C.

^{1}H NMR (500 MHz, Acetone-d_6) δ 5.41 (br, 1H), 5.08 (br, 1H). ^{19}F NMR (470 MHz, Acetone) δ -214.08, -218.13. The NMR data is matching with literature values.[10]

Perdeuterated-all-*cis*-hexafluorocyclohexane 4-3D
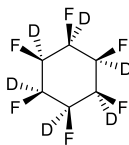
4-3-D

Compound **4-3-D** was prepared by aryl hydrogenation with modification: 2 mmol % of catalyst. Silica. (7eq), hexane (7 ml per mmol), Deuiterium (5 bar), 3 days, r.t. Reaction was performed on a 2 mmol scale, was purified by column chromatography, (Acetone/DCM; TLC on 5 % MeOH, DCM) Product obtained as a white solid (277 mg). 70 % yield. ^{2}H NMR (77 MHz, None) δ 5.23. ^{19}F NMR (470 MHz, Acetone) δ -215.05, -219.46. The NMR data is similar with reported date of its isotope analogue **4-3**. Isotope patter was observed on ^{19}F NMR caused by presence of ^{1}H impurity.

tert-Butyl (perfluorophenyl)carbamate 4-28
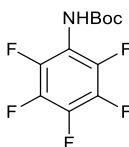
To an ice cold solution of pentalfluoroaniline **4-26** (183 mg, 1 mmol) in anhydrous THF (15 mL), NaH (60 ww%, 1.1 eq) was added slowly. The reaction mixture was stirred for 30 minutes, after which Boc$_2$O (1.5 eq.) was added slowly. The reaction was allowed to warm to room temperature. The reaction crude product was quenched with water, extracted with EtOAc, concentrated *in vacuo* and submitted to column for purification. Product was obtained as a yellow solid, the colour could be removed upon further purification by column to afford a pale white solid (82 mg), yield 30 %. m.p. 80-81 °C.

^{1}H NMR (400 MHz, Chloroform-*d*) *d* 1.47 (s, 1H); ^{19}F {^{1}H} NMR (376 MHz, Chloroform-*d*) *d* -145.8(2F), -154.49 (1F), -162.90 (2F). HRMS (EI, +P) calculated for [M+H] 284.0718, found

284.0726.

tert-Butyl ((perfluorophenyl)methyl)carbamate 4-31
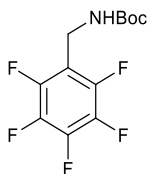
To an ice cold solution of pentalfluoromethylamine (200 mg, 1 mmol) in anhydrous THF (30 mL) , NaH (60 ww%, 1.1 eq.) wad added slowly. The reaction mixture was stirred for 30 minutes, after which Boc_2O (1.5 eq.) was added slowly. The reaction was allowed to warm to room temperature. The reaction was quenched with water, extracted with EtOAc, concentrated *in vacuo* and submitted to column for purification. Product was obtained as a white solid 110 mg, yield 37 %.

^{1}H NMR (500 MHz, Chloroform-*d*) δ 4.96 (s, 1H), 4.47 − 4.18 (m, 2H), 1.43 (d, *J* = 2.1 Hz, 11H).^{19}F NMR (471 MHz, Chloroform-*d*) δ -143.23, -154.97, -161.81.^{13}C NMR (126 MHz, Chloroform-*d*) δ 155.2, 145.2 (d, *J* = 253.6 Hz), 140.8 (d, *J* = 248.2 Hz), 137.5 (d, *J* = 252.6 Hz), 112.4, 105.4, 80.3, 32.5, 28.3.

N-(Perfluorophenyl)acetamide 4-30
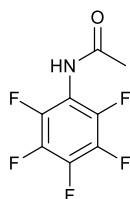
To an ice-cold solution of pentalfluoroaniline (300 mg, 1.6 mmol) in anhydrous THF (30 mL), NaH (60 ww%, 1.1 eq) were added slowly. The reaction mixture was stirred for 30 minutes, after which acetyl chloride (1.5 eq.) was added slowly. The reaction was allowed to warm to room temperature. The reaction crude product was quenched with water, extracted with EtOAc, concentrated *in vacuo* and submitted to column for purification. Product was obtained

as a yellow solid , 80 % yield.

^{1}H NMR (500 MHz, Chloroform-*d*) δ 2.37 (s, 3H).^{13}C NMR (126 MHz, Chloroform-*d*) δ 171.2, 144.4 (d, *J* = 227.3 Hz), 142.4 (d, *J* = 225.3 Hz), 138.4 (d, *J* = 253.8 Hz), 114.5, 26.1.^{19}F NMR (470 MHz, Chloroform-*d*) δ -142.80 – -145.56 (m), -150.89, -160.41 (dd, *J* = 20.9, 16.2 Hz).

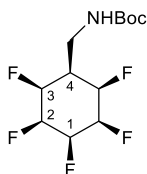**tert-Butyl (all-*cis*-2,3,4,5,6-pentafluorocyclohexyl)carbamate 4-32**
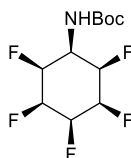
Compound **4-32** was prepared using the standard procedure for fluoro aryl hydrogenation. 4 Å MS, 72 h. Reaction was purified by column chromatography, (Acetone/DCM) Product obtained as a white solid (28 mg), 27 % yield, 170-172 °C m.p.

^{1}H NMR (500 MHz, Chloroform-*d*) δ 5.59 (s, 1H), 5.32 (d, *J* = 52.3 Hz, 1H), 5.01 (d, *J* = 49.6 Hz, 2H), 4.52 (dt, *J* = 41.8, 26.2 Hz, 2H), 3.94 (td, *J* = 30.8, 7.3 Hz, 1H), 1.47 (s, 9H).

^{19}F NMR (470 MHz, Chloroform-*d*) δ -207.88, -213.87, -213.93, -216.96. HRMS (EI, +p) *m/z* calculated for [M+Na]+ 312.1012, found 312.0999.

tert-Butyl (2-(all-*cis*-2,3,4,5,6-pentafluorocyclohexyl)ethyl)carbamate 4-34

Compound **4-34** was prepared using the standard procedure for fluoro aryl hydrogenation. 4 Å MS, 72 h. Reaction was purified by column chromatography, (Acetone/DCM) Product

obtained a white solid. 13 mg, 26 % yield, 182-184°C m.p. [2M+Na] found 629.2415 calculated 629.2413

^{1}H NMR (500 MHz, Acetone-d_6) δ 6.48 (s, 1H, NH), 5.43 (d, J = 53.8 Hz, 1H, H-1), 5.27 − 4.71 (m, 4H, H-2,H3), 3.51 (t, J = 6.6 Hz, 2H, CH2), 2.39 − 2.20 (m, 1H, H-4), 1.42 (s, 9H, Boc).
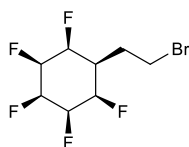
^{19}F NMR (471 MHz, Acetone) δ -205.25, -205.33, -212.91, -217.43.

^{13}C NMR (126 MHz, Acetone) δ 156.6, 87.6 (d, J= 204.8), 86.5 (d, J = 165.8), 86.2 (d, J= 192.5)77.9, 38.3, 37.3, 27.6

7.4.2 MacMillan photoredox cross coupling

General procedure for Macmillan photocoupling

Alkyl bromide: For the synthesis of alkyl bromide compound **4-39**, refer to Chapter 7.6.

To a 10 ml microwave vial with a stir bar, was added photo-catalyst Ir[dF(CF$_3$)ppy]$_2$(dtbbpy)PF$_6$ (0.01 equiv. 0.7 mg), alkyl bromide **4-39** (0.094 mmol, 1.5 eq.), aryl bromide (0.062 mmol, 1 eq.) tris(trimethylsilyl)silane (0.06 mmol, 1.0 equiv), and anhydrous sodium carbonate (20 mg, 0.2 mmol , 4 equiv.). The vial was sealed and placed under nitrogen before 5 mL of DME was added. To a separate vial was added NiCl$_2$•glyme (0.05 equiv.) and 4,4'-di-*tert*-butyl-2,2'-bipyridine (0.05 equiv). The catalyst vial was sealed, purged with nitrogen then 1 mL of DME was added. The Ni catalyst solution was sonicated for 5 minutes, after which, 0.1 mL of the solution (0.005 equv.) was syringed into the reaction vessel. The solution was degassed by

bubbling with nitrogen while stirring for 10 minutes before the LED was turned on. The reaction was stirred and irradiated with a 34 W blue LED lamp (in a photo chemical reaction box equipped with a fan) for 6 hours. The reaction was quenched by exposure to air and submitted to column directly after reaction.
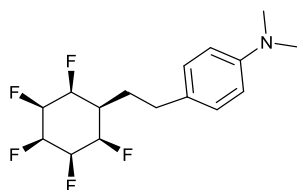
1-(4-Ethylcyclohexyl)-4-(2-((all-*cis*-2,3,4,5,6-pentafluorocyclohexyl)ethyl)benzene 4-40
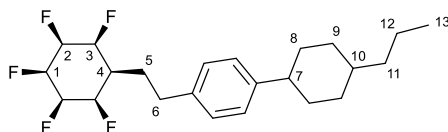
The reaction was conducted as described the general procedure for photoredox cross coupling. Product was purified by column chromatography with EtOAc:PE to a afford white crystalline product (61 mg) in 70 % yield. M.P. 222 °C.

^{1}H NMR (700 MHz, Acetone-d_6) δ 7.19 (m, 4H, Ar-H), 5.40 (d, *J* = 54.1 Hz, 1H, H-1), 5.12 (d, *J* = 50.1 Hz, 2H, H-3), 5.01 – 4.72 (m, 2H, H-2), 2.80 (t, J=7.56 Hz, 2H, H-5) 2.47 (tt, *J* = 12.1, 3.4 Hz, 1H, H-7), 2.19 – 2.10 (m, 2H, H-6), 1.87 (td, *J* = 13.9, 3.3 Hz, 4H, H11,H8,H9), 1.49 (qd, *J* = 13.4, 12.8, 3.8 Hz, 2H, H-8), 1.37, (m, 2H, H9), 1.26 – 1.20 (m, 2H, H11), 1.09 (td, *J* = 12.2, 11.7, 3.2 Hz, 2H, H-12), 0.91 (t, *J* = 7.3 Hz, 3H, H-13,).^{19}F NMR (659 MHz, Acetone) δ -204.89, -212.96, -217.42.^{13}C NMR (176 MHz, Acetone) δ 128.2, 126.8, 87.2, 44.1, 39.6, 36.9, 34.3, 33.5, 31.8, 27.7, 19.8, 13.8. FTMS +P [M+Na] obs. 425.2233 cal 425.2244.
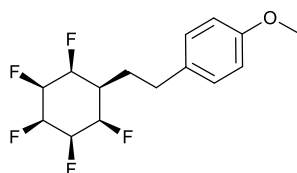
***N,N*-Dimethyl-4-(2-((all-*cis*-)-2,3,4,5,6-pentafluorocyclohexyl)ethyl)aniline 4-42**
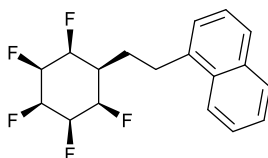

285

The reaction was carried out according to the general procedure for photoredox cross coupling. Product was obtained by purification on column chromatography (1% NEt$_3$, 5 % acetone, DCM), as a brown solid (8 mg yield), 25 %. ^{1}H NMR (500 MHz, Acetone-d_6) δ 7.33 – 7.05 (m, 4H), 5.40 (d, J = 53.3 Hz, 1H), 5.06 (d, J = 51.2 Hz, 3H), 4.88 (dd, J = 40.5, 28.3 Hz, 2H),2.10 (s, 6H) 1.88 (d, J = 7.1 Hz, 2H), 1.60 (p, J = 3.9 Hz, 2H).^{19}F NMR (470 MHz, Acetone) δ -204.89, -213.00, -217.46. TOF ESI +P cal. 321.1516 found 321.1595.

1-Methoxy-4-(2-((all-*cis*-)-2,3,4,5,6-pentafluorocyclohexyl)ethyl)benzene 4-43

The reaction was carried out according to the general procedure for photoredox cross coupling. Product was obtained by purification on column as a white solid (25 mg), 65 % yield. 118 °C m.p.^{1}H NMR (700 MHz, Acetone-d_6) δ 7.23 (dd, J = 39.7, 8.6 Hz, 2H), 6.90 (dd, J = 40.6, 8.6 Hz, 2H), 5.52 – 5.35 (m, 1H), 5.24 – 4.97 (m, 2H), 4.89 (dt, J = 40.8, 27.8 Hz, 2H), 3.79 (d, J = 18.9 Hz, 3H), 2.80 – 2.69 (m, 1H), 2.16 – 2.10 (m, 2H), 2.04 – 1.90 (m, 1H), 1.85 (dd, J = 9.2, 5.8 Hz, 1H), 1.08 (t, J = 7.4 Hz, 1H).^{19}F NMR (659 MHz, Acetone-d_6) δ -204.92, -212.73 – -213.53 (m), -217.43 (ddt, J = 53.0, 38.8, 20.1 Hz). M.p. 134, ESI TOF +p [M+Na] 331.1076 calculated 331.1091.

1-(2-((All-*cis*-)-2,3,4,5,6-Pentafluorocyclohexyl)ethyl)naphthalene 4-44
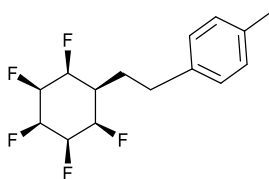

The reaction was carried out according to the general procedure of photoredox cross coupling. The product was isolated as a white solid (15 mg) from column chromatography, (20 % EtOAc),

49 % yield. M.p. 205 °C.

^{1}H NMR (700 MHz, Acetone-d_6) δ 7.86 – 7.13 (m, 8H- ArH), 5.40 (d, J = 54.3 Hz, 1H), 5.13 – 4.97 (m, 2H), 4.97 – 4.77 (m, 2H), 1.91 (s, 1H), 1.85 (dd, J = 9.2, 5.8 Hz, 2H), 1.09 (t, J = 7.4 Hz, 2H).^{19}F NMR (659 MHz, Acetone-d_6) δ -204.92 (d, J = 41.7 Hz, 2F), -213.29 (t, J = 31.3 Hz, 2F), -216.76 – -218.46 (m).

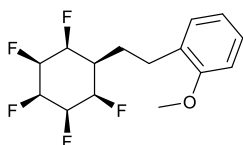**1-Methyl-4-(2-((1r,2R,3R,4s,5S,6S)-2,3,4,5,6-pentafluorocyclohexyl)ethyl)benzene 4-45**

The reaction was carried out according to the general procedure of photoredox cross coupling. Product was isolated as a white power (27 mg), 93 % yield. M.p. 55-59 °C.

^{1}H NMR (700 MHz, Acetone-d_6) δ 7.24 – 7.01 (m, 4H), 5.40 (d, J = 54.1 Hz, 1H), 5.23 – 4.74 (m, 4H), 2.82 – 2.77 (m, 1H), 2.15 – 2.12 (m, 1H), 2.07 (m, 3H), 2.04 – 1.94 (m, 1H), 1.08 (t, J = 7.4 Hz, 2H). ^{19}F NMR (659 MHz, Acetone) δ -204.89, -212.92, -213.29, -217.44. ^{13}C NMR (176 MHz, Acetone) δ 129.06, 128.22, 88.30, 87.31, 86.21, 58.06, 55.95, 37.29, 29.70, 20.10. HRMS EI + Calculated mass for [M] 292.1245. Found mass [M] 292.1233.

1-Methoxy-2-(2-((all-*cis*-)-2,3,4,5,6-pentafluorocyclohexyl)ethyl)benzene 4-46

The reaction was carried out according to the general procedure of photoredox cross coupling. Product was isolated as a white power (25 mg),78 % yield. M.p. 134, ESI TOF +p [M+Na]

331.1076 calculated 331.1091.

^{1}H NMR (700 MHz, Acetone-d_6) δ 7.21 (ddd, J = 12.1, 6.6, 2.0 Hz, 2H), 6.97 (dd, J = 8.1, 1.1 Hz, 1H), 6.90 (s, 1H), 5.40 (d, J = 54.2 Hz, 1H), 5.22 – 5.05 (m, 2H), 5.00 – 4.77 (m, 3H), 3.85 (s, 3H), 2.83 – 2.79 (m, 2H), 2.12 (s, 1H), 1.97 (d, J = 7.5 Hz, 2H), 1.09 (t, J = 7.4 Hz, 1H). ^{19}F NMR (659 MHz, Acetone) δ -204.86, -212.90, -217.42. ^{13}C NMR (176 MHz, Acetone) δ 157.5, 129.7, 129.4, 127.5, 120.5, 110.5, 88.4, 87.3, 86.2, 60.6, 54.8, 54.1, 26.6.

7.4.3 Preparation of CyF₅ amino acid and peptides

General condition for HATU coupling

To a solution of acid (0.5 mmol, 1 eq) in DMF, DIPEA (200 mg, 1. 5 mmol, 3 eq.), HATU (200 mg, 0.52 mmol, 1.04 eq) was added in sequence. The reaction mixture was stirred at room temperature for 15 minutes, after which substrate amine (0.55 mmol) was added. The reaction was stirred at room temperature overnight. After which water was added to reaction, the reaction mixture is extracted with EtOAc (50 ml), three times. (Modification if indicated: reaction could be monitored by TLC and shortened to 4 h; 1.5 eq. of HATU could be used for inactive substrates; 1 eq. of HATU is restricted to difunctional substrate amines; 1 M KOH solution was added to the reaction mixture for work up if a guanidium byproduct was generated; Brine was added during extraction if the organic layer did not separat; DCM could be used for extraction for products with poor solubility). The combined organic phase was dried over Na₂SO₄ and concentrated *in vacuo.* The crude product was purified on column chromatography to afford pure product.

Methyl (*S*)-2-((*tert*-butoxycarbonyl)amino)-3-(perfluorophenyl)propanoate 4-47
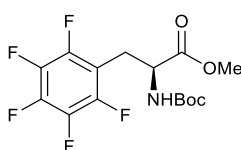
To a solution of (*S*)-2-((*tert*-butoxycarbonyl)amino)-3-(perfluorophenyl)propanoic acid **4-58** (1.00 g, 3.0 mmol, 1.0 equiv.) in a mixture of toluene:methanol (12:12 mL), was added TMS-diazomethane (3.0 mL (2M in hexane), 12.0 mmol, 2.0 equiv.) at 0 °C and stirred at r.t.. Upon completion (approx. 2 hr), the reaction was concentrated *in vacuo* and purified by silica gel column chromatography using 0-10% EtOAc in petroleum ether to afford the product as a white solid (1.02 g, quant.).

^{1}H NMR (400 MHz, Chloroform-*d*) δ 5.13 (br, NH), 4.59 (dd, *J* = 6.9 Hz, 1H, C*H*N), 3.78 (s, 3H, OMe), 3.33 (dd, *J* = 14.1, 5.4 Hz, 1H), 3.05 (dd, *J* = 14.0, 7.2 Hz, 1H), 1.39 (s, 9H). ^{19}F NMR (377 MHz, Chloroform-*d*) δ -142.21 − -142.88 (m, 2F), -155.45 (t, *J* = 20.9 Hz, 1F), -162.30 (td, *J* = 21.7, 8.0 Hz, 2F). ^{13}C NMR (101 MHz, Chloroform-*d*) δ 171.3, 154.8, 145.5 (d, *J* = 237.9 Hz), 137.4 (d, *J* = 249.6 Hz), 121.8 (d, *J* = 165.6 Hz), 110.0, 80.3, 52.8, 52.6, 28.1, 26.1.FTMS [M+Na] 392.0878. Data in accordance with literature.[11]

tert-Butyl (S)-2-((tert-butoxycarbonyl)amino)-3-(perfluorophenyl)propanoate
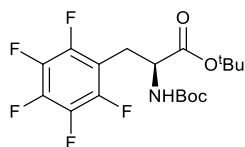
To a solution of Boc-Phe-OH **4-58** (1.112 mmol, 400 mg) in DCM (4 ml) and cyclohexane (8 ml), *tert*-Butyl 2,2,2,-trichloroacetamidate (2 eq, 0.4 ml) was added. The reaction was treated with BF$_3$·H$_2$O (0.02 ml) and stirred overnight. The reaction was quenched with 10 ml NaHCO$_3$ solution. Crude product was submitted to column chromatography to afford pure product as a white solid (242 mg). 59 % yield.

^{1}H NMR (500 MHz, Acetone-*d$_6$*) δ 6.33 (d, *J* = 8.7 Hz, 1H), 4.40 − 4.26 (m, 1H), 3.34 − 3.22 (m, 1H), 3.17 (dd, *J* = 14.1, 9.0 Hz, 1H), 1.46 (s, 7H), 1.37 (s, 7H). ^{19}F NMR (470 MHz, Acetone-*d$_6$*) δ -143.16 − -144.59 (m,2F), -159.50 (t, *J* = 20.4 Hz, 1F), -165.58 (td, *J* = 21.5 8.0 Hz, 2F).

Methyl (S)-2-((tert-butoxycarbonyl)amino)-3-((all-*cis*)-2,3,4,5,6-pentafluorocyclohexyl)propanoate 4-48
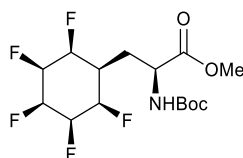
The reaction was carried out according to the general aryl hydrogenation procedure with hexane (5 ml) and 4 Å MS (2 g) per mmol, 72 h, Rh cat. (1 mol %). The product was purified on column with acetone/DCM to afford a white solid product (169 mg), 45 % yield. M.p. 170-172 °C α]$^{20}_{DD}$ = −22.5 (c = 1.0, MeOH); ^{1}H NMR (400 MHz, Methanol-d_4) δ: 5.27 (m, 1H), 5.10-4.50 (m, 5H), 4.30 (dd, J = 10.6, 4.6 Hz, 1H), 3.75 (s, 3H), 2.42 (m, 1H), 2.11 − 1.83 (m, 2H), 1.44 (s, 9H).^{13}C NMR (126 MHz, Methanol-d_4) δ: 172.9 (*C*=O), 156.9 (*C*=O), 89.5-85.2 (5 x *C*HF), 79.5 (*C*), 51.5 (*C*H$_3$), 50.9 (*C*H), 35.3-34.9 (m, 5x *C*HF), 27.8 (*C*H$_2$), 27.2 (3 x *C*H$_3$).^{19}F NMR (376 MHz, Methanol-d_4) δ: -206.1 (m, 2 x CH*F*), -212.4 (m, CH*F*), -214.0 (m, CH*F*), -218.28 (tt, J = 25.6, 10.7 Hz, CH*F*); HRMS (ESI$^+$) C$_{15}$H$_{22}$O$_4$NF$_5$Na [M+Na]$^+$ found 398.1353, requires 398.1361; ν$_{max}$/cm^{-1} 1722 (C=O), 1487 (C-H), 1234 (C-H), 867 (C-F).

(2*S*)-2-((*tert*-Butoxycarbonyl)amino)-3-*cis*-(2,3,4,5,6-pentafluorocyclohexyl)propanoic acid 4-61
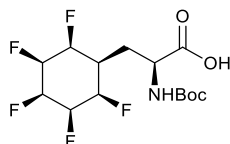

To a solution of compound **4-48** (1 mmol) in THF/H$_2$O (20 ml: 20 ml), LiOH·H$_2$O (2 eq.) was added under 0 °C, after 30 min another LiOH·H$_2$O (1 eq.) was added. The reaction was allowed to warm to r.t. and stirred for maximum 2 h. Upon completion of the reaction, 1 M HCl was

added to the reaction mixture, and the organic layer was separated. The aqueous layer was extracted with EtOAc (50 ml*2). The combined organic layer was dried over Na_2SO_4 and concentrated *in vacuo.* A white solid (343 mg) was obtained, yield 95 %. M.p. >250 °C.

$[\alpha]^{20}_{DD}$ = −13.65 (c = 0.67, MeOH); ^{1}H NMR (400 MHz, Methanol-d_4) δ: 5.27 (m, 1H), 5.114.51 (m, 4H), 4.26 (dd, J = 10.6, 4.5 Hz, 1H), 2.51 – 2.36 (m, 1H), 2.10-1.83 (m, 2H), 1.45 (s, 9H).^{13}C NMR (126 MHz, Methanol-d_4) δ: 175.5 (*C*=O), 158.3 (*C*=O), 90.9-86.7 (m, 5 x *C*HF), 80.8 (*C*), 52.2 (*C*H), 37.02-36.2 (m, *C*H), 29.5 (*C*H$_2$), 28.7 (3 x *C*H$_3$). ^{19}F NMR (377 MHz, Methanol-d_4) δ: -206.1 (m, 2 x CH*F*), -212.5 (m, CH*F*), -214.0 (m, CH*F*), -218.3 (m, CH*F*). HRMS (ESI$^-$) $C_{14}H_{19}O_4NF_5$ [M-H]$^-$ found 360.1242, requires 360.1234; v_{max}/cm^{-1} 1730 (C=O), 1699 (C-O), 1506 (C-C), 1242 (C-O), 796 (C-F).

Methyl (S)-2-amino-3-((all-*cis*)-2,3,4,5,6-pentafluorocyclohexyl)propanoate 4-62
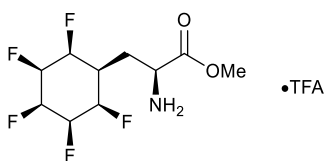
To a solution of **4-48** (1 mmol) in DCM (20 ml), TFA (1 ml) was added dropwise, the reaction was stirred at room temperature overnight, after which the reaction was concentrated *in vacuo*. The TFA was removed by leaving the crude product under high vacuum overnight. The product was used directly into next step without further purification.

^{1}H NMR (500 MHz, Methanol-d_4) δ 5.33 (d, J = 53.5 Hz, 1H), 5.21 – 4.94 (m, 3H), 4.73 (d, J = 35.9 Hz, 2H), 4.25 (s, 1H), 3.89 (s, 3H), 2.35 (m, 2H), 2.18 (t, J = 37.2 Hz, 1H). ^{19}F NMR (470 MHz, Methanol-d_4) δ -76.95 (1.5 F, TFA), -206.34 (2F), -213.33 (1F), -213.87(1F), -218.51(1F).

(S)-2-Amino-3-((all-*cis*)-2,3,4,5,6-pentafluorocyclohexyl)propanoic acid 4-51
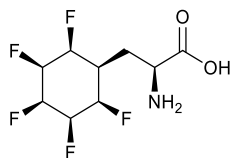
Compound **4-48** (210 mg, 0.56 mmol) was dissolved in 6 M HCl and heated under reflux for 12 hours. The water and HCl was removed *in vacuo*. A yellow solid (145 mg) was obtained as used directly without further purification for next step. Purity >90 %, by ^{19}F NMR. The product was recrystallised in MeOH to afford as a crystalline solid; m.p.> 250 °C);), $[\alpha]^{20}_{DD}$ = +20.7 (c = 0.67, MeOH); ^{1}H NMR (700 MHz, DMSO-d_6) δ: 5.37 (d, *J*= 54.3 Hz, C*H*F), 5.12-4.17 (m, 5H), 4.10 (1H, m, overlap with solvent), (2.30-2.21 ,2H) , ^{13}C NMR (176 MHz, DMSO-d_6) δ 171.0 (*C*OOH), 88.8-85.9 (*C*HF), 49.8 (*C*NH), 34.2 (CH), 27.2 (*C*H$_2$); δ -203.6 (2F), 211.9, -212.8, -216.5; v_{max}/cm^{-1} 1736 (C=O), 1717 (C-O), 1501 (N-H), 1229 (C-H), 1128 (C-O),1049 (C-N), 796 (CF).

(S)-2-((((9H-Fluoren-9-yl)methoxy)carbonyl)amino)-3-((all-*cis*)-2,3,4,5,6-pentafluorocyclohexyl)propanoic acid 4-64
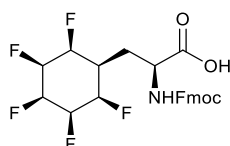
To a solution of amino acid **4-51** (235 mg, 0.9 mmol, 1 eq.) in acetonitrile (15 ml), NEt$_3$ (280 µl, 2 mmol 2 eq.) Fmoc-ONSU (337 mg, 1.1 eq.) was added. The reaction mixture was stirred at room temperature for 3h, after which the reaction was diluted with water. The aqueous layer was washed with diethyl ether, acidified by 2 M HCl and extracted with EtOAc three times. The combined EtOAc fractions were dried over Na$_2$SO$_4$ and concentrated *in vacuo*. The crude product was purified by column chromatography (10 % MeOH, DCM). Recrystallisation in MeOH/DCM is optional to remove trace Fmoc residue. Product would decompose over time, which could still be stored in the fridge over weeks. Pale yellow product (280 mg) was

obtained. Yield 64 %.

^{1}H NMR (500 MHz, Methanol-d_4) δ 7.82 (d, J = 7.5 Hz, 2H), 7.69 (t, J = 8.1 Hz, 2H), 7.41 (t, J = 7.4 Hz, 2H), 7.33 (td, J = 7.5, 1.1 Hz, 2H), 5.30 (d, J = 54.0 Hz, 1H), 5.04 (d, J = 56.0 Hz, 2H), 4.66 (ddd, J = 39.4, 26.2, 10.1 Hz, 2H), 4.43 (dd, J = 10.5, 6.7 Hz, 1H), 4.38 – 4.29 (m, 1H), 4.29 – 4.19 (m, 2H), 2.46 (dq, J = 14.2, 7.6, 5.6 Hz, 1H), 1.98 (t, J = 6.6 Hz, 2H), 1.29 (t, J = 7.3 Hz, 1H), 1.24 (t, J = 7.1 Hz, 1H). ^{19}F NMR (470 MHz, Methanol-d_4) δ -205.49 (dt, J = 42.8, 11.9 Hz), -211.77 – -212.29 (m), -213.39 (td, J = 23.9, 12.3 Hz), -217.70 (tt, J = 24.6, 11.1 Hz). ^{13}C NMR (126 MHz, MeOD) δ 157.2, 144.0, 141.2, 127.5, 126.9, 125.0, 119.7, 89.6, 87.5, 86.0, 66.5, 60.1, 46.4, 38.3, 35.2, 28.7, 25.0, 19.6, 13.2, 7.9.

**tert-Butyl((*S*)-1-(methylamino)-1-oxo-3-((all-*cis*)-2,3,4,5,6-pentafluorocyclohexyl)propan-2-yl)carbamate 4-65**
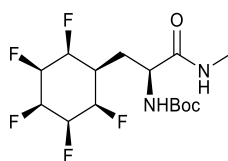
To a solution of Boc protected amino acid **4-61** (200 mg, 0.56 mmol, 1 eq.), DIPEA (290 μL, 1.7 mmol, 3 eq.) and HATU (223 mg, 0.58 mmol) were added in sequence. The reaction mixture was stirred at room temperature for 15 minutes, after which NH$_2$Me (0.6 mmol) was added. The reaction was stirred at room temperature overnight, after which water was added to reaction, and the reaction mixture was extracted with EtOAc (50 ml) three times. The combined organic phase was dried over Na$_2$SO$_4$ and concentrated *in vacuo.* The crude product was purified by column chromatography (10 %acetone/DCM) to afford pure product as a white solid (183 mg was obtained). Yield 87 %. TOF ESI +P Calculated mass of C$_{15}$H$_{24}$F$_5$N$_2$O$_3$ = 375.17016 Found mass = 375.1702.

^{1}H NMR (500 MHz, Acetone-d_6) δ 7.42 (br, 1H, NH), 6.16 (br, J = 8.9 Hz, 1H, NH), 5.41 (d, J = 54.1 Hz, 1H, CHF), 5.20 (d, J = 49.8 Hz, 2H, CHF), 4.95 – 4.71 (m, 2H, CHF), 4.38 – 4.15 (m, 1H,

CHN), 2.75 (d, J = 4.5 Hz, 3H, NMe), 2.44 – 2.23 (m, 1H, CH$_2$), 2.27 – 2.11 (m, 1H, ^{t}CH), 1.97 – 1.75 (m, 1H, CH$_2$), 1.41 (s, , 9 H, Boc). ^{19}F NMR (471 MHz, Acetone-d_6) δ -204.83 (d, J = 41.7 Hz), -205.12 (d, J = 41.4 Hz), -211.62 – -212.27 (m), -212.85 – -213.38 (m), -217.48 (d, J = 29.6 Hz). ^{13}C NMR (126 MHz, Acetone) δ 88.6 (d, J = 192 Hz), 87.6 (d. J = 199 hz) 86.9 (d, J = 204 hz), 86.4 (d, J = 165 Hz, 2 CHF overlapped), 51.6, 29.7, 29.7 (overlapped), 29.1, 27.7, 25.1

(*S*)-2-Amino-*N*-methyl-3-((all-*cis*)-2,3,4,5,6-pentafluorocyclohexyl)propenamide 4-66
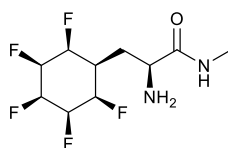
To a solution of Boc protected amino acid **4-65** (100 mg) in DCM (20 ml), TFA (1 ml) was added dropwise. The reaction was stirred at room temperature overnight, after which the DCM and TFA were removed *in vacuo* and dried on high vacuum overnight. The crude product was used in next step without further purification. Near quantitively yield. TOP ESI [M+H] calculated 274.1183 found 275.1173.

^{1}H NMR (500 MHz, Methanol-d_4) δ 5.28 (d, J = 54.2 Hz, 1H), 4.99 (dd, J = 35.4, 17.3 Hz, 2H), 4.77 – 4.54 (m, 2H), 3.44 (dd, J = 8.8, 5.6 Hz, 1H), 2.83 (d, J = 18.4 Hz, 1H), 2.76 (s, 2H), 2.17 (ddd, J = 13.9, 8.3, 6.1 Hz, 1H), 2.11 – 1.93 (m, 1H), 1.88 (dp, J = 14.6, 7.0, 6.3 Hz, 1H), 1.38 (dd, J = 9.0, 5.8 Hz, 1H). ^{19}F NMR (470 MHz, Methanol-d_4) δ -205.95 (dt, J = 23.9, 11.6 Hz), -212.88 (ddd, J = 26.7, 19.6, 10.9 Hz), -213.86 (ddd, J = 30.2, 19.7, 11.0 Hz), -218.26 (td, J = 25.7, 13.2 Hz).

(S)-2,2,3-Trimethyl-5-(((all-*cis*)-2,3,4,5,6- pentafluorocyclohexyl)methyl)imidazolidin-4-one 4-67
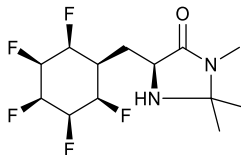
Reaction conditions were adapted from literature.[12] To a solution of amide **4-66** (50 mg, 0.175 mmol), 1 ml MeOH, 0.1 ml acetone, 20 μl triethylamine was added. The reaction was heated reflux overnight. If the reaction not completed, a Soxhelt condensor with 4 Å MS is added. After the reaction completed, the crude reaction mixture was concentrated *in vacuo* and submitted on column (20 % acetone/DCM). Product was isolated as a colourless crystal (36 mg), 65 % yield. TOF EI +P calculated mass of $C_{11}H_{12}F_5N_2O_2$ 299.08135, found mass = 299.1172.

^{1}H NMR (500 MHz, Methanol-d_4) δ 5.30 (d, *J* = 54.1 Hz, 1H), 5.14 – 4.96 (m, 2H), 4.83 – 4.44 (m, 2H), 3.72 (dd, *J* = 9.6, 5.1 Hz, 1H), 2.83 (s, 3H), 2.38 (ddd, *J* = 13.9, 8.4, 5.2 Hz, 1H), 2.29 – 2.03 (m, 1H), 1.86 (ddd, *J* = 15.1, 9.6, 6.2 Hz, 1H), 1.45 (s, 3H), 1.38 (s, 3H). ^{13}C NMR (126 MHz, MeOD) δ 89.2, 87.8, 85.7, 76.2, 55.1, 35.3, 28.7, 26.1, 24.2, 23.4.

Boc-F₅Phe-Phe-Ome 4-68
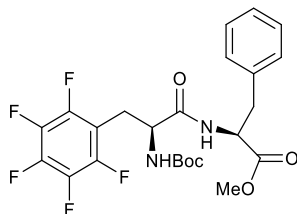
The reaction was carried out according to the standard procedure with Boc-F₅Phe-OH and MeO-Phe-NH₂. The product (300 mg) was obtained from column chromatography (2 % MeOH/DCM). 84 % yield.

<superscript>1</superscript>H NMR (500 MHz, Chloroform-*d*) δ 7.38 – 7.30 (m, 2H), 7.24 – 6.98 (m, 2H), 6.38 (br, 1H), 5.03 (brHz, 1H), 4.87 (dt, *J* = 7.9, 5.9 Hz, 1H), 4.36 (br, 1H), 3.76 (s, 3H), 3.22 (m, 1H), 3.14 (td, *J* = 13.7, 5.9 Hz, 1H), 3.04 – 2.94 (m, 1H), 1.37 (s, 9H).

<superscript>19</superscript>F NMR (470 MHz, Chloroform-*d*) δ -142.47 (dd, *J* = 22.6, 8.3 Hz), -155.73 (t, *J* = 20.9 Hz), -162.21 (td, *J* = 22.3, 8.3 Hz).

Boc-F₅Phe-Val-OMe 4-71
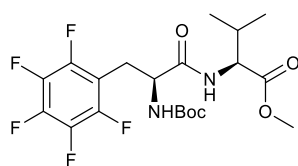
The reaction was carried out according to the standard HATU coupling procedures on a 0.7 mmol scale. White powder (188 mg) product obtained, yield 57 %.

<superscript>1</superscript>H NMR (400 MHz, Chloroform-*d*) δ 6.49 (d, *J* = 8.8 Hz, 1H), 5.17 (d, *J* = 8.9 Hz, 1H), 4.56 (dd, *J* = 8.8, 4.9 Hz, 1H), 4.39 (d, *J* = 6.3 Hz, 1H), 4.14 (q, *J* = 7.2 Hz, 2H), 3.78 (s, 3H), 3.25 (dd, *J* = 14.3, 5.2 Hz, 1H), 3.08 (dd, *J* = 14.3, 8.9 Hz, 1H), 2.33 – 2.13 (m, 1H), 2.05 – 1.98 (m, 2H), 0.94 – 0.85 (m, 6H overlapped with solvent).<superscript>19</superscript>F NMR (377 MHz, Chloroform-*d*) δ -142.41 (dd, *J* = 22.3, 8.2 Hz), -155.73 (t, *J* = 20.8 Hz), -162.19 (t, *J* = 21.9 Hz).

**Boc-CyF₅-Cha-OMe 4-69**
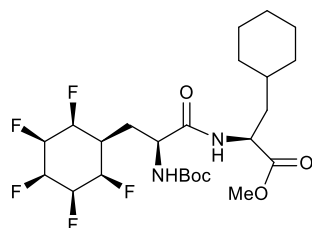
The reaction was carried out according to the standard amino acid hydrogenation conditions

on a 0.19 mmol scale.   White gel (30 mg) was isolated, 30 % yield.

^{1}H NMR (700 MHz, Acetone-d_6) δ 7.76 (d, J = 8.0 Hz, 1H), 6.29 − 6.09 (m, 1H), 5.43 (d, J = 52.8 Hz, 1H), 5.13 (d, J = 50.5 Hz, 2H), 5.02 − 4.74 (m, 3H), 4.56 (ddd, J = 10.3, 8.0, 4.9 Hz, 1H), 4.37 (q, J = 8.0 Hz, 1H), 3.69 (s, , 3H), 2.38 − 2.28 (m, 1H), 2.15 (dt, J = 7.2, 3.6 Hz, 1H), 1.97 (dd, J = 4.5, 2.1 Hz, 1H), 1.82 (d, J = 13.1 Hz, 2H), 1.74 − 1.58 (m, 8H), 1.42 (s, 9H), 1.26 − 1.11 (m, 4H). ^{19}F NMR (659 MHz, Acetone-d_6) δ -204.84 (d, J = 42.1 Hz), -204.94 − -205.25 (m), -212.53 (ddd, J = 52.9, 21.5, 10.3 Hz, 2F), -217.57 (ddt, J = 39.5, 26.9, 13.7 Hz). FTMS +P [M+Na] 551.2509 ,cal. 551.2520

Boc-CyF₅-Val-OMe 4-72
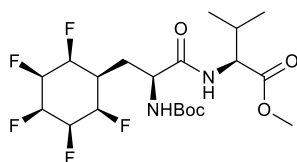
The Reaction was carried out according to the standard hydrogenation conditions at 0.21 mmol. white powder (19 mg) obtained, 20 % yield. ^{1}H NMR (700 MHz, Acetone-d_6) δ 7.75 (d, J = 8.1 Hz, 1H), 6.19 (d, J = 8.5 Hz, 1H), 5.41 (d, J = 53.0 Hz, 1H), 5.11 (d, J = 49.9 Hz, 3H), 5.02 − 4.57 (m, 2H), 4.64 − 4.33 (m, 2H), 3.67 (d, J = 2.4 Hz, 4H), 1.80 (d, J = 13.2 Hz, 2H), 1.30 (overlapped, 9H), 1.2 (overlapped, 6 H). ^{19}F NMR (659 MHz, Acetone-d_6) δ -204.29 (d, J = 40.6 Hz), -204.49 (d, J = 41.4 Hz), -211.97, -217.02.

Boc-Phe-CyF₅-OMe 4-73
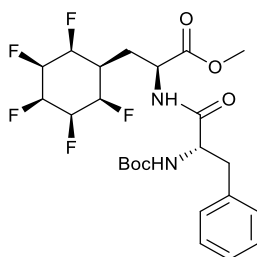
The reaction was carried out according to the standard HATU coupling conditions with MeO-CyF₅-NH₂ **4-62** and Boc-Phe-OH on 0.13 mmol scale. Product was purified by column chromatography (Acetone/DCM). Product (67 mg) was obtained as a pale-yellow gel, with presence of a DMF residue. Yield > 90 %.

^{1}H NMR (700 MHz, Chloroform-d) δ 7.32 (dd, J = 8.1, 6.6 Hz, 2H), 7.27 (t, J = 7.5 Hz, 4H), 7.20 – 7.13 (m, 2H), 6.31 (d, J = 8.0 Hz, 1H), 5.44 – 5.14 (m, 2H), 4.94 – 4.65 (m, 3H), 4.42 (ddd, J = 68.3, 40.6, 27.9 Hz, 2H), 4.05 (s, 1H), 3.15 – 2.97 (m, 2H), 2.65 (td, J = 11.3, 10.6, 6.0 Hz, 1H), 1.91 (t, J = 34.1 Hz, 1H), 1.77 (t, J = 12.5 Hz, 1H).

^{19}F NMR (659 MHz, Chloroform-d) δ -203.61 (dd, J = 77.8, 41.8 Hz), -210.40 – -211.57 (m), -212.78 – -214.01 (m), -216.28 – -217.20 (m).

^{13}C NMR (176 MHz, Chloroform-d) δ 136.1, 129.2, 129.1, 127.5, 86.7, 85.7, 77.0, 53.1, 49.5, 37.5, 36.6, 31.2, 28.4.

Tyr-Phe-CyF₅ 4-76
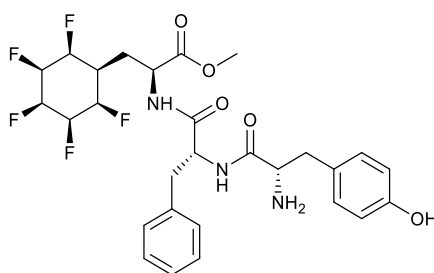
The reaction was conducted following the standard HATU coupling conditions with dipeptide **4-73**. Product was purified on column chromatography, followed Boc deprotection of TFA/DCM overnight. Product was obtained as a colourless oil (100 mg) with a residue of DMF. Conversion >80 %.

^{1}H NMR (500 MHz, Methanol-d_4) δ 7.38 – 7.20 (m, 5H), 7.04 (d, J = 8.5 Hz, 2H), 6.74 (d, J = 8.5

Hz, 2H), 5.30 (d, J = 53.6 Hz, 1H), 4.83 − 4.57 (m, 4H), 4.44 (dd, J = 8.4, 6.5 Hz, 1H), 3.73 (s, 3H), 3.62 (dd, J = 8.5, 4.9 Hz, 1H), 3.13 (dd, J = 13.9, 6.5 Hz, 1H), 3.00 − 2.91 (m, 2H), 2.61 (dd, J = 14.0, 8.5 Hz, 1H), 2.50 (ddd, J = 14.4, 10.3, 4.5 Hz, 1H), 2.09 (t, J = 34.8 Hz, 1H), 2.03 − 1.89 (m, 2H).

^{13}C NMR (176 MHz, MeOD) δ 173.8, 173.0, 164.9, 157.6, 137.9, 131.5, 130.3, 129.6, 128.4, 128.0, 116.5, 90.9, 89.8, 88.4, 87.3, 56.9, 56.7, 53.1, 50.4, 49.9, 40.38, 38.9, 38.37, 37.0, 36.1, 31.7, 29.6. The ^{13}C was assigned with HSQC and HMBC. FTMS +P 545.2025
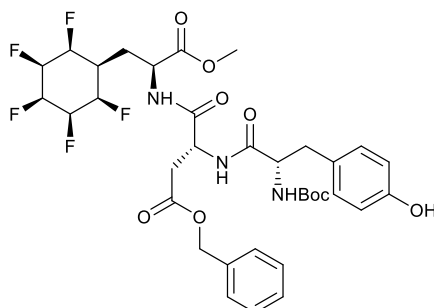
Boc-Asp(OBz0)-CyF$_5$ 4-77
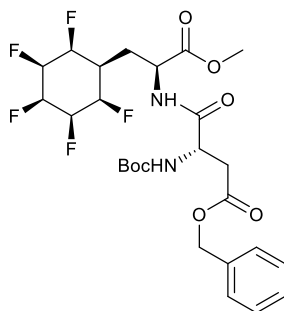
The reaction was conducted following the standard HATU coupling procedure. The product was purified by column chromatography (MeOH/DCM). The product was obtained as a colourless oil (79 mg) with a residue of DMF. The product was used directly into next step without removal of DMF. Yield about 91 %.

^{1}H NMR (700 MHz, Methanol-d_4) δ 7.47 − 7.23 (m, 5H), 5.28 (d, J = 54.1 Hz, 1H), 5.09 − 4.94 (m, 1H), 4.76 − 4.41 (m, 4H), 3.77 (d, J = 7.3 Hz, 3H), 3.33 (p, J = 1.6 Hz, 9H), 2.48 (d, J = 15.3 Hz, 1H), 1.92 (d, J = 37.6 Hz, 2H). ^{19}F NMR (659 MHz, Methanol-d_4) δ -205.89 (d, J = 30.9 Hz), -212.02 − -212.59 (m), -214.22 (dd, J = 52.5, 26.8 Hz), -218.33 (ddd, J = 38.5, 26.4, 12.4 Hz).

^{13}C NMR (176 MHz, MeOD) δ 128.2, 127.9, 127.9, 127.6, 126.6, 86.83, 85.3, 66.8, 63.8, 52.0, 51.7, 50.9, 49.4, 49.2, 37.5, 36.9, 35.5, 35.0, 34.8, 28.4, 27.3.

Tyr-Asp(OBz)-CyF₅-OMe 4-77

The reaction was carried out according to the standard HATU coupling procedure. The product was purified on column chromatography (MeOH/DCM). The product was obtained as a colourless oil (87 mg) with a trace residue of DMF, yield about 67 % . FTMS +p [M+Na] 766.2709, cal: 766.2739.

^{1}H NMR (700 MHz, Methanol-d_4) δ 7.36 (s, 1H), 7.04 (d, J = 8.3 Hz, 2H), 6.70 (d, J = 8.3 Hz, 2H), 5.27 (d, J = 54.1 Hz, 1H), 5.17 (d, J = 10.7 Hz, 2H), 5.04 (d, J = 50.6 Hz, 1H), 4.86 (s, 9H), 4.77 – 4.58 (m, 3H), 4.25 (dd, J = 9.4, 5.1 Hz, 1H), 3.77 (s, 3H), 3.00 (s, 3H), 2.82 (d, J = 5.5 Hz, 2H), 2.69 (dd, J = 14.1, 9.5 Hz, 1H), 2.50 (dd, J = 9.4, 5.4 Hz, 1H), 1.94 (d, J = 10.9 Hz, 2H), 1.37 (s, 10H).

^{19}F NMR (659 MHz, Methanol-d_4) δ -205.76 (d, J = 40.3 Hz), -211.83 – -212.72 (m), -214.25 (dd, J = 55.8, 27.0 Hz), -217.85 – -219.57 (m).

^{13}C NMR (176 MHz, MeOD) δ 172.9, 172.1, 171.2, 170.7, 163.5, 156.3, 155.8, 135.6, 130.1, 130.0, 128.2, 128.0, 127.7, 114.8, 89.2, 88.2, 86.8, 85.8, 67.0, 56.1, 53.4, 51.8, 49.4, 49.3, 48.5, 37.5, 37.0, 35.6, 34.9, 30.3, 28.4, 27.3, 27.1.

Boc-Tyr-CyF₅-OMe 4-81
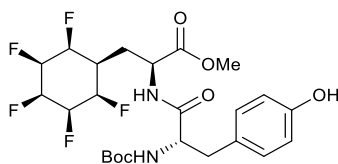
Compound **4-81** was prepared according to the standard HATU coupling procedure. Dry gel (270 mg) obtained after purification by column, with a trace residue of DMF, about 77 % yield.

^{1}H NMR (700 MHz, Methanol-d_4) δ 7.07 (d, J = 8.5 Hz, 1H), 6.72 (d, J = 8.5 Hz, 2H), 5.29 (d, J = 53.6 Hz, 1H), 5.04 (s, 1H), 4.83 (d, J = 22.3 Hz, 1H), 4.77 – 4.45 (m, 4H), 3.72 (d, J = 8.4 Hz, 3H), 2.98 – 2.90 (m, 1H), 2.79 (dd, J = 13.9, 8.3 Hz, 2H), 2.49 (dd, J = 13.5, 9.5 Hz, 1H), 1.93 (d, J = 10.8 Hz, 2H), 1.40 (s, 9H).

^{19}F NMR (659 MHz, Methanol-d_4) δ -205.84 (t, J = 38.9 Hz), -212.06 (tt, J = 32.2, 19.5, 17.4 Hz), -214.71 – -215.82 (m), -218.01 – -219.62 (m).

^{13}C NMR (176 MHz, MeOD) δ 173.21, 171.58, 156.37, 155.94, 129.96, 127.26, 121.12, 114.82, 86.86, 85.75, 56.54, 55.79, 54.64, 51.64, 37.48, 36.65, 30.68, 28.20, 28.13, 27.32.

FTMS +P ESI [M+Na] 377.1297.

Boc-Val-Tyr-CyF₅-OMe 4-83

4-83
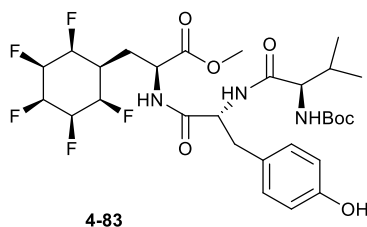
Compound **4-83** was prepared according to the standard HATU coupling. The crude product was purified by preparative TLC to afford the product as a white solid (35 mg) with a trace
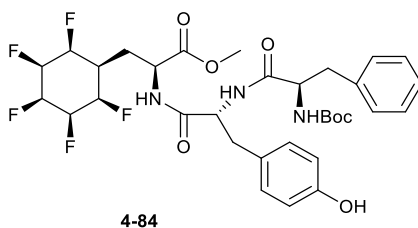
residue of DMF, yield about 46 %.   ¹H NMR (700 MHz, Methanol-d_4) δ 7.38 – 7.27 (m, 2H), 7.15 – 7.02 (m, 2H), 5.29 (d, *J* = 54.2 Hz, 1H), 4.97 (s, 1H), 4.82 – 4.57 (m, 4H), 4.37 (t, *J* = 8.2 Hz, 1H), 4.19 (dd, *J* = 6.3, 2.3 Hz, 1H), 3.78 (d, *J* = 7.7 Hz, 1H), 3.73 – 3.65 (m, 3H), 3.10 (dd, *J* = 13.9, 7.7 Hz, 1H), 3.06 – 2.98 (m, 1H), 2.49 (ddd, *J* = 14.7, 10.9, 4.1 Hz, 1H), 2.31 – 2.21 (m, 1H), 2.09 (dd, *J* = 42.3, 8.2 Hz, 1H), 1.88 (dd, *J* = 13.8, 7.1 Hz, 2H), 1.62 (d, *J* = 10.2 Hz, 1H), 1.46 (s, 9H), 1.08 (overlapped d, *J* = 6.8 Hz, 6H)

¹⁹F NMR (659 MHz, Methanol-d_4) δ -205.87 (d, *J* = 40.9 Hz), -206.08 (d, *J* = 41.0 Hz), -211.39 – -212.12 (m), -214.77 (dt, *J* = 53.7, 26.7 Hz), -218.33 (dqq, *J* = 55.7, 28.1, 16.3, 13.6 Hz).

¹³C NMR (176 MHz, MeOD) δ 172.1, 171.2, 130.1, 121.2, 86.7, 85.5, 60.3, 59.7, 55.5, 51.7, 37.5, 36.5, 36.0, 34.3, 30.7, 30.3, 29.4, 28.3, 27.3, 22.3, 18.2, 17.5, 17.3.

Boc-Phe-Tyr-CyF₅-OMe -4-84

4-84

Compound **4-84** was prepared according to the standard HATU coupling procedure. The crude product was purified by preparative TLC to afford a white solid (36 mg) as product with a trace residue of DMF, yield about 44 %.

¹H NMR (700 MHz, Methanol-d_4) δ 7.29 – 7.15 (m, 6H), 7.06 (d, *J* = 8.0 Hz, 2H), 6.77 – 6.67 (m, 2H), 5.30 (d, *J* = 54.0 Hz, 1H), 5.00 (s, 1H), 4.82 – 4.56 (m, 4H), 4.36 – 4.26 (m, 1H), 4.23 (dd, *J* = 10.0, 4.8 Hz, 1H), 3.71 (d, *J* = 13.2 Hz, 3H), 3.16 – 3.07 (m, 1H), 2.94 (dd, *J* = 13.8, 7.8 Hz, 1H), 2.76 – 2.69 (m, 1H), 2.65 (s, 3H), 2.53 – 2.44 (m, 1H), 2.10 – 1.94 (m, 1H), 1.95 – 1.87 (m, 1H), 1.27 (s, 11H).

^{19}F NMR (659 MHz, Methanol-d_4) δ -205.84, -211.76 (d, J = 175.0 Hz), -214.87 (d, J = 194.1 Hz), -218.34.

^{13}C NMR (176 MHz, MeOD) δ 156.1, 137.1, 130.1, 130.0, 128.9, 128.0, 128.0, 126.3, 114.9, 114.9, 86.5, 85.7, 56.0, 55.7, 54.7, 51.6, 37.6, 37.5, 35.8, 35.5, 34.6, 30.7, 29.3, 28.3, 28.1, 27.2.


Fmoc-Asp(O^{t}Bu)-Tyr-CyF$_5$-OMe 4-85

4-85
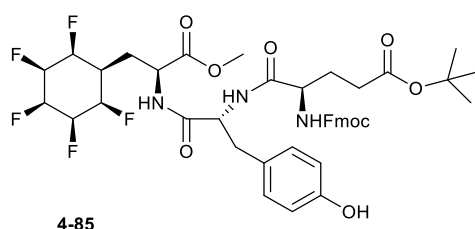
The ompound **4-85** was prepared according to the standard HATU coupling procedure. Product (52 mg) was obtained as a yellow gel, yield about 49%. ^{1}H NMR (700 MHz, Methanol-d_4) δ 8.00 (s, 1H), 7.82 (d, J = 7.6 Hz, 2H), 7.66 (t, J = 8.2 Hz, 2H), 7.41 (t, J = 7.5 Hz, 2H), 7.33 (tdd, J = 7.4, 2.6, 1.1 Hz, 2H), 7.08 – 6.99 (m, 2H), 6.76 – 6.65 (m, 2H), 5.28 (d, J = 53.9 Hz, 1H), 4.97 (d, J = 50.5 Hz, 1H), 4.79 (s, 1H), 4.77 – 4.55 (m, 3H), 4.43 (dd, J = 10.6, 6.9 Hz, 1H), 4.39 (dd, J = 8.8, 5.3 Hz, 1H), 4.35 (dd, J = 10.6, 6.7 Hz, 1H), 4.25 (dt, J = 22.0, 7.2 Hz, 2H), 3.71 (s, 3H), 2.70 (dd, J = 16.1, 5.4 Hz, 1H), 2.54 – 2.43 (m, 2H), 2.03 (d, J = 36.7 Hz, 1H), 1.91 (t, J = 13.3 Hz, 1H).

^{19}F NMR (659 MHz, Methanol-d_4) δ -205.01 – -207.20 (m), -211.94 (ddtt, J = 62.8, 45.1, 28.4, 16.5 Hz), -213.86 – -215.40 (m), -218.24 (dpd, J = 53.8, 27.0, 26.4, 13.0 Hz).

^{13}C NMR (176 MHz, MeOD) δ 172.3, 172.0, 171.5, 169.9, 163.5, 157.0, 156.0, 143.8, 143.7, 141.2, 130.0, 127.4, 127.2, 126.8, 124.8, 119.6, 114.9, 89.8, 88.6, 86.8, 86.7, 81.1, 66.7, 55.8,

51.6, 48.9, 48.1, 48.0, 48.0, 47.9, 47.8, 47.7, 47.6, 47.5, 47.4, 47.2, 46.9, 37.5, 37.0, 35.5, 34.5, 30.2, 28.4, 26.9.

Fmoc-Arg(Pbf)-Tyr-CyF₅-OMe 4-86
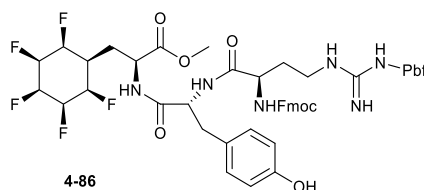
Compound **4-86** was prepared according to the standard HATU coupling procedure. The crude product was purified by preparative TLC to afford a yellow solid (20 mg) as product, with a trace residue of DMF, yield about 16 %. ^{1}H NMR (700 MHz, Acetone-d_6) δ 6.56 – 6.49 (m, 2H), 6.38 (dt, J = 14.0, 7.0 Hz, 2H), 6.12 (dt, J = 14.3, 7.4 Hz, 3H), 6.09 – 5.95 (m, 3H), 5.77 (d, J = 8.0 Hz, 2H), 5.50 – 5.37 (m, 2H), 3.98 (d, J = 54.2 Hz, 1H), 3.72 (s, 1H), 3.55 – 3.33 (m, 4H), 3.26 – 3.13 (m, 1H), 3.14 – 3.00 (m, 3H), 2.99 – 2.88 (m, 1H), 2.76 (dd, J = 8.5, 5.5 Hz, 1H), 2.48 (p, J = 6.6 Hz, 1H), 1.98 (q, J = 7.4 Hz, 2H), 1.85 (dt, J = 13.6, 6.8 Hz, 2H), 1.20 (ddd, J = 14.4, 10.6, 4.1 Hz, 1H), 0.64 (t, J = 13.1 Hz, 1H), 0.38 (dq, J = 13.8, 7.3, 5.5 Hz, 1H).

^{19}F NMR (659 MHz, Acetone-d_6) δ -206.93 (dd, J = 66.3, 42.3 Hz), -212.52 – -213.20 (m), -215.88 (p, J = 30.8, 28.4 Hz), -219.43 (dddp, J = 58.6, 43.8, 32.2, 15.6 Hz).

^{13}C NMR (176 MHz, Acetone) δ 171.1, 170.2, 162.2, 157.2, 155.8, 154.7, 142.7, 142.4, 140.0, 136.8, 131.7, 130.9, 128.7, 126.2, 126.1, 125.9, 125.5, 123.5, 123.4, 119.9, 118.3, 115.8, 113.7, 113.6, 85.5, 85.4, 85.0, 84.4, 84.3, 65.1, 54.5, 53.4, 53.3, 53.2, 50.4, 47.6, 45.8, 41.3, 41.1, 36.2, 34.6, 34.3, 29.4, 29.0, 27.5, 27.1, 26.9, 26.0, 17.1, 17.0, 16.0, 15.8, 14.6, 10.5, 9.9.

7.5 Chapter 5

7.5.1 General procedure for hydrogenation in chapter 5

Fluoroarene substrate (1 mmol), oven dried silica/ 4Å MS (1g), Rhodium CAAC catalyst (1 mmol %) and dry hexane (10ml) were added under argon to a 100 ml glass tube vessel. The reaction vessel was placed in a 150 ml stainless steel autoclave. The autoclave was pressurised and de-pressurised with 5 bar hydrogen three times before being chargedd to 50 bar of hydrogen. The reaction mixture was stirred at room temperature for 24 h or 72 h for amines, after which the autoclave was de-pressurised. The reaction mixture was flushed with DCM, acetone or methanol onto silica, dried and submitted to column chromatography.

7.5.2 Synthesis of fluorocycloalkanes

(all-*cis*)-1,2,3,4,5-Pentafluoro-6-methylcyclohexane 5-2
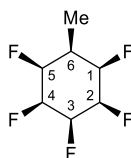
2,3,4,5,6-Pentafluoromethylbenzene (1 g, 5.49 mmol), silica gel (7 g), pentafluorotoluene (12 mg, 0.027 mmol, 0.5 mol%) and hexane (20 ml) was placed in a glass vial under nitrogen. The autoclave was pressured with hydrogen (50 bar) and stirred for 24 h. After which the crude mixture was purified directly by flush column chromatography (SiO$_2$, CH2Cl$_2$ in pentane) to give 3 (0.56 g, 3.0 mmol, 54 %) as a white crystalline solid; m.p. 182 °C; 1H NMR (400 MHz, Acetone-d6) δH 5.44-5.29 (1H, m, H-3), 5.04-4.75 (4H, overlapping m, H-1, H-2, H-4, H-5), 2.27- 2.05 (1H, m, H-6), 1.34 (3H, d J = 7.2 Hz, CH3); 19F NMR (377 MHz, Acetone-d6) δF - 205.1, -213.5, -217.5; 13C NMR (101 MHz, Acetone) δC 90.2 (CF), 88.1 (CF) , 87.7 (CF), 33.8 (C-6), 12.1 (CH3); HRMS m/z (ESI+) (calculated C7H9F5Na+ = 211.0517) found 211.0515

[M+Na]+

(all-*cis*)-1,2,3,4,5-Pentafluoro-6-(trifluoromethyl)cyclohexane 5-2CF₃
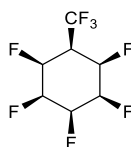

Reaction was carried out under standary hydrogenation condition. Product was obtained as a white solid (100 mg) obtained. 41 % yield. m.p. 172 °C.

^{1}H NMR (500 MHz, Acetone-d_6) δ 5.66 – 5.40 (m, 3H), 5.22 – 4.93 (m, 2H), 3.40 – 3.12 (m, 1H).

^{19}F NMR (470 MHz, Acetone-d_6) δ -206.90 (d, J = 40.5 Hz, 1F), -211.49 – -212.89 (m, 2F), -218.67 (ddtd, J = 53.7, 36.9, 26.8, 16.1 Hz, 2F).δ -66.23 (q, J = 9.2 Hz, 3F). ^{13}C NMR (126 MHz, Acetone) δ 141.4, 88.2, 86.6, 84.9, 83.3, 41.9.

FTMS ESI +P Calculated mass of $C_7H_6F_8Na_1$ = 265.0234 Found mass = 265.0234.

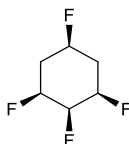**All-*cis*-1,2,3,4,5-pentafluorocyclohexane 5-15**
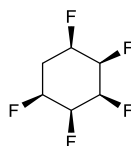
Product **5-15** was prepared by the standard hydrogenation method. The crude product was directly submitted to column chromatography with DCM to generate **5-15** as a white solid (68 mg), 39 % yield, 96 % conversion. M.p. 150-152 °C.

^{1}H NMR (318 K, 500 MHz, Methanol-d_4) δ 5.05 (dt, J = 51.5, 11.9 Hz, 1H), 4.86 – 4.67 (m, 1H),

2.49 (h, J = 10.2 Hz, 1H), 2.33 – 2.20 (m, 1H). ^{19}F NMR (213 K, 470 MHz, Methanol-d_4) δ -200.9 – -201.1 (m), -213.2 (t, J = 12.0 Hz), -219.32 (ddd, J = 12.0, 7.1, 4.8 Hz). Data matched the literature[1].
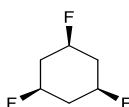
All-*cis*-1,2,3,5-tetrafluorocyclohexane 5-13

Product **5-13** was prepared by the standard hydrogenation method on a 2.13 mmol. The crude product was directly subjected to column chromatography (DCM/Pentane). A white solid (235 mg), was recovered after concentrrated *in vacuo* ,65% yiled. M.p. 84-86 °C.

^{1}H NMR (500 MHz, Chloroform-*d*) δ 5.06 (dtd, J = 54.3, 10.4, 2.1 Hz, 1H), 4.71 – 4.22 (m, 3H), 2.44 (dt, J = 11.9, 6.0 Hz, 2H), 2.35 – 2.09 (m, 2H). ^{19}F NMR (471 MHz, Chloroform-*d*) δ -183.9 (dd, J = 46.7, 8.8 Hz), -197.0 (ddd, J = 44.9, 15.6, 8.2 Hz), -216.1 – -218.2 (m). ^{13}C NMR (126 MHz, Chloroform-*d*) δ 87.5 (dt, J = 188.0, 17.9 Hz), 86.2 – 82.8 (m, overlapped), 32.1 (td, J = 21.4, 3.9 Hz). Mass FTMS +P ESI [M+Na] observed 179.0453 calculated as 179.0455.

All-*cis*-1,3,5-trifluorocyclohexane 5-11

Product **5-11** was prepared by the standard hydrogenation method on 7.6 mmol scale. The crude product was directly submitted to a column chromatography (DCM/Pentane) and the product was recovered in 60 % yield as a white solid (630 mg). M.p. 90 °C.

1H NMR (500 MHz, Methylene Chloride-d2) δ 4.58 (dtt, J = 45.8, 8.5, 3.7 Hz, 3H), 2.56 – 2.23 (m, 3H), 1.89 (h, J = 11.1 Hz, 3H).19F NMR (471 MHz, Methylene Chloride-d2) δ -181.4 (dp, J

= 48.2, 12.6 Hz). 13C NMR (126 MHz, Chloroform-d) δ 85.1 (dt, J = 176.0, 14.9 Hz), 37.8 (t, J = 20.0 Hz). All spectra and m.p match to the literature[2].
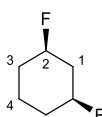
1,2,3 All-*cis* trifluoro cyclohexane 5-9
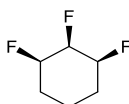
Product was prepared under standard hydrogenation conditions. The compound was flushed with diethyl ether/PE in column chromatography. The crude product was concentrated *in vacuo* to afford the product as a colourless liquid (805 mg) in 80 % yield.

^{1}H NMR (400 MHz, Chloroform-d) δ 5.01 (dtt, *J* = 53.6, 13.2, 2.1 Hz, 1H), 4.67 − 4.36 (m, 2H), 1.88 (m, 5H), 1.35 − 1.14 (m, 1H).^{19}F NMR (376 MHz, Chloroform-d) δ -188.65, -215.84. The NMR data matches with previous literature[2] .

1,3 All-*cis* difluoro cyclohexane 5-7

Product was prepared under standard hydrogenation conditions. The compound was flushed with DCM/pentane in column chromatography. The crude product was concentrated *in vacuo* to afford the product as a colourless liquid (208 mg), 70 % yield.

^{1}H NMR (700 MHz, Methylene Chloride-d_2) δ 4.62 (dtt, *J* = 47.23, 8.8, 4.0 Hz, 2H, H-2), 2.44 − 2.32 (m, 1H, H-1 eq), 1.98 − 1.88 (m, 3H, H-3 eq H-eq overlapped), 1.85 − 1.80 (m, 1H, H-1 ax), 1.58 (d, *J* = 8.5 Hz, 3H), 1.31 (m, 2H, H3-ax) 1.27 (dd, *J* = 3.4, 1.3 Hz, 1H, H-4 axial). Only

major product peaks were assigned. A 8:1 ratio of conformer was presented. ^{19}F NMR (659 MHz, CD$_2$Cl$_2$) δ -174.71. ^{13}C NMR (176 MHz, Methylene Chloride-d_2) δ 89.14 (dd, J = 173.4, 11.6 Hz), 38.58 (t, J = 19.8 Hz), 31.37 (d, J = 17.1 Hz), 17.32 (t, J = 9.9 Hz). The NMR data matches with previous literature[2] .

7.5.3 3,4,5-trifluoro-cyclohexanes

(1R,2s,3S,5r)-1,2,3-trifluoro-5-methoxycyclohexane 5-18
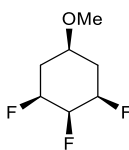
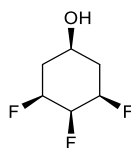Product was prepared under standard hydrogenation conditions. The reaction was carried out on a 1.5 mmol scale. The crude product was submitted to column chromatography and flushed with DCM/Pentane. The product was concentrated *in vacuo* to afford pure product (128 mg) in 64 % yield. Storage at room temperature led to sublimation in the bottle. Sublimation of clear crystal product with higher purity. M.p. 35-36 °C

^{1}H NMR (400 MHz, Chloroform-d) δ 5.09 (dt, J = 55.4, 9.4 Hz, 1H), 4.43 (dddd, J = 44.9, 25.8, 12.4, 5.0 Hz, 1H), 3.39 (s, 2H), 3.29 – 3.18 (m, 0H), 2.40 – 2.30 (m, 2H), 1.91 (p, J = 11.7 Hz, 3H). ^{19}F NMR (377 MHz, Chloroform-d) δ -194.38 (d, J = 15.2 Hz), -218.24 (t, J = 15.0 Hz). ^{13}C NMR (101 MHz, Chloroform-d) 87.99 (dt, J = 187.1, 17.9 Hz), 86.36 (ddd, J = 185.2, 18.3, 11.5 Hz), 71.50 (t, J = 15.9 Hz), 56.61, 31.18 (d, J = 19.2 Hz). FTMS +P 191.0648 obatined for [M+Na], calculate d 191.0660.

All-*cis*-3,4,5-trifluorocyclohexan-ol 5-19

The reaction was performed under the standard hydrogenation conditions on a 1 g scale. Product (648 mg) was obtained as a pale-yellow oil. Yield 62 %.

^{1}H NMR (400 MHz, Chloroform-*d*) δ 5.21 – 4.79 (m, 1H), 4.74 – 4.37 (m, 2H), 3.86 – 3.63 (m, 1H), 2.41 – 2.10 (m, 2H). ^{19}F NMR (377 MHz, Chloroform-*d*) δ -178.85 1F, -195.09 (d, *J* = 14.3 Hz, 2F). ^{13}C NMR (101 MHz, Chloroform-*d*) δ 89.6, 70.4, 35.5, 24.1. FTMS 177.0497

All-*cis*-3,4,5-trifluorocyclohexan-1-one 5-20
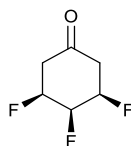
To a solution of DCM with DMSO (70 mg), oxalyl chloride (60 mg) was injected at -78 °C, after 30 min, to a compound **5-19** 50 mg was injected. After 1.5 h, Et$_3$N 0.2 ml was added. After another 1.5 h, water was added to quench the reaction. After 10 min 1 M HCl was added, then the reaction mixture was extracted with DCM. The compound was concentrated *in vacuo* to afford product contaminated with trace solvent. Product was unstable for storage.

^{1}H NMR (400 MHz, Chloroform-*d*) δ 4.90 – 4.69 (m, 1H), 4.65 – 4.45 (m, 2H), 2.35 – 2.20 (m, 2H), 2.00 – 1.86 (m, 2H). ^{19}F NMR (377 MHz, Chloroform-*d*) δ -172.58, -186.33.

All-*cis*-3,5-difluoro-1-methoxyl cyclohexane 5-16
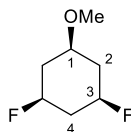
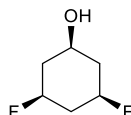Product was prepared under standard hydrogenation condition. A colourless oil (45 mg) was obtained, trace of solvent retained. Only product peaks were listed. About 30 % yield.

^{1}H NMR (700 MHz, Methylene Chloride-d_2) δ 4.58 (dddd, J = 48.3, 9.7, 5.5, 4.2 Hz, 2H, CHF), 4.03 (s, 1H, CHOMe), 3.68 (s, 3H, OMe), 2.36 – 2.24 (m, 3H, H-2, H-4, eq), 2.09 (d, J = 8.4 Hz, 1H, H-4 ax), 2.02 – 1.93 (m, 2H, H2-ax). ^{19}F NMR (659 MHz, CD$_2$Cl$_2$) δ -172.46. ^{13}C NMR (176 MHz, CD$_2$Cl$_2$) δ 90.5 (d, J = *170.7)* 41.2, 34.0, 31.4, 29.7, 18.5.

All-*cis*-difluorocyclohexan-1-ol 5-17

Product was prepared under standard hydrogenation condition. The crude product was submitted to column chromatography and flushed with DCM/pentane. A colourless oil (48 mg) was obtained as product 35 % yield.

^{1}H NMR (500 MHz, Methanol-d_4) δ 4.84 (dd, J = 18.3, 13.2, 8.8, 4.0, Hz, 2H, CHF), 4.25 (dt, J = 9.3, 5.2 Hz, 1H, CHOH), 3.97 – 3.87 (m, 3H, 3H, Heq), 3.87 – 3.75 (m, 3H, ax). ^{19}F NMR (470 MHz, MeOD) δ -176.9.

tert-Butyl ((all-cis)-3,4,5-trifluorocyclohexyl)carbamate 5-23
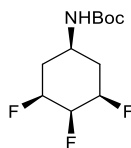
Product was prepared under standard hydrogenation condition on 4 Å MS as supporting substrate. The product was synthesis in 1 g scale reaction. The crude product was purified by column chromatography and flushed with EtOAc/Pe. Product 25 % was obtained as a white solid (250 mg), m.p. 122 °C. FTMS +P 252.1216 [M+], calculated as 252.1206

^{1}H NMR (700 MHz, Chloroform-*d*) δ 5.03 (dt, *J* = 53.8, 11.7 Hz, 1H), 4.55 (ddd, *J* = 45.0, 23.8, 11.2 Hz, 2H), 3.65 (s, 1H), 2.25 – 2.19 (m, 2H), 1.87 (m, 2H), 1.44 (s, 9H). ^{19}F NMR (659 MHz, Chloroform-*d*) δ -177.73, -193.32. ^{13}C NMR (176 MHz, Chloroform-*d*) δ 88.4, 86.2, 42.1, 32.0, 28.5

(1r,3R,4s,5S)-3,4,5-Trifluorocyclohexan-1-amine 5-24
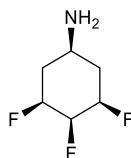
To a solution of compound **5-23** in diethyl ether, 2M HCl in dioxane was injected, the solution was stirred overnight for 12 h at room temperature. The resulted product was concentrated in vacuo to afford product **5-24** as a yellow solid. DCM was added to prevent the product decomposition. Pure dry product degraded very fast in touch with moisture from air.

^{1}H NMR (500 MHz, Chloroform-*d*) δ 5.08 (dt, *J* = 55.2, 9.9 Hz, 1H), 4.87 (dd, *J* = 52.2, 9.3 Hz, 0H), 4.47 (dddd, *J* = 45.0, 26.0, 12.1, 4.9 Hz, 1H), 2.87 – 2.72 (m, 0H), 2.13 (d, *J* = 1.2 Hz, 0H), 1.86 – 1.74 (m, 3H). ^{19}F NMR (470 MHz, Chloroform-*d*) δ -191.72 – -193.33 (m), -218.21.

^{13}C NMR (126 MHz, Chloroform-*d*) δ 87.5 (m, CHF), 67.1, 43.3 (t, *J* = 14.0 Hz), 35.3 (d, *J* = 21.4 Hz), 31.0. HRMS ESI [M+H 154.0832]

7.5.4 All-*cis*-1,3,5-trifluorocyclohexanes

(all-*cis*)-1,3,5-Trifluoro-2-(trifluoromethyl) cyclohexane 5-25
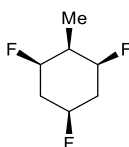
Product **5-25** was prepared by the standard hydrogenation method. The crude product was directly submitted to column chromatography with DCM/Pentane. Yield 88%. M.p.88-90 °C

^{1}H NMR (500 MHz, Chloroform-*d*) δ 4.68 (dddt, *J* = 50.1, 46.3, 7.3, 3.2 Hz, 3H), 2.47 – 2.28 (m, 2H), 2.24 – 1.91 (m, 3H), 1.20 (d, *J* = 7.1 Hz, 3H).^{19}F NMR (470 MHz, Chloroform-*d*) δ -179.2, -192.0.^{13}C NMR (126 MHz, Chloroform-*d*) δ 88.2 (d, *J* = 180.6 Hz), 84.9 (d, *J* = 175.3 Hz), 37.5 (t, *J* = 19.6 Hz), 34.8 – 33.3 (m), 10.1.

FTMS + P ESI observed [M+Na] 175.0703, calculated 175.0711.

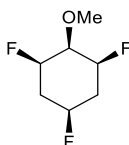**(all-*cis*)-1,3,5-Trifluoro-2-methoxycyclohexane 5-27**

Product **5-27** was prepared by the standard hydrogenation method. The crude product is directly submitted to column chromatography with DCM/Pentane. The product was isolated as a colourless oil (100 mg), Yield 47 %. The compound was cooled to -20 °C in a freezer for crystallisation.

^{1}H NMR (500 MHz, Acetone-d_6) δ 4.83 – 4.49 (m, 3H), 3.96 (td, J = 9.6, 2.5 Hz, 1H), 3.54 (s, 3H), 2.31-2.23 (m, 2H), 2.16 – 2.01 (m, 2H).^{19}F NMR (470 MHz, Acetone) δ -183.1, -195.7.

^{13}C NMR (126 MHz, Acetone-d_6) δ 88.2 (ddd, J = 181.4, 17.1, 13.0 Hz), 85.6 (dt, J = 173.4, 18.0 Hz), 78.9 (t, J = 17.0 Hz), 60.7, 55.1, 33.2 (t, J = 21.0 Hz). FTMS + P ESI observed [M+Na] 191.0652, calculated 191.0660.

(all-*cis*)-2,4,6-Trifluorocyclohexan-1-ol   5-28
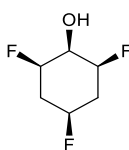
The product **5-28** was prepared by the standard hydrogenation method and purified by flush column chromatography with DCM. The product was isolated as a colourless solid (77 mg). M.p. 76 °C. Yield 35 %. ESI+p Calculated mass of [M+Na] = 177.04977. Found mass = 177.0499.

^{1}H NMR (500 MHz, Acetone-d_6) δ 4.71 – 4.46 (m, 3H), 4.18 (t, J = 15.5 Hz, 1H), 1.95 – 1.86 (m, 2H), 1.63 – 1.50 (m, 2H). ^{19}F NMR (470 MHz, Acetone) δ -196.46, -200.07.

^{13}C NMR (126 MHz, Acetone-d_6) δ 92.39 (d, J = 173.8 Hz), 90.81 (dd, J = 179.2, 8.5 Hz), 69.39 (t, J = 17.7 Hz), 25.47 (d, J = 18.6 Hz), 16.59 – 15.76 (m).

(all-*cis*)-1,3,5-Trifluoro-2-(trifluoromethyl)cyclohexane 5-26
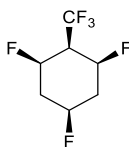
Product was prepared under standard hydrogenation condition. The crude product was submitted to column chromatography with DCM/pentane. Product was obtained as a

colourless oil (56 mg), 27 % yield.

^{1}H NMR (500 MHz, Chloroform-*d*) δ 5.17 (d, *J* = 26.9 Hz, 1H), 4.99 – 4.79 (m, 2H), 2.81 (d, *J* = 13.7 Hz, 2H), 2.26 (s, 2H), 1.77 (d, *J* = 16.7 Hz, 2H). ^{19}F NMR (470 MHz, Chloroform-*d*) δ -67.44 (t, *J* = 9.7 Hz), -67.75 (t, *J* = 9.6 Hz), -194.35 (q, *J* = 9.9 Hz), -194.96(t, 9.35 Hz).

N-((all-*cis*)-2,4,6-trifluorocyclohexyl) acetamide (5-29)

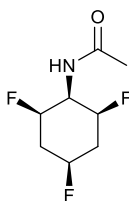Product **5-29** was prepared by the standard hydrogenation method using 2 mmol % of catalyst, hexane (7 ml) and silica (0.5 g) on a 0.5 mmol scale. The reaction time was extended to 3 days. The compound was purified over silica gel (acetone/DCM) and recrystallized in hot toluene to afford colourless needles (18 mg), 18 % yield. M.p. 126-130 °C.

^{1}H NMR (700 MHz, Toluene-d_8) δ 4.36 (overlapped, br, 2H), 4.16 (d, *J* = 47.7 Hz, 1H), 3.90 – 3.54 (m, 2H), 1.74 (d, *J* = 11.5 Hz, 3H), 1.12 (m, 2H), 0.77 (m, 2H).

^{19}F NMR (659 MHz, Toluene-d_8) δ -179.8, -196.2.^{13}C NMR (176 MHz, Tol) δ 88.3, 89.2, 84.9, 85.7, 47.8, 33.0, 24.9, 33.0 FTMS + P ESI Calculated ESI[M+Na] 218.0763 observed 218.0755.

ter*t*-Butyl (all-*cis*)-2,4,6-trifluorocyclohexyl) carbamate (5-30)
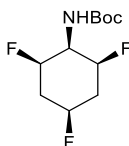
Aryl hydrogenation to generate **5-30** was carried out with 4 Å MS for 3 days on a 0.06 mmol

scale substrate scale. The product was purified over silica gel (acetone/DCM) and dried *in vacuo* to afford a white fibrous solid (6 mg), 40% yield, M.p. 160-162 °C (sub.).

^{1}H NMR (500 MHz, Acetone-d_6) δ 6.08 (s, 1H), 4.85 (ddt, *J* = 44.0, 23.8, 4.3 Hz, 4H), 4.05 (tdt, *J* = 26.5, 9.7, 3.3 Hz, 1H), 2.50 – 2.39 (m, 2H), 2.29 – 2.10 (m, 3H), 1.44 (s, 9H, ^{t}Bu). ^{19}F NMR (470 MHz, Acetone-d_6) δ -178.5, 1F, -195.3. ^{13}C NMR (126 MHz, Acetone-d_6) δ 88.2 (d, *J* = 180.6 Hz), 85.3 (dt, *J* = 174.0, 4.4 Hz), 79.6, 52.2 (t, *J* = 17.6 Hz), 34.4 (ddd, *J* = 20.3, 13.0, 7.0 Hz), 28.6.

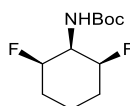FTMS + P ESI observed [M+Na] 276.1179, calculated 276.1187.

tert-Butyl ((1s,2R,6S)-2,6-difluorocyclohexyl) carbamate (5-35)

Rhodium catalyst (7 mg), *tert*-butyl (2,6-difluorphenyl) carbamate (0.2 g, 1 mmol) and activated 4 Å MS (250 mg) in a hexane (15 mL) solution were stirred under a hydrogen atmosphere under reduced pressure at 40 °C for 2 days. The product was purified by column chromatography (pentane/dichloromethane 1:1 to dichloromethane/acetone 98:2) to give **5-35** as a white solid (73 mg), about 31% yield; m.p. = 92-93 °C.

^{1}H NMR (400 MHz, Chloroform-*d*) δ 5.37 (d, *J* = 9.1 Hz, 1H, NH), 4.79 (d, *J* = 47.2 Hz, 2H, C$\underline{H}$F), 3.66 (td, *J* = 33.2, 9.7 Hz, 1H, C$\underline{H}$N), 2.28 – 2.09 (m, 2H,), 1.88 (qt, *J* = 13.5, 3.9 Hz, 1H), 1.65 – 1.48 (m, 2H), 1.45 (9H, s) 1.44 (d, *J*=12.1 Hz). ^{19}F NMR (376 MHz, Chloroform-*d*) δ -198.1. ^{13}C NMR (101 MHz, Chloroform-*d*) δ 155.5, 90.4 (d, *J* =174.7 Hz), 80.2, 52.0 (t, *J* = 17.0 Hz), 29.8 (dd, *J* = 12.6, 8.3 Hz), 28.5, 13.2. HRMS (EI, +ve) m/z calculated for C11H19NO2F2Na [M+Na]+ 258.1282, found 258.1272.

N-((all-*cis*)-2,6-difluorocyclohexyl)acetamide 5-34
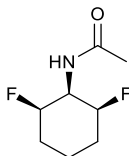
Product was prepared under standard hydrogenation conditions with modification of extend reaction time to 72 h, 50 °C heating on a 0.2 mmol scale. The crude product was purified by column (Acetone/DCM/PE). Trace of the starting 2,6 -difluorophenylacetamide was not separated from the product. Yellow gel (6 mg) was obtained. Yield about 15 %. ^{1}H NMR (500 MHz, Acetone-d_6) δ 4.19 (d, *J* = 35.9 Hz, 2H, CHF), 4.07 (m, 4H, Ac, NH overlaped), 3.34 (t, *J* = 12.2 Hz, 1H), 2.40 (d, *J* = 6.3 Hz, 3H ovlaped), 2.27 (d, *J* = 13.6 Hz, 3H overalped).^{19}F NMR (470 MHz, Acetone) δ -196.37.

7.6 Chapter 6

7.6.1 Ligand Synthesis

5.1.1.1 Methyl 2-(perfluorophenyl)acetate 6-3
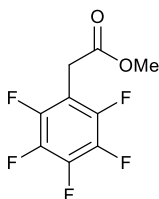
To a solution of 2-(perfluorophenyl) acetic acid (11 g, 48.6 mmol) in MeOH (200 ml), added concentrated sulfuric acid (1 ml). The reaction mixture was heated under reflux for 24 h. After the reaction mixture was cooled to room temperature, methanol was removed *in vacuo* and iced water (200 ml) was added to the mixture. The mixture was extracted with EtOAc (200 ml) twice. The combined organic layer was washed with saturated sodium bicarbonate solution, brine and dried over anhydrous sodium sulphate. The crude product was purified by column

chromatography (EtOAc/PE). The solvent was removed *in vacuo* and trace of solvent was removed by high vacuum over night to afford the product as a colourless oil which slowly turned into a white solid (10.5 g), yield 90 %. The compound NMR data agrees with the literature[13] value.

^{1}H NMR (500 MHz, Chloroform-*d*) δ 3.75 (s, 3H), 3.73 (s, 2H). ^{19}F NMR (470 MHz, Chloroform-*d*) δ -142.25 − -142.37 (dd, *J* = 21.4, 7.9 Hz)), -155.17 (t, *J* = 20.8 Hz), -162.27 (td, *J* = 21.6, 8.3 Hz). ^{13}C NMR (126 MHz, Chloroform-*d*) δ 168.9, 145.5 (d, *J* = 244.5 Hz), 140.9 (d, *J* = 254.2 Hz), 137.7 (d, *J* = 251.9 Hz), 108.2, 52.9, 27.7.

5.1.1.2 Methyl 2-((all-*cis*)-2,3,4,5,6-pentafluorocyclohexyl)acetate 6-4
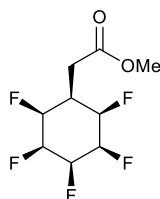
The synthesis of compound **6-4** was described in the literature [13]. In a 100 ml glass vessel, 1.00 g of compound **6-3** (4.16 mmol), 10 g of 4 Å molecule sieves, 35 ml of dry hexane and 1 mmol % catalyst **[Rh]** was added. The glass vial was placed into an autoclave under nitrogen. The autoclave was pressurised and depressurised 3 times with hydrogen before being charged to 50 bar of hydrogen. The reaction mixture was stirred for 24 h at room temperature, after which the autoclave was carefully depressurised. The suspension was filtered with celite, and washed with acetone/DCM. The solvent was removed *in vacuo* and the crude reaction mixture was purified by column chromatography (10 %acetone/DCM) to yield a white solid of **6-4** (0.588 g, 2.4 mmol), 57 % yield.

^{1}H NMR (500 MHz, Chloroform-*d*) δ 5.32(m, 1H), 4.99 (d, *J* = 49.0 Hz, 2H), 4.50 (dt, *J* = 49.6, 26.3 Hz, 2H), 3.75 (s, 3H), 2.90 (d, *J* = 6.9 Hz, 2H), 2.24 (m, 1H). ^{19}F NMR (470 MHz, Chloroform-*d*) δ -203.77, -211.52, -216.84. The NMR data matches to literature values[13].
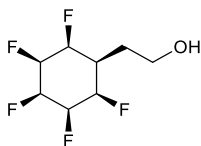
5.1.1.3 2-((all-*cis*)-2,3,4,5,6-Pentafluorocyclohexyl)ethan-1-ol 6-6

The synthesis of compound **6-6** was described in literature [13]. To a solution of compound **6-4**, 500 mg, 2.03 mmol in 20 ml THF at 0 °C, DIBAlH (1 M in hexane, 6.1 ml, 6.1 mmol 3 eq) was added dropwise. The reaction mixture was slowly wared to r.t. and was stirred for 2 h. The reaction was the ndiluted with 50 ml Et$_2$O and cooled to 0 °C, and quench by slowly addition of 0.2 ml water, 0.2 ml 15 % w/w sodium hydroxide solution and then 0.4 ml water. The reaction mixture was warmed to r.t. and stirred for 15 mins before MgSO$_4$ was added and the resulting suspension stirred for 15 mins. The suspension was filtered and washed with EtOAc. The filtrate was concentrated *in vacuo*, and the crude product was purified by flush chromatography, 10 % acetone/DCM. The purity of fraction is checked by TLC 5 % MeOH/DCM. A white solid (370 mg 1.70 mmol), 84 % yield.

^{1}H NMR (700 MHz, Methanol-d_4) δ 5.27 (d, *J* = 53.8 Hz, 1H), 4.93 (d, *J* = 52.9 Hz, 2H), 4.67 (dt, *J* = 40.5, 27.5 Hz, 2H), 3.74 (t, *J* = 6.0 Hz, 2H), 2.03 (t, *J*= 40.5 Hz, 1H, shift to 2.25 in d acetone), 1.99 (dt, *J*= 6.2, 5.8 hz, 2 H). ^{19}F NMR (659 MHz, Methanol-d_4) δ -205.83 (d, *J* = 41.4 Hz, 2F), -213.21 (m, 2F), -218.23 (m, 1F). The NMR data matches to literature values[13].

5.1.1.4 2-((all-*cis*)-2,3,4,5,6-Pentafluorocyclohexyl)acetic acid 6-5
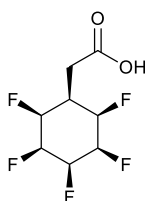
In a 100 ml round bottom flask, compound **6-4** (1 g) was dissolved in 6 M HCl (40 ml). The reaction mixture was heated under reflux overnight, after which the mixture was

concentrated *in vacuo*. The result solid in dried on high vacuum overnight to remove excess HCl and water. The crude product was used without further purification.

5.1.1.5 (all-*cis*)-1-(2-Bromoethyl)-2,3,4,5,6-pentafluorocyclohexane 6-7
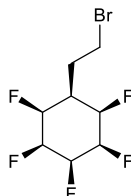
The synthesis of compound **6-7** was described in the literature [13]. To a solution of compound **6-5** (0. 4 g, 1.83 mmol, 1 eq) in 15 ml dry acetonitrile was added triphenylphosphine (1.01 g, 3.84 mmol, 2.1 eq), and slowly added carbon tetrabromide (1.28 g, 3.84 mmol, 2.1 eq.). The reaction was slightly exothermic. The reaction was stirred under nitrogen for 12 h, after which the reaction mixture was concentrated *in vacuo* and directly subjected to column chartography for purification (1:1 EtOAc/PE) to yield a white powder (326 mg), yield 64 %. The NMR data matches to literature value[13].

^{1}H NMR (700 MHz, Methanol-d_4) δ 5.28 (d, *J* = 54.4 Hz, 1H), 4.96 (d, *J* = 50.9 Hz, 2H), 4.70 (dt, *J* = 40.1, 27.5 Hz, 2H), 3.66 (t, *J* = 6.7 Hz, 2H), 2.34 (dt overlapped to q, *J* = 6.9 Hz, 2H), 2.14 (br-t, *J* = 34.5 Hz). ^{19}F NMR (659 MHz, Methanol-d_4) δ -206.13 (d, *J* = 40.7 Hz), -213.01 (m, 2F), -218.32 (m, 2F).

5.1.1.6 (all-*cis*)-1-(2-Azidoethyl)-2,3,4,5,6-pentafluorocyclohexane 6-8
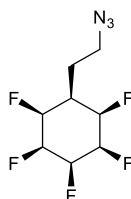
The synthesis of compound **6-8** was described in literature [13]. To a solution of compound **6-7**

(0.45 g, 1.60 mmol) in dry DMF was added sodium azide (0.21 g, 3.23 mmol). The reaction mixture was heated to 70 °C and the reaction was monitored by TLC. After 6 hours in which the starting material completely converted, the reaction was cooled to room temperature, water (30 ml) was added and the reaction mixture was extracted with EtOAc (20 ml) three times. The combined organic fraction was washed with brine, and dried over anhydrous sodium sulphate, filtered and concentrated *in vacuo*. The crude product was purified by column chromatography (2:3 EtOAc:PE) to give the product as a white needle solid (1.58 g), 99 % yield. The NMR data agrees with literature values[13].

^{1}H NMR (700 MHz, Acetone-d_6) δ 5.41 (d, J = 54.0 Hz, 1H), 5.09 (d, J = 53.0 Hz, 1H), 5.03 – 4.85 (m, 2H), 3.64 (t, J = 6.7 Hz, 2H), 2.32 – 2.14 (m, 1H), 2.09 (dt into q, J = 7.0 Hz, 2H). ^{19}F NMR (659 MHz, Acetone-d_6) δ -205.12 (d, J = 41.7 Hz), -212.67, -217.16 – -217.64 (m).

5.1.1.7 2-((all-*cis*)-2,3,4,5,6-Pentafluorocyclohexyl)ethyl 2,2,2-trichloroacetimidate 6-9
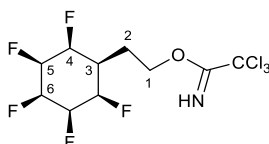
The preparation of compound **6-9** was adapted from literature[14]. To a solution of compound **6-6** (0.62 mmol, 135 mg, 1 eq.) in DCM (10 ml), added DBU (10 µl 2 eq.) at 0 °C and was stirred for 30 min. Then, trichloroacetonitrile (0.92 mmol, 1.5 eq, ~0.1 ml) was added dropwise at 0 °C. The reaction mixture was allowed to warm to room temperature and stirred overnight. The reaction mixture was concentrated *in vacuo* and submitted to column chromatography (EtOAc/PE with 1% NEt₃) to yield a white solid (157 mg, 0.43 mmol) 70 % yield. M.p. 130-134 °C. The product was degraded over 2 days.

^{1}H NMR (700 MHz, Acetone-d_6) δ 8.99 (br, 1H, N-H), 5.43 (d, J = 53.7 Hz, 1H, H-6), 5.17 (d, J = 49.8 Hz, 2H, H-4), 4.96 (dt, J = 41.3, 28.1 Hz, 2H, H-5), 4.55 (t, J = 6.1 Hz, 2H, CH2O), 2.34 (m, overlapped, 3H, H-3 and H2). ^{19}F NMR (659 MHz, Acetone-d_6) δ -205.10 (d, J = 41.44 Hz) , -

212.63, -217.54. ^{13}C NMR (126 MHz, Acetone) δ 161.0 86.7, 88.1, 87.4, 66.4, 35.4, 24.9.

5.1.1.8 (2-((all-*cis*)-2,3,4,5,6-Pentafluorocyclohexyl)ethoxy)benzene 6-13
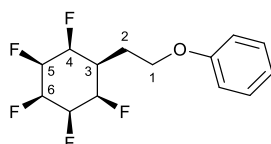
To an oven dried round bottom flask, compound **6-13** (0.4 mmol, 112 mg, 1eq), phenol (0.4 mmol, 37.6 mg 1 eq.), and potassium carbonate (0.5 mmol, 65 mg, 1.2 eq.) and DMF (5 ml) was added under nitrogen. The reaction mixture was stirred at 90 °C for 16 h. After which the reaction mixture was cooled to room temperature. The reaction mixture was poured into 20 ml water, extracted with 20 ml EtOAc three times. The combined organic layer was washed with water and brine, dried over anhydrous sodium sulphate. The crude product was concentrated *in vacuo* and submitted to column chromatography (DCM/PE 1:1) to afford a white powder 71 mg, 60 % yield, M.p. 162-164 °C.

^{1}H NMR (500 MHz, DMSO-d_6) δ 7.37 – 7.22 (m, 2H, ArH), 7.03 – 6.85 (m, 3H, ArH), 5.38 (d, J = 54.3 Hz, 1H, H6), 5.23 – 4.73 (m, 4H, H4, H5), 4.15 (t, J = 6.1 Hz, 2H, CO), 2.33 – 2.03 (m, 3H overlaped, H2 and H3).^{19}F NMR (470 MHz, DMSO-d_6) δ -203.49 (2F, F5), -211.42 (dt, J = 24.5, 5.8 Hz, 2F, F4), -216.24 (tt, J = 24.0, 11.4 Hz, 1F, F6).^{13}C NMR (126 MHz, DMSO) δ 158.9, 129.9, 121.1, 115.1, 89.0, 87.5, 86.0, 65.0, 34.9, 25.9. HRMS Calculated [M+Na] 317.0941, obs 317.0928.

5.1.1.9 4-((Trimethylsilyl)ethynyl)phenol 6-16
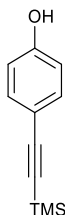
The reaction was conducted following a common Sonagashira cross coupling procedure adapted from literature[15]. In an oven dried round bottom flask, 4-iodo-phenol (4.6 mmol, 1.02 g), PdCl$_2$(PPh3)$_2$ (15 mol%, 97 mg), CuI (5 mol %, 27 mg), DIPA (30 ml), Ethynyltrimethylsilane (1 ml, 6.72 mmol) were added in sequence under argon. The reaction mixture was heated to 80 °C for 24 h, after which the reaction mixture was filter through celite, concentrated *in vacuo* and submitted to column chromatography (100% DCM) to yield a brown oil (0.788 g 4.15 mmol), 90 % yield.

^{1}H NMR (500 MHz, Chloroform-*d*) δ 7.39 – 7.34 (m, 1H), 6.79 – 6.72 (m, 1H), 0.23 (s, 4H).

The product ^{1}H NMR matches to literature values[16].

### 5.1.1.10 1-Ethynyl-4-(2-((all-*cis*)-2,3,4,5,6-pentafluorocyclohexyl)ethoxy)benzene 6-17
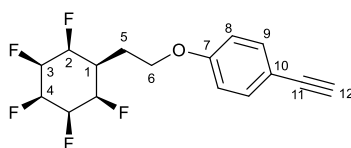
To an oven dried round bottom flask, compound **6-7** (0.5 mmol, 95 mg, 1 eq), compound **6-16** (0.5 mmol, 140 mg, 1eq), potassium carbonate (1.01 mmol, 140 mg, 2eq) and DMF (5 ml) were added under nitrogen. The reaction mixture was stirred at 90 °C for 16 h. After which the reaction mixture was cooled to room temperature. The reaction mixture was poured into water (20 ml), extracted with EtOAc (20 ml) three times. The combined organic layer was

washed with water and brine, dried over anhydrous sodium sulphate. The crude product was concentrated *in vacuo* and submitted to column chromatography (20 % EtOAc in PE) to afford a white powder (70 mg 0.22 mmol), 44 % yield. M.p. 150-152 °C

^{1}H NMR (700 MHz, Acetone-d_6) δ 7.42 (d, *J* = 8.8 Hz, 2H, H9), 6.96 (d, *J* = 8.8 Hz, 2H, H8), 5.42 (d, *J* = 54.2 Hz, 1H, C<u>H</u>F, H4), 5.14 (d, *J* = 50.5 Hz, 2H, C<u>H</u>F, H2), 5.08 – 4.81 (m, 2H, C<u>H</u>F, H3), 4.26 (t, *J* = 6.0 Hz, 2H, H6), 3.51 (s, 1H, H12), 2.38 (t, *J* = 7.7 Hz, 1H, H1), 2.30 (dt to q, *J* = 6.4 Hz, 2H, H5). ^{19}F NMR (659 MHz, Acetone-d_6) δ -205.05 (d, *J* = 40.6 Hz, 2F, F3), -212.62 (br, 2F, F2), -217.50 (br, 1F, F4). ^{13}C NMR (176 MHz, Acetone) δ 159.2 C-7, 133.3 C-9, 123.0 C-10, 114.6 C-8, 87.9 C-3, 88.0 C-4, 87.0 C-2, 83.3 C11, 77.1C-12, 64.9 C-6, 35.2 C-1, 25.7 C-5 HRMS [M+Na] 341.0941 cal, obs 341.0934

5.1.1.11 Methyl 2-(2,4,6-trifluorophenyl)acetate 6-19
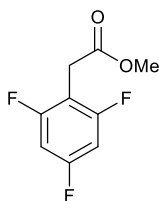
To a solution of 2-(2,4,6-trifluorophenyl)acetic acid (10.5 mmol, 2 g) in 40 ml methanol, added 0.5 ml concentrated sulphuric acid. The reaction mixture was heated under reflux for 24 hours, after which the solvent was removed *in vacuo*. The crude product was dissolved in 40 ml EtOAc, washed with sodium bicarbonate, brine and dried over anhydrous sodium sulphate. The crude product was submitted to column chromatography (EtOAc/PE) to afford a colourless oil (10.5 mmol, 2.1 g), quantitatively.

^{1}H NMR (500 MHz, Chloroform-*d*) δ 6.68 (dd, *J* = 8.7, 7.4 Hz, 2H), 3.72 (s, 3H), 3.66 (s, 2H). ^{19}F NMR (470 MHz, Chloroform-*d*) δ -109.03 (t, *J* = 5.7 Hz), -111.63 (d, *J* = 6.5 Hz). ^{13}C NMR (126 MHz, Chloroform-*d*) δ 169.9 (<u>C</u>OOMe), 162.0 (dt, *J* = 264.7, 15.6 Hz, C-4), 161.6 (ddd, *J* = 249.8, 14.8, 10.8, C-2, 6) 106.8 C-1, 100.1 (tm, *J* =28.3), 52.3 <u>OMe</u>$_2$, 27.4 CH$_2$. FTMS +P ESI observed

[M+Na] 227.0291, calculated 227.0291.

5.1.1.12 Methyl 2-((all-*cis*)-2,4,6-trifluorocyclohexyl)acetate 6-20
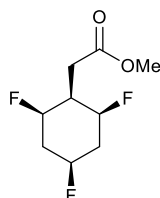
The synthesis of compound **6-20** was conducted according to the general hydrogenation conditions. In a 100 ml glass vessel, compound **6-19** (1 g, 4.9 mmol), 10 g of 4 Å molecular sieves, dry hexane (50 ml) and 1 mol % catalyst were added. The glass vial was placed into an autoclave under nitrogen. The autoclave was pressurised and depressurised 3 times with hydrogen before being charged to 50 bars of hydrogen. The reaction mixture was stirred for 24 h at room temperature, after which the autoclave was carefully depressurised. The suspension was filtered with celite, and washed with acetone/DCM. The solvent was removed *in vacuo* and the crude reaction mixture was purified by column chromatography (5 %acetone/DCM) to yield a white solid (0.8 g, 3.8 mmol), 77.7 % yield. M.p. 96 °C.

^{1}H NMR (500 MHz, Chloroform-*d*) δ 4.93 (d, *J* = 46 Hz, 1H, H4) 4.85 (d, *J* = 43.6, 2H, H2,6), 3.72 (s, 3H, OMe), 2.77 (d, *J* = 6.9 Hz, 2H, CH$_2$), 2.66 – 2.56 (m, 2H, H3,5 eq.), 2.30 (ttt, *J* = 31.9, 6.7, 3.1 Hz, 1H, H1), 1.88 (tdt, *J* = 39.4, 15.4, 3.5 Hz, 2H, H3,5 ax).
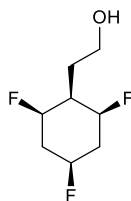
^{19}F NMR (470 MHz, Chloroform-*d*) δ -177.83 (t, *J* = 13.7 Hz), -191.47 (d, *J* = 13.7 Hz).

^{13}C NMR (126 MHz, Chloroform-*d*) δ 172.8, 87.4 (d, *J* = 178.5 Hz), 84.6 (d, *J* = 175.0 Hz), 52.0, 39.0 (t, *J* = 19.1 Hz), 34.3 (ddd, *J* = 20.7, 13.3, 7.4 Hz), 31.8 (t, *J* = 4.1 Hz).

HRMS +p [M] cal. 211.0946, obs. 211.0938.

5.1.1.13 2-((all-*cis*)-2,4,6-Trifluorocyclohexyl)ethan-1-ol 6-21

The preparation of compound **6-21** is similar to that of compound **6-6**. To a solution of compound **6-20** (420 mg, 2.00 mmol) in THF (20 ml) at 0 °C, DIBAl-H (1 M in hexane, 6.1 ml, 6.1 mmol 3 eq) was added dropwise. The reaction mixture was slowly warmed to r.t. and stirred for 2 h. The reaction was the diluted with Et_2O (50 ml), cooled to 0 °C, and quenched by slowly addition of 0.2 ml water, 0.2 ml 15 % w/w sodium hydroxide solution and then 0.4 ml water. The reaction mixture was warmed to r.t. and stirred for 15 mins before $MgSO_4$ was added and the resulting suspension was stirred for 15 mins. The suspension was filtered and washed with EtOAc. The filtrate was concentrated *in vacuo*, and the crude product was purified by flush chromatography, 10 % acetone/DCM. A white solid (0.82 mmol 150 mg) was obtained. Yield 41 %, M.p. 88-90 °C.

^{1}H NMR (700 MHz, Methanol-d_4) δ 4.86 – 4.63 (m, 3H, C$\underline{H}$F, overlaped), 3.73 (t, *J* = 6.5 Hz, 2H, C$\underline{H}_2$OH), 2.50 – 2.41 (m, 2H, C$\underline{H}_2$CH₂OH), 2.09 – 1.88 (m, 5H, cyclohexyl H, overlapped).

^{19}F NMR (659 MHz, Methanol-d_4) δ -177.90 – -179.14 (m, 1F), -191.25 – -193.33 (m, 2F).

^{13}C NMR (126 MHz, Methanol-d_4) δ 89.2 (d, *J* = 174.2 Hz), 86.7 (d, *J* = 172.5 Hz), 60.0, 39.6 (t, *J* = 19.5 Hz), 35.2 (t, *J* = 20.6 Hz), 30.8.

HRMS FTMS +P ESI [M+Na] cal. 191.0660 obs 191.0877.

5.1.1.14 (1R,2s,3S,5r)-2-(2-Bromoethyl)-1,3,5-trifluorocyclohexane 6-22
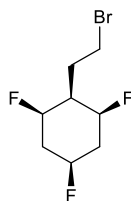
The synthesis of compound **6-22** is same as for compound **6-7**. To a solution of compound **6-21** (182 mg, 1.00 mmol, 1 eq) in 10 ml dry acetonitrile was added triphenylphosphine (550 mg, 2.1 mmol, 2.1 eq), and, slowly, carbon tetrabromide (696 mg, 2 mmol, 2.1 eq.). The reaction was slightly exothermic. The reaction was stirred under nitrogen for 12 h, after which the reaction mixture was concentrated *in vacuo* and directly subjected to column for purification (1:4 EtOAc/PE) to yield white powder (172 mg), yield 70 %.

^{1}H NMR (500 MHz, Acetone-d_6) δ 5.03 – 4.76 (m, 3H, C<u>H</u>F), 3.69 (t, *J* = 6.8 Hz, 2H, C<u>H</u>$_2$Br), 2.45 (m, 2H, H3,5 eq), 2.31 – 2.21 (m, 2H, C<u>H</u>$_2$CH$_2$Br), 2.21 – 2.14 (m, 1H, ^{t}C), 2.13 – 2.08 (m, 2H, H3,5 ax). ^{19}F NMR (471 MHz, Acetone-d_6) δ -177.66 (m, 1F), -191.17 – -192.19 (m,2 F). ^{13}C NMR (126 MHz, Acetone-d_6) δ 88.0 (d, *J* = 173.2 Hz), 85.8 (d, *J* = 173.2 Hz), 41.1 (t, *J* = 19.2 Hz), 34.7, 32.3, 31.0. HRMS [M+H] calculated 245.0153, observed 245.0610.

5.1.1.15 2-((all-*cis*)-2,4,6-Trifluorocyclohexyl)acetic acid 6-23
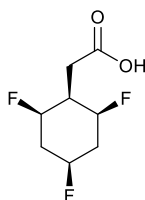
To a solution of compound **6-20** in a mixture of 20 ml THF and 20 ml H$_2$O, was added 80 mg of LiOH·H$_2$O (2 mmol, 2eq.) at 0 °C and the mixture stirred for 30 min and after which LiOH·H$_2$O (1 mmol, 1eq.) was added. The reaction mixture was warmed to r.t. and stirred for a further 2 hour. The reaction mixture was quenched with 1M HCl (10 ml) and extracted with EtOAc

(20 ml) three times. Dried over anhydrous sodium sulphate and solvent was removed *in vacuo*. A yellow solid (190 mg) was obtained. M.p. 104-106 °C. yield 97 %.

^{1}H NMR (700 MHz, Acetone-d_6) δ 4.89 (ddq, J = 47.5, 15.1, 3.6 Hz, 3H, C<u>H</u>F), 2.69 (d, J = 7.1 Hz, 2H, C<u>H</u>$_2$), 2.55 – 2.32 (m, 3H overlapped, H1 eq H3,H5), 2.19 – 1.98 (m, 2H, H3,H5 ax). ^{19}F NMR (659 MHz, Acetone-d_6) δ -177.41 (dddq, J = 63.6, 37.6, 24.7, 12.3 Hz, 1F), -191.69 (tddd, J = 55.3, 30.2, 14.4, 9.0 Hz, 2F). ^{13}C NMR (176 MHz, Acetone-d_6) δ 172.8 (<u>C</u>OOH), 87.6 (d, J = 176.3 Hz, C2,6), 84.8 C4 (d, J = 173.2 Hz), 38.6 (t, J = 18.9 Hz, C1), 33.8 (ddd, J = 20.4, 14.4, 5.9 Hz, C3,5), 31.2 <u>C</u>H$_2$. HRMS [M+Na] 219.0609 observed 219.0599.

7.6.2 Core linkage synthesis

Tetrakis(*p*-hydroxylphenyl)methane 6-26
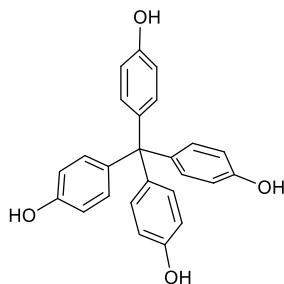
The compound **6-26** was synthesised according to a procedure adapted from the literature [17]. To a mixture of ice (6 g), concentrated sulphuric acid (2ml), Tetrakis(p-aminophenyl)methane (0.3 mmol, 114 mg) was added slowly, and the reaction mixture was stirred for 10 minutes at room temperature. CPME (9 ml) was added to the reaction mixture. An aqueous solution of sodium nitrate (1.32 mmol, 91 mg) in 3 ml H_2O was added dropwise over 10 minutes, and the reaction was refluxed for 20 min. Upon completion of reaction, the resulting solution was allowed to cool to room temperature and extracted with EtOAc and dried over $MgSO_4$. The crude product was purified by column chromatography (10-20 % methanol/DCM) to afford a pale brown solid (97 mg) 87 % yield.

^{1}H NMR (300 MHz, Methanol-d_4) δ 6.91 (d, J = 8.8 Hz, 1H), 6.63 (d, J = 8.8 Hz, 1H).

The compound date matches to literature values[18].

Tetrakis(4-trimethysilyl-ethynylphenyl)methane 6-29
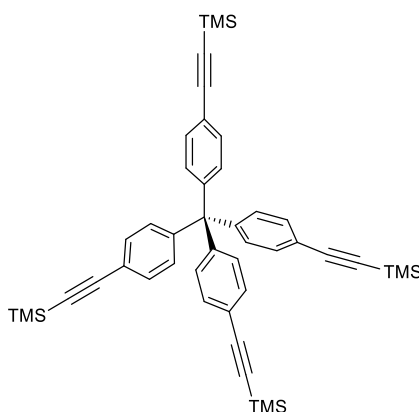
The reaction was carried out according to a literature procedure [19]. To dry triethylamine (4.5 ml), Cl$_2$Pd(PPh$_3$)$_2$ (15 mg), CuI (5 mg), tetrakis(*p*-bromophenyl)methane (0.4 mmol, 250 mg) and dry benzene (3.5 ml), was added 0.35 ml of trimethylsilylacetylene under nitrogen. After the reaction mixture was stirred for 15 minutes and a colour change was observed, the reaction mixture was heated to 80 °C and stirred for 24 h. The reaction mixture was cooled to room temperature. The solvent was evaporated *in vacuo* and the residue taken up in diethyl ether and 10 % aqueous HCl solution. The organic layer was separated, washed with water and dried over anhydrous sodium sulphate. The solution was filtered through celite, concentrated *in vacuo* and submitted to the next step without further purification.

Tetrakis(4-ethynlphenyl)methane 6-30
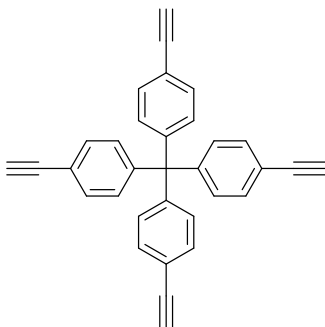
The crude product **6-29** (~0.4 mmol) obtained above, was dissolved in a solution of dry benzene (5 ml) and 8 ml dry acetonitrile. The reaction mixture was cooled to 0 °C, and 1 M TBAF (2.25 ml) in THF was added to the reaction mixture. The mixture was allowed to warm to room temperature and stirred for 2 hours. After completion of the reaction, the reaction mixture was poured into water (20 ml). The organic layer was separated, dried over anhydrous sodium sulphate, the solvent was removed *in vacuo* and the solid residue was purified by column chromatography (toluene/pentane 1:1, rf = 0.3). A white solid (57 mg) was observed after column, 34 % yield for 2 steps. The NMR data matches to literature values[19].

^{1}H NMR (700 MHz, Chloroform-*d*) δ 7.39 (d, *J* = 8.2 Hz, 2H), 7.12 (d, *J* = 8.2 Hz, 2H), 3.06 (s, 1H). ^{13}C NMR (176 MHz, Chloroform-*d*) δ 146.4, 131.8, 130.9, 120.4, 83.3 (<u>C</u>≡CH), 77.8 (C≡<u>C</u>H), 64.9 (<u>C</u>Ph₄).

4-Ethynylphenol 6-31
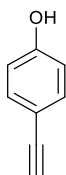
To a solution of 4-((trimethylsilyl)ethynyl)phenol (4.2 mmol, 800 mg) **6-16** in dry DCM (6 ml) , 300 mg (5.4 mmol) of KOH solution in MeOH (3ml) was added. The reaction mixture was

stirred at room temperature overnight, after which the mixture was neutralised with 2 N aqueous HCl solution (20 ml). The mixture was extracted 3 times with EtOAc (20 ml). The combined organic layer was dried over anhydrous sodium sulphate, and concentrated *in vacuo*. The residue was purified by flush column chromatography (EtOAc/PE 1:4) to yield the product as a yellow oil (455 mg), 92 % yield. The product is matching to literature value.[20] The product slowly decomposed over time and was used directly in the next step after synthesis.

^{1}H NMR (700 MHz, Methanol-d_4) δ 7.28 (d, *J* = 8.6 Hz, 2H), 6.73 (d, *J* = 8.7 Hz, 2H), 3.25 (s, 1H).

^{13}C NMR (176 MHz, MeOD) δ 159.3, 134.5, 116.4, 114.5, 84.8, 76.3.

4,4',4''-((((4-Bromophenyl)methanetriyl)tris(benzene-4,1-diyl))tris(ethyne-2,1-diyl))triphenol 6-33
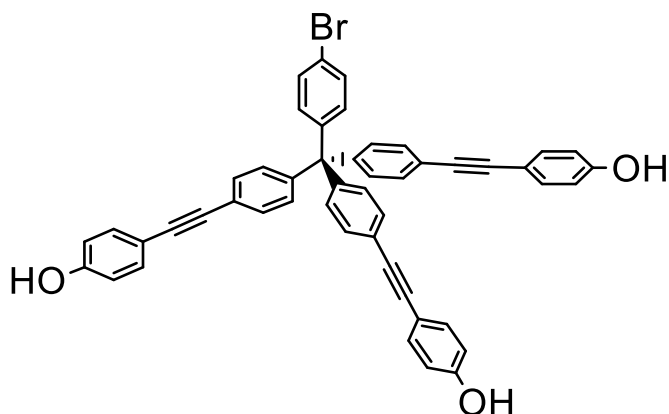
In an oven dried round bottom flask, tetrakis(*p*-bromophenyl)methane (0.157 mmol, 100 mg), PdCl$_2$(PPh$_3$)$_2$ (20 mg), CuI (5 mg), DIPA (6 ml) and 4-ethynlphenol (120mg, 1.01 mmol) were added in sequence. The reaction mixture was heated at 80 °C overnight. After the reaction was allowed to cool to room temperature, after which the reaction mixture was filtered through celite, and washed with DCM. The solvent was evaporated *in vacuo* and the crude product was submitted to column chromatography (10 % MeOH, DCM). Product 40 mg , 0.054 mmol), was isolated, 34 % yield.

¹H NMR (500 MHz, Methanol-d_4) δ 7.47 (d, *J* = 8.7 Hz, 3H), 7.42 (d, *J* = 8.5 Hz, 5H), 7.33 (dd, *J* = 8.7, 2.9 Hz, 7H), 7.19 (d, *J* = 8.6 Hz, 5H), 7.14 (d, *J* = 8.7 Hz, 2H), 6.81 – 6.73 (m, 8H).

¹³C NMR (176 MHz, Methanol-d_4) δ 160.0, 146.8, 135.1, 134.1, 133.9, 133.1, 132.1, 131.7, 130.0, 116.6, 91.1, 87.9, 73.1.

The crude reaction mixture was submitted to the next reaction without further purification.

4,4',4'',4'''-((Methanetetrayltetrakis(benzene-4,1-diyl))tetrakis(ethyne-2,1-diyl))tetraphenol 6-32
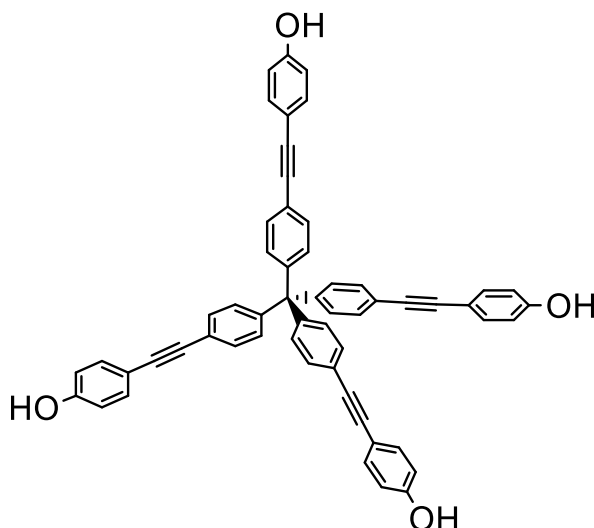
In an oven dried round bottom flask, tetrakis(*p*-bromophenyl)methane (0.157 mmol, 100 mg), PdCl$_2$(PPh$_3$)$_2$ (20 mg), CuI (5 mg), DIPA (6 ml) and 4-ethynlphenol (120mg, 1.01 mmol) was added in sequence. The reaction mixture was heated at 80 °C overnight. The reaction was allowed to cool to room temperature, after which the reaction mixture was filtered through celite, and washed with DCM. The solvent was evaporated *in vacuo* and the crude product was submitted to column chromatography (10 % MeOH, DCM). White product (30 mg) was observed, 0.038 mmol, 24 % yield.

¹H NMR (700 MHz, Methanol-d_4) δ 7.42 (d, *J* = 8.5 Hz, 1H), 7.33 (d, *J* = 8.7 Hz, 1H), 7.20 (d, *J* =

8.6 Hz, 1H), 6.77 (d, *J* = 8.7 Hz, 1H). ^{13}C NMR (176 MHz, MeOD) δ 159.2, 147.0, 134.1, 132.1, 131.7, 123.4, 116.5, 115.2, 91.1, 87.9. 66.0

1,3,5,7-Tetrabromoadamantane 6-35
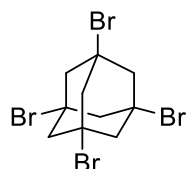
Tetrabromoadmantene was prepared by modification of the literature method[21][22]. Admante (2.5 g, 18.4 mmol) was slowly added to a mixture of bromine (9 ml) and anhydrous $AlCl_3$ (3 g, 22.9 mmol) at 0 °C. The reaction mixture was then slowly heated to 70 °C and stirred for 24 h. After the reaction mixture was cooled to room temperature, the reaction was quenched with aqueous sodium sulfite and 1M hydrochloric acid. The resulting crude product was dissolved in chloroform, washed with water and brine, dried over $MgSO_4$, concentrated *in vacuo* and recrystallised from acetic acid to give the product (4.1 g, 9.09 mmol). Yield 49.4 %

^1H NMR (500 MHz, Chloroform-*d*) δ 2.70 (s, 1H). ^{13}C NMR (126 MHz, Chloroform-*d*) δ 54.9, 54.7. The NMR data matches with the literature values[21, 22].

1,3,5,7-Tetrahydroxyadamantane 6-36
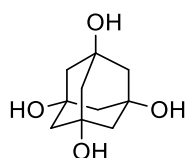
The tetrahydroxyadamantane was prepared using a literature procedure[21][22]. Compound **6-35** tetrabromoadamantane (4.43 mmol, 2 g) and $AgSO_4$ (3.06 g, 9.83 mmol) were mixed in conc. Sulphuric acid (6 ml). The suspension was slowly heated to 80 ° and stirred for 30 minutes. The reaction was then cooled to 50 °C and stirred for a further 3 h. After the reaction

was allowed to cool to room temperature, the suspension was filtered to remove the AgBr and washed with water. The filtrate was neutralised with KOH with ice to pH ~7. The water was evaporated *in vacuo*, the resulting grey solid was further dried under high vacuum, and then extracted by 100 ml of ethanol on a Soxhelt apparatus for 48 h. After removal of ethanol, the crude product was dissolved in methanol, and filtered through celite to yield a beige solid (681 mg). yield 76 %.

^{1}H NMR (700 MHz, MeOD) δ 1.61.^{13}C NMR (176 MHz, MeOD) δ 70.8, 51.4.

The NMR data matches with literature values[21,22].

1,3,5,7-Tetrakis(4-methoxyphenyl)adamantane 6-38

The compound **6-38** was synthesised according to the literature procedure[22]. A mixture of tetrahydroxyladamantane (1.5 mmol, 300 mg), TfOH (0.1 ml), anisole (10 ml) was heated to reflux in a dean stark apparatus. Then the solvent was evaporated *in vacuo*, dissolved in DCM, washed with saturated sodium bicarbonate aqueous solution, 2 M HCl, dried over anhydrous sodium sulphate, flitered through celite and concentrated *in vacuo*. The crude product was submitted to column chromotagraphy (DCM/PE 1:1, Rf = 0.28, *ortho/para* mixtures were separated in close r.f. range) to afford product (333 mg, 0.6 mmol), yield 40 %. NMR data matches with literature value[22].

^{1}H NMR (700 MHz, Chloroform-*d*) δ 7.39 (d, *J* = 8.9 Hz, 8H), 6.89 (d, *J* = 8.9 Hz, 8H), 3.80 (s,

12H), 2.09 (s, 12H). ^{13}C NMR (176 MHz, Chloroform-*d*) δ 157.9, 142.0, 126.2, 113.8, 55.4, 47.9, 38.8. Calcualted [M+Na] 583.2824 found 583.2814.

4,4',4'',4'''-(Adamantane-1,3,5,7-tetrayl)tetraphenol 6-39
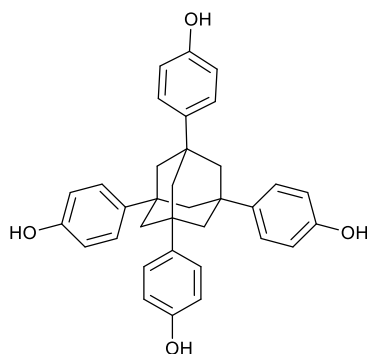
To a solution of compound **6-38** (70 mg, 0.125 mmol) in DCM (10 ml) at -78 °C, 1 M BBr$_3$ in DCM (1.5 ml, 1.5 mmol), was added dropwise. The reaction was allowed to warm to room temperature and stirred overnight. The reaction was quenched with water. The suspension was filtered and washed with water. Product was a white powder (45 mg, 0.089 mmol), Yield 71.4 %.

^{1}H NMR (500 MHz, DMSO-*d*$_6$) δ 9.15 (s, 1H), 7.30 (d, *J* = 8.8 Hz, 2H), 6.71 (d, *J* = 8.7 Hz, 2H), 1.91 (s, 3H). ^{13}C NMR (126 MHz, DMSO) δ 155.2, 140.4, 126.0, 114.8, 47.3, 38.1. Mass founded 527.2188 for [M+Na], calculated 527.2193.

Tetrakis(2-propynyloxymethyl)methane 6-43
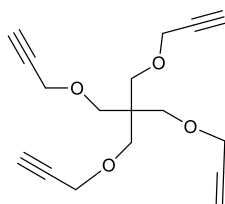
Compound **6-43** was synthesized according to a literature method[23]. Sodium hydride (240 mmol, 0.96 g, 60 % weight in mineral oil) was added to a solution of pentaerthritol (272 mg, 2mmol) in DMF (7 ml) at 0 °C and stirred for 30 minutes. Propargyl bromide (1.5 ml) was added to the reaction mixture dropwise over 30 minutes, and the solution was heated to 40 °C. After 2.5 h, an additional propargyl bromide (0.6 ml) was added dropwise, and the reaction was stirred at 50 °C for 16 h. After which the reaction was cooled to r.t. and water was added to quench the reaction. The resulting mixture was extracted with EtOAc. The combined organic layer was dried over anhydrous sodium sulfate and concentrated *in vacuo*. The crude product was submitted to column chromatography (EtOAc:PE 1:3) to the afford product desired product as white gel (394 mg, 1.37 mmol), yield 69 %. The NMR data is agreed with literature value[23].

^{1}H NMR (500 MHz, Chloroform-*d*) δ 4.12 (d, *J* = 2.4 Hz, 8H), 3.53 (s, 8H), 2.40 (t, *J* = 2.4 Hz, 4H).

^{13}C NMR (126 MHz, Chloroform-*d*) δ 80.2, 74.2, 69.2, 58.9, 44.9.

Tetrakis(azidomethyl)methane 6-45
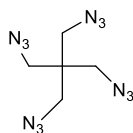
Compound **6-45** was prepared according to a literature method[24]. To an oven dried round bottom flask, pentaerythritol tetrabromide 1.34 g (3.46 mmol), DMF (20 ml), sodium azide (2.7 g, 4.15 mmol) was added slowly. The reaction mixture was stirred at 80 °C for 12 h. The reaction mixture was allowed to cooldown to room temperature, after which water (150 ml) was added. The mixture was extracted with diethyl ether (30 ml *2). The combined organic layer was dried over MgSO$_4$ and concentrated *in vacuo*. The crude product was purified by column chromatography (100 % hexane) to afford product (665 mg 2.8 mmol) stored in methanol solution, yield 80 %. Yield was calculated from internal standard.

^{1}H NMR (400 MHz, Chloroform-*d*) δ 3.34. The NMR data matches with the literature values.[24]

Tetrakis(aminomethyl)methane 6-46
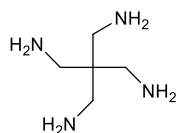
Compound **6-46** was prepared according to a literature procedure[24]. In a round bottom flask, to the solution of tetrakis(azidomethyl)methane (600 mg) in methanol (20 ml), added 10 % Pd/C (0.56 mmol, 600 mg) under nitrogen. The reaction was carefully charged with hydrogen balloon. The reaction mixture was allowed to stir for 48 hours at room temperature. After the hydrogen was released carefully, the reaction mixture was filtered through celite, and the solvent was reduced to yield desired product as a colourless oil (133 mg), yield about 40%.

^{1}H NMR (700 MHz, Chloroform-*d*) δ 2.17. ^{13}C NMR (126 MHz, DMSO) δ 44.8, 43.4. The NMR data is matched with the literature value[24].

2,2',7,7'-Tetramethoxy-9,9'-spirobifluorene 6-50
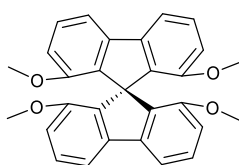
Compound **6-50** was prepared by an adapted procedure from literature[25, 26]. To a solution of 2,2',7,7'-tetrabromo-9,9'-spirobifluorine (463 mg, 0.733 mmol) in 6 ml DMF, 25 % w/w sodium methoxide solution in methanol (6 ml), CuI (140 mg) was added. The reaction mixture was heated under reflux for 24 hours. After the reaction was cooled to room temperature, DCM and then 1 M HCl was added to the mixture. The aqueous phase was extracted three times with DCM. The combined organic layer was washed with brine, dried with MgSO$_4$, and

then concentrated *in vacuo*. The solid residue was recrystallised from 10 % MeOH in DCM, filtered, and washed with MeOH to yield a colourless crystal solid (290 mg). 90 % yield.

^{1}H NMR (500 MHz, Chloroform-*d*) δ 7.62 (d, *J* = 8.4 Hz, 1H), 6.88 (dd, *J* = 8.4, 2.4 Hz, 1H), 6.24 (d, *J* = 2.4 Hz, 1H), 3.64 (s, 3H). ^{13}C NMR (126 MHz, Chloroform-*d*) δ 159.2, 150.5, 134.7, 119.9, 113.9, 109.6, 66.1, 55.6. The NMR data matches to the literature value.[26]

2,2',7,7'-Tetrahydroxyspirobifluorene 6-51
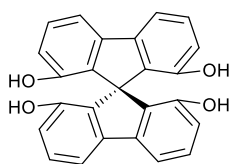
Compound **6-51** was prepared according to a literature procedure[26].

To a solution of 2,2',7,7'-tetramethoxy-9,9'-spirobifluorene (105 mg, 0.25 mmol) in 10 ml DCM at 0 °C, 1 M BBr$_3$ solution in DCM (1.1 ml, 1.1 mmol) was added dropwisely. The reaction was allowed to warm to room temperature and stirred for 3 hours. After which water was added, the reaction mixture was stirred for 10 minutes. The suspension was filtered. The resulting solid was washed with water, dissolved in diethyl ether, washed with brine and dried over MgSO$_4$. The solvent was reduced *in vacuo* to afford white solid (86 mg), yield 91 %.

^{1}H NMR (500 MHz, DMSO-*d$_6$*) δ 9.17 (s, 1H), 7.59 (d, *J* = 8.2 Hz, 1H), 6.70 (dd, *J* = 8.2, 2.3 Hz, 1H), 5.97 (d, *J* = 2.3 Hz, 1H). ^{13}C NMR (126 MHz, DMSO) δ 156.4, 150.1, 132.7, 120.0, 114.7, 110.3, 65.0. The NMR matches to literature value[26].

1,3,5,7-Tetrakis(prop-2-yn-1-yloxy)adamantane 6-37
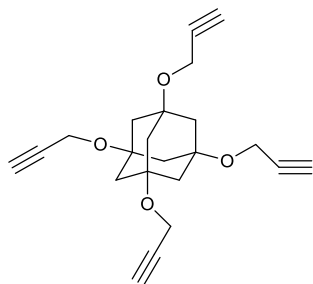
To a solution of tetrahydroxyladamantane (200 mg, 0.93 mmol) in DMF (10 ml) , sodium hydride (13.2 mmol, 528 mg, 60 % w/w in mineral oil) was added slowly at 0 °C. The reaction mixture was stirred to at room temperature for 30 minutes, after which propargyl bromide (0.6 ml) was added dropwise, and the reaction was heated to 40 °C and stirred for 2.5 h. Then an additional portion of propargyl bromide (0.3 ml) was added dropwise, and the reaction mixture was heated to 50 °C for 16 h. After the reaction was allowed to cool to room temperature, water was added to quench the reaction. The mixture was extracted with EtOAc (20 ml, 3 times). The combined organic layer was washed with water, aqueous sodium bicarbonate solution and brine, dried over anhydrous sodium sulphate, and concentrated *in vacuo*. The crude product was submitted to flush column chromatography for purification (10 % EtOAc/PE) to afford the product as a yellow oil (59 mg), 17 % yield.

^{1}H NMR (700 MHz, Chloroform-*d*) δ 4.15 (d, *J* = 2.1 Hz, 8H, CH$_2$), 2.42 (t, *J* = 2.0 Hz, 4H, C≡C-H), 1.85 (s, 12H, CH$_2$ admantane). ^{13}C NMR (176 MHz, Chloroform-*d*) δ 80.7 C-*C*≡C, 75.7 C≡*C*-H, 74.1 ^{t}C-O, 50.3, O-CH$_2$, 44.3 CH$_2$ admantane.

General Procedure for the synthesis propargyl ether core

To an oven dried round bottom flask, the tetrakis(hydroxylphenyl) (0.05 mmol), anhydrous potassium carbonate (82 mg, 0.6 mmol) and DMF (4 ml) was added, the reaction mixture was stirred at room temperature for 15 minutes. Then propargyl bromide (80 % w/w in toluene, 60 mg, 0.4 mmol) was added dropwisely. The reaction mixture was stirred and heated to 90 °C

for 24 h. After the reaction was allowed to cool to room temperature, water (20 ml) was added to the reaction mixture. The reaction mixture was extracted with 20 ml of DCM twice. The combined organic fraction washed with 20 ml of water twice, dried over anhydrous sodium sulphate and concentrated *in vacuo*. The crude product was subjected to column chromatography for purification (25 % EtOAc/PE).

Tetrakis(4-(prop-2-yn-1-yloxy)phenyl)methane 6-27

Compound **6-27** is prepared according to the general procedure for propargyl ether linkage core synthesis. Product (17 mg) was isolated as a yellow gel, 60 % yield.

^{1}H NMR (500 MHz, Methanol-d_4) δ 7.05 (d, *J* = 8.9 Hz, 1H), 6.86 (d, *J* = 8.9 Hz, 1H), 4.70 (d, *J* = 2.4 Hz, 1H), 2.93 (t, *J* = 2.4 Hz, 1H). ^{13}C NMR (126 MHz, MeOD) δ 157.2, 141.6, 133.1, 114.7, 76.7, 56.6.

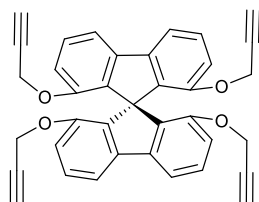**1,1,2,2-Tetrakis(4-(prop-2-yn-1-yloxy)phenyl)ethane 6-48**

Compound **6-48** was prepared according to the general procedure for propargyl ether linkage core. Product (22 mg) was obtained as a white powder, yield 50 %.

^{1}H NMR (700 MHz, Chloroform-*d*) δ 7.02 (d, *J* = 8.7 Hz, 8H), 6.72 (d, *J* = 8.7 Hz, 8H), 4.57 (s, 2H), 4.56 (d, *J* = 2.4 Hz, 8H), 2.47 (s, 4H).

^{13}C NMR (176 MHz, Chloroform-*d*) δ 155.7, 137.1, 129.5, 114.7, 78.9, 75.4, 55.9, 55.1.

1,1',8,8'-Tetrakis(prop-2-yn-1-yloxy)-9,9'-spirobi[fluorene] 6-52

Compound **6-52** was prepared according to the general procedure for propargyl ether linkage core synthesis. Product was observed as a yellow gel (8 mg), 30 % yield.

^{1}H NMR (700 MHz, Chloroform-*d*) δ 7.64 (d, *J* = 8.4 Hz, 4H), 6.96 (dd, *J* = 8.4, 2.4 Hz, 4H), 6.29 (d, *J* = 2.4 Hz, 4H), 4.51 (d, *J* = 2.4 Hz, 8H), 2.40 (s, 4H). ^{13}C NMR (176 MHz, Chloroform-*d*) δ 157.3, 150.3, 135.4, 120.1, 114.6, 111.2, 78.7, 75.6, 65.7, 56.2.

**1,3,5,7-Tetrakis(4-(prop-2-yn-1-yloxy)phenyl)adamantane 6-71**
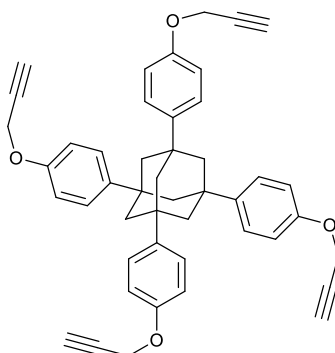
Compound **6-71** was prepared according to the general procedure for propargyl ether linkage core. Product was obtained as a white solid (34 mg), yield 39.5 %.

^{1}H NMR (700 MHz, Chloroform-*d*) δ 7.40 (d, *J* = 8.9 Hz, 1H), 6.96 (d, *J* = 8.8 Hz, 1H), 4.68 (d, *J* = 2.4 Hz, 1H), 2.51 (t, *J* = 2.4 Hz, 1H), 2.08 (s, 2H). ^{13}C NMR (176 MHz, Chloroform-*d*) δ 155.9, 142.8, 126.2, 114.8, 78.7, 75.6, 56.0, 47.8, 38.9.

7.6.3 Amide linkage scaffold synthesis

Tris(2-(all-*cis*-pentafluorocyclohexylacetamido)ethyl)amine 6-53
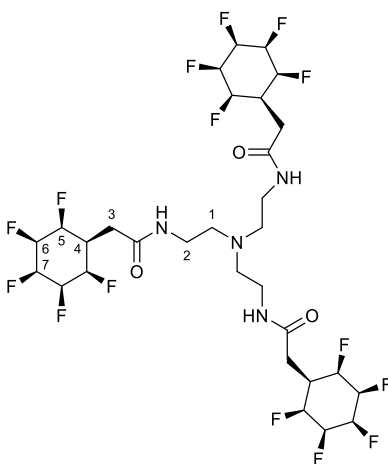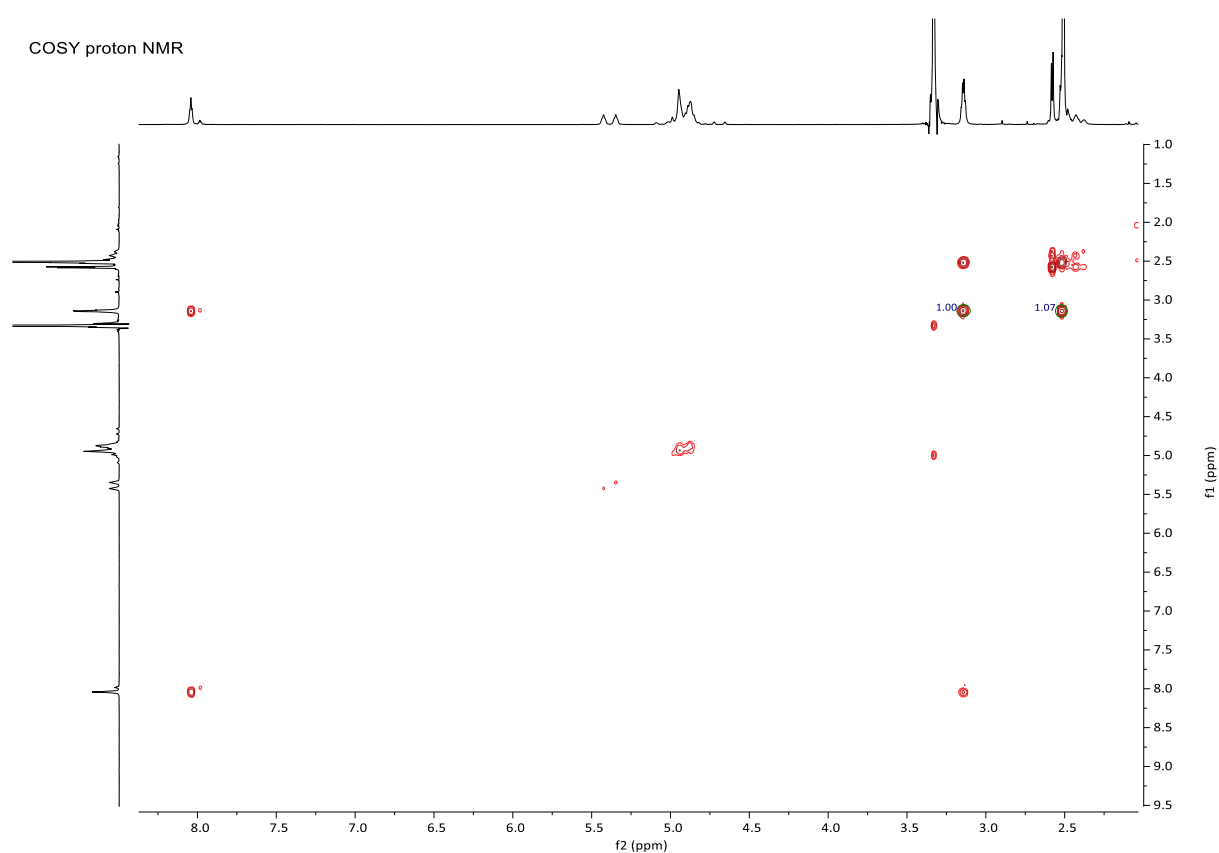

To a solution of all-*cis*-pentafluorocyclohexylacetic acid **6-5** (205 mg, 0.887 mmol) in 5 ml dry DMF, DIPEA (337 mg, 2.61 mmol), HATU (353 mg 0.93 mmol) was added in succession. The reaction mixture was stirred at room temperature for 30 min, after which, tris(2-aminoethyl)amine (26 mg, 0.1775 mmol) was added. The reaction mixture was stirred overnight. After which 20 ml water was added to the reaction mixture. The mixture was extracted with EtOAc (20 ml) three times. The combined organic layer was washed with water, brine, and concentrated *in vacuo*. The solid residue was washed with DCM, dissolved in acetone, and triturated with DCM. Higher product recovery could be archived by submitting the crude product to column chromatography (1 % MeOH, 1 % triethylamine, 5 % acetone and DCM). A white solid (110 mg) was obtained as product, yield 78%.

^{1}H NMR (700 MHz, DMSO-d_6) δ 8.03 (s, 1H, NH), 5.38 (d, J = 54.4 Hz, 1H, H7), 5.12 − 4.55 (m, 4H, CHF, H 5, 6 overlapped), 3.14 (dd, J = 6.5 Hz, 2H, H2), 2.57 (d, J = 7.4 Hz, 2H, H3), 2.52 (m, 2H, integration over cosy), 2.39 (t, J = 36.8 Hz, 1H, H4).

^{19}F NMR (659 MHz, DMSO-d_6) δ -203.73 (d, J = 39.9 Hz, 2F,F6), -210.48(2F, F5), -216.23(1F, F7)

^{13}C NMR (176 MHz, DMSO) δ 169.9 CO, 88.4 (d, J = 188.4 Hz, C5), 87.8 (d, J = 178.9 Hz, C7), 86.5 (d, J = 172.2, C6), 53.7 C1, 37.5 C2 , 34.9 C4(t, J = 18.0 Hz, C4), 33.0 , 32.0 C3.

COSY proton NMR

COSY proton NMR

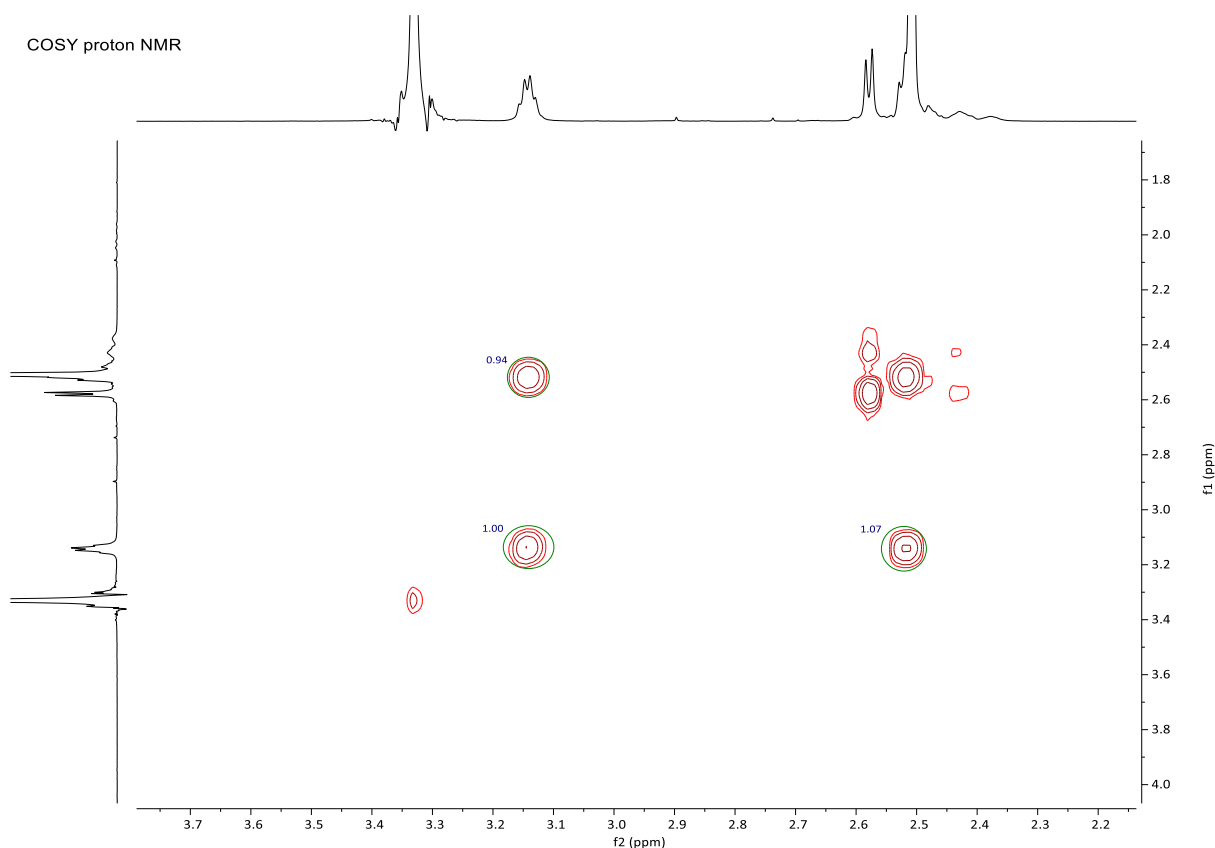**Tetrakis((all-*cis*-pentafluorocyclohexyl)acetaminomethyl)methane 6-54**
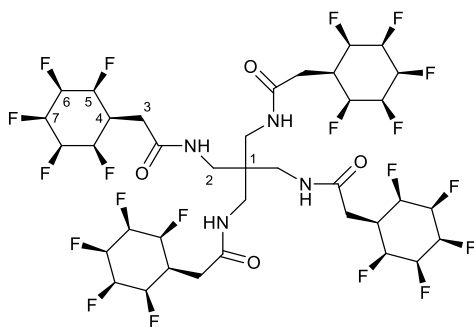
To a solution of all-*cis*-pentafluorocyclohexylacetic acid **6-5** (204 mg, 0.87 mmol) in 5 ml dry DMF, DIPEA (350 mg, 2.71 mmol), HATU (353 mg 0.93 mmol) was added in succession. The reaction mixture was stirred at room temperature for 30 min, after which Tetrakis(aminomethyl)methane (0.174 mmol, 23 mg) was added. The reaction mixture was stirred overnight. After which 20 ml water was added to the reaction mixture. The mixture was extracted with 20 ml DCM three times. The combined organic layer was washed with

water, concentrated *in vacuo*. The solid residue was submitted to column chromatography (10 % MeOH/10% Acetone/DCM) to afford crude product coeluting with DIPEA. The DIPEA was removed by wash with chloroform. Product was obtained as a white solid (48 mg), yield 28 %.

HRMS(ESI FTMS +p) Calculated [M+Na] +P FTMS ESI 1011.2941, observed 1011.2941, [2M+Na] observed as well.

^{1}H NMR (700 MHz, Acetone-d_6) δ 7.76 (t, *J* = 6.7 Hz, 1H, N*H*), 5.56 – 5.31 (d, 1H, *J* = 53.5 Hz, H7), , 5.06 (d, *J* = 50.0 Hz, H5), 5.00 (q, *J* = 40.7 Hz, H6), 3.01 (d, *J* = 6.7 Hz, 2H, H2), 2.83 (d, *J* = 7.2 Hz, 2H, H3), 2.73 – 2.58 (t, *J* = 34.6 Hz, 1H, H4).

^{19}F NMR (659 MHz, Acetone-d_6) δ -205.33 (d, *J* = 38.1 Hz, F6), -211.80, F5, -217.52, F7.

^{13}C NMR (176 MHz, Acetone) δ 172.4 *C*O, 88.0, (d, *J* = 186.3 Hz, C5), 87.5 (d, *J* = 193.5 Hz, C7), 86.5 (d, *J* = 177.8 Hz, C6), 46.1 C1, 39.6 C2, 36.0 C4, 33.1 C3.

Tetrakis((all-*cis*-pentafluorocyclohexyl)acetaminopheyl)methane 6-57
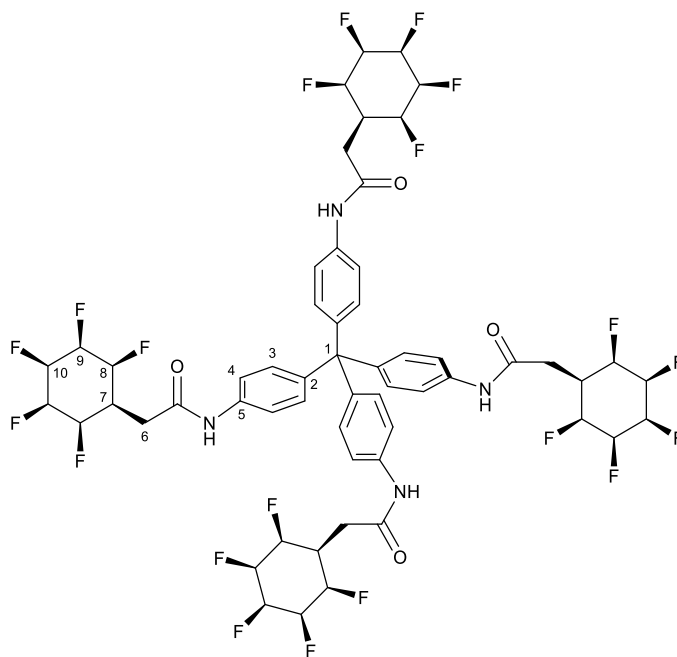
To a solution of all-*cis*-pentafluorocyclohexylacetic acid **6-5** (205 mg, 0.887 mmol) in dry DMF (5 ml), DIPEA (337 mg, 2.61 mmol), HATU (353 mg 0.93 mmol) was added in succession. The reaction mixture was stirred at room temperature for 30 min, after which, tetrakis(*p*-aminophenyl)methane (67 mg, 0.176 mmol) was added. The reaction mixture was stirred overnight. After which water (20 ml) was added to the reaction mixture. The mixture was extracted with EtOAc (20 ml) three times. The combined organic layer was washed with water, brine, concentrated *in vacuo*. The solid residue was washed with DCM, dissolved in acetone, and triturated with DCM. Higher product recovery could be archived by submiting the crude product to column chromatography (10 % MeOH in DCM). The product of white solid (110 mg) was obtained, yield about 50%.

^{1}H NMR (500 MHz, Acetone-d_6) δ 9.56 (s, 1H), 7.59 (d, *J* = 8.8 Hz, 2H), 7.13 (d, *J* = 8.8 Hz, 2H), 5.42 (d, *J* = 53.9 Hz, 1H), 5.21 − 4.68 (m, 4H), 2.92 (d, *J* = 7.2 Hz, 2H), 2.64 (t, *J* = 33.8 Hz, 1H).

^{1}H{^{19}F} NMR (500 MHz, Acetone-d_6) δ 9.54 (s, 1H), 7.59 (d, *J* = 8.5 Hz, 2H), 7.13 (d, *J* = 8.4 Hz, 2H), 5.42 (s, 1H), 5.07 (s, 1H), 4.98 (s, 1H), 2.92 (d, *J* = 7.2 Hz, 2H), 2.64 (s, 223H).

^{19}F NMR (470 MHz, Acetone-d_6) δ -205.24, -211.76 (d, *J* = 25.5 Hz), -216.34 − -218.32 (m).

^{13}C NMR (126 MHz, Acetone) δ 168.6 *C*O, 142.2 C2, 137.0 C5, 131.1 C3, 118.4 C4, 88.1 (d, *J* =184.7 Hz, C8), 87.5 (d, *J* = 194.5 Hz, C10), 86.5 (d, *J* =181.8 Hz, C9), 63.2 C1, 35.0 C7, 32.8 C6.

FTMS+p [M+Na] 1259.3556 obserbed, cal:1259.3567.

Tetrakis((all-*cis*-pentafluorocyclohexyl)acetaminopheyl)methane 6-58
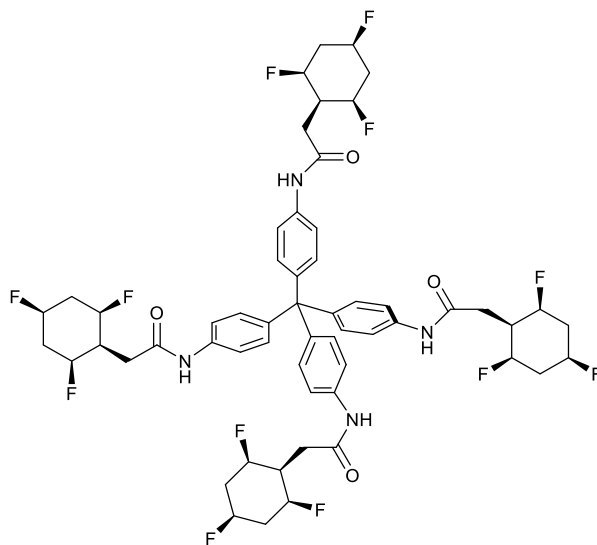
To a solution of all-*cis*-1,3,5-fluorocyclohexylacetic acid (92 mg, 0.48 mmol) in dry DMF (10 ml), DIPEA (250mg, 1.93 mmol), HATU (190 mg, 0.5 mmol) was added in succession. The reaction mixture was stirred at room temperature for 30 min, after which, tetrakis(*p*-aminophenyl)methane (38 mg, 0.1 mmol) was added. The reaction mixture was stirred overnight. After which 20 ml water was added to the reaction mixture. The mixture was extracted with 20 ml DCM three times. The combined organic layer was washed with 50 ml water twice, concentrated *in vacuo* under 50 °C. The brown oil was triturated with DCM to afford pure product (82 mg) as a pale white solid, yield 75 %.

^{1}H NMR (700 MHz, Acetonitrile-*d*$_3$) δ 8.62 (s, 4H), 7.45 (d, *J* = 8.9 Hz, 8H), 7.16 (d, *J* = 8.8 Hz, 8H), 4.83 (ddq, *J* = 50.7, 43.4, 3.3 Hz, 12H), 2.66 (d, *J* = 7.2 Hz, 8H). (solvent overlapped region was assigned by COSY/HSQC/HMBC) 2.48 (m, 8 H, H3 eq), 2.40 (t, *J* = 35.0 Hz, 1H, H-4), 1.97 (dt, *J* = 39.2, 15.1 Hz, H3 ax)
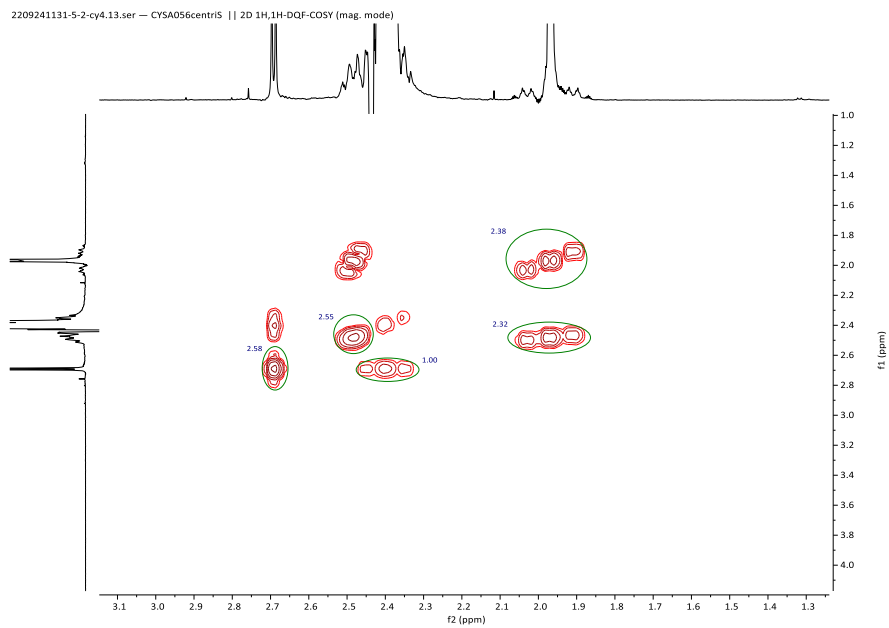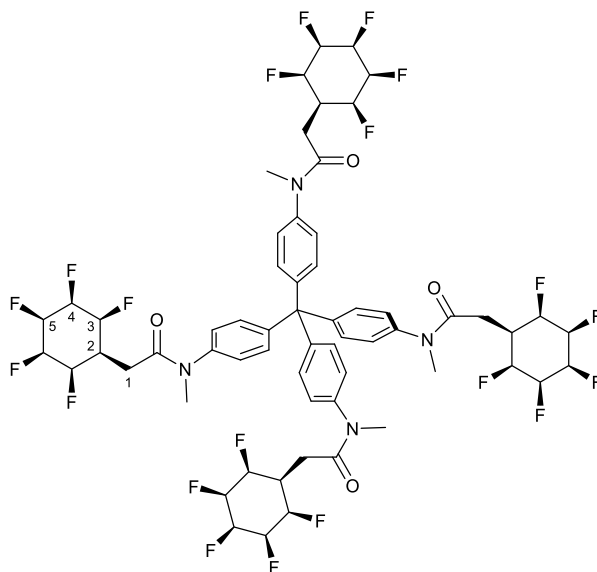
^{13}C NMR (176 MHz, Acetonitrile-d_3) δ 170.7, 143.4, 137.6, 132.0, 119.8, 89.2 (dd, J = 174.2, 4.8 Hz) , 86.3 (d, J = 171.2 Hz), 39.6 (t, J = 18.8 Hz), 34.7 (ddd, J = 20.3, 14.0, 6.3 Hz).

^{19}F NMR (659 MHz, Acetonitrile-d_3) δ -176.39 − -177.54 (m, 1F), -190.37 − -191.98 (m, 2F).

HRMS Cal [M+Na] 1115.4321, obs. 1115.4300.

Tetrakis(*N*-methyl(all-*cis*-pentafluorocyclohexyl)acetamidepheyl)methane 6-59


To an ice cooled solution of compound **6-57** (110 mg, 0.088 mmol) in DMF (5 ml), sodium hydride (0.35 mmol, 1 eq per amide, 60 % w/w in minearal oil, 15 mg) was added. The mixture was allowed to warm to room temperature and stirred for 30 minutes, after which MeI (25 µl, 0.4 mmol) was added dropwise. The reaction mixture was stirred for further 2 h. Then water was added to the reaction mixture. The mixture was extracted with EtOAc and DCM. The combined organic layer was dried over anhydrous sodium sulphate. The dried crude residue was dissolved in acetone and triturated with DCM to afford pure product as pale-yellow solid (91 mg) 80 % yield. Higher yield could be achieved by recovering product from the recrystallisation solution by column chromatography.

^{1}H NMR (700 MHz, Acetone-d_6) δ 7.34 (m, 4H, Ar-H), 5.40 (d, *J* = 53.9 Hz, 1H, C*H*F, H5), 5.17 – 4.71 (m, 4H, C*H*F, H3,H4), 3.25 (s, 3H, Me), 2.59 (m, 3H, overlap of H1, H2). ^{19}F NMR (470 MHz, Acetone-d_6) δ -205.20, -211.72, -217.47.^{13}C NMR (176 MHz, Acetone) δ 132.2 Ar, 126.7 Ar, 88.5 C3, 88.0 C5, 86.0 C4, 36.4 CH$_3$, 35.4 C2, 30.2 C1. HRMS +P [M+Na] cal. 1315.4193 obs. 1315.4176.

7.6.4 Ether linked scaffold synthesis

Tetrakis(4-(2-((all-*cis*)-2,3,4,5,6-pentafluorocyclohexyl)ethoxy)phenyl)methane 6-60
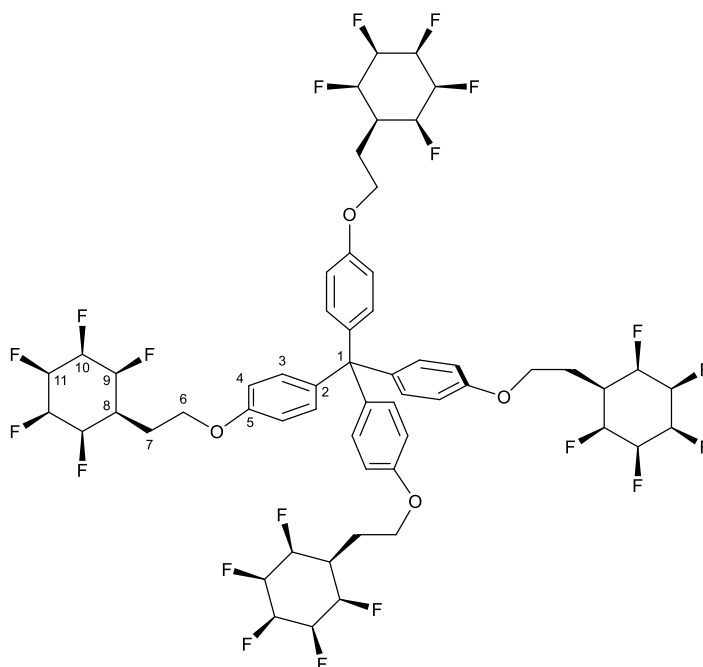
To an oven dried round bottom flask, tetrakis(*p*-hydroxylphenyl)methane (19.4 mg, 0.05 mmol, 1 eq), compound **6-7** (61.7 mg, 0.22 mmol, 4.4 eq), and potassium carbonate (30.4 mg, 0.22 mmol, 4.4 eq) and DMF (5 ml) was added under nitrogen. The reaction mixture was stirred at 90 °C for 24 h. After which the reaction mixture was cooled to room temperature. The reaction mixture was poured into water (20 ml), extracted with EtOAc (50 ml) twice. The combined organic layer was washed with water and brine, and dried over anhydrous sodium sulphate. The crude product was concentrated *in vacuo* and submitted to column chromatography (10 % Acetone in DCM) to offer a white powder, which was further purified by recrystallasation from Acetone by addition of DCM. 44 mg, 74 % yield.

^{1}H NMR (700 MHz, Acetone-d_6) δ 7.08 (d, *J* = 8.9 Hz, 2H, H-3), 6.86 (d, *J* = 8.9 Hz, 2H, H4), 5.42 (d, *J* = 54.0 Hz, 1H, H-11), 5.13 (d, *J* = 50.1 Hz, 2H, H9), 4.95 (dt, *J* = 40.3, 27.7 Hz, 2H, H10), 4.21 (t, *J* = 6.0 Hz, 2H, H-6), 2.40 (t, *J* = 35.2 Hz, 1H, H8), 2.29 (dt to q, *J* = 6.4 Hz, 2H, H7). [note,
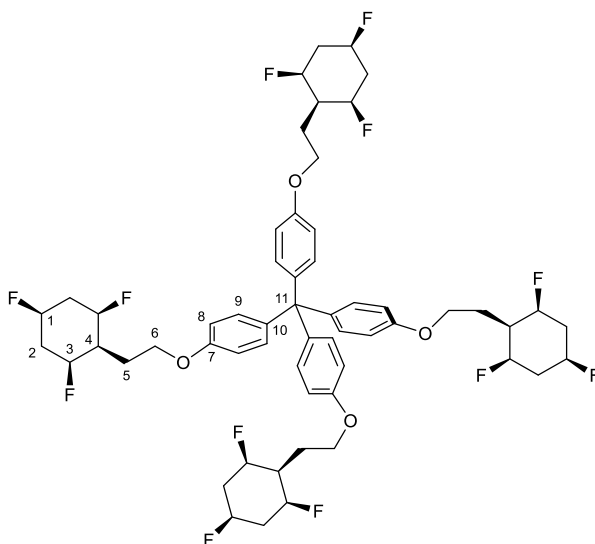
3 eq MeOH was identified]

^{19}F NMR (659 MHz, Acetone-d_6) δ -205.01 (d, J = 41.0 Hz, 2F, F10), -212.57 (m, 2F, F9), -217.21 — -217.94 (m, 1F, F11).

^{13}C NMR (176 MHz, Acetone) δ 156.8 C-5, 139.8 C-2, 131.8 C-3, 113.3 C-4, 88.3 C-9, 88.1 C-11, 86.7 C-10, 64.5 C-6, 62.1 C-1, 35.3 C-8 , 25.8 C-7

HRMS FTMS +p ESI [M+Na] Cal 1207.3757, 1207.3721 found

Tetrakis(4-(2-((all-*cis*)-2,4,6-trifluorocyclohexyl)ethoxy)phenyl)methane 6-61

To an oven dried round bottom flask, tetrakis(*p*-hydroxylphenyl)methane (6.1 mg, 0.016 mmol), compound **6-22** (20 mg, 0.08 mmol, 5 eq) and potassium carbonate (20 mg, 0.14 mmol, 9 eq) and DMF 5 ml was added under nitrogen. The reaction mixture was stirred at 90 °C for 24 h. After which the reaction mixture was cooled to room temperature. The reaction mixture was poured into water (20 ml), extracted with DCM (50 ml) twice. The combined organic layer was washed with water and brine, and dried over anhydrous sodium sulphate. The crude product was concentrated *in vacuo* and submitted to column chromatography (2 % Acetone in DCM) to afford a white powder(10 mg), yield 60 %.

¹H NMR (500 MHz, DMSO-*d*₆) δ 6.98 (d, *J* = 8.4 Hz, 2H, H-9), 6.86 (d, *J* = 8.5 Hz, 2H, H9), 4.87 (d, *J* =48.2 Hz, H-1), 4.84 (d, *J* = 47.4 Hz, H-3), 4.09 (s, 2H, H6), 2.37 (d, *J* = 12.3 Hz, 2H, H5), 2.09 – 1.85 (m, 5H, H4, H2 ax,eq overlapped).

¹⁹F NMR (470 MHz, DMSO-*d*₆) δ -175.43 (t, *J* = 12.6 Hz), -190.04 (d, *J* = 12.5 Hz).

¹³C NMR (126 MHz, DMSO) δ 156.8, 139.8, 131.8, 113.8, 88.0 (d, *J*= 187.8 Hz, C3), 85.5 (d, *J* = 152.2 Hz, C1) , 65.2, 62.4, 34.2, 34.0, 27.0.

HRMS +p [M+Na] cal.1063.4511 , obs. 1063.4547.

1,2-Bis(4-(2-((all-*cis*)-2,3,4,5,6-pentafluorocyclohexyl)ethoxy)phenyl)-1,2-bis(4-(2-((all-*cis*)-2,3,4,5,6-pentafluorocyclohexyl)ethoxy)phenyl)ethane 6-62
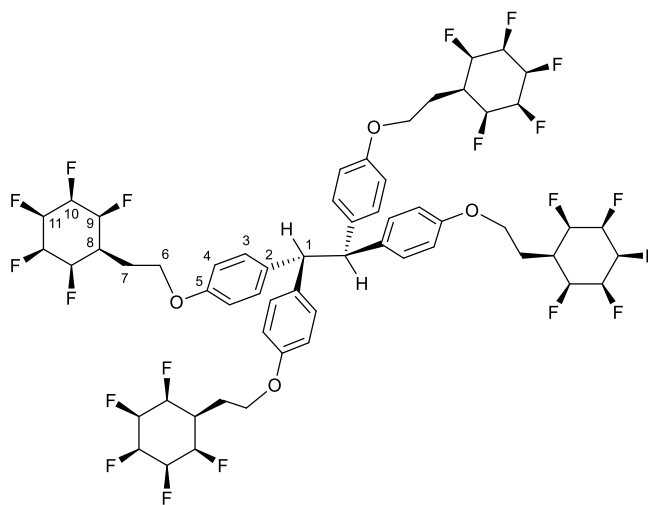
To an oven dried round bottom flask, 1,1,2,2-Tetrakis(p-hydroxyphenyl)ethane (13 mg, 0.05 mmol, 1 eq), compound **6-7** (70 mg, 0.25 mmol, 5 eq) and potassium carbonate (27.6 mg, 0.20 mmol, 4 eq) and DMF (5 ml) was added under nitrogen. The reaction mixture was stirred at 90 °C for 24 h. After which the reaction mixture was cooled to room temperature. The reaction mixture was poured into 20 ml water, extracted with 50 ml DCM twice. The combined organic layer was washed with water and brine, dried over anhydrous sodium sulphate. The crude product was concentrated *in vacuo* and submitted to column

chromatography (10 % Acetone in DCM) to afford a white powder (31 mg), yield 52 %.

^{1}H NMR (700 MHz, Acetone-d_6) δ 7.31 (d, J = 8.7 Hz, 8H), 6.70 (d, J = 8.7 Hz, 8H), 5.39 (d, J = 53.1 Hz, 4H), 5.07 (d, J = 50.8 Hz, 8H), 4.96 (s, 3H), 4.94 − 4.75 (m, 8H), 4.07 (t, J = 6.0 Hz, 8H), 2.31 (d, J = 35.1 Hz, 4H), 2.19 (q, J = 6.4 Hz, 8H).

^{19}F NMR (659 MHz, Acetone-d_6) δ -205.01 (d, J = 40.8 Hz), -212.33 − -213.03 (m), -217.17 − -217.96 (m).

^{13}C NMR (176 MHz, Acetone) δ 157.6 C-5, 138.3 C-2, 130.1 C-3, 114.9 C-4, 87.8 (d, J = 176.1, C9), 87.6 (d, J = 177.4, C-11), 86.7 (d, J = 177.4, C10), 65.3 C-6, 54.9 C-1, 36.0 C-8, 26.7 C-1.

HRMS +p [M+Na] cal. 1221.3913 obs 1221.3896

1,2-Bis(4-(2-((all-*cis*)-2,4,6-Trifluorocyclohexyl)ethoxy)phenyl)-1,2-bis(4-(2-((all-*cis*)-2,4,6-trifluorocyclohexyl)ethoxy)phenyl)ethane 6-63
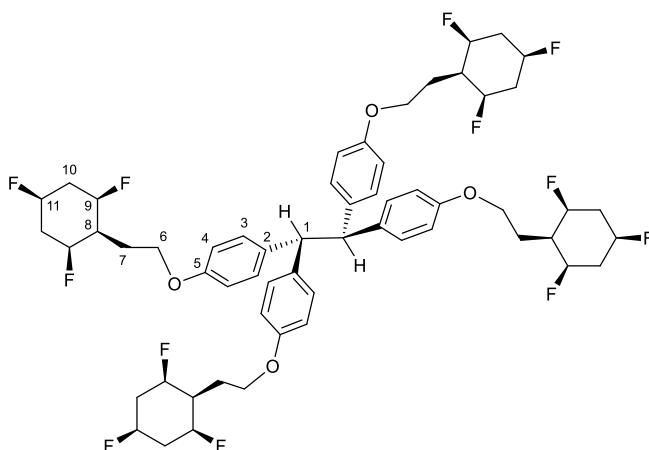
To an oven dried round bottom flask, 1,1,2,2-Tetrakis(p-hydroxyphenyl)ethane (13 mg, 0.033 mmol, 1 eq), compound **6-22** (40 mg, 0.16 mmol, 5 eq) and potassium carbonate (18 mg, 0.13 mmol, 4 eq) and DMF (5 ml) were added under nitrogen. The reaction mixture was stirred at 90 °C for 24 h. After which the reaction mixture was cooled to room temperature. The

reaction mixture was poured into 20 ml water, extracted with 50 ml DCM twice. The combined organic layer was washed with water and brine, dried over anhydrous sodium sulphate. The crude product was concentrated *in vacuo* and submitted to column chromatography (2 % Acetone in DCM) to offer product as a colourless liquid (30 mg) yield 86 %.

^{1}H NMR (700 MHz, Chloroform-*d*) δ 7.04 (d, *J* = 8.7 Hz, 1H), 6.64 (d, *J* = 8.7 Hz, 1H), 4.89 (dt, *J* = 46.7, 3.5 Hz, 1H), 4.78 (dd, *J* = 46.8, 3.5 Hz, 1H), 4.00 (t, *J* = 5.9 Hz, 1H), 2.63 – 2.54 (m, 3H), 2.16 – 2.10 (m, 2H), 2.07 – 1.93 (m, 0H), 1.80 (td, *J* = 39.9, 15.5 Hz, 2H).

^{13}C NMR (176 MHz, Chloroform-*d*) δ 156.7, 136.6, 129.4, 114.2, 87.4 (d, *J* = 177.1 Hz), 85.0 (d, *J* = 174.5 Hz), 64.4, 55.0, 38.5 (t, *J* = 19.5 Hz), 34.3 (t, *J* = 20.7 Hz), 26.9.

^{19}F NMR (659 MHz, Chloroform-*d*) δ -177.78 (dt, *J* = 47.5, 12.6 Hz, 1F, 11-F), -191.42 (tdt, *J* = 42.3, 19.3, 10.0 Hz, 2F, 9-F).

HRMS +p Cal [M+Na] 1077.4662, obs. 1077.4687.

1,1',8,8'-Tetrakis(2-((all-*cis*)-2,3,4,5,6-pentafluorocyclohexyl)ethoxy)-9,9'-spirobi[fluorene] 6-64
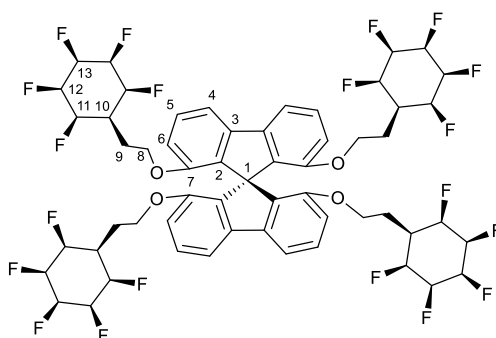
To an oven dried round bottom flask, 7.6.2.15 2,2',7,7'-Tetrahydroxyspirobifluorene (19 mg, 0.05 mmol, 1 eq), compound **6-7** (70 mg, 0.25 mmol, 5 eq.) and potassium carbonate (27.6

mg, 0.20 mmol, 4 eq) and DMF (5 ml) was added under nitrogen. The reaction mixture was stirred at 90 °C for 24 h. After which the reaction mixture was cooled to room temperature. The reaction mixture was poured into water (20 ml), extracted with DCM (50 ml) twice. The combined organic layer was washed with water and brine, dried over anhydrous sodium sulphate. The crude product was concentrated *in vacuo* and submitted to column chromatography (10 % Acetone in DCM) to offer white powder (37 mg) yield 63 %.

^{1}H NMR (700 MHz, Acetone-d_6) δ 7.80 (d, *J* = 8.4 Hz, 4H, H-4), 7.01 (dd, *J* = 8.4, 2.4 Hz, 4H, H-5), 6.21 (d, *J* = 2.3 Hz, 4H, H-6), 5.36 (d, *J* = 53.8 Hz, 4H, H-13), 5.03 (d, *J* = 50.2 Hz, 8H, H-11), 4.86 (dt, *J* = 40.6, 27.7 Hz, 8H, H-12), 4.07 (t, *J* = 6.0 Hz, 8H, H-8), 2.28 (t, *J* = 35.0 Hz, 4H, H-10), 2.18 (q, *J* = 6.4 Hz, 8H, H-9).

^{19}F NMR (659 MHz, Acetone-d_6) δ -205.05 (d, *J* = 40.8 Hz), -212.58 (dtt, *J* = 49.7, 23.5, 14.1 Hz), -217.52 (dtq, *J* = 54.5, 27.4, 16.2, 14.1 Hz).

^{13}C NMR (176 MHz, Acetone) δ 159.4 C-7, 151.3 C-3, 135.6 C-2, 121.2 C-4, 114.5 C-5, 111.4 C-6, 88.4 (d, *J* = 183.3 Hz, C11), 88.2 (d, *J* = 194.2 Hz, C13), 87.2 (d, *J* = 161.5 Hz, C-12), 66.5 C-1, 65.7 C-8, 35.8 C-10, 26.8 C9.

HRMS +p [M+Na] cal. 1203.3444, obs 1203.3433.

5.1.1.16 1,1',8,8'-Tetrakis(2-((1s,2R,4r,6S)-2,4,6-trifluorocyclohexyl)ethoxy)-9,9'-spirobi[fluorene] 6-65
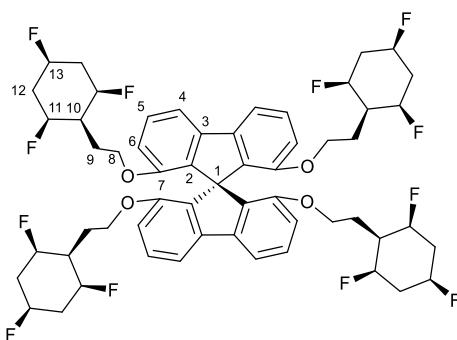
To an oven dried round bottom flask, 7.6.2.15 2,2',7,7'-Tetrahydroxyspirobifluorene (12 mg, 0.032 mmol, 1 eq), compound **6-22** (40 mg, 0.16 mmol, 5 eq.) and potassium carbonate (20 mg, 0.143 mmol, 4.3 eq) and DMF (5 ml) was added under nitrogen. The reaction mixture was stirred at 90 °C for 24 h. After which the reaction mixture was cooled to room temperature. The reaction mixture was poured into water (20 ml), and extracted with DCM (50 ml) twice. The combined organic layer was washed with water and brine, dried over anhydrous sodium sulphate. The crude product was concentrated *in vacuo* and submitted to column chromatography (2 % Acetone in DCM) to offer white powder (21 mg) yield 63 %.

^{1}H NMR (700 MHz, Acetone-d_6) δ 7.78 (d, *J* = 8.4 Hz, 1H), 6.98 (dd, *J* = 8.4, 2.4 Hz, 1H), 6.21 (d, *J* = 2.4 Hz, 1H), 4.85 (d, *J* = 48.0 Hz, 1H, H-13), 4.79 (d, *J* = 145.9 Hz, 2H, H-11),4.00 (t, *J* = 6.3 Hz, 2H, H-8), 2.36 (dd, *J* = 12.2, 3.9 Hz, 2H, H-12 eq.), 2.13 (dt, *J* = 7.1, 3.5 Hz, 1H, H10), 2.04 (m, 2H, H9), 2.00 (d,t, *J* = 31.8, 16.2 Hz, H12 ax).

^{19}F NMR (659 MHz, Acetone-d_6) δ -177.44 (dddd, *J* = 50.1, 38.1, 25.8, 12.9 Hz), -191.28 − -191.66 (m).

^{13}C NMR (176 MHz, Acetone) δ 159.5, 151.4, 135.5, 121.1, 114.6, 111.2, 88.9, 87.9, 86.3, 85.3, 66.1, 39.3, 39.2, 39.1, 27.5.

HRMS FTMS +P, observed 1059.4176, calculated 1059.4198.

Tetrakis(4-((4-(2-((all-*cis*)-2,3,4,5,6-

pentafluorocyclohexyl)ethoxy)phenyl)ethynyl)phenyl)methane 6-66
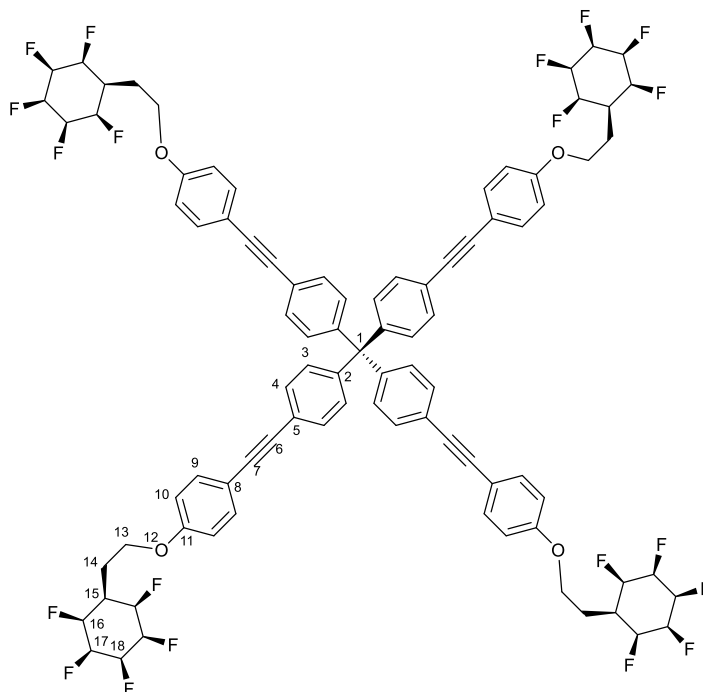
To an oven dried round bottom flask, compound **6-32** (30 mg, 0.038 mmol), compound **6-7** (106.8 mg, 0.382 mmol, 10 eq) and potassium carbonate (52 mg, 0.38mmol, 10 eq) and DMF (5 ml) were added under nitrogen. The reaction mixture was stirred at 90 °C for 72 h. After which the reaction mixture was cooled to room temperature. The reaction mixture was poured into water (20 ml), extracted with EtOAc (50 ml) twice. The combined organic layer was washed with water and brine, dried over anhydrous sodium sulphate. The crude product was concentrated *in vacuo* and submitted to column chromatography (10 % Acetone in DCM) followed by a second column (5 % Acetone in DCM) to afford white powder (26 mg), which was recrystallised from Acetone/DCM, yield 43 %. Higher yield could be achieved by first flush column with 5 % methanol, and separating the product from co-eluting compound **6-21** and **6-22**.

^{1}H NMR (700 MHz, Acetone-*d*$_6$) δ 7.50 (d, *J* = 8.6 Hz, 8H), 7.48 (d, *J* = 8.8 Hz, 8H), 7.28 (d, *J* =

8.6 Hz, 8H), 7.00 (d, *J* = 8.9 Hz, 8H), 5.42 (d, *J* = 53.9 Hz, 4H), 5.15 (d, *J* = 49.9 Hz, 8H), 4.96 (dt, *J* = 40.4, 27.9 Hz, 8H), 4.29 (t, *J* = 6.0 Hz, 8H), 2.42 (d, *J* = 35.0 Hz, 4H), 2.32 (q, *J* = 6.4 Hz, 8H).

^{19}F NMR (659 MHz, Acetone-*d$_6$*) δ -205.04 (d, *J* = 40.7 Hz, 2F, F-17), -212.60 (p, *J* = 32.3, 31.5 Hz, 2F, F16), -217.50 (dt, *J* = 55.5, 24.9 Hz, 1F, F18).

^{13}C NMR (176 MHz, Acetone) δ 160.1, 146.8, 133.9, 131.9, 131.7, 122.6, 116.1, 115.7, 90.6, 88.4, 87.8 (d, *J* = 200.0 Hz, C-16), 87.5 (d, *J* = 191.9 Hz, C-18), 86.5 (d, *J* = 170.6 Hz, C-17) ,65.7, 36.0, 26.6.

HRMS [M+Cl] -p, Cal. 1619.4800, obs 1619.4777.

4,4',4''-((4-Bromophenyl)methanetriyl)tris(((4-(2-((all-*cis*)-2,3,4,5,6-pentafluorocyclohexyl)ethoxy)phenyl)ethynyl)benzene) 6-68
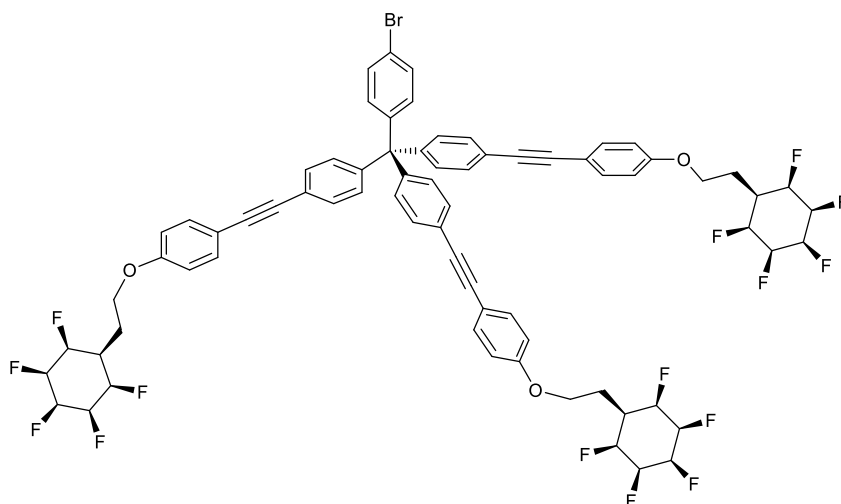
To an oven dried round bottom flask, compound **6-33** (25 mg, 0.034 mmol), compound **6-7** (50.4 mg, 0.191 mmol, 5.5 eq) and potassium carbonate (26 mg, 0.19mmol, 5.5 eq) and DMF (5 ml) were added under nitrogen. The reaction mixture was stirred at 90 °C for 72 h. After which the reaction mixture was cooled to room temperature. The reaction mixture was poured into water (20 ml), extracted with EtOAc (50 ml) twice. The combined organic layer was washed with water and brine, and dried over anhydrous sodium sulphate. The crude

product was concentrated *in vacuo* and submitted to column chromatography (10 % Acetone in DCM) to afford brown solid (20 mg) yield 43 %.

^{1}H NMR (700 MHz, Acetone-d_6) δ 7.55 – 7.46 (m, 16H), 7.29 – 7.25 (m, 6H), 7.21 (d, *J* = 8.8 Hz, 2H), 7.05 – 6.96 (m, 8H), 5.42 (d, *J* = 53.9 Hz, 4H), 5.15 (d, *J* = 49.4 Hz, 8H), 4.96 (dt, *J* = 41.1, 28.5 Hz, 9H), 4.34 – 4.16 (m, 9H), 2.42 (d, *J* = 34.7 Hz, 6H), 2.32 (q, *J* = 6.4 Hz, 9H).

^{19}F NMR (659 MHz, Acetone-d_6) δ -205.04 (d, *J* = 40.4 Hz), -212.60, -217.49.

^{13}C NMR (176 MHz, Acetone) δ 130.9, 133.9, 130.8, 132.9, 130.9, 132.8, 114.9, 88.5, 88.3, 87.1, 64.8, 35.1, 25.8

HRMS [M+Na] Cal. 1371.3207, observed 1371.3218

1,3,5,7-Tetrakis(4-(2-((all-*cis*)-2,3,4,5,6-pentafluorocyclohexyl)ethoxy)phenyl)adamantane 6-69
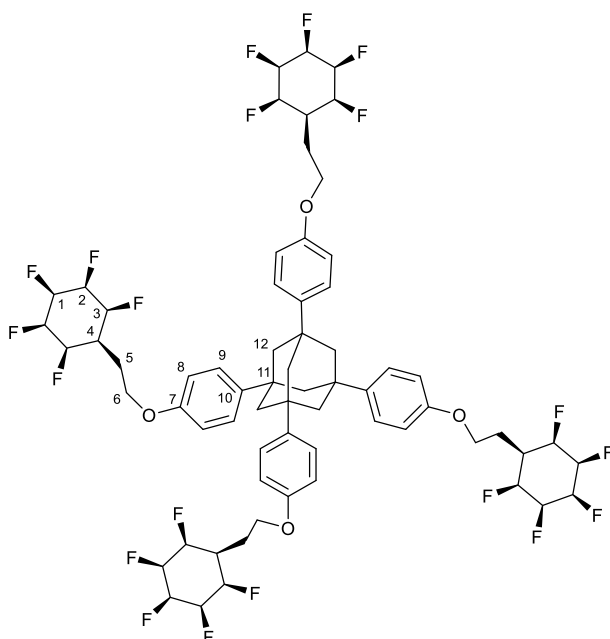
To an oven dried round bottom flask, **6-39** 4,4',4'',4'''-(adamantane-1,3,5,7-tetrayl)tetraphenol (45 mg, 0.089 mmol), compound **6-7** (124 mg, 0.446 mmol, 5 eq) and

potassium carbonate (62 mg, 0.45mmol, 5 eq) and 1.2 mg TBAI, DMF (5 ml) were added under nitrogen. The reaction mixture was stirred at 90 °C for 24 h, and then another batch of compound **6-7** was added and heated and stirred for 48 h (124 mg, 0.446 mmol, 5 eq). After which the reaction mixture was cooled to room temperature. The reaction mixture was poured into water (20 ml), extracted with EtOAc (100 ml) twice. The combined organic layer was washed with water and brine, dried over anhydrous sodium sulphate. The crude product was concentrated *in vacuo* and submitted to column chromatography (10 % Acetone in DCM). The resulting product was further purified by triturated from saturated acetone solution with DCM to afford pure product as a white powder (70 mg), 60 % yield.

^{1}H NMR (700 MHz, Acetone-d_6) δ 7.50 (d, J = 9.0 Hz, 2H, H-9), 6.94 (d, J = 8.8 Hz, 2H, H-8), 5.42 (d, J = 53.4 Hz, 1H, H-1), 5.13 (dd, J = 49.9, 5.1 Hz, 2H, H-3), 5.06 – 4.82 (m, 2H, H-2), 4.21 (t, J = 6.1 Hz, 2H, H-6), 2.38 (t, J = 35.0 Hz, 1H, H4), 2.28 (q, J = 6.4 Hz, 2H, H5), 2.09 (d, J = 10.6 Hz, 3H, H-12).

^{19}F NMR (659 MHz, Acetone-d_6) δ -204.97 (d, J = 40.8 Hz), -212.52 (td, J = 25.4, 12.9 Hz), -216.69 – -218.21 (m).

^{13}C NMR (176 MHz, Acetone) δ 157.9 C-7, 143.3 C-10, 127.0 C-9, 115.1 C8, 89.4 C-3, 88.0 C-1, 86.9 C-2, 65.4 C-6, 48.4 C-12, 36.1 C-11, 26.7 C-4.

HRMS[M+Na] Calcluated 1327.4696 obs. 1327.4690.

7.6.5 Triazole linked scaffold synthesis

General procedure for triazole linked scaffold synthesis

To a microwave tube, tetrakis-alkyne substrate (0.025 mmol, 1 eq), sodium ascorbate (6 mg, 0.06 mmol, 0.3 eq per alkyne, in 0.5 ml water solutiuon), $CuSO_4 \cdot 5H_2O$ (3.8 mg, 0.03mmol, 0.15

eq per alkyne, in 0.5 ml water solution), and azido compound **6-8** (30 mg, 0.123 mmol, 5 eq, or 1.2 eq per alkyne group), water (1 ml) and ethanol (2 ml) was added in sequence under nitrogen. If indicated, DMF/THF (2 ml) was added to dissolved the substrate. The reaction mixture was sealed under nitrogen, and heated at 65 °C for 16 h. After cooling to room temperature, the reaction mixture was centrifuged. The solid residue was washed with the indicated solvent, centrifuged, and dried under vacuum to afford the product as powder.

4,4',4',4'''-((((((1-(2-(all-*cis*)-2,3,4,5,6-Pentafluorocyclohexyl)ethyl)-1H-1,2,3-triazol-4-yl)methoxy)methyl)methane 6-72
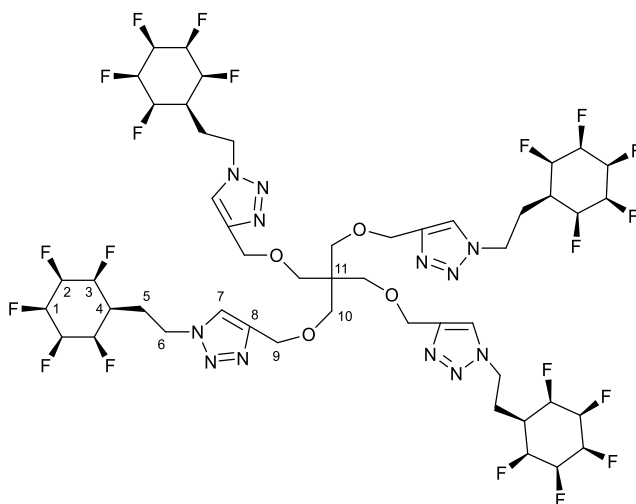
The reaction was performed in a 50 ml sealed tube on twice of scale indicated in the general procedure. After reaction finished, a brown residue was observed in the reaction mixture. The solvent of the reaction was removed by decanting. The residue was washed with water, EtOAc and DCM, then dissolved in acetone. The crude product was concentrated *in vacuo* to afford pure product (55 mg) as a brown gel. Yield 87 %.

^{1}H NMR (700 MHz, Acetone-d_6) δ 5.41 (d, *J* = 53.7 Hz, 1H), 5.14 (d, *J* = 49.7 Hz, 2H), 4.92 (dt, *J* = 36.2, 25.9 Hz, 2H), 4.68 (s, 1H), 4.50 (s, 2H), 3.44 (s, 2H), 2.45 (d, *J* = 7.2 Hz, 2H).
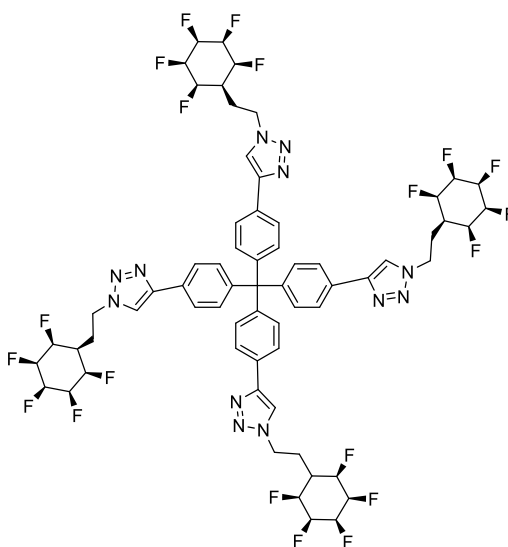
^{13}C NMR (176 MHz, Acetone) δ 145.0 C-8, 123.2, C-7, 87.6(d, *J* = 50.1 Hz, C-3) 87.5 (d, *J* = 51.8

Hz, C-1), 86.6 (d, J = 38.3 Hz, C-2), 69.0 C-10, 64.6 C-9, 46.7 C6, 45.1 C-11, 35.3 C-4, 26.8 C-5,

^{19}F NMR (659 MHz, Acetone-d_6) δ -205.13, -212.63, -217.53.

HRMS [M+Na] +p cal. 1283.4439, obs. 1283.4420.

Tetrakis(4-(1-(2-((all-*cis*)-2,3,4,5,6-pentafluorocyclohexyl)ethyl)-1H-1,2,3-triazol-4-yl)phenyl)methane 6-73

The preparation was conducted according to the general procedure described above. After reaction finished, the suspension was centrifuged. The residue solid was washed with water, and DCM to afford the product (31 mg), 89 % yield.

^{1}H NMR (700 MHz, DMSO-d_6) δ 8.63 (s, 1H), 7.81 (d, J = 8.4 Hz, 1H), 7.34 (d, J = 8.2 Hz, 1H), 5.36 (d, J = 54.6 Hz, 1H), 5.08 (d, J = 50.2 Hz, 2H), 4.86 (dt, J = 43.1, 29.4 Hz, 2H), 4.61 (t, J = 7.1 Hz, 2H), 2.29 (q, J = 7.2 Hz, 2H), 1.91 (t, J = 34.6 Hz, 1H).

^{19}F NMR (659 MHz, DMSO-d_6) δ -203.63 (d, J = 40.3 Hz), -211.58 (t, J = 34.5 Hz), -215.96 − -216.75 (m).

13C NMR (176 MHz, DMSO) δ 146.3, 146.2, 131.1, 129.1, 125.3, 121.9, 87.8 (d, *J* = 168.5 Hz), 87.8 (d, *J* =185.4), 86.7 (d, *J* = 182.0 Hz), 65.1, 44.0, 35.2, 26.8,

HRMS +p Cal [M+Cu] 1451.4041, obs 1450.4032.

Tetrakis(4-((1-(2-((all-*cis*)-2,3,4,5,6-pentafluorocyclohexyl)ethyl)-1H-1,2,3-triazol-4-yl)methoxy)phenyl)methane 6-74
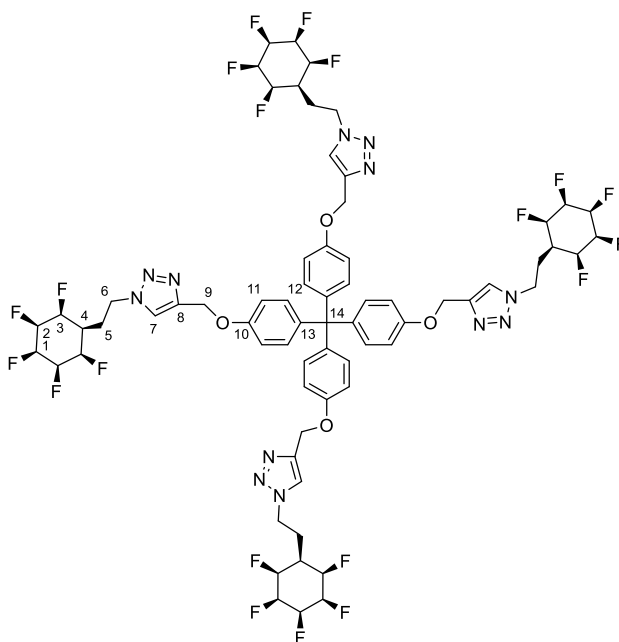
The preparation was conducted according to the general procedure described above, DCM 2 ml was added to the starting material. After the reaction finished, the suspension was centrifuged. The residue solid was washed with water, acetone and DCM to afford the product (34 mg), 98 % yield.

 1H NMR (700 MHz, DMSO-*d*₆) δ 8.32 (s, 1H, H-7), 6.99 (q, *J* = 8.8 Hz, 4H, H-12), 5.37 (d, *J* = 54.1 Hz, 1H, H-1), 5.11 (s, 2H, H-9), 5.07 (m, 2H, H-3), 4.88 (q, *J* = 29.7 Hz, 2H, H-2), 4.58 (t, *J* = 7.1 Hz, 2H, H-6), 2.26 (d, *J* = 7.4 Hz, 2H, H-5), 2.01 – 1.85 (m, 1H, H4).

19F NMR (659 MHz, DMSO-*d*₆) δ -203.64 (d, *J* = 39.8 Hz), -211.63, -216.29 (d, *J* = 47.2 Hz).

^{13}C NMR (176 MHz, DMSO) δ 156.1, 143.2, 139.4, 131.5, 124.7, 113.5, 88.0, 87.0, 85.7, 61.1, 46.5, 26.4.

HRMS FTMS +P, ESI, cal [M+Cu] 1571.4463, obs 1571.4460.

1,1,2,2-Tetrakis(4-((1-(2-((all-*cis*)-2,3,4,5,6-pentafluorocyclohexyl)ethyl)-1H-1,2,3-triazol-4-yl)methoxy)phenyl)ethane 6-75
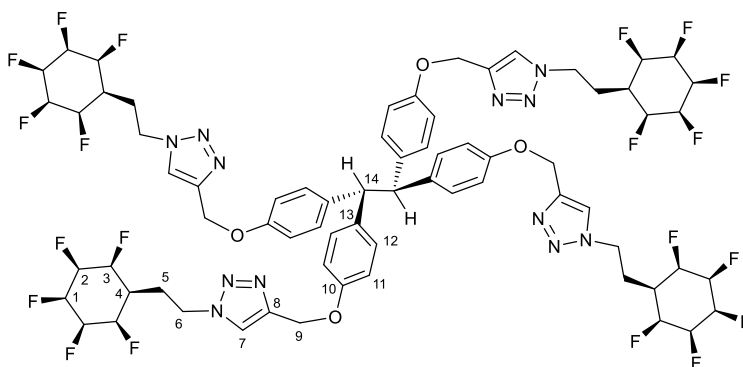
The preparation was conducted according to the general procedure, with additional THF (1 ml) to the starting material. Product (35 mg) was obtained, yield 92 %.

^{1}H NMR (700 MHz, DMSO-d_6) δ 8.23 (s, 4H, H-7), 7.32 (d, J = 8.7 Hz, 8H, H-12), 6.78 (d, J = 8.2 Hz, 8H, H-11), 5.36 (d, J = 53.9 Hz, 4H, H-1), 5.06 (d, J = 50.1 Hz, 8H, H-3), 4.97 (s, 10H, H-9, H-14 overlapped), 4.92 − 4.72 (m, 8H, H-2), 4.54 (t, J = 7.2 Hz, 8H, H-6), 2.23 (q, J = 7.3 Hz, 8H, H-5), 1.92 (t, J = 37.0 Hz, 4H, H-4).

^{19}F NMR (659 MHz, DMSO-d_6) δ -203.66 (d, J = 39.9 Hz), -211.29 − -212.26 (m), -215.95 − -216.83 (m).

^{13}C NMR (176 MHz, DMSO) δ 156.1, 143.3, 137.9, 129.8, 125.0, 114.4, 88.3, 88.2, 87.1, 61.3, 53.4, 47.1, 35.1, 26.8

Calculated for [M+Cu] 1585.4620, obs 1585.4580.

1,1',8,8'-Tetrakis((1-(2-((all-*cis*)-2,3,4,5,6-pentafluorocyclohexyl)ethyl)-1H-1,2,3-triazol-4-yl)methoxy)-9,9'-spirobi[fluorene] 6-76
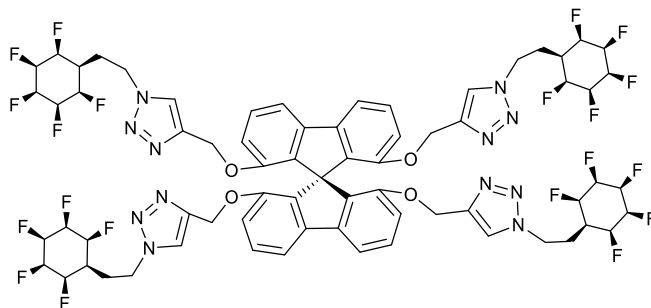
The preparation was conducted according to the general procedure, starting alkyne (8 mg 0.015 mmol used), with additional DMF (1 ml) added. Product (15 mg) obtained, yield 66 %.

^{1}H NMR (700 MHz, DMSO-d_6) δ 8.18 (s, 1H), 7.85 (d, J = 8.4 Hz, 1H), 7.10 (dd, J = 8.4, 2.4 Hz, 1H), 6.18 (d, J = 2.4 Hz, 1H), 5.35 (d, J = 55.0 Hz, 1H), 5.03 (d, J = 61.8 Hz, 4H), 4.95 – 4.70 (m, 2H), 4.52 (t, J = 7.1 Hz, 2H), 2.20 (q, J = 7.3 Hz, 2H), 1.88 (t, J = 35.7 Hz, 1H).

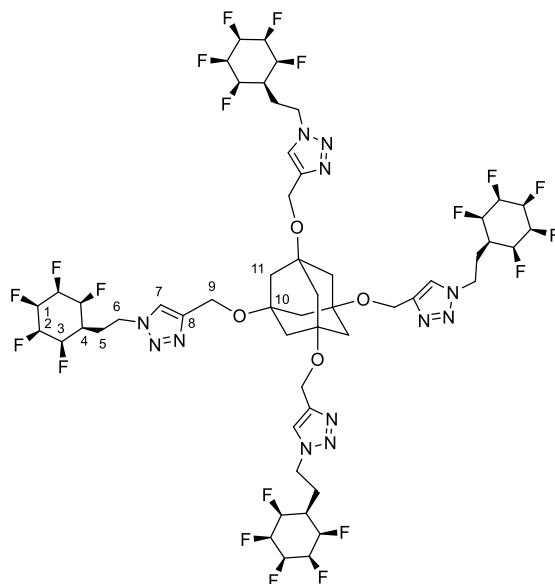^{19}F NMR (659 MHz, DMSO-d_6) δ -203.67 (d, J = 36.8 Hz), -211.69, -216.30.

^{13}C NMR (176 MHz, DMSO) δ 158.0, 150.5,143.1, 134.8, 124.7, 121.2, 114.3, 110.9, 88.,3 87.0, 88.2, 66.1, 61.7, 46.8, 35.1, 26.8,

HRMS [M+Cu] +p, cal 1567.4150 obs 1567.4130.

4,4',4'',4'''-((Adamantane-1,3,5,7-tetrayltetrakis(oxy))tetrakis(methylene))tetrakis(1-(2-((all-*cis*)-2,3,4,5,6-pentafluorocyclohexyl)ethyl)-1H-1,2,3-triazole) 6-77

The reaction was conducted according to the general procedure. Product (13 mg) was obtained. Product was washed with water, DCM, 10% acetone in DCM, and EtOAc. Yield 39 %.

^{1}H NMR (700 MHz, DMSO-d_6) δ 8.13 (s, 1H, H-7), 5.37 (d, *J* = 54.5 Hz, 1H, H-1), 5.07 (d, *J* = 50.6 Hz, 2H, H3), 4.97 – 4.73 (m, 2H, H-2), 4.59 (s, 2H, H-9), 4.54 (t, *J* = 7.2 Hz, 2H, H-6), 2.24 (q, *J* = 7.3 Hz, 2H, H-5), 1.97 (t, *J* = 35.6 Hz, 1H, H-4), 1.88 (s, 3H, H-11).

^{19}F NMR (659 MHz, DMSO-d_6) δ -203.63 (d, *J* = 40.6 Hz), -211.28 – -212.07 (m), -215.48 – -216.46 (m).

^{13}C NMR (176 MHz, DMSO) δ 145.6, 124.1, 88.3, 88.4, 87.0, 75.5, 55.6, 46.8, 44.1, 35.2, 26.9

HRMS FTMS -p calculated [M+Cu] 1387.4150, obs. 1387.4104.

4,4',4'',4'''-(((Adamantane-1,3,5,7-tetrayltetrakis(benzene-4,1-diyl))tetrakis(oxy))tetrakis(methylene))tetrakis(1-(2-((all-*cis*)-2,3,4,5,6-pentafluorocyclohexyl)ethyl)-1H-1,2,3-triazole) 6-78
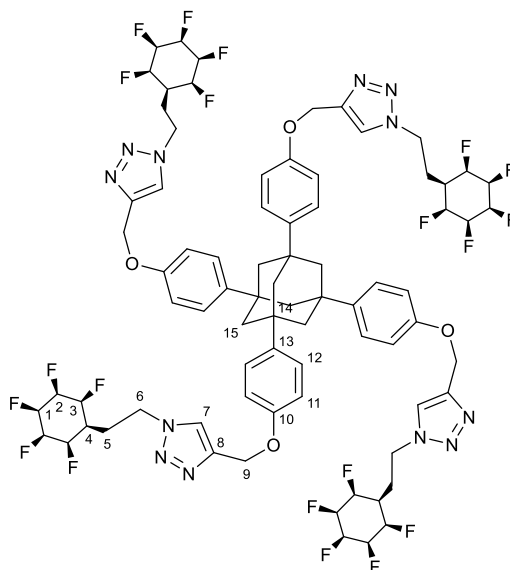
Compound **6-78** was prepared according to the general procedure, DMF (1 ml) was added. Starting material alkyne (13 mg, 0.02 mmol) was used. Product (27 mg) was isolated by wash with MeOH, DCM. Yield 83 %

^{1}H NMR (700 MHz, DMSO-*d*6) δ 8.31 (s, 1H, H-7), 7.47 (d, *J* = 8.9 Hz, 1H, H-12), 7.00 (d, *J* = 8.9 Hz, 1H, H-11), 5.37 (d, *J* = 53.4 Hz, 1H, H-1), 5.12 (s, 2H, H-9), 4.96 – 4.77 (m, 2H, H-2), 4.57 (t, *J* = 7.2 Hz, 2H, H-6), 2.25 (q, *J* = 7.2 Hz, 2H, H-5), 2.00 (m, 4H, H4 and H-15). ^{19}F NMR (659 MHz, DMSO-*d*6) δ -203.63 (d, *J* = 40.3 Hz), -211.65, -216.29. ^{13}C NMR (176 MHz, DMSO) δ 156.6, 143.4, 142.8, 126.7, 124.8, 114.7, 88.1, 87.3, 87.2, 61.5, 47.5, 46.8, 38.9, 35.3, 26.8.

HRMS [M+Cu] FTMS -P , 1692.5436 obs 1062.5395.

7.7 References

1. H. E. Gottlieb, V. Kotlyar and A. Nudelman, *J. Org. Chem.*, 1997, **62**, 7512-7515.

2. M. P. Wiesenfeldt, Z. Nairoukh, W. Li and F. Glorius, *Science*, 2017, **357**, 908-912.

3. Y. Wei, B. Rao, X. Cong and X. Zeng, *J. Am. Chem. Soc.*, 2015, **137**, 9250-9253.

4. M. S. Baker and S. T. Phillips, *J. Am. Chem. Soc.*, 2011, **133**, 5170-5173.

5. X.-j. Qiao, X. Hou, W.-h. Fang, X.-f. Bao and G.-l. Chen, *J. Am. Chem. Soc.*, 2015, **27**, 899-904.

6. F. Leroux, E. Castagnetti and M. Schlosser, *J. Org. Chem.*, 2003, **68**, 4693-4699.

7. W. Kitching, H. A. Olszowy, G. M. Drew and W. Adcock, *J. Org. Chem.*, 1982, **47**, 5153-5156.

8. D. L. Mattern, *J. Org. Chem.*, 1984, **49**, 3051-3053.

9. A. Kütt, V. Movchun, T. Rodima, T. Dansauer, E. B. Rusanov, I. Leito, I. Kaljurand, J. Koppel, V. Pihl, I. Koppel, G. Ovsjannikov, L. Toom, M. Mishima, M. Medebielle, E. Lork, G.-V. Röschenthaler, I. A. Koppel and A. A. Kolomeitsev, *J. Org. Chem.*, 2008, **73**, 2607-2620.

10. N. S. Keddie, A. M. Z. Slawin, T. Lebl, D. Philp and D. O'Hagan, *Nat. Chem.*, 2015, **7**, 483-488.

11. P. P. Geurink, N. Liu, M. P. Spaans, S. L. Downey, A. M. C. H. van den Nieuwendijk, G. A. van der Marel, A. F. Kisselev, B. I. Florea and H. S. Overkleeft, *J. Med. Chem.*, 2010, **53**, 2319-2323.

12. Deepa and S. Singh, *Adv. Synth. Catal.*, 2021, **363**, 629-656.

13. J. L. Clark, R. M. Neyyappadath, C. Yu, A. M. Z. Slawin, D. B. Cordes and D. O'Hagan, *Chem. - Eur. J.*, 2021, **27**, 16000-16005.

14. S. J. Kim, Y. Oh, H. Park, S. Oh and H. Kim, *Bull. Korean Chem. Soc.*, 2015, **36**, 1897-1899.

15. H. Tsuji, G. Cantagrel, Y. Ueda, T. Chen, L.-J. Wan and E. Nakamura, *Chem. - Asian J.*, 2013, **8**, 2377-2382.

16. S. A. Hudson, K. J. McLean, S. Surade, Y.-Q. Yang, D. Leys, A. Ciulli, A. W. Munro and C. Abell, *Angew. Chem. Int. Ed.*, 2012, **51**, 9311-9316.

17. T. Taniguchi, M. Imoto, M. Takeda, T. Nakai, M. Mihara, T. Iwai, T. Ito, T. Mizuno, A. Nomoto and A. Ogawa, *Heteroat. Chem*, 2015, **26**, 411-416.

18. E. Díez-Barra, R. González, P. Sánchez-Verdú and J. Tolosa, *Tetrahedron*, 2004, **60**, 1563-1569.

19. E. Galoppini and R. Gilardi, *Chem. Commun.*, 1999, DOI: 10.1039/A807993E, 173-174.

20. J. Krauss, U. Kopp and F. Bracher, *Z. Naturforsch., B*, 2015, **70**, 637-641.

21. F. M. Menger and V. A. Migulin, *J. Org. Chem.*, 1999, **64**, 8916-8921.

22. A. Schwenger, W. Frey and C. Richert, *Chem. - Eur. J.*, 2015, **21**, 8781-8789.

23. G.-j. Liu, Y. Zhang, L. Zhou, L.-y. Jia, G. Jiang, G.-w. Xing and S. Wang, *Chem. Commun.*, 2019, **55**, 9869-9872.

24. R. Butera, A. Shrinidhi, K. Kurpiewska, J. Kalinowska-Tłuścik and A. Dömling, *Chem. Commun.*, 2020, **56**, 10662-10665.

25. L. Pop, F. Dumitru, N. D. Hădade, Y.-M. Legrand, A. van der Lee, M. Barboiu and I. Grosu, *Org. Lett.*, 2015, **17**, 3494-3497.

26. S. Néron, M. Morency, L. Chen, T. Maris, D. Rochefort, R. Iftimie and J. D. Wuest, *J. Org. Chem.*, 2022, **87**, 7673-7695.